FROM SINGLE STEM CELLS TO ORGANOIDS, ORGAN REPAIR, AND PUBLIC HEALTH

EDITED BY: Lon J. Van Winkle, Philip Iannaccone and Rebecca Ryznar
PUBLISHED IN: Frontiers in Cell and Developmental Biology and
Frontiers in Genetics

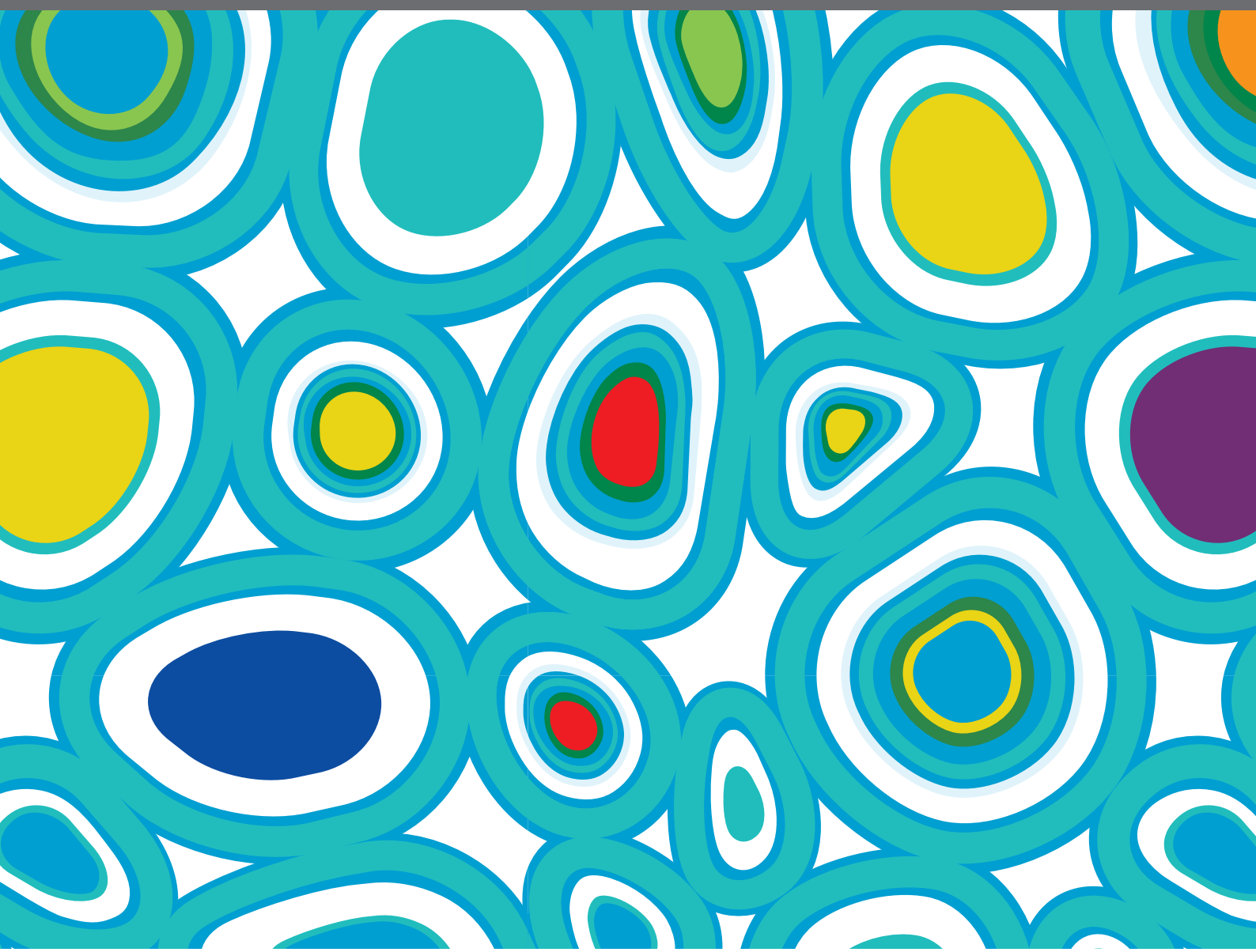

frontiers Research Topics

ISSN 1664-8714
ISBN 978-2-88974-624-8
DOI 10.3389/978-2-88974-624-8

About Frontiers

Frontiers is more than just an open-access publisher of scholarly articles: it is a pioneering approach to the world of academia, radically improving the way scholarly research is managed. The grand vision of Frontiers is a world where all people have an equal opportunity to seek, share and generate knowledge. Frontiers provides immediate and permanent online open access to all its publications, but this alone is not enough to realize our grand goals.

Frontiers Journal Series

The Frontiers Journal Series is a multi-tier and interdisciplinary set of open-access, online journals, promising a paradigm shift from the current review, selection and dissemination processes in academic publishing. All Frontiers journals are driven by researchers for researchers; therefore, they constitute a service to the scholarly community. At the same time, the Frontiers Journal Series operates on a revolutionary invention, the tiered publishing system, initially addressing specific communities of scholars, and gradually climbing up to broader public understanding, thus serving the interests of the lay society, too.

Dedication to Quality

Each Frontiers article is a landmark of the highest quality, thanks to genuinely collaborative interactions between authors and review editors, who include some of the world's best academicians. Research must be certified by peers before entering a stream of knowledge that may eventually reach the public - and shape society; therefore, Frontiers only applies the most rigorous and unbiased reviews.
Frontiers revolutionizes research publishing by freely delivering the most outstanding research, evaluated with no bias from both the academic and social point of view. By applying the most advanced information technologies, Frontiers is catapulting scholarly publishing into a new generation.

What are Frontiers Research Topics?

Frontiers Research Topics are very popular trademarks of the Frontiers Journals Series: they are collections of at least ten articles, all centered on a particular subject. With their unique mix of varied contributions from Original Research to Review Articles, Frontiers Research Topics unify the most influential researchers, the latest key findings and historical advances in a hot research area! Find out more on how to host your own Frontiers Research Topic or contribute to one as an author by contacting the Frontiers Editorial Office: frontiersin.org/about/contact

FROM SINGLE STEM CELLS TO ORGANOIDS, ORGAN REPAIR, AND PUBLIC HEALTH

Topic Editors:
Lon J. Van Winkle, Rocky Vista University, United States
Philip Iannaccone, Northwestern University, United States
Rebecca Ryznar, Rocky Vista University, United States

Citation: Van Winkle, L. J., Iannaccone, P., Ryznar, R., eds. (2022). From Single Stem Cells to Organoids, Organ Repair, and Public Health.
Lausanne: Frontiers Media SA. doi: 10.3389/978-2-88974-624-8

Table of Contents

frontiers in Cell and Developmental Biology

EDITORIAL
published: 11 February 2022
doi: 10.3389/fcell.2022.849889

Editorial: From Single Stem Cells to Organoids, Organ Repair, and Public Health

Lon J. Van Winkle[1,2]*, *Rebecca J. Ryznar*[3] *and Philip M. Iannaccone*[4]

[1]Department of Biochemistry, Midwestern University, Downers Grove, IL, United States, [2]Department of Medical Humanities, Rocky Vista University, Parker, CO, United States, [3]Molecular Biology, Department of Biomedical Sciences, Rocky Vista University, Parker, CO, United States, [4]Department of Pediatrics and Pathology, Northwestern University's Feinberg School of Medicine, Stanley Manne Children's Research Institute, Lurie Children's Hospital, Chicago, IL, United States

Keywords: drug therapy, organoid, public health, single-cell analysis, stem cells

Editorial on the Research Topic

From Single Stem Cells to Organoids, Organ Repair, and Public Health

INTRODUCTION

Teratocarcinomas were shown more than 50 years ago to harbor stem cells that differentiate into components of all three germ layers. Soon, pluripotent cells were obtained from preimplantation embryos and were induced to form three dimensional structures, embryoid bodies recapitulating normal embryonic development. Producing induced pluripotent stem cells (iPSCs) or using adult stem cells, along with directed differentiation is used to develop organized three-dimensional bodies known as organoids that duplicate normal tissues both biochemically and physiologically. When produced from disease state iPSCs, organoids can be used to investigate pathogenesis and therapy. Finally, the regulated heterogeneity of cells as they develop into organoids can now be investigated using single cell RNA sequencing and other emerging genomic technologies. Papers contributed to this Research Topic describe how stem cells and organoids may eventually foster public health.

POSSIBLE CONTRIBUTIONS OF ORGANOIDS TO PUBLIC HEALTH

In their review, Heremans et al. described work to study tissues comprising the human female reproductive tract using organoids derived from healthy or diseased tissues. Biobanking, gene-editing and multi-omics, tissue and organ regeneration, interactions with pathogens, drug testing, and precision therapy all can be evaluated using these models. The authors describe models and conditions needed to maintain healthy tissues or alternatively produce disease states, such as endometriosis and endometrial cancer.

Zhang et al. consider the ways in which intestinal organoid (IO) technology provides new opportunities to study intestinal cell differentiation, interactions, organogenesis, and function. Moreover, IOs are used to study inflammatory bowel disease, colorectal cancers and other malignancies, gastrointestinal infections, and genetic diseases including cystic fibrosis. These authors also describe current shortcomings of organoid research using bibliometric analyses, including the absence of other pertinent structures, such as the vascular system and associated cells, and they recommend that co-culture systems be developed. The organoids block external effectors, such as drugs, from reaching the apical side of the IOs, an important future research direction.

OPEN ACCESS

Edited by:
Atsushi Asakura,
University of Minnesota Twin Cities, United States

Reviewed by:
Jorge Munera,
Medical University of South Carolina, United States

****Correspondence:***
Lon J. Van Winkle
lvanwi@midwestern.edu

Specialty section:
This article was submitted to Stem Cell Research, a section of the journal Frontiers in Cell and Developmental Biology

Received: *06 January 2022*
Accepted: *24 January 2022*
Published: *11 February 2022*

Citation:
Van Winkle LJ, Ryznar RJ and Iannaccone PM (2022) Editorial: From Single Stem Cells to Organoids, Organ Repair, and Public Health. Front. Cell Dev. Biol. 10:849889. doi: 10.3389/fcell.2022.849889

In their mini review, Sun et al. discuss skin complexity and components, such as hair follicles and sweat glands, that are missing from most efforts to generate functional human skin *in vitro*. Human skin production *in vitro* is an important source of tissues for therapy and study. Of particular interest is regeneration of eccrine sweat glands in human skin produced *in vitro* (and as discussed by Lin et al. in their review). Multiple signaling pathways, that govern cellular differentiation into eccrine sweat gland cells, are discussed. Sun et al. discuss the sources of skin cells and skin organoids, the microenvironment for these cells and the challenges and opportunities involved in producing skin organoids that are multifunctional.

In their review, Fernandes et al. describe the use of human and nonhuman iPSCs to generate mini-brain organoids to probe the complexity of human-specific brain development and human brain evolution. Organoids can be generated representing different brain regions, allowing the study of interactions between combinations in culture. A multiplicity of genes important to brain development are differentially expressed spatiotemporally in humans vs. nonhuman primates. The transcriptome can be manipulated and perturbed in brain organoids using gene editing technologies. These studies will reveal not only how mechanisms of brain development differ among species and unique mechanisms driving brain disorder pathophysiology, but also processes, such as neoteny, that have been employed during human brain evolution.

In their research article, Erni et al. used cochlear organoid cultures and other means, such as explants of the organ of Corti, to show that two novel gamma-secretase inhibitors, termed CPD3 and CPD8, increased cochlear hair cell numbers. Their preclinical data support the notion that CPD3 might be used to restore hearing in clinical trials. Since hair cell degeneration is a major contributor to hearing loss among five percent of people in the world, successful therapeutic development would substantially improve the health of affected individuals and public health in general.

USE OF STEM CELLS DIRECTLY TO PROMOTE HUMAN HEALTH

Three research articles report successful efforts to produce and utilize stem cells clinically. First, Chakritbudsabong et al., showed that exogenous LIN28 supports porcine iPSC pluripotency and proliferation. Successful porcine iPSC production has lagged that of other species and prevented establishment of this model of human development and differentiation. Organs derived from porcine iPSCs might be used eventually to help to produce organs for human transplant. Moreover, porcine iPSCs will help improve veterinary medicine therapies and agricultural production.

For humans, Rabesandratana et al. demonstrated that hiPSCs can be used to generate retinal ganglion cells (RGCs). This use of hiPSCs is important because RGCs themselves are not easily located and grown *in vitro*. RGCs produced from hiPSCs survived for nearly a month when the authors injected them into the vitreous of mice experiencing optic neuropathy. Thus, these RGCs might eventually be used to promote human health by preventing or even reversing blindness.

Lan et al. describe how exosomes produced by bone marrow stem cells (BMSCs) foster their own osteogenic differentiation on titanium surfaces. This differentiation is essential to the successful production of dental implants and is impeded by medical conditions like diabetes, osteoporosis, and others. Loss of teeth from deterioration or accident leads to malocclusion, difficulty eating, and significant bone loss in the jaw. Ameliorating these effects will improve the health of millions of people with obvious impacts on the public health.

Three review papers also describe the possible use of stem cells directly to promote human health. To treat type 1 diabetes mellitus, beta-cell function can be restored through islet transplantation. The supply of beta-cells is, of course, limited by donor availability. However, Szlachcic et al. consider how an inexhaustible supply of beta-cells might be produced from hiPSCs. These authors consider how single-cell RNA sequencing (scRNA-Seq) could be used better to understand normal pancreas development and, specifically, beta-cell differentiation. This understanding might then be used to produce better sources of beta-cells for individuals from whom the hiPSCs were derived. The consequences of such technology for worldwide public health could be enormous, since the costs of diabetes, as measured both monetarily and regarding human suffering, are extremely large. In 2020, the cost to care for persons in the US with type 1 diabetes was projected to be $203 billion over a ten-year period (Sussman, M., Benner, J., Haller, M. J., Rewers, M., and Griffiths, R. (2020). Estimated lifetime economic burden of type 1 diabetes. *Diabetes technology and therapeutics* 22, 121–130).

Similarly, mesenchymal stem cells (MSCs) transplantation could be used to treat premature ovarian failure (POF), as described in the review by Wang et al. The incidence of POF has increased to about ten percent of women in recent years apparently owing, in part, to greater life stresses. MSC transplantation in animals has restored ovarian function, apparently through their differentiation into oocytes, and makes us optimistic that fertility can be restored in this way in women with POF. MSCs have already been used clinical to treat many human diseases including blood, skin, and cardiovascular disorders.

Liver injury, regeneration, and diseases, including cancer, might also be fostered/treatable by properly activating stem cells. Several types of cells are involved in liver regeneration, and their balanced regulation is essential to this process. For example, c-kit positive hepatocytes, oval cells, and bile epithelial cells promote liver repair by differentiating into different types of cells depending on the nature of the injury. But c-kit positive mast cells are associated with primary sclerosing cholangitis, and c-kit overexpression may result in malignancy. Hence, Wang et al. concluded that c-kit is "a double-edged sword in liver regeneration and diseases."

AUTHOR CONTRIBUTIONS

LJV wrote the initial draft, and PMI and RJR edited the draft extensively.

Conflict of Interest: The authors declare that the research was conducted in the absence of any commercial or financial relationships that could be construed as a potential conflict of interest.

Publisher's Note: All claims expressed in this article are solely those of the authors and do not necessarily represent those of their affiliated organizations, or those of the publisher, the editors and the reviewers. Any product that may be evaluated in this article, or claim that may be made by its manufacturer, is not guaranteed or endorsed by the publisher.

frontiers in Cell and Developmental Biology

ORIGINAL RESEARCH
published: 27 October 2020
doi: 10.3389/fcell.2020.585675

Generation of a Transplantable Population of Human iPSC-Derived Retinal Ganglion Cells

Oriane Rabesandratana[1], Antoine Chaffiol[1], Antoine Mialot[1], Amélie Slembrouck-Brec[1], Corentin Joffrois[1], Céline Nanteau[1], Amélie Rodrigues[1], Giuliana Gagliardi[1], Sacha Reichman[1], José-Alain Sahel[1,2,3], Alain Chédotal[1], Jens Duebel[1], Olivier Goureau[1] and Gael Orieux[1]**

[1] Institut de la Vision, Sorbonne Université, INSERM, CNRS, Paris, France, [2] CHNO des Quinze-Vingts, INSERM-DHOS CIC 1423, Paris, France, [3] Department of Ophthalmology, The University of Pittsburgh School of Medicine, Pittsburgh, PA, United States

OPEN ACCESS

Edited by:
Lon J. Van Winkle,
Rocky Vista University, United States

Reviewed by:
Zi-Bing Jin,
Capital Medical University, China
Melissa R. Andrews,
University of Southampton,
United Kingdom

***Correspondence:**
Gael Orieux
gael.orieux@sorbonne-universite.fr
Olivier Goureau
olivier.goureau@inserm.fr

Specialty section:
This article was submitted to Stem Cell Research, a section of the journal Frontiers in Cell and Developmental Biology

Received: 21 July 2020
Accepted: 24 September 2020
Published: 27 October 2020

Citation:
Rabesandratana O, Chaffiol A, Mialot A, Slembrouck-Brec A, Joffrois C, Nanteau C, Rodrigues A, Gagliardi G, Reichman S, Sahel J-A, Chédotal A, Duebel J, Goureau O and Orieux G (2020) Generation of a Transplantable Population of Human iPSC-Derived Retinal Ganglion Cells. Front. Cell Dev. Biol. 8:585675. doi: 10.3389/fcell.2020.585675

Optic neuropathies are a major cause of visual impairment due to retinal ganglion cell (RGC) degeneration. Human induced-pluripotent stem cells (iPSCs) represent a powerful tool for studying both human RGC development and RGC-related pathological mechanisms. Because RGC loss can be massive before the diagnosis of visual impairment, cell replacement is one of the most encouraging strategies. The present work describes the generation of functional RGCs from iPSCs based on innovative 3D/2D stepwise differentiation protocol. We demonstrate that targeting the cell surface marker THY1 is an effective strategy to select transplantable RGCs. By generating a fluorescent GFP reporter iPSC line to follow transplanted cells, we provide evidence that THY1-positive RGCs injected into the vitreous of mice with optic neuropathy can survive up to 1 month, intermingled with the host RGC layer. These data support the usefulness of iPSC-derived RGC exploration as a potential future therapeutic strategy for optic nerve regeneration.

Keywords: retinal ganglion cells, induced pluripotent stem cells, retinal organoids, cell transplantation, optic nerve injury

INTRODUCTION

Retinal ganglion cells (RGCs) play a major role in the visual function in transmitting visual information from the retina through the optic nerve and optic tract to the brain structures dedicated to processing visual information. RGC impairment is a common feature in many pathologies leading to visual loss, generally referred to as optic neuropathies such as Leber's hereditary optic neuropathy (LHON), and dominant optic atrophy or glaucoma, which is the second cause of blindness in the world (Jonas et al., 2017). Elevated intraocular pressure (IOP) is considered an important risk factor for glaucoma and most of the treatment strategies aim at reducing IOP. However, despite treatments, RGC degeneration and visual loss still progress in some patients

leading to irreversible blindness (Susanna et al., 2015; Greco et al., 2016). Moreover, some patients are diagnosed at a late stage of the disease when many RGCs have already been lost. In hereditary optic neuropathies, RGC loss mainly occurs in young patients, notably LHON-patients with no effective treatment to date (Newman, 2012; Carelli et al., 2017).

Human RGCs are difficult to access and grow *in vitro* (Zhang et al., 2010). Therefore, human pluripotent stem cells (hPSCs) represent one of the most promising sources of human RGCs. Recent development of methods guiding the differentiation of hPSCs toward specific retinal lineages, including RGCs, has emerged as a powerful strategy for disease modeling, drug screening, and gene or cell therapy (Llonch et al., 2018; Rabesandratana et al., 2018; Miltner and La Torre, 2019; Ahmad et al., 2020). Previous studies have demonstrated the ability to differentiate RGCs from plated hPSC-derived embryoid bodies (Riazifar et al., 2014; Sluch et al., 2015; Gill et al., 2016; Teotia et al., 2017). Based on initial protocols developed with mouse and human ESCs (Eiraku et al., 2011; Nakano et al., 2012), different groups including ours developed three-dimensional (3D) culture systems recapitulating key steps of retinal development and allowing the generation of self-organizing retinal organoids containing RGCs (Reichman et al., 2014; Zhong et al., 2014; Maekawa et al., 2015; Ohlemacher et al., 2016; Fligor et al., 2018). Very recently, RGCs were differentiated from human induced pluripotent stem cells (hiPSCs) using a chemically defined medium resulting in dual SMAD and Wnt inhibition bypassing retinal organoid formation (Chavali et al., 2020). Patient-specific iPSCs can be useful to better characterize the pathogenesis and molecular mechanisms of different inherited optic neuropathies (Chen et al., 2016; Ohlemacher et al., 2016; Wu et al., 2018; VanderWall et al., 2020). iPSC-derived RGCs also offer opportunities to identify molecules with therapeutic potential (Chen et al., 2016; Sluch et al., 2017) or to evaluate the efficiency of rescue strategies (Hung et al., 2016; Wong et al., 2017). Finally, hPSC-derived RGCs could be used for cell therapy even if many obstacles need to be overcome before any clinical application, such as the refractory nature of the central nervous system to axonal regeneration that could impede the reconnection of new RGC axons to their visual targets (Fischer et al., 2017; Laha et al., 2017). The ability to purify hPSC-derived RGCs from other cell types and to eliminate any residual proliferative cells is also a critical point to obtain a population of transplantable cells. Genetic engineering has been used to facilitate RGC isolation employing RGC-specific reporter gene or RGC-specific cell surface marker (Sluch et al., 2015; Kobayashi et al., 2018).

Based on our good manufacturing practice (GMP)-compliant retinal differentiation protocol (Reichman et al., 2017), we demonstrate that RGCs cultured in 2D conditions after dissociation of early retinal organoids derived from hiPSCs strongly express the cell surface antigen THY1 (also known as CD90). Here, we report a molecular and functional characterization of iPSC-derived RGCs and demonstrate the ability to enrich the RGC population using a THY1-based magnetic-activated cell sorting (MACS) strategy. Transplantation of enriched THY1-positive RGCs derived from a new fluorescent GFP reporter iPSC line in a mouse model of RGC degeneration supports the convenience of our culture and selection strategy when studying the potential of hPSC-derived RGCs for cell therapy for optic neuropathies.

MATERIALS AND METHODS

Animals

Eleven to 13-week-old adult female C57/BL6J mice were used in this study (Envigo). Animals were kept on a 12-h light/12-h dark cycle and allowed to eat and drink *ad libitum* (certified animal facility of the "Institut de la Vision"; agreement number A751202). All experiments were carried out in strict accordance with the Association for Research in Vision and Ophthalmology statement for animal research in ophthalmology. Moreover, all protocols were approved by the local ethical committee (Charles Darwin Ethical Committee for Animal Experimentation C2EA-05) in strict accordance with French and European regulation for animal use in research (authorization number #9061).

Human Induced Pluripotent Stem Cell Cultures

Two established human iPSC lines, hiPSC-2 and hiPSC line-5f, derived, respectively, from dermal fibroblasts (Reichman et al., 2014) and retinal Müller glial cells (Slembrouck-Brec et al., 2019) were cultured as previously described (Reichman et al., 2017). The fluorescent reporter iPSC line adeno-associated virus integration site 1 (AAVS1):CrxP_H2BmCherry-hiPSC line (Gagliardi et al., 2018) has also been used for specific experiments. Briefly, hiPSC lines were cultured on feeder-free conditions on truncated recombinant human vitronectin rhVTN-N (Thermo Fisher Scientific) in Essential 8^{TM} medium (Thermo Fisher Scientific). Cells were routinely cultured at 37°C in a standard 5% CO_2/95% air incubator with a daily medium change.

Generation of Human Reporter AAVS1::CAG-P_EGFP hiPSC Line

We used pX330-U6-Chimeric_BB-CBh-hSpCas9 (addgene#42230) (Cong et al., 2013) to construct the CRISPR/Cas9 vector by annealing and ligating in *Bbs*I sites an oligonucleotide pairs (5′-CACCGGGGCCACTAGGGACAG GAT-3′/3′-CCCCGGTGATCCCTGTCCTACAAA-5′) encoding a 20-nt AAVS1 guide sequence according to the protocol of Ran et al. (2013). We used the AAV–CAGGS–EGFP plasmid (Addgene #22212) (Hockemeyer et al., 2009) containing Puromycin-resistant gene and EGFP under the control of CMV early enhancer/chicken β actin (CAG) promoter between AAVS1 homology arms of 800 bp each (HA-L and HA-R). Plasmids are prepared using a Plasmid Midiprep kit (Macherey–Nagel) and verified for identity and integrity by restriction digest and gel electrophoresis before storage at 1–2 mg/ml in sterile Tris buffer (pH 8.0). The generation of stable cell clones was performed as previously described (Gagliardi et al., 2018). The hiPSC

line-5f clone was grown for 24 h in six-well plates before overnight transfection at 37°C with CRISPR/Cas9 and donor plasmids using FuGene HD (ratio 1:1:5; Promega). Two days after transfection, selection of recombinant cells was started in the presence of 0.25 μg/ml puromycin (Thermo Fisher Scientific) for the first 48 h; the concentration of puromycin was then increased to 0.5 μg/ml until picking of single colonies. Genomic DNA from puromycin-resistant clones was extracted with NucleoSpin Tissue kit (Macherey–Nagel) according to the manufacturer instruction. Correct reporter integration was evaluated by PCR using a forward primer upstream to the left arm of AAVS1 of recombination and a reverse primer either within the reporter cassette or in the AAVS1 right homologous arm. The PCR was composed of 32 cycles including three successive steps at 95°C, 60°C, and 72°C, respectively, for 30 s, 30 s, and 2 min. The genotype was finally visualized after migration of the DNA in a 1.2% agarose gel. After validation by sequencing, one homozygous reporter integration cell line was selected, and pluripotent status was validated by immunostaining for pluripotency markers, and the integrity of the karyotype was verified by SNP genotyping using Illumina's Infinium HumanCore-24 Bead Chips (Illumina, Inc., San Diego, CA, United States) at Integragen (Évry, France) (Slembrouck-Brec et al., 2019).

Retinal Differentiation

Retinal differentiation was based on our previously established protocol with adherent human iPSCs (Reichman et al., 2017; Slembrouck-Brec et al., 2019). After 56 days of differentiation (D56), retinal organoids were collected and enzymatically dissociated with papain (Worthington, WOLS03126) as previously described (Reichman et al., 2017). Retinal organoids were incubated with preactivated papain (1 U for 10^6cells) in Ringer solution during 30 min at 37°C, and then gently pipetted up and down to obtain uniform cell suspension. Dissociated retinal cell suspension was plated at a density of 100,000 cells/cm^2 onto either 6-, 24- (Corning, 3528), 48- (Greiner bio-one), or 96-well plates (Cellvis) previously coated with poly-D-lysine (Sigma-Aldrich) and laminin (Sigma-Aldrich), respectively, at 2 and 1 μg/cm^2. Dissociated retinal cells were cultured in retinal differentiation medium (RDM) composed of DMEM/F12 plus B27 supplement (Reichman et al., 2017), with medium changed every 2–3 days for 1 week after plating.

Cryopreservation of Retinal Organoids

Up to 12 retinal organoids at D45 were suspended in 250 μl of cold CryoStem freezing medium (CliniSciences) and frozen in a 1.5-ml cryogenic tube (Sarstedt) placed in isopropanol-based Mr. Frosty freezing container (Thermo Fisher Scientific) at −80°C for a minimum of 4 h. Frozen tubes were kept in a −150°C freezer for long-term storage. Frozen retinal structures were thawed quickly at 37°C in a water bath and resuspended in pre-warmed dedicated media for downstream investigations.

Magnetic-Activated Cell Sorting

One week after enzymatic dissociation at D56, dissociated retinal cells were carefully detached from the plates by incubation with previously activated papain protocol (1 U for 10^6 cells) for 15 min at 37°C. To remove residual aggregates, deoxyribonuclease I from bovine pancreas (Sigma-Aldrich) was added into cell suspensions, before filtering through a 30-mm strainer (Miltenyi Biotec) prehydrated with 1 ml of RDM. Cell suspension was centrifuged for 10 min at 300 *g* and resuspended in MACS buffer (80 μl up to 2.10^7 cells) for 30 min at 4°C to block non-specific binding sites. Next, cells were incubated with anti-mouse IgG1 MicroBeads (Miltenyi Biotec) coupled with human THY1 antibody for 15 min at 4°C at a dilution of 1:5 for a ratio up to 2.10^7 cells. The cells were washed by adding 2 ml of MACS buffer, centrifuged at 10 min at 300 × *g* and resuspended in 500 μl of MACS buffer (MACS BSA solution) supplemented with 1:20 MACS separation buffer (Miltenyi Biotec). Cell suspension was applied once onto a pre-equilibrated MS column (Miltenyi Biotec) fixed to a MiniMACS^{TM} separator (Miltenyi Biotec). The flow-through containing unlabeled cells was collected and then applied a second time onto the separation column to optimize the selection. The column was washed twice with 500 μl of MACS buffer. The positive fraction was eluted with 1 ml of MACS buffer following removal of the column from the magnet.

Flow Cytometry

After THY1 MACS, all unsorted and sorted THY1 retinal cell fractions were resuspended to a final volume of 1 ml in MACS buffer. Then they were incubated with FITC-conjugated THY1 primary antibody for at least 30 min, at 4°C, in the dark. To exclude dead cells, propidium iodide was added to the cells at a final concentration of 1 μg/ml, incubated for 10 min at 4°C in the dark. Background fluorescence and non-specific binding were measured using unstained cells and mouse IgG1 FITC-conjugated isotypic antibody control (R&D systems) with a concentration of 5 μl/test up to 10^6 cells. Samples were analyzed without additional washings. Analysis was performed with FC500 Flow Cytometer (Beckman Coulter). Flow cytometry data were analyzed using FlowJo software (TreeStar). A minimum of four independent biological experiments were performed for flow cytometry.

Multi-Electrode Array Recordings

Whole retinal organoids were chopped at D56 and plated onto a multi-electrode array (MEA) chip (MEA256 100/30 iR-ITO, Multi Channel Systems, Germany) facing the electrodes and coated with poly-D-lysine/laminin to promote adhesion onto the electrodes. Organoid fragments were maintained during 2–3 weeks in RDM at 37°C in a standard 5% CO_2/95% air incubator, with medium changed every 2–3 days until electrophysiological recordings. During MEA recordings, the organoids were continuously perfused with oxygenized (95% O_2, 5% CO_2) Ames medium (Sigma-Aldrich) at 34°C at a rate of 1–2 ml/min (Garita-Hernandez et al., 2019). Raw extracellular RGC activity was amplified and sampled at 20 kHz. Resulting data was stored and filtered with a 200-Hz high-pass filter

for subsequent offline analysis using Spike2 software v.7 (CED Co., United Kingdom). Single-unit data were obtained using a combination of template matching and cluster grouping based on principal component analysis of the waveforms. Each recording lasted for at least 30 min.

Single-Cell Electrophysiological Recordings

Patch-clamp electrodes were made from borosilicate glass (BF100-50-10, Sutter Instruments) and pulled to 6–9 MΩ. Pipettes were filled with 115 mM K Gluconate, 10 mM KCl, 1 mM $MgCl_2$, 0.5 mM $CaCl_2$, 1.5 mM EGTA, 10 mM HEPES, and 4 mM ATP–Na_2 (pH 7.2). An Axon MultiClamp 700B amplifier was used for whole-cell patch-clamp and extracellular recordings. Retinal cells were recorded 2–3 weeks after plating, either in voltage-clamp configuration and clamped at −60 mV (with 10 mV steps from −100 to +40 mV), or in current-clamp configuration (with current injections from −20 to +100 pA). Extracellular recordings were also performed, with electrodes filled with Ames' solution. During recordings, cells were perfused with oxygenized (95% O_2, 5% CO_2) Ames' medium (Sigma-Aldrich) at 34°C at a rate of 1.5 ml/min.

RNA Extractions and TaqMan Assays

Total RNAs were extracted using NucleoSpin RNA XS kit (Macherey–Nagel) according to the manufacturer's protocol, and RNA yields and quality were checked with a NanoDrop spectrophotometer. cDNA was synthesized from 250 ng of mRNA using the QuantiTect reverse transcription kit (Qiagen, 205313) following manufacturer's recommendations. Synthesized cDNA was then diluted at 1/20 in DNase-free water before performing quantitative PCR. qPCR analysis was performed on an Applied Biosystems Real-Time PCR machine (7500 Fast System) with custom TaqMan® Array 96-Well Fast plates (Thermo Fischer Scientific) and TaqMan® Gene expression Master Mix (Thermo Fischer Scientific) following manufacturer's instructions. All primers and MGB probes labeled with FAM™ (carboxyfluorescein) for amplification (**Supplementary Table S1**) were purchased from Thermo Fischer Scientific. Results were normalized against 18S, and quantification of gene expression was based on the Delta Ct Method in three minimum independent biological experiments.

Tissue Fixation and Cryosection

For eye cup collecting, animals were deeply anesthetized by intraperitoneal injection of ketamine (Ketamidor; Axience; 100 mg/kg) and xylazine (Nerfasin® Vet; Axience; 10 mg/kg) before transcardiac perfusion with 100 ml of 4% paraformaldehyde at 4°C. Retinal organoids and mouse eye cups were fixed (or postfixed) for 20 min in 4% paraformaldehyde at 4°C and washed in PBS. Structures were incubated at 4°C in PBS/30% sucrose solution for at least 2 h. Structures were embedded in a solution of PBS/7.5% gelatine/10% sucrose and frozen in isopentane at −55°C. For further analysis, 10- and 14-μm-thick cryosections were collected, respectively, for retinal organoids and mouse eye cups. Dissociated retinal cells on coverslips (WPI) or on glass-bottomed 96-well plates (Cellvis) were fixed with 4% paraformaldehyde for 15 min before immunostaining.

Immunostaining, Imaging, and Quantification

After washes with PBS, non-specific binding sites were blocked for 1 h at room temperature with a PBS solution containing 0.2% gelatine and 0.1% Triton X-100 (blocking buffer) and then overnight at 4°C with the primary antibody (**Supplementary Table S2**) diluted in blocking buffer. Slides were washed three times in PBS with 0.1% Tween and then incubated for 1 h at room temperature with appropriate secondary antibodies conjugated with either Alexa Fluor 488, 594, or 647 (**Supplementary Table S2**) diluted at 1:800 in blocking buffer with 4′,6-diamidino-2-phenylindole (DAPI) diluted at 1:1,000 to counterstain the nuclei. Specifically, for mouse eye cups, sections were incubated in two drops of Mouse IgG blocking reagent (Vector laboratories) diluted in 2.5 ml of PBS for 1 h at room temperature to block endogenous mouse antibody in the tissue section in anticipation of mouse antibody-based immunostaining.

Cell death was detected using the *In Situ* Cell Death Detection kit, TMR (Roche), according the to the manufacturer's instruction.

Fluorescent staining signals were captured with an Olympus FV1000. Acquisitions were done with a variable step size according to objective magnification (1.64 μm at ×20; 0.61 μm at ×40; 0.48 μm at ×60). Images were analyzed with FIJI/ImageJ software, and each illustration corresponds to a Z-projection of all X-Y optical sections.

Quantification of cell density immunoreactive for specific markers has been performed by automatic counting using ArrayScan VTI HCS Reader® station with the HCS iDev Cell® studio software 6.6.0. (Thermo Fischer Scientific). A minimum of 72 areas (0.83 mm^2 each) were counted for each condition of dissociated retinal cells per experiment. For a few markers, manual quantification was realized on the FIJI/ImageJ software. Quantification is expressed as mean ± S.E.M and corresponds to a minimum of four independent biological experiments for automatic or manual counting.

Optic Nerve Crush Mouse Model

Animals were anesthetized by intraperitoneal injection of ketamine (Ketamidor; Axience; 100 mg/kg) and xylazine (Nerfasin® Vet; Axience; 10 mg/kg). Buprenorphine (Buprecare, Axience; 0.05 mg/kg) was also administrated before the surgery to provide additional analgesia. Oxybuprocaine (THEA) was also administered locally on the operated eye. Under a stereoscopic microscope, the left eye ball was bulging with Dumont fine forceps (Fine Science Tools, n° 11252-30) to expose the optic nerve. The optic nerve was crushed a few millimeters behind the eye by compression for 5 s with Dumont #5 – mirror finish forceps (Fine Science Tools, n° 11252-23). Lubrital (Dechra) was used to avoid dry eyes until waking up.

Transplantation of Human-iPSC-Derived RGCs

Mice were first anesthetized by 5% isoflurane (Isoflurin; Axience) inhalation for 2 min and were maintained in deep anesthesia with 2% isoflurane inhalation. Oxybuprocaine was also administered locally before transplantation. Cell suspension (1 μl) containing 200,000 cells in MACS buffer was delivered by intravitreal injection. Injection was performed using a micropump (UltraMicroPump III with Micro4 Controller; World Precision Instruments). Cells were delivered at 150 nl/s using a 10-μl NanoFil syringe with a 33G beveled tip (NanoFil). From 1 week before transplantation to the end of the follow-up, mice were maintained under immunosuppression through cyclosporine treatment (210 mg/l) in the drinking water. A total of 27 female mice were analyzed 1 week after transplantation (n = 17 animals with grafted THY1-positive cells; n = 4 animals with grafted unsorted cells) and 4 weeks after transplantation (n = 6 animals with grafted THY1-positive cells).

Statistical Analysis

"n" corresponds to the number of organoids, animals, or images from each independent differentiation; "N" indicates the number of independent experiments performed (e.g., the number of independent retinal differentiations). All statistical analyses are based on at least three independent experiments. Data were averaged and expressed with means ± SEM. Statistical analysis was performed using Prism 7 (GraphPad software) with appropriate statistical tests including Mann–Whitney test, ordinary one-way, two-way ANOVA, or Kruskal–Wallis test followed when necessary by multiple comparison test (*post hoc* analysis) such as Dunn's (multiple comparison with one control group) or Tukey's test (comparison between all groups). P values lower than 0.05 led to the rejection of the null hypothesis (H0) and to consider the difference statistically significant.

RESULTS

Absence of THY1 Expression in Human-Induced Pluripotent Stem Cell-Derived Retinal Organoids

Because THY1 is considered as a specific marker of RGC in a retinal context (Barnstable and Dräger, 1984), we first sought to determine, using our previously GMP-compatible protocol (Reichman et al., 2017), the expression of this cell surface marker during the differentiation of hiPSC-derived retinal organoids in floating conditions. RT-qPCR analysis revealed a low increase in *THY1* expression in maturating organoids between D42 and D84 contrasting with the transient increase in *BRN3A* expression that demonstrated the generation of RGCs during this period (**Figure 1A**) ($n \geq 30$ organoids from $N \geq 3$ differentiations; $^{**}p < 0.01$, Kruskal–Wallis test followed by Dunn's multiple comparison). The transient expression of *BRN3A* can be explained by RGC loss in floating culture conditions (Reichman et al., 2014; Zhong et al., 2014; Capowski et al., 2019). Immunofluorescence analysis showed that numerous immunoreactive cells for specific RGC markers (BRN3A, RBPMS, and HuC/D) are present in floating retinal organoids at D56, D70, and D84, while their density decreased at D98 (**Figure 1B**) and became undetectable at later stages as previously described (Reichman et al., 2014). By contrast, the photoreceptor population was clearly traceable at D98 according to CRX and Recoverin (RCVRN) expression ruling out a global and non-specific cell loss (**Supplementary Figure S1**). This observation confirmed the data obtained by RT-qPCR and revealed the progressive RGC loss over long-term retinal organoid maturation. Surprisingly, immunofluorescence analysis did not detect expression of THY1 in retinal organoids between D42 and D98 (**Figure 1B**) despite the gene expression detected at mRNA level by RT-qPCR (**Figure 1A**).

In order to evaluate the functional maturation of presumed hiPSC-derived RGCs, and considering that retinal cells capable of emitting large spikes are overwhelmingly RGCs, we performed multi-electrode array (MEA) recordings from organoids cultured on MEA chipsets for 2 weeks (**Figure 1C**). Spiking activity was recorded at the surface of four out of seven MEA chipset, and the average spiking activity of individual cells was 0.37 ± 0.13 Hz (mean ± SEM; N = 4 out of seven experiments, n = 10 responding electrodes).

Promotion of Human-iPSC-Derived RGC Survival and Maturation in Adherent Conditions

Since targeting THY1 would be useful to isolate the RGC population, we aimed at inducing RGC maturation to trigger THY1 expression at protein level. For this purpose, we developed a two-stepwise retinal differentiation protocol to promote survival and maturation of RGCs (**Figure 2A**). Retinal organoids were dissociated after 8 weeks of differentiation (D56), and cell suspension was seeded back onto an adherent substrate for 1 week and maintained in RDM medium to enhance RGC survival and maturation. After 1 week, the dissociated retinal cells showed a typical neuronal morphology (**Figure 2B**). Most cells were identified as RGCs by the co-expression of BRN3A and THY1 (**Figure 2C**), or the co-expression of PAX6 with RBPMS or βIII-tubulin (**Figure 2C**; Fournier and McKerracher, 1997; Zhang et al., 2010; Rodriguez et al., 2014; Li et al., 2017). The co-expression of CRX and RCVRN in some cells confirmed that differentiating photoreceptors were also present (**Figure 2C**). RT-qPCR analysis revealed a higher expression of *BRN3A* and *RBPMS* in retinal cells 1 week after plating compared to D56 organoids (**Figure 2D**) ($n \geq 30$ organoids from $N \geq 3$ differentiations; $^{*}p < 0.05$, Mann–Whitney test) and a weak but not statistically significant increase in *THY1* expression (**Figure 2D**) ($n \geq 30$ organoids from $N \geq 3$ differentiations). All these results confirmed an enrichment of maturating RGCs over other retinal cell populations in these adherent conditions.

Functional maturation of RGCs was further evaluated by single-cell electrophysiological recordings (**Figure 3**). Twenty out of sixty-one RGCs, defined by morphological criteria

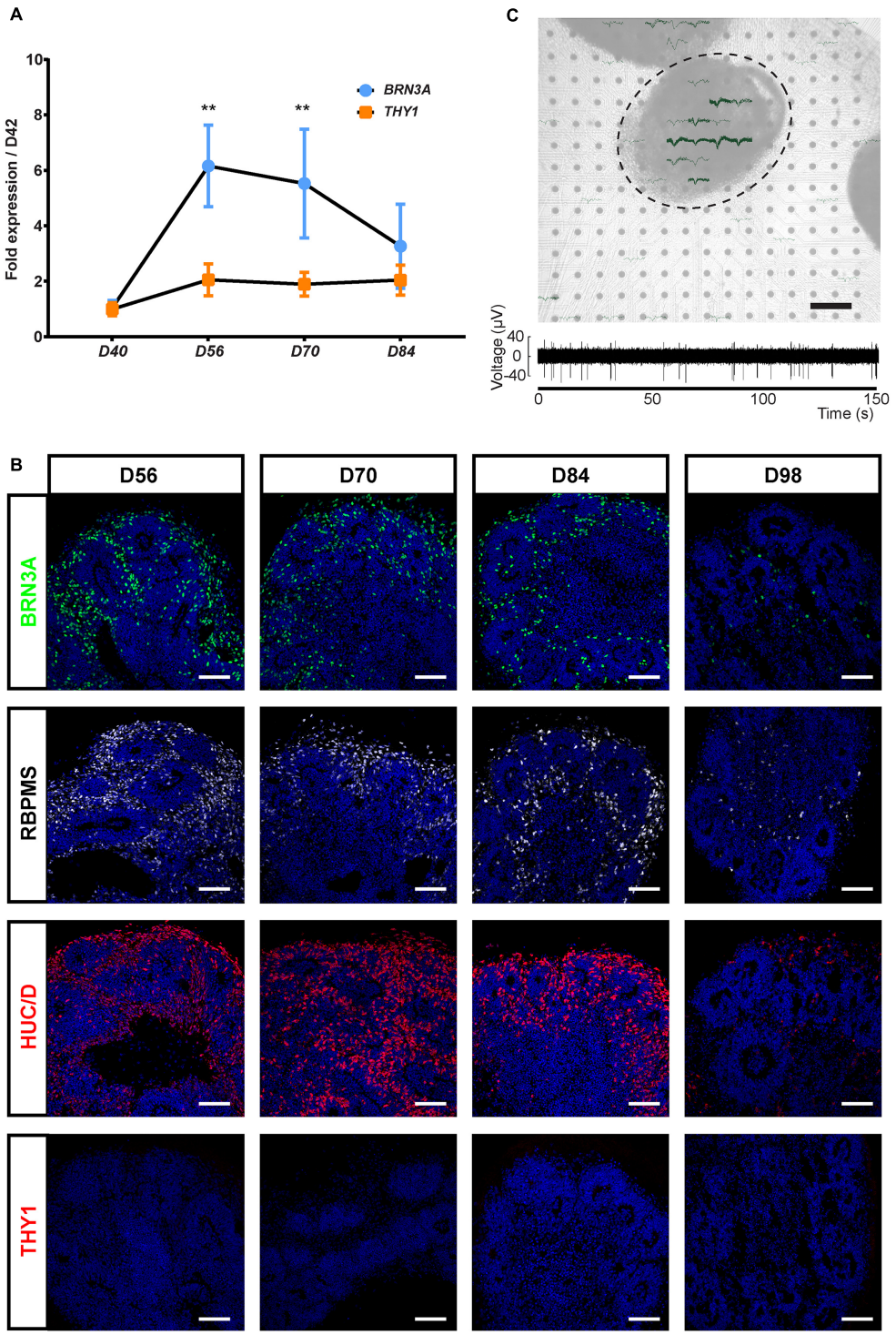

FIGURE 1 | Characterization of the retinal ganglion cell (RGC) population in human induced pluripotent stem cell (hiPSC)-derived retinal organoids. **(A)** RT-qPCR analysis of *BRN3A* and *THY1* during differentiation between D42 and D84 (mean ± SEM; $N = 3$ differentiations per time point; $n \geq 10$ organoids/differentiation). Gene expression at each time point is indicated relative to organoids at D42. $^{**}p < 0.01$, Kruskal–Wallis test followed by Dunn's multiple comparison. **(B)** Immunostaining showing the expression of BRN3A, RBPMS, HuC/D, and the absence of THY1 immunoreactivity in sections of retinal organoids, from D56 to D98. Nuclei were counterstained with DAPI (blue). Scale bars, 100 µm. **(C)** Top, infrared image displaying an organoid cultured on a 256-recording site (gray dots) MEA chipset. Electrical activity showed as superimposed waveforms is observed at the level of the organoid ($N = 7$ independent experiments including 10 electrodes showing electrical activity). Scale bar, 200 µm. Bottom, raw data trace example of a recorded neuron from the same organoid exhibiting spontaneous firing activity.

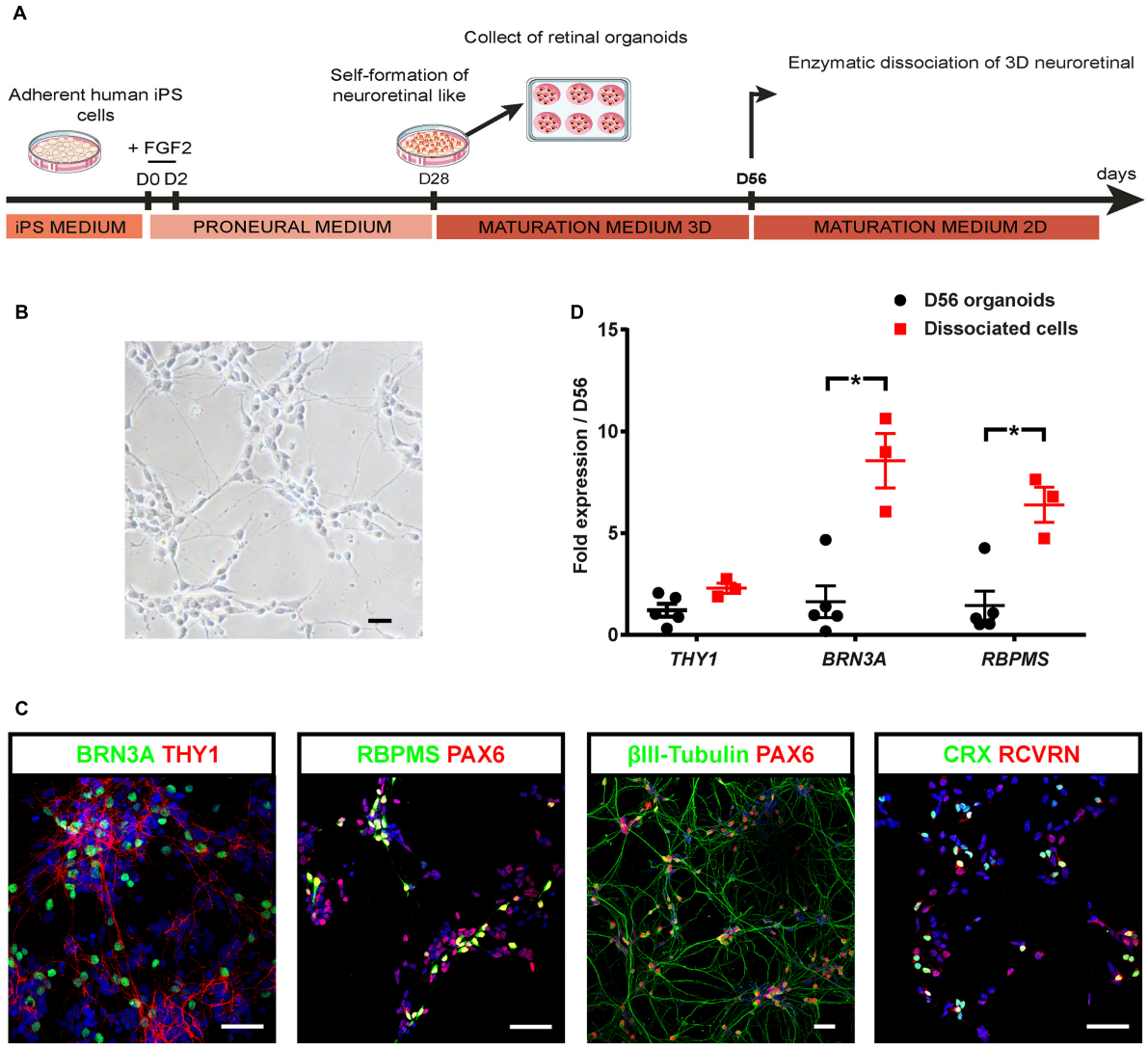

FIGURE 2 | Optimization of hiPSC-derived RGCs differentiation. **(A)** Schematic diagram illustrating the protocol for RGC differentiation from hiPSC-derived retinal organoids. **(B)** Phase-contrast micrograph of retinal cells 1 week after plating of dissociated cells derived from D56 organoids; scale bar, 50 μm. **(C)** Immunostaining on dissociated cells derived from D56 retinal organoids, showing the co-expression of BRN3A and THY1, or PAX6 with RBPMS, or βIII-tubulin allowing the identification of RGCs 1 week after plating. Photoreceptors are also identified according to CRX and recoverin (RCVRN) expression. Nuclei staining with DAPI in blue; scale bars, 50 μm. **(D)** RT-qPCR analysis of *THY1*, *BRN3A*, and *RBPMS* in D56 organoids and in retinal cells 1 week after plating (mean ± SEM; $N = 3$ differentiations per time point; $n \geq 10$ organoids/differentiations). Gene expression at each time point is indicated relative to D56 organoids. $^*p < 0.05$, Mann–Whitney test).

and recorded extracellularly showed spontaneous spiking (**Figure 3A**). The resting membrane potential was similar for all recording cells (−43.2 ± 2.1 mV; mean ± SEM), and the mean firing frequency was 0.31 ± 0.07 Hz (mean ± SEM; $n = 20$ out of 61 recorded cells from $N = 9$ differentiations). Voltage-gated sodium channels that mediate fast depolarization in neurons are responsible for initiation of the action potential (Marban et al., 1998). Patch-clamp recordings revealed fast inward ionic currents in a majority of putative RGCs (**Figure 3B**) ($n = 15$ out of 22 patched cells) and a voltage-dependence of these currents with an inward peak of activity at −20 mV. Because the majority of recorded cells were not spontaneously spiking, we injected positive current pulses during 500 ms leading to firing activity in the majority of recorded cells (**Figure 3C**) ($n = 7$ out of 10 cells). Firing response ranged from 1 to 10 action potentials per stimulation. Furthermore, in order to check if cells expressed functional glutamate receptors, we puffed glutamic acid (1 mM) and managed to record inward slow currents in response to the stimulation (**Figure 3D**) ($n = 3$ technical replicates). In order to better characterize the identity of recording cells, we performed similar experiments using our previously described CrxP_H2BmCherry reporter hiPSC line (Gagliardi et al., 2018). This allowed the identification of photoreceptors according to the expression of the mCherry

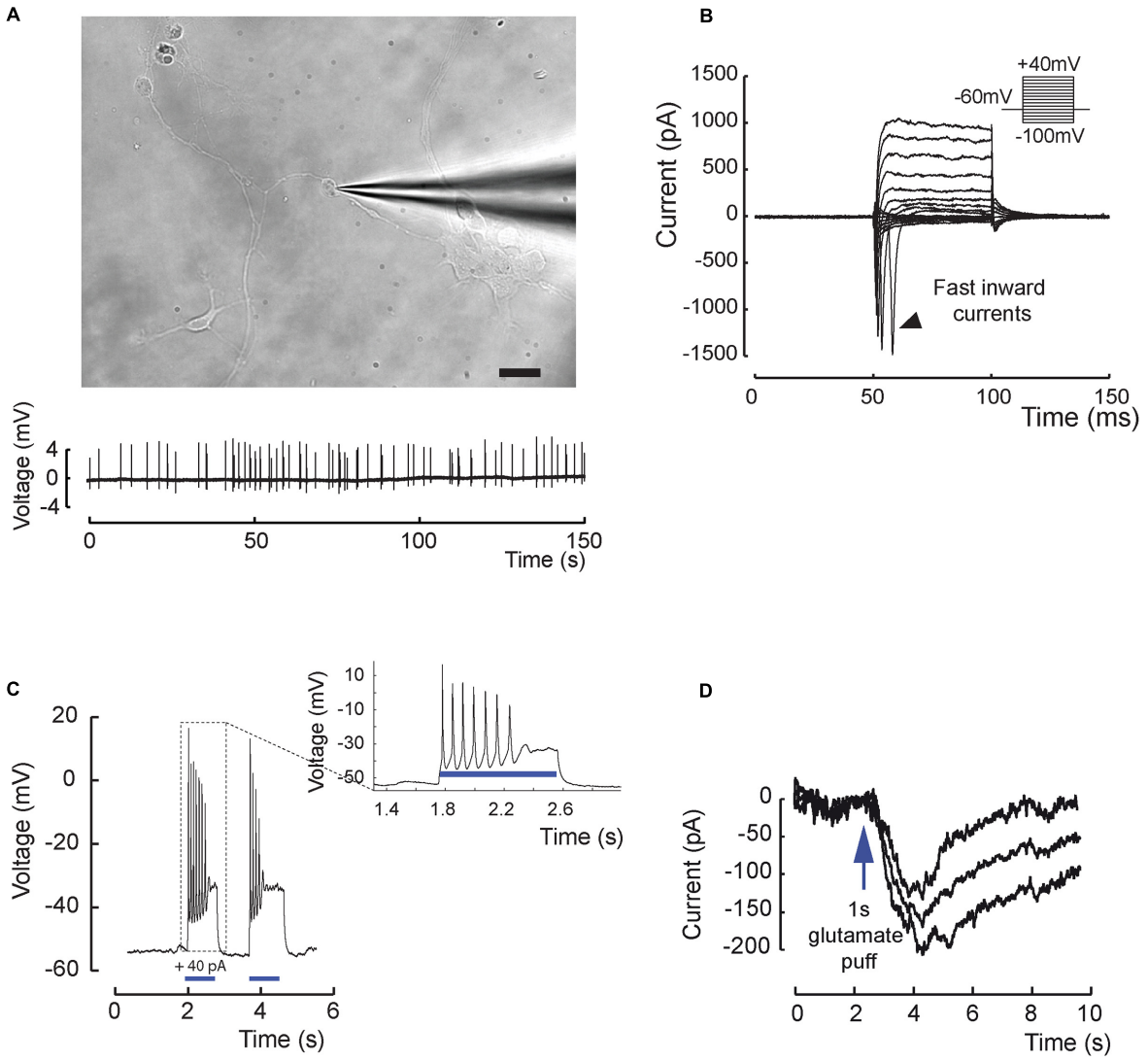

FIGURE 3 | Excitability and electrical properties of hiPSC-derived RGC-like cells after differentiation in 2D. **(A)** Top, infrared image of a recording electrode in contact with a RGC 3 weeks after plating of retinal cells derived from D56 organoid Scale bar, 20 μm. Bottom, example of an extracellular recording from the same cell displaying spontaneous firing activity (0.31 ± 0.07 Hz; mean ± SEM; *N* = 9; *n* = 20 out of 61 recorded cells). **(B)** Whole-cell patch-clamp recording of a representative cell in voltage-clamp mode. Current responses to voltage steps are obtained by stepping the membrane potential from –100 to +40 mV in 10 mV increments. Note the presence of fast inward currents (arrow head); (*N* = 5; *n* = 15 out of 22 recorded cells). **(C)** Whole-cell patch-clamp recording in current-clamp mode. Injecting positive current (40 pA) in the cell (blue bars) leads to firing activity (*N* = 5; *n* = 7 out of 10 recorded cells). **(D)** Recording in one cell of a long inward current evoked by glutamic acid (1 mM) application and compatible with a synaptic current; this response has been reproduced three times.

fluorescent protein (**Figure 4A**). As expected, patch-clamp recordings showed that mCherry/CRX-positive photoreceptors failed to evoke fast inward currents (**Figures 4B,C**) (n = 7) and never evoked spike after current injection (**Figure 4D**) (n = 7). By contrast, mCherry/CRX-negative cells (classified as RGCs based on additional morphological criteria) displayed fast inward currents (**Figures 4B,E**) (n = 4) and evoked spikes after current injections (**Figure 4F**) (n = 3 out of 4). The resting membrane potential was similar for all recording cells, ranging from −38.3 ± 3.1 mV (mean ± SEM; CRX-positive cells) to −42.7 ± 4 mV (mean ± SEM; RGC-like CRX-negative cells). Based on these morphological and functional criteria, we demonstrated that RGCs isolated from retinal organoids can survive and mature in adherent mixed retinal cell cultures.

Enrichment of RGCs by MACS Based on THY1 Expression in Adherent Cells From Dissociated Organoids

Since the transplantation of hiPSC-derived RGCs represents one objective for future applications to treat optic neuropathies, we aimed to discard non-RGCs from the whole-cell population even though an enrichment in RGCs was already observed in our adherent cell culture conditions (**Figure 2**). For this

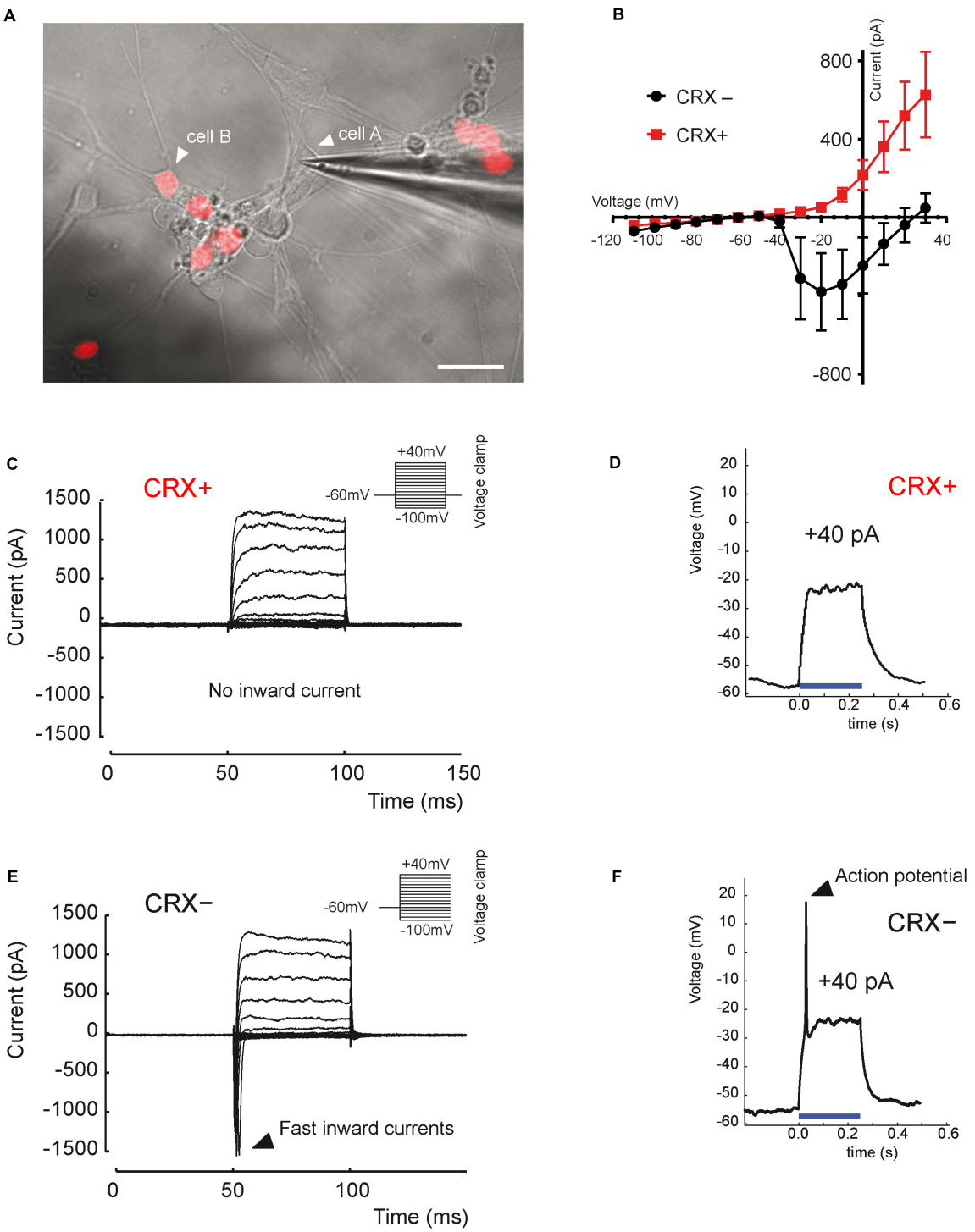

FIGURE 4 | Distinct electrical properties of hiPSC-derived RGCs and hiPSC-derived CRX-positive photoreceptors. **(A)** Infrared image of a monolayer of retinal cells derived from D56 organoid generated from the adeno-associated virus integration site 1 (AAVS1):CrxP_H2BmCherry hiPSC line, 3 weeks after plating. Epifluorescence images revealing mCherry+ cells corresponding to CRX+ photoreceptors are superimposed (white arrow head on cell A; a recording electrode is in contact with a mCherry– (CRX–) non-photoreceptor cell showing an RGC morphology (white arrow head on cell A). Scale bar: 25 μm. **(B)** Mean current–voltage (I–V) relationship curve of CRX– (black curve) and CRX+ (red curve) cells, calculated as the minimum current value observed during the first 10 ms of each voltage step. Fast inward currents peaking around –20 mV are only visible for CRX– cells (mean ± SEM; $N = 3$; $n = 7$). **(C,E)** Current responses to voltage steps of CRX+ **(C)** and CRX– **(E)** representative cells by stepping the membrane potential from –100 to +40 mV in 10-mV increments ($N = 3$; $n = 11$). Only CRX– cells displayed fast inward currents. **(D,F)** Voltage responses of CRX+ **(D)** and CRX– **(F)** representative retinal cells to a +40-pA current injection (blue line). Evoked action potentials were observed only in CRX– cells ($N = 3$; $n = 4$).

purpose, 1 week after plating of dissociated retinal organoid cells, we performed MACS using THY1 antibody-coupled magnetic MicroBeads. In order to evaluate the enrichment of RGCs, unsorted and MAC-sorted fractions were submitted to flow cytometry to quantify THY1-positive cells. Flow cytometry analysis confirmed an RGC enrichment after 7 days in adherent cell culture conditions, with 60.48 ± 0.14% of THY1-positive cells in the unsorted fraction (**Figure 5A**) (mean ± SEM; $n = 198$ organoids; $N = 3$ independent experiments). We showed that the MACS-positive fraction containing 78.03 ± 1.47% of THY1-positive cells was significantly enriched compared to MACS-negative fraction containing 15.11 ± 3.77% of THY1-positive cells (**Figures 5B,C**) (mean ± SEM; $N = 3$; $^{**}p < 0.01$; one-way ANOVA followed by Dunn's multiple comparison test). Cell viability of MAC-sorted cells was assessed by flow cytometry using the apoptotic marker YOPRO (**Figure 5D**) showing a high survival rate in both THY1-positive and negative fractions (91.63 ± 0.62% and 92.5 ± 1.08%, respectively; $N = 3$; $n = 308$), similar to the living cell ratio before MACS (95.1 ± 2.19% in unsorted fraction; $N = 3$; two-way ANOVA).

In order to confirm the identity of sorted cells (**Figure 6A**), we performed immunofluorescence analysis on cells from the different MACS fractions 2 days after plating (**Figure 6B**). As expected, the MACS-positive fraction was enriched in cells expressing specific RGC markers (THY1, BRN3A, RBPMS, HuC/D) (**Figure 6B**). Quantitative analysis revealed a significant

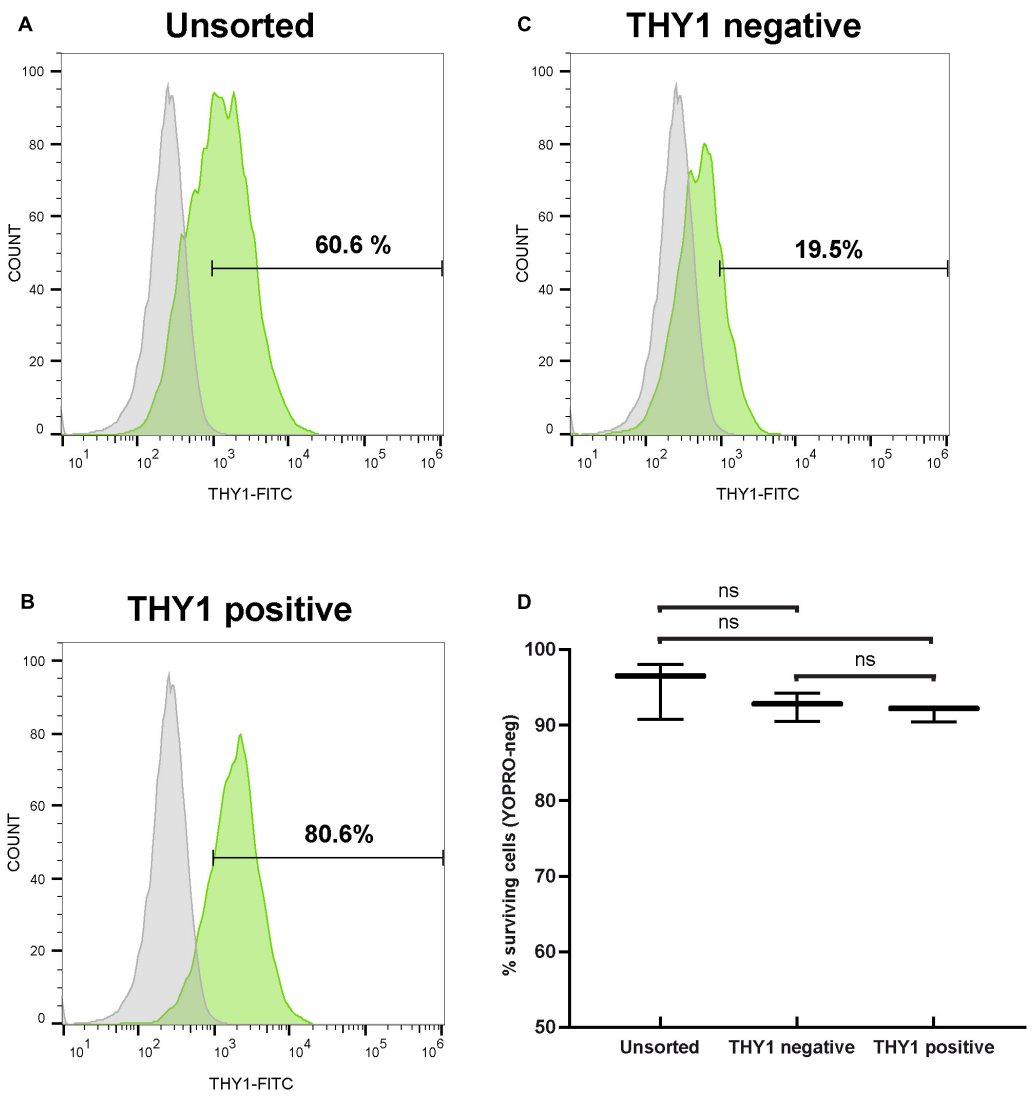

FIGURE 5 | Selection of hiPSC-derived RGCs by targeting THY1. **(A–C)** One representative THY1 flow cytometry analysis plot of the different fractions before **(A)** and after magnetic-activated cell sorting (MACS) (**B:** THY1-positive fraction; **(C):** THY1-negative fraction). Fluorescence intensity indicative of FITC-conjugated THY1 primary antibody binding is shown on the *x*-axis. Specific staining in green; Non-specific binding was estimated by incubation with a mouse IgG1 FITC-conjugated isotypic antibody (in gray). **(D)** Quantitative analysis by flow cytometry of living cells (YOPRO-negative) on unsorted, THY1-negative, and THY1-positive fractions from retinal organoid-derived dissociated cells, 1 week after plating (min to max; $N = 3$ differentiations; $n = 308$ organoids; ns: not statistically significant two-way ANOVA followed by Tukey's multiple comparison test).

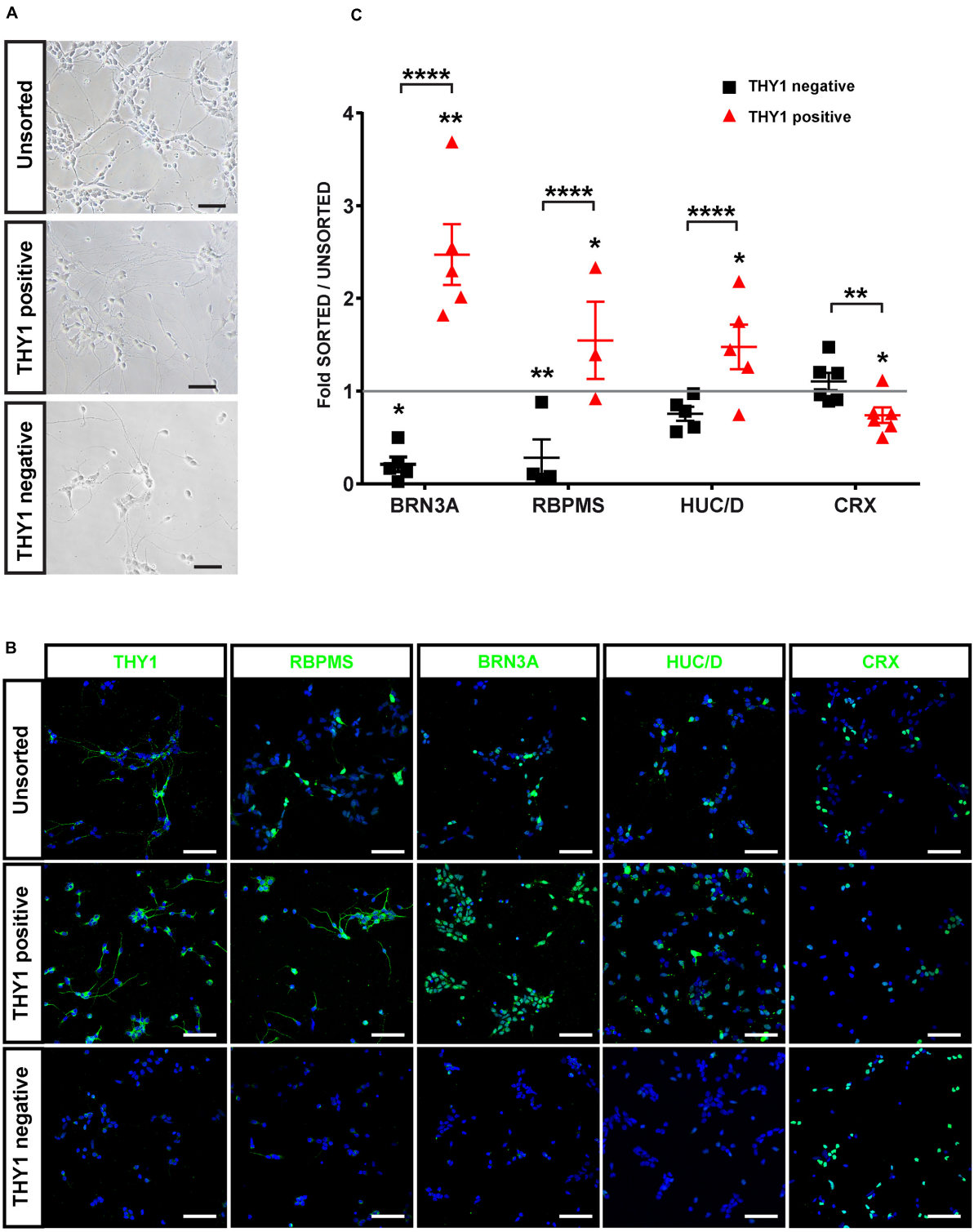

FIGURE 6 | Characterization of hiPSC-derived RGCs after THY1-targeted MACS. **(A)** Phase-contrast and brightfield micrographs illustrate the morphology of dissociated cells from D56 retinal organoids 1 week after plating (unsorted) and 2 days after MACS (THY1-positive and THY1-negative fractions). Scale bars: 50 μm. **(B)** Immunofluorescence analysis of RGC markers (THY1, RBPMS, BRN3A, and HuC/D) and photoreceptor marker CRX in unsorted, THY1-positive, and THY-negative fractions (cell nuclei staining with DAPI in blue). Scale bars: 50 μm. **(C)** Quantitative analysis using ArrayScan of RGCs and photoreceptors in adherent cell cultures of unsorted, THY1-negative, and THY1-positive fractions, 2 days after plating (mean ± SEM; $*p < 0.05$, $**p < 0.01$, $****p < 0.0001$; Dunn's multiple comparisons test after global Kruskal–Wallis test; $N \geq 4$). Asterisks positioned above scatter plots refer to comparison with the unsorted fraction (gray line); asterisks above square bracket refer to comparison between positive and negative fractions.

enrichment in BRN3A-positive cells (+147% ± 38%) in the THY1-sorted cell population compared to the unsorted fraction and a significant depletion in the negative fraction (−80 ± 8%) (**Figure 6C**) (mean ± SEM; $n = 671$ organoids from $N = 5$ differentiations; $^{**}p < 0.01$, Kruskal–Wallis test followed by Tukey's multiple comparison test). This enrichment was confirmed by the increase in 55 ± 11.5% and 48 ± 7.7% of RBPMS-positive cells and HuC/D-positive cells, respectively, compared to the unsorted fraction (**Figure 6C**) (mean ± SEM; $N = 5$ experiments; $^{****}p < 0.0001$, Kruskal–Wallis test followed by Tukey's multiple comparison test). In contrast, the MACS-positive fraction was partially depleted in CRX-positive photoreceptor cells (**Figures 6B,C**) (−24 ± 8.3% compared to the unsorted fraction; mean ± SEM; $N = 6$; $n = 731$ organoids; $^{*}p < 0.05$, Kruskal–Wallis test followed by Tukey's multiple comparison test). To demonstrate that this selection strategy was not dependent on the hiPSC line used for generation of retinal organoids, we carried out additional immunostaining with another previously characterized hiPSC line (hiPSC-2) derived from human dermal fibroblasts (Reichman et al., 2014). Using different markers of RGCs (THY1, HuC/D, and RBPMS), we confirmed an enrichment of RGCs in the THY1-sorted fraction (**Supplementary Figure S2**). In contrast, RCVRN-positive photoreceptors detected in the unsorted fraction were very rarely observed in the THY1-sorted fraction (**Supplementary Figure S2**).

With the perspective of developing cell therapy applications for optic neuropathies, we tested the ability to cryopreserve dissociated cells before or after THY1-targeted MACS. Dissociated cells before cell sorting (unsorted fraction) and MAC-sorted cells were immediately frozen, thawed 1 week later, and cell viability was assessed by flow cytometry using the apoptotic marker YOPRO. Quantitative analysis demonstrated an important decrease in cell viability in freeze–thawed cell population, both in unsorted (51.4 ± 5.2%; $N = 3$) and THY1-sorted (24.5 ± 0.5%; $N = 3$) fractions compared to corresponding fresh-cell fractions: 99.4 ± 0.3% and 94.5 ± 1.2% for unsorted and THY1-sorted fraction, respectively ($n = 395$ organoids from $N = 3$ experiments; $^{****}p < 0.0001$, two-way ANOVA followed by Tukey's multiple comparison test). These results ruled out the possibility to use this approach for banking THY1-targeted MACS retinal cells. Having already validated the possibility to cryopreserve retinal organoids (around D85-D100) without affecting photoreceptor differentiation after thawing (Gagliardi et al., 2018), we tested the possibility, as an alternative solution, to isolate RGCs from young freeze–thawed organoids (**Figure 7**). Retinal organoids frozen at D45 of differentiation were thawed and put back into floating culture for 1 week before dissociation. Retinal cells were then cultured an additional week in adherent conditions (**Figure 7A**). Immunostaining demonstrated that most cells exhibited an RGC profile with the expression of specific neuronal, retinal, and RGC markers such as βIII-tubulin, PAX6, BRN3A, or THY1 (**Figure 7B**). In these conditions, THY1-targeted MACS was still efficient as demonstrated by immunostaining on the sorted fraction in which a majority of the cells expressed BRN3A, RBPMS, and THY1 (**Figure 7B**). One week after dissociation, quantitative analysis of YOPRO labeling by flow cytometry demonstrated that freeze–thawing of retinal organoids did not affect cell viability in dissociated cells (unsorted cells) from freeze–thawed organoids (97.43 ± 0.74%; $N = 3$) (**Figure 7C**) compared to fresh organoids (95.1 ± 2.19; $N = 3$) (**Figure 5D**). A high survival rate was also observed after MACS (**Figure 7C**) (93.90 ± 0.76% in positive fraction and 93.93 ± 1.09% in negative fraction; $N = 3$) even though cell viability was slightly lower compared to unsorted cells ($n = 380$ organoids; $N = 3$ experiments; $^{*}p < 0.05$, two-way ANOVA followed by Tukey's multiple comparison test). These results suggested that performing THY1-targeted MACS on retinal dissociated cells derived from previously cryopreserved organoids could provide a good solution to obtain readily transplantable cells and overcome the obstacle of direct cryopreservation of THY1-targeted MACS retinal cells.

Generation and Retinal Differentiation of Human Reporter AAVS1::CAG-P_EGFP iPSC Line

For potential validation of cell replacement strategies, we engineered a fluorescent reporter human iPSC line (**Supplementary Figure S3**) from hiPSC line-5f (Slembrouck-Brec et al., 2019) enabling the production of fluorescent retinal cells that could be easily identified after transplantation. We used the CRISPR-Cas9 knock-in strategy (Cong et al., 2013; Gagliardi et al., 2018) to generate an hiPSC reporter line in which the fluorescent protein EGFP under the control of ubiquitous CAG promoter is inserted into the "safe harbor" AAVS1 site (**Supplementary Figure S3A**). Among the five puromycin-resistant selected clones (**Supplementary Figure S3B**), we selected a clone carrying a copy of the insert in both AAVS1 loci (CAG-c2), for further retinal differentiation. The iPSC line genomic integrity was confirmed by SNP genotyping (**Supplementary Figure S3C**). As expected, the iPSC colonies expressed GFP and the pluripotency markers OCT4, SSEA4, SOX2, and NANOG (**Supplementary Figures S3D,E**). When overgrowing AAVS1:CAG-P-EGFP iPSCs were switched to a differentiation medium, self-forming neuro-retinal structures could be observed 4 weeks after the initiation of differentiation (**Figure 8A**). Endogenous GFP signal was visible in D56 retinal organoids in floating cultures (**Figure 8B**). Immunostaining for GFP on cryosections of retinal organoids confirmed the expression of the transgene in all retinal cells (**Figures 8C,D**). Co-immunostaining with specific RGC markers (BRN3A and PAX6) in D56 organoids (**Figure 8C**) or photoreceptor markers (CRX and RCVRN) in D130 organoids (**Figure 8D**) confirmed that GFP is expressed in differentiating retinal neurons.

Applying the double-stepwise selection of RGCs (adherent culture of dissociated cells from D56 retinal organoids combined with THY1-targeted MACS) to GFP-positive retinal organoids, allowed an enrichment in cells expressing RGC markers (RBPMS, BRN3A, THY1, and ISLET1) in the MACS-positive fraction compared to unsorted cells and MACS-negative fraction (**Figure 8E**). As expected, the MACS-positive fraction was markedly depleted in photoreceptor cells identified with both CRX and RCVRN antibodies, while they were mainly found in

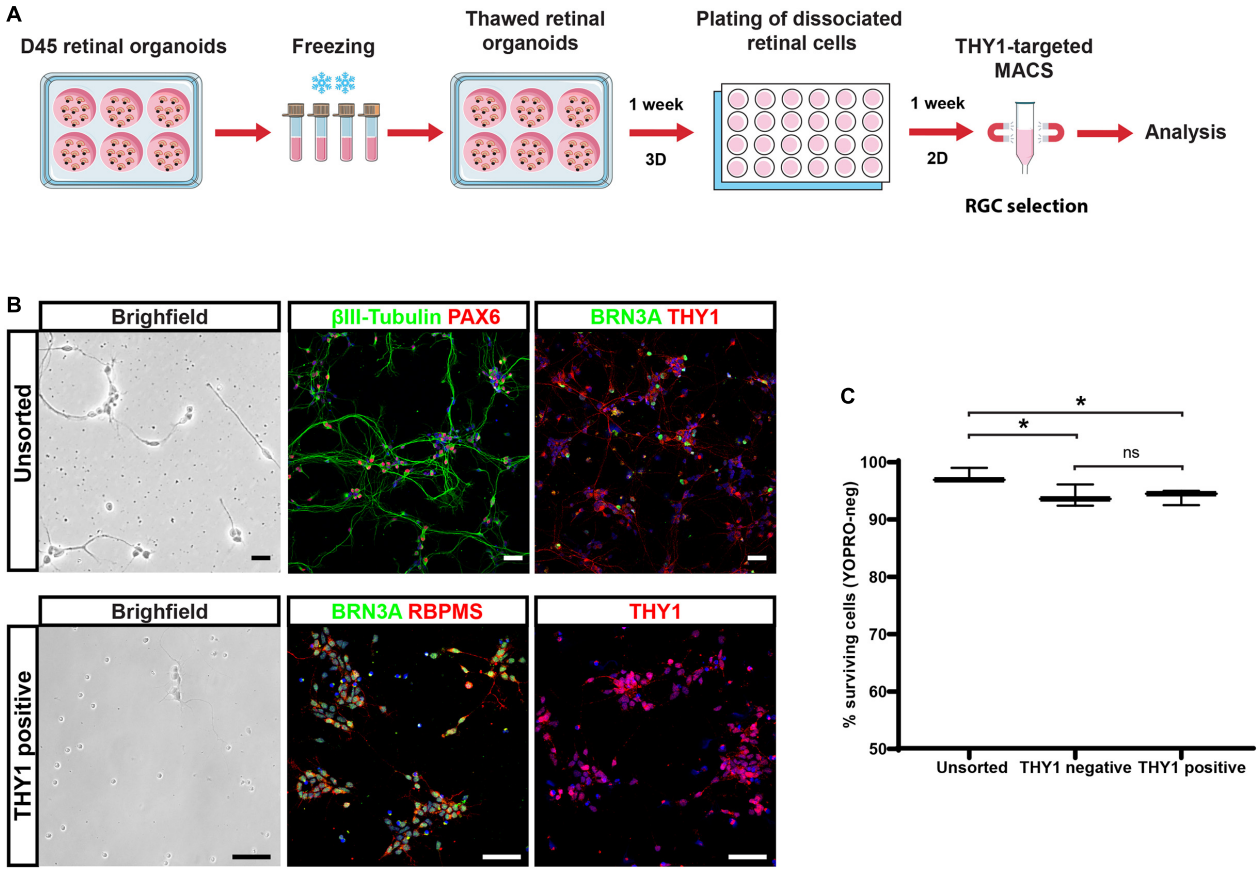

FIGURE 7 | Selection of hiPSC-derived RGCs from cryopreserved retinal organoids. **(A)** Schematic diagram illustrating the protocol for the selection of THY1-targeted hiPSC-derived RGCs from cryopreserved hiPSC-derived retinal organoids. **(B)** Phase-contrast and brightfield micrograph and immunostaining for RGC markers, βIII-tubulin, BRN3A, PAX6, RBPMS, or THY1 in unsorted or THY1-sorted cells from dissociated freeze–thawed organoids (cell nuclei staining with DAPI in blue). Scale bars: 50 μm. **(C)** Quantitative analysis by flow cytometry of living cells (YOPRO negative) on unsorted, THY1-negative, and THY1-positive fractions, 1 week after plating, of dissociated cells derived from freeze–thawed retinal organoids (min to max; $N = 3$ differentiation; $n = 380$ organoids; $^*p < 0.05$, two-way ANOVA followed by Tukey's multiple comparison test).

the MACS-negative fraction (**Figure 8E**). These results confirm that our optimized protocol for RGC generation and enrichment from human retinal organoids is suitable for different hiPSC lines.

Transplantation of Unsorted and THY1-Positive Retinal Cells Into a Mouse Model of Optic Nerve Injury

Next, we sought to study the transplantation competence of hiPSC-derived RGCs in a host environment recapitulating degenerative conditions of RGCs. Progressive loss of optic nerve fibers was induced by the optic nerve crush (ONC) model (Park et al., 2008; McKinnon et al., 2009). ONC was confirmed after tracing RGC axons through intravitreal injection of Alexa-555-conjugated cholera-toxin subunit B (CTB) (**Figure 9A**). ONC was followed by a progressive loss of endogenous RGCs visualized after 4 weeks (**Figure 9B**). Unsorted cells (200,000) (**Figure 9C**) or THY1-sorted cells (**Figures 9D–F**) derived from GFP-expressing retinal organoids were injected into the vitreous space close to the host ganglion cell layer (GCL) 4 weeks after ONC. One week after transplantation in immunosuppressed animals, GFP-positive cells were found in 75% of eyes injected with unsorted cells ($n = 3$ out of 4) and 59% of eyes injected with THY1-sorted cells ($n = 10$ out of 17 mice; $N = 3$ experiments). GFP-positive injected cells in the vitreous were clearly identified by the expression of human-specific marker hNA (**Figures 9C,D**). Most human grafted GFP-positive cells co-expressed RBPMS (**Figures 9C,D**), and only some expressed BRN3A and THY1 (**Figure 9D** and **Supplementary Figure S4**) in accordance with the previous demonstration that BRN3A is expressed in an RGC subpopulation (Badea et al., 2009). In order to exclude the possibility that injected cells engaged in apoptosis, we performed TUNEL assay (**Figure 9D**). Quantification of TUNEL-positive cells revealed that 15.82 ± 4.98% of GFP-positive cells were TUNEL positive demonstrating that most grafted cells were alive (**Figure 9D**) ($n = 9$). Among the animals injected with THY1-sorted cells and displaying human cells in the vitreous, nine showed GFP-positive cells intermingled with the host GCL. In these animals, some double-positive RBPMS/GFP-injected RGCs

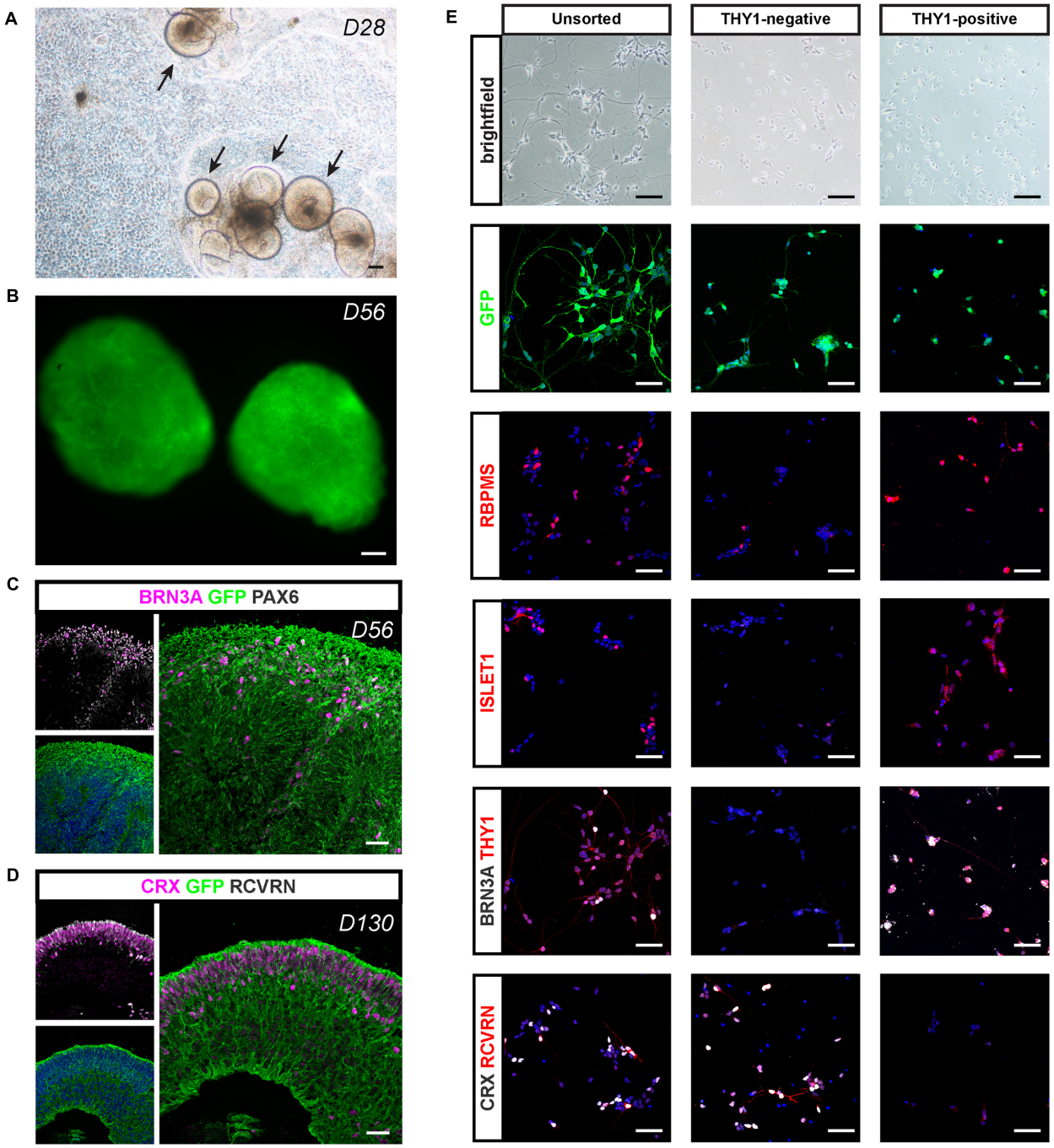

FIGURE 8 | Retinal differentiation and selection of THY1-positive RGCs using a AAVS1:CAG-P_EGFP hiPSC line. **(A)** Phase-contrast and brightfield micrograph showing emergence of D28 retinal organoids from differentiating AAVS1:CAG-P_EGFP hiPSCs. Scale bar: 200 μm. **(B)** Endogenous GFP expression in D56 retinal organoids. Scale bar: 200 μm. **(C,D)** Immunostaining showing the expression of GFP in all retinal organoid cells. **(C)** RGCs are identified at D56 according to the co-expression of PAX6 and BRN3A. **(D)** Co-expression of CRX and recoverin (RCVRN) corresponds to photoreceptors in D130 organoids. Scale bars: 30 μm. **(E)** RGC characterization in unsorted, THY1– and THY1+ fractions according to the expression of RBPMS, ISLET1, BRN3A, and THY1. Immunostaining for CRX and RCVRN enables photoreceptor identification. Scale bars: 50 μm.

migrated in the remaining GCL (**Figures 9C,D**). Interestingly, GFP/hNA double-positive cells were still present 4 weeks after injection of THY1-sorted cells in half of the transplanted animals (n = 3 out of 6) under immunosuppressive treatment. Transplanted cells were distributed either as small cell clusters close to the retina (**Figure 9E**) or as small number of cells, intermingled with the host GCL (**Figure 9F**). Despite no evidence of neurite outgrowth, the majority of surviving

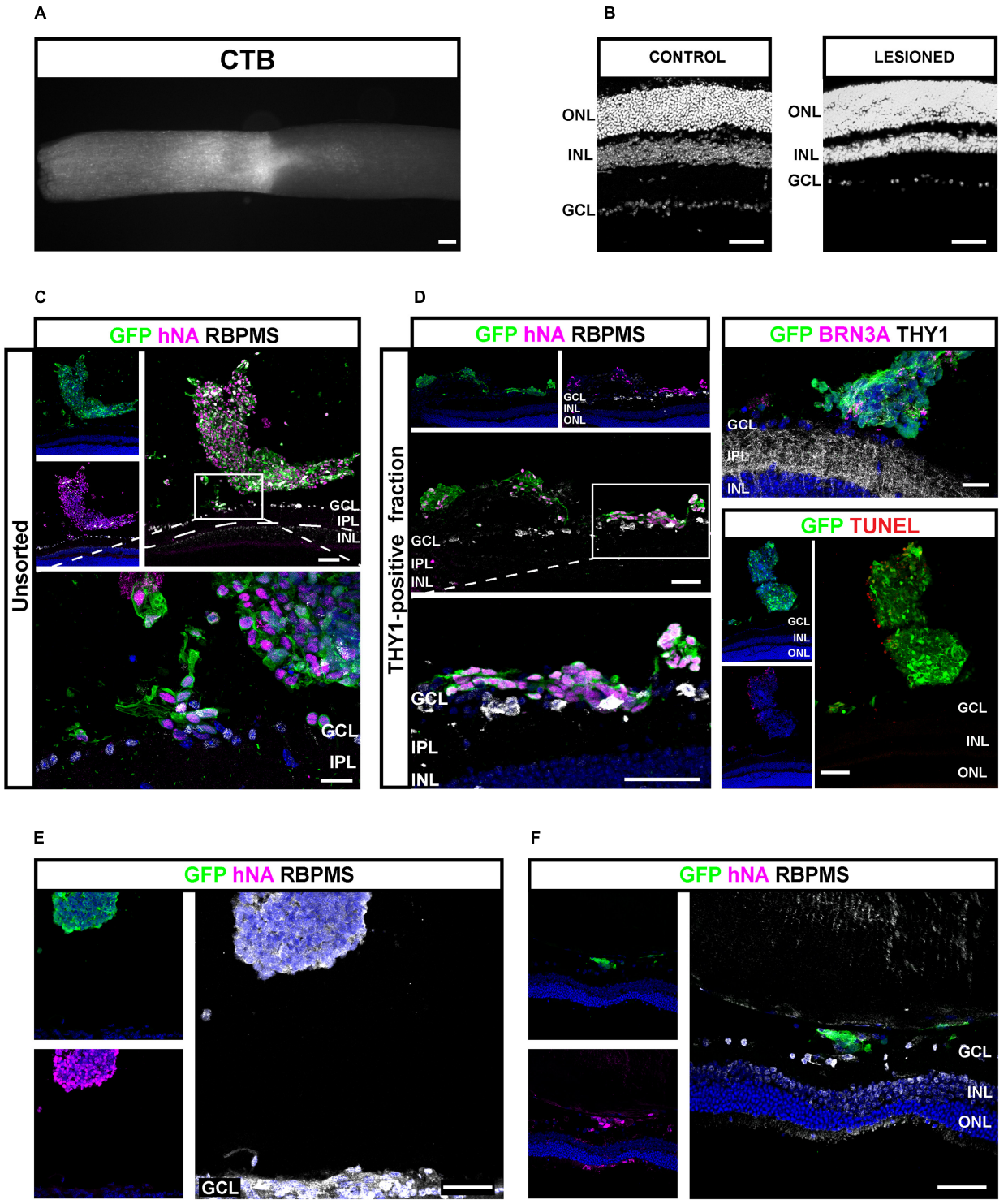

FIGURE 9 | Injection of hiPSC-derived RGCs in the vitreous of optic nerve crush mice model. **(A)** Alexa 555-conjugated CTB-β-labeled optic nerve crush revealing the lesion site. Scale bar: 100 μm. **(B)** DAPI staining showing the RGC loss in the GCL 5 weeks after optic nerve crush. Scale bar: 100 μm. **(C–F)** Immunostaining in retinal sections from mice grafted with unsorted **(C)** or MAC-sorted THY1-positive fractions **(D)** 1 week after transplantations, and MAC-sorted THY1-positive cells **(E,F)** 4 weeks after transplantations. The delimitated areas indicate the location of high-magnification image below. Transplanted cells are identified according to GFP and human marker hNA immunoreactivity **(C–F)**. RGCs are identified according to BRN3A **(D)** or RBPMS expression **(C–F)**. Notice the close apposition of transplanted cells to GCL **(D)**. Evaluation of cell death among engrafted cells was performed according to TUNEL labeling **(D)**. Notice the small number of TUNEL-positive cells. Scale bars: 100 μm **(A–D)** or 50 μm **(E,F)**. GCL, ganglion cell layer; INL, inner nuclear layer; IPL, inner plexiform layer; ONL, outer nuclear layer.

cells were identified as RGCs according to RBPMS expression (**Figures 9E,F**).

DISCUSSION

In the current study, we have developed a two-step process to optimize the differentiation and the isolation of RGCs from hiPSC-derived retinal organoids. As previously reported in different retinal organoids (Reichman et al., 2014; Zhong et al., 2014), we demonstrated an increase in the RGC population from D42 with a peak around D56 before a progressive loss of these cells. The RGC loss starting before their advanced maturation, as shown by the absence of THY1 immunoreactivity, was likely due to the absence of projection targets and to the floating culture condition, the latter representing a strong hindrance to axon outgrowth outside the organoids, as previously observed with an RGC fluorescent reporter iPSC line (Capowski et al., 2019). Beyond the morphological and molecular features of RGCs, the functional maturation, such as the ability of RGCs to trigger action potentials, is an important issue. By using MEA recording, we detected relatively low spontaneous activity, which does not exclude that more RGCs would be able to fire in response to stimulation. Moreover, scattered distribution of RGCs in the core of retinal organoids may limit suitable contacts with the recording electrodes required for an optimal recording. Despite these technical issues, the possibility to detect spiking activity in retinal organoids suggests that RGCs initiated a maturation process. RGCs are massively predominant among the spiking retinal cells. However, it cannot be totally excluded that some other retinal cells, such as a few amacrine cells, are at the origin of some recorded spikes.

In order to promote RGC survival and functional maturation, retinal organoids have been dissociated at D56, a stage of development at which many RGCs are present, and retinal cells were replated onto an adherent substrate. In agreement with previous studies, the adherent culture of retinal cells allowed RGCs to grow extensions showing βIII-tubulin or THY1 immunoreactivity (Ohlemacher et al., 2016; Li et al., 2017; Fligor et al., 2018; Langer et al., 2018; Chavali et al., 2020). The capacity of neurons such as RGCs to trigger an action potential depends on different hallmarks including the expression of specific voltage-gated channels and, importantly, a resting membrane potential (V_{rest}) allowing their activation (Catterall, 2012). This crucial point is illustrated by a recent study showing that only hiPSC-derived RGCs displaying an adequately negative V_{rest} were able to spike (Teotia et al., 2019). In the present study, the V_{rest} was approximatively −43 mV, a slightly more depolarized value than that reported by Riazifar et al. (2014) or Chavali et al. (2020) in hiPSC-derived RGC-like cells, but lower than that observed by Teotia et al. (2019). Consistent with previous studies (Teotia et al., 2019; VanderWall et al., 2019), we demonstrated that 3 weeks after plating, the mature RGCs, in contrast to photoreceptors, displayed voltage-gated ionic currents enabling these RGCs to evoke spikes after stimulation and to spontaneously fire. The ability of RGCs to trigger action potentials is an important issue for future transplantation applications since electrical activity has been shown to be important for both RGC development (Assali et al., 2014) and regeneration (Lim et al., 2016). Interestingly, MAC-sorted RGCs displayed very weak voltage-gated fast inward currents that were insufficient to allow the generation of an action potential (data not shown), suggesting that functional maturation of RGCs could be improved in the presence of other non-RGC retinal cells. Similar observations have been nicely reported for hiPSC-derived RGCs co-cultured with astrocytes by VanderWall et al. (2019).

The cell sorting method based on the specific expression of a cell surface marker is useful for the enrichment of a specific cell type, allowing for instance, transcriptomic analysis (Daniszewski et al., 2018). In the present study, we demonstrated that adherent culture conditions of dissociated cells from D56 retinal organoids are sufficient to enrich in RGCs more than 60%, according to THY1 expression, 1 week after plating. The second step of RGC enrichment using THY1-targeted MACS allowed to reach up to almost 80% of RGCs, corresponding to a similar enrichment than previously reported with another RGC differentiation protocol (Gill et al., 2016). To improve MACS efficiency, retinal cell culture after plating could be extended in order to obtain more mature RGCs expressing a higher level of THY1. However, for future cell transplantation, the ontogenetic stage of donor cells should be a critical point. The ability of RGCs to integrate the host tissue according to the specific developmental stage is poorly documented, but it was shown in rodents that RGCs isolated from adult retina failed to integrate the host retina after intravitreal injection unlike RGCs isolated from early postnatal donors (Hertz et al., 2014; Venugopalan et al., 2016). An excessive stage of differentiation of engrafted cells could also explain integration failure observed in normal mouse retina with RGC-like cells derived from mouse iPSC overexpressing Atoh7 in order to bias RGC differentiation toward RGC lineage (Chen et al., 2010). In order to efficiently select RGCs, other strategies using engineered reporter cell line expressing fluorescent protein or a cell surface selection marker have been proposed (Sluch et al., 2015, 2017). However, engineered reporter cell lines may not be suitable for the development of clinically compatible stem cell-based therapies.

One major advantage of the separation strategy presented here relies on the possible transfer of our entire protocol to GMP-compatible conditions. Indeed, our differentiation protocol is based on a feeder-free iPSC culture system and uses exclusively chemically defined xeno-free compounds. Furthermore, the GMP-compliant MACS enrichment is already used in clinical trials (Menasché et al., 2015). We also demonstrated that MACS targeting THY1 expression could be performed using cryopreserved organoids, ensuring the possibility to store the organoids at the appropriate stage of differentiation for downstream applications. Targeting other specific RGC cell surface markers such as CD184 or CD171 (Aparicio et al., 2017) could be an interesting alternative to improve RGC enrichment compared to THY1 targeting.

Transplantation studies demonstrated that THY1-enriched retinal cells survived in the vitreous up to 4 weeks after injection. Cells were found in the eyes of 59% of transplanted animals

1 week after intravitreal injection and 50% of transplanted animals 4 weeks post-injection. The limited efficacy of the immunosuppressive regimen could explain the limited number of animals where human cells can be detected, even though we cannot formally rule out some technical issues related to intravitreal injections. Administration of an immunosuppressant in drinking water is classically used and has demonstrated its efficiency (Jensen et al., 2012; Kamao et al., 2014; Ben M'Barek et al., 2017) but can yield partial success because of the inconsistent blood immunosuppressant levels (Jensen et al., 2012). However, the success ratio of transplantation is comparable and even slightly higher to the one (43%) reported with intravitreal injection of postnatal rat RGCs in normal mice (Venugopalan et al., 2016). TUNEL experiments demonstrated that the majority of injected cells were alive and immunostaining with specific RGC markers and specific antibodies for human antigen confirmed that most of the injected human cells were RGCs. Many engrafted cells were observed as trapped in the vitreous. Nevertheless, in a few animals, the engrafted cells intermingled with host retina. Although further experiments are needed to clearly demonstrate their integration into the host retina, our data are consistent with previous studies reporting 10% integration efficiency of postnatal rat RGCs (Venugopalan et al., 2016). A recent study suggested that retinal progenitors derived from human embryonic stem cells (hESCs) could differentiate into RGC-like cells in the host GCL 4 weeks after transplantation in NMDA-injured retina, but no morphological maturation was reported (Wang et al., 2019). However, injection of a cell population that may contain mitotic cells seems hazardous, with the risk of cell hyperproliferation within the vitreous. Very recently, intravitreal injection of hESC-derived RGC-like cells has been performed in normal, non-injured adult rat eye showing some survival and migration of transplanted cells into the host GCL (Zhang et al., 2019). Some donor cells displayed β-III-tubulin labeling suggesting initiation of maturation, but according to the authors, donor cells failed to express specific RGC marker such as RBPMS. In our study, transplanted cells did not harbor neurite elongation, even at 4 weeks after transplantation, in contrast to the observation made by Venugopalan et al. (2016) with transplantation of rat postnatal RGCs. These authors reported that 3 weeks after transplantation, some engrafted cells harbored neurite elongation on the retinal surface with diverse dendrite architecture demonstrating that RGC could morphologically mature after transplantation. Slower kinetics of human development could explain that transplanted cells failed to harbor significant neurite outgrowth, and increasing the delay after transplantation of hiPSC-derived RGCs would be useful to explore the ability of RGCs to extend axons and dendrites and to establish synaptic contacts with bipolar and amacrine cells in our model of optic nerve injury. RGC scattering in the vitreous after injection has been frequently reported (Hertz et al., 2014; Becker et al., 2016). Co-injection with trophic factors supporting axon growth would be also useful. Interestingly, hiPSC-derived RGCs have been shown to be responsive to various factors such as BDNF (Fligor et al., 2018). In order to facilitate cell migration in the vitreous to reach the retinal surface, it would be useful to limit the aggregation of transplanted cells with the use of specific injectable hydrogels (Pakulska et al., 2012). The inner limiting membrane, and more generally the extracellular matrix, could also limit cell integration into the GCL layer. Co-injection with a specific enzyme, such as chondroitinase, should facilitate both migration and integration of transplanted cells, as it has been reported for the injection of Muller glial cell-derived RGC-like cells (Singhal et al., 2012).

Attachment of the grafted cells onto the host retina surface is also a critical point. The absence of physical support possibly limits the survival and differentiation of the injected cells. Some recent studies demonstrated that engineered scaffolds or biomaterials can stimulate RGC axon outgrowth *in vitro* (Kador et al., 2014; Sluch et al., 2015; Li et al., 2017; Yang et al., 2017). Introducing a RGC-scaffold biomaterial into the eye would be a real progress compared to an injection of cell suspension as reported recently in rabbits and monkeys (Li et al., 2017). In summary, we report the optimization of RGC generation derived from hPSCs compatible with GMP manufacturing required for future cell replacement therapies. To the best of our knowledge, this is the first "proof of concept" of a successful transplantation of isolated hPSC-derived RGCs in a mouse model of optic neuropathy.

DATA AVAILABILITY STATEMENT

The data used to support the findings of this study are available from the corresponding author upon request.

ETHICS STATEMENT

The animal study was reviewed and approved by the Charles Darwin Ethical Committee for Animal Experimentation C2EA-05.

AUTHOR CONTRIBUTIONS

OR conducted the conception and design, collection and assembly of data, data analysis and interpretation, manuscript writing, and final approval of the manuscript. ACha carried out the collection and assembly of data, data analysis and interpretation, and final approval of the manuscript. AM was carried out the collection and assembly of data, data analysis, and interpretation. CJ was involved in the collection and assembly of data. AS-B, CN, and AR were contributed to the provision of study materials. GG and SR were involved in the provision of study materials and data analysis and interpretation. J-AS contributed to administrative and financial support. JD contributed to data analysis and interpretation. AChe

contributed to the data analysis and interpretation, and final approval of the manuscript. OG was involved in the conception and design, data analysis and interpretation, manuscript writing and final approval of the manuscript, and financial support. GO was responsible for the conception and design, collection and assembly of data, data analysis and interpretation, manuscript writing and final approval of the manuscript, and financial support. All authors contributed to the article and approved the submitted version.

FUNDING

This work was supported by grants from the ANR (ANR-17-CE18-0004-01-EyePS), UNADEV-Aviesan (Diseases of the vision, origins and treatments) and Retina France Association. This work was also performed in the frame of the LABEX LIFESENSES (ANR-10-LABX-65) within the Programme Investissements d'Avenir (ANR-11-IDEX-0004-02) and IHU FOReSIGHT (ANR-18-IAHU-01). OR was a recipient of a Ph.D. fellowship from Fédération des Aveugles de France.

ACKNOWLEDGMENTS

We are grateful to J. Dégardin, M. Simonutti, and the staff of Animal and Phenotyping facilities for help. We thank S. Fouquet from the Imaging facility, L. Riancho from the FACS facility, and A. Potey from the High Content Screening facility. We also thank E. Meloni for her technical assistance and K. Marazova for critical reading.

SUPPLEMENTARY MATERIAL

The Supplementary Material for this article can be found online at: https://www.frontiersin.org/articles/10.3389/fcell.2020.585675/full#supplementary-material

REFERENCES

Ahmad, I., Teotia, P., Erickson, H., and Xia, X. (2020). Recapitulating developmental mechanisms for retinal regeneration. *Prog. Retin. Eye Res.* 76:100824. doi: 10.1016/j.preteyeres.2019.100824

Aparicio, J. G., Hopp, H., Choi, A., Mandayam Comar, J., Liao, V. C., Harutyunyan, N., et al. (2017). Temporal expression of CD184(CXCR4) and CD171(L1CAM) identifies distinct early developmental stages of human retinal ganglion cells in embryonic stem cell derived retina. *Exp. Eye Res.* 154, 177–189. doi: 10.1016/j.exer.2016.11.013

Assali, A., Gaspar, P., and Rebsam, A. (2014). Activity dependent mechanisms of visual map formation - From retinal waves to molecular regulators. *Semin. Cell Dev. Biol.* 35, 136–146. doi: 10.1016/j.semcdb.2014.08.008

Badea, T. C., Cahill, H., Ecker, J., Hattar, S., and Nathans, J. (2009). Distinct roles of transcription factors brn3a and brn3b in controlling the development, morphology, and function of retinal ganglion cells. *Neuron* 61, 852–864. doi: 10.1016/j.neuron.2009.01.020

Barnstable, C. J., and Dräger, U. C. (1984). Thy-1 antigen: a ganglion cell specific marker in rodent retina. *Neuroscience* 11, 847–855. doi: 10.1016/0306-4522(84)90195-7

Becker, S., Eastlake, K., Jayaram, H., Jones, M. F., Brown, R. A., McLellan, G. J., et al. (2016). Allogeneic transplantation of müller-derived retinal ganglion cells improves retinal function in a feline model of ganglion cell depletion. *Stem Cells Transl. Med.* 5, 192–205. doi: 10.5966/sctm.2015-0125

Ben M'Barek, K., Habeler, W., Plancheron, A., Jarraya, M., Regent, F., et al. (2017). Human ESC-derived retinal epithelial cell sheets potentiate rescue of photoreceptor cell loss in rats with retinal degeneration. *Sci. Transl. Med.* 9:eaai7471. doi: 10.1126/scitranslmed.aai7471

Capowski, E. E., Samimi, K., Mayerl, S. J., Phillips, M. J., Pinilla, I., Howden, S. E., et al. (2019). Reproducibility and staging of 3D human retinal organoids across multiple pluripotent stem cell lines. *Development* 146:dev171686. doi: 10.1242/dev.171686

Carelli, V., La Morgia, C., Ross-Cisneros, F. N., and Sadun, A. A. (2017). Optic neuropathies: the tip of the neurodegeneration iceberg. *Hum. Mol. Genet.* 26, R139–R150. doi: 10.1093/hmg/ddx273

Catterall, W. A. (2012). Voltage-gated sodium channels at 60: structure, function and pathophysiology. *J. Physiol.* 590, 2577–2589. doi: 10.1113/jphysiol.2011.224204

Chavali, V. R. M., Haider, N., Rathi, S., Vrathasha, V., Alapati, T., He, J., et al. (2020). Dual SMAD inhibition and Wnt inhibition enable efficient and reproducible differentiations of induced pluripotent stem cells into retinal ganglion cells. *Sci. Rep.* 10:11828. doi: 10.1038/s41598-020-68811-8

Chen, J., Riazifar, H., Guan, M.-X., and Huang, T. (2016). Modeling autosomal dominant optic atrophy using induced pluripotent stem cells and identifying potential therapeutic targets. *Stem Cell Res. Ther.* 7:2. doi: 10.1186/s13287-015-0264-1

Chen, M., Chen, Q., Sun, X., Shen, W., Liu, B., Zhong, X., et al. (2010). Generation of retinal ganglion-like cells from reprogrammed mouse fibroblasts. *Invest. Ophthalmol. Vis. Sci.* 51, 5970–5978. doi: 10.1167/iovs.09-4504

Cong, L., Ran, F. A., Cox, D., Lin, S., Barretto, R., Habib, N., et al. (2013). Multiplex genome engineering using CRISPR/Cas systems. *Science* 339, 819–823. doi: 10.1126/science.1231143

Daniszewski, M., Senabouth, A., Nguyen, Q. H., Crombie, D. E., Lukowski, S. W., Kulkarni, T., et al. (2018). Single cell RNA sequencing of stem cell-derived retinal ganglion cells. *Sci. Data* 5:180013. doi: 10.1038/sdata.2018.13

Eiraku, M., Takata, N., Ishibashi, H., Kawada, M., Sakakura, E., Okuda, S., et al. (2011). Self-organizing optic-cup morphogenesis in three-dimensional culture. *Nature* 472, 51–56. doi: 10.1038/nature09941

Fischer, D., Harvey, A. R., Pernet, V., Lemmon, V. P., and Park, K. K. (2017). Optic nerve regeneration in mammals: regenerated or spared axons? *Exp. Neurol.* 296, 83–88. doi: 10.1016/j.expneurol.2017.07.008

Fligor, C. M., Langer, K. B., Sridhar, A., Ren, Y., Shields, P. K., Edler, M. C., et al. (2018). Three-dimensional retinal organoids facilitate the investigation of retinal ganglion cell development, organization and neurite outgrowth from human pluripotent stem cells. *Sci. Rep.* 8:14520. doi: 10.1038/s41598-018-32871-8

Fournier, A. E., and McKerracher, L. (1997). Expression of specific tubulin isotypes increases during regeneration of injured CNS neurons, but not after the application of brain-derived neurotrophic factor (BDNF). *J. Neurosci.* 17, 4623–4632. doi: 10.1523/JNEUROSCI.17-12-04623.1997

Gagliardi, G., Ben, M., Barek, K., Chaffiol, A., Slembrouck-Brec, A., Conart, J.-B., et al. (2018). Characterization and transplantation of CD73-positive photoreceptors isolated from human iPSC-derived retinal organoids. *Stem Cell Rep.* 11, 665–680. doi: 10.1016/j.stemcr.2018.07.005

Garita-Hernandez, M., Lampič, M., Chaffiol, A., Guibbal, L., Routet, F., Santos-Ferreira, T., et al. (2019). Restoration of visual function by transplantation of optogenetically engineered photoreceptors. *Nat. Commun.* 10:4524. doi: 10.1038/s41467-019-12330-2

Gill, K. P., Hung, S. S. C., Sharov, A., Lo, C. Y., Needham, K., Lidgerwood, G. E., et al. (2016). Enriched retinal ganglion cells derived from human embryonic stem cells. *Sci. Rep.* 6:30552. doi: 10.1038/srep30552

Greco, A., Rizzo, M. I., De Virgilio, A., Gallo, A., Fusconi, M., and de Vincentiis, M. (2016). Emerging concepts in glaucoma and review of the literature. *Am. J. Med.* 129, 1000.e7–1000.e13. doi: 10.1016/j.amjmed.2016.03.038

Hertz, J., Qu, B., Hu, Y., Patel, R. D., Valenzuela, D. A., and Goldberg, J. L. (2014). Survival and integration of developing and progenitor-derived retinal

ganglion cells following transplantation. *Cell Transplant.* 23, 855–872. doi: 10.3727/096368913X667024

Hockemeyer, D., Soldner, F., Beard, C., Gao, Q., Mitalipova, M., DeKelver, R. C., et al. (2009). Efficient targeting of expressed and silent genes in human ESCs and iPSCs using zinc-finger nucleases. *Nat. Biotechnol.* 27, 851–857. doi: 10.1038/nbt.1562

Hung, S. S. C., Van Bergen, N. J., Jackson, S., Liang, H., Mackey, D. A., Hernández, D., et al. (2016). Study of mitochondrial respiratory defects on reprogramming to human induced pluripotent stem cells. *Aging* 8, 945–957. doi: 10.18632/aging.100950

Jensen, M. B., Krishnaney-Davison, R., Cohen, L. K., and Zhang, S.-C. (2012). Injected versus oral cyclosporine for human neural progenitor grafting in rats. *J. Stem Cell Res. Ther. Suppl.* 10:003. doi: 10.4172/2157-7633.S10-003

Jonas, J. B., Aung, T., Bourne, R. R., Bron, A. M., Ritch, R., and Panda-Jonas, S. (2017). Glaucoma. *Lancet* 390, 2183–2193. doi: 10.1016/S0140-6736(17)31469-1

Kador, K. E., Alsehli, H. S., Zindell, A. N., Lau, L. W., Andreopoulos, F. M., Watson, B. D., et al. (2014). Retinal ganglion cell polarization using immobilized guidance cues on a tissue-engineered scaffold. *Acta Biomater.* 10, 4939–4946. doi: 10.1016/j.actbio.2014.08.032

Kamao, H., Mandai, M., Okamoto, S., Sakai, N., Suga, A., Sugita, S., et al. (2014). Characterization of human induced pluripotent stem cell-derived retinal pigment epithelium cell sheets aiming for clinical application. *Stem Cell Rep.* 2, 205–218. doi: 10.1016/j.stemcr.2013.12.007

Kobayashi, W., Onishi, A., Tu, H., Takihara, Y., Matsumura, M., Tsujimoto, K., et al. (2018). Culture systems of dissociated mouse and human pluripotent stem cell-derived retinal ganglion cells purified by two-step immunopanning. *Invest. Ophthalmol. Vis. Sci.* 59, 776–787. doi: 10.1167/iovs.17-22406

Laha, B., Stafford, B. K., and Huberman, A. D. (2017). Regenerating optic pathways from the eye to the brain. *Science* 356, 1031–1034. doi: 10.1126/science.aal5060

Langer, K. B., Ohlemacher, S. K., Phillips, M. J., Fligor, C. M., Jiang, P., Gamm, D. M., et al. (2018). Retinal ganglion cell diversity and subtype specification from human pluripotent stem cells. *Stem Cell Rep.* 10, 1282–1293. doi: 10.1016/j.stemcr.2018.02.010

Li, K., Zhong, X., Yang, S., Luo, Z., Li, K., Liu, Y., et al. (2017). HiPSC-derived retinal ganglion cells grow dendritic arbors and functional axons on a tissue-engineered scaffold. *Acta Biomater.* 54, 117–127. doi: 10.1016/j.actbio.2017.02.032

Lim, J. H. A., Stafford, B. K., Nguyen, P. L., Lien, B. V., Wang, C., Zukor, K., et al. (2016). Neural activity promotes long-distance, target-specific regeneration of adult retinal axons. *Nat. Neurosci.* 19, 1073–1084. doi: 10.1038/nn.4340

Llonch, S., Carido, M., and Ader, M. (2018). Organoid technology for retinal repair. *Dev. Biol.* 433, 132–143. doi: 10.1016/j.ydbio.2017.09.028

Maekawa, Y., Onishi, A., Matsushita, K., Koide, N., Mandai, M., Suzuma, K., et al. (2015). Optimized culture system to induce neurite outgrowth from retinal ganglion cells in three-dimensional retinal aggregates differentiated from mouse and human embryonic stem cells. *Curr. Eye Res.* 41, 558–568. doi: 10.3109/02713683.2015.1038359

Marban, E., Yamagishi, T., and Tomaselli, G. F. (1998). Structure and function of voltage-gated sodium channels. *J. Physiol.* 508, 647–657. doi: 10.1111/j.1469-7793.1998.647bp.x

McKinnon, S. J., Schlamp, C. L., and Nickells, R. W. (2009). Mouse models of retinal ganglion cell death and glaucoma. *Exp. Eye Res.* 88, 816–824. doi: 10.1016/j.exer.2008.12.002

Menasché, P., Vanneaux, V., Hagège, A., Bel, A., Cholley, B., Cacciapuoti, I., et al. (2015). Human embryonic stem cell-derived cardiac progenitors for severe heart failure treatment: first clinical case report. *Eur. Heart J.* 36, 2011–2017. doi: 10.1093/eurheartj/ehv189

Miltner, A. M., and La Torre, A. (2019). Retinal ganglion cell replacement: current status and challenges ahead. *Dev. Dyn.* 248, 118–128. doi: 10.1002/dvdy.24672

Nakano, T., Ando, S., Takata, N., Kawada, M., Muguruma, K., Sekiguchi, K., et al. (2012). Self-formation of optic cups and storable stratified neural retina from human ESCs. *Cell Stem Cell* 10, 771–785. doi: 10.1016/j.stem.2012.05.009

Newman, N. J. (2012). Treatment of hereditary optic neuropathies. *Nat. Rev. Neurol.* 8, 545–556. doi: 10.1038/nrneurol.2012.167

Ohlemacher, S. K., Sridhar, A., Xiao, Y., Hochstetler, A. E., Sarfarazi, M., Cummins, T. R., et al. (2016). Stepwise differentiation of retinal ganglion cells from human pluripotent stem cells enables analysis of glaucomatous neurodegeneration. *Stem Cells* 34, 1553–1562. doi: 10.1002/stem.2356

Pakulska, M. M., Ballios, B. G., and Shoichet, M. S. (2012). Injectable hydrogels for central nervous system therapy. *Biomed. Mater.* 7:024101. doi: 10.1088/1748-6041/7/2/024101

Park, K. K., Liu, K., Hu, Y., Smith, P. D., Wang, C., Cai, B., et al. (2008). Promoting axon regeneration in the adult CNS by modulation of the PTEN/mTOR pathway. *Science* 322, 963–966. doi: 10.1126/science.1161566

Rabesandratana, O., Goureau, O., and Orieux, G. (2018). Pluripotent stem cell-based approaches to explore and treat optic neuropathies. *Front. Neurosci.* 12:651. doi: 10.3389/fnins.2018.00651

Ran, F. A., Hsu, P. D., Wright, J., Agarwala, V., Scott, D. A., and Zhang, F. (2013). Genome engineering using the CRISPR-Cas9 system. *Nat. Protoc.* 8, 2281–2308. doi: 10.1038/nprot.2013.143

Reichman, S., Slembrouck, A., Gagliardi, G., Chaffiol, A., Terray, A., Nanteau, C., et al. (2017). Generation of storable retinal organoids and retinal pigmented epithelium from adherent human iPS cells in xeno-free and feeder-free conditions. *Stem Cells* 35, 1176–1188. doi: 10.1002/stem.2586

Reichman, S., Terray, A., Slembrouck, A., Nanteau, C., Orieux, G., Habeler, W., et al. (2014). From confluent human iPS cells to self-forming neural retina and retinal pigmented epithelium. *Proc. Natl. Acad. Sci. U.S.A.* 111, 8518–8523. doi: 10.1073/pnas.1324212111

Riazifar, H., Jia, Y., Chen, J., Lynch, G., and Huang, T. (2014). Chemically induced specification of retinal ganglion cells from human embryonic and induced pluripotent stem cells. *Stem Cells Transl. Med.* 3, 424–432. doi: 10.5966/sctm.2013-0147

Rodriguez, A. R., de Sevilla Müller, L. P., and Brecha, N. C. (2014). The RNA binding protein RBPMS is a selective marker of ganglion cells in the mammalian retina. *J. Comp. Neurol.* 522, 1411–1443. doi: 10.1002/cne.23521

Singhal, S., Bhatia, B., Jayaram, H., Becker, S., Jones, M. F., Cottrill, P. B., et al. (2012). Human Müller glia with stem cell characteristics differentiate into retinal ganglion cell (RGC) precursors in vitro and partially restore RGC function in vivo following transplantation. *Stem Cells Transl. Med.* 1, 188–199. doi: 10.5966/sctm.2011-0005

Slembrouck-Brec, A., Rodrigues, A., Rabesandratana, O., Gagliardi, G., Nanteau, C., Fouquet, S., et al. (2019). Reprogramming of adult retinal müller glial cells into human-induced pluripotent stem cells as an efficient source of retinal cells. *Stem Cells Int.* 2019, 1–13. doi: 10.1155/2019/7858796

Sluch, V. M., Chamling, X., Liu, M. M., Berlinicke, C. A., Cheng, J., Mitchell, K. L., et al. (2017). Enhanced stem cell differentiation and immunopurification of genome engineered human retinal ganglion cells. *Stem Cells Transl. Med.* 6, 1972–1986. doi: 10.1002/sctm.17-0059

Sluch, V. M., Davis, C.-H. O., Ranganathan, V., Kerr, J. M., Krick, K., Martin, R., et al. (2015). Differentiation of human ESCs to retinal ganglion cells using a CRISPR engineered reporter cell line. *Sci. Rep.* 5:16595. doi: 10.1038/srep16595

Susanna, R., De Moraes, C. G., Cioffi, G. A., and Ritch, R. (2015). Why do people (still) go blind from glaucoma? *Transl. Vis. Sci. Technol.* 4:1. doi: 10.1167/tvst.4.2.1

Teotia, P., Chopra, D. A., Dravid, S. M., Van Hook, M. J., Qiu, F., Morrison, J., et al. (2017). Generation of functional human retinal ganglion cells with target specificity from pluripotent stem cells by chemically defined recapitulation of developmental mechanism. *Stem Cells* 35, 572–585. doi: 10.1002/stem.2513

Teotia, P., Van Hook, M. J., Fischer, D., and Ahmad, I. (2019). Human retinal ganglion cell axon regeneration by recapitulating developmental mechanisms: effects of recruitment of the mTOR pathway. *Development* 146:dev178012. doi: 10.1242/dev.178012

VanderWall, K. B., Huang, K.-C., Pan, Y., Lavekar, S. S., Fligor, C. M., Allsop, A. R., et al. (2020). Retinal ganglion cells with a glaucoma OPTN(E50K) mutation exhibit neurodegenerative phenotypes when derived from three-dimensional retinal organoids. *Stem Cell Rep.* 15, 52–66. doi: 10.1016/j.stemcr.2020.05.009

VanderWall, K. B., Vij, R., Ohlemacher, S. K., Sridhar, A., Fligor, C. M., Feder, E. M., et al. (2019). Astrocytes regulate the development and maturation of retinal ganglion cells derived from human pluripotent stem cells. *Stem Cell Rep.* 12, 201–212. doi: 10.1016/j.stemcr.2018.12.010

Venugopalan, P., Wang, Y., Nguyen, T., Huang, A., Muller, K. J., and Goldberg, J. L. (2016). Transplanted neurons integrate into adult retinas and respond to light. *Nat. Commun.* 7:10472. doi: 10.1038/ncomms10472

Wang, S.-T., Chen, L., Zhang, P., Wang, X., Sun, Y., Ma, L., et al. (2019). Transplantation of retinal progenitor cells from optic cup-like structures differentiated from human embryonic stem cells in vitro and in vivo generation of retinal ganglion-like cells. *Stem Cells Dev.* 28, 258–267. doi: 10.1089/scd.2018.0076

Wong, R. C. B., Lim, S. Y., Hung, S. S. C., Jackson, S., Khan, S., Van Bergen, N. J., et al. (2017). Mitochondrial replacement in an iPSC model of Leber's hereditary optic neuropathy. *Aging* 9, 1341–1350. doi: 10.18632/aging.101231

Wu, Y.-R., Wang, A.-G., Chen, Y.-T., Yarmishyn, A. A., Buddhakosai, W., Yang, T.-C., et al. (2018). Bioactivity and gene expression profiles of hiPSC-generated retinal ganglion cells in MT-ND4 mutated Leber's hereditary optic neuropathy. *Exp. Cell Res.* 363, 299–309. doi: 10.1016/j.yexcr.2018.01.020

Yang, T.-C., Chuang, J.-H., Buddhakosai, W., Wu, W.-J., Lee, C.-J., Chen, W.-S., et al. (2017). Elongation of axon extension for human ipsc-derived retinal ganglion cells by a nano-imprinted scaffold. *Int. J. Mol. Sci.* 18:2013. doi: 10.3390/ijms18092013

Zhang, X., Tenerelli, K., Wu, S., Xia, X., Yokota, S., Sun, C., et al. (2019). Cell transplantation of retinal ganglion cells derived from hESCs. *Restor. Neurol. Neurosci.* 38, 131–140. doi: 10.3233/RNN-190941

Zhang, X.-M., Li Liu, D. T., Chiang, S. W.-Y., Choy, K.-W., Pang, C.-P., Lam, D. S.-C., et al. (2010). Immunopanning purification and long-term culture of human retinal ganglion cells. *Mol. Vis.* 16, 2867–2872.

Zhong, X., Gutierrez, C., Xue, T., Hampton, C., Vergara, M. N., Cao, L.-H., et al. (2014). Generation of three-dimensional retinal tissue with functional photoreceptors from human iPSCs. *Nat. Commun.* 5:4047. doi: 10.1038/ncomms5047

Conflict of Interest: The authors declare that the research was conducted in the absence of any commercial or financial relationships that could be construed as a potential conflict of interest.

frontiers in Cell and Developmental Biology

ORIGINAL RESEARCH
published: 05 November 2020
doi: 10.3389/fcell.2020.583234

Exosomes Enhance Adhesion and Osteogenic Differentiation of Initial Bone Marrow Stem Cells on Titanium Surfaces

Yanhua Lan, Qianrui Jin, Huizhi Xie, Chengxi Yan, Yi Ye, Xiaomin Zhao, Zhuo Chen and Zhijian Xie**

Key Laboratory of Oral Biomedical Research of Zhejiang Province, The Affiliated Hospital of Stomatology, School of Stomatology, Zhejiang University School of Medicine, Hangzhou, China

OPEN ACCESS

Edited by:
Philip Iannaccone, Northwestern University, United States

Reviewed by:
Tetsuya S. Tanaka, Elixirgen Scientific, Inc., United States
Gianpaolo Papaccio, Second University of Naples, Italy

***Correspondence:**
Zhijian Xie
xzj66@zju.edu.cn
Zhuo Chen
zoechen@zju.edu.cn

Specialty section:
This article was submitted to Stem Cell Research, a section of the journal Frontiers in Cell and Developmental Biology

Received: *14 July 2020*
Accepted: *07 October 2020*
Published: *05 November 2020*

Citation:
Lan Y, Jin Q, Xie H, Yan C, Ye Y, Zhao X, Chen Z and Xie Z (2020) Exosomes Enhance Adhesion and Osteogenic Differentiation of Initial Bone Marrow Stem Cells on Titanium Surfaces. Front. Cell Dev. Biol. 8:583234. doi: 10.3389/fcell.2020.583234

Successful osseointegration involves the biological behavior of bone marrow stem cells (BMSCs) on an implant surface; however, the role of BMSC-derived extracellular vesicles (EVs)/exosomes in osseointegration is little known. This study aimed to: (i) explore the interaction force between exosomes (Exo) and cells on a titanium surface; (ii) discuss whether the morphology and biological behavior of BMSCs are affected by exosomes; and (iii) preliminarily investigate the mechanism by which exosomes regulate cells on Ti surface. Exosomes secreted by rat BMSCs were collected by ultracentrifugation and analyzed using transmission electron microscopy and nanoparticle tracking analysis. Confocal fluorescence microscopy, scanning electron microscopy, Cell Counting Kit-8 (CCK-8), quantitative real-time polymerase chain reaction techniques, and alkaline phosphatase bioactivity, Alizarin Red staining, and quantification were used to investigate the exosomes that adhere to the Ti plates under different treatments as well as the morphological change, adhesion, spread, and differentiation of BMSCs. We found that exosomes were efficiently internalized and could regulate cell morphology and promoted the adhesion, spreading, and osteogenic differentiation of BMSCs. These were achieved partly by activating the RhoA/ROCK signaling pathway. Our discovery presents a new insight into the positive regulatory effect of exosomes on the biological behaviors of BMSCs on Ti surface and provides a novel route to modify the surface of a Ti implant.

Keywords: osseointegration, cell–material interaction, exosomes, titanium, bone marrow stem cells

INTRODUCTION

Dental implants have become an alternative for replacing missing teeth, which are essential for patients looking to restore dental esthetics and function. Fast and effective osseointegration is central to the success of dental implant therapy (Cervino et al., 2019). Successful osseointegration benefits from improved surface modification methods. Studies related to the implant surface have

increased exponentially, largely focusing on two aspects: abiotic methods (chemical and physical methods) based on surface engineering (Kuroda et al., 2002; Omar et al., 2016) and biotic methods (cells, polypeptide, covalent grafting, and etc.) that alter the implant surface with functional biomaterials (Zhang et al., 2011; Liu et al., 2017). The advantages of biotic implant modification, such as high osteoinduction capability, biocompatibility, and biodegradability, are required in many cases for biomedical applications (Geetha et al., 2008). However, the use of these traditional biotic implant modifications has several disadvantages, such as explosive release, immunogenicity, instability, and easy degradation. Recently, it has been proven that nanoscale materials that show novel physical, chemical, and biological properties with high stability could be efficient alternatives to increased cell responses, bone conduction, and osseointegration (Wang Y. et al., 2018).

Osseointegration and the maintenance of bone homeostasis on the bone–implant contact (BIC) mostly rely on cell-to-cell and cell-to-material communication, and this osseointegration process is directed by complex biological mechanisms that involve many cells and their secreted signaling factors (Nagasawa et al., 2016). Bone marrow stem cells (BMSCs) play an essential role in some key processes of osseointegration involving osteoinduction, osteogenesis, and bone reparative mechanism (Won et al., 2017). *In vitro* and *in vivo* studies suggest that various "tiny pieces of matter" (secreted by cells) such as cytokines, chemokines, growth factors, and others are implicated in the regulation of BMSC biological behavior. However, little is known about events in the interaction and regulation of cell-derived secretome products and the biological behavior of BMSCs.

Exosomes (Exo), specifically defined as the 50- to 200-nm vesicles that are secreted by multiple cells, have been reported to be present in biological fluids and are involved in multiple physiological and pathological processes. Exosomes are now considered an additional mechanism for intercellular communication, allowing cells to exchange proteins, lipids, and genetic material (van Niel et al., 2018). Among the multifarious exosomes, mesenchymal stem cell exosomes (MSC-exosomes) have attracted great attention as they have recently been identified as possibly functioning as regulators of various treatments, especially tissue engineering, and tissue regeneration.

Mesenchymal stem cell-exosomes, like most exosomes that carry informative cargo from the MSC to targeted cells, influence fundamental cellular processes including apoptosis, proliferation, migration, and lineage-specific differentiation (Brennan et al., 2020). Within the field of orthopedics and dentistry, MSC-exosomes regulate the osteogenic differentiation of MSCs by transferring vital materials, such as osteogenesis-related protein and microRNAs (Wang X. et al., 2018). Moreover, many studies have shown that multiple regulatory factors and complex signaling pathways involved in the process of osteogenesis differentiation are regulated by MSC-exosomes. Specific pathways including Wnt, BMP, PI3K/Akt, insulin, TGFβ, and calcium signaling pathways may be affected by MSC-exosomes (Cooper et al., 2019; Wei et al., 2019; Zhang et al., 2020). In aggregate, these researches demonstrate that MSC-exosomes carry much information that impacts key gene activation for osteogenesis including SATB2, Runx2, Dlx5, and Osterix (Osx; Fang et al., 2015; Huang et al., 2017). Despite extensive research, a clear picture is yet to emerge on how MSC-exosomes regulate cell biological behavior and differentiation, especially in materials frequently used for implant application.

Exosomes are certainly nanoscale intercellular messengers secreted by cells to deliver biological signals. Thus, the "if and how" they regulate the behavior of BMSCs on titanium (Ti) or other materials have become interesting and intriguing (Al-Sowayan et al., 2020). Furthermore, considering the outstanding properties of exosomes (natural origin, cargo representing a rich source of factors, and low immunogenicity), there may be a novel strategy to promote the activity of BMSCs in the process of osseointegration by introducing exosomes.

Therefore, the purposes of this study were to: (i) explore the form of the interaction force between exosomes and cells in a Ti environment; (ii) discuss whether the morphology and biological behavior of BMSCs are affected by exosomes; and (iii) preliminarily trace the internal molecular mechanism of this regulation on a Ti surface.

MATERIALS AND METHODS

Treatments With Titanium

Pure Ti plates (grade 4, 10 × 10 mm, 1-mm thickness; Guangci Medical Appliance Company, Zhejiang, China) were polished by grinding using silicon carbide (*SiC*) abrasive paper (#320 to #1600 grit sizes). Acid-etched Ti plates were treated as described in Zhang et al. (2011). Pure Ti plates were sand-blasted, rinsed with acetone, ultrasonic cleaned in 75% alcohol and distilled water, and dried under nitrogen flow. Ti plates were then treated with a solution containing hydrofluoric acid (HF) and HNO_3 followed by treatment with a solution containing HCl and H_2SO_4. On the other hand, the acid–alkali Ti plates were treated as follows (Jin et al., 2017). The Ti plates were treated with a solution containing HF and HNO_3, ultrasonically cleaned in 75% alcohol and distilled water, and treated with a solution containing 5 M NaOH for 30 min. Then, the Ti plates were heated to 450°C, kept for 1 h, and cooled to room temperature (25°C) naturally. All Ti plates were sterilized by ultraviolet (UV) radiation before use in the experiment. The experiment exclusively investigated the adsorption and biological effects of exosomes on BMSCs cultured on a Ti surface (**Figure 1**).

rBMSC Extraction, Culture, and Conditioned Medium Collection

Rats were sacrificed by an overdose of chloral hydrate to obtain rat bone marrow stem cells (rBMSCs) for culture. These cultures were prepared according to the protocol developed in Caplan Laboratory and previously carried out in our laboratory (Ke et al., 2016). The experimental procedures were approved by the Ethics Committee for Animal Research at Zhejiang University (ethics approval number: ZJU20200075). In brief, the tibia and femur, without attached tissues, were excised under sterile conditions. Subsequently, bone marrow was extracted using an injection of basal growth medium (BGM) consisting of

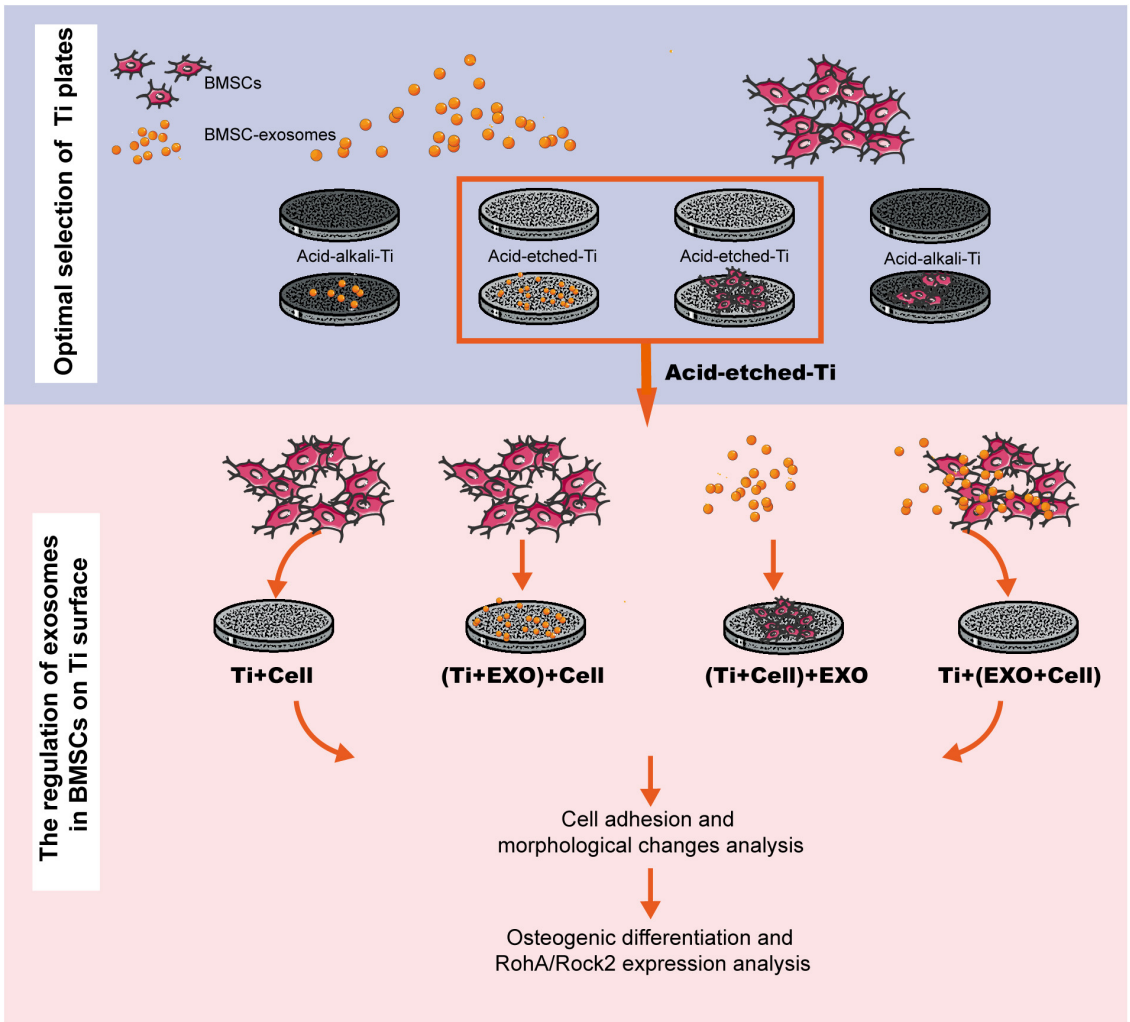

FIGURE 1 | Experimental flowchart. This workflow is divided into two steps: selecting a favorable adsorption material for exosomes and cells and investigating the regulation of exosomes in bone marrow stem cells (BMSCs) on Ti surfaces in three different combinations. BMSC-derived exosomes (*Exo*).

α-MEM medium (HyClone, UT, United States) with 10% fetal bovine serum (FBS; Gibco, New York, United States), 100 U/ml penicillin, and 100 μg/ml streptomycin. rBMSCs from passages 3–5 were used in this experiment. When cells were needed for differentiation into osteocytes, the rBMSCs were cultured in an osteogenic differentiation medium supplemented with 10 mM β-glycerophosphate, 50 μg/ml ascorbic acid, and 10^{-8} M dexamethasone (Sigma-Aldrich Co., St. Louis, United States). Besides, adenoviral vectors encoding a green fluorescent protein (Ad-GFP; GeneChem Co. Ltd., Shanghai, China) were used at a multiplicity of transduction of 100 for a clear presentation of the morphology of BMSCs.

Characterization of r-BMSCs by Flow Cytometry

Attached cells were trypsinized and detached from the polystyrene flask and separately incubated with the phycoerythrin-conjugated anti-rat antibodies, anti-CD29, anti-CD90, anti-CD45, and anti-CD34 (Biolegend, United States), for 30 min at room temperature. Then, the cells were washed twice with phosphate-buffered saline (PBS), centrifuged (1,500 rpm, 5 min) at room temperature, and resuspended in PBS. The cells were adjusted to a concentration of 5×10^5 cells/100 μl. Flow cytometric analysis was carried out using FACScan system (BD Becton Dickinson, United States).

Isolation of Exosomes

Before exosomes were extracted from rBMSCs, a fresh serum-free medium was introduced after cell attachment. A cell-conditioned medium was obtained from the rBMSCs cultured for 2 days in a medium without added serum and subjected to differential centrifugation (300 × *g*, 10 min; 2,000 × *g*, 10 min; and 10,000 × *g*, 30 min) at 4°C and filtered through a 0.45-μm membrane to remove large debris and dead cells. Then, the exosomes were pelleted by ultracentrifugation at 100,000 × *g* for

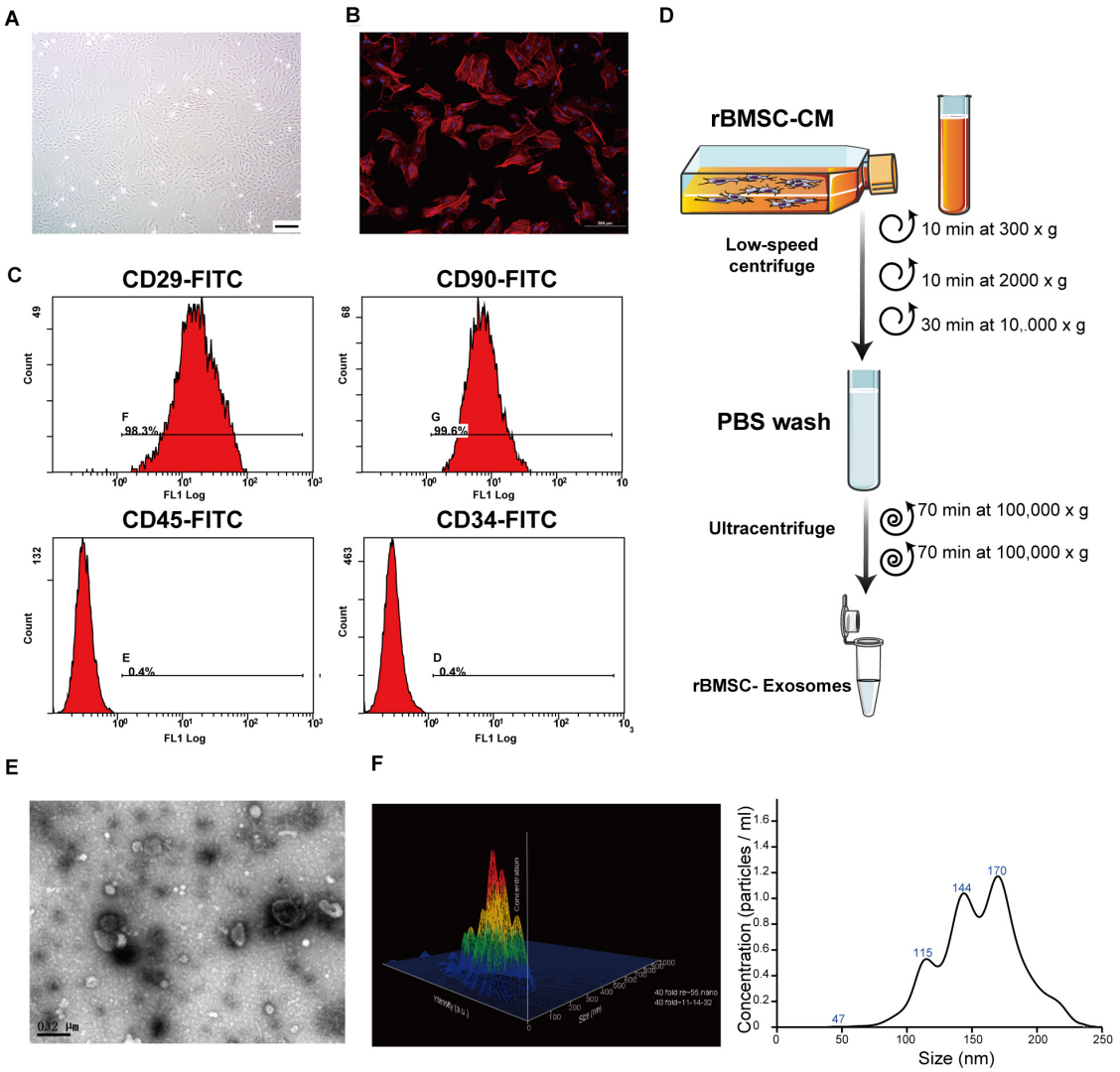

FIGURE 2 | Rat bone marrow stem cell (rBMSC) and exosome identification. **(A)** Typical photograph of spindle-shaped rBMSCs (undifferentiated) under an inverted microscope (*scale bar*, 50 μm). **(B)** Identification of rBMSC morphology through confocal microscopy (*scale bar*, 200 μm). **(C)** Flow cytometric analysis to identify rat BMSCs. The presence of rBMSCs was confirmed by positive staining for CD29 and CD90 as well as negative staining for CD34 and CD45. *CD*, cluster of differentiation. **(D)** Exosome purification protocol: collect conditioned medium from rBMSCs, use low-speed centrifugation and filtration to remove dead cells and debris, and wash contaminating proteins using an ultracentrifuge. **(E)** Representative image of exosome morphology as captured by transmission electron microscopy (TEM; *scale bar*, 200 nm). **(F)** Measurement of the particle size distribution of exosomes by nanoparticle transport analysis (NTA).

140 min at 4°C using a 70 Ti rotor (Beckman Coulter, Fullerton, United States; Théry et al., 2006). Finally, the supernatant was removed and the pellet resuspended in cold PBS throughout the ultracentrifugation step trials. A schematic of the exosome sample preparation method is shown (**Figure 2D**).

Characterization of Exosomes

After collecting the isolated exosomes, their morphology was observed using transmission electron microscopy (TEM). In brief, the exosomes were fixed with 4% paraformaldehyde (PFA, 1:1; Alfa Aesar, United States), then loaded onto a TEM copper grid, and washed with PBS, 1% glutaraldehyde, and distilled water. Exosome samples were next incubated with 4% uranyl acetate and visualized under a Tecnai 12 BioTWIN TEM (FEI/Phillips, United States) at 100 kV. Additionally, the number and the size distribution of exosomes were analyzed by nanoparticle trafficking analysis (NTA) using a NanoSight NS300 system (Malvern, United Kingdom) according to the manufacturer's instructions. In brief, the exosome samples were diluted, resuspended in 1 ml PBS, and reinjected into the device (Liao et al., 2019).

Optimal Selection of Ti Plates

The protein concentration of exosomes was determined using a bicinchoninic acid (BCA) assay with a standard curve (Biyuntian Biotech Company, Shanghai, China). The concentration of each

exosome sample was measured and adjusted to 100 μg/ml using cold PBS. One milliliter of the exosome solution was added dropwise to the surface of different Ti plates (two groups: acid-etched Ti and acid–alkali Ti). After 5 min of incubation at 4°C, the exosomes were immobilized on the surface of the Ti plates. The remaining solution was removed, collected, and the protein concentration determined to calculate the quantitative detection of the adsorption of exosomes by different Ti plates. rBMSCs were seeded at a low density (5,000 cells/plate) and grown overnight in order to screen and quantify exosome-regulated adhesion behavior of rBMSCs on two types of Ti surfaces.

Inoculate BMSC and BMSC-Exosome on Ti Plates

To examine the regulatory role of exosomes on rBMSCs cultured on Ti plates, the rBMSCs and exosomes were seeded on acid-etched Ti plates in four different combinations (**Figure 1**): Ti + Cell group: 100 μl cell suspension (2×10^5 cells/ml); (Ti + Exo) + Cell group: 100 μl of exosome suspension (100 μg/ml) was seeded after 12 h incubation at 37°C, 100 μl cell suspension; (Ti + Cell) + Exo group: 100 μl cell suspension was seeded 12 h before, 100 μl exosome suspension; and Ti + (Exo + Cell) group: 100 μl cell suspension and 100 μl exosome suspension were premixed before being added on Ti plates. The suspension was dropped onto the surface of Ti and allowed to settle for 15 min before the addition of a culture medium.

Confocal Fluorescence Microscopy and Image Analysis

Purified exosomes were labeled using PKH67 green fluorescent cell linker (PKH67GL-1KT; Sigma-Aldrich Co.) according to the manufacturer's instructions and then added to low-density rBMSC suspensions (5,000 cells/10 μg exosome) in each Ti plate. After 6 h of incubation, the Ti plates were washed three times in PBS and then fixed with 4% paraformaldehyde. The cell F-actin was visualized using rhodamine–phalloidin (Cytoskeleton Inc., Denver, United States). The nuclei were stained using DAPI (Sigma-Aldrich) following the manufacturer's recommended protocol.

Observation of Adherent Cells on Ti Plates Using Scanning Electron Microscopy

The adhesion of rBMSCs and the physical location and interactions between the cells and exosomes on the Ti surface were evaluated using a field-emission scanning electron microscope (FE-SEM; SU8010, Hitachi, Tokyo, Japan). In summary, the acid-etched Ti plates loaded with cells and exosome samples were fixed in 2% paraformaldehyde at 4°C for 15 min, washed with 0.15 M sodium cocoate buffer, and stained with 1% osmium tetraoxide for 2 h. After rinsing with the buffer, the samples were dehydrated through an ethanol series (30 min each in 50, 60, 70, 80, 90, 95, 100%, and dry ethanol) and dried in the air before gold sputter coating and observation (Wang Y. et al., 2018).

ALP Bioactivity

Alkaline phosphatase (ALP) bioactivity was examined by ALP staining and ALP activity testing after 7 days. For ALP staining, the acid-etched Ti plates loaded with cells and exosome samples were fixed in 4% paraformaldehyde and stained using a BCIP/NBT ALP color development kit (Biyuntian, China), then washed with PBS and photographed. ALP activity was determined using the LabAssay ALP kit (Wako Pure Chemical Industries, Japan) according to the manufacturer's instructions. Total cellular proteins were determined using the BCA protein assay and the absorbance at 405 nm was measured with a Microplate reader (Thermo Fisher Scientific).

Alizarin Red Staining and Quantification

Alizarin Red S stain was used for staining mineralized nodules. Briefly, the Ti plates loaded with cells and exosome samples were fixed in 4% paraformaldehyde and stained by 2% Alizarin Red S for 30 min. For quantification of Alizarin Red S staining, the samples were fixed in 70% ethanol for 1 h, then washed three times with dH_2O and stained with 0.5% Alizarin Red S solution (*w*/*v*, pH 4.2). The stain was desorbed with 10% cetylpyridinium chloride for 30 min and the absorbance at 562 nm was measured.

Cell Adhesion and Spread

Two methods were used to investigate the initial adhesion behavior of rBMSCs on the Ti plates. One method involved counting the attached cell numbers by counting the number of DAPI-stained nuclei in five random fields, expressed as the average number of the positively labeled cells per unit area of view. Then, the numbers of adherent cells in the co-culture setting with/without exosomes were indirectly quantified using the Cell Counting Kit-8 (CCK-8; Dojindo Laboratories, Kumamoto, Japan). Next, the spreading area of the cells was calculated using ImageJ analysis software. The average cell spreading area was calculated as S = Subtotal/Number of Nuclei, where Subtotal is the total cell spreading area on the image.

Quantitative Real-Time Polymerase Chain Reaction

The expression levels of cell adhesion, spreading, and osteogenic genes were evaluated using quantitative real-time polymerase chain reaction (qRT-PCR) for marker genes including the ras homolog family member A (RhoA), Rho-associated coiled-coil containing protein kinase 2 (ROCK2), Osterix (Osx), osteocalcin (OCN), and ALP in rBMSCs. Total RNA was isolated and purified using an RNeasy kit (Qiagen GmbH, Hilden, Germany). Complementary DNAs (cDNAs) were synthesized using a PrimeScript RT Master Mix (Takara Bio, Osaka, Japan). qPCR analysis was performed in duplicate for each sample in a 10-μl reaction using a CFX384 real-time system (Bio-Rad Laboratories, California, United States) with an SYBR Green I kit (Takara City, Osaka, Japan). All the expression levels of the target gene were normalized to those of the housekeeping gene, GAPDH. The primer sequences used are listed in **Supplementary Table 1**.

Statistics

All tests were repeated three times with two parallel runs for each assay, for a total of six runs, and the results presented as means ± standard deviation. Independent *t* test statistics were computed using SPSS version 19.0 (SPSS, Chicago, United States) and the *p* value set at 0.05.

RESULTS

Characterization of rBMSC and Exosomes

To comprehensively characterize the purified nanoparticles derived from rBMSCs, TEM, and NTA were employed. All exosomes are derived from donor cells (rBMSCs) in good condition, which appeared spindle-like in shape on the tissue culture plate (**Figures 2A,B**). The cell surface markers were determined by flow cytometry analysis to identify rBMSCs. The rBMSCs were confirmed by high percentages of positive staining for CD29 (98.3%) and CD90 (99.6%) as well as by low percentages of staining for CD34 (0.4%) and CD45 (0.4%; **Figure 2C**). The morphology of the BMSC-derived exosomes was first confirmed in the TEM image (**Figure 2E**), which revealed that the exosomes were 100- to 200-nm spherical particles with a complete membrane structure and similar shape to a biconcave-discoid, fitting the recognized characteristics of exosomes. The size distribution of the nanoparticles in exosomes is shown in a relative-intensity three-dimensional plot, which is characterized by NTA (**Figure 2F**). The concentration of exosomes was 3×10^8 particles/ml and the mean diameter of the particles was 163.7 ± 1.6 nm, as measured by the NTA system. Taken together, these data suggest that the nanoparticles are exosomes.

The Different Morphologies and Adsorption Capacity of Titanium Surface Under Acid or Acid–Alkali Treatments

For qualitative and quantitative evaluation, the adsorption capacities of two Ti surfaces (acid-etched and acid–alkali) were evaluated by SEM and protein quantification analysis of the leaching solution. Ti plates were sandblasted and acid-etched to obtain an irregular and rough surface with macro- and micro-pits similar to those commonly used in commercial dental implants (**Figure 3A**, 1–4). SEM images of the nanostructures were prepared using Ti wet corrosion in 5 M NaOH aqueous solution at 450°C. Porous nanowire networks were formed on the acid–alkali Ti surface. The nanowire networks were entangled, featuring a coralline-like morphology at a low magnification with a multilayered overlapping stamen shape at a high magnification (**Figure 3A**). To our surprise, such a complex morphology was unfavorable to the adherence of exosomes and cells when comparing with acid-etched surface (**Figures 3A,B**). It is clear from the pictures that the number of adherent exosomes on the acid-etched Ti surface was about two times greater than that on the acid–alkali Ti surface (**Figure 3D**). The acid-etched Ti surface has advantages over the numbers of cells and exosomes per counting area (**Figures 3C,E**) as well as the mean spreading area of the cells. Therefore, the acid-etched Ti plates were selected for subsequent experiments due to this greater ability to adsorb exosomes and cells. To sum up, acid-etched Ti has a stronger adsorption of exosomes and is therefore more likely to lead to the effective realization of the potential of exosomes.

Exosomes Induce Morphological Changes in BMSCs

To understand whether the physical interactions occurred preferentially between exosomes and cells, we next carefully observed them when both were present on the Ti surface. Based on our experimental results listed above and pilot experiments, the acid-etched Ti plates were chosen for subsequent experiments. Interestingly, as we observed in the low-magnification SEM images of the Ti surface, the exosomes were more likely to adhere to the surface of the cells while it was hard to see exosomes that adhered to the Ti surface away from the cell body. Moreover, changes in the cell morphology induced by exosome treatment were particularly obvious in the Ti + (Exo + Cell) group, including elongated, spindle-shaped morphology, pseudopodia formation, and increased cell scattering (**Figure 4A**). In contrast, cells showed no/decreased microvilli or filopodia- and lamellipodia-like structures on the Ti surface without exosomes. These results indicate that exosomes are more inclined to bind and be internalized by cells on the Ti surface. In addition, the adhesion and spreading of rBMSCs on the Ti surface were stimulated with the addition of exosomes (**Figures 4B,C**).

Exosomes Promote BMSC Adhesion and Spread on Ti Surfaces

Having shown that exosomes are efficiently internalized by cells, we then investigated whether exosomes play a role in the adhesion and spread of rBMSCs. We first proved that an interaction occurred between the cells and exosomes by tracing exosomes after co-culturing for 12 h and immunofluorescent staining in all the experimental groups (**Figure 5A**). Surprisingly, approximately 80–90% of cell-endocytosed exosomes without statistical differences were found regardless of the sequence of exosome treatment (**Figure 5B**). Then, the cell adhesion was directly and indirectly quantified by confocal microscope counting (**Figure 5D**) and CCK-8 assay (**Figure 5C**), respectively. Similarly, cell spread was calculated using ImageJ analysis software (**Figure 5E**). Over the same culture time, when observed by a microscope, the number of adhered cells in the Ti + (Exo + Cell) group was significantly more than that in the no-exosome group (**Figure 5A**). Also, rBMSCs in the Ti + (Exo + Cell) group with exosomes showed a significantly higher optical density (OD) value, which means an increased number of live cells (**Figure 5C**). The consistent results of the metabolic activity measurement and quantitative morphological assessment of the live cells were observed in the number of adherent rBMSCs. A similar result was obtained: under culture conditions in the presence of exosomes, treated rBMSCs displayed a dramatically increased adhesion to Ti surfaces compared with the control (**Figure 5D**). The cell spread

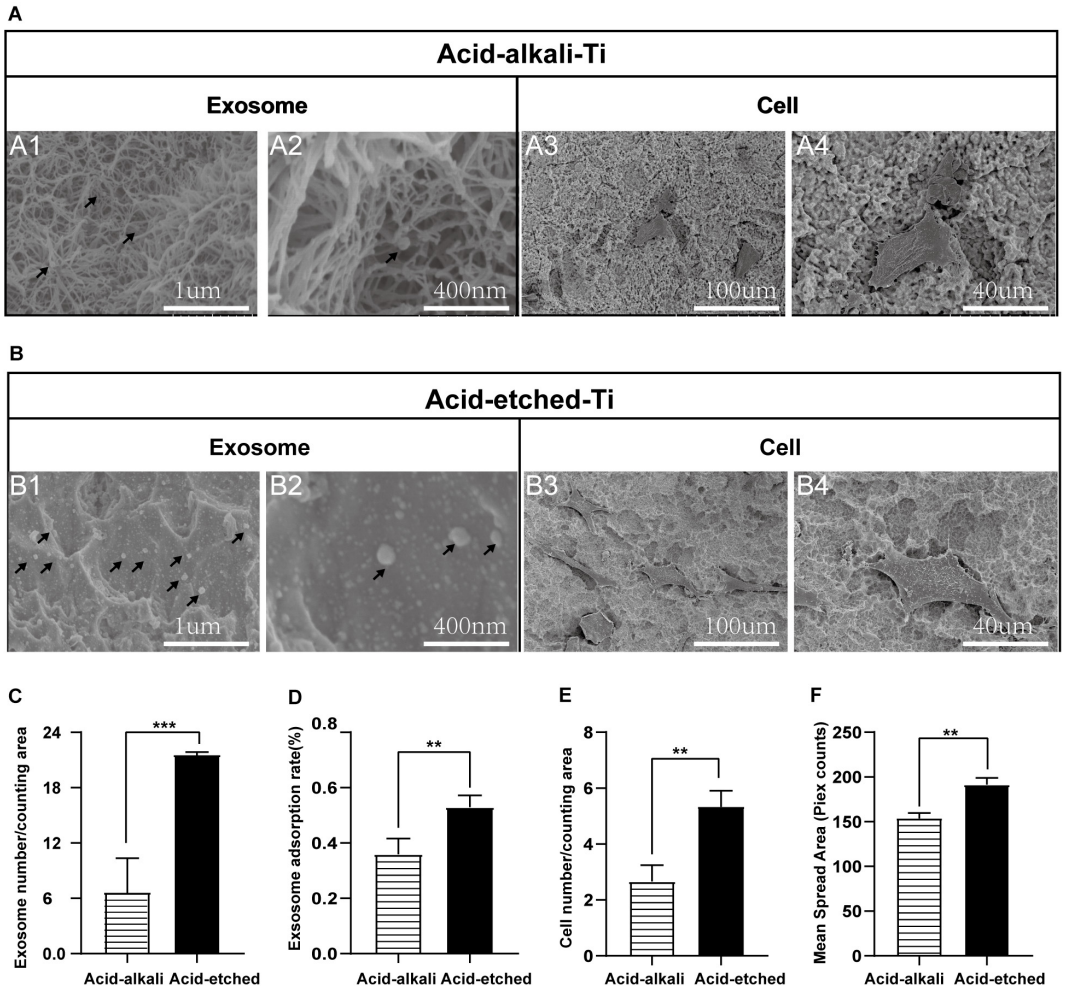

FIGURE 3 | Rat bone marrow stem cell (rBMSC) and BMSC-exosomes adhesion rates on the acid-etched Ti and acid–alkali Ti plates. **(A)** SEM images: Exosomes and cells on acid–alkali Ti surfaces (*scale bar*: *A1*, 1 μm; *A2*, 400 nm; *A3*, 100 μm; and A4, 40 μm). **(B)** SEM images: Exosomes and cells on acid-etched Ti surfaces (*scale bar*: *B1* 1 μm; *B2*, 400 nm; *B3*, 100 μm; and *B4*, 40 μm). **(C)** The number of exosomes was counted under SEM. **(D)** The adherence intensities of exosomes were quantified. The protein concentration indicated the quantity of exosomes adhering to the Ti surface. **(E)** The number of rBMSC cells was counted under SEM. **(F)** The average steady-state spreading area of each rBMSC was quantified using ImageJ. The results are presented as the mean ± standard error of the mean, $n = 3$. $^{*}p < 0.05$; $^{**}p <$'0.01, $^{***}p < 0.001$. The *black arrow* indicates exosomes adhering to the Ti surface.

was evaluated by measuring the mean spreading area of each cell (**Figure 5E**). The cell spreading area was significantly greater on exosomes than on the control Ti surface. In summary, the consistent results of the metabolic activity and quantitative morphological of cells were observed in the number of adherent rBMSCs, which indicated that exosomes had obvious cell tropism and contributed to the adhesion of rBMSCs on Ti surfaces.

The Expression of Selected Adherence and Osteogenic Differentiation Markers in rBMSCs on Ti Surfaces Were Upregulated by Exosomes

We next asked whether exosomes could contribute to the osteogenic differentiation of BMSCs and whether cytoskeletal changes were relevant. Exosomes significantly upregulated the rBMSC expression of cell adhesion, spread, and migration compared to those on the control Ti (**Figures 6A,B**). Especially in the Ti + (Cell + Exo) group, the effect was more pronounced. In comparison with the Ti group, the expression levels of RhoA and its downstream molecule ROCK2 were both up to nearly 2 and 1.5 times higher, respectively.

Osteogenesis-related genes' (Osx, OCN, and ALP) mRNA expressions in rBMSCs co-cultured with exosomes were determined by real-time PCR (**Figures 6C–E**). At 6 days, all selected osteogenic genes were upregulated on the Ti with exosomes. Increases of Osx, OCN, and ALP ranging from 1.5 to 2 times in the Ti + (Cell + Exo) group were observed when compared with the other three groups. To summarize, exosome treatment promoted the upregulation of RhoA and ROCK2, which indicates activation of the

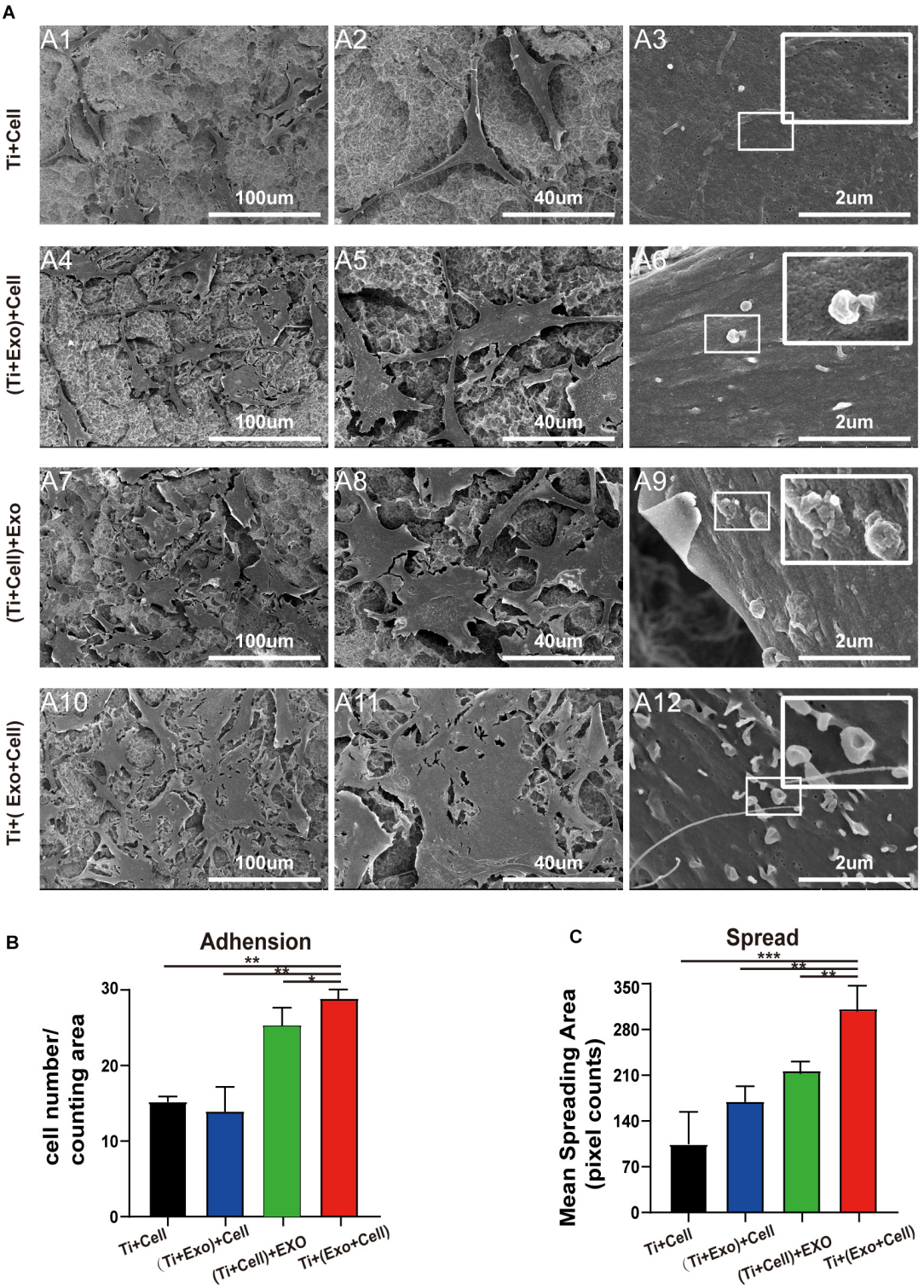

FIGURE 4 | SEM images of adherent rat bone marrow stem cells (rBMSCs) under different treatments of exosomes. **(A)** No exosomes appear on the control surface and adherent cells. In the Ti + (Exo + Cell) group, rBMSCs with longer and more numerous microvilli are detected in the presence of exosomes compared with the other three groups. The high-magnification image shows the endocytosis of exosomes by BMSCs (*scale bar*: *A1*, *A4*, *A7*, and *A10*, 100 μm; *A2*, *A5*, *A8*, and *A11*, 40 μm; *A3*, *A6*, *A9*, and *A12*, 2 μm). **(B)** The number of attached cells was counted under SEM. **(C)** The average steady-state spreading area of each rBMSC was quantified using ImageJ. The results are presented as the mean ± standard error of the mean, $n = 3$. *$p < 0.05$; **$p < 0.01$, ***$p < 0.001$. *ns*, not significant; *Exo*, exosomes.

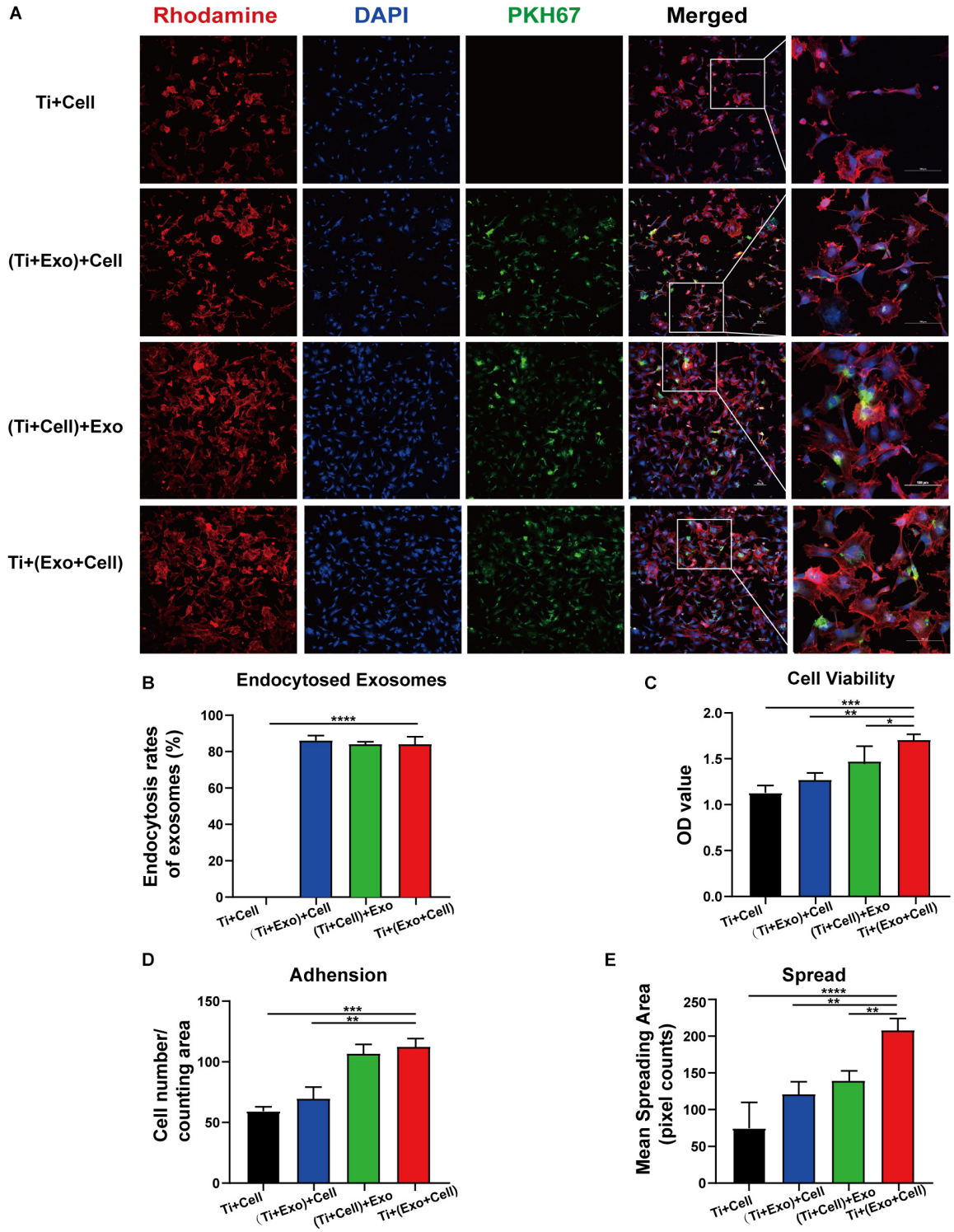

FIGURE 5 | Exosomes specifically bind to rat bone marrow stem cells (rBMSCs) and promote the adherence of rBMSCs onto Ti surfaces. The cells with or without exosome treatment were imaged using a confocal microscope. **(A)** rBMSCs incubated with or without PKH67-labeled exosomes (*green*) for 12 h. The nuclei of rBMSCs were stained using DAPI (*blue*), while the actin cytoskeleton was stained using phalloidin–rhodamine (*red*). *Scale bar*, 100 μm. **(B)** *Bars* represent the exosome endocytosis rates given as (number of cells containing exosomes/number of cell in each region) × 100. **(C)** The cell viability of adherent cells was measured using a CCK-8 assay after 12 h. **(D)** The number of attached cells was counted under a microscope. **(E)** The average steady-state spreading area of each rBMSC was quantified using ImageJ. The results are presented as the mean ± standard error of the mean, $n = 3$. $^{*}p < 0.05$, $^{**}p < 0.01$, $^{***}p < 0.001$, $^{****}p < 0.0001$. *ns*, not significant; *Exo*, exosomes.

RhoA–ROCK pathway. Moreover, exosomes promoted significant ALP, Osx, and OCN temporal upregulation by day 6 in the osteogenic differentiation medium, especially when they were premixed with rBMSCs in the Ti + (Cell + Exo) group.

Bone mineralization resulting from calcium deposition is known as a late marker in osteogenic differentiation. The results of the Alizarin Red and ALP staining and quantitation (**Figures 6F,G′**) illustrated that there were more calcified nodules and higher ALP staining intensity when co-cultured

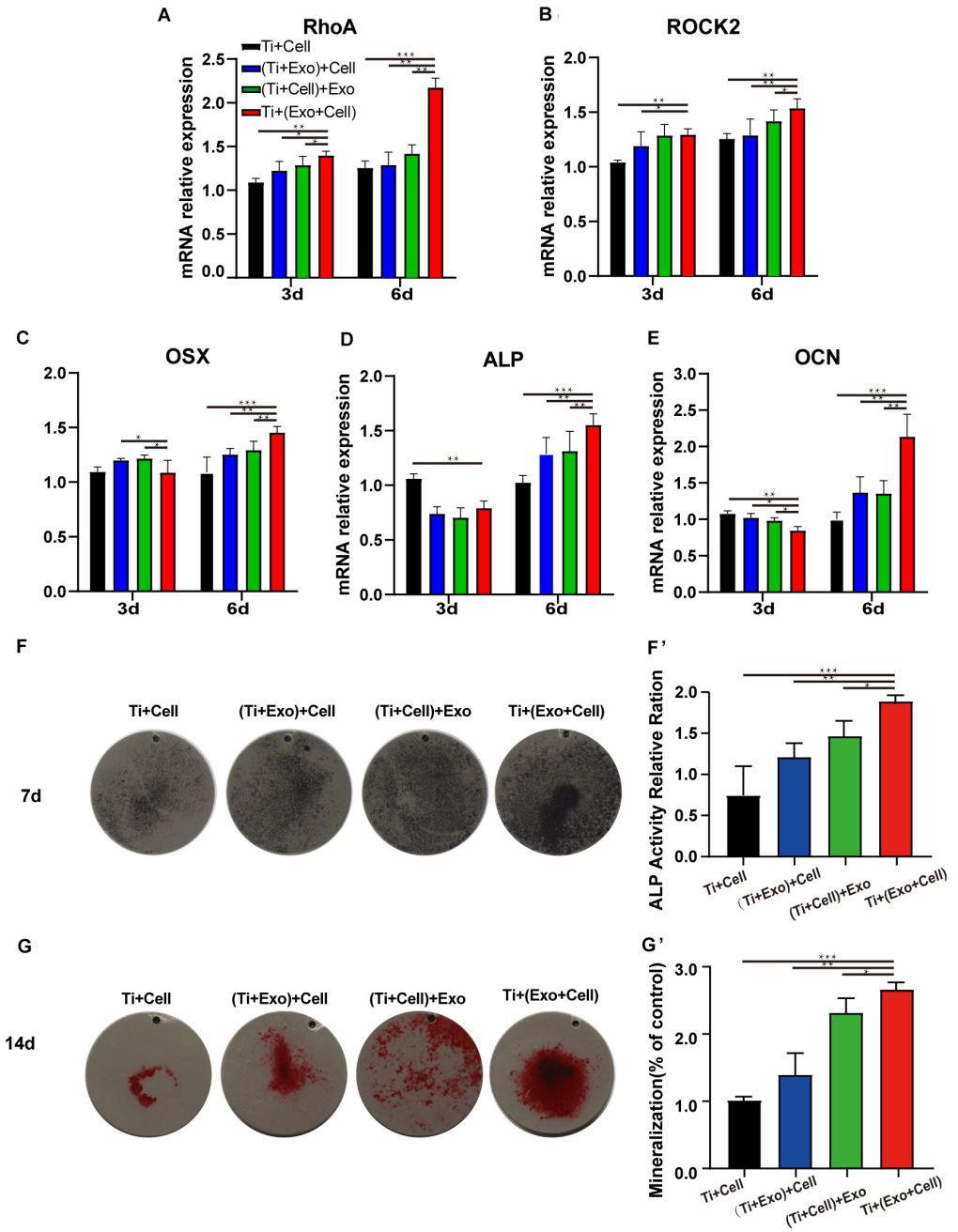

FIGURE 6 | Exosomes induce elevated expressions of genes related to cell adhesion (RhoA and ROCK2), improving osteogenesis in rat bone marrow stem cells (rBMSCs). The levels of gene expression of the cell adhesion markers RhoA **(A)** and ROCK2 **(B)** and the osteogenic differentiation markers Osterix **(C)**, ALP **(D)**, and OCN **(E)** in rBMSCs on Ti surfaces at different treatments of exosomes were analyzed. **(F)** The formation of mineralized nodules was then observed by Alizarin Red S staining. **(G, G′)** The quantitative alkaline phosphatase (ALP) assay was a parallel experiment to ALP staining. **(F, F′)** Alizarin Red staining was measured and quantification is shown on the *right*. The results are presented as the mean ± standard error of the mean, $n = 3$. $^{*}p < 0.05$; $^{**}p < 0.01$, $^{***}p < 0.001$. *ns*, not significant; *Exo*, exosomes.

with exosomes. These effects were most apparent in the Ti + (Cell + Exo) group. The ALP and Alizarin Red quantitations were elevated around 1.8- and 2.2-fold, respectively.

DISCUSSION

Effective integration of dental implants requires the chronological processes of osteoinduction, osteoconduction, and osseointegration (Albrektsson and Johansson, 2001). Cell-to-cell and cell-to-material communications are indispensable to these osseointegration processes, especially in the early stages (Smeets et al., 2016). Of interest in this study, we investigated the exosome trafficking between cells that take part in the regulation of the biological behaviors of BMSCs on the Ti surface. Here, cell adherence, spread, and osteogenic differentiation, which are crucial biological behaviors in the process of osseointegration, were evaluated. The main finding of the present work was that exosomes efficiently internalized and modulated cell biological behaviors on the Ti surface, most likely by activating the RhoA–ROCK pathway.

Firstly, we observed that exosomes have preferences for a special landing position. Our results suggest that the affinity of exosomes was strongest for cells, weaker with an abiotic surface, and quite reduced on an acid–alkali Ti surface compared to acid-etched Ti. The authors concluded that better adhesion might result from the physicochemical properties of materials and, more specifically, the different affinity with water and surface charge. One possible reason is that the acid–alkali Ti surface usually shows a lower water contact angle, which means higher surface energy, better wettability, and, thus, stronger hydrophilicity (Hoshino et al., 2015). However, exosomes have an intrinsic favorable lipid and surface protein composition, leading to an easier adherence to hydrophobic followed by super-hydrophilic substrates. Another possible reason is that the exosomes which demonstrated negative zeta potential values of about −10 to −50 mV (Maroto et al., 2017) tend to be more attracted to the positively charged surface and might be more prone to trapping on the acid-etched Ti surface (with a large number of protons) easily. Experiments show that the acid–alkali Ti, which is widely accepted and clinically used, has better performance in exosome adhesion. The results of the study support the use of acid–alkali Ti as a good system to study exosome-based modification of Ti surfaces.

In our following study, we found that exosomes and cells produced a very interesting attractive interaction when there were coexisting BMSC–exosomes in the cell milieu. We observed that the sequence of addition of exosomes and cells led to a different cell behavior promoted by exosomes. Compared to the other two sequences, the premix maximizes the effect of adhesion and spreading, wherein the full contact and interaction between the exosomes and cells are feasible. More interestingly, a common point in these observations is that this interaction appears to be cell tropism. Exosomes present where the cells reside, but are not sufficient to affect the positions the cells adhered to. However, Wang et al. (2020) found that exosome-triggered effects mainly occur when the exosomes are immobilized on the surface, but do not occur when exosomes are provided in suspension. This may be partially explained by the direct exposure of the assembled exosomes on the smooth surface of titanium. In contrast to the previous work, titanium with an acid-etched surface and three-dimensional structure was examined in the present study, which is more commonly used in clinical practice. These exosomes likely stuck to cells to mediate the cell adhesion and migration to the Ti surface. The spatial location relation between the exosomes and cells was determined for the cellular uptake of exosomes (**Figures 4**, **5**). This phenomenon that exosomes are easily internalized by cells was first identified in cancer studies and is called "efficient cellular internalization." This same feature (with four other features: long circulation, enhanced tumor accumulation, deep tumor penetration, and drug release) makes exosomes a novel tool in non-invasive anticancer therapy (Yong et al., 2020). However, this phenomenon exists not only in the tumor microenvironment but also on the Ti surface. Although the mechanisms of the processes remain unclear, they might shed light on previous studies in the field of tumor biology. The proposed mechanism of enhanced efficient cellular internalization can be attributed to the following three aspects: (i) as Smyth et al. (2014) have shown, in addition to the lipid component, the unique protein composition of exosomes promotes their internalization in cancer cells. Evidence indicated that ligand–receptor binding played an important role in promoting cellular internalization (van Dongen et al., 2016). (ii) There are some targeting ligands expressed on exosomes that are responsible for efficient cellular internalization. For example, it has been demonstrated that glycans and the soluble ligand CCL18 on extracellular vesicles (EVs) derived from cells mediated the interaction between exosomes and cancer cells (Islam et al., 2019). (iii) Extracellular matrix remodeling (ECM) is another cytosolic protein that plays an important role in efficient cellular internalization. Hoshino et al. have pointed out that the unique exosome integrin interaction with the cell-related ECM could mediate exosome uptake in specific target organ cells. In this case, ECM can be treated as a "zipper" between the exosomes and integrin on target cells (Hoshino et al., 2015). We set out to understand the efficient cellular internalization of exosomes. Exosomes also play an important role at the interface between the implant and bone tissue. The finding implies that exosomes may have advantages of targeting and specificity as bioactive-based materials (Zhou et al., 2020).

Of great importance is that exosomes are not only internalized by cells but also possess a robust capacity to affect the cell morphology and cell adhesion on the Ti surface (Wei et al., 2019). The number of mast cells was significantly higher on the Ti surface with the treatment of exosomes. Adherent rBMSCs on the Ti surface with exosomes appeared more stretched and larger than those on the control Ti surfaces. Concurrently, significant morphological characteristics (more triangular or polygonal and branched and filopodia-rich) of the rBMSCs were observed. Cell morphology contributes as a descriptor, indicator, or intermediate factor in characterizing cell material interactions and reflects the integrative effect of many distinct processes and signaling pathways across different scales, and it may be a valuable descriptor of cell behaviors

in differentiation and function (Marklein et al., 2016; Islam et al., 2019). For example, the study of Marklein et al. (2016) found that cell morphology could also serve as a predictor of the fate of progenitor cells. This beneficial effect is promoted by the exosome-mediated factor communication, which led to cell cytoskeleton rearrangement, adhesion, spread, and differentiation. However, the precise mechanisms for the enhanced exosome-related MSC spreading and adhesion are not clear yet. One possibility is the exosome-mediated transfer of molecular signaling among cells. A candidate may be RhoA, a molecule facilitating cytoskeleton remodeling and formation of adherens junctions. Through its effect on ROCK-mediated cytoskeletal tension, RhoA directly mediates the shape-related control of lineage stereotypes. As McBeath et al. (2004) said, controlling RhoA activity could even replace the need for soluble differentiation factors that caused osteogenesis. We did find that the expressions of RhoA and ROCK2 significantly increased under the treatment of exosomes, which is in line with our hypothesis. Furthermore, as suggested by previous studies, the phenomenon can be further explained by the transfer of an important signaling molecule. Wang et al. (2020) using proteomic analysis, suggested that MSC-exosomes carry a robust profile of cell adhesion molecules and signaling molecules, such as integrins, cadherins, and fibronectins. In the present study, we demonstrate that exosomes can regulate cell behaviors by upgrading the activation of the RhoA–ROCK pathway, but what triggers the signaling pathway requires further exploration.

Besides its adhesion impact, compelling evidence indicates the great potential of BMSC-exosomes for bone tissue engineering. The mechanism of the effect of exosomes on the increase of BMSC spreading and adhesion is still unclear. It is reasonably believed that osteogenic differentiation is related to the development of cell density (Pena et al., 2019), especially as we have previously shown that exosomes promote BMSC adhesion and cell–cell contact. Several studies suggest that cell density, which impacts cell–cell contacts and the concentration of paracrine factors, plays a role (Kempf et al., 2014). Moreover, a positive combined effect of adhesion and proliferation was found in some previous *in vitro* studies on different biomaterial surfaces (Reher et al., 2017). As the metal implants persist for the long term, the progress of dental implant osseointegration is distinct from normal bone defect repair. Highlighted as a key in this study is the efficient cell adhesion and spreading on the Ti surface. The secretion and the reciprocal exchange of exosomes between adherent cells and free cells in the bone/implant interface are also noteworthy. Therefore, another tentative role we present here is this exosome-dependent control of lineage commitment that is mediated by RhoA activity, and specifically *via* its effects on ROCK-mediated cytoskeletal tension. RhoA GTPase and RhoA/ROCK signaling, as a central regulator of contractility in many cells, has been proven to be critical to proliferation and differentiation in numerous studies. RhoA GTPase is even sufficient to mediate the switch in human mesenchymal stem cell (hMSC) commitment between adipogenic and osteogenic fates. The activation of RhoA can facilitate cytoskeleton remodeling (cell spreading), formation of adherens junctions, and downstream integrin signaling, such as TGF-β (Wang et al., 2012), ERK/Runx2, and the Wnt/PCP signaling pathway, which serve notable roles in osteogenic differentiation (Khatiwala et al., 2009; Li et al., 2015). All these imply that the activation of the RhoA/ROCK signaling pathway supports the preferential commitment of the progenitor cells to osteogenic differentiation, which may elucidate the mechanism of exosome treatment for new bone formation from a novel perspective.

Despite the interesting attraction between exosomes and cells and the obvious changes in the behavior of MSCs on Ti surfaces, these results are limited to the conventional single-cell model, especially considering that implant osseointegration is a complex process that involves osteogenesis, osteoinduction, osteoconduction, and remodeling of bone (Qin et al., 2016; Li et al., 2017). This complicated process involves multiple cells such as stem cells, osteoclasts/osteoblasts, and monocytes/macrophages (Sima and Glogauer, 2003). As the recruitment of monocytes/macrophages is crucial in the early stage of osseointegration, studies on the function of exosomes in monocyte–macrophage systems would be critical and interesting (Kang et al., 2020). Another issue that merits further study is whether the same exosomes have different roles in various cellular contexts: for example, whether the exosomes derived from BMSCs have different effects on stem cells, osteoblasts, and osteoclasts.

Even though exosome-based modification of implant surfaces is in its infancy, it exhibits promising prospects to enhance bone–implant integration, especially for patients with preexisting systemic illnesses. In order to achieve exosome implant coating and successful assembly on the titanium surface, the coating technique should be investigated and improved. More research is required to determine the optimum exosome concentration for coatings. The initial binding of exosomes might be stabilized by the antibody/ligand binding, like a covalent bond on the chemically modified titanium surfaces *via* intentional biological modification. Patients with systemic diseases such as diabetes and osteoporosis, having a lower implant survival, might benefit from these implants coated with exosomes due to the docking of exosomes to their parent cells, which suggests a more precise approach to treatment (Tsolaki et al., 2009).

Overall, we demonstrated the ability of exosomes to target cells and change their biological behaviors, which is an opportunity that opens up new ways to devise targeted therapies to facilitate the osseointegration of a dental implant. Our research described three important findings (**Figure 7**): (i) BMSC-exosomes derived by either adherent cells or suspension cells can be internalized efficiently by cells and to change the biological behaviors of cells. (ii) When exosomes are ingested by suspension cells, they advance cell attachment to the Ti surface. (iii) When exosomes are ingested by adherent cells or have been bound to cells as a whole and adhered to a Ti surface, they promote cell spreading and osteogenic differentiation. All these findings present new insights into the regulatory role of exosomes on

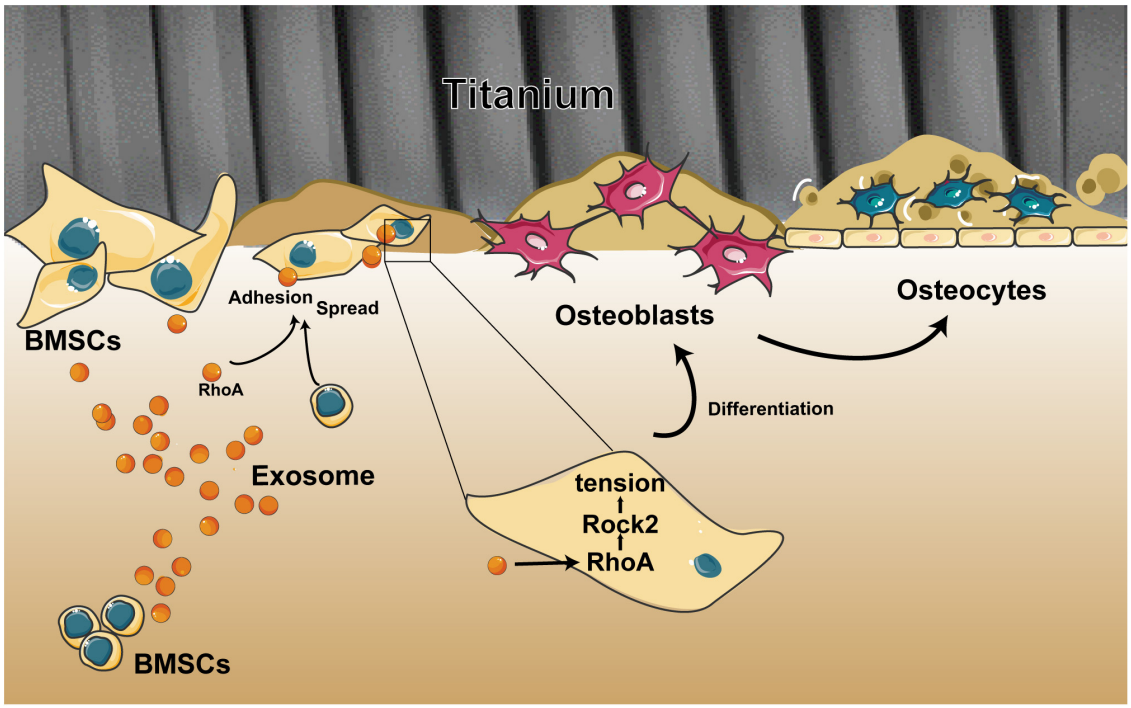

FIGURE 7 | Schematic of the multiple effects of exosomes on rat bone marrow stem cells (MSCs) on a Ti surface. Free/adhered BMSCs release exosomes. These BMSC-exosomes identify homologous cells, aid in efficient cellular internalization, and promote the adhesion, spread, and osteogenesis differentiation of BMSCs on the Ti surface.

cells on a Ti surface and provide a novel way to modify the surface of Ti implants.

CONCLUSION

To conclude, we report that exosomes exhibit efficient cellular internalization and take part in the regulation of cell morphology as well as biological behaviors. Our results demonstrate the novel insight that exosomes can promote the activity of BMSCs in the process of implant osseointegration and could be used for implant surface modification. Further experiments are required to investigate the functional roles of exosomes derived from diverse cells in a more complex model system to study the dynamics and regulation of multicellular populations.

DATA AVAILABILITY STATEMENT

The raw data supporting the conclusions of this article will be made available by the authors, without undue reservation.

ETHICS STATEMENT

The animal study was reviewed and approved by the Ethics Committee for Animal Research at Zhejiang University (Ethics approval number: ZJU20200075).

AUTHOR CONTRIBUTIONS

ZX and ZC conceived and designed the experiments. YL, QJ, HX, and CY performed the experiments. YL and YY analyzed the data. YL and XZ wrote the first draft of the manuscript. All authors contributed to manuscript revision and read and approved the submitted version.

FUNDING

This research was funded by grants from the National Natural Science Foundation of China (grant nos. 81771118 and 81800934); National Key R&D Program of China (grant no. 2018YFC1105103); and Zhejiang Provincial Natural Science Foundation of China (grant no. LY19H140004).

ACKNOWLEDGMENTS

We are grateful to the Imaging Center of Zhejiang University School of Medicine for their assistance in confocal microscopy.

SUPPLEMENTARY MATERIAL

The Supplementary Material for this article can be found online at: https://www.frontiersin.org/articles/10.3389/fcell.2020.583234/full#supplementary-material

REFERENCES

Albrektsson, T., and Johansson, C. (2001). Osteoinduction, osteoconduction and osseointegration. *Eur. Spine J.* 10, S96–S101. doi: 10.1007/978-3-642-56071-2_3

Al-Sowayan, B., Alammari, F., and Alshareeda, A. (2020). Preparing the bone tissue regeneration ground by exosomes: from diagnosis to therapy. *Molecules* 25:E4205. doi: 10.3390/molecules25184205

Brennan, M. Á, Layrolle, P., and Mooney, D. J. (2020). Biomaterials functionalized with MSC secreted extracellular vesicles and soluble factors for tissue regeneration. *Adv. Funct. Mater.* 30:1909125. doi: 10.1002/adfm.201909125

Cervino, G., Fiorillo, L., Iannello, G., Santonocito, D., Risitano, G., Cicciù, M., et al. (2019). Sandblasted and acid etched titanium dental implant surfaces systematic review and confocal microscopy evaluation. *Materials* 12:1763. doi: 10.3390/ma12111763

Cooper, L. F., Ravindran, S., Huang, C.-C., and Kang, M. (2019). A role for exosomes in craniofacial tissue engineering and regeneration. *Front. Physiol.* 10:1569. doi: 10.3389/fphys.2019.01569

Fang, S., Deng, Y., Gu, P., and Fan, X. (2015). Micrornas regulate bone development and regeneration. *Int. J. Mol. Sci.* 16, 8227–8253. doi: 10.3390/ijms16048227

Geetha, M., Singh, A. K., Asokamani, R., and Gogia, A. K. (2008). Ti based biomaterials, the ultimate choice for orthopaedic implants - A review. *Prog. Mater. Sci.* 54, 397–425. doi: 10.1016/j.pmatsci.2008.06.004

Hoshino, A., Costa-Silva, B., Shen, T. L., Rodrigues, G., Hashimoto, A., Tesic Mark, M., et al. (2015). Tumour exosome integrins determine organotropic metastasis. *Nature* 527, 329–335. doi: 10.1038/nature15756

Huang, C., Geng, J., and Jiang, S. (2017). MicroRNAs in regulation of osteogenic differentiation of mesenchymal stem cells. *Cell Tissue Res.* 368, 229–238. doi: 10.1007/s00441-016-2462-2

Islam, M. K., Syed, P., Lehtinen, L., Leivo, J., Gidwani, K., Wittfooth, S., et al. (2019). A nanoparticle-based approach for the detection of extracellular vesicles. *Sci. Rep.* 9:10038. doi: 10.1038/s41598-019-46395-2

Jin, S., Shin, E., and Hong, J. (2017). TiO_2 nanowire networks prepared by titanium corrosion and their application to bendable dye-sensitized solar cells. *Nanomaterials* 7:315. doi: 10.3390/nano7100315

Kang, M., Huang, C. C., Lu, Y., Shirazi, S., Gajendrareddy, P., Ravindran, S., et al. (2020). Bone regeneration is mediated by macrophage extracellular vesicles. *Bone* 3:115627. doi: 10.1016/j.bone.2020.115627

Ke, K., Li, Q., Yang, X., Xie, Z., Wang, Y., Shi, J., et al. (2016). Asperosaponin vi promotes bone marrow stromal cell osteogenic differentiation through the pi3k/akt signaling pathway in an osteoporosis model. *Sci. Rep.* 6:35233. doi: 10.1038/srep35233

Kempf, H., Olmer, R., Kropp, C., Rückert, M., Jara-Avaca, M., Robles-Diaz, D., et al. (2014). Controlling expansion and cardiomyogenic differentiation of human pluripotent stem cells in scalable suspension culture. *Stem Cell Rep.* 3, 1132–1146. doi: 10.1016/j.stemcr.2014.09.017

Khatiwala, C. B., Kim, P. D., Peyton, S. R., and Putnam, A. J. (2009). Ecm compliance regulates osteogenesis by influencing mapk signaling downstream of rhoa and rock. *J. Bone Miner. Res.* 24, 886–898. doi: 10.1359/jbmr.081240

Kuroda, K., Ichino, R., Okido, M., and Takai, O. (2002). Hydroxyapatite coating on titanium by thermal substrate method in aqueous solution. *J. Biomed. Mater. Res.* 59, 390–397. doi: 10.1002/jbm.10002

Li, J., Hu, C., Han, L., Liu, L., Jing, W., Tang, W., et al. (2015). Mir-154-5p regulates osteogenic differentiation of adipose-derived mesenchymal stem cells under tensile stress through the wnt/pcp pathway by targeting wnt11. *Bone* 75, 130–141. doi: 10.1016/j.bone.2015.05.003

Li, J., Huang, Z., Chen, L., Tang, X., Fang, Y., and Liu, L. (2017). Restoration of bone defects using modified heterogeneous deproteinized bone seeded with bone marrow mesenchymal stem cells. *Am. J. Transl. Res.* 9, 3200–3211.

Liao, Z., Luo, R., Li, G., Song, Y., Zhan, S., Zhao, K., et al. (2019). Exosomes from mesenchymal stem cells modulate endoplasmic reticulum stress to protect against nucleus pulposus cell death and ameliorate intervertebral disc degeneration in vivo. *Theranostics* 9, 4084–4100. doi: 10.7150/thno.33638

Liu, C., Zhou, Y., Sun, M., Li, Q., Dong, L., Ma, L., et al. (2017). Light-induced cell alignment and harvest for anisotropic cell sheet technology. *ACS Appl. Mater. Interfaces* 9, 36513–36524. doi: 10.1021/acsami.7b07202

Marklein, R. A., Lo Surdo, J. L., Bellayr, I. H., Godil, S. A., Puri, R. K., and Bauer, S. R. (2016). High content imaging of early morphological signatures predicts long term mineralization capacity of human mesenchymal stem cells upon osteogenic induction. *Stem Cells Stem Cells* 34, 935–947. doi: 10.1002/stem.2322

Maroto, R., Zhao, Y., Jamaluddin, M., Popov, V. L., Wang, H., Kalubowilage, M., et al. (2017). Effects of storage temperature on airway exosome integrity for diagnostic and functional analyses. *J. Extracell. Vesicles* 6:1359478. doi: 10.1080/20013078.2017.1359478

McBeath, R., Pirone, D. M., Nelson, C. M., Bhadriraju, K., and Chen, C. S. (2004). Cell shape, cytoskeletal tension, and rhoa regulate stem cell lineage commitment. *Dev. Cell.* 6, 483–495. doi: 10.1016/s1534-5807(04)00075-9

Nagasawa, M., Cooper, L. F., Ogino, Y., Mendonca, D., Liang, R., Yang, S., et al. (2016). Topography influences adherent cell regulation of osteoclastogenesis. *J. Dent. Res.* 95, 319–326. doi: 10.1177/0022034515616760

Omar, S. A., Ballarre, J., and Ceré, S. (2016). Protection and functionalization of aisi 316 l stainless steel for orthopedic implants: hybrid coating and sol gel glasses by spray to promote bioactivity. *Electrochim. Acta* 203, 309–315. doi: 10.1016/j.electacta.2016.01.051

Pena, C. D., Zhang, S., Majeska, R., Venkatesh, T., and Vazquez, M. (2019). Invertebrate retinal progenitors as regenerative models in a microfluidic system. *Cells* 8:1301. doi: 10.3390/cells8101301

Qin, Y., Wang, L., Gao, Z., Chen, G., and Zhang, C. (2016). Bone marrow stromal/stem cell-derived extracellular vesicles regulate osteoblast activity and differentiation in vitro and promote bone regeneration in vivo. *Sci. Rep.* 6:21961. doi: 10.1038/srep21961

Reher, D., Klink, B., Deutsch, A., and Voss-Böhme, A. (2017). Cell adhesion heterogeneity reinforces tumour cell dissemination: novel insights from a mathematical model. *Biol. Direct.* 12:18. doi: 10.1186/s13062-017-0188-z

Sima, C., and Glogauer, M. (2003). Macrophage subsets and osteoimmunology: tuning of the immunological recognition and effector systems that maintain alveolar bone. *Periodontology* 63, 80–101. doi: 10.1111/prd.12032

Smeets, R., Stadlinger, B., Schwarz, F., Beck-Broichsitter, B., Jung, O., Precht, C., et al. (2016). Impact of dental implant surface modifications on osseointegration. *Biomed. Res. Int.* 2016:6285620.

Smyth, T. J., Redzic, J. S., Graner, M. W., and Anchordoquy, T. J. (2014). Examination of the specificity of tumor cell derived exosomes with tumor cells in vitro. *Biochim. Biophys. Acta* 1838, 2954–2965. doi: 10.1016/j.bbamem.2014.07.026

Théry, C., Amigorena, S., Raposo, G., and Clayton, A. (2006). Isolation and characterization of exosomes from cell culture supernatants and biological fluids. *Curr. Protoc. Cell Biol.* 30, 3.22.1–3.22.29. doi: 10.1002/0471143030.cb0322s30

Tsolaki, I. N., Madianos, P. N., and Vrotsos, J. A. (2009). Outcomes of dental implants in osteoporotic patients. A literature review. *J. Prosthodont.* 18, 309–323. doi: 10.1111/j.1532-849X.2008.00433.x

van Dongen, H. M., Masoumi, N., Witwer, K. W., and Pegtel, D. M. (2016). Extracellular vesicles exploit viral entry routes for cargo delivery. *Microbiol. Mol. Biol. Rev.* 80, 369–386. doi: 10.1128/MMBR.00063-15

van Niel, G., D'Angelo, G., and Raposo, G. (2018). Shedding light on the cell biology of extracellular vesicles. *Nat. Rev. Mol. Cell. Biol.* 19, 213–228. doi: 10.1038/nrm.2017.125

Wang, X., Omar, O., Vazirisani, F., Thomsen, P., and Ekström, K. (2018). Mesenchymal stem cell-derived exosomes have altered microrna profiles and induce osteogenic differentiation depending on the stage of differentiation. *PLoS One* 13:e0193059. doi: 10.1371/journal.pone.0193059

Wang, X., Shah, F. A., Vazirisani, F., Johansson, A., Palmquist, A., Omar, O., et al. (2020). Exosomes influence the behavior of human mesenchymal stem cells on titanium surfaces. *Biomaterials* 230:119571. doi: 10.1016/j.biomaterials.2019.119571

Wang, Y., Zhang, C., Xu, W. J., Wang, B. X., Lan, Y. H., Yu, M., et al. (2018). The effect of surface immobilized nbd peptide on osteoclastogenesis of rough titanium plates in vitro and osseointegration of rough titanium implants in ovariectomized rats in vivo. *RSC Adv.* 8, 22853–22865. doi: 10.1039/C8RA03116A

Wang, Y. K., Yu, X., Cohen, D. M., Wozniak, M. A., Yang, M. T., Gao, L., et al. (2012). Bone morphogenetic protein-2-induced signaling and osteogenesis is regulated by cell shape, rhoa/rock, and

cytoskeletal tension. *Stem Cells Dev.* 21, 1176–1186. doi: 10.1089/scd.2011.0293

Wei, F., Li, M., Crawford, R., Zhou, Y., and Xiao, Y. (2019). Exosome-integrated titanium oxide nanotubes for targeted bone regeneration. *Acta Biomater.* 86, 480–492. doi: 10.1016/j.actbio.2019.01.006

Wei, Y., Tang, C., Zhang, J., Li, Z., Zhang, X., Miron, R. J., et al. (2019). Extracellular vesicles derived from the mid-to-late stage of osteoblast differentiation markedly enhance osteogenesis in vitro and in vivo. *Biochem. Biophys. Res. Commun.* 514, 252–258. doi: 10.1016/j.bbrc.2019.04.029

Won, S., Huh, Y. H., Cho, L. R., Lee, H. S., Byon, E. S., and Park, C. J. (2017). Cellular response of human bone marrow derived mesenchymal stem cells to titanium surfaces implanted with calcium and magnesium ions. *Tissue Eng. Regen. Med.* 14, 123–131. doi: 10.1007/s13770-017-0028-3

Yong, T., Wang, D., Li, X., Yan, Y., Hu, J., Gan, L., et al. (2020). Extracellular vesicles for tumor targeting delivery based on five features principle. *J. Control. Release* 322, 555–565. doi: 10.1016/j.jconrel.2020.03.039

Zhang, E. W., Wang, Y. B., Shuai, K. G., Gao, F., Bai, Y. J., Cheng, Y., et al. (2011). In vitro and in vivo evaluation of sla titanium surfaces with further alkali or hydrogen peroxide and heat treatment. *Biomed. Mater.* 6:025001. doi: 10.1088/1748-6041/6/2/025001

Zhang, L., Jiao, G., Ren, S., Zhang, X., Li, C., Wu, W., et al. (2020). Exosomes from bone marrow mesenchymal stem cells enhance fracture healing through the promotion of osteogenesis and angiogenesis in a rat model of nonunion. *Stem Cell Res. Ther.* 11:38. doi: 10.1186/s13287-020-1562-9

Zhou, Q., Cai, Y., and Lin, X. (2020). The dual character of exosomes in osteoarthritis: antagonists and therapeutic agents. *Acta Biomater.* 105, 15–25. doi: 10.1016/j.actbio.2020.01.040

Conflict of Interest: The authors declare that the research was conducted in the absence of any commercial or financial relationships that could be construed as a potential conflict of interest.

frontiers in Genetics

REVIEW
published: 02 February 2021
doi: 10.3389/fgene.2021.598855

C-Kit, a Double-Edged Sword in Liver Regeneration and Diseases

Weina Wang, Liyan Shui, Yanning Liu and Min Zheng**

State Key Laboratory for Diagnosis and Treatment of Infectious Diseases, National Clinical Research Center for Infectious Diseases, Collaborative Innovation Center for Diagnosis and Treatment of Infectious Diseases, The First Affiliated Hospital, College of Medicine, Zhejiang University, Hangzhou, China

Previous studies have reported an important role of c-kit in embryogenesis and adulthood. Activation of the SCF/KIT signal transduction pathway is customarily linked to cell proliferation, migration and survival thus influence hematopoiesis, pigmentation, and spermatogenesis. The role of c-kit in the liver is controversial, it is however argued that it is a double-edged sword in liver regeneration and diseases. First, liver c-kit$^+$ cells, including oval cells, bile epithelial cells, and part of hepatocytes, participate in liver tissue repair by regenerating target cells according to the type of liver injury. At the same time, c-kit$^+$ mast cells, act as immature progenitors in circulation, playing a critical role in liver fibrosis. Furthermore, c-kit is also a proto-oncogene. Notably, c-kit overexpression regulates gastrointestinal stromal tumors. Various studies have explored on c-kit and hepatocellular carcinoma, nevertheless, the intricate roles of c-kit in the liver are largely understudied. Herein, we extensively summarize previous studies geared toward providing hints for future clinical and basic research.

Keywords: c-kit, liver regeneration, stem cell, liver disease, HCC

OPEN ACCESS

Edited by:
Lon J. Van Winkle, Rocky Vista University, United States

Reviewed by:
Isabel Fabregat, Institut d'Investigacio Biomedica de Bellvitge (IDIBELL), Spain
Lindsey Kennedy, Indiana University Bloomington, United States

****Correspondence:***
Yanning Liu
liuyanning@zju.edu.cn
Min Zheng
minzheng@zju.edu.cn

Specialty section:
This article was submitted to Stem Cell Research, a section of the journal Frontiers in Genetics

Received: *25 August 2020*
Accepted: *08 January 2021*
Published: *02 February 2021*

Citation:
Wang W, Shui L, Liu Y and Zheng M (2021) C-Kit, a Double-Edged Sword in Liver Regeneration and Diseases. Front. Genet. 12:598855. doi: 10.3389/fgene.2021.598855

INTRODUCTION

C-kit also known as CD117, is a type III receptor tyrosine kinase coded by the KIT gene. It has a stem cell growth factor (SCF) as its ligand, hence referred to as the stem cell growth factor receptor (SCFR) (Fujio et al., 1996). C-kit is encoded by white spotting (W) locus with more than 30 mutations while SCF is encoded by steel (Sl) locus also with natural mutations (Lev et al., 1994). In mice, total loss of c-kit or SCF function causes embryonic lethal, however, mice with one of these mutations (W or Sl mice) can survive.

Previous studies have demonstrated the fundamental role of c-kit in embryogenesis and adulthood. C-kit can be detected in several normal cells including, hematopoietic stem cells (HSCs), oval cells, intestinal cells of Cajal, germ cells, melanocytes among others. Activation of the SCF/c-kit signal transduction pathway is usually linked to cell proliferation, migration, and survival, and thus regulate crucial functions in hematopoiesis, pigmentation, and spermatogenesis (Besmer et al., 1993). The liver is the only visceral organ that possesses the capacity to regenerate. As long as 30–35% of the liver remains, the remnant liver will undergo hyperplasia until the normal liver is re-established. Approximately 20% of hepatocytes located mainly at the periportal and pericentral regions express c-kit located with a weak staining intensity participates in liver regeneration (Yushkov et al., 2011). Hepatic resident stem cells and bone marrow-derived stem cells (BMSCs), both of which express c-kit, can differentiate into various cells according to the specific injuries.

Moreover, transplantation of c-kit positive (c-kit$^+$) oval cells, and BMSCs is a potential factor of improving liver regeneration.

Under pathological conditions, excessive c-kit signaling is often associated with tumor formation and progression in gastrointestinal stromal tumors (GISTs), melanoma, small cell lung carcinoma, testicular carcinoma, etc. Imatinib, a relatively selective tyrosine inhibitor, is a target particularly of BCR-ABL, platelet-derived growth factor receptor (PDGFR), and c-kit. Imatinib is commonly used in the treatment of GIST. Piebaldism is a rare autosomal dominant disorder in which interstitial cells of Cajal are lost due to the loss-of-function mutation of c-kit (Giebel and Spritz, 1991). In liver, c-kit$^+$ oval cells malignant transformation might be one of the possible mechanisms of hepatocarcinogenesis (Fang et al., 2004). Moreover, c-kit mutation or overexpression has been reported in hepatocellular carcinomas (HCC) (Potti et al., 2003; Yan et al., 2018). Besides, c-kit$^+$ mast cells play a key role in fibrogenesis, specifically in cholestatic/biliary diseases associated with fibrosis.

Nonetheless, the complex roles of c-kit and liver are largely understudied, therefore, this review broadly summarizes previous research to provide clues for future basic and clinical studies.

IDENTIFICATION OF C-KIT$^+$ CELLS IN THE LIVER

Several cell surface markers have been utilized to identify stem/progenitor cells of the liver, such as c-kit, CD34, Thy-1 (Lemmer et al., 1998; Petersen et al., 1998; Baumann et al., 1999; Crosby et al., 2001). Even without a characteristic marker for liver progenitor cells, previous studies used c-kit as a potential marker for liver stem/progenitor cells (Fujio et al., 1994; Fujio et al., 1996; Baumann et al., 1999). Adult hepatic stem cells, also termed oval cells, express both SCF and c-kit (Fujio et al., 1994). While the proliferation of hepatocytes is inhibited, KIT-mediated signal transduction activates oval cells which then produce hepatocytes and bile epithelial cells (BECs) (Matsusaka et al., 1999). Besides, c-kit is expressed in oval cells and BECs (Fujio et al., 1996), whereas only 20% of hepatocytes located mainly at the periportal and pericentral regions express c-kit with a weak staining intensity (Yushkov et al., 2011). Moreover, liver sinusoidal endothelial cells (LSECs) are known to express c-kit (Luna et al., 2004). On the other hand, c-kit can be detected in early hematopoietic cells, mast cells, and dendritic cells. And c-kit$^+$ mast cells are closely related to primary sclerosing cholangitis (PSC) (Metcalfe et al., 1997; Ishii et al., 2005; Ray et al., 2010). Kupffer cells and hepatic stellate cells are negative for c-kit (Ikarashi et al., 2013; Fu et al., 2015).

C-KIT AND LIVER REGENERATION

The liver is the only visceral organ with the capacity to regenerate. Liver c-kit$^+$ cells, including part of hepatocytes, BECs, and oval cells participate in liver regeneration by differentiating into different types of cells depending on the type of the injury. Moreover, c-kit$^+$ hematopoietic stem/progenitor cells (HSCs/HPCs) participate in liver regeneration. SCF/KIT signal transduction system regulates cell proliferation and survival. This review explains the relationship between c-kit and liver regeneration based on different types of cells (**Figure 1**).

Hepatocytes

Stem cell growth factor is localized in hepatocytes surrounding the BECs. And c-kit expressed with a weak staining intensity in 20% of hepatocytes located mainly at the periportal and pericentral regions (Yushkov et al., 2011).

Partial hepatectomy (PH) is the most common model used to study liver regeneration. After PH, mature hepatocytes proliferation leads to liver regeneration. Following PH, there is a significant decline in liver SCF levels and an increase in serum SCF levels during the first 24 h (Ren et al., 2003). The level of liver SCF mRNA was upregulated from the 24th hour to the 7th day (Meng et al., 2012). The number of c-kit$^+$ hepatocytes increased after PH, including medium and high staining intensity (Yushkov et al., 2011). In addition, exogenous SCF promotes the proliferation of primary hepatocytes in humans and mice (Meng et al., 2012). Moreover, a study by Ren et al. linked the interleukin-6 (IL-6) enzyme and tumor necrosis factor-α (TNF-α) with the SCF/C-kit in mice in 70% PH model. Results suggested that IL-6 stimulates the production and release of SCF, then SCF interacts with c-kit in activating the signal transducer and activator of transcription 3 (stat3) signal pathway thereby inducing hepatocyte proliferation (Ren et al., 2003; **Figure 2**). Besides, TNF-α-induced hepatocyte proliferation was partially mediated via SCF/c-kit, and the SCF-induced hepatocyte proliferation might also be mediated by the stat3 signal pathway (Ren et al., 2008; **Figure 2**). The possible mechanism occurs after acute injury where solubilized SCF is released and interact with c-kit, causing proliferation of the surrounding hepatocytes.

Acetaminophen or Tylenol overdose has become the most prevalent cause of acute liver failure in the United States (Larson et al., 2005). Overdose produces serious acute liver toxicity, leading to hepatocyte necrosis, acute liver failure, and even death. Acetaminophen (APAP) model is a widely used animal experimental model of drug-induced hepatic injury. Data from an examination by Hu and Colletti et al. on the c-kit and SCF expression of C57BL/6J mice, shows that c-kit mRNA increase begins at 6 h and peaks after 48 h of overdose APAP treated, while SCF mRNA increase begins at 6 h and peaks at 16 h post-administration. Treatment with exogenous SCF significantly reduces the mortality of mice in 750 mg/kg APAP model. These findings suggest that SCF/KIT's function in the APAP model might be mainly through increasing proliferation of hepatocyte and inhibiting hepatocyte apoptosis. Exogenous SCF activating c-kit and Akt, results in an increase in B cell lymphoma-2 (Bcl-2) protein and inhibiting hepatocyte apoptosis (Hu and Colletti, 2008; **Figure 2**). In contrast, inhibiting c-kit will increase the mortality of the lethal dose APAP-treated model (Nassar et al., 2009; Shaker, 2014). In summary, these results indicate that c-kit is an important molecule in liver recovery according to the APAP

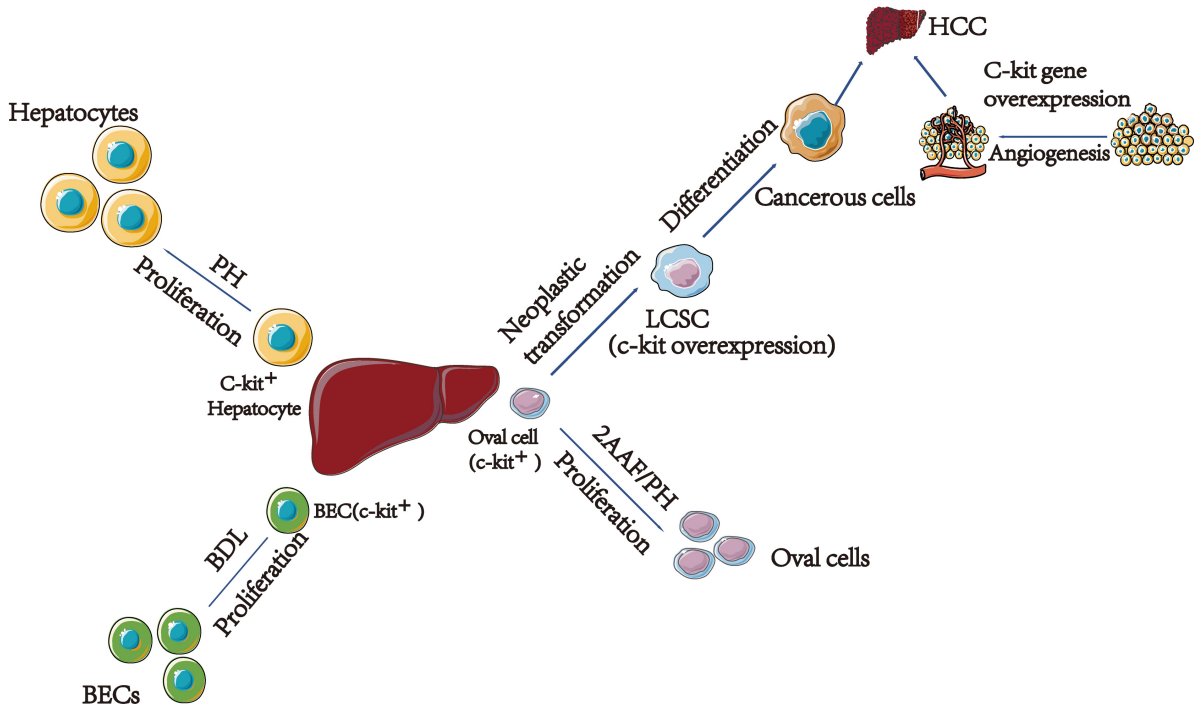

FIGURE 1 | The relationship between c-kit and different type of cells in liver regeneration and cancer. (1) C-kit express in 20% hepatocytes. After acute injury, solubilized SCF released and interact with c-kit, leading surrounding hepatocytes prolifer8ation. (2) In young rats after BDL, SCF bind to c-kit, leading to activation of the MAPK pathway; finally, BECs proliferation. (3) C-kit play a vital role in HCC. On the one hand, oval cells transformed to LCSCs are related with the c-kit gene overexpression. On the other hand, c-kit might associate with HCC by participating in angiogenesis. PH, Partial Hepatectomy; BEC, Bile Epithelial Cell; BDL, Bile Duct Ligation; 2AAF/PH, 2-Acetylaminofluorene/Partial Hepatectomy; LCSC, Liver Cancer Stem Cell; HCC, Hepatocellular Carcinoma.

model. Activation of the SCF/KIT system causes an increase in hepatocyte proliferation and a decrease in hepatocyte apoptosis.

Bile Epithelial Cells

Studies argue that the proliferation of BEC is associated with c-kit. A study by Fujio et al. (1996) reported that SCF and c-kit are co-expressed in BEC during the embryonic and adult stages of rat's liver. Elsewhere, Omori et al. demonstrated that BECs in young liver react differently with adult liver in the bile duct ligation (BDL) model. In the liver of a young rat with 5 weeks of age, there is an upregulation in the expression of SCF and c-kit after BDL is performed. But in the adult liver of rats after BDL, no upregulation of SCF and c-kit is observed. And the pattern of BECs in young liver response to bile stasis is similar to that of the early stage of oval cell activation (Omori et al., 1997). Evidence reported by Satake et al. show that both SCF and c-kit are up-regulated in BECs in young rats after BDL, SCF binds to c-kit, causing the activation of the Ras/Raf/mitogen-activated protein kinase (MAPK) pathway, hence the proliferation of bile epithelial cells (**Figure 2**). Nevertheless, in the adult rats, KIT-mediated signal transduction plays a mirror role due to the low expression of SCF/c-kit (Satake et al., 2003).

Oval Cells

Oval cells are the progenitor cells of the liver with c-kit as one of its markers (Crosby et al., 2001). Normally, after PH, mature hepatocytes proliferate causing liver regeneration. However, if PH is performed when the replicative ability of mature hepatocytes is impaired, there will occur proliferation and differentiation of oval cells (Thorgeirsson, 1996). PH integrated with 2-acetylaminofluorene (2-AAF)/PH is the model utilized to investigate the liver regeneration capability via oval cells. Further reports by Fujio et al. (1994) showed that in the embryonic and adult rats, both SCF and c-kit were expressed in oval cells. After 2-AAF/PH, the level of SCF transcripts increased within 12 h and reached a peak at day 4, the level of c-kit mRNA was upregulated from 12th hour to 11th day (Fujio et al., 1994). Additionally, Matsusaka et al. used Ws/Ws rats with 2-AAF/PH model to evaluate the role of SCF/KIT in the development of oval cells. Their results demonstrated that in at least one rat under the 2-AAF/PH model, KIT-mediated signal transduction activates the oval cells. However, in the proliferative activity and determining the phenotype of oval cells, the SCF/KIT signal transduction system plays a minor role (Matsusaka et al., 1999).

Circulating Progenitor Cells

Circulating endothelial progenitors (CEPs) originated from bone marrow with markers c-kit or CD133. By combining bone marrow transplant with 70% PH, the investigators concluded that CEPs contribute to liver regeneration by differentiating into liver vasculature, and exogenous VEGF accelerates liver regeneration by increasing the recruitment of CEPs in 70%

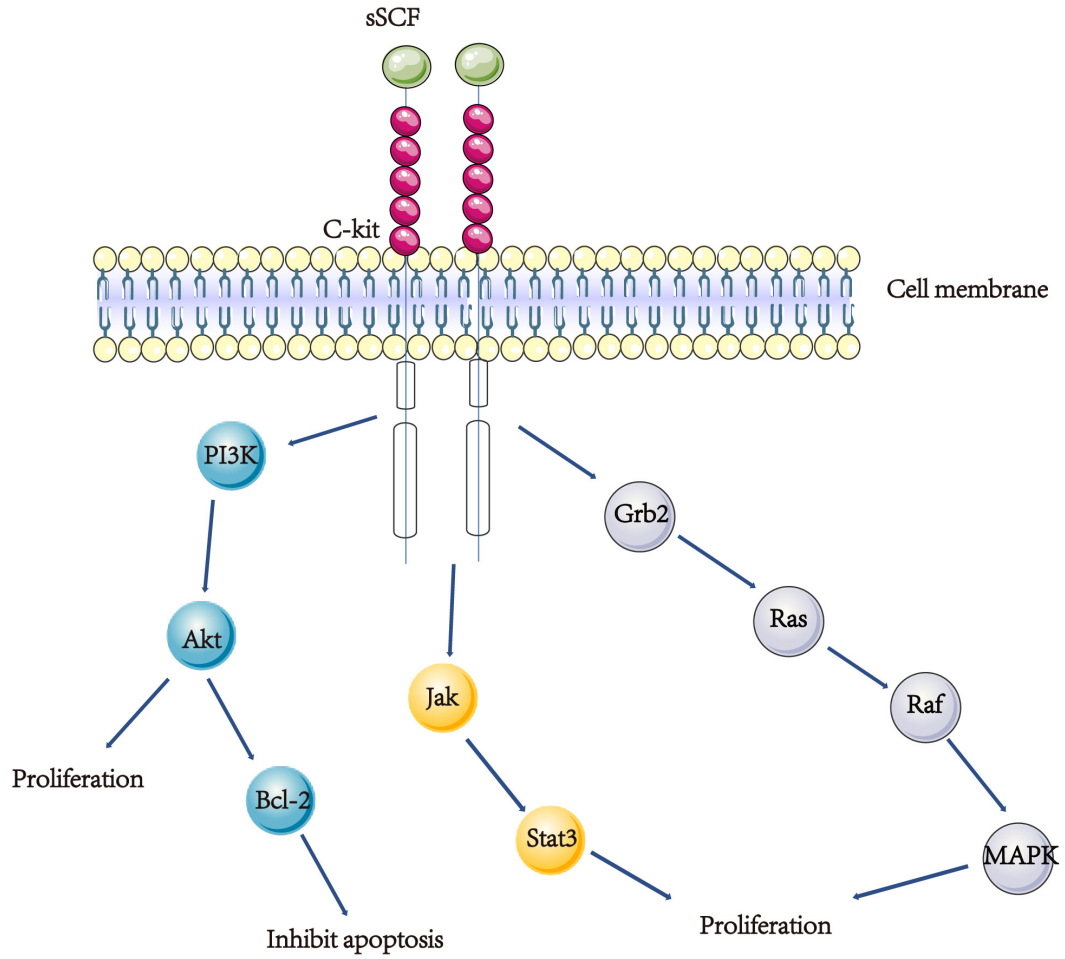

FIGURE 2 | A scheme showing the SCF/KIT signal transduction. (1) SCF/KIT function in the APAP model might be mainly through increasing proliferation of hepatocyte and inhibiting hepatocyte apoptosis. Exogenous SCF activating c-kit and Akt, results in an increase in Bcl-2 protein and inhibiting hepatocyte apoptosis. (2) IL-6 stimulates the production and release of SCF, then SCF interacts with c-kit in activating the stat3 signal pathway thereby inducing hepatocyte proliferation. (3) Both SCF and c-kit are up-regulated in BECs in young rats after BDL, SCF binds to c-kit, causing the activation of the Ras/Raf/MAPK pathway, hence the proliferation of bile epithelial cells.

PH model (Beaudry et al., 2007; **Figure 3A**). Moreover, a study by Si et al. found that there were relatively more $CD45^{+}Lin^{-}C\text{-}Kit^{+}$ HSCs/HPCs recruited in wide type (WT) liver than chemokine (C-C motif) receptor2 knock out ($CCR2^{-/-}$) after APAP-induced injury. More importantly, after administration with exogenous $CD45^{+}Lin^{-}C\text{-}Kit^{+}$ HSCs/HPCs, WT had greater resolution of APAP-induced injury than $CCR2^{-/-}$ mice, and these HSCs/HPCs express the macrophage M2 (repair phenotype) genes characteristic (Si et al., 2010; **Figure 3B**).

In summary, liver regeneration is a complex process, with multiple mechanisms and pathways, current literatures suggest that c-kit regulates liver regeneration. On the one hand, activation of the SCF/KIT signal transduction system leads to hepatocytes proliferation and apoptosis inhibition, BECs proliferation and oval cells activation. On the other hand, $c\text{-}kit^{+}$ progenitor cells contribute to liver regeneration by differentiating into liver vasculature or alternatively activated macrophages.

C-KIT AND LIVER DISEASES

C-kit is expressed on HSCs/HPCs and mast cells, and several liver diseases are relevant to c-kit. A strong relationship was observed between c-kit and primary liver cancer, besides, $c\text{-}kit^{+}$ mast cells also participate in fibrogenesis. This section extensively summarizes the relationship.

Primary Liver Cancer

Liver cancer is the fourth leading cause of cancer death among sexes combined globally (Bray et al., 2018). Evidence shows that liver stem/progenitor cells are the potential source of HCC, also called liver cancer stem cells (LCSCs) (Dumble et al., 2002; Fujii et al., 2008). It is believed that the liver stem cells transformed into LCSCs are linked with the overexpression of the c-kit gene (Chen et al., 2007; Yan et al., 2018). The SCF/c-kit signal transduction system participates in the activation and proliferation of oval cells. On the other hand, overexpression

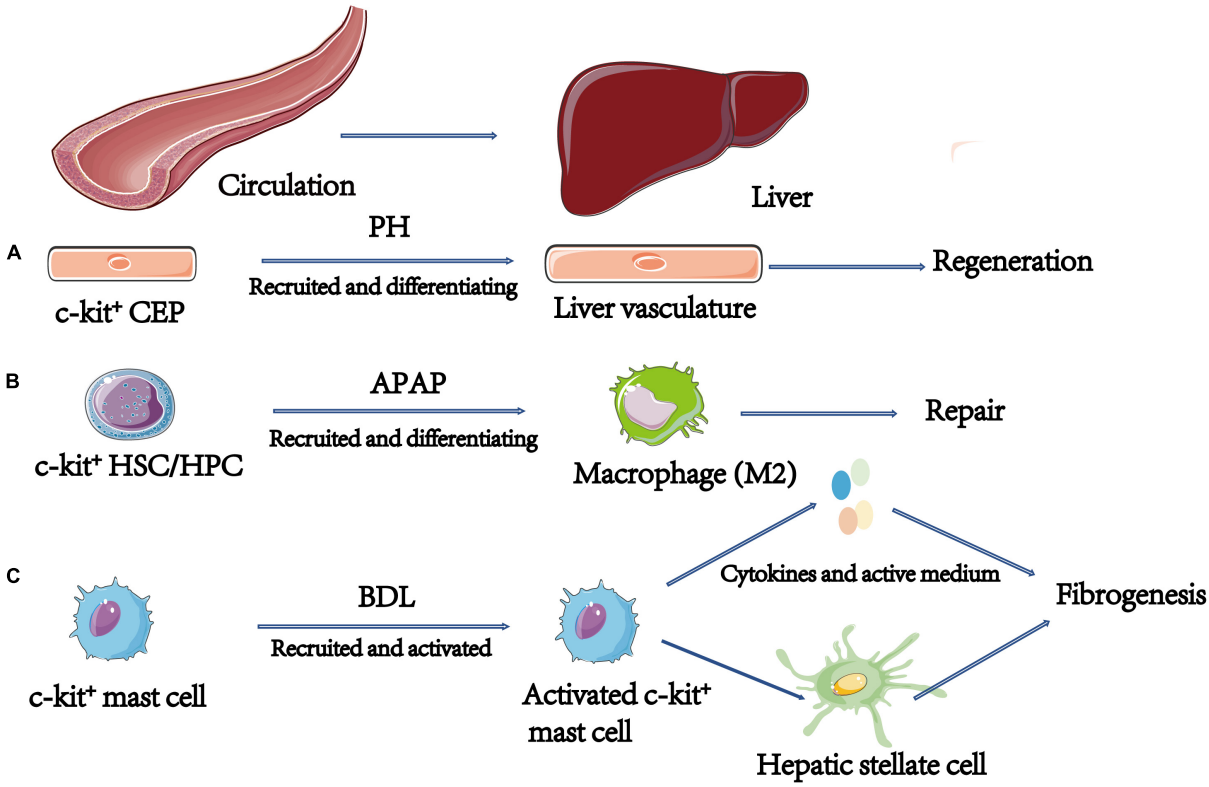

FIGURE 3 | The role of c-kit$^+$ circulating progenitor cells in liver diseases. **(A)** By combined bone marrow transplant with 70% PH, the investigators conclude that CEPs contribute to liver regeneration by differentiating into liver vasculature. **(B)** In APAP model, c-kit$^+$ HSCs/HPCs were recruited into liver and these HSCs/HPCs express the macrophage M2 (repair phenotype) genes characteristic. **(C)** Cholestatic/biliary diseases-associated fibrosis. Damaged BECs express and secrete SCF to recruit mast cells, then mast cells migrate to the damage area and contribute to fibrogenesis. C-kit$^+$ mast cells play a key role in fibrogenesis mainly through expressing fibrosis-associated factors including tryptase, b-FGF and TNF-α. HSCs/HPCs, Hematopoietic Stem/Progenitor Cells; CEPs, Circulating Endothelial Progenitors.

of c-kit is relevant with micro-vessel density, therefore, c-kit might be associated with HCC by participating in angiogenesis (Yan et al., 2018). Concerning the hepatitis B virus (HBV) or hepatitis C virus (HCV) induced HCC, c-kit is involved. PreS1 protein of HBV stimulates the appearance and self-renewal of LCSCs by activating the expression of c-kit and is confirmed in human hepatoma cells and HCC tissues (Liu et al., 2017). And in HCV infection patients, c-kit overexpression is observed (Kwon et al., 2015; Nazzal et al., 2020). Data shows that HCV core protein upregulates the expression of c-kit in hepatocytes, inducing the epithelial-mesenchymal transition, and extends the life span of cells (Kwon et al., 2015). Further, evidence recommends that liver stem/progenitor cells are the potential source of intrahepatic cholangiocarcinoma (ICC) and SCF/c-kit system might contribute to ICC by promoting cell proliferation and survival (Nomoto et al., 2006; Komuta et al., 2008; Mansuroglu et al., 2009b). Again, several lines of evidence attest that liver stem/progenitor cells are the potential source of HCC-ICC (Tanaka et al., 2005; Zhang et al., 2008). And the recent classification of digestive system tumor (5th edition) by the World Health Organization (WHO) also agrees with this concept. A different follow-up model indicates that the recurrence of HCC-ICC after hepatectomy is associated with the expression of c-kit in both tumor and non-tumor livers (Cai et al., 2012).

HCC is the most prevalent primary liver cancer, accounting for 85∼90% of primary liver cancers. However, the positive rate of HCC has not been precisely clarified. A research executed by Chung et al. (2005) examined the protein expression of c-kit in 86 human HCC specimens. The results demonstrated that among the 86 specimens, 22 (25.6%) were positive. According to an article published by Yan et al. (2018), the percentage of positive c-kit expression is 48.1% in 206 HCC cases. Nevertheless, Becker et al. (2007) collected 258 human HCC samples and c-kit immunohistochemistry was performed, results reported that only 6 (2.3%) samples were positive. There are many reasons attributed to these results among them, antibody specificity (Went et al., 2004), cellular heterogeneity, different stages of cell differentiation, etc. In summary, more cases need to be included and more detailed etiology should be classified. Epidemiological data shows that ICC accounts for 15% of primary liver cancer, second to the HCC (Shaib et al., 2005). Clinicopathological study on c-kit positive immunohistochemistry staining of human ICC sample (1/32), suggesting that ICC originates from hepatic stem cell (Liu et al., 2004). Certainly, only one c-kit positive

among 32 samples could not clarify the origin of ICC, implying that other mechanisms might also exist. Therefore, more cases need to be collected in future studies before a single-cell RNA sequence can be performed, this might solve the problem of origin. A study by Xu et al. (2018) showed that NCAM$^+$ c-kit$^+$ subset cells in RBE cell lines might have properties of hepatic progenitor cells. And NCAM combined with c-Kit might be a valuable marker for isolating and purifying ICC stem/progenitor cells. Therefore, c-kit can be a candidate marker of ICC stem/progenitor cells used in single cell RNA sequence in the future. HCC-ICC is a rare subtype of primary liver cancer with poor prognosis, comprising <1% of all liver carcinomas, and epidemiological data shows it accounts for 1.6–6.5% of surgically resected primary liver cancer (Koh et al., 2005; Yu et al., 2011; Akiba et al., 2013). Unlike the low c-kit positive rate of HCC, the presence of the c-kit in HCC-ICC is 71.4% (10/14), which might explain the poor prognosis of HCC-ICC (Yu et al., 2011).

In addition, it is reported that there is positive feedback in transforming growth factor β (TGF-β) and c-kit, which induce carcinogenesis in HepG2 cells. TGF-β activated SMAD2 transcriptionally induces SCF expression, SCF expression and secretion result in stimulation of the c-kit receptor, followed by activation of JAK1/STAT3 signaling. p^{Tyr705}STAT3 trans-locates to the nucleus where it binds directly to the TGF-β ligand gene, positively regulating its expression. Following activation of secreted TGF-β precursor, it can activate the TGF-β receptor. Disruption of the TGF-β/KIT signaling loop on the level of the SCF/STAT3 axis restores TGF-β tumor suppressor function by inhibition of epithelial-mesenchymal transition (EMT), tumor cell migration, and invasion, and restoration of its cell cycle inhibitory functions (Rojas et al., 2016). Besides, a recent study showed that in HCV-infected patients, their c-kit gene mutation in exons 9 but not 11, are often bound up with high-viremia HCV. And these patients might be resistant to TGF-β, thus promoting the development of HCC (El-Houseini et al., 2019). These studies indicate that TGF-β/KIT signaling plays an important role in the development of HCC and is a key target for the prevention and treatment of HCC.

Hepatic Fibrosis

Hepatic fibrosis is a wound healing process involving multiple cell types. There are many causes of liver fibrosis, including viral, alcoholic, cholestasis, etc. The role of c-kit in liver fibrosis is quite complex. Mast cells increase in liver fibrosis, but decrease in other chronic liver diseases, suggesting that mast cells take part in fibrogenesis particularly in cholestatic/biliary diseases (Weiskirchen et al., 2019).

Cholestatic/Biliary Diseases-Associated Fibrosis

Most of hematopoietic cells lose expression of c-kit when they mature, except mast cells and dendritic cells. Mast cells are derived from the bone marrow, and they act as immature progenitors in circulation. In the liver, mast cells are primarily located in the periportal area. Primary sclerosing cholangitis (PSC) or primary biliary cirrhosis is an autoimmune disease characterized by infiltration of mast cell (Nakamura et al., 1997; Ishii et al., 2005). In contrast, there is no significant increase in acute viral or drug-induced hepatitis (Yamashiro et al., 1998).

PSC is a disease characterized by infiltration of mast cell, biliary damage, and liver fibrosis. SCF/KIT signaling plays a critical role in the development of mast cell, survival and homing. Animal models have shown that inhibiting the c-kit system releases allergic reactions in the lungs (Berlin et al., 2004). In the liver, data suggests that c-kit$^+$ mast cells play a key role in fibrogenesis from the early stage of PSC (Ishii et al., 2005; Meadows et al., 2019). First, damaged BECs express and secrete SCF to recruit mast cells. Secondly, mast cells migrate to the damaged area and cause fibrogenesis. Therefore, c-kit$^+$ mast cells contribute to fibrogenesis primarily through expressing fibrosis-associated factors including tryptase, basic fibroblast growth factor (b-FGF), and TNF-α (Kanbe et al., 2000; Gaca et al., 2002; **Figure 3C**). BDL-induced biliary hyperplasia, hepatic injury, and fibrosis are reduced in Kit^{W-sh} mice, which are mast cell deficient (Hargrove et al., 2017). As for ameliorating progression of PSC, targeting mast cell infiltration might be an efficient option. Furthermore, in systemic mastocytosis, mastocytosis-derived extracellular vesicles transfer c-kit to liver stellate cells, causing activation, proliferation, cytokine production, and differentiation of liver stellate cells (Kim et al., 2018). This might be an alternative mechanism of c-kit$^+$ mast cells-induced fibrogenesis.

Additionally, mast cells take part in the progress of biliary atresia (BA). It is reported that the increased mast cells adversely affects liver function, perhaps through type I allergic reaction (Uddin Ahmed et al., 2000). However, there is no specific study about the SCF/c-kit system and BA. Given the relationship between mast cells and BA, SCF/c-kit system should be considered.

Other Chronic Liver Diseases-Associated Fibrosis

The number of mast cells in other chronic liver diseases-associated fibrosis is increased, and the intensity of c-kit immunostaining is slightly higher in cirrhotic non-tumorous liver than in non-cirrhotic non-tumorous liver, but the relationship between c-kit and fibrosis has not been extensively evaluated (Mansuroglu et al., 2009a). C-kit expressed in fibroblasts and SCF/c-kit plays a vital role in scar pathogenesis, thus we can use a c-kit selective inhibitor to block it (Mukhopadhyay et al., 2011).

In summary, the role of c-kit in liver fibrosis is obscure. In cholestatic/biliary diseases-associated fibrosis, c-kit$^+$ mast cells regulate fibrogenesis. However, in other chronic liver diseases-associated fibrosis, despite the increase of mast cells, the relationship between c-kit and fibrosis is largely understudied. Therefore, further studies are necessary to elaborate on the relationship between c-kit and hepatic fibrosis.

Other Liver Diseases

The roles of c-kit$^+$ cells in chronic hepatitis B and C have been described in HCC (Kara et al., 2008; Kwon et al., 2015; Liu et al., 2017; Nazzal et al., 2020). Also, it is reported that there is an increase of mast cells in alcoholic hepatitis, but reports on the

relationship between c-kit and alcoholic hepatitis are insufficient (Farrell et al., 1995). Alcoholic hepatitis impairs intestinal barrier and activate the mast cell causing fibrogenesis (Ferrier et al., 2006). Besides, a study by Hisada et al. (2017) mentioned that the percentage of c-kit$^+$ cells was dramatically decreased in alcohol-fed rats compared to non-alcohol-fed rats. These findings indicate that BMSCs might be damaged by the consumption of alcohol. Nonetheless, the relationship between c-kit$^+$ cells and alcohol has not been fully elucidated, hence this represents an important topic for future research.

In summary, c-kit is relevant to primary liver cancer. It is believed that liver stem cells transformed into LCSCs are linked with the overexpression of the c-kit gene, causing liver cancer. Besides, c-kit$^+$ mast cells participate in fibrogenesis particularly in cholestatic/biliary diseases. C-kit$^+$ mast cells contribute to fibrogenesis primarily through expressing fibrosis-associated factors.

CLINICAL IMPLICATIONS OF C-KIT IN LIVER

The Role of C-Kit in Diagnosis and Prognosis

Few reports are suggested that c-kit can be used as a diagnostic factor in liver diseases. For instance, Kara et al. (2008) recommended that c-kit can be used as an early diagnostic factor for HBV-related HCC. However, it is unclear whether c-kit can be used as an indicator in HCC caused by other factors. Furthermore, it is reported that c-kit$^+$ mast cells increase after liver allograft rejection (El-Refaie and Burt, 2005), but the increased c-kit$^+$ mast cells cannot distinguish rejection from recurrent HCV infection in transplantation of liver (Doria et al., 2006). Seemingly, c-kit is a good prognostic parameter in several diseases. First, one article has mentioned that c-kit can be used as a prognostic factor for HCC (Chung et al., 2005). Moreover, Yan et al. suggested that c-kit is an independent prognostic indicator for HBV-related HCC patients. In addition, Kaplan–Meier survival analysis shows that the c-kit expression was linked to poor disease-free survival (DFS) ($P < 0.001$) in HBV-related HCC patients (Yan et al., 2018). Besides, in a cohort of 70 HCC-ICC patients who underwent resection for treatment, overall survival (OS) and DFS were associated with expression of c-kit in both tumor and non-tumor livers (Cai et al., 2012). Secondly, the increased number of c-kit$^+$ mast cells in chronic HCV patients might be used as an indicator of liver fibrosis (Koruk et al., 2011). Thirdly, it is reported that the number of mast cells adversely affects liver function in biliary atresia, but the authors did not stain mast cells with c-kit. Therefore, more patients should be enrolled when conducting c-kit$^+$ mast cell statistics (Uddin Ahmed et al., 2000). Finally, due to the role of c-kit$^+$ mast cells in fibrogenesis among PSC patients and animal models, the number of c-kit$^+$ mast cells might reflect the prognosis of PSC patients (Ishii et al., 2005; Meadows et al., 2019). However, only 4 samples were observed, therefore more clinical data need to be counted.

The Role of C-Kit$^+$ Cell in Stem Cell Therapy

Oval cell transplantation after liver transplantation might be useful for liver regeneration. A study by Li et al. (2013) isolated oval cells, of which 99.8% were positive for c-kit. After primary culture, oval cells were injected into the rats who underwent liver transplantation. Data shows that compared to controls, oval cell transplantation significantly improved the liver function, prolonged median survival time and reduced acute allograft rejection (Li et al., 2013).

BMSCs are closely related to liver fibrosis. In carbon tetrachloride (CCl4)-induced liver fibrosis mice, the differentiation potential of circulation of endothelial progenitor cells (EPCs) is attenuated due to the impairment of the endothelial lineage differentiation potential of bone marrow-C-kit$^+$, Sca-1$^+$, and Lin$^-$(BM-KSL) cells (Shirakura et al., 2011). Transplantation of HSCs has been reported to be effective in mice. Some authors proved that CCl4 treated liver fibrosis mice administered with the HSCs (Lin$^-$Sca-1$^+$c-kit$^+$) had less fibrosis and better liver function compared with the group not inject (Cho et al., 2011). Moreover, King et al. arrived at the same conclusion and pointed out that HSCs (Lin$^-$Sca-1$^+$c-kit$^+$) participate in anti-fibrotic by promoting the recruitment of endogenous macrophages and neutrophils. And the retention of HSCs can be increased by reducing sphingosine-1-phosphate (S1P) signaling to antifibrosis (King et al., 2017). Furthermore, it has been reported that in CCl4-induced liver injury, transplantation of very small embryonic-like stem cells (VSELs), which express c-kit, directly into the liver can significantly lower the levels of serum alanine aminotransferase (ALT) and aspartate aminotransferase (AST) (Chen et al., 2015). Transplantation of BMSCs has been reported to be effective in humans. Research by Terai et al. reported 9 patients with liver cirrhosis that received the therapy of autologous bone marrow cell infusion (ABMI). The cell characteristics were confirmed by fluorescence-activated cell sorting analysis (CD34$^+$, CD45$^+$, c-kit$^+$). And after infusing, significantly improved serum albumin levels and total protein were witnessed. Besides, significant improvements in Child-Pugh scores were observed (Terai et al., 2006; **Figure 4**).

By and large, we can speculate that c-kit$^+$ oval cell transplantation might be useful in therapeutic liver regeneration after orthotopic liver transplantation. And c-kit$^+$ BMSCs or HSCs transplantation is a promising treatment of patients with liver cirrhosis. Nevertheless, considering the role of c-kit in liver cancer, further studies are essential to evaluate the relationship between c-kit$^+$ cell, hepatic fibrosis, and liver cancer. Additionally, we summarized the clinical implications of c-kit in liver (**Table 1**).

Targeted Inhibition of C-Kit in Liver Diseases

Besides its implication in prognosis and stem cell therapy, overexpression of c-kit in liver primary cancer has potential therapeutic implications because it can inhibit the kinase activity of c-kit. Imatinib mesylate (STI-571 or Gleevecs) is a relatively selective tyrosine inhibitor of BCR-ABL, PDGF-R, and c-kit,

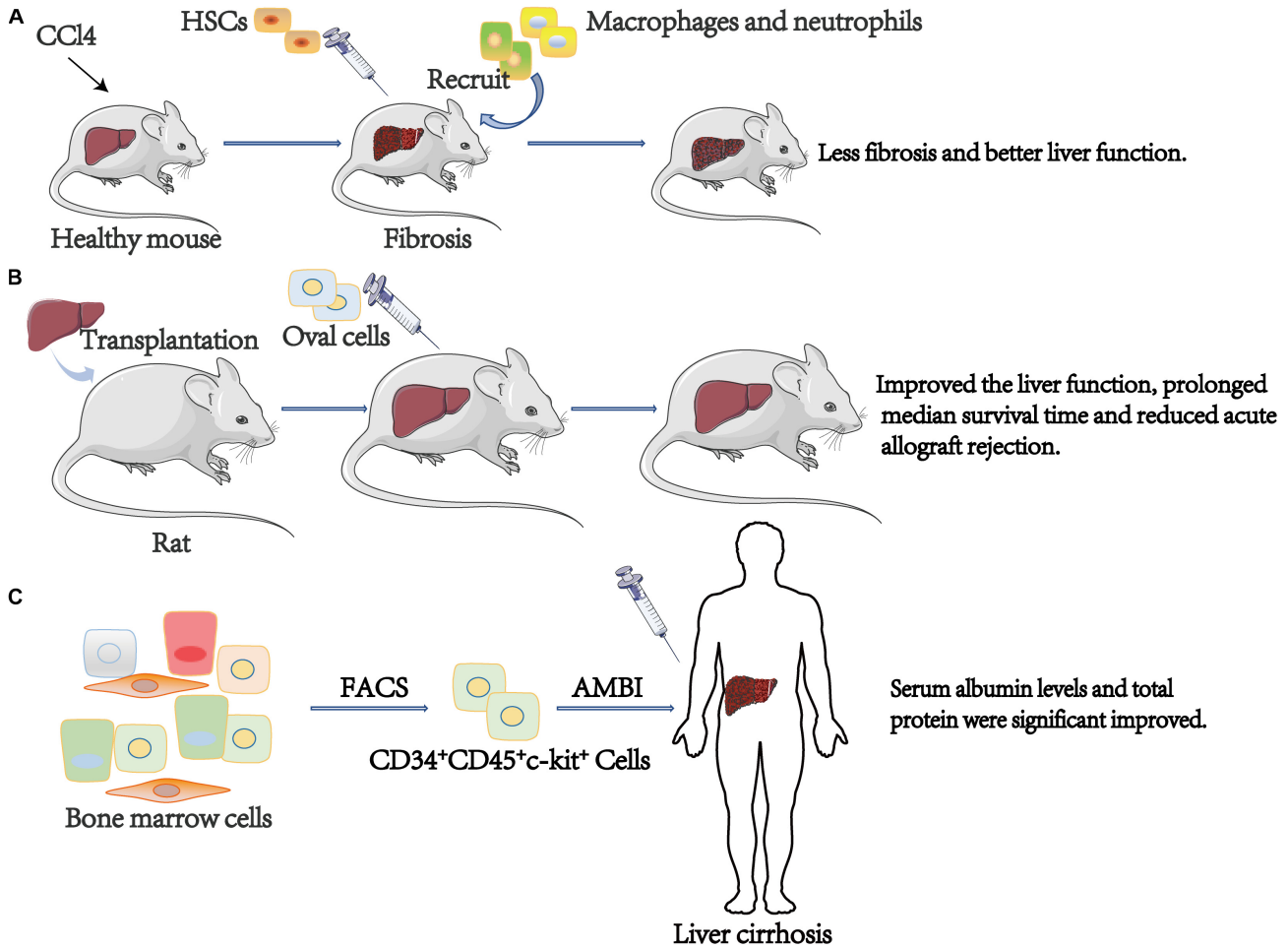

FIGURE 4 | The role of c-kit$^+$ cell in stem cell therapy. **(A)** CCl4 treated liver fibrosis mice administered with the HSCs (Lin$^-$Sca-1$^+$c-kit$^+$) had less fibrosis and better liver function compared with the group not inject. **(B)** Compare to controls, oval cells transplantation significantly improved the liver function, prolonged median survival time and reduced acute allograft rejection. **(C)** After infusing, significantly improved serum albumin levels and total protein were observed. ABMI, Autologous Bone Marrow cell Infusion.

which is usually used in the treatment of chronic myelocytic leukemia (CML) and GIST. Animal experiments point out that imatinib treatment can inhibit c-kit-expressing liver progenitor cells proliferation and early fibrosis induced by short-term choline-deficient, ethionine-supplemented (CDE) diet. In the long run, imatinib treatment can reduce the degree of fibrosis and significantly inhibit the formation of tumor (Knight et al., 2008). Furthermore, Nazzal et al. recently showed that HCC-patient-derived xenograft (PDX) tumors respond well following imatinib treatment. Treatment of HCC-PDX xenograft tumor-bearing mice with imatinib significantly reduced tumor growth and c-kit downstream molecules expression (Nazzal et al., 2020). In clinical, Becker et al. (2007) discovered that the positive rate of c-kit is 2.3% and that there was no role for imatinib. Similarly, in a clinical phase II trial of imatinib, Eckel et al. (2005) found no positive case for c-kit among 15 HCC patients, and imatinib showed no therapeutic effect. Another phase II study of imatinib in unresectable HCC concluded that imatinib is unsuitable as a monotherapy in the treatment of unresectable HCC (Lin et al., 2008). Interestingly, Ramadori et al. (2004) effectively treated one HCC patient with imatinib. Sorafenib is a multi-kinase inhibitor that is broadly applied in unresectable HCC as a first-line treatment. C-kit is among the molecular targets of sorafenib. In one case report, a patient diagnosed with HCC-ICC and highly c-kit positive, responded to sorafenib (Seino et al., 2014). As we know, sorafenib targets c-kit, and the high concentration of soluble c-kit group has a greater response to sorafenib than the low concentration group (Llovet et al., 2012). Since primary liver tumors are regulated by multiple signaling pathways, imatinib is hardly used in patients with HCC. But going by the results of sorafenib and imatinib, the c-kit pathway should be of concern. Additionally, we summarized c-kit signal involved drugs and clinical trials in unresectable hepatocellular carcinoma(uHCC)(**Table 2**).

On the other hand, due to the role of c-kit$^+$ mast cells in cholestatic/biliary diseases-associated fibrosis, c-kit

receptor tyrosine inhibitor can be used to prevent fibrosis. It is reported that a c-kit/PDGF receptor tyrosine kinase inhibitor-masitinib, plays an effective role in the treatment of corticosteroid-dependent asthma by inhibiting c-kit$^+$ mast cells (Humbert et al., 2009). However, to validate these findings, further *in vitro* and *in vivo* experiments are essential.

SUMMARY AND FUTURE PERSPECTIVES

The role of c-kit in the liver is conflicting, it is a two-edged sword in liver regeneration and diseases. First, as a liver stem cell marker, c-kit$^+$ cells, such as oval cells, BECs, and part of

TABLE 1 | Clinical implications of c-kit in liver.

Clinical implications				References
Diagnosis/ prognosis	**Conclusions**			
	C-kit can be used as an early diagnostic factor for HBV-related HCC.			Kara et al., 2008
	C-kit$^+$ mast cells increase after liver allograft rejection, but the increased c-kit$^+$ mast cells cannot distinguish rejection from recurrent HCV infection in transplantation of liver.			El-Refaie and Burt, 2005; Doria et al., 2006
	C-kit can be used as a prognostic factor for HCC. Moreover, c-kit is an independent prognostic indicator for HBV-related HCC patients.			Chung et al., 2005; Cai et al., 2012; Yan et al., 2018
	The increased number of c-kit$^+$ mast cells in chronic HCV patients might be used as an indicator of liver fibrosis.			Koruk et al., 2011
	The number of c-kit$^+$ mast cells might reflect the prognosis of PSC patients.			Ishii et al., 2005; Meadows et al., 2019
Treatment	**Species/model**	**Stem cell therapy**	**Results**	
	Rats/underwent liver transplantation	Oval cells (99.8% c-kit$^+$)	Significantly improved the liver function, prolonged median survival time and reduced acute allograft rejection	Li et al., 2013
	Mice/CCl4 induced liver fibrosis	HSCs (Lin$^-$Sca-1$^+$c-kit$^+$)	Less fibrosis and better liver function compared with the group not inject	Cho et al., 2011
	Mice/CCl4 induced liver fibrosis	HSCs (Lin$^-$Sca-1$^+$c-kit$^+$)	Participate in anti-fibrotic by promoting the recruitment of endogenous macrophages and neutrophils.	King et al., 2017
	Mice/CCl4-induced liver injured	VSELs (Lin$^-$Sca-1$^+$c-kit$^+$CD45$^-$)	Lower the levels of ALT and AST	Chen et al., 2015
	Humans/Liver cirrhosis	Bone marrow cell (CD34$^+$, CD45$^+$, c-kit$^+$)	Significantly improved serum albumin levels and total protein	Terai et al., 2006

TABLE 2 | C-kit signal involved drugs and clinical trials in unresectable hepatocellular carcinoma.

Drug	Targets	Trial for uHCC		References
		Status	**Phase**	
Sorafenib	VEGFR1-3, PDGFR-β, c-KIT, RET, FLT-3, RAF	First-line treatment		Llovet et al., 2008; Cheng et al., 2009; Pressiani et al., 2013
Lenvatinib	VEGFR1-3, FGFR1-4, c-kit, RET, PDGF-β	First-line treatment		Kudo et al., 2018
Regorafenib	VEGFR1-3, c-Kit, TIE-2, PDGFR-β, FGFR-1, RAF-1, BRAF, p38	Second-line treatment		Bruix et al., 2017
Anlotinib	VEGFR2/3, FGFR1-4, PDGFRα/β, c-kit, Ret	Ongoing	II	Clinicaltrials.gov
Sunitinib	PDGFR, VEGFR1-2, c-kit, FLT3, RET	Unsuccessful	II	Faivre et al., 2009
Dovitinib	FGFR1&3, VEGFR1-3, PDGFR-β, c-kit	Unsuccessful	II	Cheng et al., 2016
Axitinib	VEGFR1-3, c-kit, PDGFR	Unsuccessful	II	Kang et al., 2015
Imatinib	Bcr-Abl, PDGFR, c-kit	Unsuccessful	II	Lin et al., 2008

hepatocytes are closely linked to liver regeneration. And c-kit signaling participates in cell proliferation, migration, and survival based on different types of cells. At the final stage of chronic liver cirrhosis, liver transplantation is the most effective treatment. But there are many challenges such as limited donors, surgical complications, etc. And c-kit$^+$ BMSCs or HSCs transplantation is a potential treatment of patients in the final stage of chronic liver cirrhosis. Nevertheless, further research is crucial to explore the relationship between c-kit$^+$ cell, hepatic fibrosis, and liver cancer. Secondly, mast cells express c-kit, and damaged BECs express and secrete SCF to recruit c-kit$^+$ mast cells, resulting in fibrogenesis. Eventually, c-kit also is a proto-oncogene, and its overexpression is associated with primary liver cancer. Sorafenib, a multi-kinase inhibitor with c-kit included, is used as a first-line treatment for HCC. Since primary liver tumors are regulated by multiple signaling pathways, imatinib is hardly used in patients with HCC. But going by the results of sorafenib and imatinib, the c-kit pathway should be of concern.

Conventional research methods cannot reveal the dynamic process of stem cell differentiation *in vivo*, but genetic lineage tracing can address this challenge. Previously, we used Kit-CreERxRosa26-RFP mouse to trace the role of c-kit$^+$ stem/progenitor cells in vascular injury-induced neointimal lesions, and found that c-kit$^+$ cells are majorly converted to immune-inflammatory cells during neointima formation (Chen et al., 2018). Another laboratory utilized Kit$^{MerCreMer/+}$x Rosa26-eGFP lineage-tracing mouse to examine endothelial cell formation in the heart (Vagnozzi et al., 2020). Furthermore, several laboratories used single-cell RNA sequences to reveal the cell heterogeneity of the liver, including all liver cells, immune cells, and cancer stem cells (Zheng et al., 2018; Aizarani et al., 2019; Zhang et al., 2019). Recently, lineage-tracing combine RNA sequence analysis has revealed the mechanisms of endothelial repair by progenitors (Deng et al., 2020). In future research, this technology can be adopted in the liver to expose the role of c-kit$^+$ cells in various liver diseases.

AUTHOR CONTRIBUTIONS

WW wrote the manuscript and prepared figures. MZ, YL, and LS provided the expert comments and edited the manuscript. All authors reviewed the manuscript.

FUNDING

This work was supported by the State S&T Project of 13th Five Year (No. 2018ZX10302206), the National Natural Science Foundation of China (No. 81871646), and the Key R&D Projects of Zhejiang Province (2018C03019).

REFERENCES

Aizarani, N., Saviano, A., Sagar, M. L., Durand, S., and Herman, J. S. (2019). A human liver cell atlas reveals heterogeneity and epithelial progenitors. *Nature* 572, 199–204. doi: 10.1038/s41586-019-1373-2

Akiba, J., Nakashima, O., Hattori, S., Tanikawa, K., Takenaka, M., Nakayama, M., et al. (2013). Clinicopathologic analysis of combined hepatocellular-cholangiocarcinoma according to the latest WHO classification. *Am. J. Surg. Pathol.* 37, 496–505. doi: 10.1097/PAS.0b013e31827332b0

Baumann, U., Crosby, H. A., Ramani, P., Kelly, D. A., and Strain, A. J. (1999). Expression of the stem cell factor receptor c-kit in normal and diseased pediatric liver: identification of a human hepatic progenitor cell? *Hepatology* 30, 112–117. doi: 10.1002/hep.510300140

Beaudry, P., Hida, Y., Udagawa, T., Alwayn, I. P., Greene, A. K., Arsenault, D., et al. (2007). Endothelial progenitor cells contribute to accelerated liver regeneration. *J. Pediatr. Surg.* 42, 1190–1198. doi: 10.1016/j.jpedsurg.2007.02.034

Becker, G., Schmitt-Graeff, A., Ertelt, V., Blum, H. E., and Allgaier, H. P. (2007). CD117 (c-kit) expression in human hepatocellular carcinoma. *Clin. Oncol.* 19, 204–208. doi: 10.1016/j.clon.2006.12.009

Berlin, A. A., Lincoln, P., Tomkinson, A., and Lukacs, N. W. (2004). Inhibition of stem cell factor reduces pulmonary cytokine levels during allergic airway responses. *Clin. Exp. Immunol.* 136, 15–20. doi: 10.1111/j.1365-2249.2004.02404.x

Besmer, P., Manova, K., Duttlinger, R., Huang, E. J., Packer, A., Gyssler, C., et al. (1993). The kit-ligand (steel factor) and its receptor c-kit/W: pleiotropic roles in gametogenesis and melanogenesis. *Dev. Suppl.* 119, 125–137.

Bray, F., Ferlay, J., Soerjomataram, I., Siegel, R. L., Torre, L. A., and Jemal, A. (2018). Global cancer statistics 2018: GLOBOCAN estimates of incidence and mortality worldwide for 36 cancers in 185 countries. *CA Cancer J. Clin.* 68, 394–424. doi: 10.3322/caac.21492

Bruix, J., Qin, S., Merle, P., Granito, A., Huang, Y. H., Bodoky, G., et al. (2017). Regorafenib for patients with hepatocellular carcinoma who progressed on sorafenib treatment (RESORCE): a randomised, double-blind, placebo-controlled, phase 3 trial. *Lancet* 389, 56–66. doi: 10.1016/S0140-6736(16)32453-9

Cai, X., Zhai, J., Kaplan, D. E., Zhang, Y., Zhou, L., Chen, X., et al. (2012). Background progenitor activation is associated with recurrence after hepatectomy of combined hepatocellular-cholangiocarcinoma. *Hepatology* 56, 1804–1816. doi: 10.1002/hep.25874

Chen, L., Shen, R., Ye, Y., Pu, X. A., Liu, X., Duan, W., et al. (2007). Precancerous stem cells have the potential for both benign and malignant differentiation. *PLoS One* 2:e293. doi: 10.1371/journal.pone.0000293

Chen, Q., Yang, M., Wu, H., Zhou, J., Wang, W., Zhang, H., et al. (2018). Genetic lineage tracing analysis of c-kit(+) stem/progenitor cells revealed a contribution to vascular injury-induced neointimal lesions. *J. Mol. Cell Cardiol.* 121, 277–286. doi: 10.1016/j.yjmcc.2018.07.252

Chen, Z. H., Lv, X., Dai, H., Liu, C., Lou, D., Chen, R., et al. (2015). Hepatic regenerative potential of mouse bone marrow very small embryonic-like stem cells. *J. Cell Physiol.* 230, 1852–1861. doi: 10.1002/jcp.24913

Cheng, A. L., Kang, Y. K., Chen, Z., Tsao, C. J., Qin, S., Kim, J. S., et al. (2009). Efficacy and safety of sorafenib in patients in the Asia-Pacific region with advanced hepatocellular carcinoma: a phase III randomised, double-blind, placebo-controlled trial. *Lancet Oncol.* 10, 25–34. doi: 10.1016/S1470-2045(08)70285-7

Cheng, A. L., Thongprasert, S., Lim, H. Y., Sukeepaisarnjaroen, W., Yang, T. S., Wu, C. C., et al. (2016). Randomized, open-label phase 2 study comparing frontline dovitinib versus sorafenib in patients with advanced hepatocellular carcinoma. *Hepatology* 64, 774–784. doi: 10.1002/hep.28600

Cho, K. A., Lim, G. W., Joo, S. Y., Woo, S. Y., Seoh, J. Y., Cho, S. J., et al. (2011). Transplantation of bone marrow cells reduces CCl4 -induced liver fibrosis in mice. *Liver Int.* 31, 932–939. doi: 10.1111/j.1478-3231.2010.02364.x

Chung, C. Y., Yeh, K. T., Hsu, N. C., Chang, J. H., Lin, J. T., Horng, H. C., et al. (2005). Expression of c-kit protooncogene in human hepatocellular carcinoma. *Cancer Lett.* 217, 231–236. doi: 10.1016/j.canlet.2004.06.045

Crosby, H. A., Kelly, D. A., and Strain, A. J. (2001). Human hepatic stem-like cells isolated using c-kit or CD34 can differentiate into biliary epithelium. *Gastroenterology* 120, 534–544. doi: 10.1053/gast.2001.21175

Deng, J., Ni, Z., Gu, W., Chen, Q., Nowak, W. N., Chen, T., et al. (2020). Single-cell gene profiling and lineage tracing analyses revealed novel mechanisms

of endothelial repair by progenitors. *Cell Mol. Life Sci.* 77, 5299–5320. doi: 10.1007/s00018-020-03480-4

Doria, C., di Francesco, F., Marino, I. R., Ramirez, C. B., Frank, A., Iaria, M., et al. (2006). c-Kit-positive mast cells in portal tracts cannot be used to distinguish acute cellular rejection from recurrent hepatitis C infection in liver allografts. *Transpl. Proc.* 38, 3597–3600. doi: 10.1016/j.transproceed.2006.10.175

Dumble, M. L., Croager, E. J., Yeoh, G. C., and Quail, E. A. (2002). Generation and characterization of p53 null transformed hepatic progenitor cells: oval cells give rise to hepatocellular carcinoma. *Carcinogenesis* 23, 435–445. doi: 10.1093/carcin/23.3.435

Eckel, F., von Delius, S., Mayr, M., Dobritz, M., Fend, F., Hosius, C., et al. (2005). Pharmacokinetic and clinical phase II trial of imatinib in patients with impaired liver function and advanced hepatocellular carcinoma. *Oncology* 69, 363–371. doi: 10.1159/000089990

El-Houseini, M. E., Ismail, A., Abdelaal, A. A., El-Habashy, A. H., Abdallah, Z. F., Mohamed, M. Z., et al. (2019). Role of TGF-beta1 and C-Kit mutations in the development of Hepatocellular carcinoma in hepatitis C virus-infected patients: in vitro study. *Biochemistry* 84, 941–953. doi: 10.1134/S0006297919080108

El-Refaie, A. M., and Burt, A. D. (2005). Mast cells and c-Kit expression in liver allograft rejection. *Histopathology* 47, 375–381. doi: 10.1111/j.1365-2559.2005.02239.x

Faivre, S., Raymond, E., Boucher, E., Douillard, J., Lim, H. Y., Kim, J. S., et al. (2009). Safety and efficacy of sunitinib in patients with advanced hepatocellular carcinoma: an open-label, multicentre, phase II study. *Lancet Oncol.* 10, 794–800. doi: 10.1016/S1470-2045(09)70171-8

Fang, C. H., Gong, J. Q., and Zhang, W. (2004). Function of oval cells in hepatocellular carcinoma in rats. *World J. Gastroenterol.* 10, 2482–2487. doi: 10.3748/wjg.v10.i17.2482

Farrell, D. J., Hines, J. E., Walls, A. F., Kelly, P. J., Bennett, M. K., and Burt, A. D. (1995). Intrahepatic mast-cells in chronic liver-diseases. *Hepatology* 22, 1175–1181. doi: 10.1002/hep.1840220425

Ferrier, L., Berard, F., Debrauwer, L., Chabo, C., Langella, P., Bueno, L., et al. (2006). Impairment of the intestinal barrier by ethanol involves enteric microflora and mast cell activation in rodents. *Am. J. Pathol.* 168, 1148–1154. doi: 10.2353/ajpath.2006.050617

Fu, S., Wang, F., Cao, Y., Huang, Q., Xiao, J., Yang, C., et al. (2015). Telocytes in human liver fibrosis. *J. Cell Mol. Med.* 19, 676–683. doi: 10.1111/jcmm.12542

Fujii, T., Zen, Y., Harada, K., Niwa, H., Masuda, S., Kaizaki, Y., et al. (2008). Participation of liver cancer stem/progenitor cells in tumorigenesis of scirrhous hepatocellular carcinoma–human and cell culture study. *Hum. Pathol.* 39, 1185–1196. doi: 10.1016/j.humpath.2007.12.010

Fujio, K., Evarts, R. P., Hu, Z., Marsden, E. R., and Thorgeirsson, S. S. (1994). Expression of stem cell factor and its receptor, c-kit, during liver regeneration from putative stem cells in adult rat. *Lab. Invest.* 70, 511–516.

Fujio, K., Hu, Z., Evarts, R. P., Marsden, E. R., Niu, C. H., and Thorgeirsson, S. S. (1996). Coexpression of stem cell factor and c-kit in embryonic and adult liver. *Exp. Cell Res.* 224, 243–250. doi: 10.1006/excr.1996.0134

Gaca, M. D., Zhou, X., and Benyon, R. C. (2002). Regulation of hepatic stellate cell proliferation and collagen synthesis by proteinase-activated receptors. *J. Hepatol.* 36, 362–369. doi: 10.1016/s0168-8278(01)00285-9

Giebel, L. B., and Spritz, R. A. (1991). Mutation of the KIT (mast/stem cell growth factor receptor) protooncogene in human piebaldism. *Proc. Natl. Acad. Sci. U.S.A.* 88, 8696–8699. doi: 10.1073/pnas.88.19.8696

Hargrove, L., Kennedy, L., Demieville, J., Jones, H., Meng, F., DeMorrow, S., et al. (2017). Bile duct ligation-induced biliary hyperplasia, hepatic injury, and fibrosis are reduced in mast cell-deficient Kit(W-sh) mice. *Hepatology* 65, 1991–2004.

Hisada, M., Zhang, X., Ota, Y., Cameron, A. M., Burdick, J., Gao, B., et al. (2017). Fibrosis in small syngeneic rat liver grafts because of damaged bone marrow stem cells from chronic alcohol consumption. *Liver Transpl.* 23, 1564–1576. doi: 10.1002/lt.24820

Hu, B., and Colletti, L. M. (2008). Stem cell factor and c-kit are involved in hepatic recovery after acetaminophen-induced liver injury in mice. *Am. J. Physiol. Gastrointest. Liver Physiol.* 295, G45–G53. doi: 10.1152/ajpgi.00024.2008

Humbert, M., de Blay, F., Garcia, G., Prud'homme, A., Leroyer, C., Magnan, A., et al. (2009). Masitinib, a c-kit/PDGF receptor tyrosine kinase inhibitor, improves disease control in severe corticosteroid-dependent asthmatics. *Allergy* 64, 1194–1201. doi: 10.1111/j.1398-9995.2009.02122.x

Ikarashi, M., Nakashima, H., Kinoshita, M., Sato, A., Nakashima, M., Miyazaki, H., et al. (2013). Distinct development and functions of resident and recruited liver Kupffer cells/macrophages. *J. Leukoc. Biol.* 94, 1325–1336. doi: 10.1189/jlb.0313144

Ishii, M., Iwai, M., Harada, Y., Morikawa, T., Okanoue, T., Kishikawa, T., et al. (2005). A role of mast cells for hepatic fibrosis in primary sclerosing cholangitis. *Hepatol. Res.* 31, 127–131. doi: 10.1016/j.hepres.2005.01.007

Kanbe, N., Kurosawa, M., Nagata, H., Yamashita, T., Kurimoto, F., and Miyachi, Y. (2000). Production of fibrogenic cytokines by cord blood-derived cultured human mast cells. *J. Allergy Clin. Immunol.* 106(1 Pt 2), S85–S90. doi: 10.1067/mai.2000.106777

Kang, Y. K., Yau, T., Park, J. W., Lim, H. Y., Lee, T. Y., Obi, S., et al. (2015). Randomized phase II study of axitinib versus placebo plus best supportive care in second-line treatment of advanced hepatocellular carcinoma. *Ann. Oncol.* 26, 2457–2463. doi: 10.1093/annonc/mdv388

Kara, B., Doran, F., Kara, I. O., Akkiz, H., and Sandikci, M. (2008). Expression of c-kit protooncogen in hepatitis B virus-induced chronic hepatitis, cirrhosis and hepatocellular carcinoma: has it a diagnostic role? *Int. J. Clin. Pract.* 62, 1206–1211. doi: 10.1111/j.1742-1241.2007.01675.x

Kim, D. K., Cho, Y. E., Komarow, H. D., Bandara, G., Song, B. J., Olivera, A., et al. (2018). Mastocytosis-derived extracellular vesicles exhibit a mast cell signature, transfer KIT to stellate cells, and promote their activation. *Proc. Natl. Acad. Sci. U.S.A.* 115, E10692–E10701. doi: 10.1073/pnas.1809938115

King, A., Houlihan, D. D., Kavanagh, D., Haldar, D., Luu, N., Owen, A., et al. (2017). Sphingosine-1-phosphate prevents egress of hematopoietic stem cells from liver to reduce fibrosis. *Gastroenterology* 153, 233–248.e16. doi: 10.1053/j.gastro.2017.03.022

Knight, B., Tirnitz-Parker, J. E., and Olynyk, J. K. (2008). C-kit inhibition by imatinib mesylate attenuates progenitor cell expansion and inhibits liver tumor formation in mice. *Gastroenterology* 135, 969–979.e1. doi: 10.1053/j.gastro.2008.05.077

Koh, K. C., Lee, H., Choi, M. S., Lee, J. H., Paik, S. W., Yoo, B. C., et al. (2005). Clinicopathologic features and prognosis of combined hepatocellular cholangiocarcinoma. *Am. J. Surg.* 189, 120–125. doi: 10.1016/j.amjsurg.2004.03.018

Komuta, M., Spee, B., Vander Borght, S., De Vos, R., Verslype, C., Aerts, R., et al. (2008). Clinicopathological study on cholangiolocellular carcinoma suggesting hepatic progenitor cell origin. *Hepatology* 47, 1544–1556. doi: 10.1002/hep.22238

Koruk, S. T., Ozardali, I., Dincoglu, D., and Bitiren, M. (2011). Increased liver mast cells in patients with chronic hepatitis C. *Indian J. Pathol. Microbiol.* 54, 736–740. doi: 10.4103/0377-4929.91510

Kudo, M., Finn, R. S., Qin, S., Han, K. H., Ikeda, K., Piscaglia, F., et al. (2018). Lenvatinib versus sorafenib in first-line treatment of patients with unresectable hepatocellular carcinoma: a randomised phase 3 non-inferiority trial. *Lancet* 391, 1163–1173. doi: 10.1016/S0140-6736(18)30207-1

Kwon, Y. C., Bose, S. K., Steele, R., Meyer, K., Di Bisceglie, A. M., Ray, R. B., et al. (2015). Promotion of cancer stem-like cell properties in hepatitis C virus-infected hepatocytes. *J. Virol.* 89, 11549–11556. doi: 10.1128/JVI.01946-15

Larson, A. M., Polson, J., Fontana, R. J., Davern, T. J., Lalani, E., Hynan, L. S., et al. (2005). Acetaminophen-induced acute liver failure: results of a United States multicenter, prospective study. *Hepatology* 42, 1364–1372. doi: 10.1002/hep.20948

Lemmer, E. R., Shepard, E. G., Blakolmer, K., Kirsch, R. E., and Robson, S. C. (1998). Isolation from human fetal liver of cells co-expressing CD34 haematopoietic stem cell and CAM 5.2 pancytokeratin markers. *J. Hepatol.* 29, 450–454. doi: 10.1016/s0168-8278(98)80064-0

Lev, S., Blechman, J. M., Givol, D., and Yarden, Y. (1994). Steel factor and c-kit protooncogene: genetic lessons in signal transduction. *Crit. Rev. Oncog.* 5, 141–168. doi: 10.1615/critrevoncog.v5.i2-3.30

Li, Z., Chen, J., Li, L., Ran, J. H., Liu, J., Gao, T. X., et al. (2013). In vitro proliferation and differentiation of hepatic oval cells and their potential capacity for intrahepatic transplantation. *Braz. J. Med. Biol. Res.* 46, 681–688. doi: 10.1590/1414-431X20132620

Lin, A. Y., Fisher, G. A., So, S., Tang, C., and Levitt, L. (2008). Phase II study of imatinib in unresectable hepatocellular carcinoma. *Am. J. Clin. Oncol.* 31, 84–88. doi: 10.1097/COC.0b013e3181131db9

Liu, C., Wang, J., and Ou, Q. J. (2004). Possible stem cell origin of human cholangiocarcinoma. *World J. Gastroenterol.* 10, 3374–3376. doi: 10.3748/wjg.v10.i22.3374

Liu, Z., Dai, X., Wang, T., Zhang, C., Zhang, W., Zhang, W., et al. (2017). Hepatitis B virus PreS1 facilitates hepatocellular carcinoma development by promoting appearance and self-renewal of liver cancer stem cells. *Cancer Lett.* 400, 149–160. doi: 10.1016/j.canlet.2017.04.017

Llovet, J. M., Pena, C. E., Lathia, C. D., Shan, M., Meinhardt, G., Bruix, J., et al. (2012). Plasma biomarkers as predictors of outcome in patients with advanced hepatocellular carcinoma. *Clin. Cancer Res.* 18, 2290–2300. doi: 10.1158/1078-0432.CCR-11-2175

Llovet, J. M., Ricci, S., Mazzaferro, V., Hilgard, P., Gane, E., Blanc, J. F., et al. (2008). Sorafenib in advanced hepatocellular carcinoma. *N. Engl. J. Med.* 359, 378–390. doi: 10.1056/NEJMoa0708857

Luna, G., Paez, J., and Cardier, J. E. (2004). Expression of the hematopoietic stem cell antigen Sca-1 (LY-6A/E) in liver sinusoidal endothelial cells: possible function of Sca-1 in endothelial cells. *Stem Cells Dev.* 13, 528–535. doi: 10.1089/scd.2004.13.528

Mansuroglu, T., Baumhoer, D., Dudas, J., Haller, F., Cameron, S., Lorf, T., et al. (2009a). Expression of stem cell factor receptor c-kit in human nontumoral and tumoral hepatic cells. *Eur. J. Gastroenterol. Hepatol.* 21, 1206–1211. doi: 10.1097/MEG.0b013e328317f4ef

Mansuroglu, T., Ramadori, P., Dudas, J., Malik, I., Hammerich, K., Fuzesi, L., et al. (2009b). Expression of stem cell factor and its receptor c-Kit during the development of intrahepatic cholangiocarcinoma. *Lab. Invest.* 89, 562–574. doi: 10.1038/labinvest.2009.15

Matsusaka, S., Tsujimura, T., Toyosaka, A., Nakasho, K., Sugihara, A., Okamoto, E., et al. (1999). Role of c-kit receptor tyrosine kinase in development of oval cells in the rat 2-acetylaminofluorene/partial hepatectomy model. *Hepatology* 29, 670–676. doi: 10.1002/hep.510290304

Meadows, V., Kennedy, L., Hargrove, L., Demieville, J., Meng, F., Virani, S., et al. (2019). Downregulation of hepatic stem cell factor by vivo-morpholino treatment inhibits mast cell migration and decreases biliary damage/senescence and liver fibrosis in Mdr2(-/-) mice. *Biochim. Biophys. Acta Mol. Basis Dis.* 1865:165557. doi: 10.1016/j.bbadis.2019.165557

Meng, F., Francis, H., Glaser, S., Han, Y., DeMorrow, S., Stokes, A., et al. (2012). Role of stem cell factor and granulocyte colony-stimulating factor in remodeling during liver regeneration. *Hepatology* 55, 209–221. doi: 10.1002/hep.24673

Metcalfe, D. D., Baram, D., and Mekori, Y. A. (1997). Mast cells. *Physiol. Rev.* 77, 1033–1079. doi: 10.1152/physrev.1997.77.4.1033

Mukhopadhyay, A., Do, D. V., Ong, C. T., Khoo, Y. T., Masilamani, J., Chan, S. Y., et al. (2011). The role of stem cell factor and c-KIT in keloid pathogenesis: do tyrosine kinase inhibitors have a potential therapeutic role? *Br. J. Dermatol.* 164, 372–386. doi: 10.1111/j.1365-2133.2010.10035.x

Nakamura, A., Yamazaki, K., Suzuki, K., and Sato, S. (1997). Increased portal tract infiltration of mast cells and eosinophils in primary biliary cirrhosis. *Am. J. Gastroenterol.* 92, 2245–2249.

Nassar, I., Pasupati, T., Judson, J. P., and Segarra, I. (2009). Reduced exposure of imatinib after coadministration with acetaminophen in mice. *Indian J. Pharmacol.* 41, 167–172. doi: 10.4103/0253-7613.56071

Nazzal, M., Sur, S., Steele, R., Khatun, M., Patra, T., Phillips, N., et al. (2020). Establishment of a patient-derived xenograft tumor from hepatitis C-associated liver cancer and evaluation of imatinib treatment efficacy. *Hepatology* 72, 379–388. doi: 10.1002/hep.31298

Nomoto, K., Tsuneyama, K., Cheng, C., Takahashi, H., Hori, R., Murai, Y., et al. (2006). Intrahepatic cholangiocarcinoma arising in cirrhotic liver frequently expressed p63-positive basal/stem-cell phenotype. *Pathol. Res. Pract.* 202, 71–76. doi: 10.1016/j.prp.2005.10.011

Omori, M., Evarts, R. P., Omori, N., Hu, Z., Marsden, E. R., and Thorgeirsson, S. S. (1997). Expression of alpha-fetoprotein and stem cell factor/c-kit system in bile duct ligated young rats. *Hepatology* 25, 1115–1122. doi: 10.1002/hep.510250512

Petersen, B. E., Goff, J. P., Greenberger, J. S., and Michalopoulos, G. K. (1998). Hepatic oval cells express the hematopoietic stem cell marker Thy-1 in the rat. *Hepatology* 27, 433–445. doi: 10.1002/hep.510270218

Potti, A., Ganti, A. K., Tendulkar, K., Chitajallu, S., Sholes, K., Koch, M., et al. (2003). HER-2/neu and CD117 (C-kit) overexpression in hepatocellular and pancreatic carcinoma. *Anticancer Res.* 23, 2671–2674.

Pressiani, T., Boni, C., Rimassa, L., Labianca, R., Fagiuoli, S., Salvagni, S., et al. (2013). Sorafenib in patients with Child-Pugh class A and B advanced hepatocellular carcinoma: a prospective feasibility analysis. *Ann. Oncol.* 24, 406–411. doi: 10.1093/annonc/mds343

Ramadori, G., Fuzesi, L., Grabbe, E., Pieler, T., and Armbrust, T. (2004). Successful treatment of hepatocellular carcinoma with the tyrosine kinase inhibitor imatinib in a patient with liver cirrhosis. *Anticancer Drugs* 15, 405–409. doi: 10.1097/00001813-200404000-00014

Ray, P., Krishnamoorthy, N., Oriss, T. B., and Ray, A. (2010). Signaling of c-kit in dendritic cells influences adaptive immunity. *Ann. N.Y. Acad. Sci.* 1183, 104–122. doi: 10.1111/j.1749-6632.2009.05122.x

Ren, X., Hogaboam, C., Carpenter, A., and Colletti, L. (2003). Stem cell factor restores hepatocyte proliferation in IL-6 knockout mice following 70% hepatectomy. *J. Clin. Invest.* 112, 1407–1418. doi: 10.1172/JCI17391

Ren, X., Hu, B., and Colletti, L. (2008). Stem cell factor and its receptor, c-kit, are important for hepatocyte proliferation in wild-type and tumor necrosis factor receptor-1 knockout mice after 70% hepatectomy. *Surgery* 143, 790–802. doi: 10.1016/j.surg.2008.03.021

Rojas, A., Zhang, P., Wang, Y., Foo, W. C., Munoz, N. M., Xiao, L., et al. (2016). A Positive TGF-beta/c-KIT feedback loop drives tumor progression in advanced primary liver cancer. *Neoplasia* 18, 371–386. doi: 10.1016/j.neo.2016.04.002

Satake, M., Shimano, K., Yamamoto, T., Okaya, A., Iwasaki, T., Kakihana, M., et al. (2003). Role of c-kit receptor tyrosine kinase-mediated signal transduction during proliferation of bile epithelial cells in young rats after ligation of bile duct: a study using Ws/Ws c-kit mutant rats. *J. Hepatol.* 39, 86–92. doi: 10.1016/s0168-8278(03)00149-1

Seino, S., Tsuchiya, A., and Watanabe, M. (2014). A rare primary liver tumor that responded to sorafenib. *Gastroenterology* 147, 1226–1227. doi: 10.1053/j.gastro.2014.07.035

Shaib, Y. H., El-Serag, H. B., Davila, J. A., Morgan, R., and McGlynn, K. A. (2005). Risk factors of intrahepatic cholangiocarcinoma in the United States: a case-control study. *Gastroenterology* 128, 620–626. doi: 10.1053/j.gastro.2004.12.048

Shaker, M. E. (2014). Nilotinib interferes with the signalling pathways implicated in acetaminophen hepatotoxicity. *Basic Clin. Pharmacol. Toxicol.* 114, 263–270. doi: 10.1111/bcpt.12144

Shirakura, K., Masuda, H., Kwon, S. M., Obi, S., Ito, R., Shizuno, T., et al. (2011). Impaired function of bone marrow-derived endothelial progenitor cells in murine liver fibrosis. *Biosci. Trends* 5, 77–82. doi: 10.5582/bst.2011.v5.2.77

Si, Y., Tsou, C. L., Croft, K., and Charo, I. F. (2010). CCR2 mediates hematopoietic stem and progenitor cell trafficking to sites of inflammation in mice. *J. Clin. Invest.* 120, 1192–1203. doi: 10.1172/JCI40310

Tanaka, S., Yamamoto, T., Tanaka, H., Kodai, S., Ogawa, M., Ichikawa, T., et al. (2005). Potentiality of combined hepatocellular and intrahepatic cholangiocellular carcinoma originating from a hepatic precursor cell: immunohistochemical evidence. *Hepatol. Res.* 32, 52–57. doi: 10.1016/j.hepres.2005.01.012

Terai, S., Ishikawa, T., Omori, K., Aoyama, K., Marumoto, Y., Urata, Y., et al. (2006). Improved liver function in patients with liver cirrhosis after autologous bone marrow cell infusion therapy. *Stem Cells* 24, 2292–2298. doi: 10.1634/stemcells.2005-0542

Thorgeirsson, S. S. (1996). Hepatic stem cells in liver regeneration. *FASEB J.* 10, 1249–1256.

Uddin Ahmed, A. F., Ohtani, H., Nio, M., Funaki, N., Sasaki, H., Nagura, H., et al. (2000). Intrahepatic mast cell population correlates with clinical outcome in Biliary atresia. *J. Pediatr. Surg.* 35, 1762–1765. doi: 10.1053/jpsu.2000.19245

Vagnozzi, R. J., Maillet, M., Sargent, M. A., Khalil, H., Johansen, A. K. Z., Schwanekamp, J. A., et al. (2020). An acute immune response underlies the benefit of cardiac stem cell therapy. *Nature* 577, 405–409. doi: 10.1038/s41586-019-1802-2

Weiskirchen, R., Meurer, S. K., Liedtke, C., and Huber, M. (2019). Mast cells in liver fibrogenesis. *Cells* 8:1429. doi: 10.3390/cells8111429

Went, P. T., Dirnhofer, S., Bundi, M., Mirlacher, M., Schraml, P., Mangialaio, S., et al. (2004). Prevalence of KIT expression in human tumors. *J. Clin. Oncol.* 22, 4514–4522. doi: 10.1200/JCO.2004.10.125

Xu, J., Tan, Y., Shao, X., Zhang, C., He, Y., Wang, J., et al. (2018). Evaluation of NCAM and c-Kit as hepatic progenitor cell markers for intrahepatic

cholangiocarcinomas. *Pathol. Res. Pract.* 214, 2011–2017. doi: 10.1016/j.prp.2018.09.005

Yamashiro, M., Kouda, W., Kono, N., Tsuneyama, K., Matsui, O., and Nakanuma, Y. (1998). Distribution of intrahepatic mast cells in various hepatobiliary disorders - An immunohistochemical study. *Virchows Arch.* 433, 471–479. doi: 10.1007/s004280050276

Yan, W., Zhu, Z., Pan, F., Huang, A., and Dai, G. H. (2018). Overexpression of c-kit(CD117), relevant with microvessel density, is an independent survival prognostic factor for patients with HBV-related hepatocellular carcinoma. *Oncol. Targets Ther.* 11, 1285–1292. doi: 10.2147/OTT.S157545

Yu, X. H., Xu, L. B., Zeng, H., Zhang, R., Wang, J., and Liu, C. (2011). Clinicopathological analysis of 14 patients with combined hepatocellular carcinoma and cholangiocarcinoma. *Hepatobil. Pancreat. Dis. Int.* 10, 620–625. doi: 10.1016/s1499-3872(11)60105-7

Yushkov, B. G., Danilova, I. G., Ponezheva, Zh B, Brykina, I. A., Abidov, M. T., and Kalyuzhin, O. V. (2011). Modulation of reparative regeneration and CD117 expression by liver cells after partial hepatectomy in mice. *Bull. Exp. Biol. Med.* 150, 352–354. doi: 10.1007/s10517-011-1140-3

Zhang, F., Chen, X. P., Zhang, W., Dong, H. H., Xiang, S., Zhang, W. G., et al. (2008). Combined hepatocellular cholangiocarcinoma originating from hepatic progenitor cells: immunohistochemical and double-fluorescence immunostaining evidence. *Histopathology* 52, 224–232. doi: 10.1111/j.1365-2559.2007.02929.x

Zhang, Q., He, Y., Luo, N., Patel, S. J., Han, Y., Gao, R., et al. (2019). Landscape and dynamics of single immune cells in hepatocellular carcinoma. *Cell* 179, 829–845.e20. doi: 10.1016/j.cell.2019.10.003

Zheng, H., Pomyen, Y., Hernandez, M. O., Li, C., Livak, F., Tang, W., et al. (2018). Single-cell analysis reveals cancer stem cell heterogeneity in hepatocellular carcinoma. *Hepatology* 68, 127–140. doi: 10.1002/hep.29778

Conflict of Interest: The authors declare that the research was conducted in the absence of any commercial or financial relationships that could be construed as a potential conflict of interest.

frontiers in Cell and Developmental Biology

REVIEW
published: 20 April 2021
doi: 10.3389/fcell.2021.661472

Organoids of the Female Reproductive Tract: Innovative Tools to Study Desired to Unwelcome Processes

*Ruben Heremans[1,2,3], Ziga Jan[1,2,4], Dirk Timmerman[2,3] and Hugo Vankelecom[1]**

[1] *Laboratory of Tissue Plasticity in Health and Disease, Cluster of Stem Cell and Developmental Biology, Department of Development and Regeneration, KU Leuven (University of Leuven), Leuven, Belgium,* [2] *Cluster Woman and Child, Department of Development and Regeneration, KU Leuven, Leuven, Belgium,* [3] *Department of Obstetrics and Gynecology, University Hospitals, KU Leuven, Leuven, Belgium,* [4] *Department of Gynecology, Klinikum Klagenfurt, Klagenfurt, Austria*

The pelviperineal organs of the female reproductive tract form an essential cornerstone of human procreation. The system comprises the ectodermal external genitalia, the Müllerian upper-vaginal, cervical, endometrial and oviductal derivatives, and the endodermal ovaries. Each of these organs presents with a unique course of biological development as well as of malignant degeneration. For many decades, various preclinical *in vitro* models have been employed to study female reproductive organ (patho-)biology, however, facing important shortcomings of limited expandability, loss of representativeness and inadequate translatability to the clinic. The recent emergence of 3D organoid models has propelled the field forward by generating powerful research tools that *in vitro* replicate healthy as well as diseased human tissues and are amenable to state-of-the-art experimental interventions. Here, we in detail review organoid modeling of the different female reproductive organs from healthy and tumorigenic backgrounds, and project perspectives for both scientists and clinicians.

Keywords: organoids, gynecology, reproduction, cancer modeling, women's health

OPEN ACCESS

Edited by:
Lon J. Van Winkle,
Rocky Vista University, United States

Reviewed by:
Aitor Aguirre,
Michigan State University, United States
Taisen Iguchi,
Graduate University for Advanced Studies (Sokendai), Japan

****Correspondence:***
Hugo Vankelecom
hugo.vankelecom@kuleuven.be

Specialty section:
This article was submitted to Stem Cell Research, a section of the journal Frontiers in Cell and Developmental Biology

Received: *30 January 2021*
Accepted: *22 March 2021*
Published: *20 April 2021*

Citation:
Heremans R, Jan Z, Timmerman D and Vankelecom H (2021) Organoids of the Female Reproductive Tract: Innovative Tools to Study Desired to Unwelcome Processes. Front. Cell Dev. Biol. 9:661472. doi: 10.3389/fcell.2021.661472

INTRODUCTION

The female reproductive system serves a unique purpose as it harbors the beginning of life, but, conversely, also risks to bring about the very end of it. The embryonic etiology of these closely related tissues are threefold (Brauer, 2009; Mutter and Robboy, 2014). The vulva and lower third of the vagina arise from ectoderm. The tissues making up the actual female reproductive tract (FRT), including upper two-thirds of the vagina, cervix, uterus, endometrium and fallopian tubes (FT), are mesodermal derivatives whereas the ovaries originate from the endoderm. Each of these tissues is epitomized by its unique patterns of development, proliferation and differentiation. Importantly, to serve their reproductive purpose, these tissues rely on the self-renewing capacity of their constituents (Patterson and Pru, 2013). However, it is in their efforts that allow for life to begin, by fulfilling transportation functions, supporting implantation and serving as barriers from internal and external stressors and pathogens, that its constituents risk cellular deregulation due to threatening impacts such as hormonal dysregulation, infections or auto-immune diseases, which may ultimately result in carcinogenesis (Hanahan and Weinberg, 2011; Visvader, 2011).

In general, insight in tissue development, homeostasis and disease has been obtained from several research models that throughout the years have become more complex and representative, and even personalized (Schutgens and Clevers, 2020). For many years, hypothesis testing for tissues of the FRT has relied on two-dimensional (2D) models (such as cell lines) that have stood alongside short-term three-dimensional (3D) *in vitro* cell-culture (such as spheroids) and *in vivo* explant systems [such as patient-derived xenografts (PDXs)] (Adissu et al., 2007; Gargett et al., 2016; **Figure 1**). It took until 2009, however, for the prospect of a complete transition into use of long-term 3D *in vitro* cell-culturing methods to be envisioned. The intestine was the first of many organs to have its stem cell niche analyzed and have expansion and differentiation pathways charted by means of a self-forming and -organizing, tissue stem cell-derived culturing system called "*organoids*" (Ootani et al., 2009; Sato et al., 2009). The insights brought about by this novel technology, reliant on the use of a gel-based substitute for the local extracellular matrix (ECM) and supplementation of feeder- and serum-free stem cell niche-supporting factors, were manifold (Kleinman et al., 1986). This system was the first to show defined use of growth and regulatory factors required by the stem cell niche, thereby discarding the need for highly variable and ill-defined serum supplements (Clevers et al., 2014). Contrary to 2D cell lines, organoids proved to remain morphologically, genomically and transcriptomically stable over a long period of time and serial passaging. This novel culturing method thereby allowed for spatiotemporal tracking (i.e., how various specific cell types occupy different positions within tissues and how their positions alter through time) of developing organs, requiring only the bare minimum of starting (patient) material. Rapidly and effectively, the complex biology of the epithelial compartment of the intestine was analyzed for the entire spectrum spanning healthy to diseased conditions (Sato et al., 2009, 2011; van de Wetering et al., 2015; Hibiya et al., 2017). Although revolutionizing human research, organoids were only replicating the tissue's epithelium. This drawback of lacking the organ's stromal, vascular and immune cells and their interplay was readily overcome by the development of various *in vitro* co-culturing as well as *in vivo* transplant modalities (Nozaki et al., 2016; Roper et al., 2017; Dijkstra et al., 2018). Overall, more reliably than other experimental models, organoids enable a wide variety of basic, translational and clinical research prospects such as deciphering the heterogeneous make-up of tissues via multi-omic analyses, unraveling host tissue-pathogen interactions, and advancing precision and regenerative medicine using cryopreserved and biobanked organoid lines (**Figure 2**). Organoids are also amenable to cutting-edge experimental technologies such as CRISPR-Cas9 gene editing, and can be efficiently subjected to live imaging (Kim et al., 2021).

In this review, we aim to systematically list the efforts made in the field of organoid research for the tissues that make up the human FRT. We provide a systematic overview of the organoid models developed and the growth media that detail the niche requirements ranging from healthy to diseased states. We critically appraise their validity and scrutinize reports for investigated applications. Taken together, we aim to highlight the specific benefits of organoid technology in the setting of desired and unwelcome processes of the human FRT.

VULVA

The vulva, that consists of labia majora, mons pubis, labia minora, clitoris and vestibulum, acts as a gatekeeping structure and serves as a first line of defense in order to protect the FRT against extracorporeal stressors. Being an ectodermal derivative, the vulva is shaped as urogenital or cloacal folds through cellular expansion of its underlying mesodermal compartment (Brauer, 2009). As in other tissues (Sato et al., 2011), this epithelium serves not only as a mechanical scaffold, but also as a source for paracrine crosstalk that shapes the specialized cellular niche, thereby anchoring and supporting resident stem cells. To date, no organoids have been derived from appendages of the human perineal or vulvar region (**Table 1** and **Supplementary Table 1**). Insights on vulvar homeostasis and disease can, however, be inferred from organoid studies exploring skin because the vulva, forming the exterior ending of the FRT, is largely covered with skin epithelium (Lei et al., 2017; Gupta et al., 2018; Boonekamp et al., 2019; Diao et al., 2019). Lei et al. (2017) elucidated the spatiotemporal component in mouse epidermal development using organoids, thereby unveiling which transcriptional pathways are consecutively activated during each phase of skin development. Boonekamp et al. (2019) established an organoid system for long-term expansion of murine keratinocytes and were able to initiate and maintain cultures from stem cells with various gene signatures. The fact that these organoids were amenable to genetic manipulation may draw a parallel toward prospective vulvar organoids in which gene alterations may be studied as, for instance, occurring during chronic inflammation (e.g., lichen sclerosus or lichen planus) or infection (e.g., candidosis or herpes genitalis) or in driver genes involved in blistering diseases (e.g., epidermolysis bullosa or pemphigus vulgaris) and carcinogenesis (e.g., basocellular or squamous vulvar cancer). Organoids may also be particularly useful for drug screening in order to find (new) drug targets and drugs that can mitigate the undesired vulvar diseases. On the vulva like on skin, sweat glands serve as gatekeepers for bacterial colonization, waste excretion and body-temperature maintenance. These glands are therefore important elements to explore when trying to understand vulvar (microbial) homeostasis. Diao et al. (2019) generated an organoid culture system for epidermal sweat glands, which may pave the way to vulvar sweat gland-derived organoids. Gupta et al. (2018) studied epithelial–mesenchymal interactions in composite organoids obtained by co-culturing human dermal papilla spheroids, hair follicle keratinocytes and stem cells in a hydrogel-based microenvironment. Taken together, vulva-derived organoids will be powerful tools to help understanding normal epithelium biology and microbiome interaction, and specific vulvotropic diseases such as genital infections and cancers (e.g., vulvar squamous cell carcinoma), as well as to provide a potential means for tissue regeneration after debilitating surgery (e.g., radical vulvectomy).

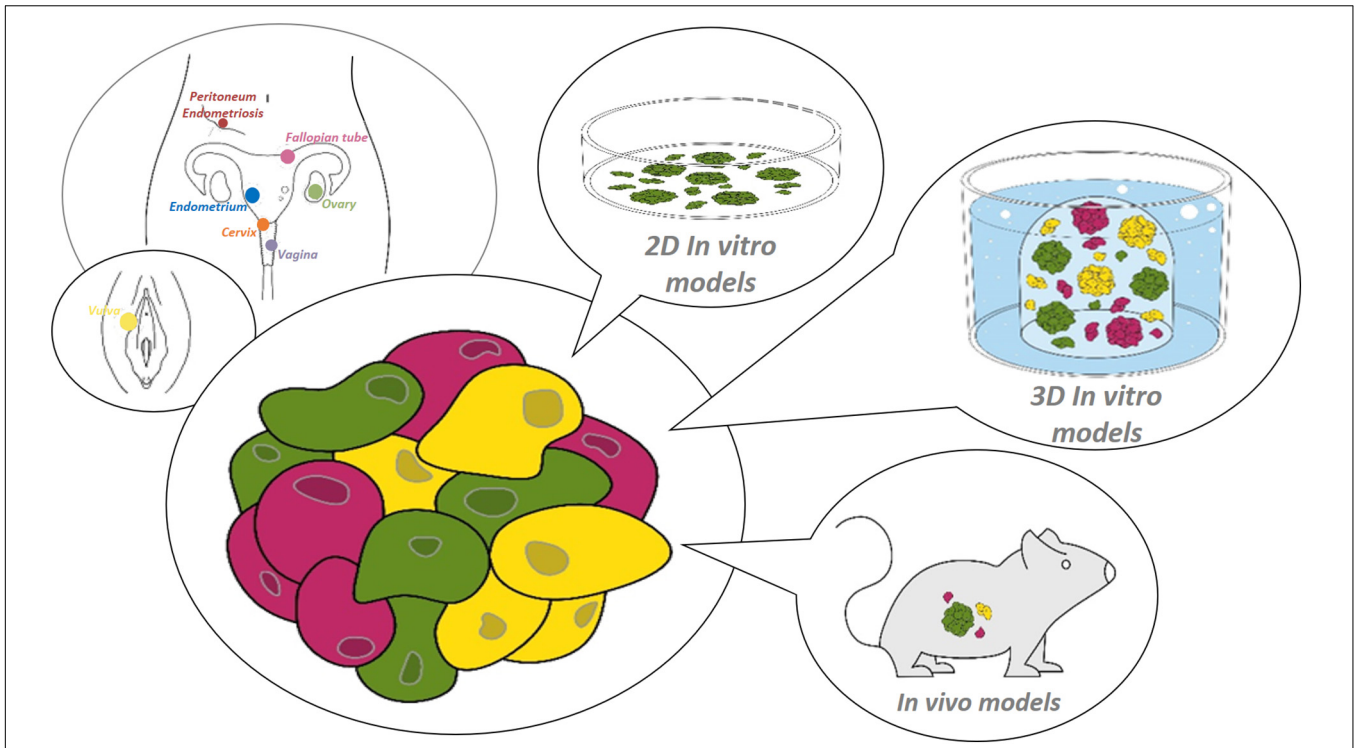

FIGURE 1 | Research models for the female reproductive tract. Starting from healthy or diseased tissue from the site of interest within the female reproductive tract (from distal to proximal: vulva, vagina, cervix, endometrium, fallopian tube, ovary and peritoneum/endometriosis), (patho-)physiology can be studied using various preclinical 2D or 3D *in vitro*, or *in vivo* models.

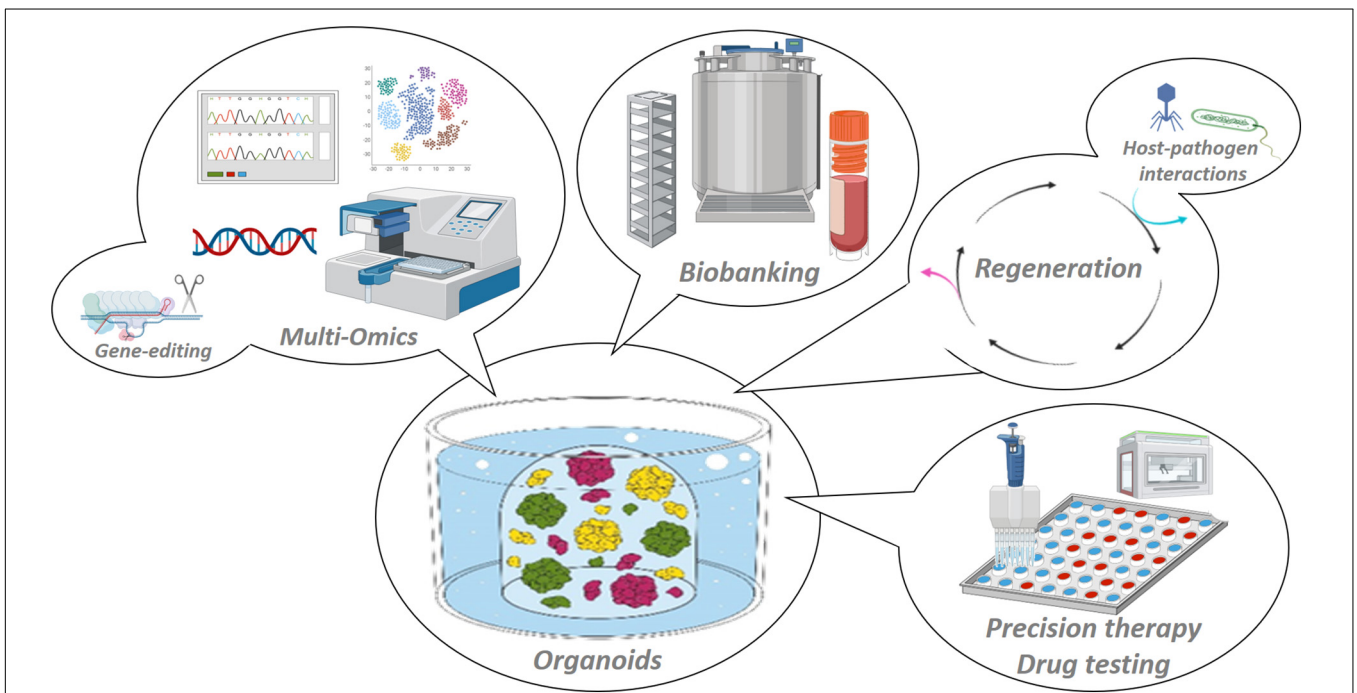

FIGURE 2 | Applications of organoid model systems. Organoids are stable 3D *in vitro* representations of the tissue of origin that adequately recapitulate tissue (patho-)biology, and are amenable to manifold basic and (pre-)clinical research applications such as multi-omic scrutiny and gene-editing, host–pathogen interaction mapping and regenerative medicine, biobanking and high-throughput drug testing toward patient-tailored treatments.

TABLE 1 | Main findings and applications of human female reproductive tract organoid studies.

Organoids of human . . .	Author, year	Main findings	Applications
VULVA	NA	NA	NA
VAGINA	NA	NA	NA
CERVIX	Chumduri et al., 2018, 2021	• Differential niche requirements for squamous and columnar cervical organoids suggest cervical homeostasis is determined by stromal Wnt signaling rather than epithelial transition. • Squamous cancers probably originate from $CK5^+$, adenocarcinomas from $CK7^+CK8^+$ cells.	Characterization, biobanking
	Maru et al., 2019a	Establishment of cervical clear cell carcinoma organoids	Characterization, biobanking, xenografting, drug screening
	Maru et al., 2020	Establishment of normal and metaplastic cervical organoids from the squamocolumnar junctional zone	Characterization, biobanking
ENDOMETRIUM			
Healthy endometrium	Turco et al., 2017	• Establishment of endometrial organoids of all phases of menstrual cycle and decidual changes. • Endometrial organoids are clonogenic and bipotent.	Characterization, optimization, biobanking,
	Boretto et al., 2017	Establishment of endometrial organoids of all phases of menstrual cycle. • Human endometrial organoids express *LGR4* and *LGR5* and WNT ligands are endogenously expressed. • Endometrial organoids mimic the menstrual cycle in a dish.	Characterization, optimization, biobanking
	Haider et al., 2018	• Establishment of trophoblast organoids. • Wnt signaling promotes villous but not extravillous trophoblast formation.	Characterization, optimization, biobanking
	Turco et al., 2018	Establishment of trophoblast organoids	Characterization, optimization, biobanking
	Fitzgerald et al., 2019	• Validation of endometrial organoid model. • Deepened understanding of gene expression upon hormonal stimulation.	Characterization, biobanking
	Hennes et al., 2019	• Validation of endometrial organoid model. • Mechanosensitive ion channels (e.g., PIEZO1) are expressed in endometrial organoids.	Characterization, mechanical stimulation, patch clamping, calcium imaging, drug screening,
	Haider et al., 2019	• Validation of endometrial organoid model. • Estrogen and NOTCH signaling drive ciliogenesis.	Characterization, biobanking, drug screening
	Luddi et al., 2020	• Validation of endometrial organoid model. • Receptivity marker glycodelin A differs between healthy and endometriosis-affected endometrium.	Characterization
	Cochrane et al., 2020	• Validation of endometrial organoid model. • Differentiation of secretory and ciliated epithelial cell populations in endometrial organoids.	
	Marinić et al., 2020	Endometrial gland organoid derivation from term placentas	Characterization
Adenomyosis and endometriosis	Boretto et al., 2019	• Establishment of endometriosis organoid model. • *LGR6* is upregulated in endometriosis organoids. • Inflammatory and cancer-associated genes/traits are found in endometriosis organoids.	Characterization, optimization, biobanking, xenografting, drug screening
	Esfandiari et al., 2021	Validation of endometriosis organoid model	Characterization
Endometrial hyperplasia and cancer	Dasari et al., 2017	Verteporfin as promising therapeutic agent for endometrial cancer.	Characterization, drug screening
	Girda et al., 2017	• Establishment of endometrial cancer organoid model. • Novel STAT3 inhibitors as potent anticancer agent.	Characterization, drug screening
	Pauli et al., 2017	Combination of buparlisib with olaparib as optimal treatments in endometrial organoid and PDX models.	Characterization, biobanking, drug screening, xenografting
	Boretto et al., 2019	• Establishment of endometrial cancer (-predisposed) organoid models. • Significant differences compared to healthy endometrium in PIEZO1 and transient receptor potential channels.	Characterization, optimization, biobanking, xenografting, drug screening, calcium imaging, patch clamping

(Continued)

TABLE 1 | Continued

Organoids of human . . .	Author, year	Main findings	Applications
	Maru et al., 2019b	Establishment of endometrial cancer organoid model.	Characterization, optimization, biobanking, drug screening
FALLOPIAN TUBES	Kessler et al., 2015	• Establishment of healthy fallopian tube organoid model. • Fallopian tube stemness is Wnt- and NOTCH-dependent.	Characterization, optimization, biobanking
	Kessler et al., 2019	*Chlamydia* infection can be mimicked in oviductal organoids and increases DNA hypermethylation and stemness.	Characterization
	Kopper et al., 2019	• Establishment of healthy fallopian tube organoid model from BRCA germline mutation carriers. • Strong Wnt dependency in fallopian tube organoids.	Characterization, optimization, biobanking, drug screening, gene-editing
	de Witte et al., 2020	• Fallopian/ovarian cancer organoid response matches patient's clinical response. • Intra- as well as inter-patient drug response heterogeneity.	Characterization, optimization, biobanking, drug screening, clinical correlation
	Hoffmann et al., 2020	• Triple knock-down oviductal organoids show ovarian cancer traits. • Medium optimized for ovarian cancer organoids promotes stemness in modified oviductal organoids. • Modified organoids thrive in Wnt-free environment.	Characterization, optimization, biobanking, drug screening, clinical correlation
	Rose et al., 2020	• Fimbrial ends of the oviducts possess the highest organoid-forming capacity. • Aldehyde dehydrogenase-positive cells replicate with higher frequency and form larger structures.	Characterization,
OVARIES	Hill et al., 2018	• Establishment of short-term ovarian cancer organoids. • Functional assays of homologous repair deficiency outperform isolated assessment of mutational profiles.	Characterization, drug screening
	Kopper et al., 2019	• Establishment of (predisposed) healthy and diseased ovarian organoid model. • Importance of heregulin-β1 (neuregulin-1) and low WNT environment.	Characterization, optimization, biobanking, drug screening, xenografting
	Maru et al., 2019b	Establishment of ovarian cancer organoid model	Characterization, optimization, biobanking, drug screening
	de Witte et al., 2020	• Fallopian/ovarian cancer organoid response matches patient's clinical response. • Intra- as well as inter-patient drug response heterogeneity.	Characterization, optimization, biobanking, drug screening, clinical correlation
	Hoffmann et al., 2020	Ovarian cancer organoids require low-Wnt environment	Characterization, optimization, biobanking, drug screening, clinical correlation
	Maenhoudt et al., 2020	• Establishment of ovarian cancer organoid model. • Importance of heregulin-β1 (neuregulin-1).	Characterization, optimization, biobanking, drug screening
	Chen et al., 2020	Establishment of short-term organoids/spheroids model from malignant effusion fluids	Characterization, biobanking, drug screening
	Nanki et al., 2020	Establishment of ovarian cancer organoid model	Characterization, drug screening
	Zhang et al., 2020	Establishment of ovarian cancer organoid model	Characterization, drug screening

VAGINA

Like for the vulva, most of our current understanding on vaginal development and regeneration is construed from 2D primary cell culture and animal experiments (Bulmer, 1957; Mutter and Robboy, 2014). Mouse studies have been essential in conveying the importance of a transformative interplay between the epithelium and its underlying stroma, revealing that the stroma eventually induces cytodifferentiation of pseudostratified columnar to squamous epithelium and shapes the morphology of the overlying epithelium (Cunha, 1976; Robboy et al., 1982; Iguchi et al., 1983; Tsai and Bern, 1991; Miyagawa and Iguchi, 2015). Several mouse-derived 2D cell culture and *in vivo* studies later underscored the role of hormone receptor genes and hinted on the possible contribution of the Wnt/β-catenin pathway to vaginal proliferation and differentiation (Iguchi et al., 1983; Tsai and Bern, 1991; Nakamura et al., 2012; Miyagawa and Iguchi, 2015; Mehta et al., 2016; Li et al., 2018). Only recently, the pivotal function of the latter pathway in vaginal epithelium became elegantly clear. After discovering new bona fide markers of different subpopulations in mouse vaginal epithelium, including potential stem cell populations, Ali et al. succeeded in establishing an expandable, genomically stable 3D organoid culturing system (Ali et al., 2020). After embedding single-cell suspensions in basement membrane extract, the sole requirements appeared to be the addition of epidermal growth factor (EGF), transforming growth factor β receptor (TGF-βR) kinase inhibitor, and Rho-associated protein kinase (ROCK) inhibitor (ROCKi). EGF

and TGF-βR kinase inhibitor were important throughout the whole culturing process and served as (stem cell) mitogens, whereas ROCKi was used mainly during passaging and seeding steps to prevent anoikis of the single cells. The importance of Wnt and BMP signaling in maintenance of the stem cell niche was accentuated by the positive correlation between organoid-forming capacity and concentrations of supplemented Wnt3a and R-Spondin-3 (RSPO3), both Wnt pathway activators, and of Noggin, a BMP inhibitor. Inversely, inhibiting Wnt *O*-acyltransferase Porcupine (PORCN) activity, needed for Wnt ligand maturation and secretion, via IWP-2 halted organoid growth and multiplication. Pulse labeling of cells expressing Wnt target and regulator axis inhibition protein 2 (AXIN2) in doxycycline-inducible AXIN2^{rtTA}/tetO^{Cre}/lacZ$^{fl/+}$ mice led to understand that these cells give rise to all other epithelial cell lineages of vaginal epithelium in mice. Unfortunately, to the best of our knowledge, no data on vaginal epithelium stem cells are available in humans (**Table 1** and **Supplementary Table 1**). Considering that vaginal epithelium, together with the vulva, represents the first line of defense against pathogenic colonization or infection of the reproductive organs, human vaginal organoids would allow us to gather better understanding of how these human cells interact with micro-organisms on a (sub-)cellular level. In addition, by co-culturing organoids with associated stroma, a more thorough comprehension could be obtained of the signaling cascade that causes and maintains vaginal atrophy. If eventually applied in a system that also encompasses the immune and vascular system, a more purposeful narrative could be written for pathogenesis and drug discovery in vaginal cancers. Owing to their rarity and proximity of the vulva and cervix, vaginal cancers are either treated as cervical or vulvar entities and not a single treatment algorithm is set out to deal with vaginal cancers focusing on their intrinsic characteristics. Therefore, a model that allows understanding, expanding and biobanking these rare cancers would be invaluable to gynecological cancer research (de Martel et al., 2017). Once more, organoid technology may prove here to bridge the gap between bench and bedside.

CERVIX

The uterine cervix is the final frontier between a stressor-laden, entropic external environment and the well-organized, homeostatic internal conditions at the locus of implantation. Yet, more than any other compartment of the FRT, the focus of cervical research lies not in its impact on fertility, but in its risk of oncogenic transformation. It is still the most prevalent gynecological cancer worldwide. It is infection-driven, most notably with oncogenic strains of human papillomavirus (HPV) (zur Hausen et al., 1974; de Sanjose et al., 2010; de Martel et al., 2017; Bray et al., 2018). However, not all tissue-resident cells are equally prone to malignant transformation. The cervix initially comprises two distinct native epithelia with a dynamic interface that give rise to an area consisting of a third, transformative epithelium that displays traits of both precursors (**Figure 3**). The ectocervix is marked by a stratified, non-keratinizing epithelium similar to that of the vagina. The endocervix is an evident extension of the endometrium consisting of a single line of columnar, mucus-secreting cells, sparsely interspersed with ciliated cells. Starting from the original squamocolumnar junction (SCJ) and due to the acidity of the vaginal compared to the endocervical environment, transformative pathways are activated in bipotent progenitor, so-called "reserve" cells, subjacent to columnar cells to replace and replenish the exposed surface with metaplastic squamous epithelium (Herfs et al., 2013; Malpica, 2014). Even though carcinomas arising from both epithelia display only minute differences in clinical risk factors and majority of dedicated HPV types, much is still to be elucidated on how they pathogenetically diverge (Berrington de González et al., 2004; Bray et al., 2005; de Sanjose et al., 2010; Patterson and Pru, 2013; Deng et al., 2018; Stewart et al., 2019). It has been postulated that cytokeratin (CK-) 7-positive stem cells residing at the SCJ, may represent a cell population in which cervical carcinogenesis originates (Herfs et al., 2012, 2013). Current understanding of cervical cancer cells has been acquired owing to the efforts of Gey et al. (1952) who established the renowned "HeLa" cancer cell line from an aggressive clone of cervical adenocarcinoma, named after its patient donor Henrietta Lacks. In general, the establishment of cervical cancer cell lines provided important stepping stones toward more insight into molecular and genetic cancer pathways, but these 2D cell-line models suffer from major shortcomings. First, only highly aggressive tumors can be readily established in cell lines (Gartler, 1968; Sandberg and Ernberg, 2005). Second, the tumor niche is only poorly recapitulated, using undefined supplements such as chicken plasma, bovine embryo extract and human placental cord serum, or more in general, serum (Gartler, 1968; Sandberg and Ernberg, 2005). Third, clonal selection (with loss of tumor original heterogeneous composition), genetic drift and contamination by other cell lines, all severely compromise their use as representative cancer research models (Gartler, 1968; Sandberg and Ernberg, 2005). Since cervical cancer is a predominantly infection-mediated disease, scientists turned to HPV-transfected (immortalized) keratinocytes and direct (epi-)genetic analysis on patient samples to study its pathogenesis, thereby unveiling roles for pathways impacting apoptosis and cell-cycle inhibition (Dyson et al., 1989; Scheffner et al., 1990; Tsuda et al., 2003; Cancer Genome Atlas Research Network, 2017). The importance of three-dimensionality in studying HPV life cycle was underpinned by the application of a raft culture method encompassing immortalized human foreskin keratinocytes on a dermal-equivalent support at air–liquid interface, allowing to study short-term events in the non-productive stages of HPV transmission, as well as impact of viral persistence and replication in the process of tissue stratification and differentiation (Flores et al., 1999). Co-culturing with immune cells allowed for a still better approximation of the genital mucosal microenvironment (Delvenne et al., 2001). A further advanced 3D set-up, using ECM-bound virions to infect primary foreskin keratinocytes and subsequently culturing these ensembles as rafts, recapitulated the earliest events of HPV infection as well as viral persistence, disease progression and

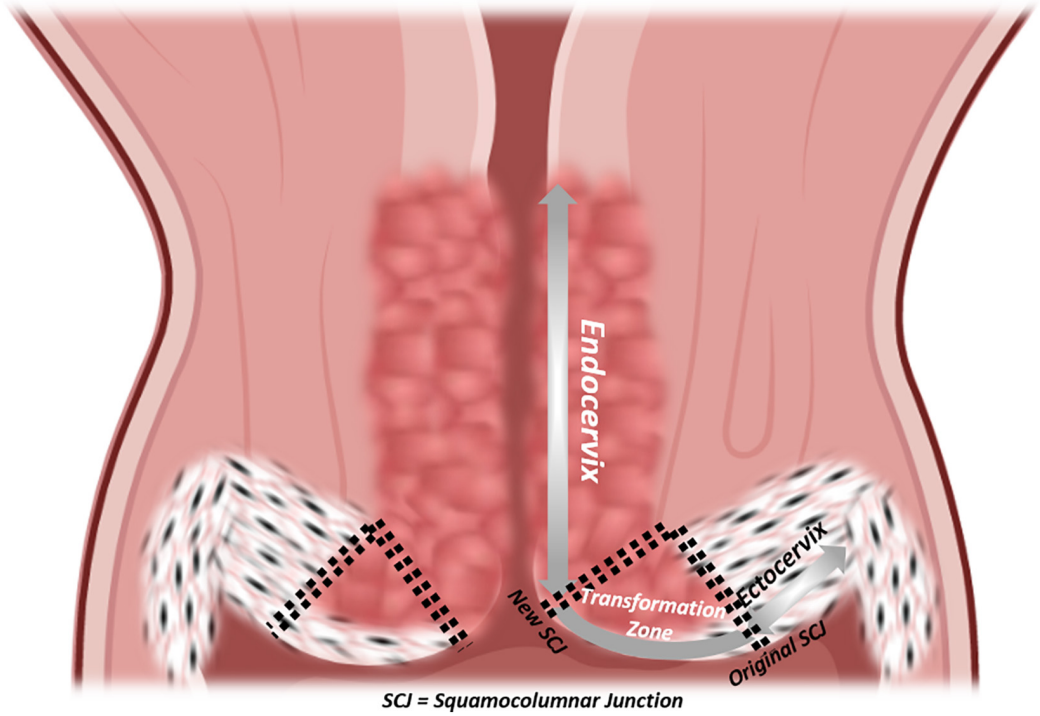

FIGURE 3 | Epithelial histology of the cervix. Coronal section of the cervix with a detailed visualization of epithelia, from vagina to isthmus: ectocervix, original squamocolumnar junction (SCJ), new SCJ, endocervix.

viral invasion, thereby providing invaluable insights in the first steps of viral infection and unveiling which viral transcripts are sequentially activated (Bienkowska-Haba et al., 2018). However, a specific fibroblast feeder cells providing stromal signals were used in these models which may be overcome by applying 3D organoid technology (**Table 1** and **Supplementary Table 1**). Recently, Maru et al. (2020) succeeded in establishing cervical organoids from a limited number of patient-derived biopsies in a medium supplemented with RSPO1, Noggin, EGF, ROCKi and the Notch ligand Jagged-1. The organoid cells expressed validated SCJ markers more robustly than classic cell lines and displayed both differentiated endo- and ectocervical cell types. Chumduri et al. (2018, 2021) generated endocervical-like, long-term expandable organoids from ecto- and endocervical patient samples, dependent on the presence of Wnt agonists (RSPO1 and WNT3A). They showed differentiation potential toward an ectocervical phenotype by activating the cAMP pathway and hinted toward different originating cells (i.e., squamous cancers from $CK7^+$ and adenocarcinomas from $CK7^+CK8^+$ cells). Maru et al. (2019a,b) were also able to establish organoids from a cervical clear cell carcinoma using their previously published culture conditions for other gynecological cancers. This organoid line, as well as endometrial and ovarian cancer organoids, were subjected to tailored drug therapy and grown as xenografts in the dorsal skin of immunocompromised nude mice (Maru et al., 2019a,b). However, although orthotopic xenograft models have previously been advocated as promising tools to model cervical cancer (Hoffmann et al., 2010), there are main limitations including lack of translatability because of species differences in stromal and immune cell interactions (in the PDX model, originating from mouse), the take rate mostly limited to aggressive subtypes, and the highly time- and animal-consuming aspects. Organoid technology may overcome some of these hurdles, as an impetus to still more advanced co-culture systems including immune cells. For instance, much remains to be learned about the effect of the genital mucosal microenvironment on virus-specific effector and suppressor immune responses and their impact on lesion pathogenesis.

ENDOMETRIUM

Healthy Endometrium

The multilayered inner lining of the uterus plays a pivotal role in human reproduction. Its make-up is tightly regulated by the hypothalamic-pituitary-gonadal axis and, in order to serve its primordial purposes of embryonic implantation and nourishment, it undergoes monthly reiterative cycles of proliferation, differentiation and menstrual shedding (Yin and Ma, 2005). This mucosal lining lies in continuity with that of the endocervix at the proximal side and FT at the distal end, and consists of glands, stroma, blood vessels and immune cells. Histologically subdivided, the endometrium consists of the - durably present - *lamina basalis* deeply and adjacent to the myometrium, and the - menstrually shed - *lamina functionalis* more superficially (**Figure 4**). The

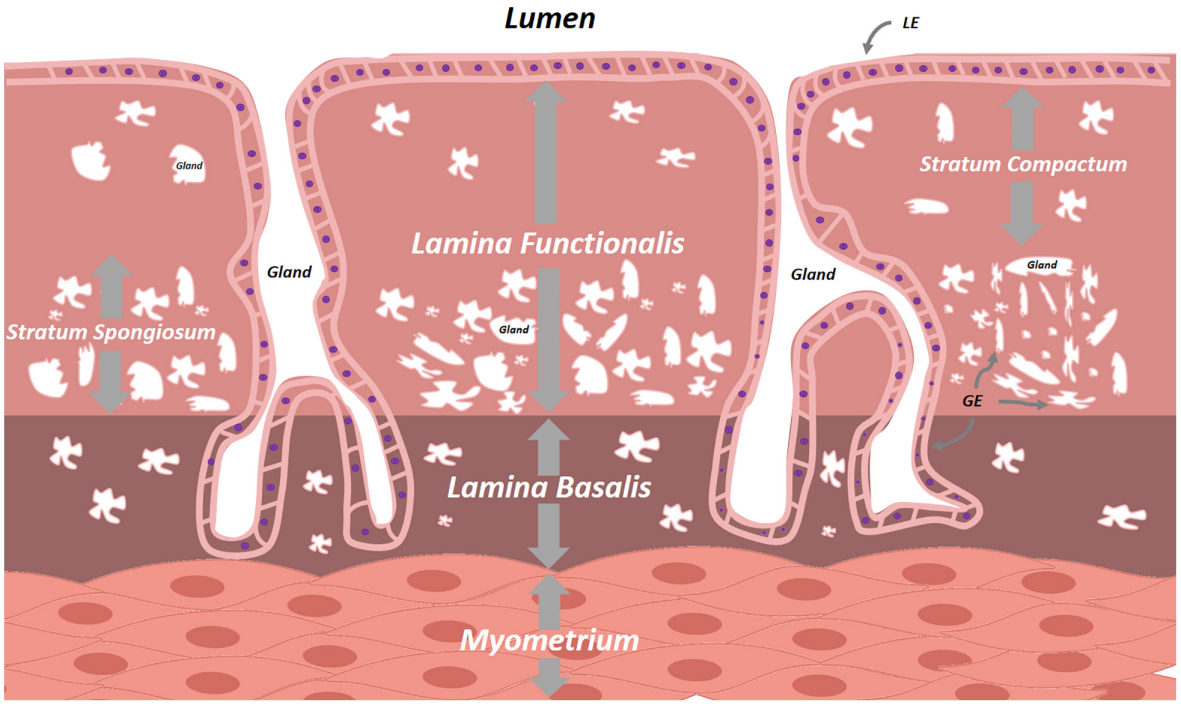

FIGURE 4 | Schematic overview of the endometrium. The cyclically replenished *lamina functionalis* divides into the superficial *stratum compactum* and the deeper *stratum spongiosum*. The persistent *lamina basalis* lies between the *lamina functionalis* and the uterine myometrium. Both lamina contain epithelial cells interspersed with varying densities of stromal cells. LE, luminal epithelium, GE, glandular epithelium.

lamina functionalis, containing luminal epithelium (LE) and glandular epithelium (GE), organizes into both a deeper lying *stratum spongiosum*, marked by numerous glands and ensuing loose stromal organization, and a superficial, less glandular and thereby stromally dense, *stratum compactum*. Whether the monthly regeneration of the endometrium is driven by endometrial stem cells, remains unclear and actively debated. Several epithelial and stromal stem cell candidates have been proposed, including long-term label-retaining cells, endometrial side population cells, perivascular CD146+, platelet-derived growth factor receptor-β (PDGFR-β+) and sushi domain containing-2 (SUSD2+) cells, and AXIN2+ cells, the latter identified by lineage tracing in mice and found responsible for tissue regeneration (Cunha, 1976; Robboy et al., 1982; Gray et al., 2001; Patterson and Pru, 2013; Gargett et al., 2016; Tempest et al., 2018; Syed et al., 2020). In addition, contribution of bone marrow-derived (endometrial progenitor) cells has also been suggested during the cyclic regeneration. Many questions and controversies remain regarding potential (hierarchical) relationship between the various stem cell candidates, and several of these findings in mice have not been translated into human. Apart from comparative ungulate, rodent or primate studies, understanding of regeneration-involved signaling pathways between cells, or between cells and ECM, sprouted from direct immunohistochemical (IHC) time-point analyses in human tissue (Snijders et al., 1992; Thiet et al., 1994; Jones et al., 1998; Aflatoonian et al., 2007). Also here, 3D models, cultured in basement membrane mimics, would be highly interesting to decipher these cellular processes and crosstalks. Iguchi et al. (1985) were able to dissociate luminal mouse endometrium from its fibromuscular stromal surroundings and seed these cells on collagen gel matrices in serum-free conditions. Cultures were short-lived, but the endometrial cells demonstrated apicobasal polarity and were characterized by spherical outgrowth and sheet- and/or duct-like extrusions, reminiscent of adenogenesis *in vivo*. Rinehart et al. (1988) seeded 3D endometrial glands in 50% Matrigel on Matrigel-coated plates. However, the 3D structures spread out into 2D monolayer colonies with columnar aspect, apicobasal polarity and preserved intercellular connections, but were not deeply characterized. Moreover, the medium, albeit serum-free, was not entirely chemically defined as 10% was made up of conditioned medium of the RL95-2 endometrial carcinoma cell line. Efforts by other groups showed persistent requirement of low amounts of serum, were hampered by the inability of long-term maintenance or expansion, and did not adequately recapitulate the endometrium as observed *in vivo* (Bentin-Ley et al., 1994; Bläuer et al., 2005, 2008). Only recently, human endometrium-derived organoids were successfully derived, using a defined culture medium (Boretto et al., 2017; Turco et al., 2017; Haider et al., 2019) (**Table 1** and **Supplementary Table 2**). Activation of Wnt/β-catenin signaling with RSPO1 (or CHIR99021, an inhibitor of β-catenin degradation) proved indispensable. This is in line with the proposed role of Wnt in uterus development and adenogenesis (uterine gland formation), recently supported by *in vivo* lineage tracing of AXIN2+ cells,

assigning these cells as plausible stem cell candidates in mouse uterus (Syed et al., 2020).

Different from mouse endometrial organoids, development and culture of human organoids did not require exogenous WNT3A. Inhibition of BMP (Noggin) and TGF-β/Alk (A83-01) pathways was indispensable, plausibly quenching differentiation of the organoid-driving stem cells (Boretto et al., 2017). Cultures furthermore benefited from the mitogens EGF and fibroblast growth factor 10 (FGF10), the endometrium-proliferative hormone 17β-estradiol (E2), insulin transduction activation (insulin-transferrin-selenium, ITS), and inhibition of p38 MAPK (SB202190 [p38i]), of reactive oxygen species (*N*-Acetyl-L-Cysteine [NAC]), of ROCK (Y-27632 [ROCKi]) and of sirtuin (nicotinamide [NAM]). By exposure to a specific hormone treatment protocol encompassing E2 and progesterone (P4), organoids mimicked the full menstrual cycle as well as incipient decidualization (**Table 1** and **Supplementary Table 3**). The robustness of the endometrial organoid platform has been validated by IHC, electron microscopy, array Comparative Genomic Hybridization (aCGH) and transcriptome analysis and, in addition, ion channel functionality and ciliogenesis was demonstrated using these organoid systems (Fitzgerald et al., 2019; Haider et al., 2019; Hennes et al., 2019; Cochrane et al., 2020; Bui et al., 2020; Luddi et al., 2020; Syed et al., 2020). Two groups achieved to derive organoids from trophoblasts, offering the appealing possibility to study trophoblast-endometrium crosstalk *in vitro* (Haider et al., 2018; Turco et al., 2018). Organoid medium of both studies only showed minimal differences, highlighting the importance of EGF, Wnt activation (RSPO, CHIR99021, and prostaglandin E2 [PGE2]) and inhibition of TGF-β signaling (A83-01) (Haider et al., 2018; Turco et al., 2018; **Table 1** and **Supplementary Table 3**). Interestingly, Noggin was not required, but Haider et al. (2018) retained it to limit differentiation. With only few medium alterations compared to trophoblast organoid culturing, Marinić et al. (2020) were able to derive endometrial gland organoids from term placentas which showed proper hormone responsiveness and molecular patterns distinct from the endometrial stromal cells, initially also present in the term placenta samples.

Taken together, these recent realizations have provided an interesting new port of entry in pregnancy research. The organoid models may generate unprecedented insight in the signal transduction cascade at both maternal and fetal side during embryo apposition, implantation and outgrowth, may impart in-depth understanding of the pathways leading to fetal growth restriction and pre-eclampsia, and may lead us to a better apprehension of genetic placental aberrations found at chorionic villus sampling (such as confined placental mosaicisms). Also, the organoid platform may provide insight in developmental biology of iatrogenically arrested pregnancies nesting in cesarean scar tissue or uterine niches, and shed light on unsolved questions in infertility research such as non-receptive endometria or recurrent implantation failure.

Adenomyosis and Endometriosis

Adenomyosis and endometriosis have been put forward as two distinct entities within the same continuum. Both conditions essentially display benign endometrial epithelium and stroma outside the uterine cavity, but affect different patient groups and are thought to arise through different pathogenic mechanisms. Adenomyosis boils down to the presence of ectopic endometrial tissue within the uterine wall that is fully confined within hypertrophic myometrium, supposedly owing to invagination (Frankl, 1925; Emge, 1962; Leyendecker et al., 2009). In endometriosis, endometrial tissue and cells are believed to translocate toward the peritoneal cavity by means of retrograde menstrual flow, after which they generate ectopic deposits on peritoneum and/or internal organs (Sampson, 1921, 1927; Leyendecker et al., 2009). For both diseases, however, alternative explanations - among which metaplasia is the most notable -, have been considered to remedy few remaining clinical shortcomings of the translocation theories (Gruenwald, 1942; Vannuccini et al., 2017; García-Solares et al., 2018; Koninckx et al., 2019). Valuable insights on mechanisms underlying pathogenesis and progression of both diseases have been obtained from non-human primate studies given that endometriosis naturally occurs only in this species with histopathological features consistent with the human disease (D'Hooghe et al., 1991, 1992; Fazleabas, 2010; Donnez et al., 2013). Although providing longitudinal insights in important primary endpoints such as fertility and pain-related behavior, this research approach suffers from multiple limitations including strong ethical concerns, labor-intensity and costliness, and still faces species-specific translatability restraints. Again, a myriad of mouse and *in vitro* cell culture models have been used to study endometriosis (Habiba, 2016; Greaves et al., 2017), however, encountering clear shortcomings including the inability to reproduce patient variability as well as phenotypic heterogeneity between different stages and types of endometriosis, and logically also species differences with endometriosis not natively occurring in mouse. The establishment by our group of robustly expandable 3D organoids from human endometriotic lesions, as well as from the (eutopic) endometrium of the same patients, provides more appropriate study models (Boretto et al., 2017, 2019; **Table 1** and **Supplementary Table 2**). Organoid development efficiency appeared somewhat lower than from healthy endometrium, likely secondary to the harsher experimental conditions needed to dissociate the endometriotic lesion. Medium components were similar. Organoids were developed from different endometriosis types (including superficial and deep peritoneal lesions) and different severity stages. Transplantation of the endometriotic organoids into the renal capsule of immunocompromised mice, or more orthotopically by intraperitoneal injection, resulted in outgrowth of representative lesions (Boretto et al., 2019). Recently, Esfandiari et al. (2021) also developed organoids from endometriotic biopsies and showed that methylation patterns from the primary tissue were robustly recapitulated. Now, to fully recapitulate the inflammatory character and immunological dysregulation of endometriosis, epithelial organoid cultures should be enriched with stromal cells that also play a role in endometriosis, and further with endothelial and immune cells, while provided with a scaffold that allows for angiogenesis, neurogenesis and immune cell influx. Such efforts should also be applied to adenomyosis, for which epithelial organoids have not

yet been described. Before, a co-culture model of adenomyotic epithelial cells, stromal cells and myocytes has been reported (Mehasseb et al., 2010).

Endometrial Hyperplasia and Cancer

Endometrial cancer (EC) is the second most common tumor of the FRT and its incidence is rising incessantly in industrialized countries, subjecting women to cancer- and therapy-related risks (Bray et al., 2018; Zhang et al., 2019b). EC is a heterogenic constellation of diseases for which etiopathogenesis has historically been dichotomized into two groups based on clinico-histological characteristics (Bokhman, 1983). Type I tumors were postulated to be estrogen-mediated, well-to-moderately differentiated endometrioid lesions on a background of juxtaposed hyperplasia in younger women. Type II EC referred to poorly differentiated tumors of endometrioid or non-endometrioid histology arising in a milieu of endometrial atrophy and were claimed to be estrogen-independent. There is also an important role for hereditary syndromes such as Lynch syndrome, that can result in endometrial cancers of both categories as well as a multitude of extra-uterine malignancies (Lynch et al., 2015). Sequencing efforts by The Cancer Genome Atlas (TCGA) Research Network later fine-tuned the knowledge of EC-related mutations and allowed for a more precise (i.e., resulting in superior distinction of low- versus high-risk EC) molecular classification that is outside the scope of this review (Cancer Genome Atlas Research Network, 2013).

To date, the identity of the primordially affected cells in humans is still unknown. Syed et al. (2020) advanced AXIN2+ (stem) cells in mice to be EC-initiating cells upon oncogenic transformation. Before, most insights were drawn from patient EC-derived cell lines such as Ishikawa and ECC-1 (well-differentiated), RL95-2, HEC1A and HEC1B (moderately differentiated), and KLE and AN3CA (metastatic, poorly differentiated) (Van Nyen et al., 2018). Genomic profiling showed their comparative and temporal stability with respect to copy number aberrations and EC-associated point mutations, but intra-tumor heterogeneity was lost in cell lines. Mouse xenograft models, starting from these cell lines or primary tumors (105–107) showed fair engraftment rates of about 60% although aggressive subtypes are more efficient in growing out (Wang et al., 2010; Cabrera et al., 2012; Korch et al., 2012). The xenografts showed 90% genetic similarity with the tumor (Depreeuw et al., 2015), displaying only low numbers of newly acquired SCNAs, but genetic drift was still observed (Ben-David et al., 2017). Further limitations of EC PDX are the inability to replicate full intra-tumor heterogeneity, to mimic the tumor micro-environment as mouse stroma gradually replaces the human stroma present in the transplanted tumor, the absence of immunomodulatory responses and difficulties to correctly simulate patient drug-responses (Depreeuw et al., 2015). With respect to representativeness, another step in this direction was taken by implementing 3D culturing techniques, as exemplified by spheroid cultures which were instrumental to uncover altered metabolism, polarity and drug susceptibility (Chitcholtan et al., 2012, 2013). Spheroid constructs have been applied to study carcinogenesis, either in isolation or as element in a co-culture or explant model (Hashimoto et al., 2017; Goad et al., 2018; Al-Juboori et al., 2019). To provide a more accurate rendering of EC, research groups embarked on establishing organoids from EC tumor samples (Dasari et al., 2017; Girda et al., 2017; Pauli et al., 2017; Turco et al., 2017; Boretto et al., 2019; **Table 1** and **Supplementary Table 2**). Organoid development was achieved, reliant on the typical factors such as RSPO1, Noggin, EGF, FGF2, FGF10, A83-01, NAC, and NAM, further promoted by addition of insulin-like growth factor 1 (IGF1), hepatocyte growth factor (HGF) and lipids. Importantly, it was necessary to lower p38i concentration to favor organoid growth from tumor cells above growth from healthy cells, also often present in the original biopsy. Interleukin-6 (IL6) and (non-)essential amino acids were also tested, but proved less important (Boretto et al., 2019). In addition to IHC and gene-expression characterization of the tumor organoids for endometrium/EC markers like estrogen receptor-α (ERα), progesterone receptor (PR), CK AE1/AE3, CK7, CK20, mucin 1 (MUC1), SRY-Box transcription factor 17 (SOX17), cluster of differentiation 10 (CD10), CD44 and/or aldehyde dehydrogenase 1 (ALDH1), two studies also defined and validated genomics and transcriptomics of the EC-derived organoids (Pauli et al., 2017; Boretto et al., 2019). Based on recapitulated mutations in AT-rich interaction domain 1A (*ARID1A*), β-Catenin (*CTNNB1*), F-box and WD repeat domain containing protein 7 (*FBXW7*), human epidermal growth factor receptor 2 (*HER2*), Polymerase-ε exonuclease domain (*POLE*) and phosphatase and tensin homolog (*PTEN*), organoids were tested for sensitivity to classic chemotherapeutics (5-fluorouracil, carboplatin, paclitaxel and doxorubicin), phosphoinositide 3-kinase (PI3K) inhibitors (apitolisib, buparlisib), inhibitors of mammalian target of rapamycin (mTOR) (everolimus), and histone deacetylase (HDAC) inhibitors (vorinostat, belinostat). Our group showed the organoids' ability to reproduce the phenotype of the spectrum of endometrial states, i.e., from healthy, over simple and complex hyperplasia with and without atypia, to cancerous endometrium, and to recapitulate mutations of Lynch syndrome patients (Boretto et al., 2019). Now that the necessary backbone is provided, next-generation organoid-based models can be developed including co-culture systems, which will lend themselves to extensive, or rather focused, drug testing and cutting-edge gene-editing exploration.

FALLOPIAN TUBES

The FT (or oviducts), functioning as relay between uterus and ovaries, consist of four zones with distinct histological architecture, i.e., the fimbriated and funneled infundibulum, the tortuous ampulla, the muscular isthmus and the circular and myometrialized interstitial/intramural portions (**Figure 5A**). In order to provide an appropriate environment for gamete conditioning, fertilization and ovum nutrition, and to allow proper transit of the zygote, secretory, ciliary and muscular functions of the different parts are aligned (Jarboe, 2014).

Since the first *in vitro* culturing of oviductal cells (McComb et al., 1986), several tactics have been applied to overcome their rapid senescence, loss of polarization, fibroblast overgrowth

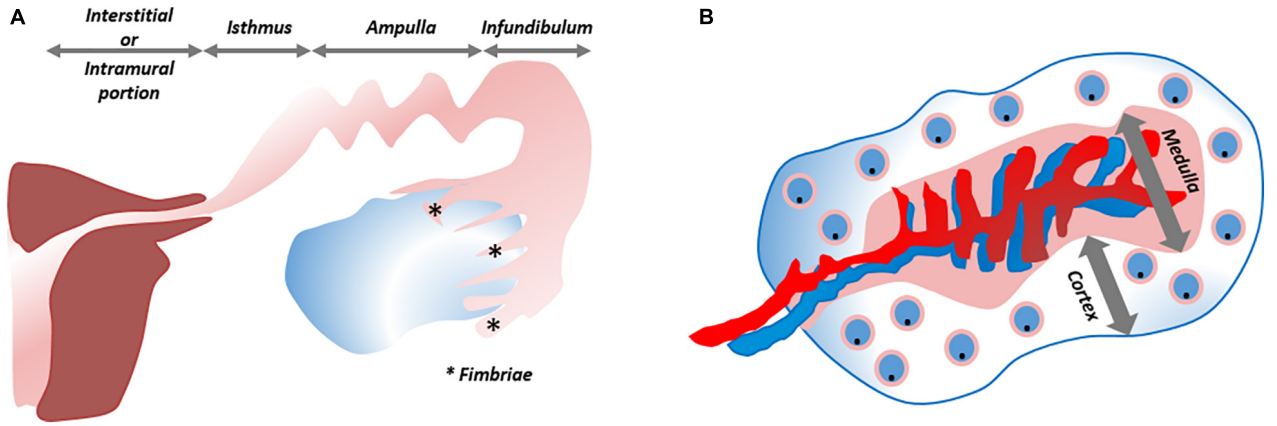

FIGURE 5 | Schematic overview of fallopian tube and ovary. **(A)** The fallopian tube consists of four zones with distinct histological architecture, from distal to proximal: infundibulum with its fimbriae (*), ampulla, isthmus and interstitial/intramural portion. **(B)** The ovary is divided into a cortical region in which the oocytes/follicles develop and the medulla that contains the larger blood vessels. ***Refers to "Fimbriae".

and deciliation/dedifferentiation (Henriksen et al., 1990; Ando et al., 2000; Levanon et al., 2010; Karst et al., 2011). Karst et al. (2011) immortalized 2D-grown oviductal cells, and showed their tumorigenicity upon injection in immunocompromised mice. Using a transwell approach, the same group also cultured non-immortalized fimbrial FT epithelial cells at air/liquid interface, thereby replicating typical structural, proteomic and secretomic features, and providing insight into DNA damage repair kinetics (Levanon et al., 2010). To surmount the yet limited propagation of this system, and the failure to simulate the oviducts' tubular folded architecture, further advanced 3D constructs were generated by placing minced mouse or baboon oviducts in alginate matrix, exposed to a precisely defined cocktail of hormones and growth factors (King et al., 2011). The immersed cells expressed the FT markers oviductin (OVGP1), paired box 8 (PAX8), E-cadherin, CK8 and acetylated tubulin (in cilia), and phenocopied the normal cell proliferation rate of the healthy donor. The main drawback was the limited culturing capacity (only for 7 days). The identification of label-retaining, putative stem cells in the distal oviduct of mice formed the impetus toward 3D organoid modeling using Matrigel (Wang et al., 2012). Grown under serum-free conditions, requiring only FGF2 and EGF, the organoid cells remained in an undifferentiated, slow-proliferative state for at least 10 weeks. Adding serum nudged cells to differentiate into various Müllerian derivatives, as exemplified by different expression patterns of ERα, PR, CD44, and progestagen associated endometrial protein (PAEP), and by the formation of hollow tubal structures through budding-out of the differentiating organoids. Kessler et al. (2015) were the first to develop organoids from human epithelial (epithelial cell adhesion molecule (EpCAM+) FT cells (**Table 1** and **Supplementary Table 4**). Wnt potentiation was indispensable for organoid propagation, and the Wnt-boosting LGR6 emerged as potential FT stem cell marker. Interestingly, *LGR6* expression was also found upregulated in endometriotic organoids when compared to healthy endometrium organoids (Boretto et al., 2019). Optimal expansion of FT organoids required WNT3A, RSPO1, EGF, FGF10, TGF-βr kinase inhibitor (SB431542) and Noggin. Both secretory and ciliated cells were present, giving credence to the possible existence of a common bipotent stem cell. Notch inhibition by use of a γ-secretase inhibitor propelled ciliogenesis (Kessler et al., 2015), as later also found in endometrial organoids (Haider et al., 2019). It was also demonstrated that the fimbrial ends of the oviducts possess the highest organoid-forming capacity, both in mouse (Xie et al., 2018) and human (Rose et al., 2020), and that human fimbrial ALDH+ cells replicate with higher frequency and form larger structures (Rose et al., 2020). Co-culturing of FT epithelial cells with FT stromal cells and endothelial (HUVEC) cells formed more complex organoid structures (Chang et al., 2020). FT epithelial cells could also be derived from induced pluripotent stem cells (iPSC) in which first an intermediate mesoderm state was induced, subsequently differentiated toward a FT phenotype *via* suppletion of WNT4 (or WNT3A), follistatin, E2 and P4 (Yucer et al., 2017).

The FT organoids were applied to explore the origin of ovarian cancer (OC) and to model infections with specific pathogens. Kopper et al. (2019) defined the optimal culture conditions to obtain organoids from both healthy FT and ovarian surface epithelium (OSE), alongside organoids from a broad spectrum of OC subtypes including high-risk patients with germline mutations in breast cancer types 1 and 2 susceptibility genes (BRCA1/2), thus allowing to study how their (unaffected) FT-derived organoids relates to OC. Organoid formation from FT, OSE, and OC required equal amounts of RSPO1, Noggin, NAC, NAM, A83-01, and ROCKi. Organoid derivation from healthy FT as compared to healthy OSE asked for less Wnt, but similar EGF levels. Maintenance of OSE organoids additionally needed forskolin, hydrocortisone, E2 and the tyrosine kinase activator heregulin-β1 in amounts equivalent to OC organoids. Kopper et al. (2019) were able to further optimize OC organoid formation efficiency by reducting of EGF and adding FGF10. Moreover, it was observed that only a subset of OC benefited from Wnt supplementation, moreover added at lower concentrations than for organoid derivation

from FT and OSE. Hoffmann et al. (2020) knocked down p53, PTEN and retinoblastoma (RB) tumor suppressor genes in FT organoids resulting in genomic instability, reduced apicobasal polarity, and larger and polymorphic nuclei compared to healthy controls. The modified organoids showed similarity to organoids derived from high-grade serous OC (HGSOC). In addition to sharing prominent morphological characteristics (such as nuclear atypia, increased DNA damage and altered epithelial organization) and transcriptomic traits (such as congruent upregulation of proto-oncogenes and downregulation of Wnt signaling), the medium optimized for HGSOC-derived organoids also promoted stemness in the modified FT organoids. Head-to-head comparisons between genetically rewired mouse FT and ovarian organoids supported that HGSOC can be derived from both cell populations, which may underlie HGSOC clinical heterogeneity, evidenced by differences in transcriptome, tumor kinetics and drug responses (Zhang et al., 2019a; Lõhmussaar et al., 2020). It has been proposed before that fimbrial ends of the FT form an equally important site of ovarian tumorigenesis (Dubeau, 1999; Karnezis et al., 2017). Thus, the FT organoids platform will allow researchers to delve deeper into the minimal (epi-)genetic requirements for oviductal tumorigenesis, using, amongst others, modern gene-editing techniques.

Acute and chronic salpingeal infections may cause progressive pelvic inflammatory disease and subsequent ectopic pregnancies and/or subfertility. With the emergence of multidrug-resistant sexually transmitted diseases, it is of paramount importance to have preclinical models to study host-microbe interplay, query treatments for infections, and develop regenerative therapies in case of surgical resections (Harris et al., 2018). Infection with *Chlamydia trachomatis* has recently been modeled in human FT organoids as well as in mouse endometrial organoids (Kessler et al., 2019; Bishop et al., 2020). Acute infection triggered a sustained response of inflammation and homeostatic repair. Infected cells containing bacterial inclusions extruded into the organoid lumen, after which adjacent cells compensatorily repleted their inlet. Owing to organoid longevity, also chronic chlamydiosis, known for its subclinical presentation, could be studied. Chronic infection of the organoids could model trace effects of infection, convalescence and reinfection, resulting in significantly increased organoid-forming capacity and increased EpCAM expression, even after successful treatment and curation of the chronic infection. A shift toward a less differentiated, secretory phenotype and epigenetic rewiring akin to aging are features reminiscent of OC.

OVARIES

The ovaries, consisting of a central medulla, peripheral cortex and overlying serosa, serve two main purposes: steroidogenesis and iterative oocyte maturation with subsequent transmission into the FT. The cortical region houses the developing oocytes/follicles (White et al., 2012; **Figure 5B**). It has been speculated many times that oogonial stem cells ("cortical reserve") may exist, but this hypothesis remains controversial and heavily debated. Cells expressing extracellular DEAD-box polypeptide 4 (ecDDX4) have been advanced as stem cell candidates, but recent single-cell omics identified these ecDDX4+ cells as perivascular cells (Fan et al., 2019; Wagner et al., 2020). To date, the Zuckerman axiom that a fixed number of oocytes is present and available throughout a woman's lifetime still stands (Zuckerman, 1951). Regarding the cortex-bordering OSE, organoid studies, as described above, may eventually lead to the identification of the OSE stem cells, which may also lie at the origin of epithelial ovarian cancer (EOC). With more than half of affected women succumbing to this disease, EOC is considered the most lethal gynecological cancer. This high death-to-incidence ratio is attributable to the fact that the majority of cases are diagnosed in advanced stages of disease, and due to rapid recurrences (Prat and FIGO Committee on Gynecologic Oncology, 2014; Lheureux et al., 2019). EOC is more than a single entity and comprises serous, mucinous, endometrioid and clear cell histological signatures. Exact origin and downstream pathobiology remain debated. As previously mentioned, both FT epithelium and OSE have been proposed and validated as originating tissues for EOC (Dubeau, 1999; Jarboe, 2014; Coscia et al., 2016; Karnezis et al., 2017; Zhang et al., 2019a; Hoffmann et al., 2020; Lõhmussaar et al., 2020). One-fifth of the patients are genetically predisposed (Walsh et al., 2011; Toss et al., 2015), and advancements in genetic testing, biomarker discovery and preclinical models are enabling the application of personalized therapies. Cell lines of EOC, used as preclinical models, suffer from genetic drift, cross-contamination and misidentification (Sandberg and Ernberg, 2005; Korch et al., 2012; Domcke et al., 2013). In particular, SK-OV-3 and A2780, the two most utilized cell lines to emulate HGSOC, lack its typical *TP53* mutation and distinctive somatic copy number alterations (SCNA). Instead, they harbor mutations typical for other histotypes (e.g., *ARID1A* and *PTEN*) (148). Given this incongruity as well as poor translatability with regards to clinical response, these cell lines are not highly apt as preclinical model of HGSOC (Matsuo et al., 2010). Xenografts grown from the cell lines face the same dire fate (Bobbs et al., 2015). Transgenic mouse models, although allowing to query early events in ovarian tumorigenesis, insufficiently recapitulate the full genomic landscape of HGSOC (Bobbs et al., 2015). Patient-derived xenografts in immunodeficient mice reproduce relevant HGSOC complications such as tumor invasion, expansion and metastasis, and retain histologic and genomic characteristics (at least at early passage), but lack the immune component (Dobbin et al., 2014; Weroha et al., 2014; Bobbs et al., 2015). In order to better reproduce tumor complexity, *in vitro* 3D spheroid models have been developed. Differentially expressed genes, altered tumor kinetics and more translatable drug responses have been noted using spheroids as compared to 2D cell lines (Zietarska et al., 2007; Raghavan et al., 2015). Immune and stromal components were added to scrutinize cancer stem cell pathways and cellular interactions (Raghavan et al., 2019). Spheroids were also used to study progression from normal OSE to preinvasive phenotypes (e.g., by tracking depolarization, disorganized stratification, overexpression of cancer markers and ultimately degradation of the subjacent basement membrane) (Kwong et al., 2009).

Studying these first steps from normal to invasive phenotype required OSE cells to be cultured in Matrigel-coated wells while suspended in a serum-containing medium supplemented with 2% Matrigel and continuously exposed to tumor necrosis factor α (TNF-α). The importance of TNF-α supports the association of tumorigenesis with chronic inflammation. The spheroids arose by aggregation, not by self-organization, and could not be maintained beyond 40 days. Nevertheless, the short-term 3D spheroid cultures were more representative than 2D setups when assessing OC drug sensitivities (Jabs et al., 2017).

Significant progress in OC modeling was generated by the development of organoids from OC as mentioned above. Organoid lines were established from a wide variety of OC, ranging from borderline tumors to invasive OC of various grades, stages and histologies (Kopper et al., 2019; **Table 1** and **Supplementary Table 4**). A preceding study showed that organoid establishment was feasible without forskolin, hydrocortisone, E2, heregulin-β1 and ROCKi but required FGF2, PGE2 and p38i, although organoid maintenance was only short-term and the study focused mainly on HGSOC (Hill et al., 2018). Subsequent studies emphasized the importance of heregulin-β1 (neuregulin-1) and low WNT environment for long-term EOC organoid expansion (Hoffmann et al., 2020; Maenhoudt et al., 2020). The OC-derived organoids mirrored the (epi-)genomic and transcriptomic landscape of their native tissue and exemplified tumor heterogeneity at different sites of metastatic disease (Kopper et al., 2019). Organoid gene transcript clustering provided arguments for the hypothesis that borderline tumor may transition into OC. Organoids were amenable to gene-editing, xenografting and drug-sensitivity profiling (Hill et al., 2018; Kopper et al., 2019; Maru et al., 2019b; Phan et al., 2019; Chen et al., 2020; Hoffmann et al., 2020; Lõhmussaar et al., 2020; Maenhoudt et al., 2020). Hill et al. (2018) functionally studied HGSOC-specific homologous recombination deficiency (HRD) and replication fork instability, and observed that functional assays (i.e., drug-testing) systematically outperformed the data obtained from mutational profiles alone, moreover in keeping with the parallel clinical reality. Further developments were achieved to circumvent the possible interference of the gel-based scaffold with drug diffusion (using resuspended organoids) and to apply the organoid platform in high-throughput settings (Maru et al., 2019b; Phan et al., 2019). Drug sensitivity was linked to well-recapitulated individual (epi-)genomic and transcriptomic profiles (Phan et al., 2019; Chen et al., 2020; de Witte et al., 2020; Nanki et al., 2020; Zhang et al., 2020). To a further extent, the organoids reliably simulated intra- and inter-patient drug response heterogeneity and were able to predict useful therapeutic agents in the majority of cases, longitudinally compared to patient-wide clinical outcomes albeit retrospectively (de Witte et al., 2020). These findings put us at the brink of a new era in which the predictive value of OC-derived organoids will be prospectively tested in clinical trials. The prospect of more complex organoid models also encompassing immune, stromal and/or vascular cells, raises the hope to in the future test clinically relevant drugs that tackle neo-angiogenesis and tumor immunology. Indeed, short-term 3D spheroid co-cultures of HGSOC cells with immune cells have shown sensitivity to immune checkpoint inhibitors (Wan et al., 2020).

CONCLUDING REMARKS

Over the past decades, we have witnessed an important paradigm shift in preclinical modeling of healthy and diseased tissues. With respect to the organs of the female reproductive system concentrated in and near the pelvis, organoids have gradually assumed a pivotal position in research. Considering their efficient establishment and propagation, their amenability to state-of-the-art techniques (such as gene-editing and single-cell omics), their *in vivo* transplantability and their positive translational power, this promising technology has spurred an invaluable amount of *in vitro* and *in vivo* realizations. Organoids provide an unprecedented opportunity to practice personalized medicine. The most important hurdle that lies ahead is to further enrich the established organoid culturing systems, by adding stromal, vascular and immune components to still better mimic real-life conditions. Rightfully wielding this momentum by means of parallel clinical trials (Vlachogiannis et al., 2018; Ooft et al., 2019) will now be of paramount importance to further close the gap between bench and bedside.

AUTHOR CONTRIBUTIONS

RH devised the idea, performed the literature search, and wrote the manuscript. ZJ performed a simultaneous and focused organoid-specific literature search. RH and ZJ independently constructed the tables. RH designed and adapted the figures. HV amended and co-wrote the manuscript. DT and HV provided funding and essential insights to produce this manuscript. All authors critically appraised the manuscript, which was finalized by RH.

FUNDING

This work was supported by grants from the KU Leuven Research Fund and from the FWO-Flanders (Belgium). DT is a Senior Clinical Investigator of the FWO.

ACKNOWLEDGMENTS

We would like to thank all present and former lab members and clinical associates for insightful discussions. We would also like to thank Miha Gašperin for his help in the initial conceptualization of the organoid overview figures, which we later amended and fine-tuned.

SUPPLEMENTARY MATERIAL

The Supplementary Material for this article can be found online at: https://www.frontiersin.org/articles/10.3389/fcell.2021.661472/full#supplementary-material

Supplementary Table 1 | Recruitment details and medium compositions of human vulvar, vaginal and cervical organoid studies.

Supplementary Table 2 | Recruitment details and medium compositions of human endometrial organoid studies.

Supplementary Table 3 | Recruitment details and medium compositions of pregnancy-related organoid studies.

Supplementary Table 4 | Recruitment details and medium compositions of human ovarian organoid studies.

REFERENCES

Adissu, H. A., Asem, E. K., and Lelièvre, S. A. (2007). Three-dimensional cell culture to model epithelia in the female reproductive system. *Reprod. Sci.* 14(Suppl. 8), 11–19. doi: 10.1177/1933719107310872

Aflatoonian, R., Tuckerman, E., Elliott, S. L., Bruce, C., Aflatoonian, A., Li, T. C., et al. (2007). Menstrual cycle-dependent changes of toll-like receptors in endometrium. *Hum. Reprod.* 22, 586–593. doi: 10.1093/humrep/del388

Ali, A., Syed, S. M., Jamaluddin, M., Colino-Sanguino, Y., Gallego-Ortega, D., and Tanwar, P. S. (2020). Cell lineage tracing identifies hormone-regulated and Wnt-responsive vaginal epithelial stem cells. *Cell Rep.* 30, 1463–1477.e7. doi: 10.1016/j.celrep.2020.01.003

Al-Juboori, A., Ghosh, A., Jamaluddin, M., Kumar, M., Sahoo, S. S., Syed, S. M., et al. (2019). Proteomic analysis of stromal and epithelial cell communications in human endometrial cancer using a unique 3D co-culture model. *Proteomics* 19: e1800448. doi: 10.1002/pmic.201800448

Ando, H., Kobayashi, M., Toda, S., Kikkawa, F., Masahashi, T., and Mizutani, S. (2000). Establishment of a ciliated epithelial cell line from human Fallopian tube. *Hum. Reprod.* 15, 1597–1603. doi: 10.1093/humrep/15.7.1597

Ben-David, U., Ha, G., Tseng, Y. Y., Greenwald, N. F., Oh, C., Shih, J., et al. (2017). Patient-derived xenografts undergo mouse-specific tumor evolution. *Nat. Genet.* 49, 1567–1575. doi: 10.1038/ng.3967

Bentin-Ley, U., Pedersen, B., Lindenberg, S., Larsen, J. F., Hamberger, L., and Horn, T. (1994). Isolation and culture of human endometrial cells in a three-dimensional culture system. *J. Reprod. Fertil.* 101, 327–332. doi: 10.1530/jrf.0.1010327

Berrington de González, A., Sweetland, S., and Green, J. (2004). Comparison of risk factors for squamous cell and adenocarcinomas of the cervix: a meta-analysis. *Br. J. Cancer.* 90, 1787–1791. doi: 10.1038/sj.bjc.6601764

Bienkowska-Haba, M., Luszczek, W., Myers, J. E., Keiffer, T. R., DiGiuseppe, S., Polk, P., et al. (2018). A new cell culture model to genetically dissect the complete human papillomavirus life cycle. *PLoS Pathog.* 14:e1006846. doi: 10.1371/journal.ppat.1006846

Bishop, R. C., Boretto, M., Rutkowski, M. R., Vankelecom, H., and Derré, I. (2020). Murine endometrial organoids to model *Chlamydia* infection. *Front. Cell. Infect. Microbiol.* 10:416. doi: 10.3389/fcimb.2020.00416

Bläuer, M., Heinonen, P. K., Martikainen, P. M., Tomás, E., and Ylikomi, T. (2005). A novel organotypic culture model for normal human endometrium: regulation of epithelial cell proliferation by estradiol and medroxyprogesterone acetate. *Hum. Reprod.* 20, 864–871. doi: 10.1093/humrep/deh722

Bläuer, M., Heinonen, P. K., Rovio, P., and Ylikomi, T. (2008). Effects of tamoxifen and raloxifene on normal human endometrial cells in an organotypic in vitro model. *Eur. J. Pharmacol.* 592, 13–18. doi: 10.1016/j.ejphar.2008.06.091

Bobbs, A. S., Cole, J. M., and Cowden Dahl, K. D. (2015). Emerging and evolving ovarian cancer animal models. *Cancer Growth Metastasis* 8(Suppl. 1), 29–36. doi: 10.4137/CGM.S21221

Bokhman, J. V. (1983). Two pathogenetic types of endometrial carcinoma. *Gynecol. Oncol.* 15, 10–17. doi: 10.1016/0090-8258(83)90111-7

Boonekamp, K. E., Kretzschmar, K., Wiener, D. J., Asra, P., Derakhshan, S., Puschhof, J., et al. (2019). Long-term expansion and differentiation of adult murine epidermal stem cells in 3D organoid cultures. *Proc. Natl. Acad. Sci. U.S.A.* 116, 14630–14638. doi: 10.1073/pnas.1715272116

Boretto, M., Cox, B., Noben, M., Hendriks, N., Fassbender, A., Roose, H., et al. (2017). Development of organoids from mouse and human endometrium showing endometrial epithelium physiology and long-term expandability. *Development* 144, 1775–1786. doi: 10.1242/dev.148478

Boretto, M., Maenhoudt, N., Luo, X., Hennes, A., Boeckx, B., Bui, B., et al. (2019). Patient-derived organoids from endometrial disease capture clinical heterogeneity and are amenable to drug screening. *Nat. Cell Biol.* 21, 1041–1051. doi: 10.1038/s41556-019-0360-z

Brauer, P. R. (2009). "Development of the urogenital system," in *Larsen's Human Embryology*, 4th Edn, eds G. C. Schoenwolf, S. B. Bleyl, P. R. Brauer, and P. H. Francis-West (Philadelphia, PA: Churchill Livingstone), 479–541.

Bray, F., Carstensen, B., Møller, H., Zappa, M., Zakelj, M. P., Lawrence, G., et al. (2005). Incidence trends of adenocarcinoma of the cervix in 13 European countries. *Cancer Epidemiol. Biomarkers Prev.* 14, 2191–2199. doi: 10.1158/1055-9965.EPI-05-0231

Bray, F., Ferlay, J., Soerjomataram, I., Siegel, R. L., Torre, L. A., and Jemal, A. (2018). Global cancer statistics 2018: GLOBOCAN estimates of incidence and mortality worldwide for 36 cancers in 185 countries. *CA Cancer J. Clin.* 68, 394–424. doi: 10.3322/caac.21492

Bui, B. N., Boretto, M., Kobayashi, H., van Hoesel, M., Steba, G. S., van Hoogenhuijze, N., et al. (2020). Organoids can be established reliably from cryopreserved biopsy catheter-derived endometrial tissue of infertile women. *Reprod. Biomed. Online* 41, 465–473. doi: 10.1016/j.rbmo.2020.03.019

Bulmer, D. (1957). The development of the human vagina. *J. Anat.* 91, 490–509.

Cabrera, S., Llauradó, M., Castellví, J., Fernandez, Y., Alameda, F., Colás, E., et al. (2012). Generation and characterization of orthotopic murine models for endometrial cancer. *Clin. Exp. Metastasis* 29, 217–227. doi: 10.1007/s10585-011-9444-2

Cancer Genome Atlas Research Network (2013). Integrated genomic characterization of endometrial carcinoma. *Nature* 497, 67–73. doi: 10.1038/nature12113

Cancer Genome Atlas Research Network (2017). Integrated genomic and molecular characterization of cervical cancer. *Nature* 543, 378–384. doi: 10.1038/nature21386

Chang, Y. H., Chu, T. Y., and Ding, D. C. (2020). Human fallopian tube epithelial cells exhibit stemness features, self-renewal capacity, and Wnt-related organoid formation. *J. Biomed. Sci.* 27:32. doi: 10.1186/s12929-019-0602-1

Chen, H., Gotimer, K., De Souza, C., Tepper, C. G., Karnezis, A. N., Leiserowitz, G. S., et al. (2020). Short-term organoid culture for drug sensitivity testing of high-grade serous carcinoma. *Gynecol. Oncol.* 157, 783–792. doi: 10.1016/j.ygyno.2020.03.026

Chitcholtan, K., Asselin, E., Parent, S., Sykes, P. H., and Evans, J. J. (2013). Differences in growth properties of endometrial cancer in three dimensional (3D) culture and 2D cell monolayer. *Exp. Cell Res.* 319, 75–87. doi: 10.1016/j.yexcr.2012.09.012

Chitcholtan, K., Sykes, P. H., and Evans, J. J. (2012). The resistance of intracellular mediators to doxorubicin and cisplatin are distinct in 3D and 2D endometrial cancer. *J. Transl. Med.* 10:38. doi: 10.1186/1479-5876-10-38

Chumduri, C., Gurumurthy, R. K., Berger, H., Dietrich, O., Kumar, N., Koster, S., et al. (2021). Opposing Wnt signals regulate cervical squamocolumnar homeostasis and emergence of metaplasia. *Nat. Cell Biol.* 23, 184–197. doi: 10.1038/s41556-020-00619-0

Chumduri, C., Gurumurthy, R. K., Berger, H., Koster, S., Brinkmann, V., Klemm, U., et al. (2018). Transition of Wnt signaling microenvironment delineates the squamo-columnar junction and emergence of squamous metaplasia of the cervix. *bioRxiv* [Preprint] doi: 10.1101/443770

Clevers, H., Loh, K. M., and Nusse, R. (2014). Stem cell signaling. An integral program for tissue renewal and regeneration: Wnt signaling and stem cell control. *Science* 346:1248012. doi: 10.1126/science.1248012

Cochrane, D. R., Campbell, K. R., Greening, K., Ho, G. C., Hopkins, J., Bui, M., et al. (2020). Single cell transcriptomes of normal endometrial derived organoids uncover novel cell type markers and cryptic differentiation of primary tumours. *J. Pathol.* 252, 201–214. doi: 10.1002/path.5511

Coscia, F., Watters, K. M., Curtis, M., Eckert, M. A., Chiang, C. Y., Tyanova, S., et al. (2016). Integrative proteomic profiling of ovarian cancer cell lines reveals precursor cell associated proteins and functional status. *Nat. Commun.* 7:12645. doi: 10.1038/ncomms12645

Cunha, G. R. (1976). Stromal induction and specification of morphogenesis and cytodifferentiation of the epithelia of the Mullerian ducts and urogenital sinus

during development of the uterus and vagina in mice. *J. Exp. Zool.* 196, 361–370. doi: 10.1002/jez.1401960310

Dasari, V. R., Mazack, V., Feng, W., Nash, J., Carey, D. J., and Gogoi, R. (2017). Verteporfin exhibits YAP-independent anti-proliferative and cytotoxic effects in endometrial cancer cells. *Oncotarget* 8, 28628–28640. doi: 10.18632/oncotarget.15614

de Martel, C., Plummer, M., Vignat, J., and Franceschi, S. (2017). Worldwide burden of cancer attributable to HPV by site, country and HPV type. *Int. J. Cancer* 141, 664–670. doi: 10.1002/ijc.30716

de Sanjose, S., Quint, W. G., Alemany, L., Geraets, D. T., Klaustermeier, J. E., Lloveras, B., et al. (2010). Human papillomavirus genotype attribution in invasive cervical cancer: a retrospective cross-sectional worldwide study. *Lancet Oncol.* 11, 1048–1056. doi: 10.1016/S1470-2045(10)70230-8

de Witte, C. J., Espejo Valle-Inclan, J., Hami, N., Lõhmussaar, K., Kopper, O., Vreuls, C., et al. (2020). Patient-derived ovarian cancer organoids mimic clinical response and exhibit heterogeneous inter- and intrapatient drug responses. *Cell Rep.* 31:107762. doi: 10.1016/j.celrep.2020.107762

Delvenne, P., Hubert, P., Jacobs, N., Giannini, S. L., Havard, L., Renard, I., et al. (2001). The organotypic culture of HPV-transformed keratinocytes: an effective in vitro model for the development of new immunotherapeutic approaches for mucosal (pre)neoplastic lesions. *Vaccine* 19, 2557–2564. doi: 10.1016/s0264-410x(00)00489-8

Deng, H., Hillpot, E., Mondal, S., Khurana, K. K., and Woodworth, C. D. (2018). HPV16-immortalized cells from human transformation zone and endocervix are more dysplastic than ectocervical cells in organotypic culture. *Sci. Rep.* 8:15402. doi: 10.1038/s41598-018-33865-2

Depreeuw, J., Hermans, E., Schrauwen, S., Annibali, D., Coenegrachts, L., Thomas, D., et al. (2015). Characterization of patient-derived tumor xenograft models of endometrial cancer for preclinical evaluation of targeted therapies. *Gynecol. Oncol.* 139, 118–126. doi: 10.1016/j.ygyno.2015.07.104

D'Hooghe, T. M., Bambra, C. S., Cornillie, F. J., Isahakia, M., and Koninckx, P. R. (1991). Prevalence and laparoscopic appearance of spontaneous endometriosis in the baboon (*Papio anubis, Papio cynocephalus*). *Biol. Reprod.* 45, 411–416. doi: 10.1095/biolreprod45.3.411

D'Hooghe, T. M., Bambra, C. S., Isahakia, M., and Koninckx, P. R. (1992). Evolution of spontaneous endometriosis in the baboon (*Papio anubis, Papio cynocephalus*) over a 12-month period. *Fertil. Steril.* 58, 409–412. doi: 10.1016/S0015-0282(16)55190-5

Diao, J., Liu, J., Wang, S., Chang, M., Wang, X., Guo, B., et al. (2019). Sweat gland organoids contribute to cutaneous wound healing and sweat gland regeneration. *Cell Death Dis.* 10:238. doi: 10.1038/s41419-019-1485-5

Dijkstra, K. K., Cattaneo, C. M., Weeber, F., Chalabi, M., van de Haar, J., Fanchi, L. F., et al. (2018). Generation of tumor-reactive T cells by co-culture of peripheral blood lymphocytes and tumor organoids. *Cell* 174, 1586–1598.e12. doi: 10.1016/j.cell.2018.07.009

Dobbin, Z. C., Katre, A. A., Steg, A. D., Erickson, B. K., Shah, M. M., Alvarez, R. D., et al. (2014). Using heterogeneity of the patient-derived xenograft model to identify the chemoresistant population in ovarian cancer. *Oncotarget* 5, 8750–8764. doi: 10.18632/oncotarget.2373

Domcke, S., Sinha, R., Levine, D. A., Sander, C., and Schultz, N. (2013). Evaluating cell lines as tumour models by comparison of genomic profiles. *Nat. Commun.* 4:2126. doi: 10.1038/ncomms3126

Donnez, O., Van Langendonckt, A., Defrère, S., Colette, S., Van Kerk, O., Dehoux, J. P., et al. (2013). Induction of endometriotic nodules in an experimental baboon model mimicking human deep nodular lesions. *Fertil. Steril.* 99, 783–789.e3. doi: 10.1016/j.fertnstert.2012.10.032

Dubeau, L. (1999). The cell of origin of ovarian epithelial tumors and the ovarian surface epithelium dogma: does the emperor have no clothes? *Gynecol. Oncol.* 72, 437–442. doi: 10.1006/gyno.1998.5275

Dyson, N., Howley, P. M., Münger, K., and Harlow, E. (1989). The human papilloma virus-16 E7 oncoprotein is able to bind to the retinoblastoma gene product. *Science* 243, 934–937. doi: 10.1126/science.2537532

Emge, L. A. (1962). The elusive adenomyosis of the uterus. Its historical past and its present state of recognition. *Am. J. Obstet. Gynecol.* 83, 1541–1563. doi: 10.1016/0002-9378(62)90170-9

Esfandiari, F., Favaedi, R., Heidari-Khoei, H., Chitsazian, F., Yari, S., Piryaei, A., et al. (2021). Insight into epigenetics of human endometriosis organoids: DNA methylation analysis of HOX genes and their cofactors. *Fertil. Steril.* 115, 125–137. doi: 10.1016/j.fertnstert.2020.08.1398

Fan, X., Bialecka, M., Moustakas, I., Lam, E., Torrens-Juaneda, V., Borggreven, N. V., et al. (2019). Single-cell reconstruction of follicular remodeling in the human adult ovary. *Nat. Commun.* 10:3164. doi: 10.1038/s41467-019-11036-9

Fazleabas, A. T. (2010). Progesterone resistance in a baboon model of endometriosis. *Semin. Reprod. Med.* 28, 75–80. doi: 10.1055/s-0029-1242997

Fitzgerald, H. C., Dhakal, P., Behura, S. K., Schust, D. J., and Spencer, T. E. (2019). Self-renewing endometrial epithelial organoids of the human uterus. *Proc. Natl. Acad. Sci. U.S.A.* 116, 23132–23142. doi: 10.1073/pnas.1915389116

Flores, E. R., Allen-Hoffmann, B. L., Lee, D., Sattler, C. A., and Lambert, P. F. (1999). Establishment of the human papillomavirus type 16 (HPV-16) life cycle in an immortalized human foreskin keratinocyte cell line. *Virology* 262, 344–354. doi: 10.1006/viro.1999.9868

Frankl, O. (1925). Adenomyosis uteri. *Am. J. Obstet. Gynecol.* 10, 680–684.

García-Solares, J., Donnez, J., Donnez, O., and Dolmans, M. M. (2018). Pathogenesis of uterine adenomyosis: invagination or metaplasia? *Fertil. Steril.* 109, 371–379. doi: 10.1016/j.fertnstert.2017.12.030

Gargett, C. E., Schwab, K. E., and Deane, J. A. (2016). Endometrial stem/progenitor cells: the first 10 years. *Hum. Reprod. Update* 22, 137–163. doi: 10.1093/humupd/dmv051

Gartler, S. M. (1968). Apparent Hela cell contamination of human heteroploid cell lines. *Nature* 217, 750–751. doi: 10.1038/217750a0

Gey, G. O., Coffmann, W. D., and Kubicek, M. T. (1952). Tissue culture studies of the proliferative capacity of cervical carcinoma and normal epithelium. *Cancer Res.* 12, 264–265.

Girda, E., Huang, E. C., Leiserowitz, G. S., and Smith, L. H. (2017). The use of endometrial cancer patient-derived organoid culture for drug sensitivity testing is feasible. *Int. J. Gynecol. Cancer* 27, 1701–1707. doi: 10.1097/IGC.0000000000001061

Goad, J., Ko, Y. A., Kumar, M., Jamaluddin, M., and Tanwar, P. S. (2018). Oestrogen fuels the growth of endometrial hyperplastic lesions initiated by overactive Wnt/β-catenin signalling. *Carcinogenesis* 39, 1105–1116. doi: 10.1093/carcin/bgy079

Gray, C. A., Bartol, F. F., Tarleton, B. J., Wiley, A. A., Johnson, G. A., Bazer, F. W., et al. (2001). Developmental biology of uterine glands. *Biol. Reprod.* 65, 1311–1323. doi: 10.1095/biolreprod65.5.1311

Greaves, E., Critchley, H., Horne, A. W., and Saunders, P. (2017). Relevant human tissue resources and laboratory models for use in endometriosis research. *Acta Obstet. Gynecol. Scand.* 96, 644–658. doi: 10.1111/aogs.13119

Gruenwald, P. (1942). Origin of endometriosis from the mesenchyme of the celomic walls. *Am. J. Obstet. Gynecol.* 44, 470–474.

Gupta, A. C., Chawla, S., Hegde, A., Singh, D., Bandyopadhyay, B., Lakshmanan, C. C., et al. (2018). Establishment of an in vitro organoid model of dermal papilla of human hair follicle. *J. Cell. Phys.* 233, 9015–9030. doi: 10.1002/jcp.26853

Habiba, M. (2016). "The animal model of adenomyosis," in *Uterine Adenomyosis*, 1st Edn, eds M. Habiba and G. Benagiano (Cham: Springer), 123–127.

Haider, S., Gamperl, M., Burkard, T. R., Kunihs, V., Kaindl, U., Junttila, S., et al. (2019). Estrogen signaling drives ciliogenesis in human endometrial organoids. *Endocrinology* 160, 2282–2297. doi: 10.1210/en.2019-00314

Haider, S., Meinhardt, G., Saleh, L., Kunihs, V., Gamperl, M., Kaindl, U., et al. (2018). Self-renewing trophoblast organoids recapitulate the developmental program of the early human placenta. *Stem Cell Rep.* 11, 537–551. doi: 10.1016/j.stemcr.2018.07.004

Hanahan, D., and Weinberg, R. A. (2011). Hallmarks of cancer: the next generation. *Cell* 144, 646–674. doi: 10.1016/j.cell.2011.02.013

Harris, S. R., Cole, M. J., Spiteri, G., Sánchez-Busó, L., Golparian, D., Jacobsson, S., et al. (2018). Public health surveillance of multidrug-resistant clones of *Neisseria gonorrhoeae* in Europe: a genomic survey. *Lancet Infect. Dis.* 18, 758–768. doi: 10.1016/S1473-3099(18)30225-1

Hashimoto, S., Tabuchi, Y., Yurino, H., Hirohashi, Y., Deshimaru, S., Asano, T., et al. (2017). Comprehensive single-cell transcriptome analysis reveals heterogeneity in endometrioid adenocarcinoma tissues. *Sci. Rep.* 7:14225. doi: 10.1038/s41598-017-14676-3

Hennes, A., Held, K., Boretto, M., De Clercq, K., Van den Eynde, C., Vanhie, A., et al. (2019). Functional expression of the mechanosensitive PIEZO1 channel

in primary endometrial epithelial cells and endometrial organoids. *Sci. Rep.* 9:1779. doi: 10.1038/s41598-018-38376-8

Henriksen, T., Tanbo, T., Abyholm, T., Oppedal, B. R., Claussen, O. P., and Hovig, T. (1990). Epithelial cells from human fallopian tube in culture. *Hum. Reprod.* 5, 25–31. doi: 10.1093/oxfordjournals.humrep.a137034

Herfs, M., Vargas, S. O., Yamamoto, Y., Howitt, B. E., Nucci, M. R., Hornick, J. L., et al. (2013). A novel blueprint for 'top down' differentiation defines the cervical squamocolumnar junction during development, reproductive life, and neoplasia. *J. Pathol.* 229, 460–468. doi: 10.1002/path.4110

Herfs, M., Yamamoto, Y., Laury, A., Wang, X., Nucci, M. R., McLaughlin-Drubin, M. E., et al. (2012). A discrete population of squamocolumnar junction cells implicated in the pathogenesis of cervical cancer. *Proc. Natl. Acad. Sci. U.S.A.* 109, 10516–10521. doi: 10.1073/pnas.1202684109

Hibiya, S., Tsuchiya, K., Hayashi, R., Fukushima, K., Horita, N., Watanabe, S., et al. (2017). Long-term inflammation transforms intestinal epithelial cells of colonic organoids. *J. Crohns Colitis* 11, 621–630. doi: 10.1093/ecco-jcc/jjw186

Hill, S. J., Decker, B., Roberts, E. A., Horowitz, N. S., Muto, M. G., Worley, M. J. Jr., et al. (2018). Prediction of DNA repair inhibitor response in short-term patient-derived ovarian cancer organoids. *Cancer Discov.* 8, 1404–1421. doi: 10.1158/2159-8290.CD-18-0474

Hoffmann, C., Bachran, C., Stanke, J., Elezkurtaj, S., Kaufmann, A. M., Fuchs, H., et al. (2010). Creation and characterization of a xenograft model for human cervical cancer. *Gynecol. Oncol.* 118, 76–80. doi: 10.1016/j.ygyno.2010.03.019

Hoffmann, K., Berger, H., Kulbe, H., Thillainadarasan, S., Mollenkopf, H. J., Zemojtel, T., et al. (2020). Stable expansion of high-grade serous ovarian cancer organoids requires a low-Wnt environment. *EMBO J.* 39:e104013. doi: 10.15252/embj.2019104013

Iguchi, T., Uchima, F.-D. A., Ostrander, P. L., and Bern, H. A. (1983). Growth of normal mouse vaginal epithelial cells in and on collagen gels. *Proc. Natl. Acad. Sci. U.S.A.* 80, 3743–3747.

Iguchi, T., Uchima, F.-D. A., Ostrander, P. L., Hamamoto, S. T., and Bern, H. A. (1985). Proliferation of normal mouse uterine luminal epithelial cells in serum-free collagen gel culture. *Proc. Jpn. Acad. Ser. B Phys. Biol. Sci.* 61, 292–295.

Jabs, J., Zickgraf, F. M., Park, J., Wagner, S., Jiang, X., Jechow, K., et al. (2017). Screening drug effects in patient-derived cancer cells links organoid responses to genome alterations. *Mol. Syst. Biol.* 13:955. doi: 10.15252/msb.20177697

Jarboe, E. A. (2014). "Fallopian tube," in *Pathology of the Female Reproductive Tract*, 3rd Edn, eds G. L. Mutter and J. Prat (London: Churchill Livingstone), 459–486.

Jones, R. L., Critchley, H. O., Brooks, J., Jabbour, H. N., and McNeilly, A. S. (1998). Localization and temporal expression of prolactin receptor in human endometrium. *J. Endocrinol. Metab.* 83, 258–262. doi: 10.1210/jcem.83.1.4506

Karnezis, A. N., Cho, K. R., Gilks, C. B., Pearce, C. L., and Huntsman, D. G. (2017). The disparate origins of ovarian cancers: pathogenesis and prevention strategies. *Nat. Rev. Cancer* 17, 65–74. doi: 10.1038/nrc.2016.113

Karst, A. M., Levanon, K., and Drapkin, R. (2011). Modeling high-grade serous ovarian carcinogenesis from the fallopian tube. *Proc. Natl. Acad. Sci. U.S.A.* 108, 7547–7552. doi: 10.1073/pnas.1017300108

Kessler, M., Hoffmann, K., Brinkmann, V., Thieck, O., Jackisch, S., Toelle, B., et al. (2015). The Notch and Wnt pathways regulate stemness and differentiation in human fallopian tube organoids. *Nat. Commun.* 6:8989. doi: 10.1038/ncomms9989

Kessler, M., Hoffmann, K., Fritsche, K., Brinkmann, V., Mollenkopf, H. J., Thieck, O., et al. (2019). Chronic *Chlamydia* infection in human organoids increases stemness and promotes age-dependent CpG methylation. *Nat. Commun.* 10:1194. doi: 10.1038/s41467-019-09144-7

Kim, M., Fevre, C., Lavina, M., Disson, O., and Lecuit, M. (2021). Live imaging reveals *Listeria* hijacking of E-cadherin recycling as it crosses the intestinal barrier. *Curr. Biol.* 31, 1037–1047.e4. doi: 10.1016/j.cub.2020.11.041

King, S. M., Hilliard, T. S., Wu, L. Y., Jaffe, R. C., Fazleabas, A. T., and Burdette, J. E. (2011). The impact of ovulation on fallopian tube epithelial cells: evaluating three hypotheses connecting ovulation and serous ovarian cancer. *Endocr. Relat. Cancer* 18, 627–642. doi: 10.1530/ERC-11-0107

Kleinman, H. K., McGarvey, M. L., Hassell, J. R., Star, V. L., Cannon, F. B., Laurie, G. W., et al. (1986). Basement membrane complexes with biological activity. *Biochemistry* 25, 312–318. doi: 10.1021/bi00350a005

Koninckx, P. R., Ussia, A., Adamyan, L., Wattiez, A., Gomel, V., and Martin, D. C. (2019). Pathogenesis of endometriosis: the genetic/epigenetic theory. *Fertil. Steril.* 111, 327–340. doi: 10.1016/j.fertnstert.2018.10.013

Kopper, O., de Witte, C. J., Lõhmussaar, K., Valle-Inclan, J. E., Hami, N., Kester, L., et al. (2019). An organoid platform for ovarian cancer captures intra- and interpatient heterogeneity. *Nat. Med.* 25, 838–849. doi: 10.1038/s41591-019-0422-6

Korch, C., Spillman, M. A., Jackson, T. A., Jacobsen, B. M., Murphy, S. K., Lessey, B. A., et al. (2012). DNA profiling analysis of endometrial and ovarian cell lines reveals misidentification, redundancy and contamination. *Gynecol. Oncol.* 127, 241–248. doi: 10.1016/j.ygyno.2012.06.017

Kwong, J., Chan, F. L., Wong, K. K., Birrer, M. J., Archibald, K. M., Balkwill, F. R., et al. (2009). Inflammatory cytokine tumor necrosis factor alpha confers precancerous phenotype in an organoid model of normal human ovarian surface epithelial cells. *Neoplasia* 11, 529–541. doi: 10.1593/neo.09112

Lei, M., Schumacher, L. J., Lai, Y. C., Juan, W. T., Yeh, C. Y., Wu, P., et al. (2017). Self-organization process in newborn skin organoid formation inspires strategy to restore hair regeneration of adult cells. *Proc. Natl. Acad. Sci. U.S.A.* 114, E7101–E7110. doi: 10.1073/pnas.1700475114

Levanon, K., Ng, V., Piao, H. Y., Zhang, Y., Chang, M. C., Roh, M. H., et al. (2010). Primary ex vivo cultures of human fallopian tube epithelium as a model for serous ovarian carcinogenesis. *Oncogene* 29, 1103–1113. doi: 10.1038/onc.2009.402

Leyendecker, G., Wildt, L., and Mall, G. (2009). The pathophysiology of endometriosis and adenomyosis: tissue injury and repair. *Arch. Gynecol. Obstet.* 280, 529–538. doi: 10.1007/s00404-009-1191-0

Lheureux, S., Gourley, C., Vergote, I., and Oza, A. M. (2019). Epithelial ovarian cancer. *Lancet* 393, 1240–1253. doi: 10.1016/S0140-6736(18)32552-2

Li, S., Herrera, G. G., Tam, K. K., Lizarraga, J. S., Beedle, M. T., and Winuthayanon, W. (2018). Estrogen action in the epithelial cells of the mouse vagina regulates neutrophil infiltration and vaginal tissue integrity. *Sci. Rep.* 8:11247. doi: 10.1038/s41598-018-29423-5

Lõhmussaar, K., Kopper, O., Korving, J., Begthel, H., Vreuls, C., van Es, J. H., et al. (2020). Assessing the origin of high-grade serous ovarian cancer using CRISPR-modification of mouse organoids. *Nat. Commun.* 11:2660. doi: 10.1038/s41467-020-16432-0

Luddi, A., Pavone, V., Semplici, B., Governini, L., Criscuoli, M., Paccagnini, E., et al. (2020). Organoids of human endometrium: a powerful *in vitro* model for the endometrium-embryo cross-talk at the implantation site. *Cells* 9:1121. doi: 10.3390/cells9051121

Lynch, H. T., Snyder, C. L., Shaw, T. G., Heinen, C. D., and Hitchins, M. P. (2015). Milestones of Lynch syndrome: 1895-2015. *Nat. Rev. Cancer* 15, 181–194. doi: 10.1038/nrc3878

Maenhoudt, N., Defraye, C., Boretto, M., Jan, Z., Heremans, R., Boeckx, B., et al. (2020). Developing organoids from ovarian cancer as experimental and preclinical models. *Stem Cell Reports.* 14, 717–729. doi: 10.1016/j.stemcr.2020.03.004

Malpica, A. (2014). "Cervical benign and non-neoplastic conditions," in *Pathology of the Female Reproductive Tract*, 3rd Edn, eds G. L. Mutter and J. Prat (London: Churchill Livingstone), 160–187.

Marinić, M., Rana, S., and Lynch, V. J. (2020). Derivation of endometrial gland organoids from term placenta. *Placenta* 101, 75–79. doi: 10.1016/j.placenta.2020.08.017

Maru, Y., Kawata, A., Taguchi, A., Ishii, Y., Baba, S., Mori, M., et al. (2020). Establishment and molecular phenotyping of organoids from the squamocolumnar junction region of the uterine cervix. *Cancers (Basel)* 12:694. doi: 10.3390/cancers12030694

Maru, Y., Tanaka, N., Ebisawa, K., Odaka, A., Sugiyama, T., Itami, M., et al. (2019a). Establishment and characterization of patient-derived organoids from a young patient with cervical clear cell carcinoma. *Cancer Sci.* 110, 2992–3005. doi: 10.1111/cas.14119

Maru, Y., Tanaka, N., Itami, M., and Hippo, Y. (2019b). Efficient use of patient-derived organoids as a preclinical model for gynecologic tumors. *Gynecol. Oncol.* 154, 189–198. doi: 10.1016/j.ygyno.2019.05.005

Matsuo, K., Eno, M. L., Im, D. D., Rosenshein, N. B., and Sood, A. K. (2010). Clinical relevance of extent of extreme drug resistance in epithelial ovarian carcinoma. *Gynecol. Oncol.* 116, 61–65. doi: 10.1016/j.ygyno.2009.09.018

McComb, P., Langley, L., Villalon, M., and Verdugo, P. (1986). The oviductal cilia and Kartagener's syndrome. *Fertil. Steril.* 46, 412–416. doi: 10.1016/S0015-0282(16)49578-6

Mehasseb, M. K., Taylor, A. H., Pringle, J. H., Bell, S. C., and Habiba, M. (2010). Enhanced invasion of stromal cells from adenomyosis in a three-dimensional coculture model is augmented by the presence of myocytes from affected uteri. *Fertil. Steril.* 94, 2547–2551. doi: 10.1016/j.fertnstert.2010.04.016

Mehta, F. F., Son, J., Hewitt, S. C., Jang, E., Lydon, J. P., Korach, K. S., et al. (2016). Distinct functions and regulation of epithelial progesterone receptor in the mouse cervix, vagina, and uterus. *Oncotarget* 7, 17455–17467. doi: 10.18632/oncotarget.8159

Miyagawa, S., and Iguchi, T. (2015). Epithelial estrogen receptor 1 intrinsically mediates squamous differentiation in the mouse vagina. *Proc. Natl. Acad. Sci. U.S.A.* 112, 12986–12991. doi: 10.1073/pnas.1513550112

Mutter, G. L., and Robboy, S. J. (2014). "Embryology," in *Pathology of the Female Reproductive Tract*, 3rd Edn, eds G. L. Mutter and J. Prat (London: Churchill Livingstone), 1–17.

Nakamura, T., Miyagawa, S., Katsu, Y., Watanabe, H., Mizutani, T., Sato, T., et al. (2012). Wnt family genes and their modulation in the ovary-independent and persistent vaginal epithelial cell proliferation and keratinization induced by neonatal diethylstilbestrol exposure in mice. *Toxicology* 296, 13–19. doi: 10.1016/j.tox.2012.02.010

Nanki, Y., Chiyoda, T., Hirasawa, A., Ookubo, A., Itoh, M., Ueno, M., et al. (2020). Patient-derived ovarian cancer organoids capture the genomic profiles of primary tumours applicable for drug sensitivity and resistance testing. *Sci. Rep.* 10:12581. doi: 10.1038/s41598-020-69488-9

Nozaki, K., Mochizuki, W., Matsumoto, Y., Matsumoto, T., Fukuda, M., Mizutani, T., et al. (2016). Co-culture with intestinal epithelial organoids allows efficient expansion and motility analysis of intraepithelial lymphocytes. *J. Gastroenterol.* 51, 206–213. doi: 10.1007/s00535-016-1170-8

Ooft, S. N., Weeber, F., Dijkstra, K. K., McLean, C. M., Kaing, S., van Werkhoven, E., et al. (2019). Patient-derived organoids can predict response to chemotherapy in metastatic colorectal cancer patients. *Sci. Transl. Med.* 11:eaay2574. doi: 10.1126/scitranslmed.aay2574

Ootani, A., Li, X., Sangiorgi, E., Ho, Q. T., Ueno, H., Toda, S., et al. (2009). Sustained in vitro intestinal epithelial culture within a Wnt-dependent stem cell niche. *Nat. Med.* 15, 701–706. doi: 10.1038/nm.1951

Patterson, A. L., and Pru, J. K. (2013). Long-term label retaining cells localize to distinct regions within the female reproductive epithelium. *Cell Cycle* 12, 2888–2898. doi: 10.4161/cc.25917

Pauli, C., Hopkins, B. D., Prandi, D., Shaw, R., Fedrizzi, T., Sboner, A., et al. (2017). Personalized *in vitro* and *in vivo* cancer models to guide precision medicine. *Cancer Discov.* 7, 462–477. doi: 10.1158/2159-8290.CD-16-1154

Phan, N., Hong, J. J., Tofig, B., Mapua, M., Elashoff, D., Moatamed, N. A., et al. (2019). A simple high-throughput approach identifies actionable drug sensitivities in patient-derived tumor organoids. *Commun. Biol.* 2:78. doi: 10.1038/s42003-019-0305-x

Prat, J., and FIGO Committee on Gynecologic Oncology (2014). Staging classification for cancer of the ovary, fallopian tube, and peritoneum. *Int. J. Gynaecol. Obstet.* 124, 1–5. doi: 10.1016/j.ijgo.2013.10.001

Raghavan, S., Mehta, P., Xie, Y., Lei, Y. L., and Mehta, G. (2019). Ovarian cancer stem cells and macrophages reciprocally interact through the WNT pathway to promote pro-tumoral and malignant phenotypes in 3D engineered microenvironments. *J. Immunother. Cancer* 7:190. doi: 10.1186/s40425-019-0666-1

Raghavan, S., Ward, M. R., Rowley, K. R., Wold, R. M., Takayama, S., Buckanovich, R. J., et al. (2015). Formation of stable small cell number three-dimensional ovarian cancer spheroids using hanging drop arrays for preclinical drug sensitivity assays. *Gynecol. Oncol.* 138, 181–189. doi: 10.1016/j.ygyno.2015.04.014

Rinehart, C. A. Jr., Lyn-Cook, B. D., and Kaufman, D. G. (1988). Gland formation from human endometrial epithelial cells in vitro. *In Vitro Cell. Dev. Biol.* 24, 1037–1041. doi: 10.1007/BF02620878

Robboy, S. J., Taguchi, O., and Cunha, G. R. (1982). Normal development of the human female reproductive tract and alterations resulting from experimental exposure to diethylstilbestrol. *Hum. Pathol.* 13, 190–198. doi: 10.1016/s0046-8177(82)80177-9

Roper, J., Tammela, T., Cetinbas, N. M., Akkad, A., Roghanian, A., Rickelt, S., et al. (2017). In vivo genome editing and organoid transplantation models of colorectal cancer and metastasis. *Nat. Biotechnol.* 35, 569–576. doi: 10.1038/nbt.3836

Rose, I. M., Bidarimath, M., Webster, A., Godwin, A. K., Flesken-Nikitin, A., and Nikitin, A. Y. (2020). WNT and inflammatory signaling distinguish human Fallopian tube epithelial cell populations. *Sci. Rep.* 10:9837. doi: 10.1038/s41598-020-66556-y

Sampson, J. A. (1921). Perforating hemorrhagic (Chocolate) cysts of the ovary: their importance and especially their relation to pelvic adenomas of endometrial type ("adenomyoma" of the uterus, rectovaginal septum, sigmoid, etc.). *Arch. Surg.* 3, 245–323. doi: 10.1001/archsurg.1921.01110080003001

Sampson, J. A. (1927). Peritoneal endometriosis due to the menstrual dissemination of endometrial tissue into the peritoneal cavity. *Am. J. Obstet. Gynecol.* 14, 422–469. doi: 10.1016/S0002-9378(15)30003-X

Sandberg, R., and Ernberg, I. (2005). Assessment of tumor characteristic gene expression in cell lines using a tissue similarity index (TSI). *Proc. Natl. Acad. Sci. U.S.A.* 102, 2052–2057. doi: 10.1073/pnas.0408105102

Sato, T., Stange, D. E., Ferrante, M., Vries, R. G., Van Es, J. H., Van den Brink, S., et al. (2011). Long-term expansion of epithelial organoids from human colon, adenoma, adenocarcinoma, and Barrett's epithelium. *Gastroenterology* 141, 1762–1772. doi: 10.1053/j.gastro.2011.07.050

Sato, T., Vries, R. G., Snippert, H. J., van de Wetering, M., Barker, N., Stange, D. E., et al. (2009). Single Lgr5 stem cells build crypt-villus structures in vitro without a mesenchymal niche. *Nature* 459, 262–265. doi: 10.1038/nature07935

Scheffner, M., Werness, B. A., Huibregtse, J. M., Levine, A. J., and Howley, P. M. (1990). The E6 oncoprotein encoded by human papillomavirus types 16 and 18 promotes the degradation of p53. *Cell* 63, 1129–1136. doi: 10.1016/0092-8674(90)90409-8

Schutgens, F., and Clevers, H. (2020). Human organoids: tools for understanding biology and treating diseases. *Annu. Rev. Pathol.* 15, 211–234. doi: 10.1146/annurev-pathmechdis-012419-032611

Snijders, M. P., de Goeij, A. F., Debets-Te Baerts, M. J., Rousch, M. J., Koudstaal, J., and Bosman, F. T. (1992). Immunocytochemical analysis of oestrogen receptors and progesterone receptors in the human uterus throughout the menstrual cycle and after the menopause. *J. Reprod. Fertil.* 94, 363–371. doi: 10.1530/jrf.0.0940363

Stewart, C., Crum, C. P., McCluggage, W. G., Park, K. J., Rutgers, J. K., Oliva, E., et al. (2019). Guidelines to aid in the distinction of endometrial and endocervical carcinomas, and the distinction of independent primary carcinomas of the endometrium and adnexa from metastatic spread between these and other sites. *Int. J. Gynecol. Pathol.* 38, S75–S92. doi: 10.1097/PGP.0000000000000553

Syed, S. M., Kumar, M., Ghosh, A., Tomasetig, F., Ali, A., Whan, R. M., et al. (2020). Endometrial Axin2+ cells drive epithelial homeostasis, regeneration, and cancer following oncogenic transformation. *Cell Stem Cell* 26, 64–80.e13. doi: 10.1016/j.stem.2019.11.012

Tempest, N., Maclean, A., and Hapangama, D. K. (2018). Endometrial stem cell markers: current concepts and unresolved questions. *Int. J. Mol. Sci.* 19:3240. doi: 10.3390/ijms19103240

Thiet, M. P., Osathanondh, R., and Yeh, J. (1994). Localization and timing of appearance of insulin, insulin-like growth factor-I, and their receptors in the human fetal müllerian tract. *Am. J. Obstet. Gynecol.* 170, 152–156. doi: 10.1016/s0002-9378(94)70401-5

Toss, A., Tomasello, C., Razzaboni, E., Contu, G., Grandi, G., Cagnacci, A., et al. (2015). Hereditary ovarian cancer: not only BRCA 1 and 2 genes. *Biomed. Res. Int.* 2015:341723. doi: 10.1155/2015/341723

Tsai, P. S., and Bern, H. A. (1991). Estrogen-independent growth of mouse vaginal epithelium in organ culture. *J. Exp. Zool.* 259, 238–245. doi: 10.1002/jez.1402590213

Tsuda, H., Hashiguchi, Y., Nishimura, S., Kawamura, N., Inoue, T., and Yamamoto, K. (2003). Relationship between HPV typing and abnormality of G1 cell cycle regulators in cervical neoplasm. *Gynecol. Oncol.* 91, 476–485. doi: 10.1016/j.ygyno.2003.08.019

Turco, M. Y., Gardner, L., Hughes, J., Cindrova-Davies, T., Gomez, M. J., Farrell, L., et al. (2017). Long-term, hormone-responsive organoid cultures of human endometrium in a chemically defined medium. *Nat. Cell Biol.* 19, 568–577. doi: 10.1038/ncb3516

Turco, M. Y., Gardner, L., Kay, R. G., Hamilton, R. S., Prater, M., Hollinshead, M. S., et al. (2018). Trophoblast organoids as a model for maternal-fetal interactions during human placentation. *Nature* 564, 263–267. doi: 10.1038/s41586-018-0753-3

van de Wetering, M., Francies, H. E., Francis, J. M., Bounova, G., Iorio, F., Pronk, A., et al. (2015). Prospective derivation of a living organoid biobank of colorectal cancer patients. *Cell* 161, 933–945. doi: 10.1016/j.cell.2015.03.053

Van Nyen, T., Moiola, C. P., Colas, E., Annibali, D., and Amant, F. (2018). Modeling endometrial cancer: past, present, and future. *Int. J. Mol. Sci.* 19:2348. doi: 10.3390/ijms19082348

Vannuccini, S., Tosti, C., Carmona, F., Huang, S. J., Chapron, C., Guo, S. W., et al. (2017). Pathogenesis of adenomyosis: an update on molecular mechanisms. *Reprod. Biomed. Online* 35, 592–601. doi: 10.1016/j.rbmo.2017.06.016

Visvader, J. E. (2011). Cells of origin in cancer. *Nature* 469, 314–322. doi: 10.1038/nature09781

Vlachogiannis, G., Hedayat, S., Vatsiou, A., Jamin, Y., Fernández-Mateos, J., Khan, K., et al. (2018). Patient-derived organoids model treatment response of metastatic gastrointestinal cancers. *Science* 359, 920–926. doi: 10.1126/science.aao2774

Wagner, M., Yoshihara, M., Douagi, I., Damdimopoulos, A., Panula, S., Petropoulos, S., et al. (2020). Single-cell analysis of human ovarian cortex identifies distinct cell populations but no oogonial stem cells. *Nat. Commun.* 11:1147. doi: 10.1038/s41467-020-14936-3

Walsh, T., Casadei, S., Lee, M. K., Pennil, C. C., Nord, A. S., Thornton, A. M., et al. (2011). Mutations in 12 genes for inherited ovarian, fallopian tube, and peritoneal carcinoma identified by massively parallel sequencing. *Proc. Natl. Acad. Sci. U.S.A.* 108, 18032–18037. doi: 10.1073/pnas.1115052108

Wan, C., Keany, M. P., Dong, H., Al-Alem, L. F., Pandya, U. M., Lazo, S., et al. (2020). Enhanced efficacy of simultaneous PD-1 and PD-L1 immune checkpoint blockade in high grade serous ovarian cancer. *Cancer Res.* 81, 158–173. doi: 10.1158/0008-5472.CAN-20-1674

Wang, Y., Sacchetti, A., van Dijk, M. R., van der Zee, M., van der Horst, P. H., Joosten, R., et al. (2012). Identification of quiescent, stem-like cells in the distal female reproductive tract. *PLoS One* 7:e40691. doi: 10.1371/journal.pone.0040691

Wang, Y., Yang, D., Cogdell, D., Hu, L., Xue, F., Broaddus, R., et al. (2010). Genomic characterization of gene copy-number aberrations in endometrial carcinoma cell lines derived from endometrioid-type endometrial adenocarcinoma. *Technol. Cancer Res. Treat.* 9, 179–189. doi: 10.1177/153303461000900207

Weroha, S. J., Becker, M. A., Enderica-Gonzalez, S., Harrington, S. C., Oberg, A. L., Maurer, M. J., et al. (2014). Tumorgrafts as in vivo surrogates for women with ovarian cancer. *Clin. Cancer Res.* 20, 1288–1297. doi: 10.1158/1078-0432.CCR-13-2611

White, Y. A., Woods, D. C., Takai, Y., Ishihara, O., Seki, H., and Tilly, J. L. (2012). Oocyte formation by mitotically active germ cells purified from ovaries of reproductive-age women. *Nat. Med.* 18, 413–421. doi: 10.1038/nm.2669

Xie, Y., Park, E. S., Xiang, D., and Li, Z. (2018). Long-term organoid culture reveals enrichment of organoid-forming epithelial cells in the fimbrial portion of mouse fallopian tube. *Stem Cell Res.* 32, 51–60. doi: 10.1016/j.scr.2018.08.021

Yin, Y., and Ma, L. (2005). Development of the mammalian female reproductive tract. *J. Biochem.* 137, 677–683. doi: 10.1093/jb/mvi087

Yucer, N., Holzapfel, M., Jenkins Vogel, T., Lenaeus, L., Ornelas, L., Laury, A., et al. (2017). Directed differentiation of human induced pluripotent stem cells into fallopian tube epithelium. *Sci. Rep.* 7:10741. doi: 10.1038/s41598-017-05519-2

Zhang, S., Dolgalev, I., Zhang, T., Ran, H., Levine, D. A., and Neel, B. G. (2019a). Both fallopian tube and ovarian surface epithelium are cells-of-origin for high-grade serous ovarian carcinoma. *Nat. Commun.* 10:5367. doi: 10.1038/s41467-019-13116-2

Zhang, S., Gong, T. T., Liu, F. H., Jiang, Y. T., Sun, H., Ma, X. X., et al. (2019b). Global, regional, and national burden of endometrial cancer, 1990-2017: results from the global burden of disease study, 2017. *Front. Oncol.* 9:1440. doi: 10.3389/fonc.2019.01440

Zhang, S., Iyer, S., Ran, H., Dolgalev, I., Gu, S., Wei, W., et al. (2020). Genetically defined, syngeneic organoid platform for developing combination therapies for ovarian cancer. *Cancer Discov.* 11, 362–383. doi: 10.1158/2159-8290.CD-20-0455

Zietarska, M., Maugard, C. M., Filali-Mouhim, A., Alam-Fahmy, M., Tonin, P. N., Provencher, D. M., et al. (2007). Molecular description of a 3D in vitro model for the study of epithelial ovarian cancer (EOC). *Mol. Carcinog.* 46, 872–885. doi: 10.1002/mc.20315

Zuckerman, S. (1951). The number of oocytes in the mature ovary. *Rec. Prog. Horm. Res.* 6, 63–108.

zur Hausen, H., Meinhof, W., Scheiber, W., and Bornkamm, G. W. (1974). Attempts to detect virus-secific DNA in human tumors. I. Nucleic acid hybridizations with complementary RNA of human wart virus. *Int. J. Cancer* 13, 650–656. doi: 10.1002/ijc.2910130509

Conflict of Interest: The authors declare that the research was conducted in the absence of any commercial or financial relationships that could be construed as a potential conflict of interest.

frontiers in Cell and Developmental Biology

REVIEW
published: 29 April 2021
doi: 10.3389/fcell.2021.629212

Endocrine Pancreas Development and Dysfunction Through the Lens of Single-Cell RNA-Sequencing

*Wojciech J. Szlachcic[1], Natalia Ziojla[1], Dorota K. Kizewska[1], Marcelina Kempa[1] and Malgorzata Borowiak[1,2]**

[1] Department of Gene Expression, Institute of Molecular Biology and Biotechnology, Faculty of Biology, Adam Mickiewicz University, Poznań, Poland, [2] Department of Molecular and Cellular Biology, Baylor College of Medicine, Houston, TX, United States

OPEN ACCESS

Edited by:
Philip Iannaccone, Northwestern University, United States

Reviewed by:
Haiting Ma, Whitehead Institute for Biomedical Research, United States
Borhane Guezguez, German Cancer Consortium, German Cancer Research Center (DKFZ), Germany

***Correspondence:**
Malgorzata Borowiak
borowiak@bcm.edu;
malbor3@amu.edu.pl

Specialty section:
This article was submitted to Stem Cell Research, a section of the journal Frontiers in Cell and Developmental Biology

Received: *13 November 2020*
Accepted: *06 April 2021*
Published: *29 April 2021*

Citation:
Szlachcic WJ, Ziojla N, Kizewska DK, Kempa M and Borowiak M (2021) Endocrine Pancreas Development and Dysfunction Through the Lens of Single-Cell RNA-Sequencing. Front. Cell Dev. Biol. 9:629212. doi: 10.3389/fcell.2021.629212

A chronic inability to maintain blood glucose homeostasis leads to diabetes, which can damage multiple organs. The pancreatic islets regulate blood glucose levels through the coordinated action of islet cell-secreted hormones, with the insulin released by β-cells playing a crucial role in this process. Diabetes is caused by insufficient insulin secretion due to β-cell loss, or a pancreatic dysfunction. The restoration of a functional β-cell mass might, therefore, offer a cure. To this end, major efforts are underway to generate human β-cells *de novo, in vitro,* or *in vivo*. The efficient generation of functional β-cells requires a comprehensive knowledge of pancreas development, including the mechanisms driving cell fate decisions or endocrine cell maturation. Rapid progress in single-cell RNA sequencing (scRNA-Seq) technologies has brought a new dimension to pancreas development research. These methods can capture the transcriptomes of thousands of individual cells, including rare cell types, subtypes, and transient states. With such massive datasets, it is possible to infer the developmental trajectories of cell transitions and gene regulatory pathways. Here, we summarize recent advances in our understanding of endocrine pancreas development and function from scRNA-Seq studies on developing and adult pancreas and human endocrine differentiation models. We also discuss recent scRNA-Seq findings for the pathological pancreas in diabetes, and their implications for better treatment.

Keywords: single-cell RNA sequencing, pancreas development, stem cell pancreatic differentiation, beta cell development and maturation, diabetes

PANCREAS AND DIABETES

The pancreas is a glandular organ with crucial roles in digestion (exocrine activity) and glucose homeostasis (endocrine activity). The main mass of the exocrine compartment consists of the *acini*. The acinar cells secrete enzymes involved in the digestion of proteins (trypsinogen, chymotrypsinogen), fats (lipase, phospholipase, cholesterol esterase), and carbohydrates (amylase). These enzymes are produced in an inactive form, stored as granules known as zymogens, and are released into the ducts as required; these ducts eventually converge into the main duct, via which the pancreatic juice drains directly into the duodenum (Alexandre-Heymann et al., 2019).

The exocrine cells occupy a large proportion of the pancreas, whereas the endocrine compartment consists of cell clusters known as the islets of Langerhans (about 100 μm in diameter) dispersed throughout the organ. Crosstalk between the different cell types comprising the islets (α-, β-, δ-, ε-, and PP-cells) regulates glucose homeostasis, by controlling the secretion of cell-specific hormones (Benitez et al., 2012). The most abundant cells in the pancreatic islets (up to 90% per islet) are the α- and β-cells. The β-cells secrete insulin in response to an increase in serum glucose concentration. Insulin facilitates the uptake of glucose from the blood by cells in peripheral tissues, for use as an energy source (in muscles), or storage as glycogen (in hepatocytes) and thus the insulin decreases serum glucose levels. By contrast, the α-cells secrete glucagon, which increases blood sugar levels by stimulating the release of glucose from glycogen in hepatocytes (Benitez et al., 2012). The hormones secreted by the other islet cells regulate the function of α- and β-cells, and their own functions, in a paracrine manner. The δ-cells secrete somatostatin, which regulates the functions of both α- and β-cells by binding to the somatostatin receptors expressed on their membranes (Braun et al., 2010; Benitez et al., 2012; Gromada et al., 2018). The PP-cells produce and release pancreatic polypeptide, which reduces the secretion of glucagon from α-cells (Aragón et al., 2015). The ε-cells, a rare population within the islet (<1% in adult human islets), release ghrelin to stimulate somatostatin secretion and inhibit insulin secretion (Dominguez Gutierrez et al., 2018). Insufficient paracrine regulation within the islets may lead to the long-term disruption of glucose balance, resulting in a chronic metabolic disease, diabetes mellitus.

Diabetes is considered a disease of civilization. It affected over 425 million people worldwide in 2017, and the number of people with diabetes is predicted to increase to 642 million by 2040 (idf.org, Velazco-Cruz et al., 2019). The various types of diabetes differ in etiology and molecular background. However, the hallmark of this disease is insufficient insulin secretion due to β-cell loss resulting from autoimmune attack, as in type 1 diabetes (T1D), or an impairment of the β-cell function or insulin resistance built up by peripheral tissues, as in type 2 diabetes (T2D) (American Diabetes and Association, 2013; Johannesson et al., 2015). Most patients with diabetes have type 1 or type 2 disease, but there is also another rare type of diabetes (accounting for 1–2% cases): maturity-onset diabetes of the young (MODY), which is caused by a single gene mutation. MODY patients are usually diagnosed in late childhood or early adulthood, have a strong family history of diabetes, lack autoantibodies against pancreatic antigens, and have normal body weight. MODY manifests as various abnormalities of β-cell function and can be further classified into subtypes on the basis of the gene mutated (Gardner and Tai, 2012). Many of the causal genes for MODY encode factors involved in pancreas development, suggesting that this form of diabetes may be a developmental disease.

Current therapeutic strategies for diabetes aim to control carbohydrate homeostasis, mostly through the delivery of exogenous insulin, the use of drugs to stimulate insulin production and secretion by the diminishing β-cell mass, and therapeutic agents inhibiting glucagon secretion (Marín-Peñalver et al., 2016). A healthy lifestyle, including an appropriate diet and physical activity, is also promoted in addition to pharmacological treatment. These approaches might stabilize blood glucose levels but are often imprecise and burdensome for patients. For example, insulin treatment requires multiple injections per day of an exact amount of insulin (Tan et al., 2019), making it challenging to maintain correct glucose homeostasis over long periods. Therefore, patients with diabetes often develop secondary diseases affecting multiple organs, including cardiovascular or renal functions, which may reduce their lifespan and quality of life. There is, thus, a pressing need to identify a cure for diabetes, or better treatments, to free patients from the inconvenience and risks associated with this highly prevalent disease.

One attractive idea is the restoration of a functional β-cell pool in the patient (Zhou and Melton, 2018). Proof-of-principle studies have shown that islet transplantation can lead to independence from exogenous insulin in people with diabetes (Bellin et al., 2012; Moore et al., 2015). Ready-to-transplant islets containing insulin-secreting cells are obtained from cadaveric donors. However, this source of cells is limited, due to a shortage of donors and suboptimal islet isolation procedures (Shapiro et al., 2006; Bellin et al., 2012). Xenotransplantation with immunocompetent porcine islets, a potentially unlimited source of β-cells, has been proposed as a means of solving this problem. However, the risk of transmitting endogenous porcine retroviruses to patients and the high inflammatory response to animal islets have prevented the transfer of this approach into clinical practice (van der Windt et al., 2012; Rashid et al., 2014; Moore et al., 2015).

Recent advances in regenerative medicine based on the use of β-cells differentiated *in vitro* from pluripotent stem cells (PSCs) have raised the possibility of an inexhaustible source of β-cells (Johannesson et al., 2015). Application of the knowledge obtained in classical biology studies, including knockout or lineage tracing experiment has led to the *de novo* derivation of β-cells, resulting in improvements in glucose homeostasis in diabetic mice (Pagliuca et al., 2014; Rezania et al., 2014; Russ et al., 2015; Nair et al., 2019).

Moreover, in addition to their possible use in cell replacement therapies for diabetes, PSC-derived β-cells could be used as a platform for disease modeling and drug screening. The *in vivo* transdifferentiation of other cell types into β-cells has also been proposed as an alternative to transplantation. In mouse T1D models, almost complete β-cell loss triggered the transdifferentiation of α- or δ-cells into insulin-producing cells (Thorel et al., 2010; Bru-Tari et al., 2019). Furthermore, pancreatic acinar cells and endocrine cells in the intestine or stomach can be transdifferentiated into insulin-secreting cells (Zhou et al., 2008; Li et al., 2014; Ariyachet et al., 2016). However, the transdifferentiation efficiency is low, the long-term stability of newly formed β-cells is uncertain, and our understanding of this process remains incomplete (Collombat et al., 2009; Courtney et al., 2013; Wilcox et al., 2013; Chera et al., 2014; Li et al., 2017; Furuyama et al., 2019).

Significant progress has been made toward the efficient *in vitro* or *in vivo* production of clinically relevant, functional β-cells, but this aim has yet to be achieved. *In vitro* pancreatic differentiation or *in vivo* transdifferentiation require an understanding of pancreas development, derived from extensive and meticulous research on transgenic animal models and cell lines.

PANCREAS DEVELOPMENT

The pancreas develops from the endoderm-derived primitive digestive tube. The gut tube separates into the foregut, midgut and hindgut, and pancreatic specification occurs in the duodenal loop, at the border between foregut and midgut (Wells and Melton, 2000; Lawson and Schoenwolf, 2003). Approximately 29–33 days post-conception (dpc) in humans, and at embryonic day 9.5–10 (E9.5-E10) in mice, the primary transition begins with gut tube budding, leading to the appearance of two pancreatic buds on the dorsal and ventral sides of the duodenal loop. The expression of pancreatic and duodenal homeobox 1 (PDX1) (Offield et al., 1996; Burlison et al., 2008), SRY-box transcription factor 9 (SOX9) (Lynn et al., 2007), and pancreas associated transcription factor 1A (PTF1A) (Krapp et al., 1998; Kawaguchi et al., 2002; Burlison et al., 2008) marks the multipotent pancreatic progenitors (MPs) within the buds. These MPs give rise to all pancreatic cell types. Subsequently, in the 6th week of human development and at E11-12 in mice, the buds bulge, and the ventral bud flips to the other side of the gut tube and fuses with the dorsal bud (Jeon et al., 2009). Progressive branching morphogenesis establishes the trunk (ductal body) and the tip (ductal termini) domains between the 10th and 14th weeks in humans, and at E13.5 in mice. This event marks the start of the so-called secondary transition in pancreatic development. The PTF1A$^+$ and PDX1$^+$ cells in the tip domain are initially multipotent, but they acquire an acinar fate bias during secondary transition (Zhou et al., 2007). The trunk domain contains PDX1$^+$, SOX9$^+$, and NKX6.1$^+$, bipotent progenitors (BPs) that generate duct-like structures and endocrine progenitors (Jennings et al., 2015). The endocrine progenitors (EPs) arise from trunk domain cells lacking SOX9 and expressing neurogenin-3 (NEUROG3). The NEUROG3 transcription factor is necessary and sufficient for endocrine cell lineage specification (Gradwohl et al., 2000; Gu et al., 2002; Sheets et al., 2018) and activates downstream transcription factors essential for endocrine specification, such as neuronal differentiation 1 (NEUROD1), INSM transcriptional repressor 1 (INSM1), Iroquois homeobox 1 (IRX1), regulatory factor X6 (RFX6), and paired box 4 (PAX4). In mice, NEUROG3 is expressed in a biphasic manner. The first wave of NEUROG3 expression is associated with the emergence of pro-α-cells, from E8.5 to E11 (Larsson, 1998; Villasenor et al., 2008). The second wave of high NEUROG3 expression, from E13.5 to E17.5, leads to the generation of multiple endocrine cell types (Gradwohl et al., 2000; Schwitzgebel et al., 2000; Villasenor et al., 2008). In humans, NEUROG3 expression increases at 47–52 dpc, coinciding with the appearance of the first insulin-expressing cells, and peaks at 8–10 weeks of development (Jennings et al., 2013). All five types of pancreatic endocrine cells arise from NEUROG3$^+$ EPs. A unique combination of transcription factors triggers islet cell type-specific gene regulatory networks in EPs and represses alternative networks, resulting in the formation of cells producing specific hormones.

SINGLE-CELL RNA SEQUENCING TECHNOLOGY

Tremendous efforts have been made to identify the principal transcription factors and signaling pathways driving pancreas development. However, conventional research methods may miss subtle molecular events, such as cell state transitions, and cellular heterogeneity, a knowledge of which is necessary for the fine-tuning of β-cell production and for understanding the molecular mechanisms underlying diabetes. These gaps in our knowledge can be bridged by the use of rapidly evolving single-cell transcriptomics (scRNA-Seq) and other single-cell omics technologies.

Global gene expression analysis by RNA-Seq became a very common technology in studies on pancreas development and disease. Yet, bulk gene expression analysis by RNA-Seq provides information about average levels of gene expression for all cells. Thus, with bulk RNA-Seq, it is almost impossible to detect continuous cell-state transitions, the cell fate bifurcations, transient molecular events, or rare cell types and subpopulations. In contrast, scRNA-Seq enables to define the transcriptome of individual cells within the studied tissue, organ, or in cell cultures. Cells are grouped into clusters based on transcriptomic similarities. The extraction of a cell type of interest from a larger dataset makes it possible to identify discrete cell subtypes of subpopulations, potentially reflecting subsequent also maturation steps. Individual cells can also be ordered in pseudotime, reflecting their putative sequential appearance, and aligned along linear developmental trajectories (Cannoodt et al., 2016; Qiu X. et al., 2017; Street et al., 2018; Tritschler et al., 2019; Van den Berge et al., 2020). Within these trajectories, it is possible to identify branching points for cell fate decisions. Moreover, the dynamics of cell state transitions can be inferred from RNA velocity (La Manno et al., 2018; Bergen et al., 2020). For each cell state or pseudotime point, transcripts, signaling pathways, and gene ontology terms displaying enrichment can be identified. A pseudodynamics method, in which whole cell populations are placed along pseudotime trajectories, was also proposed for the inference of developmental population dynamics from scRNA-Seq data (Fischer et al., 2019). Alternatively, a gene-centric approach can be used to align each gene expression over pseudotime, and cluster genes with similar patterns of behavior into regulons (Van de Sande et al., 2020). Each cell type can then be defined by its regulons. The strengths and limitations of pseudotime analyses have been recently discussed in detail elsewhere (Tritschler et al., 2019). Therefore, the principal advantage of scRNA-Seq is that it facilitates creation of novel scientific hypotheses, depending on the research goal, through a plethora of rapidly evolving bioinformatics tools (Efremova and Teichmann, 2020; Wu and Zhang, 2020). Yet, these hypotheses

are based on a glimpse into complex biological systems, might be an artifact of bioinformatic analysis and have to be further validated by other methods.

Since the first publication relating to scRNA-Seq in 2009 (Tang et al., 2009), single-cell techniques have rapidly evolved, and a multitude of sequencing platforms and bioinformatics tools for data analysis have been developed (Svensson et al., 2018). The platforms that initially dominated this sector, such as Smart-Seq (Ramsköld et al., 2012; Picelli et al., 2013), used flow-activated cell separation (FACS) to separate individual cells. A C1 Fluidigm microfluidics system was subsequently adapted to separate cells into reaction chambers on a chip. These low-throughput methods enabled to sequence hundreds of cells at a time and were relatively costly because of limited sample pooling. In more advanced platforms, such as the widely used Drop-seq (Macosko et al., 2015), inDrops (Klein et al., 2015), and 10× Genomics Chromium (Zheng et al., 2017), single cells are encapsulated in microfluidic drops. The mRNAs of individual cells are then tagged with a unique barcode sequence, allowing multiplexing. Droplet-based methods generally enable to sequence hundreds of thousands of cells in parallel and generate a number of reads similar to that for bulk RNA sequencing. However, the total read number must then be divided by the number of cells used in the experiment, and the use of larger numbers of cells results in a lower sequencing depth (Zhang et al., 2020). The detection limit for scRNA-Seq is, thus, much lower than that for bulk RNA-Seq (Mawla and Huising, 2019). Low-abundance RNAs therefore frequently remain undetected, due to technical noise, sequencing depth, or an actual biological effect (Lähnemann et al., 2020). Fewer than 100 transcripts are commonly detected in all β-cells, for example (Mawla and Huising, 2019). Nevertheless, a β-cell pool can be constituted based on a reasonable correlation with the corresponding bulk RNA-Seq data. The overrepresentation of highly abundant transcripts, such as that for insulin (INS) in the endocrine pancreas, for example, may also hinder the detection of less abundant transcripts. High-abundance transcripts might also be a source of biological contamination when free-floating mRNA is captured in a droplet (Macosko et al., 2015) and for example endocrine gene transcripts have been found to be abundant even in non-endocrine cells, probably due to contamination (Marquina-Sanchez et al., 2020). The use of cross-species spike-ins in samples can overcome this problem. The examples mentioned, and multiple other experimental and analytical limitations of scRNA-Seq have been discussed in detail elsewhere (Luecken and Theis, 2019; Mawla and Huising, 2019; Tritschler et al., 2019; Lähnemann et al., 2020). Despite these challenges, scRNA-Seq has already established itself as a valuable tool for developmental biology. A growing number of scRNA-Seq studies on endocrine pancreas development (summarized in **Supplementary Table 1**) have shown that at different developmental stages cell types, traditionally identified by a few markers, consist of heterogeneous cell populations reflecting continuous maturation or transitions between stages, and cell fate bias (**Figure 1**). Below, we will discuss examples of the corroboration and extension of our understanding of pancreas development by scRNA-Seq.

NOVEL INSIGHT INTO ENDOCRINE PANCREAS DEVELOPMENT FROM SINGLE-CELL RNA-SEQ

Epithelial Multipotent Progenitors

Numerous knockout studies in mice have suggested that MPs expressing Pdx1, Sox9, and Ptf1a form a homogeneous population, in which each MP has a similar developmental potential. Recently, the scRNA-Seq of E9.5–E17.5 pancreas revealed the existence of three consecutive subpopulations of *Pdx1*$^+$ *Sox9*$^+$ MPs: MP−early, MP−late, and tip-like cells (Yu et al., 2019). Previously undetected MP−early cells, expressing *Nr2f2* but not *Ptf1a,* were found at E9.5 and, by E10.5, were succeeded by a *Ptf1a*$^+$ *Nr2f2*$^-$ MP-late population. Immunofluorescence staining confirmed the expression of NR2F2 in PDX1$^+$ cells in the E9.5 pancreas, but not E10.5. The scRNA-Seq identify MP-early cells as a direct source of the first wave of *Neurog3*$^+$ cells at E9.5, with these cells developing into α-cells (Yu et al., 2019). Consistent with this finding, lineage tracing and single-cell qPCR (sc-qPCR) showed that *Ptf1a*$^+$ cells were rarely ancestors of the first *Neurog3*$^+$ cells in the E9.5 pancreas (Larsen et al., 2017). Thus, the MP-early cells are probably the first pancreatic cells and serve as a branching point for cell fate decisions.

After MP expansion, branching morphogenesis begins at E12.5 driven by tip cells, self-renewing progenitors present at the ductal termini. Tip progenitors display stage-dependent multipotency (Zhou et al., 2007; Larsen et al., 2017; Sznurkowska et al., 2018). scRNA-Seq revealed that, by E11.5, the MP-late cluster gives rise to the tip-like progenitors expressing *Cpa1*, a marker of tip and acinar cells, and *Sox9*, a marker of the trunk and ducts (Yu et al., 2019). The *Cpa1*$^+$ cells remain multipotent until E12.5-E13.5, yielding trunk and acinar cells, while from E13.5-E14.5 are restricted to the acinar lineage (Sznurkowska et al., 2018; Bastidas-Ponce et al., 2019; Yu et al., 2019). The identification of *Cpa1*$^+$ multipotent tip cells in these scRNA-Seq experiments thus confirmed and extended a discovery made in an extensive *in situ* hybridization screen of over 1,100 transcription factors in mouse embryonic pancreas, followed by lineage tracing of Cpa1$^+$ progeny (Zhou et al., 2007). Interestingly, a rare population of multipotent PDX1$^+$/ALK3$^+$/CAII- progenitors was recently identified by scRNA-Seq in adult human ducts (Qadir et al., 2020). Upon transplantation under the mouse kidney capsule, these progenitors differentiated into acinar, ductal, and endocrine cells. The resemblance of these cells to the human and mouse MPs present during development remains unclear and could have implications for their therapeutic application.

Bipotent Progenitors

scRNA-Seq analyses supported by embryonic pancreas staining identified new markers of trunk BPs: Anxa2 in mice (Yu et al., 2019) and Dcdc2a in both mice and humans (Scavuzzo et al., 2018). Furthermore, scRNA-Seq revealed that early trunk cells arise between E11.5-12.5 and bifurcate at E14.5 to generate either pro-ductal or pro-EP trunk cell intermediate subpopulations, the

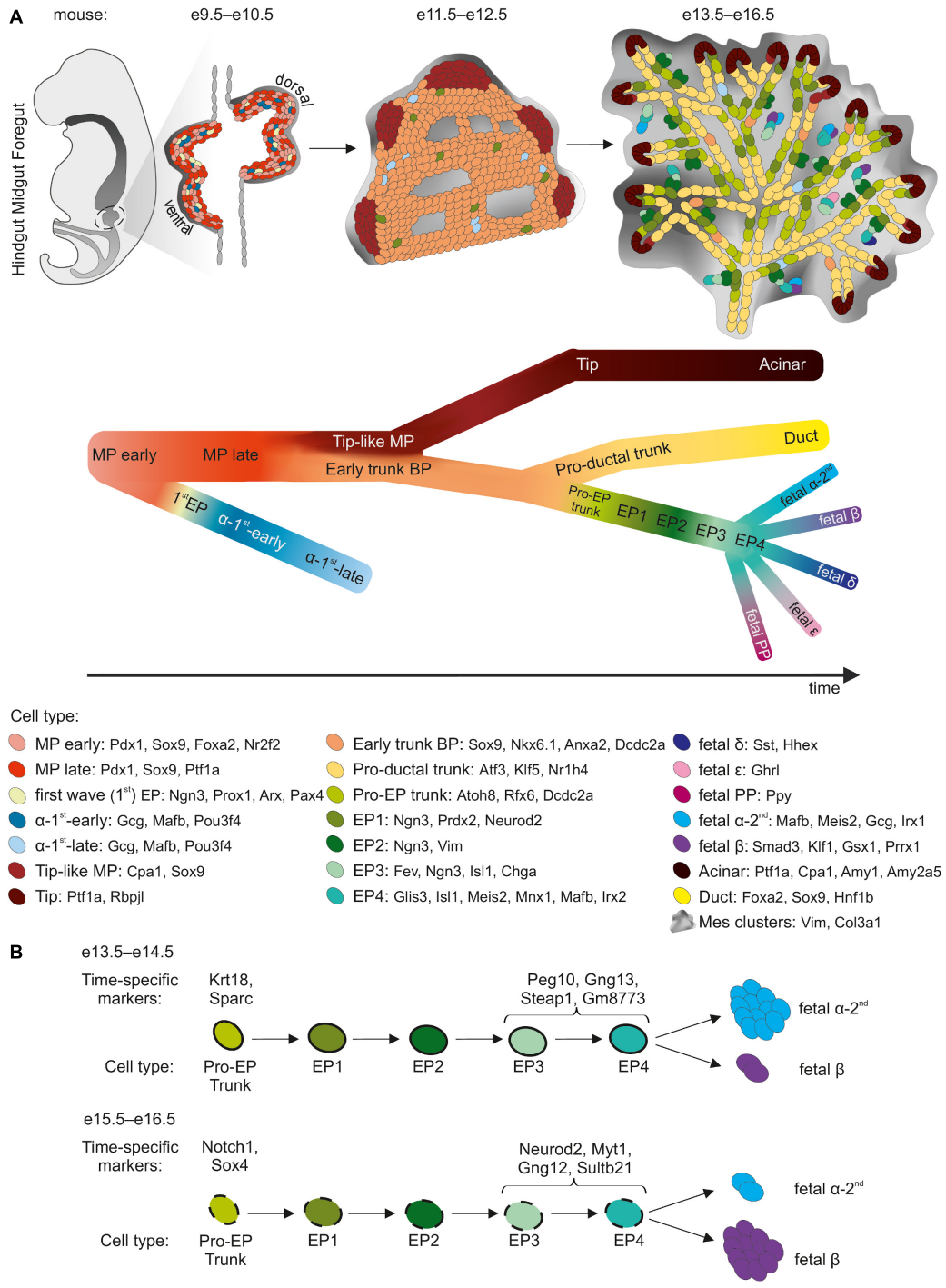

FIGURE 1 | sc-RNA-Seq insight into murine pancreatic development. **(A)** Three major morphogenesis transitions in pancreatic development are shown. Cell types with cell specific markers are listed in the legend below. The black arrow indicates the developmental trajectory. MP, multipotent progenitors; BP, bipotent progenitors; EP, endocrine progenitors. **(B)** Developmental trajectory of Pro-EP trunk and EP cells as they differentiate at e13.5–e14.5 preferably into α-cells, and at e15.5–e16.5 preferably into β-cells. Time point-specific markers are listed above the scheme.

cells of this latter population already displaying low levels of *Neurog3* expression (Yu et al., 2019). Simultaneously, the pro-EP E14.5 BPs develop into either EPs or transcriptionally distinct BPs at E16.5 (Scavuzzo et al., 2018). The change in BPs between E14.5 and E16.5 may already reflect a bias toward either an α- or a β-cell fate, as observed in scRNA-Seq experiments (see section "Endocrine Progenitors"). If this is indeed the case, then the change in endocrine cell type must be decided before the

onset of Neurog3 expression. This scenario is supported by a another scRNA-Seq study revealing that methylation patterns in the UR2 promoter region of the *Arx* gene, encoding transcription factor determining β- vs. α-cell fate (Dhawan et al., 2011), are established before the expression of its regulator, Neurog3 (Liu et al., 2019). When highly methylated by the Dnmt1 DNA methyltransferase, UR2 adopts an α-cell fate (Liu et al., 2019). Another example supporting for pre-Neurog3 priming is the *Amotl2* gene, which is enriched in pro-β-fate E16.5 compared to pro-α- E14.5 BPs (Scavuzzo et al., 2018), and which is expressed in similar pattern as *Neurog3* (Scavuzzo et al., 2018; Bastidas-Ponce et al., 2019; van Gurp et al., 2019). Amotl2, a Hippo pathway component, inhibits the Notch and canonical Wnt pathways, induces a loss of polarity, and promotes endothelial cell motility (Wang et al., 2011; Zhao et al., 2011; Li et al., 2012; Mojallal et al., 2014). The Notch and canonical Wnt pathways block EP specification (Jensen et al., 2000; Cebola et al., 2015; Rosado-Olivieri et al., 2019; Sharon et al., 2019a). Amotl2 may, therefore, regulate EP specification upstream from Neurog3. *AMOTL2* knockdown in human ESC-derived BP stage cells increases the *GCG* and decreases *INS* expression at the endocrine cell stage. The early differences in Amotl2 expression between pro-α and pro-β BPs may reflect differences in behavior between developing endocrine lineages during delamination, reflecting further spatial organization within islets.

The Wnt, Notch, and Bmp pathways are key regulators of pancreatic endocrine cell development. However, we still do not fully understand signaling pathways regulating endocrine lineage specification. The ERK pathway, for example, was not known to be involved in this process, but scRNA-Seq revealed ERK signaling downregulation when BPs developed into early EPs (Yu et al., 2019). Immunostaining confirmed that pERK was expressed in Neurog3^{low} pro-EP trunk cells but not in Neurog3^{high} EP cells in E14.5 pancreas. Furthermore, transient MAPK/ERK pathway suppression by a small molecule (U0126) in E13.5 pancreatic explants increased the proportion of *Ins1*$^{+}$ and *Gcg*$^{+}$ cells (Yu et al., 2019). Thus, scRNA-Seq has identified the MAPK/ERK pathway as a regulator of mouse endocrine specification. Further studies are required to confirm that ERK signaling enhances human β-cell differentiation *in vitro*.

Endocrine Progenitors

A combination of lineage tracing and sc-qPCR revealed that as many as 50% of E9.5 pancreatic cells are biased toward the endocrine lineage (Larsen et al., 2017), corresponding to the first wave of endocrine differentiation. By scRNA-Seq, endocrine differentiation from *Ptf1a*$^{-}$ MP-early cells has been observed at E9.5, with the emergence of *Neurog3*$^{+}$ progenitors ("pre−α−first cells"), which further mature from the α−first−early cells at E10.5 to a diverse population of more mature α−first−late cells by E11.5-E13.5 (Yu et al., 2019). The α-first-cells were also identified at E12.5 in a separate study (Bastidas-Ponce et al., 2019). These α−first-cells differ significantly from those of the second wave and have a specific gene signature (Bastidas-Ponce et al., 2019; Yu et al., 2019). The role of the first-wave α-like cells remains unclear, as these cells are not found at later stages in mice. It remains to be determined whether they acquire the characteristics of second-wave α-cells, or undergo apoptosis. A combination of lineage tracing and scRNA-Seq could address some of these questions.

During the second wave at E13.5-E17.5, EPs rapidly transit toward distinct endocrine fates, but multiple subpopulations representing subsequent maturation stages have consistently been identified by scRNA-Seq (Byrnes et al., 2018; Scavuzzo et al., 2018; Bastidas-Ponce et al., 2019; Yu et al., 2019). Importantly, cells with low levels of *Neurog3* expression were detected within the tip, trunk/BPs, and ductal clusters, suggesting that EPs emerge in different domains within the pancreas. The earliest EPs give rise to other EP subpopulations as *Neurog3* expression peaks, followed by late subpopulations with the extinction of *Neurog3* expression. The identification of early, *Neurog3*-Low EPs corroborates lineage-tracing results, showing that these cells as proliferating, long-lived cells (Schonhoff et al., 2004; Bechard et al., 2016). Lineage tracing also indicated despite the priming of *Neurog3*-Low cells for an endocrine fate, they may sometimes acquire a ductal or acinar fate. Thus, *Neurog3*-Low cells must either retain some multipotency or dedifferentiate (Bechard et al., 2016).

On their route to becoming endocrine islet cells, EPs delaminate from the epithelium into the surrounding mesenchyme. It is generally thought that individual delaminated EPs cross the mesenchyme, maturing into endocrine cells, and then aggregate into islets (Larsen and Grapin-Botton, 2017). An alternative model was recently proposed, in which EPs do not fully delaminate from the epithelial cord, instead forming budding peninsula-like structures attached to the cord (Sharon et al., 2019b). In this model, α-committed EPs arise first, lining the peninsula border, followed by β-committed EPs, which bud into the interior of the peninsula. This model is consistent with the final architecture of mouse and small human islets. It has been suggested that large human islets are formed by the coalescence of smaller islets. Peninsula-like buds have also been observed at the EP stage of human ESC differentiation (Sharon et al., 2019b). We have captured a small transient early EP subpopulation of Neurog3^{+} cells from E14.5 mouse pancreas. This N14_2 subpopulation displays a strong enrichment in the expression of epithelial-to-mesenchymal (EMT) genes, including vimentin (*Vim*), possibly reflecting the delamination process (Scavuzzo et al., 2018). These markers are lost in late-EPs and endocrine cells (Scavuzzo et al., 2018; Sharon et al., 2019b). Early EPs undergo a remodeling of adherens and tight junctions. Expression of the epithelial marker E-cadherin therefore transiently decreases but is not entirely abolished (Bakhti et al., 2019; Sharon et al., 2019b). This finding provides conclusive support for the hypothesis that EPs turn on delamination and EMT programs only partially, to enable them to move out of the epithelial cord whilst retaining epithelial characteristics ensuring their attachment to the epithelial cord during islet formation, without individual cells traveling through the mesenchyme.

A *Procr*$^{+}$ pancreatic population was recently identified by scRNA-Seq in 8 week-old adult mice (Wang D. et al., 2020). These *Procr*$^{+}$ cells have a transcriptional profile similar to that of the E14.5 N14_2 subpopulation, with similar EMT characteristics and *Procr* expression (Scavuzzo et al., 2018), and to

a subpopulation identified by another E14.5 pancreas scRNA-Seq study (Byrnes et al., 2018). Procr is a surface marker of adult stem cells in other mouse tissues, but not in the pancreas (Wang et al., 2015; Yu et al., 2016; Fares et al., 2017). The Procr+ cells in adult mouse pancreas no longer express *Neurog3* but are pre-endocrine descendants of Neurog3$^+$ progenitors and can give rise to α-, β-, δ-, and PP-cells in adult mice (Wang D. et al., 2020). When cocultured with endothelial cells, Procr+ cells expand *in vitro,* forming 3D clusters and differentiating into functional islet-like organoids. Upon transplantation, these organoids rescue streptozotocin-induced hyperglycemia in mice. The Procr$^+$ cells were the first EP-like adult cells to be cultured long-term *in vitro*. It would be interesting to delineate the ancestry relationship between the fetal Neurog3$^+$Procr$^+$ and adult Neurog3$^-$Procr$^+$ pancreatic cells and identify their human counterparts.

The late EPs, in which *Neurog3* expression is decreasing, are marked by high levels of *Fev* expression (Byrnes et al., 2018; Scavuzzo et al., 2018; Bastidas-Ponce et al., 2019; van Gurp et al., 2019; Yu et al., 2019). Fev is a transcription factor activated downstream from Neurog3 in the developing pancreas (Miyatsuka et al., 2009). The *FEV*$^+$ population in present in the fetal pancreas, human ESC-derived EPs, and immature endocrine cells (Krentz et al., 2018; Ramond et al., 2018; Veres et al., 2019; Augsornworawat et al., 2020). The *Fev*$^+$ late-EPs display an activation of endocrine cell genes including the *Chga*, *Isl1*, *Irx2,* and *Mafb* (Scavuzzo et al., 2018; Yu et al., 2019). Fev$^+$ cells may, therefore, represent an intermediate cell state between Neurog3$^+$ EPs and more mature endocrine cells.

scRNA-Seq studies have collectively shown that the pancreatic EP subcluster based on developmental stage can be broken down into at least four subpopulations: from early to late EPs. Moreover, these studies have revealed that EPs differ in terms of development potential, displaying a distinct propensity for the generation of α- or β-cells. Several markers have been proposed for the identification of EPs biased toward a specific endocrine cell type. For example, it has been suggested that *Peg10* and *Gng12,* which are expressed in *Fev*$^+$ cells at E14.5, could be used to characterize pro-α- and pro-β-EPs, respectively (Byrnes et al., 2018). *Myt1* was recently identified as a marker with enhanced expression in a late EP developmental trajectory branch leading to a β-cell fate (Liu et al., 2019). Lineage-tracing experiments have shown that Neurog3$^+$/Myt1$^+$ cells are less likely to differentiate into α-cells. However, neither *Neurog3* promoter-driven *Myt1* overexpression nor knockout has a major effect on the β- to α-cell ratio. Interestingly, scRNA-Seq studies of *Neurog3*$^+$*/Myt1*$^+$ and *Neurog3*$^+$*/Myt1*$^-$ EPs led to the discovery of a *Dnmt1*-driven increased in the methylation of the UR2 promoter of the *Arx* as a functional characteristic of *Neurog3*$^+$*/Myt1*$^+$ EPs inhibiting the α-cell fate acquisition (Liu et al., 2019).

EPs are formed continually during the secondary transition, with differences between those formed on different embryonic days (Scavuzzo et al., 2018; Bastidas-Ponce et al., 2019). We have shown that EPs born at E14.5 differ from those born at E16.5 in terms of their transcriptome and epigenome, with the latter revealed by ATAC-Seq (Scavuzzo et al., 2018). This heterogeneity reflects the bias of E14.5 EPs toward α-cells, whereas E16.5 EPs preferentially differentiate into β-cells. This finding is consistent with that of a previous report, in which a conditional, tamoxifen-induced reconstitution of Neurog3 in *Pdx1*$^+$ cells in *Neurog3*$^{-/-}$ mice revealed an age-dependent shift in the EP fate from a pro-α to a pro-β bias (Johansson et al., 2007). Other scRNA-Seq have also shown a temporal bias in the formation of α- and β-cells during the second wave of endocrinogenesis (Bastidas-Ponce et al., 2019; Yu et al., 2019). Moreover, E14.5 early EPs are present in the tips, whereas, after plexus-to-duct transition at E16.5, early EPs are found almost exclusively in the trunk domain. It remains unclear whether the tip-derived EPs are biased toward an α-cell fate, whereas trunk-derived EPs are biased toward a β-cell fate, which would be consistent with the timeline of EP and endocrine cell emergence.

Importantly, scRNA-Seq identified genes with similar patterns of expression throughout the generation, maturation and transition of EPs into specific endocrine lineages, revealing new candidate regulators of pancreas development. The use of single-cell technology also made it possible to capture rare early born rare endocrine cell types (i.e., δ-, ε-, and PP-cells) (Byrnes et al., 2018; Krentz et al., 2018; Bastidas-Ponce et al., 2019; Sharon et al., 2019b), and decipher the molecular blueprints of these populations. Moreover, scRNA-Seq confirmed a progressive loss of proliferation capacity and exit from the cell cycle in EPs and their progeny (Krentz et al., 2018; Scavuzzo et al., 2018; Bastidas-Ponce et al., 2019; van Gurp et al., 2019; Yu et al., 2019). The intriguing connection between the neuronal and pancreatic endocrine cell development programs (Arntfield and van der Kooy, 2011) has also been further extended by scRNA-Seq, through the identification of genes with previously known roles in the developing brain but not in the pancreas (Krentz et al., 2018; Bastidas-Ponce et al., 2019).

Endocrine Cell Maturation

Newborn endocrine cells mature to become fully functional adult cells. Two scRNA-Seq-based studies focused on endocrine cell maturation, analyzing β-cells (both studies) and α-cells (one of these studies) from *Ins1* and *Gcg* reporter strains, respectively, in E17.5—P60 mice (Qiu W.-L. et al., 2017; Zeng et al., 2017). A progressive maturation of β- and α-cells was observed, with the expected loss of known markers of immature endocrine cells and gain of mature endocrine cells markers, together with a decrease in the proportion of proliferative cells. However, these two cell types appear to have different maturation dynamics. β-cells mature steadily over time, with a progressive loss of immature cells, the acquisition of more mature states, and the generation of different postnatal subpopulations. A small population of immature β-cells is retained in adult mice, as revealed by both lineage tracing and scRNA-Seq (Bader et al., 2016; Sachs et al., 2020). By contrast, all postnatal α-cells (P9–P60) cluster together, indistinguishably, separately from E17.5-P0 cells, suggesting that the maturation end-state is acquired earlier in α-cells (Qiu W.-L. et al., 2017). Human endocrine cells display a similar differential pattern of maturation, as shown by a comparison of β- and α-cells from a newborn, toddlers (10 months–4 years old), adolescents, and adults (Avrahami et al., 2020). Newborn β-cells clustered separately from maturing β-cells from toddlers or older individuals. These results for

newborns were obtained with cells from a single donor, but they may nevertheless indicate that β-cells do not become functional until after birth. This may be because blood glucose levels are regulated directly by the mother's cells during gestation. The β-cells of toddlers retain multiple characteristics of immature cells, such as activated TNF and Notch signaling. By contrast, α-cells from the islets of individuals of all ages, from toddlers to adults, were indistinguishable, and displayed a pattern of gene expression common to immature, newborn α-cells, suggesting that maturation involves less pronounced transcriptomic changes in α-cells than in β-cells. This finding may also reflect the greater plasticity and regeneration potential of α-cells *in vivo*. Indeed, α-cells can transdifferentiate into β-cells, in a process driven by FOXO1 inhibition (Chera et al., 2014), or the activation of GABA receptor signaling, which can also be induced by artemisinins, a class of antimalarial drugs (Li et al., 2017). ScRNA-Seq provided evidence of α-cell dedifferentiation in mouse and human islets *ex vivo*, when these islets were treated with FOXO inhibitor, GABA or artemisinin drug, artemether (Marquina-Sanchez et al., 2020). However, FOXO inhibition is not specific to α-cells. It also induces β-cell dedifferentiation, preventing the use of this pathway to restore β-cell mass in situations in which not all β-cells are lost. Detailed comparison of transcriptomes during α- and β-cell maturation might identify cell type-specific maturation factors for the refinement of induced maturation and transdifferentiation.

The markers of immature β-cells include retinol binding protein 4 (*Rbp4*) (Qiu W.-L. et al., 2017; Zeng et al., 2017), which is also highly abundant in the β-cell subpopulations present in the adult human pancreas (Segerstolpe et al., 2016; Mawla and Huising, 2019; Camunas-Soler et al., 2020). A combination of single-cell patch-clamp electrophysiology and scRNA-Seq (Patch-Seq) revealed that the RBP4-rich β-cells in the adult human pancreas have reduced functionality, which manifests in lower levels of Na^+ channel activity and exocytosis (Camunas-Soler et al., 2020). As revealed by another scRNA-Seq study, *Rbp4* levels are also high in surviving β-cells in a multiple-low-dose model of streptozotocin-induced diabetes (mSTZ) in mice (Sachs et al., 2020). Together with the observed alterations to other pathways in these mSTZ-β-cells, these findings suggest that β-cells dedifferentiate to generate the $Rbp4^+$ population in pharmacologically induced diabetes.

Maturing β-cells display a decrease in mTORC1 signaling and pro-proliferative gene expression, and changes to amino-acid metabolism, mitochondrial respiration, and reactive oxidative species response gene expression (Zeng et al., 2017). Similar changes in mTORC1 and mitochondrial metabolism are associated with the poor proliferation capacity of immature β-cells, due to a misfolding mutation in proinsulin, responsible for neonatal diabetes (Balboa et al., 2018).

The Developing Pancreatic Niche

The embryonic pancreas receives mechanical and chemical signals from surrounding tissues and non-epithelial cells within the pancreas. These signals jointly drive development, regulating the expansion and differentiation of progenitors (reviewed in detail by Cozzitorto and Spagnoli, 2019). For example, mesenchyme was shown to be required for pancreas development as long ago as the 1960s (Golosow and Grobstein, 1962). More recently, the use of sophisticated transgenic mouse models has made it possible to separate out the various developmental roles of the mesenchyme at different timepoints (Landsman et al., 2011) and to identify mesenchyme subpopulations with different pro-endocrine potentials (Cozzitorto et al., 2020). Mesenchymal niche-derived factors are beneficial for hPSC differentiation into pancreatic endocrine cells (Guo et al., 2013; Russ et al., 2016; Mamidi et al., 2018; Cozzitorto et al., 2020). Finally, coculture with mesenchyme promotes the self-renewal of mouse ESC-derived $Ngn3^+$ progenitors (Sneddon et al., 2012).

scRNA-Seq studies focused initially on the pancreatic epithelium, but also have shed light on the mesenchymal compartment, revealing its heterogeneity at E12.5-E18.5 (Byrnes et al., 2018; Krentz et al., 2018; Scavuzzo et al., 2018). These studies (Byrnes et al., 2018; Scavuzzo et al., 2018) identified similar mesenchymal populations in the E14.5 pancreas: the largest cluster, consisting of archetypal proliferating mesenchyme cells, a few smaller mesenchymal clusters, myofibroblast-like stellate cells, and proliferating and non-proliferating mesothelial populations. Mesenchymal clusters were differentially enriched in secreted factors. One cluster is enriched in Wnt signaling agonists, chemokines, and ACE2, and another expresses TGFβ, Hippo, and Id pathway components, suggesting different functions for these two clusters. Another mesenchymal cluster in the E12.5-E14.5 pancreas is enriched in the NKX2-5 transcription factor and represents the splenopancreatic mesenchyme surrounding the pancreatic buds showed to be essential for endocrine lineage specification (Hecksher-Sørensen et al., 2004; Cozzitorto et al., 2020). Pseudotime analysis from E12.5-E17.5 suggested that mesothelial cells are the progenitors of mesenchyme subpopulations and stellate cells (Byrnes et al., 2018). This function had already been demonstrated in other organs but had never before been shown for the pancreas. A comparison of E12.5, E14.5, and E17.5 scRNSeq datasets revealed that the mesenchymal subpopulations changed, through differentiation and maturation, or simply disappeared during the course of development (Byrnes et al., 2018), corroborating earlier findings for transgenic models. Between E15.5 and E18.5, the mesenchyme also becomes less heterogeneous (Krentz et al., 2018). It would be interesting to elucidate the developmental role of each mesenchymal subtype, by studying the interactions of each subtype with other pancreatic cell types.

INSIGHT INTO HUMAN PANCREAS DEVELOPMENT FROM PLURIPOTENT MODELS

The sequence of developmental events is highly conserved between species, but there are nevertheless interspecies differences in pancreatogenesis (Nair and Hebrok, 2015). For example, NEUROG3 is transiently and robustly expressed, in two waves, in mice (Gradwohl et al., 2000; Schwitzgebel et al., 2000; Gu et al., 2002), whereas human NEUROG3 expression occurs in single wave (Lyttle et al., 2008; Jennings et al., 2013;

Salisbury et al., 2014). The embryonic islet cells of mice are mostly monohormonal, whereas a large proportion of human islet cells are initially polyhormonal (Bocian-Sobkowska et al., 1999; Herrera, 2000; Riedel et al., 2012). Moreover, a comparison of scRNA-Seq of mouse and human β- and α-cells revealed differential expression of multiple genes between these species (Xin et al., 2016). These examples highlight the need to confirm any findings obtained in mice in human models.

Ethical restrictions limit studies on human embryos. As a result, the *in vitro* hPSC differentiation has become a powerful tool to study human pancreatic development. Current hPSC differentiation protocols focus on the generation of functional β-cells, but other endocrine cell types and polyhormonal cells also arise during differentiation (Pagliuca et al., 2014; Rezania et al., 2014; Cogger et al., 2017; Nair et al., 2019; Velazco-Cruz et al., 2019). The *in vitro* differentiation aims to mimic the subsequent embryogenesis stages of β-cell development, by modulating the signaling pathways triggered during this process, including signals arising from non-epithelial pancreatic niche cells not directly incorporated into protocols. The use of suspension (3D) protocols results in a microenvironment more closely resembling *in vivo* embryogenesis than that generated by the planar (2D) cultures initially used. This approach also increases the functionality of hPSC-derived β-cells (Russ et al., 2015; Millman et al., 2016; Velazco-Cruz et al., 2019). *In vitro* differentiation as 3D spheroids is also widely used for the generation of other endoderm derivatives, such as intestine or lung cells (Workman et al., 2016; Múnera et al., 2017; Yamamoto et al., 2017; Miller et al., 2019).

The outcome of hPSC pancreatic differentiation is usually assessed by determining the proportion of cells expressing a limited number of stage-specific markers. As an endpoint assay, the β-cell functionality is evaluated either *in vitro* (in terms of glucose-stimulated insulin secretion) or *in vivo* (the ability to restore glucose homeostasis in diabetic mice). However, scRNA-Seq on the developing pancreas have revealed progenitor heterogeneity, including early acquired biases toward progeny lineages and continuous changes in cell state. The use of single-cell omics approaches to study subsequent steps of human *in vitro* pancreatic development more closely would improve the control of pancreas engineering, paving the way for clinical applications.

To this end, scRNA-Seq has been used to specify populations at different stages during 2D and 3D β-cell differentiation (Krentz et al., 2018; Sharon et al., 2019a; Veres et al., 2019). The 3D protocols used in these studies included six stages, with PDX1$^+$ pancreatic progenitors (PP1) forming at the end of stage 3 (8 days of differentiation, efficiency > 90%), PDX1$^+$/NKX6-1$^+$ progenitors (PP2) at the end of stage 4 (5 more days, ∼60% efficiency), and immature NKX6-1$^+$/C-PEP$^+$ endocrine cells (EN) forming at the end of stage 5 (7 more days), followed by reaggregation to promote maturation into functional β-cells (SC-β) after seven or more additional days. At the PP1 stage, the PDX1$^+$ population was rather homogeneous, with the exception of a discrete PDX1$^+$ subpopulation undergoing mitosis, corresponding to high differentiation efficiency at this stage (Veres et al., 2019). At the PP2 stage, PDX1$^+$/NKX6-1$^+$ progenitors constituted the largest population, including a proliferating subpopulation, followed by EPs (NEUROG3$^+$ and FEV$^+$ISL$^-$ populations), first α-like cells, and a rare SST$^+$/HHEX$^+$ δ-like population. The presence of EPs and their derivatives at this early stage indicates a precocious induction, before the NKX6-1 expression (Russ et al., 2016; Sharon et al., 2019a), and the initiation of an α-like differentiation, probably leading to bihormonal GCG$^+$/INS$^+$ cells. NEUROG3$^+$NKX6-1$^-$ and NKX6-1$^-$ endocrine cells were also detected early in 2D pancreatic differentiation by sc-qPCR and scRNA-Seq (Petersen et al., 2017; Krentz et al., 2018). The endpoint endocrine cells were mostly polyhormonal and immature relative to adult human islet cells. It would be interesting to determine whether these cells correspond to the first wave of α-cells from mouse early MPs, which has yet to be clearly demonstrated in human pancreas development, or to the second wave of endocrine differentiation, in which α-cells precede β-cells.

scRNA-Seq revealed that PP2 stage progenitors express BMP pathway genes. BMP blocks the precocious induction of *NEUROG3*, whereas BMP inhibition promotes this induction (Sharon et al., 2019a). BMP inhibitors were widely included in the early 2D and 3D differentiation protocols. scRNA-Seq also revealed an enrichment in canonical Wnt pathway components in PPs relative to endocrine-committed cells. By contrast, endocrine cell clusters display an enrichment in APC, which inhibits Wnt, suggesting that Wnt signaling may suppress endocrine induction (Sharon et al., 2019a). Indeed, the preservation of Wnt activity in *Neurog3*$^+$ cells, via conditional Cre-mediated APC KO, blocks their differentiation into endocrine cells in mice (Sharon et al., 2019a). Conversely, the Wnt inhibition at the EN stage substantially increases the efficiency of C-PEP$^+$/NKX6.1$^+$ cell derivation (Sharon et al., 2019a).

Unexpectedly, scRNA-Seq identified a novel endocrine population arising from *NEUROG3*$^+$ progenitors during the EN stage, along with immature β-, α- and rare δ-like cells (Veres et al., 2019). The cells of this SC-EC population, resemble enterochromaffin cells, a serotonin-producing chemosensor gut cell type (Grün et al., 2015; Haber et al., 2017). SC-ECs have a frequency similar to that of SC-β cells (Veres et al., 2019) and can be identified by scRNA-Seq in 2D differentiation (Krentz et al., 2018; Augsornworawat et al., 2020). SC-ECs appear to be closely related to SC-β cells, which can also produce serotonin *in vivo* (Almaça et al., 2016). They also have a similar developmental program to common *NEUROG3*$^+$ progenitors, suggesting possible misdifferentiation *in vitro*, as these cells do not seem to arise in the pancreas *in vivo* (Veres et al., 2019; Augsornworawat et al., 2020). Moreover, enterochromaffin marker genes were induced in a β-cell dedifferentiation model (Lu et al., 2018; Veres et al., 2019), again pointing to a close relationship between the two cell types. SC-ECs express *CHGA*, *NKX6-1*, and low levels of *INS,* but they do not express *GCG* (Veres et al., 2019), suggesting possible misalignment with β-cells in immunostaining-based assays. The depletion of SC-ECs with the CD49a surface marker, identified by scRNA-Seq as characteristic of SC-β population, results in an enrichment in SC-β cells and promotes their maturation (Veres et al., 2019). Other groups have similarly observed that reaggregation

(based on the INS-GFP reporter) or simple cluster resizing promotes the *in vitro* β-cell maturation (Nair et al., 2019; Velazco-Cruz et al., 2019). As enrichment for β-like cells based on a surface marker or reporters cannot be applied to clinical-grade preparations, it would be desirable to block SC-EC during differentiation. Single-cell transcriptomics has provided insight into the bifurcation event, during which common NEUROG3$^+$ progenitors split into two groups destined to become either SC-EC or SC-β cells; over 300 genes displaying enriched expression in one particular branch were identified (Veres et al., 2019), providing a possible starting point for protocol refinement.

Interestingly, scRNA-Seq also revealed that significant proliferative non-endocrine populations appear first at the EP stage and then at the endocrine maturation stage. These non-endocrine cells develop into ductal, acinar and mesenchymal cell-like populations (Veres et al., 2019), implying that some of the PDX1$^+$/NKX6-1$^+$ cells at the PP2 stage retain or regain multipotency. This hypothesis is supported by lineage-tracing in mice showing that early progenitors with Neurog3 low expression retain a small degree of multipotency (Bechard et al., 2016). The 3D sphere dissociation and reaggregation at EP stage purifies endocrine cells from non-endocrine populations (Veres et al., 2019). However, protocol refinement to block non-endocrine commitment would probably increase the yield of functional β-cells.

Mechanosignaling from the mesenchyme is critical for PP fates (Mamidi et al., 2018). During development, the mesenchymal extracellular matrix triggers F-actin depolymerization, leading to the recruitment of YAP1 to the cytoplasm, impeding its nuclear function in the blocking of *NEUROG3* expression together with Notch. scRNA-Seq was used to investigate the involvement of cytoskeleton remodeling in EP induction (Hogrebe et al., 2020). In the experimental conditions used, almost all the adherent multipotent PDX1$^+$ progenitors developed into PDX1$^+$/NKX6-1 BPs within 5 days. However, F-actin depolymerization by latrunculin A greatly decreases the proportion of PP2 (about 20% of all cells) and stimulates precocious EP differentiation (about 50%) without the NKX6-1 induction, and leads to the an undefined endodermal fate (about 26%), probably non-pancreatic. Conversely, reinforcement of the F-actin skeleton by nocodazole treatment shifted differentiation toward exocrine-like progenitors (about 66% of all cells). The application of latrunculin A during the first day of a seven-consecutive day stage in which BPs differentiate into EPs and immature endocrine cells leads to the efficient generation of functional β-cells from various cell lines, mostly in 2D protocols. Lantrunculin-induced cytoskeleton alterations also affect differentiation into other primitive gut descendants, such as intestine and liver cells, suggesting that the possible mechanosignaling mechanisms common to the development of other endodermal organs (Hogrebe et al., 2020). The SC-β cells generated by planar protocols are functional *in vitro* and rescue STZ-induced diabetes in mice similarly to human islets. However, these SC-β cells retain multiple transcriptomic and functional features of juvenile, immature β-cells, and are thus different from human adult islets (Augsornworawat et al., 2020; Hogrebe et al., 2020). *In vivo*, SC-β cells further mature toward a more human islet-like state, as revealed by scRNA-Seq 6 months after transplantation (Augsornworawat et al., 2020). A closer look at the pathways active in grafted SC-β, might reveal novel candidate regulators of maturation.

The advent of CRISPR technology has increased the accessibility of genetically engineered hPSCs, allowing the manipulation of known or putative regulators of development for their function assessment in the human context. Again, scRNA-Seq may facilitate characterization of the mutation consequences. Russell et al. recently assessed the developmental role of MAFB (Russell et al., 2020), a transcription factor that binds to crucial β-cell genes, including *INS* and *PDX1* (Nishimura et al., 2006; Vanhoose et al., 2008). This is particularly interesting given the differential expression of *MAFB* between species. It is expressed in human adult α-, β- and δ-cells (Fang et al., 2019; Avrahami et al., 2020), whereas it is expressed solely in α-cells in adult mice, its expression in β-cells being lost upon maturation of these cells (Qiu W.-L. et al., 2017; Zeng et al., 2017). MAFB murine KO results in a quantitative and functional α-cell deficiency, whereas β-cell development is only delayed (Katoh et al., 2018). As demonstrated by scRNA-Seq, MAFB KO does not affect hPSC-to-EP differentiation; instead, it blocks α- and β-cell specification, leading to the induction of rare endocrine lineages, such as δ-cells, PP-cells, gastrin$^+$ and peptide YY$^+$ cells (Russell et al., 2020). No link has been established between MAFB mutations and diabetes, but many other genes have been shown to cause monogenic forms of diabetes. Thus, hPSC lines with KOs of these genes, and patient-derived iPSCs are potentially invaluable models for research into pancreas development and diabetes pathogenesis.

β-cells initially proliferate, exiting the cell cycle once they have matured (Kulkarni et al., 2012). However, a low level of proliferation is maintained in adulthood, to allow for β-cell mass maintenance (Bader et al., 2016). The identification of rare adult β-cells capable of proliferating, and the characterization of triggers and signaling pathways via which β-cells re-enter the cell cycle are of considerable interest, as a way of replenishing these cells in diabetes patients *in vivo,* and of increasing the yield of *in vitro*-derived β-cells. The YAP pathway was shown to induce SC-β cell proliferation (Rosado-Olivieri et al., 2019). Rosado-Olivieri made use of this discovery to force SC-β-cells to re-enter the cell cycle, and then used scRNA-Seq to identify the enriched pathways, as putative proliferation drivers (Rosado-Olivieri et al., 2020). One of the identified drivers was the leukemia inhibitory factor (LIF) pathway, acting through JAK/STAT and the CEBPD transcription factor. LIF induces the proliferation of mouse β-cells *in vivo*, human islets grafted into murine kidneys, and SC-β-cells. Interestingly, LIF receptor (*LIFR*)-positive β-cells constitute a small (less than 20%) subpopulation of cells with a distinct transcriptomic profile among SC-β cells or adult human islets (Rosado-Olivieri et al., 2020).

In addition to β-cell degeneration, α-cell dysfunction may also underlie diabetes progression (Gromada et al., 2018; Yosten, 2018). In the T1D treatment, α-cells are essential for the tight control of islet hormone secretion, and for the regulation of glucose levels, but most studies to date have focused on the generation of β-cells. Early NEUROG3

induction in PDX1$^+$/NKX6-1$^-$ progenitors leads exclusively to the generation of α-like bihormonal cells. BMP inhibition has therefore been used to enhance this induction, resulting in the efficient generation of functional α-like cells, known as SC-α cells (Peterson et al., 2020). The bihormonal α-like cells (pre-α cells) express both GCG and INS, but pro-insulin is not processed to generate mature insulin in these cells (Peterson et al., 2020). Bihormonal α-like cells are transiently present during human pancreatic development and in diseases, such as diabetes (Riedel et al., 2012; Md Moin et al., 2016). The pre-α cells eventually mature into monohormonal GCG$^+$ cells. *In vitro,* the functional maturation of these cells is efficiently promoted PKC activator treatment during stage 6. By contrast, the pre-α-cells maturation into monohormonal SC-α cells was rare in prior protocols for β-cell maturation. A comparison of the transcriptomes of individual pre-α-cells and mature SC-α cells revealed a subtle maturation process, with the silencing of stress-related and insulin secretion pathways and the induction of glucagon release [(Peterson et al., 2020). Studies based on pre-α-cell transplantation (Augsornworawat et al., 2020) have suggested that SC-α cells undergo further maturation in mice. Such a transplantation model could be used to identify regulators of α-cell maturation, leading to further refinement of the *in vitro* derivation protocol.

DIABETES

scRNA-seq provides insight into the diabetes-induced dysfunction of each islet cell type and subtype, making it possible to identify pathway dysregulations undetectable with bulk RNA-seq. Main studies that used scRNA-Seq to identify pathways involved in diabetes or obesity are summarized in **Supplementary Table 2**. In the initial studies, T2D-related transcriptional alterations were found not only in β-cells, but also in other islet and non-endocrine cells (Segerstolpe et al., 2016; Xin et al., 2016; Lawlor et al., 2017). In addition, there is growing evidence to suggest that adult endocrine cell populations are not homogeneous (**Supplementary Table 2**) and that the ratios of the various subpopulations change in pathogenic situations. Adult β-cells differ in terms of their phenotypic, proliferative, and functional characteristics, and these cells may have different sensitivities to glucose. Multiple molecular markers have been proposed for the characterization of β-cell heterogeneity (Dominguez-Gutierrez et al., 2019). For example, a small population of β-cells with pacemaker properties, called hub cells, has been identified (Johnston et al., 2016). These cells with immature characteristics are indispensable for the islet-wide coordinated response to glucose and are specifically targeted by diabetic stress. scRNA-Seq could, therefore, potentially reveal alterations in specific subpopulations.

A comparison of the transcripts dysregulated in T2D from multiple studies revealed a minimal overlap of genes, possibly due to the limited numbers of donors and of sequenced cells (Wang and Kaestner, 2019). As only a fraction of the cells may be affected by disease, and changes in the expression of individual genes may be subtle, transcriptional dysregulation may be masked by natural variation between individuals. Fang et al. therefore developed the RePACT (regressing principal components for the assembly of continuous trajectory) strategy, in which changes in cellular heterogeneity in a context of obesity or T2D were treated as a development-like pseudotime trajectory (Fang et al., 2019). The combination of this approach with high-throughput scRNA-Seq resulted in the identification of discrete affected β-cell subpopulations, the comparison of which increased statistical power and made it possible to detect changes in gene expression common to obesity and T2D and changes specific to each of these conditions. The common alterations included an upregulation of hypoxia-related genes and a downregulation of aerobic respiration-related genes. *INS* was also one of the genes deregulated, displaying upregulation in obesity but downregulation in T2D, confirming previous scRNA-Seq findings (Segerstolpe et al., 2016). Other genes with inverse patterns of expression in obesity and T2D included two ferritin genes, *FTL* and *FTH1*, encoding proteins involved in intracellular iron metabolism (Fang et al., 2019). This finding is consistent with the observation that obese patients have low serum iron levels, whereas high serum iron levels are a risk factor for T2D (Simcox and McClain, 2013). In addition, a combination of the RePACT approach and a CRISPR screen identified known and unknown insulin regulators in T2D and obesity trajectories, including Mau2-Nipbl cohesin loading complex, a new *INS* gene transcription regulator, and the NuA4/Tip60 HAT complex, a new insulin secretion regulator, with possible roles in diabetes development (Fang et al., 2019).

Another insight into compensatory mechanisms related to β-cell physiology in T2D was provided by a powerful multimodal approach, in which single-cell transcriptomes for endocrine cells were coupled with exocytosis measurements, for the estimation of glucose-dependent insulin secretion with Patch-Seq technology (Camunas-Soler et al., 2020). Multiple genes with expression patterns positively or negatively correlated with exocytosis in healthy cells were inversely correlated with exocytosis in individuals with T2D. These results suggest that damaged islet cells display changes in functionality-related transcript levels with increases in blood glucose levels, but that their response is weak. One of the mechanisms thought to underlie this phenomenon is an increase in inflammation due to the insufficient degradation of ETV1 and STAT3 by COP1 ubiquitin ligase (Suriben et al., 2015; Nordmann et al., 2017). Indeed, ETV1 knockdown increases exocytosis β-cells from T2D patients, but not in healthy β-cells (Camunas-Soler et al., 2020). It has been suggested that hyperglycemia-induced inflammation triggers endocrine cell dedifferentiation in T2D and T1D (Talchai et al., 2012; Cinti et al., 2016; Nordmann et al., 2017; Bensellam et al., 2018; Seiron et al., 2019). In support of this dedifferentiation model, single-cell studies performed by the group of Kaestner have shown that the gene expression patterns of α- and β-cells from T2D individuals are similar to that of juvenile, immature cells, suggesting that damage to endocrine cells triggers dedifferentiation (Wang et al., 2016; Avrahami et al., 2020). Furthermore, a comparison of the transcriptome of immature or mature β-cells from healthy, developing mice with that of β-cells surviving mSTZ, revealed a reversion to an embryonic immature β-cell-like state

(Sachs et al., 2020). Years after the onset of T1D, only a few β-cells prevail in most patients (Keenan et al., 2010; Oram et al., 2015), suggesting that β-cell redifferentiation is a promising strategy for the treatment of T1D and T2D.

Dedifferentiation probably involves epigenetic mechanisms. Based on CHIP-Seq and scRNA-Seq in mice, Lu et al. recently identified a loss of polycomb repressor complex (PRC2) function as the underlying cause of adult β-cell identity loss (Lu et al., 2018). They confirmed the PRC2 dysfunction in T2D islets. Mechanistically, the dysregulation of PRC2 in β-cells triggers epigenetic remodeling at specific loci in the β-cell genome in the context of a high-fat diet, in mice with a loss of PRC2 function, resulting in an increase in transcriptional entropy, with the ectopic expression of bivalent loci and an explicit loss of the acetylation of β-cell-specific transcription factors (Lu et al., 2018). The re-activation of bivalent loci characteristic of immature β-cells in human newborns has also been observed in T2D β-cells (Avrahami et al., 2020).

Diabetes induced by stress-activated β-cell dedifferentiation may be reinforced by the inhibition of FOXO1 signaling (Talchai et al., 2012). scRNA-Seq in *ex vivo* mouse and human islets treated with FOXO1 inhibitor demonstrated β-cell dedifferentiation revealed as similar dedifferentiation of α-cells (Marquina-Sanchez et al., 2020). In juvenile mice depleted of β-cells, FOXO1 inhibition also results in δ-cell dedifferentiation to such an extent that these cells can undergo endocrine lineage specification (Chera et al., 2014). A recent study by Sachs and colleagues showed that combined treatment with PEGylated-insulin and GLP-1-estrogen conjugate reverses STZ-induced diabetes, mainly by inducing the proliferation and redifferentiation of dedifferentiated β-cells (Sachs et al., 2020). The FOXO1 and MAPK pathways were implicated in this process.

iPSCs derived from diabetic patients are a powerful tool for studies of pathogenesis and efforts to develop effective treatments. In T2D or monogenic diabetes, patient iPSC-derived β-cells or islets can be used for autologous transplantation (after genetic correction in the case of monogenic diabetes). For studies on the mechanisms underlying disease, candidate gene mutations can be introduced into healthy PSCs. Progress in diabetes research through studies using human PSC models has been described in detail elsewhere (Balboa et al., 2018). More recently, scRNA-Seq has been used to determine the precise effects on β-cell differentiation of mutations in patient-derived iPSCs (Balboa et al., 2018; Maxwell et al., 2020). Notably, iPSCs carrying mutations have been compared to genetically corrected isogenic lines, a method of decreasing intra-iPSC line variability. In a first study, iPSCs with a heterozygous *INS* C96Y mutation resulting in proinsulin misfolding and neonatal diabetes differentiated into β-like cells less efficiently than their counterparts with a corrected mutation. scRNA-Seq revealed high levels of endoplasmic reticulum (ER) stress, low levels of mTORC1 signaling, and mitochondrial alterations, which together resulted in early proliferation defects in cells with misfolded C96Y proinsulin, where were validated following the transplantation of these cells into mice (Balboa et al., 2018). The restoration of mTORC1 signaling in a mouse model of insulin misfolding, the Akita mouse, rescued neonatal β-cell proliferation defects and aggravated the diabetic phenotype (Riahi et al., 2018). These studies together identify mTORC1 signaling as a potential treatment target in neonatal diabetes, although any treatment would need to be applied very early in life to be effective. In another study, the CRISPR-Cas9 system was used to correct a diabetes-causing pathogenic variant of the Wolfram syndrome 1 (WFS1) gene in iPSCs derived from a patient with Wolfram syndrome (WS) (Maxwell et al., 2020). This correction improved the differentiation and maturation of SC-β cells relative to uncorrected isogenic cells, including their ability to secrete insulin in a dynamic manner following stimulation with glucose *in vitro,* and it reversed diabetes following the transplantation of corrected cells into a diabetic mouse. A comparison of scRNA-Seq transcriptomes from corrected and uncorrected iPSCs at the mature endocrine cell stage revealed substantial misdifferentiation, with an expansion of the non-pancreatic and acinar lineages at the expense of SC-β, α-, and δ-cells, and most of the remaining endocrine cells being enterochromaffin cells. Patient SC-β cells experienced higher levels of ER and mitochondrial stress than corrected cells, and displayed higher levels of expression for apoptosis markers, as generally observed in cases of WFS1 gene deficiency (Fonseca et al., 2005, 2010; Yamada et al., 2006) and consistent with a previous Wolfram Syndrome iPSC study (Shang et al., 2014). Collectively, scRNA-Seq has greatly extended our knowledge of the mechanisms involved in endocrine cell dedifferentiation in diabetes, paving the way for β-cell mass restoration.

NON-DIABETIC DISEASES OF PANCREAS

In this review we mainly focus on endocrine pancreas, however, diabetes is often strictly linked to other prevalent pancreatic conditions, like cancer and pancreatitis. These conditions share a common feature—the long-term pancreatic inflammation and, together with obesity, significantly increase risk to develop each other (Paternoster and Falasca, 2020). Pancreatic ductal adenocarcinoma (PDAC) is one of the leading death-causing cancer types worldwide, yet early malignancy markers allowing detection and treatment at pre-metastatic stage and prior to drug resistance acquisition are missing (Storz and Crawford, 2020). PDAC develops from benign lesions through a complex interplay between transformed exocrine cells and microenvironment, as it has been thoroughly reviewed elsewhere (Bulle and Lim, 2020; Storz and Crawford, 2020). The two essential components for PDAC development are: (1) acquisition of an oncogenic mutation by acinar or ductal cells, with KRAS oncogene counting for 90% of cases; (2) inflammation within microenvironment which drives early lesion development. Multiple scRNA-Seq studies in PDAC mouse models and human tumor samples shed light on tumor cell identity and heterogeneity, as well as tumor microenvironment (TME), including role of cancer associated fibroblasts (CAFs) and immune landscape, and cross-talk between tumor and TME (Ting et al., 2014; Bernard et al., 2019; Elyada et al., 2019; Hosein et al., 2019; Ligorio et al., 2019;

Peng et al., 2019; Dominguez et al., 2020; Hwang et al., 2020; Lee et al., 2020; Schlesinger et al., 2020; Steele et al., 2020; Zhou et al., 2021). These studies showed that intra-tumor heterogeneity identified by scRNA-Seq is reliable as a prognostic marker and can be used for personalized treatment choice. Importantly, scRNA-Seq on samples collected by fine-needle low-input biopsies is sufficient as diagnostic tool (Lee et al., 2020; Steele et al., 2020). Moreover, these studies revealed acquisition of immunosuppressive TME during neoplastic progression, which allow to further focus on mechanisms beyond this phenomenon.

PDAC can develop when control over a physiological regeneration of exocrine pancreas fails (Storz, 2017). The regeneration is driven by a reversible process of acinar cells dedifferentiation into duct-like exocrine progenitors (acinar-to-ductal metaplasia, ADM), and the transitional, plastic populations were observed in adult human pancreata and PDAC samples by scRNA-Seq (Qadir et al., 2020; Zhou et al., 2021) and single-nucleus RNA-Seq (sNuc-Seq) (Tosti et al., 2021). The irreversible dedifferentiation and unrestrained proliferation of these progenitors leads to pancreatic intraepithelial neoplastic lesions (PanIN) and eventually PDAC (Storz, 2017). Regenerating gene protein (REG) family-enriched acinar cells were identified as promoting ADM and PanIN growth (Gironella et al., 2013; Liu et al., 2015). A small proportion of REG+ population was identified by scRNA-Seq also in non-disease pancreata (Muraro et al., 2016; Tosti et al., 2021), and enriched in low-grade lesions (Bernard et al., 2019) and PDAC (Schlesinger et al., 2020). A recent sNuc-Seq study identified REG+ cells as the only exocrine cluster in a pancreatitis sample, whereas they were minority in healthy pancreas and not present in neonatal pancreas (Tosti et al., 2021). *In situ* sequencing revealed that these cells reside near macrophages, possibly modulating immune response (Tosti et al., 2021). Moreover, research on PDAC, pre-metastatic PanIN and intraductal papillary-mucinous neoplasms, identified transition of KRT19+ ductal populations along tumor development, where MUC5AC-rich clusters are present in benign lesions, and MUC5B+ metaplastic populations marks pancreatitis and PDAC (Bernard et al., 2019; Peng et al., 2019; Schlesinger et al., 2020; Tosti et al., 2021).

Several recent scRNA-Seq studies focused on role of TME components, for example CAFs, in PDAC development. CAFs are actively involved in tumor growth, metastasis and drug resistance in various types of cancers (Bulle and Lim, 2020; Hosein et al., 2020). Myofibroblastic myCAFs and inflammatory iCAFs were recently described as two subtypes present in PDAC and originating from activated pancreatic stellate cells (Öhlund et al., 2017). These cells were robustly identified at different stages of lesion development by multiple scRNA-Seq studies (Bernard et al., 2019; Elyada et al., 2019; Hosein et al., 2019; Ligorio et al., 2019; Peng et al., 2019; Dominguez et al., 2020). Moreover, a novel subpopulation of antigen presenting CAFs (apCAFs) was discovered by scRNA-Seq study (Elyada et al., 2019) and further confirmed by others (Hosein et al., 2019; Dominguez et al., 2020; Lee et al., 2020; Zhou et al., 2021). The scRNA-Seq data led to further insights into CAFs roles in tumor development, e.g., changes the subtypes proportions during lesion progression and after drug treatment (Bernard et al., 2019; Dominguez et al., 2020; Zhou et al., 2021), immunosuppressive roles of iCAFs and apCAFs (Bernard et al., 2019; Elyada et al., 2019), identification of CAF-specific prognostic markers like LRRC15^{+} (Dominguez et al., 2020), identification of TGFβ as CAF-released signal inducing metastatic and proliferative PDAC phenotype run by MAPK and STAT3 pathways (Ligorio et al., 2019), and suggested CAFs plasticity as a potential therapeutic target (Feldmann et al., 2021). These advanced scRNA-seq studies together provided valuable input into the molecular mechanism of PDAC, and provided novel candidate targets for treatment.

DISCUSSION: CONCLUDING REMARKS AND FUTURE PERSPECTIVES

Many studies have shown that scRNA-Seq technology has the power to confirm and extend the fundamental findings obtained with traditional research approaches. Moreover, the datasets generated by different research groups, with platforms using advanced and less advanced technologies, or different patterns of cell-type enrichment, have generally been similar, after variability in sensitivity, technical noise, and data processing methods has been taken into account. Multiple datasets for the developing pancreas have made it possible to identify equivalent, previously unknown pancreatic subpopulations. Furthermore, the use of novel bioinformatic tools to re-analyze existing datasets and integrate them into a single model may reveal details that had previously been missed. For example, the integration of adult pancreas datasets resolved clusters of sporadic populations, such as ε, Schwann, mast and macrophage cells, that had remained undetected in the individual datasets (Stuart et al., 2019).

The ultimate aim of endocrine pancreatic research is the development of better treatments or cures for diabetes. In this context, an increasing number of scRNA-Seq studies are identifying candidate regulatory genes and pathways beyond the development and pathogenesis of diabetes, for which further validation is required. The curated data for the developing pancreas will make it possible to refine *in vitro* and *in vivo* methods for manipulating pancreatic endocrine cell identity and expansion. For example, ligand-receptor connectome analyses can be performed on existing time-series datasets including pancreatic niche components, to identify time-dependent, specific niche-derived signals influencing cell-fate decisions (Byrnes et al., 2018; Scavuzzo et al., 2018). The power of such systems biology approaches was recently demonstrated in an elegant study by Han et al., in which the authors used scRNA-Seq to reveal complex interactions, including some involving signaling pathways, between the gut tube endoderm and mesoderm at E8.5-E9.5 (Han et al., 2020). In the human context, scRNA-Seq has highlighted a number of obstacles to the robust generation of functional human β-cells, including: (1) the precocious differentiation of NKX6-1^{-} pancreatic progenitors, (2) the incomplete commitment of PDX1^{+}NKX6-1^{+} cells to an endocrine fate, and (3) misdifferentiation into enterochromaffin-like cells (**Figure 2A**). An analysis of the bifurcation events underlying these unwanted fates, even with existing datasets, might yield sufficient candidate regulators for the improvement

of *in vitro* differentiation. For example, the discovery of precocious α-cell specification led to the development of a protocol for functional SC-α cell generation (Peterson et al., 2020). The combination of α- and β-cells derived from cell-specific protocols into single islets could also improve *in vivo* maturation and function.

Single-cell research on tissues from diabetic patients, and in human and mouse genetic models, has identified multiple pathways involved in endocrine failure in the pancreas. In particular, such studies have highlighted the occurrence of stress-related mature cell identity loss in surviving endocrine cells, resulting in dysfunctional β-cells unable to respond correctly to glucose stimulation (**Figure 2B**). The use of single-cell omics approaches has shown that treatment with PEGylated-insulin and GLP-1-estrogen conjugate stimulates β-cell redifferentiation and restores β-cell mass by proliferation, rendering this approach potentially very promising for the treatment of T1D and T2D. Immature endocrine cells have been observed in post-mortem tissues from patients, diabetic mouse models and following specific dedifferentiation-inducing treatments in cell and mouse models. But what if, in some cases of diabetes, the observed immature endocrine cells result from defective

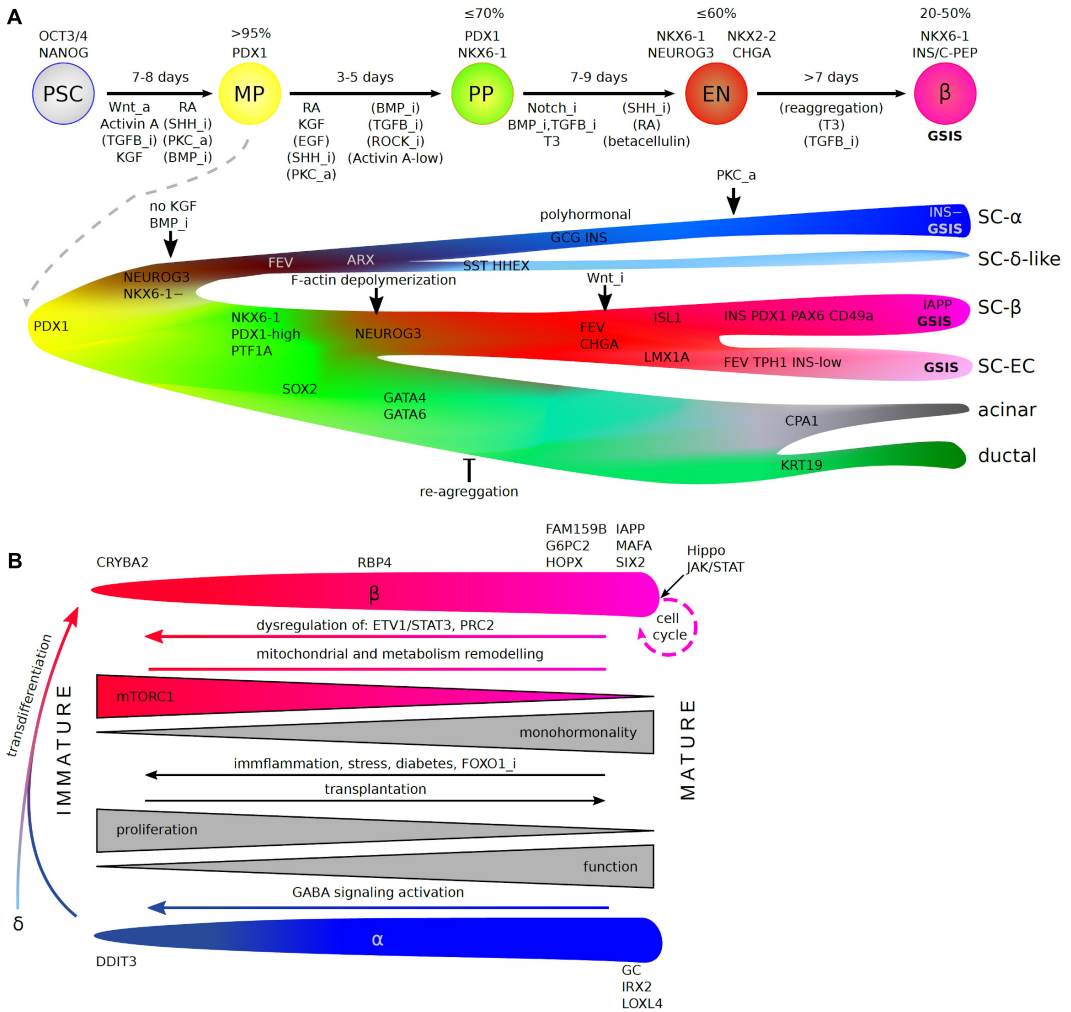

FIGURE 2 | scRNA-Seq insight into *in vitro* hPSC differentiation toward human pancreatic β-cells **(A)** and endocrine cell maturation **(B)**. **(A)** *(Top)* Stages of differentiation protocols (arrows), which recapitulate consecutive pancreas development steps *in vivo* (circles). Denoted are: a length of each stage (above arrows, in days), genes commonly used to estimate differentiation efficiency (% + for stage markers out of all cells), and pathways that are inhibited ("_i") or activated ("_a") during each stage (below arrows). Pathways without brackets are essential for the process and applied in all commonly used protocols, while brackets indicate pathways regulated in a fraction of protocols. PSC—pluripotent stem cells, MP—multipotent progenitors, BP—bipotent progenitors, EN—endocrine lineage (endocrine progenitors and immature endocrine cells), β—β-cells, GSIS—glucose stimulated insulin secretion. *(Bottom)* A detailed view on the differentiation based on scRNA-Seq reveals the origin of non-β-cell specific populations that deteriorate differentiation efficiency and points to branching at which the protocols could be refined. Factors identified in scRNA-Seq studies that improve specific lineage choices are denoted. SC—stem cell-derived, EC—enterochromaffin cells. **(B)** Maturation of β- and α- cells including molecular changes and marker genes along the process. Dedifferentiation (reverse arrows), transdifferentation, and re-entering cell cycle are possible as physiological compensatory mechanisms, in pathology and when artificially forced by identified factors, with potential use in medicine.

pancreas development rather than dedifferentiation? Studies of iPSCs from neonatal diabetes and WS1 patients pointed to defective differentiation *in vitro* and multiple MODY-causing genes. Indeed, defects of pancreatic development have recently been implicated in the pathogenesis of T2D (Perng et al., 2019; Stein et al., 2019) and T1D (Phillips et al., 2017). It may appear counterintuitive to attribute a developmental character to diseases of adulthood, but late-onset neurodegenerative diseases provide an example supporting the consideration of similar hypotheses for diabetes. There are multiple lines of evidence to suggest that neurodegenerative diseases of adults, such as Huntington's disease (Wiatr et al., 2017), Parkinson's disease (Schwamborn, 2018) and Alzheimer's disease (Arendt et al., 2017), are not solely neurodegenerative, but also have a neurodevelopmental component. In Huntington's disease, abnormal neural development is observed during the hPSC differentiation (Conforti et al., 2018; Smith-Geater et al., 2020) and in affected fetuses and children, years before the disease onset (van der Plas et al., 2019; Barnat et al., 2020). These findings suggest that the disease persists in a latent phase for years, during which compensatory mechanisms within the organ prevent the onset of disease. Similarly, for diabetes, immature or misdifferentiated islets might be more prone to environmental stress induced by an unhealthy lifestyle and impaired glucose homeostasis. Indeed, the pacemaker-like hub β-cells, are preferentially targeted by diabetic stress, leading to functional failure of the whole islet (Johnston et al., 2016). Limited self-renewal of β-cells might lead to a temporary replenishment of the β-cell pool, but the number of these cells gradually declines, eventually leading to diabetes, with an onset earlier or later in life, depending on the strength of the developmental deficits and environmental stress. Research in presymptomatic patients is almost impossible, but these subtle changes in endocrine cell maturity could be evaluated with single-cell approaches in mouse or human PSC-derived pancreatic models. If such developmental defects are found to underlie diabetes, it may be possible to develop a pre-onset treatment for patients with a known genetic or environmental predisposition to diabetes.

The ongoing development of scRNA-Seq technologies is improving sequencing yields and depths, facilitating more accurate biological inference (Ding et al., 2020). It is particularly difficult to study individual cells in the pancreas, due to the high hydrolytic enzyme content of the exocrine cells. The almost

TABLE 1 | Insights into endocrine pancreas development and cellular identity maintenance from scRNA-Seq studies.

Key questions	*In vitro*	*In vivo*
First wave endocrine differentiation	– Human α-cells (SC-α) arise prematurely from *NKX6-1-/NEUROG3+* progenitors during Stage 4 – SC-α cells can be efficiently enriched and matured *in vitro* and *in vivo*	– Mouse first wave α-cells arise from early *Pdx1+/Sox9+/Ptf1a-/Nr2f2+* MPs – Fate and function unknown
Cell fate determination	– Subpopulations of progenitors are present during differentiation – Regulation at identified bifurcation points increase efficiency of differentiation	– Subpopulations of progenitors (MPs, BPs, EPs) are present, representing subsequent developmental stages as well as cell fate biases – Progenitors can be primed for a specific cell fate choice earlier than expected (e.g., for endocrine before *Neurog3* expression)
Islet formation	– Peninsula-like structures arise during human PSC 3D differentiation	– The peninsula theory: in mice primary islets are formed by emerging endocrine cells, adjacent to epithelium, without individual cells undergoing complete EMT
Pancreatic niche	– Mesenchymal-like cells present during human endocrine differentiation	– Mesenchyme is molecularly and functionally heterogeneous during mouse development – Heterogeneity is lower in adulthood but raises in stress and disease
Polyhormonal cells	– *GCG+/INS+* immature α-cells from Stage 4	– Transiently present in human developing pancreas and in diabetes – Not confirmed yet by scRNA-Seq
	– *TPH1+/INS^{low}/GCG*-enterochromaffin-like cells (SC-EC) from Stage 5	– Not observed in developing/adult human pancreas
Functional maturation	– Transcriptomic changes correlate with functional maturation	– Transcriptomic changes correlate with age
Progenitors in adulthood	– *LIFR+* SC-β cell subpopulation re-enters cell cycle upon LIF exposure – Mouse *Procr+* cells can be expanded *ex vivo*	– *LIFR+* β-cell subpopulation capable of re-entering cell cycle present in mice and human – Multipotent progenitors present in mouse endocrine compartment (*Procr+* cells) and human ducts (*PDX1+/ALK3+/CAII- cells*)
Adult cells plasticity	– Dedifferentiation can be pharmacologically induced *in vitro* and *ex vivo*	– Adult endocrine and exocrine cells can dedifferentiate upon chronic stress (e.g., inflammation), upon pharmacological induction and in disease
Specificity of endocrine differentiation	– Fine-tuning of specific endocrine cell type derivation through signaling regulation at identified bifurcation points (see **Figure 2**)	

exclusive removal of the exocrine pancreas hinders scRNA-Seq research on acinar and ductal cells in the adult pancreas. Methods for overcoming these limitations are emerging, such as snap-freezing of the dissected pancreas followed by single-nucleus RNA-Seq (Tosti et al., 2021). This is also important in the context of a limited availability of biological material, from T1D patients for example, as the use of frozen tissues extends this availability. Also, pancreatic differentiation of patient-specific iPSCs offers alternative platform to study transcriptomes of T1D specific single islet cells. Moreover, single-cell omics techniques other than scRNA-Seq have been developed and their application in combination with scRNA-Seq adds additional layers of information to the existing data (Efremova and Teichmann, 2020), as for Patch-Seq, for example (Camunas-Soler et al., 2020). Furthermore, scRNA-Seq can be combined with scDNA barcoding, using CRISPR for lineage tracing (Raj et al., 2018; Spanjaard et al., 2018), or with sc-epigenetics (Ai et al., 2019; Chen et al., 2019; Li et al., 2019; Rooijers et al., 2019; Zhu et al., 2019). Single-cell proteomics is also being extensively developed (Goltsev et al., 2018; Gut et al., 2018; Saka et al., 2019; Labib et al., 2020). *In situ* single-cell sequencing methods can identify spatial connections between cell types of interest that may be particularly useful for further inferences concerning the structural development of the pancreas or niche and pancreas crosstalk. The *in situ* sequencing of cytoplasmic transcripts can be performed on the same tissue preparations as used for single-nucleus RNA-Seq (Tosti et al., 2021). In summary, pancreas research has already greatly benefited from scRNA-Seq (**Table 1**). The refined analysis of already curated datasets and the use of emerging technologies will boost progress toward the development of new therapies for diabetes.

AUTHOR CONTRIBUTIONS

All authors analyzed literature, discussed findings, and wrote part of the manuscript. MB and WS did final editing.

FUNDING

This work was supported by the McNair Medical Institute, National Science Center (OPUS UMO-2O19/33/B/NZ3/01226), National Science Center (Polonez UMO-2015/19/P/NZ3/03452 and UE Horizon 2020 MSCA grant 665778), the Foundation for Polish Science –TEAM—program financed by the European Union within the European Regional Development. Fund TEAM to MB, National Science Center–Miniatura (2018/02/X/NZ3/02157) to WS and the AMU Dean's Grant for Ph.D. students (GDWB-02/2018) to NZ.

ACKNOWLEDGMENTS

We would like to thank Julie Sappa for expert text editing.

SUPPLEMENTARY MATERIAL

The Supplementary Material for this article can be found online at: https://www.frontiersin.org/articles/10.3389/fcell.2021.629212/full#supplementary-material. The following scRNA-Seq studies are not discussed in the manuscript, but are included in Supplementary Tables: (Grün et al., 2016; Wollny et al., 2016; Stanescu et al., 2017; Wang J. et al., 2020).

REFERENCES

Ai, S., Xiong, H., Li, C. C., Luo, Y., Shi, Q., Liu, Y., et al. (2019). Profiling chromatin states using single-cell itChIP-seq. *Nat. Cell Biol.* 21, 1164–1172. doi: 10.1038/s41556-019-0383-5

Alexandre-Heymann, L., Mallone, R., Boitard, C., Scharfmann, R., and Larger, E. (2019). Structure and function of the exocrine pancreas in patients with type 1 diabetes. *Rev. Endocr. Metab. Disord.* 20, 129–149.

Almaça, J., Molina, J., Menegaz, D., Pronin, A. N., Tamayo, A., Slepak, V., et al. (2016). Human beta cells produce and release serotonin to inhibit glucagon secretion from alpha cells. *Cell Rep.* 17, 3281–3291. doi: 10.1016/j.celrep.2016.11.072

American Diabetes and Association (2013). Diagnosis and classification of diabetes mellitus. *Diabetes Care* 36(Suppl. 1), S67–S74.

Aragón, F., Karaca, M., Novials, A., Maldonado, R., Maechler, P., and Rubí, B. (2015). Pancreatic polypeptide regulates glucagon release through PPYR1 receptors expressed in mouse and human alpha-cells. *Biochim. Biophys. Acta* 1850, 343–351. doi: 10.1016/j.bbagen.2014.11.005

Arendt, T., Stieler, J., and Ueberham, U. (2017). Is sporadic Alzheimer's disease a developmental disorder? *J. Neurochem.* 143, 396–408. doi: 10.1111/jnc.14036

Ariyachet, C., Tovaglieri, A., Xiang, G., Lu, J., Shah, M. S., Richmond, C. A., et al. (2016). Reprogrammed stomach tissue as a renewable source of functional β cells for blood glucose regulation. *Cell Stem Cell* 18, 410–421. doi: 10.1016/j.stem.2016.01.003

Arntfield, M. E., and van der Kooy, D. (2011). β-Cell evolution: how the pancreas borrowed from the brain: the shared toolbox of genes expressed by neural and pancreatic endocrine cells may reflect their evolutionary relationship. *BioEssays News Rev. Mol. Cell. Dev. Biol.* 33, 582–587. doi: 10.1002/bies.201100015

Augsornworawat, P., Maxwell, K. G., Velazco-Cruz, L., and Millman, J. R. (2020). Single-cell transcriptome profiling reveals β cell maturation in stem cell-derived islets after transplantation. *Cell Rep.* 32:108067. doi: 10.1016/j.celrep.2020.108067

Avrahami, D., Wang, Y. J., Schug, J., Feleke, E., Gao, L., Liu, C., et al. (2020). Single-cell transcriptomics of human islet ontogeny defines the molecular basis of β-cell dedifferentiation in T2D. *Mol. Metab.* 42:101057. doi: 10.1016/j.molmet.2020.101057

Bader, E., Migliorini, A., Gegg, M., Moruzzi, N., Gerdes, J., Roscioni, S. S., et al. (2016). Identification of proliferative and mature β-cells in the islets of Langerhans. *Nature* 535, 430–434. doi: 10.1038/nature18624

Bakhti, M., Scheibner, K., Tritschler, S., Bastidas-Ponce, A., Tarquis-Medina, M., Theis, F. J., et al. (2019). Establishment of a high-resolution 3D modeling system for studying pancreatic epithelial cell biology in vitro. *Mol. Metab.* 30, 16–29. doi: 10.1016/j.molmet.2019.09.005

Balboa, D., Saarimäki-Vire, J., Borshagovski, D., Survila, M., Lindholm, P., Galli, E., et al. (2018). Insulin mutations impair beta-cell development in a patient-derived iPSC model of neonatal diabetes. *eLife* 7:e38519.

Barnat, M., Capizzi, M., Aparicio, E., Boluda, S., Wennagel, D., Kacher, R., et al. (2020). Huntington's disease alters human neurodevelopment. *Science* 369, 787–793.

Bastidas-Ponce, A., Tritschler, S., Dony, L., Scheibner, K., Tarquis-Medina, M., Salinno, C., et al. (2019). Comprehensive single cell mRNA profiling reveals a detailed roadmap for pancreatic endocrinogenesis. *Dev. Camb. Engl.* 146:dev173849. doi: 10.1242/dev.173849

Bechard, M. E., Bankaitis, E. D., Hipkens, S. B., Ustione, A., Piston, D. W., Yang, Y.-P., et al. (2016). Precommitment low-level Neurog3 expression defines a long-lived mitotic endocrine-biased progenitor pool that drives production of endocrine-committed cells. *Genes Dev.* 30, 1852–1865. doi: 10.1101/gad.284729.116

Bellin, M. D., Barton, F. B., Heitman, A., Harmon, J. V., Kandaswamy, R., Balamurugan, A. N., et al. (2012). Potent induction immunotherapy promotes long-term insulin independence after islet transplantation in type 1 diabetes. *Am. J. Transplant. Off. J. Am. Soc. Transplant. Am. Soc. Transpl. Surg.* 12, 1576–1583. doi: 10.1111/j.1600-6143.2011.03977.x

Benitez, C. M., Goodyer, W. R., and Kim, S. K. (2012). Deconstructing pancreas developmental biology. *Cold Spring Harb. Perspect. Biol.* 4:a012401. doi: 10.1101/cshperspect.a012401

Bensellam, M., Jonas, J.-C., and Laybutt, D. R. (2018). Mechanisms of β-cell dedifferentiation in diabetes: recent findings and future research directions. *J. Endocrinol.* 236, R109–R143.

Bergen, V., Lange, M., Peidli, S., Wolf, F. A., and Theis, F. J. (2020). Generalizing RNA velocity to transient cell states through dynamical modeling. *Nat. Biotechnol.* 38, 1408–1414. doi: 10.1038/s41587-020-0591-3

Bernard, V., Semaan, A., Huang, J., San Lucas, F. A., Mulu, F. C., Stephens, B. M., et al. (2019). Single-cell transcriptomics of pancreatic cancer precursors demonstrates epithelial and microenvironmental heterogeneity as an early event in neoplastic progression. *Clin. Cancer Res. Off. J. Am. Assoc. Cancer Res.* 25, 2194–2205. doi: 10.1158/1078-0432.ccr-18-1955

Bocian-Sobkowska, J., Zabel, M., Wozniak, W., and Surdyk-Zasada, J. (1999). Polyhormonal aspect of the endocrine cells of the human fetal pancreas. *Histochem. Cell Biol.* 112, 147–153. doi: 10.1007/s004180050401

Braun, M., Ramracheya, R., Bengtsson, M., Clark, A., Walker, J. N., Johnson, P. R., et al. (2010). Gamma-aminobutyric acid (GABA) is an autocrine excitatory transmitter in human pancreatic beta-cells. *Diabetes* 59, 1694–1701. doi: 10.2337/db09-0797

Bru-Tari, E., Cobo-Vuilleumier, N., Alonso-Magdalena, P., Dos Santos, R. S., Marroqui, L., Nadal, A., et al. (2019). Pancreatic alpha-cell mass in the early-onset and advanced stage of a mouse model of experimental autoimmune diabetes. *Sci. Rep.* 9:9515.

Bulle, A., and Lim, K.-H. (2020). Beyond just a tight fortress: contribution of stroma to epithelial-mesenchymal transition in pancreatic cancer. *Signal Transduct. Target. Ther.* 5:249.

Burlison, J. S., Long, Q., Fujitani, Y., Wright, C. V. E., and Magnuson, M. A. (2008). Pdx-1 and Ptf1a concurrently determine fate specification of pancreatic multipotent progenitor cells. *Dev. Biol.* 316, 74–86. doi: 10.1016/j.ydbio.2008.01.011

Byrnes, L. E., Wong, D. M., Subramaniam, M., Meyer, N. P., Gilchrist, C. L., Knox, S. M., et al. (2018). Lineage dynamics of murine pancreatic development at single-cell resolution. *Nat. Commun.* 9:3922.

Camunas-Soler, J., Dai, X.-Q., Hang, Y., Bautista, A., Lyon, J., Suzuki, K., et al. (2020). Patch-seq links single-cell transcriptomes to human islet dysfunction in diabetes. *Cell Metab.* 31, 1017.e4–1031.e4.

Cannoodt, R., Saelens, W., and Saeys, Y. (2016). Computational methods for trajectory inference from single-cell transcriptomics. *Eur. J. Immunol.* 46, 2496–2506. doi: 10.1002/eji.201646347

Cebola, I., Rodríguez-Seguí, S. A., Cho, C. H.-H., Bessa, J., Rovira, M., Luengo, M., et al. (2015). TEAD and YAP regulate the enhancer network of human embryonic pancreatic progenitors. *Nat. Cell Biol.* 17, 615–626. doi: 10.1038/ncb3160

Chen, S., Lake, B. B., and Zhang, K. (2019). High-throughput sequencing of the transcriptome and chromatin accessibility in the same cell. *Nat. Biotechnol.* 37, 1452–1457. doi: 10.1038/s41587-019-0290-0

Chera, S., Baronnier, D., Ghila, L., Cigliola, V., Jensen, J. N., Gu, G., et al. (2014). Diabetes recovery by age-dependent conversion of pancreatic δ-cells into insulin producers. *Nature* 514, 503–507. doi: 10.1038/nature13633

Cinti, F., Bouchi, R., Kim-Muller, J. Y., Ohmura, Y., Sandoval, P. R., Masini, M., et al. (2016). Evidence of β-cell dedifferentiation in human type 2 diabetes. *J. Clin. Endocrinol. Metab.* 101, 1044–1054. doi: 10.1210/jc.2015-2860

Cogger, K. F., Sinha, A., Sarangi, F., McGaugh, E. C., Saunders, D., Dorrell, C., et al. (2017). Glycoprotein 2 is a specific cell surface marker of human pancreatic progenitors. *Nat. Commun.* 8:331.

Collombat, P., Xu, X., Ravassard, P., Sosa-Pineda, B., Dussaud, S., Billestrup, N., et al. (2009). The ectopic expression of Pax4 in the mouse pancreas converts progenitor cells into alpha and subsequently beta cells. *Cell* 138, 449–462. doi: 10.1016/s9999-9994(09)20391-6

Conforti, P., Besusso, D., Bocchi, V. D., Faedo, A., Cesana, E., Rossetti, G., et al. (2018). Faulty neuronal determination and cell polarization are reverted by modulating HD early phenotypes. *Proc. Natl. Acad. Sci. U.S.A.* 115, E762–E771.

Courtney, M., Gjernes, E., Druelle, N., Ravaud, C., Vieira, A., Ben-Othman, N., et al. (2013). The inactivation of Arx in pancreatic α-cells triggers their neogenesis and conversion into functional β-like cells. *PLoS Genet.* 9:e1003934. doi: 10.1371/journal.pgen.1003934

Cozzitorto, C., and Spagnoli, F. M. (2019). Pancreas organogenesis: the interplay between surrounding microenvironment(s) and epithelium-intrinsic factors. *Curr. Top. Dev. Biol.* 132, 221–256. doi: 10.1016/bs.ctdb.2018.12.005

Cozzitorto, C., Mueller, L., Ruzittu, S., Mah, N., Willnow, D., Darrigrand, J.-F., et al. (2020). A specialized niche in the pancreatic microenvironment promotes endocrine differentiation. *Dev. Cell.* 55, 150.e6–162.e6.

Dhawan, S., Georgia, S., Tschen, S.-I., Fan, G., and Bhushan, A. (2011). Pancreatic β cell identity is maintained by DNA methylationmediated repression of Arx. *Dev. Cell* 20, 419–429. doi: 10.1016/j.devcel.2011.03.012

Ding, J., Adiconis, X., Simmons, S. K., Kowalczyk, M. S., Hession, C. C., Marjanovic, N. D., et al. (2020). Systematic comparison of single-cell and single-nucleus RNA-sequencing methods. *Nat. Biotechnol.* 38, 737–746.

Dominguez Gutierrez, G., Kim, J., Lee, A.-H., Tong, J., Niu, J., Gray, S. M., et al. (2018). Gene signature of the human pancreatic ε cell. *Endocrinology* 159, 4023–4032.

Dominguez, C. X., Müller, S., Keerthivasan, S., Koeppen, H., Hung, J., Gierke, S., et al. (2020). Single-cell RNA sequencing reveals stromal evolution into LRRC15+ myofibroblasts as a determinant of patient response to cancer immunotherapy. *Cancer Discov.* 10, 232–253. doi: 10.1158/2159-8290.cd-19-0644

Dominguez-Gutierrez, G., Xin, Y., and Gromada, J. (2019). Heterogeneity of human pancreatic β-cells. *Mol. Metab.* 27S, S7–S14.

Efremova, M., and Teichmann, S. A. (2020). Computational methods for single-cell omics across modalities. *Nat. Methods* 17, 14–17. doi: 10.1038/s41592-019-0692-4

Elyada, E., Bolisetty, M., Laise, P., Flynn, W. F., Courtois, E. T., Burkhart, R. A., et al. (2019). Cross-species single-cell analysis of pancreatic ductal adenocarcinoma reveals antigen-presenting cancer-associated fibroblasts. *Cancer Discov.* 9, 1102–1123. doi: 10.1158/2159-8290.cd-19-0094

Fang, Z., Weng, C., Li, H., Tao, R., Mai, W., Liu, X., et al. (2019). Single-cell heterogeneity analysis and CRISPR screen identify key β-cell-specific disease genes. *Cell Rep.* 26, 3132.e7–3144.e7.

Fares, I., Chagraoui, J., Lehnertz, B., MacRae, T., Mayotte, N., Tomellini, E., et al. (2017). EPCR expression marks UM171-expanded CD34+ cord blood stem cells. *Blood* 129, 3344–3351. doi: 10.1182/blood-2016-11-750729

Feldmann, K., Maurer, C., Peschke, K., Teller, S., Schuck, K., Steiger, K., et al. (2021). Mesenchymal plasticity regulated by Prrx1 drives aggressive pancreatic cancer biology. *Gastroenterology* 160, 346.e24–361.e24.

Fischer, D. S., Fiedler, A. K., Kernfeld, E. M., Genga, R. M. J., Bastidas-Ponce, A., Bakhti, M., et al. (2019). Inferring population dynamics from single-cell RNA-sequencing time series data. *Nat. Biotechnol.* 37, 461–468. doi: 10.1038/s41587-019-0088-0

Fonseca, S. G., Fukuma, M., Lipson, K. L., Nguyen, L. X., Allen, J. R., Oka, Y., et al. (2005). WFS1 is a novel component of the unfolded protein response and maintains homeostasis of the endoplasmic reticulum in pancreatic beta-cells. *J. Biol. Chem.* 280, 39609–39615. doi: 10.1074/jbc.m507426200

Fonseca, S. G., Ishigaki, S., Oslowski, C. M., Lu, S., Lipson, K. L., Ghosh, R., et al. (2010). Wolfram syndrome 1 gene negatively regulates ER stress signaling in rodent and human cells. *J. Clin. Invest.* 120, 744–755. doi: 10.1172/jci39678

Furuyama, K., Chera, S., van Gurp, L., Oropeza, D., Ghila, L., Damond, N., et al. (2019). Diabetes relief in mice by glucose-sensing insulin-secreting human α-cells. *Nature* 567, 43–48. doi: 10.1038/s41586-019-0942-8

Gardner, D. S., and Tai, E. S. (2012). Clinical features and treatment of maturity onset diabetes of the young (MODY). *Diabetes Metab. Syndr. Obes. Targets Ther.* 5, 101–108. doi: 10.2147/dmso.s23353

Gironella, M., Calvo, C., Fernández, A., Closa, D., Iovanna, J. L., Rosello-Catafau, J., et al. (2013). Reg3β deficiency impairs pancreatic tumor growth by skewing macrophage polarization. *Cancer Res.* 73, 5682–5694. doi: 10.1158/0008-5472.can-12-3057

Golosow, N., and Grobstein, C. (1962). Epitheliomesenchymal interaction in pancreatic morphogenesis. *Dev. Biol.* 4, 242–255. doi: 10.1016/0012-1606(62)90042-8

Goltsev, Y., Samusik, N., Kennedy-Darling, J., Bhate, S., Hale, M., Vazquez, G., et al. (2018). Deep profiling of mouse splenic architecture with CODEX multiplexed imaging. *Cell* 174, 968.e15–981.e15.

Gradwohl, G., Dierich, A., LeMeur, M., and Guillemot, F. (2000). neurogenin3 is required for the development of the four endocrine cell lineages of the pancreas. *Proc. Natl. Acad. Sci. U.S.A.* 97, 1607–1611. doi: 10.1073/pnas.97.4.1607

Gromada, J., Chabosseau, P., and Rutter, G. A. (2018). The α-cell in diabetes mellitus. *Nat. Rev. Endocrinol.* 14, 694–704.

Grün, D., Lyubimova, A., Kester, L., Wiebrands, K., Basak, O., Sasaki, N., et al. (2015). Single-cell messenger RNA sequencing reveals rare intestinal cell types. *Nature* 525, 251–255. doi: 10.1038/nature14966

Grün, D., Muraro, M. J., Boisset, J.-C., Wiebrands, K., Lyubimova, A., Dharmadhikari, G., et al. (2016). De novo prediction of stem cell identity using single-cell transcriptome data. *Cell Stem Cell* 19, 266–277. doi: 10.1016/j.stem.2016.05.010

Gu, G., Dubauskaite, J., and Melton, D. A. (2002). Direct evidence for the pancreatic lineage: NGN3+ cells are islet progenitors and are distinct from duct progenitors. *Dev. Camb. Engl.* 129, 2447–2457.

Guo, T., Landsman, L., Li, N., and Hebrok, M. (2013). Factors expressed by murine embryonic pancreatic mesenchyme enhance generation of insulin-producing cells from hESCs. *Diabetes* 62, 1581–1592. doi: 10.2337/db12-0167

Gut, G., Herrmann, M. D., and Pelkmans, L. (2018). Multiplexed protein maps link subcellular organization to cellular states. *Science* 361:eaar7042. doi: 10.1126/science.aar7042

Haber, A. L., Biton, M., Rogel, N., Herbst, R. H., Shekhar, K., Smillie, C., et al. (2017). A single-cell survey of the small intestinal epithelium. *Nature* 551, 333–339.

Han, L., Chaturvedi, P., Kishimoto, K., Koike, H., Nasr, T., Iwasawa, K., et al. (2020). Single cell transcriptomics identifies a signaling network coordinating endoderm and mesoderm diversification during foregut organogenesis. *Nat. Commun.* 11:4158.

Hecksher-Sørensen, J., Watson, R. P., Lettice, L. A., Serup, P., Eley, L., De Angelis, C., et al. (2004). The splanchnic mesodermal plate directs spleen and pancreatic laterality, and is regulated by Bapx1/Nkx3.2. *Dev. Camb. Engl.* 131, 4665–4675. doi: 10.1242/dev.01364

Herrera, P. L. (2000). Adult insulin- and glucagon-producing cells differentiate from two independent cell lineages. *Dev. Camb. Engl.* 127, 2317–2322.

Hogrebe, N. J., Augsornworawat, P., Maxwell, K. G., Velazco-Cruz, L., and Millman, J. R. (2020). Targeting the cytoskeleton to direct pancreatic differentiation of human pluripotent stem cells. *Nat. Biotechnol.* 38, 460–470. doi: 10.1038/s41587-020-0430-6

Hosein, A. N., Brekken, R. A., and Maitra, A. (2020). Pancreatic cancer stroma: an update on therapeutic targeting strategies. *Nat. Rev. Gastroenterol. Hepatol.* 17, 487–505. doi: 10.1038/s41575-020-0300-1

Hosein, A. N., Huang, H., Wang, Z., Parmar, K., Du, W., Huang, J., et al. (2019). Cellular heterogeneity during mouse pancreatic ductal adenocarcinoma progression at single-cell resolution. *JCI Insight* 5:e129212.

Hwang, W. L., Jagadeesh, K. A., Guo, J. A., Hoffman, H. I., Yadollahpour, P., Mohan, R., et al. (2020). Single-nucleus and spatial transcriptomics of archival pancreatic cancer reveals multi-compartment reprogramming after neoadjuvant treatment. *BioRxiv* doi: 10.1053/j.gastro.2020.11.010

Jennings, R. E., Berry, A. A., Kirkwood-Wilson, R., Roberts, N. A., Hearn, T., Salisbury, R. J., et al. (2013). Development of the human pancreas from foregut to endocrine commitment. *Diabetes* 62, 3514–3522. doi: 10.2337/db12-1479

Jennings, R. E., Berry, A. A., Strutt, J. P., Gerrard, D. T., and Hanley, N. A. (2015). Human pancreas development. *Dev. Camb. Engl.* 142, 3126–3137.

Jensen, J., Pedersen, E. E., Galante, P., Hald, J., Heller, R. S., Ishibashi, M., et al. (2000). Control of endodermal endocrine development by Hes-1. *Nat. Genet.* 24, 36–44. doi: 10.1038/71657

Jeon, J., Correa-Medina, M., Ricordi, C., Edlund, H., and Diez, J. A. (2009). Endocrine cell clustering during human pancreas development. *J. Histochem. Cytochem. Off. J. Histochem. Soc.* 57, 811–824. doi: 10.1369/jhc.2009.953307

Johannesson, B., Sui, L., Freytes, D. O., Creusot, R. J., and Egli, D. (2015). Toward beta cell replacement for diabetes. *EMBO J.* 34, 841–855. doi: 10.15252/embj.201490685

Johansson, K. A., Dursun, U., Jordan, N., Gu, G., Beermann, F., Gradwohl, G., et al. (2007). Temporal control of neurogenin3 activity in pancreas progenitors reveals competence windows for the generation of different endocrine cell types. *Dev. Cell* 12, 457–465. doi: 10.1016/j.devcel.2007.02.010

Johnston, N. R., Mitchell, R. K., Haythorne, E., Pessoa, M. P., Semplici, F., Ferrer, J., et al. (2016). Beta cell hubs dictate pancreatic islet responses to glucose. *Cell Metab.* 24, 389–401. doi: 10.1016/j.cmet.2016.06.020

Katoh, M. C., Jung, Y., Ugboma, C. M., Shimbo, M., Kuno, A., Basha, W. A., et al. (2018). MafB is critical for glucagon production and secretion in mouse pancreatic α cells in vivo. *Mol. Cell. Biol.* 38, e504–e517.

Kawaguchi, Y., Cooper, B., Gannon, M., Ray, M., MacDonald, R. J., and Wright, C. V. E. (2002). The role of the transcriptional regulator Ptf1a in converting intestinal to pancreatic progenitors. *Nat. Genet.* 32, 128–134. doi: 10.1038/ng959

Keenan, H. A., Sun, J. K., Levine, J., Doria, A., Aiello, L. P., Eisenbarth, G., et al. (2010). Residual insulin production and pancreatic ß-cell turnover after 50 years of diabetes: Joslin medalist study. *Diabetes* 59, 2846–2853. doi: 10.2337/db10-0676

Klein, A. M., Mazutis, L., Akartuna, I., Tallapragada, N., Veres, A., Li, V., et al. (2015). Droplet barcoding for single-cell transcriptomics applied to embryonic stem cells. *Cell* 161, 1187–1201. doi: 10.1016/j.cell.2015.04.044

Krapp, A., Knöfler, M., Ledermann, B., Bürki, K., Berney, C., Zoerkler, N., et al. (1998). The bHLH protein PTF1-p48 is essential for the formation of the exocrine and the correct spatial organization of the endocrine pancreas. *Genes Dev.* 12, 3752–3763. doi: 10.1101/gad.12.23.3752

Krentz, N. A. J., Lee, M. Y. Y., Xu, E. E., Sproul, S. L. J., Maslova, A., Sasaki, S., et al. (2018). Single-cell transcriptome profiling of mouse and hESC-derived pancreatic progenitors. *Stem Cell Rep.* 11, 1551–1564. doi: 10.1016/j.stemcr.2018.11.008

Kulkarni, R. N., Mizrachi, E.-B., Ocana, A. G., and Stewart, A. F. (2012). Human β-cell proliferation and intracellular signaling: driving in the dark without a road map. *Diabetes* 61, 2205–2213. doi: 10.2337/db12-0018

La Manno, G., Soldatov, R., Zeisel, A., Braun, E., Hochgerner, H., Petukhov, V., et al. (2018). RNA velocity of single cells. *Nature* 560, 494–498.

Labib, M., Wang, Z., Ahmed, S. U., Mohamadi, R. M., Duong, B., Green, B., et al. (2020). Tracking the expression of therapeutic protein targets in rare cells by antibody-mediated nanoparticle labelling and magnetic sorting. *Nat. Biomed. Eng.* 5, 41–52. doi: 10.1038/s41551-020-0590-1

Lähnemann, D., Köster, J., Szczurek, E., McCarthy, D. J., Hicks, S. C., Robinson, M. D., et al. (2020). Eleven grand challenges in single-cell data science. *Genome Biol.* 21:31.

Landsman, L., Nijagal, A., Whitchurch, T. J., Vanderlaan, R. L., Zimmer, W. E., Mackenzie, T. C., et al. (2011). Pancreatic mesenchyme regulates epithelial organogenesis throughout development. *PLoS Biol.* 9:e1001143. doi: 10.1371/journal.pbio.1001143

Larsen, H. L., and Grapin-Botton, A. (2017). The molecular and morphogenetic basis of pancreas organogenesis. *Semin. Cell Dev. Biol.* 66, 51–68. doi: 10.1016/j.semcdb.2017.01.005

Larsen, H. L., Martín-Coll, L., Nielsen, A. V., Wright, C. V. E., Trusina, A., Kim, Y. H., et al. (2017). Stochastic priming and spatial cues orchestrate heterogeneous clonal contribution to mouse pancreas organogenesis. *Nat. Commun.* 8:605.

Larsson, L. I. (1998). On the development of the islets of Langerhans. *Microsc. Res. Technol.* 43, 284–291.

Lawlor, N., George, J., Bolisetty, M., Kursawe, R., Sun, L., Sivakamasundari, V., et al. (2017). Single-cell transcriptomes identify human islet cell signatures and reveal cell-type-specific expression changes in type 2 diabetes. *Genome Res.* 27, 208–222. doi: 10.1101/gr.212720.116

Lawson, A., and Schoenwolf, G. C. (2003). Epiblast and primitive-streak origins of the endoderm in the gastrulating chick embryo. *Dev. Camb. Engl.* 130, 3491–3501. doi: 10.1242/dev.00579

Lee, J. J., Bernard, V., Semaan, A., Monberg, M. E., Huang, J., Stephens, B. M., et al. (2020). Elucidation of tumor-stromal heterogeneity and the ligand-receptor

interactome by single cell transcriptomics in real-world pancreatic cancer biopsies. *BioRxiv* doi: 10.1101/2020.07.28.225813

Li, G., Liu, Y., Zhang, Y., Kubo, N., Yu, M., Fang, R., et al. (2019). Joint profiling of DNA methylation and chromatin architecture in single cells. *Nat. Methods* 16, 991–993. doi: 10.1038/s41592-019-0502-z

Li, J., Casteels, T., Frogne, T., Ingvorsen, C., Honoré, C., Courtney, M., et al. (2017). Artemisinins target GABAA receptor signaling and impair α cell identity. *Cell* 168, 86.e15–100.e15.

Li, W., Cavelti-Weder, C., Zhang, Y., Zhang, Y., Clement, K., Donovan, S., et al. (2014). Long-term persistence and development of induced pancreatic beta cells generated by lineage conversion of acinar cells. *Nat. Biotechnol.* 32, 1223–1230. doi: 10.1038/nbt.3082

Li, Z., Wang, Y., Zhang, M., Xu, P., Huang, H., Wu, D., et al. (2012). The Amotl2 gene inhibits Wnt/β-catenin signaling and regulates embryonic development in zebrafish. *J. Biol. Chem.* 287, 13005–13015. doi: 10.1074/jbc.m112.347419

Ligorio, M., Sil, S., Malagon-Lopez, J., Nieman, L. T., Misale, S., Di Pilato, M., et al. (2019). Stromal microenvironment shapes the intratumoral architecture of pancreatic cancer. *Cell* 178, 160.e27–175.e27.

Liu, J., Banerjee, A., Herring, C. A., Attalla, J., Hu, R., Xu, Y., et al. (2019). Neurog3-independent methylation is the earliest detectable mark distinguishing pancreatic progenitor identity. *Dev. Cell* 48, 49.e7–63.e7.

Liu, X., Wang, J., Wang, H., Yin, G., Liu, Y., Lei, X., et al. (2015). REG3A accelerates pancreatic cancer cell growth under IL-6-associated inflammatory condition: involvement of a REG3A-JAK2/STAT3 positive feedback loop. *Cancer Lett.* 362, 45–60. doi: 10.1016/j.canlet.2015.03.014

Lu, T. T.-H., Heyne, S., Dror, E., Casas, E., Leonhardt, L., Boenke, T., et al. (2018). The polycomb-dependent epigenome controls β cell dysfunction, dedifferentiation, and diabetes. *Cell Metab.* 27, 1294.e7–1308.e7.

Luecken, M. D., and Theis, F. J. (2019). Current best practices in single-cell RNA-seq analysis: a tutorial. *Mol. Syst. Biol.* 15:e8746.

Lynn, F. C., Smith, S. B., Wilson, M. E., Yang, K. Y., Nekrep, N., and German, M. S. (2007). Sox9 coordinates a transcriptional network in pancreatic progenitor cells. *Proc. Natl. Acad. Sci. U.S.A.* 104, 10500–10505. doi: 10.1073/pnas.0704054104

Lyttle, B. M., Li, J., Krishnamurthy, M., Fellows, F., Wheeler, M. B., Goodyer, C. G., et al. (2008). Transcription factor expression in the developing human fetal endocrine pancreas. *Diabetologia* 51, 1169–1180. doi: 10.1007/s00125-008-1006-z

Macosko, E. Z., Basu, A., Satija, R., Nemesh, J., Shekhar, K., Goldman, M., et al. (2015). Highly parallel genome-wide expression profiling of individual cells using nanoliter droplets. *Cell* 161, 1202–1214. doi: 10.1016/j.cell.2015.05.002

Mamidi, A., Prawiro, C., Seymour, P. A., de Lichtenberg, K. H., Jackson, A., Serup, P., et al. (2018). Mechanosignalling via integrins directs fate decisions of pancreatic progenitors. *Nature* 564, 114–118. doi: 10.1038/s41586-018-0762-2

Marín-Peñalver, J. J., Martín-Timón, I., Sevillano-Collantes, C., and Del Cañizo-Gómez, F. J. (2016). Update on the treatment of type 2 diabetes mellitus. *World J. Diabetes* 7, 354–395.

Marquina-Sanchez, B., Fortelny, N., Farlik, M., Vieira, A., Collombat, P., Bock, C., et al. (2020). Single-cell RNA-seq with spike-in cells enables accurate quantification of cell-specific drug effects in pancreatic islets. *Genome Biol.* 21:106.

Mawla, A. M., and Huising, M. O. (2019). Navigating the depths and avoiding the shallows of pancreatic islet cell transcriptomes. *Diabetes* 68, 1380–1393. doi: 10.2337/dbi18-0019

Maxwell, K. G., Augsornworawat, P., Velazco-Cruz, L., Kim, M. H., Asada, R., Hogrebe, N. J., et al. (2020). Gene-edited human stem cell-derived β cells from a patient with monogenic diabetes reverse preexisting diabetes in mice. *Sci. Transl. Med.* 12:eaax9106. doi: 10.1126/scitranslmed.aax9106

Md Moin, A. S., Dhawan, S., Cory, M., Butler, P. C., Rizza, R. A., and Butler, A. E. (2016). Increased frequency of hormone negative and polyhormonal endocrine cells in lean individuals with type 2 diabetes. *J. Clin. Endocrinol. Metab.* 101, 3628–3636. doi: 10.1210/jc.2016-2496

Miller, A. J., Dye, B. R., Ferrer-Torres, D., Hill, D. R., Overeem, A. W., Shea, L. D., et al. (2019). Generation of lung organoids from human pluripotent stem cells in vitro. *Nat. Protoc.* 14, 518–540.

Millman, J. R., Xie, C., Van Dervort, A., Gürtler, M., Pagliuca, F. W., and Melton, D. A. (2016). Generation of stem cell-derived β-cells from patients with type 1 diabetes. *Nat. Commun.* 7:11463.

Miyatsuka, T., Li, Z., and German, M. S. (2009). Chronology of islet differentiation revealed by temporal cell labeling. *Diabetes* 58, 1863–1868. doi: 10.2337/db09-0390

Mojallal, M., Zheng, Y., Hultin, S., Audebert, S., van Harn, T., Johnsson, P., et al. (2014). AmotL2 disrupts apical-basal cell polarity and promotes tumour invasion. *Nat. Commun.* 5:4557.

Moore, S. J., Gala-Lopez, B. L., Pepper, A. R., Pawlick, R. L., and Shapiro, A. J. (2015). Bioengineered stem cells as an alternative for islet cell transplantation. *World J. Transplant.* 5, 1–10. doi: 10.5500/wjt.v5.i1.1

Múnera, J. O., Sundaram, N., Rankin, S. A., Hill, D., Watson, C., Mahe, M., et al. (2017). Differentiation of human pluripotent stem cells into colonic organoids via transient activation of BMP signaling. *Cell Stem Cell* 21, 51.e6–64.e6.

Muraro, M. J., Dharmadhikari, G., Grün, D., Groen, N., Dielen, T., Jansen, E., et al. (2016). A single-cell transcriptome atlas of the human pancreas. *Cell Syst.* 3, 385.e3–394.e3.

Nair, G. G., Liu, J. S., Russ, H. A., Tran, S., Saxton, M. S., Chen, R., et al. (2019). Recapitulating endocrine cell clustering in culture promotes maturation of human stem-cell-derived β cells. *Nat. Cell Biol.* 21, 263–274. doi: 10.1038/s41556-018-0271-4

Nair, G., and Hebrok, M. (2015). Islet formation in mice and men: lessons for the generation of functional insulin-producing β-cells from human pluripotent stem cells. *Curr. Opin. Genet. Dev.* 32, 171–180. doi: 10.1016/j.gde.2015.03.004

Nishimura, W., Kondo, T., Salameh, T., El Khattabi, I., Dodge, R., Bonner-Weir, S., et al. (2006). A switch from MafB to MafA expression accompanies differentiation to pancreatic beta-cells. *Dev. Biol.* 293, 526–539. doi: 10.1016/j.ydbio.2006.02.028

Nordmann, T. M., Dror, E., Schulze, F., Traub, S., Berishvili, E., Barbieux, C., et al. (2017). The role of inflammation in β-cell dedifferentiation. *Sci. Rep.* 7:6285.

Offield, M. F., Jetton, T. L., Labosky, P. A., Ray, M., Stein, R. W., Magnuson, M. A., et al. (1996). PDX-1 is required for pancreatic outgrowth and differentiation of the rostral duodenum. *Dev. Camb. Engl.* 122, 983–995.

Öhlund, D., Handly-Santana, A., Biffi, G., Elyada, E., Almeida, A. S., Ponz-Sarvise, M., et al. (2017). Distinct populations of inflammatory fibroblasts and myofibroblasts in pancreatic cancer. *J. Exp. Med.* 214, 579–596. doi: 10.1084/jem.20162024

Oram, R. A., McDonald, T. J., Shields, B. M., Hudson, M. M., Shepherd, M. H., Hammersley, S., et al. (2015). Most people with long-duration type 1 diabetes in a large population-based study are insulin microsecretors. *Diabetes Care* 38, 323–328. doi: 10.2337/dc14-0871

Pagliuca, F. W., Millman, J. R., Gürtler, M., Segel, M., Van Dervort, A., Ryu, J. H., et al. (2014). Generation of functional human pancreatic β cells in vitro. *Cell* 159, 428–439. doi: 10.1016/j.cell.2014.09.040

Paternoster, S., and Falasca, M. (2020). The intricate relationship between diabetes, obesity and pancreatic cancer. *Biochim. Biophys. Acta Rev. Cancer* 1873:188326. doi: 10.1016/j.bbcan.2019.188326

Peng, J., Sun, B.-F., Chen, C.-Y., Zhou, J.-Y., Chen, Y.-S., Chen, H., et al. (2019). Single-cell RNA-seq highlights intra-tumoral heterogeneity and malignant progression in pancreatic ductal adenocarcinoma. *Cell Res.* 29, 725–738. doi: 10.1038/s41422-019-0195-y

Perng, W., Oken, E., and Dabelea, D. (2019). Developmental overnutrition and obesity and type 2 diabetes in offspring. *Diabetologia* 62, 1779–1788. doi: 10.1007/s00125-019-4914-1

Petersen, M. B. K., Azad, A., Ingvorsen, C., Hess, K., Hansson, M., Grapin-Botton, A., et al. (2017). Single-cell gene expression analysis of a human ESC model of pancreatic endocrine development reveals different paths to β-cell differentiation. *Stem Cell Rep.* 9, 1246–1261. doi: 10.1016/j.stemcr.2017.08.009

Peterson, Q. P., Veres, A., Chen, L., Slama, M. Q., Kenty, J. H. R., Hassoun, S., et al. (2020). A method for the generation of human stem cell-derived alpha cells. *Nat. Commun.* 11:2241.

Phillips, J. E., Couper, J. J., Penno, M. A. S., Harrison, L. C., Endia Study, and Group. (2017). Type 1 diabetes: a disease of developmental origins. *Pediatr. Diabetes* 18, 417–421. doi: 10.1111/pedi.12425

Picelli, S., Björklund, ÅK., Faridani, O. R., Sagasser, S., Winberg, G., and Sandberg, R. (2013). Smart-seq2 for sensitive full-length transcriptome profiling in single cells. *Nat. Methods* 10, 1096–1098. doi: 10.1038/nmeth.2639

Qadir, M. M. F., Álvarez-Cubela, S., Klein, D., van Dijk, J., Muñiz-Anquela, R., Moreno-Hernández, Y. B., et al. (2020). Single-cell resolution analysis of the

human pancreatic ductal progenitor cell niche. *Proc. Natl. Acad. Sci. U.S.A.* 117, 10876–10887. doi: 10.1073/pnas.1918314117

Qiu, W.-L., Zhang, Y.-W., Feng, Y., Li, L.-C., Yang, L., and Xu, C.-R. (2017). Deciphering pancreatic islet β cell and α cell maturation pathways and characteristic features at the single-cell level. *Cell Metab.* 25, 1194.e4–1205.e4.

Qiu, X., Mao, Q., Tang, Y., Wang, L., Chawla, R., Pliner, H. A., et al. (2017). Reversed graph embedding resolves complex single-cell trajectories. *Nat. Methods* 14, 979–982. doi: 10.1038/nmeth.4402

Raj, B., Wagner, D. E., McKenna, A., Pandey, S., Klein, A. M., Shendure, J., et al. (2018). Simultaneous single-cell profiling of lineages and cell types in the vertebrate brain. *Nat. Biotechnol.* 36, 442–450. doi: 10.1038/nbt.4103

Ramond, C., Beydag-Tasöz, B. S., Azad, A., van de Bunt, M., Petersen, M. B. K., Beer, N. L., et al. (2018). Understanding human fetal pancreas development using subpopulation sorting, RNA sequencing and single-cell profiling. *Dev. Camb. Engl.* 145, dev165480. doi: 10.1242/dev.165480

Ramsköld, D., Luo, S., Wang, Y.-C., Li, R., Deng, Q., Faridani, O. R., et al. (2012). Full-length mRNA-Seq from single-cell levels of RNA and individual circulating tumor cells. *Nat. Biotechnol.* 30, 777–782. doi: 10.1038/nbt.2282

Rashid, T., Kobayashi, T., and Nakauchi, H. (2014). Revisiting the flight of Icarus: making human organs from PSCs with large animal chimeras. *Cell Stem Cell* 15, 406–409. doi: 10.1016/j.stem.2014.09.013

Rezania, A., Bruin, J. E., Arora, P., Rubin, A., Batushansky, I., Asadi, A., et al. (2014). Reversal of diabetes with insulin-producing cells derived in vitro from human pluripotent stem cells. *Nat. Biotechnol.* 32, 1121–1133. doi: 10.1038/nbt.3033

Riahi, Y., Israeli, T., Yeroslaviz, R., Chimenez, S., Avrahami, D., Stolovich-Rain, M., et al. (2018). Inhibition of mTORC1 by ER stress impairs neonatal β-cell expansion and predisposes to diabetes in the Akita mouse. *eLife* 7:e38472.

Riedel, M. J., Asadi, A., Wang, R., Ao, Z., Warnock, G. L., and Kieffer, T. J. (2012). Immunohistochemical characterisation of cells co-producing insulin and glucagon in the developing human pancreas. *Diabetologia* 55, 372–381. doi: 10.1007/s00125-011-2344-9

Rooijers, K., Markodimitraki, C. M., Rang, F. J., de Vries, S. S., Chialastri, A., de Luca, K. L., et al. (2019). Simultaneous quantification of protein-DNA contacts and transcriptomes in single cells. *Nat. Biotechnol.* 37, 766–772. doi: 10.1038/s41587-019-0150-y

Rosado-Olivieri, E. A., Aigha, I. I., Kenty, J. H., and Melton, D. A. (2020). Identification of a LIF-responsive, replication-competent subpopulation of human β cells. *Cell Metab.* 31, 327.e6–338.e6.

Rosado-Olivieri, E. A., Anderson, K., Kenty, J. H., and Melton, D. A. (2019). YAP inhibition enhances the differentiation of functional stem cell-derived insulin-producing β cells. *Nat. Commun.* 10:1464.

Russ, H. A., Landsman, L., Moss, C. L., Higdon, R., Greer, R. L., Kaihara, K., et al. (2016). Dynamic proteomic analysis of pancreatic mesenchyme reveals novel factors that enhance human embryonic stem cell to pancreatic cell differentiation. *Stem Cells Int.* 2016:6183562.

Russ, H. A., Parent, A. V., Ringler, J. J., Hennings, T. G., Nair, G. G., Shveygert, M., et al. (2015). Controlled induction of human pancreatic progenitors produces functional beta-like cells in vitro. *Embo J.* 34, 1759–1772. doi: 10.15252/embj.201591058

Russell, R., Carnese, P. P., Hennings, T. G., Walker, E. M., Russ, H. A., Liu, J. S., et al. (2020). Loss of the transcription factor MAFB limits β-cell derivation from human PSCs. *Nat. Commun.* 11:2742.

Sachs, S., Bastidas-Ponce, A., Tritschler, S., Bakhti, M., Böttcher, A., Sánchez-Garrido, M. A., et al. (2020). Targeted pharmacological therapy restores β-cell function for diabetes remission. *Nat. Metab.* 2, 192–209. doi: 10.1038/s42255-020-0171-3

Saka, S. K., Wang, Y., Kishi, J. Y., Zhu, A., Zeng, Y., Xie, W., et al. (2019). Immuno-SABER enables highly multiplexed and amplified protein imaging in tissues. *Nat. Biotechnol.* 37, 1080–1090. doi: 10.1038/s41587-019-0207-y

Salisbury, R. J., Blaylock, J., Berry, A. A., Jennings, R. E., De Krijger, R., Piper Hanley, K., et al. (2014). The window period of NEUROGENIN3 during human gestation. *Islets* 6:e954436. doi: 10.4161/19382014.2014.954436

Scavuzzo, M. A., Hill, M. C., Chmielowiec, J., Yang, D., Teaw, J., Sheng, K., et al. (2018). Endocrine lineage biases arise in temporally distinct endocrine progenitors during pancreatic morphogenesis. *Nat. Commun.* 9:3356.

Schlesinger, Y., Yosefov-Levi, O., Kolodkin-Gal, D., Granit, R. Z., Peters, L., Kalifa, R., et al. (2020). Single-cell transcriptomes of pancreatic preinvasive lesions and cancer reveal acinar metaplastic cells' heterogeneity. *Nat. Commun.* 11:4516.

Schonhoff, S. E., Giel-Moloney, M., and Leiter, A. B. (2004). Neurogenin 3-expressing progenitor cells in the gastrointestinal tract differentiate into both endocrine and non-endocrine cell types. *Dev. Biol.* 270, 443–454. doi: 10.1016/j.ydbio.2004.03.013

Schwamborn, J. C. (2018). Is Parkinson's disease a neurodevelopmental disorder and will brain organoids help us to understand it? *Stem Cells Dev.* 27, 968–975. doi: 10.1089/scd.2017.0289

Schwitzgebel, V. M., Scheel, D. W., Conners, J. R., Kalamaras, J., Lee, J. E., Anderson, D. J., et al. (2000). Expression of neurogenin3 reveals an islet cell precursor population in the pancreas. *Dev. Camb. Engl.* 127, 3533–3542.

Segerstolpe, Å, Palasantza, A., Eliasson, P., Andersson, E.-M., Andréasson, A.-C., Sun, X., et al. (2016). Single-cell transcriptome profiling of human pancreatic islets in health and type 2 diabetes. *Cell Metab.* 24, 593–607. doi: 10.1016/j.cmet.2016.08.020

Seiron, P., Wiberg, A., Kuric, E., Krogvold, L., Jahnsen, F. L., Dahl-Jørgensen, K., et al. (2019). Characterisation of the endocrine pancreas in type 1 diabetes: islet size is maintained but islet number is markedly reduced. *J. Pathol. Clin. Res.* 5, 248–255. doi: 10.1002/cjp2.140

Shang, L., Hua, H., Foo, K., Martinez, H., Watanabe, K., Zimmer, M., et al. (2014). β-cell dysfunction due to increased ER stress in a stem cell model of Wolfram syndrome. *Diabetes* 63, 923–933. doi: 10.2337/db13-0717

Shapiro, A. M. J., Ricordi, C., Hering, B. J., Auchincloss, H., Lindblad, R., Robertson, R. P., et al. (2006). International trial of the Edmonton protocol for islet transplantation. *N. Engl. J. Med.* 355, 1318–1330.

Sharon, N., Chawla, R., Mueller, J., Vanderhooft, J., Whitehorn, L. J., Rosenthal, B., et al. (2019b). A peninsular structure coordinates asynchronous differentiation with morphogenesis to generate pancreatic islets. *Cell* 176, 790.e13–804.e13.

Sharon, N., Vanderhooft, J., Straubhaar, J., Mueller, J., Chawla, R., Zhou, Q., et al. (2019a). Wnt signaling separates the progenitor and endocrine compartments during pancreas development. *Cell Rep.* 27, 2281.e5–2291.e5.

Sheets, T. P., Park, K.-E., Park, C.-H., Swift, S. M., Powell, A., Donovan, D. M., et al. (2018). Targeted mutation of NGN3 gene disrupts pancreatic endocrine cell development in pigs. *Sci. Rep.* 8:3582.

Simcox, J. A., and McClain, D. A. (2013). Iron and diabetes risk. *Cell Metab.* 17, 329–341. doi: 10.1016/j.cmet.2013.02.007

Smith-Geater, C., Hernandez, S. J., Lim, R. G., Adam, M., Wu, J., Stocksdale, J. T., et al. (2020). Aberrant development corrected in adult-onset huntington's disease ipsc-derived neuronal cultures via WNT signaling modulation. *Stem Cell Rep.* 14, 406–419. doi: 10.1016/j.stemcr.2020.01.015

Sneddon, J. B., Borowiak, M., and Melton, D. A. (2012). Self-renewal of embryonic-stem-cell-derived progenitors by organ-matched mesenchyme. *Nature* 491, 765–768. doi: 10.1038/nature11463

Spanjaard, B., Hu, B., Mitic, N., Olivares-Chauvet, P., Janjuha, S., Ninov, N., et al. (2018). Simultaneous lineage tracing and cell-type identification using CRISPR-Cas9-induced genetic scars. *Nat. Biotechnol.* 36, 469–473. doi: 10.1038/nbt.4124

Stanescu, D. E., Yu, R., Won, K.-J., and Stoffers, D. A. (2017). Single cell transcriptomic profiling of mouse pancreatic progenitors. *Physiol. Genomics* 49, 105–114. doi: 10.1152/physiolgenomics.00114.2016

Steele, N. G., Carpenter, E. S., Kemp, S. B., Sirihorachai, V. R., The, S., Delrosario, L., et al. (2020). Multimodal mapping of the tumor and peripheral blood immune landscape in human pancreatic cancer. *Nat. Cancer* 1, 1097–1112.

Stein, A. D., Obrutu, O. E., Behere, R. V., and Yajnik, C. S. (2019). Developmental undernutrition, offspring obesity and type 2 diabetes. *Diabetologia* 62, 1773–1778. doi: 10.1007/s00125-019-4930-1

Storz, P. (2017). Acinar cell plasticity and development of pancreatic ductal adenocarcinoma. *Nat. Rev. Gastroenterol. Hepatol.* 14, 296–304. doi: 10.1038/nrgastro.2017.12

Storz, P., and Crawford, H. C. (2020). Carcinogenesis of pancreatic ductal adenocarcinoma. *Gastroenterology* 158, 2072–2081. doi: 10.1053/j.gastro.2020.02.059

Street, K., Risso, D., Fletcher, R. B., Das, D., Ngai, J., Yosef, N., et al. (2018). Slingshot: cell lineage and pseudotime inference for single-cell transcriptomics. *BMC Genomics* 19:477. doi: 10.1186/s12864-018-4772-0

Stuart, T., Butler, A., Hoffman, P., Hafemeister, C., Papalexi, E., Mauck, W. M., et al. (2019). Comprehensive integration of single-cell data. *Cell* 177, 1888.e21–1902.e21.

Suriben, R., Kaihara, K. A., Paolino, M., Reichelt, M., Kummerfeld, S. K., Modrusan, Z., et al. (2015). β-Cell insulin secretion requires the ubiquitin ligase COP1. *Cell* 163, 1457–1467. doi: 10.1016/j.cell.2015.10.076

Svensson, V., Vento-Tormo, R., and Teichmann, S. A. (2018). Exponential scaling of single-cell RNA-seq in the past decade. *Nat. Protoc.* 13, 599–604. doi: 10.1038/nprot.2017.149

Sznurkowska, M. K., Hannezo, E., Azzarelli, R., Rulands, S., Nestorowa, S., Hindley, C. J., et al. (2018). Defining lineage potential and fate behavior of precursors during pancreas development. *Dev. Cell* 46, 360.e5–375.e5.

Talchai, C., Xuan, S., Lin, H. V., Sussel, L., and Accili, D. (2012). Pancreatic β cell dedifferentiation as a mechanism of diabetic β cell failure. *Cell* 150, 1223–1234. doi: 10.1016/j.cell.2012.07.029

Tan, S. Y., Mei Wong, J. L., Sim, Y. J., Wong, S. S., Mohamed Elhassan, S. A., Tan, S. H., et al. (2019). Type 1 and 2 diabetes mellitus: a review on current treatment approach and gene therapy as potential intervention. *Diabetes Metab. Syndr.* 13, 364–372. doi: 10.1016/j.dsx.2018.10.008

Tang, F., Barbacioru, C., Wang, Y., Nordman, E., Lee, C., Xu, N., et al. (2009). mRNA-Seq whole-transcriptome analysis of a single cell. *Nat. Methods* 6, 377–382. doi: 10.1038/nmeth.1315

Thorel, F., Népote, V., Avril, I., Kohno, K., Desgraz, R., Chera, S., et al. (2010). Conversion of adult pancreatic alpha-cells to beta-cells after extreme beta-cell loss. *Nature* 464, 1149–1154.

Ting, D. T., Wittner, B. S., Ligorio, M., Vincent Jordan, N., Shah, A. M., Miyamoto, D. T., et al. (2014). Single-cell RNA sequencing identifies extracellular matrix gene expression by pancreatic circulating tumor cells. *Cell Rep.* 8, 1905–1918. doi: 10.1016/j.celrep.2014.08.029

Tosti, L., Hang, Y., Debnath, O., Tiesmeyer, S., Trefzer, T., Steiger, K., et al. (2021). Single-nucleus and in situ RNA-sequencing reveal cell topographies in the human pancreas. *Gastroenterology* 160, 1330.e11–1344.e11.

Tritschler, S., Büttner, M., Fischer, D. S., Lange, M., Bergen, V., Lickert, H., et al. (2019). Concepts and limitations for learning developmental trajectories from single cell genomics. *Dev. Camb. Engl.* 146:dev170506. doi: 10.1242/dev.170506

Van de Sande, B., Flerin, C., Davie, K., De Waegeneer, M., Hulselmans, G., Aibar, S., et al. (2020). A scalable SCENIC workflow for single-cell gene regulatory network analysis. *Nat. Protoc.* 15, 2247–2276. doi: 10.1038/s41596-020-0336-2

Van den Berge, K., Roux, de Bézieux, H., Street, K., Saelens, W., Cannoodt, R., et al. (2020). Trajectory-based differential expression analysis for single-cell sequencing data. *Nat. Commun.* 11:1201.

van der Plas, E., Langbehn, D. R., Conrad, A. L., Koscik, T. R., Tereshchenko, A., Epping, E. A., et al. (2019). Abnormal brain development in child and adolescent carriers of mutant huntingtin. *Neurology* 93, e1021–e1030.

van der Windt, D. J., Bottino, R., Kumar, G., Wijkstrom, M., Hara, H., Ezzelarab, M., et al. (2012). Clinical islet xenotransplantation: how close are we? *Diabetes* 61, 3046–3055. doi: 10.2337/db12-0033

van Gurp, L., Muraro, M. J., Dielen, T., Seneby, L., Dharmadhikari, G., Gradwohl, G., et al. (2019). A transcriptomic roadmap to alpha- and beta cell differentiation in the embryonic pancreas. *Dev. Camb. Engl.* 146:dev173716. doi: 10.1242/dev.173716

Vanhoose, A. M., Samaras, S., Artner, I., Henderson, E., Hang, Y., and Stein, R. (2008). MafA and MafB regulate Pdx1 transcription through the Area II control region in pancreatic beta cells. *J. Biol. Chem.* 283, 22612–22619. doi: 10.1074/jbc.m802902200

Velazco-Cruz, L., Song, J., Maxwell, K. G., Goedegebuure, M. M., Augsornworawat, P., Hogrebe, N. J., et al. (2019). Acquisition of dynamic function in human stem cell-derived β cells. *Stem Cell Rep.* 12, 351–365. doi: 10.1016/j.stemcr.2018.12.012

Veres, A., Faust, A. L., Bushnell, H. L., Engquist, E. N., Kenty, J. H.-R., Harb, G., et al. (2019). Charting cellular identity during human in vitro β-cell differentiation. *Nature* 569, 368–373. doi: 10.1038/s41586-019-1168-5

Villasenor, A., Chong, D. C., and Cleaver, O. (2008). Biphasic Ngn3 expression in the developing pancreas. *Dev. Dyn. Off. Publ. Am. Assoc. Anat.* 237, 3270–3279. doi: 10.1002/dvdy.21740

Wang, D., Cai, C., Dong, X., Yu, Q. C., Zhang, X.-O., Yang, L., et al. (2015). Identification of multipotent mammary stem cells by protein C receptor expression. *Nature* 517, 81–84. doi: 10.1038/nature13851

Wang, D., Wang, J., Bai, L., Pan, H., Feng, H., Clevers, H., et al. (2020). Long-term expansion of pancreatic islet organoids from resident procr+ progenitors. *Cell* 180, 1198.e19–1211.e19.

Wang, J., Yuan, R., Zhu, X., and Ao, P. (2020). Adaptive landscape shaped by core endogenous network coordinates complex early progenitor fate commitments in embryonic pancreas. *Sci. Rep.* 10:1112.

Wang, Y. J., and Kaestner, K. H. (2019). Single-Cell RNA-Seq of the pancreatic islets–a promise not yet fulfilled? *Cell Metab.* 29, 539–544. doi: 10.1016/j.cmet.2018.11.016

Wang, Y. J., Schug, J., Won, K.-J., Liu, C., Naji, A., Avrahami, D., et al. (2016). Single-cell transcriptomics of the human endocrine pancreas. *Diabetes* 65, 3028–3038. doi: 10.2337/db16-0405

Wang, Y., Li, Z., Xu, P., Huang, L., Tong, J., Huang, H., et al. (2011). Angiomotin-like2 gene (amotl2) is required for migration and proliferation of endothelial cells during angiogenesis. *J. Biol. Chem.* 286, 41095–41104. doi: 10.1074/jbc.m111.296806

Wells, J. M., and Melton, D. A. (2000). Early mouse endoderm is patterned by soluble factors from adjacent germ layers. *Dev. Camb. Engl.* 127, 1563–1572.

Wiatr, K., Szlachcic, W. J., Trzeciak, M., Figlerowicz, M., and Figiel, M. (2017). Huntington disease as a neurodevelopmental disorder and early signs of the disease in stem cells. *Mol. Neurobiol.* 55, 3351–3371. doi: 10.1007/s12035-017-0477-7

Wilcox, C. L., Terry, N. A., Walp, E. R., Lee, R. A., and May, C. L. (2013). Pancreatic α-cell specific deletion of mouse Arx leads to α-cell identity loss. *PLoS One* 8:e66214. doi: 10.1371/journal.pone.0066214

Wollny, D., Zhao, S., Everlien, I., Lun, X., Brunken, J., Brüne, D., et al. (2016). Single-cell analysis uncovers clonal acinar cell heterogeneity in the adult pancreas. *Dev. Cell* 39, 289–301. doi: 10.1016/j.devcel.2016.10.002

Workman, M. J., Mahe, M. M., Trisno, S., Poling, H. M., Watson, C. L., Sundaram, N., et al. (2016). Engineered human pluripotent-stem-cell-derived intestinal tissues with a functional enteric nervous system. *Nat. Med.* 23, 49–59. doi: 10.1038/nm.4233

Wu, Y., and Zhang, K. (2020). Tools for the analysis of high-dimensional single-cell RNA sequencing data. *Nat. Rev. Nephrol.* 16, 408–421. doi: 10.1038/s41581-020-0262-0

Xin, Y., Kim, J., Okamoto, H., Ni, M., Wei, Y., Adler, C., et al. (2016). RNA sequencing of single human islet cells reveals type 2 diabetes genes. *Cell Metab.* 24, 608–615. doi: 10.1016/j.cmet.2016.08.018

Yamada, T., Ishihara, H., Tamura, A., Takahashi, R., Yamaguchi, S., Takei, D., et al. (2006). WFS1-deficiency increases endoplasmic reticulum stress, impairs cell cycle progression and triggers the apoptotic pathway specifically in pancreatic beta-cells. *Hum. Mol. Genet.* 15, 1600–1609. doi: 10.1093/hmg/ddl081

Yamamoto, Y., Gotoh, S., Korogi, Y., Seki, M., Konishi, S., Ikeo, S., et al. (2017). Long-term expansion of alveolar stem cells derived from human iPS cells in organoids. *Nat. Methods* 14, 1097–1106. doi: 10.1038/nmeth.4448

Yosten, G. L. C. (2018). Alpha cell dysfunction in type 1 diabetes. *Peptides* 100, 54–60. doi: 10.1016/j.peptides.2017.12.001

Yu, Q. C., Song, W., Wang, D., and Zeng, Y. A. (2016). Identification of blood vascular endothelial stem cells by the expression of protein C receptor. *Cell Res.* 26, 1079–1098. doi: 10.1038/cr.2016.85

Yu, X.-X., Qiu, W.-L., Yang, L., Zhang, Y., He, M.-Y., Li, L.-C., et al. (2019). Defining multistep cell fate decision pathways during pancreatic development at single-cell resolution. *Embo J.* 38:e100164.

Zeng, C., Mulas, F., Sui, Y., Guan, T., Miller, N., Tan, Y., et al. (2017). Pseudotemporal ordering of single cells reveals metabolic control of postnatal β cell proliferation. *Cell Metab.* 25, 1160.e11–1175.e11.

Zhang, M. J., Ntranos, V., and Tse, D. (2020). Determining sequencing depth in a single-cell RNA-seq experiment. *Nat. Commun.* 11:774.

Zhao, B., Li, L., Lu, Q., Wang, L. H., Liu, C.-Y., Lei, Q., et al. (2011). Angiomotin is a novel Hippo pathway component that inhibits YAP oncoprotein. *Genes Dev.* 25, 51–63. doi: 10.1101/gad.2000111

Zheng, G. X. Y., Terry, J. M., Belgrader, P., Ryvkin, P., Bent, Z. W., Wilson, R., et al. (2017). Massively parallel digital transcriptional profiling of single cells. *Nat. Commun.* 8:14049.

Zhou, D. C., Jayasinghe, R. G., Herndon, J. M., Storrs, E., Mo, C.-K., Wu, Y., et al. (2021). Spatial drivers and pre-cancer populations collaborate with the microenvironment in untreated and chemo-resistant pancreatic cancer. *BioRxiv* doi: 10.1101/2021.01.13.426413

Zhou, Q., and Melton, D. A. (2018). Pancreas regeneration. *Nature* 557, 351–358.

Zhou, Q., Brown, J., Kanarek, A., Rajagopal, J., and Melton, D. A. (2008). In vivo reprogramming of adult pancreatic exocrine cells to beta-cells. *Nature* 455, 627–632.

Zhou, Q., Law, A. C., Rajagopal, J., Anderson, W. J., Gray, P. A., and Melton, D. A. (2007). A multipotent progenitor domain guides pancreatic organogenesis. *Dev. Cell* 13, 103–114. doi: 10.1016/j.devcel.2007.06.001

Zhu, C., Yu, M., Huang, H., Juric, I., Abnousi, A., Hu, R., et al. (2019). An ultra high-throughput method for single-cell joint analysis of open chromatin and transcriptome. *Nat. Struct. Mol. Biol.* 26, 1063–1070. doi: 10.1038/s41594-019-0323-x

Conflict of Interest: The authors declare that the research was conducted in the absence of any commercial or financial relationships that could be construed as a potential conflict of interest.

frontiers in Cell and Developmental Biology

ORIGINAL RESEARCH
published: 20 July 2021
doi: 10.3389/fcell.2021.709286

Exogenous LIN28 Is Required for the Maintenance of Self-Renewal and Pluripotency in Presumptive Porcine-Induced Pluripotent Stem Cells

*Warunya Chakritbudsabong[1,2,3], Somjit Chaiwattanarungruengpaisan[4], Ladawan Sariya[4], Sirikron Pamonsupornvichit[4], Joao N. Ferreira[5], Panithi Sukho[1,2], Dulyatad Gronsang[3], Theerawat Tharasanit[6], Andras Dinnyes[7,8,9] and Sasitorn Rungarunlert[1,3]**

[1] Laboratory of Cellular Biomedicine and Veterinary Medicine, Faculty of Veterinary Science, Mahidol University, Nakhon Pathom, Thailand, [2] Department of Clinical Sciences and Public Health, Faculty of Veterinary Science, Mahidol University, Nakhon Pathom, Thailand, [3] Department of Preclinic and Applied Animal Science, Faculty of Veterinary Science, Mahidol University, Nakhon Pathom, Thailand, [4] The Monitoring and Surveillance Center for Zoonotic Diseases in Wildlife and Exotic Animals (MOZWE), Faculty of Veterinary Science, Mahidol University, Nakhon Pathom, Thailand, [5] Exocrine Gland Biology and Regeneration Research Group, Faculty of Dentistry, Chulalongkorn University, Bangkok, Thailand, [6] Department of Obstetrics, Gynecology and Reproduction, Faculty of Veterinary Science, Chulalongkorn University, Bangkok, Thailand, [7] BioTalentum Ltd., Gödöllő, Hungary, [8] Department of Physiology and Animal Health, Institute of Physiology and Animal Health, Hungarian University of Agriculture and Life Sciences, Gödöllő, Hungary, [9] College of Life Sciences, Sichuan University, Chengdu, China

OPEN ACCESS

Edited by:
Lon J. Van Winkle, Rocky Vista University, United States

Reviewed by:
Heiner Niemann, Hannover Medical School, Germany
Gianpaolo Papaccio, Second University of Naples, Italy

***Correspondence:**
Sasitorn Rungarunlert
sasitorn.run@mahidol.edu

Specialty section:
This article was submitted to Stem Cell Research, a section of the journal Frontiers in Cell and Developmental Biology

Received: *13 May 2021*
Accepted: *18 June 2021*
Published: *20 July 2021*

Citation:
Chakritbudsabong W, Chaiwattanarungruengpaisan S, Sariya L, Pamonsupornvichit S, Ferreira JN, Sukho P, Gronsang D, Tharasanit T, Dinnyes A and Rungarunlert S (2021) Exogenous LIN28 Is Required for the Maintenance of Self-Renewal and Pluripotency in Presumptive Porcine-Induced Pluripotent Stem Cells. Front. Cell Dev. Biol. 9:709286. doi: 10.3389/fcell.2021.709286

Porcine species have been used in preclinical transplantation models for assessing the efficiency and safety of transplants before their application in human trials. Porcine-induced pluripotent stem cells (piPSCs) are traditionally established using four transcription factors (4TF): OCT4, SOX2, KLF4, and C-MYC. However, the inefficiencies in the reprogramming of piPSCs and the maintenance of their self-renewal and pluripotency remain challenges to be resolved. LIN28 was demonstrated to play a vital role in the induction of pluripotency in humans. To investigate whether this factor is similarly required by piPSCs, the effects of adding LIN28 to the 4TF induction method (5F approach) on the efficiency of piPSC reprogramming and maintenance of self-renewal and pluripotency were examined. Using a retroviral vector, porcine fetal fibroblasts were transfected with human OCT4, SOX2, KLF4, and C-MYC with or without LIN28. The colony morphology and chromosomal stability of these piPSC lines were examined and their pluripotency properties were characterized by investigating both their expression of pluripotency-associated genes and proteins and *in vitro* and *in vivo* differentiation capabilities. Alkaline phosphatase assay revealed the reprogramming efficiencies to be 0.33 and 0.17% for the 4TF and 5TF approaches, respectively, but the maintenance of self-renewal and pluripotency until passage 40 was 6.67 and 100%, respectively. Most of the 4TF-piPSC colonies were flat in shape, showed weak positivity for alkaline phosphatase, and expressed a significantly high level of SSEA-4 protein, except for one cell line (VSMUi001-A) whose properties were similar to those of the 5TF-piPSCs; that is, tightly packed and dome-like in shape, markedly positive for alkaline phosphatase, and

expressing endogenous pluripotency genes (*pOCT4, pSOX2, pNANOG,* and *pLIN28*), significantly high levels of pluripotent proteins (OCT4, SOX2, NANOG, LIN28, and SSEA-1), and a significantly low level of SSEA-4 protein. VSMUi001-A and all 5F-piPSC lines formed embryoid bodies, underwent spontaneous cardiogenic differentiation with cardiac beating, expressed cardiomyocyte markers, and developed teratomas. In conclusion, in addition to the 4TF, LIN28 is required for the effective induction of piPSCs and the maintenance of their long-term self-renewal and pluripotency toward the development of all germ layers. These piPSCs have the potential applicability for veterinary science.

Keywords: LIN28, reprogramming, induced pluripotent stem cells, porcine, self-renewal, pluripotency, differentiation, cardiomyocytes

INTRODUCTION

The development of genetic reprogramming tools for generating induced pluripotent stem cells (iPSCs) from somatic cells is a promising strategy in regenerative medicine. The iPSC cultures can provide limitless sources of cells for biomedical research, disease modeling, drug discovery and screening, toxicity testing, and patient-specific cell transplantation (Takahashi et al., 2007; Yu et al., 2007; Singh et al., 2015). However, iPSC transplants must undergo various stages of animal testing of their efficiency and safety before they can be applied to humans. Because *Sus scrofa* species (domestic pigs) have similar anatomical, physiological, and immunological attributes to humans (Hall, 2008; Groenen et al., 2012; Moradi et al., 2019), they have been widely used as test models in preclinical transplantation medicine (Harding et al., 2013) and especially in myocardial therapy (Li et al., 2013). Moreover, piPSCs would produce available cell resources to study embryonic development and cell differentiation of these species for screening and establishing desired traits for sustainable agricultural production for veterinary medicine. Therefore, piPSCs are innovative therapies for veterinary medicine (Su et al., 2020).

Porcine iPSCs (piPSCs) are typically generated using both viral-based integration and non-integration methods. Although most piPSCs are established using four transcription factors (4TF)–octamer-binding transcription factor 4 (OCT4), SRY-box transcription factor 2 (SOX2), Kruppel-like factor 4 (KLF4), and MYC proto-oncogene, basic helix–loop–helix transcription factor (C-MYC)–which are introduced *via* retroviral vector transduction, the reprogramming efficiency is lower than that for mouse iPSCs (miPSCs) and human iPSCs (hiPSCs) (Esteban et al., 2009; Ezashi et al., 2009; Wu et al., 2009). It was previously found that hiPSCs could be efficiently reprogrammed using a viral method expressing the 4TF OCT4, SOX2, Lin-28 (LIN28), and Nanog homeobox (NANOG) (Yu et al., 2007). Subsequently, Tanabe et al. (2013) combined LIN28 with the 4TF approach for generating hiPSCs and reported a significant increase in the number of colonies produced and that LIN28 had supported complete cell reprogramming. The endogenous LIN28 was activated later during the reprogramming of the hiPSCs while maturation was taking place and therefore also improved the maturation of the cells (Tanabe et al., 2013). Aside from improving hiPSC colony formation, LIN28 overexpression could enhance the efficiency of hiPSC derivation. Conversely, the depletion of endogenous LIN28 decreased the efficiency of miPSC reprogramming (Zhang J. et al., 2016). Moreover, LIN28 promoted high reprogramming efficiency during miPSC generation by inducing an increase in the rate of cell division (Hanna et al., 2009).

LIN28, an RNA-binding protein found in nucleolus precursor bodies during embryogenesis (Vogt et al., 2012), has two paralogs: LIN28A and LIN28B. The expression of LIN28 in an embryo is restricted to some differentiated cells, such as cardiomyocytes, epithelial cells of the lung and kidney, and neuroepithelial cells (Yang and Moss, 2003). In adult cells, LIN28 remains expressed in kidney epithelial cells, cardiomyocytes, skeletal myocytes, and red blood cells (Tsialikas and Romer-Seibert, 2015). LIN28 plays an essential role in both embryonic stem cell (ESC) and iPSC self-renewal and also promotes the number of ESCs and their proliferation (Xu et al., 2009). When LIN28 is highly upregulated, it binds to both pri- and pre-*let-7* microRNAs, thereby inhibiting the maturation of *let-7* and restraining the differentiation of iPSCs (Shyh-Chang and Daley, 2013). When mouse ESCs differentiate, the expression of LIN28 is downregulated. It was demonstrated that LIN28 could regulate glucose and amino acid metabolism in both ESCs and iPSCs, where the lack of LIN28 decreased nucleotide and glucose metabolism in the stem cells and inhibited their proliferation (Nguyen and Zhu, 2015).

LIN28 has already been used together with core embryonic TFs to generate miPSCs and hiPSCs. In 2017, our group registered the establishment of one piPSC line reprogrammed from porcine fetal fibroblasts (PFFs) with the addition of LIN28 to OSKM (hOCT4, hSOX2, hKLF4, and hC-MYC) TF (Chakritbudsabong et al., 2017). However, no comparison was performed to understand the reprogramming advantages of 5TF (OSKM with Lin28) over 4TF (OSKM without Lin28). Hence, a comparative study is deemed necessary. This current study was carried out to investigate the effects of LIN28 addition to the traditional 4TF on the efficiencies of piPSC generation and reprogramming. Additionally, the biological effects of LIN28 on piPSC self-renewal and pluripotency were evaluated. Our findings provide a solution for improving the induction and reprogramming

efficiencies of piPSCs and the maintenance of their self-renewal and pluripotency and allow for the effective scale-up production of piPSC-derived cardiomyocytes for application in research studies on cardiovascular diseases and treatments.

MATERIALS AND METHODS

Ethics Statement

The Institutional Animal Care and Use Committee at the Faculty of Veterinary Science, Mahidol University, Thailand, approved the experimental use of animals (Approval ID: VSMU-2012-57).

Animals

A male porcine fetus (at embryonic day 28) from a crossbred pig (Large White/Landrace × Duroc) was procured from a certified farm at Ratchaburi Province, Thailand. Pregnant ICR mice at 13–14 days post-coitum were used for the generation of feeder cells, and 6-weeks-old female nude mice (BALB/cAJcl-nu/nu) were used for testing the formation of teratomas. All mice were purchased from Nomura Siam International Co., Ltd., Bangkok, Thailand.

Reagents

All cell culture reagents and chemical compounds were obtained from Thermo Fisher Scientific (Waltham, MA, United States) and Sigma-Aldrich (St. Louis, MO, United States), respectively, unless otherwise stated.

Cell Culture

Porcine fetal fibroblasts from the porcine fetus were prepared using standard procedures (Cheng et al., 2012). The GP2-293 cells (a HEK 293-based retroviral packaging cell line), PFFs, and mitomycin C-inactivated mouse embryonic fibroblasts (iMEFs) were maintained in fibroblast medium made up of Dulbecco's modified Eagle's medium (DMEM)-high glucose supplemented with 10% fetal bovine serum (cat. no. SV30160, Hyclone, Logan, UT, United States), 1% GlutaMAX™, and 1% antibiotic-antimycotic solution. The piPSC lines were cultured in piPSC medium made up of DMEM/F-12 supplemented with 10% Knockout™ serum replacement, 10% fetal bovine serum (cat no. SH30070, Hyclone, Logan, UT, United States), 1% GlutaMAX™, 1% antibiotic-antimycotic solution, 0.1 mM non-essential amino acids, 0.1 mM 2-mercaptoethanol, 1,000 U/mL mouse leukemia inhibitory factor (LIF; ESG1107, Millipore, Burlington, MA, United States), and 10 ng/mL human basic fibroblast growth factor (bFGF; 233-FB-025/CF, R&D Systems, Minneapolis, MN, United States). The piPSCs were maintained on iMEF and passaged using 1% TrypLE™ Select every 2 days. The cells were cultured in differentiation medium (piPSC medium without LIF and bFGF) to induce their differentiation into all three germ layers and cardiomyocytes. All cells were incubated in a humidified incubator under 5% CO_2 at 37°C. The piPSC medium was changed daily, whereas the differentiation medium was changed every 2 days.

Retroviral Vector Transduction and piPSC Generation

The retroviral vector transduction and piPSC generation were performed according to the protocols described in a previous report (Esteban et al., 2009). Two different reprogramming factor combinations were used: 4TF, and 4TF plus LIN28 (i.e., 5TF). In brief, GP2-293 cells were seeded at 2×10^6 cells in 100 mm dishes. After 24 h, pMX plasmids carrying the human monocistronic reprogramming factors (4TF or 5TF) were transfected into the GP2-293 cells using the calcium phosphate transfection protocol. The supernatant with virus particles was collected at 48 and 72 h after transduction, filtered through a 0.45 μm membrane (Millipore), and then directly used to infect the PFFs. At day 2 post-reprogramming, the PFFs were dissociated with 0.25% trypsin-EDTA solution and re-seeded in six-well plates containing iMEFs and piPSC medium. At days 9–15 post-reprogramming, primary colonies with an ESC-like morphology were separated mechanically into small fractions using a Pasteur pipette and transferred to a Falcon® IVF one-well dish with iMEFs (**Figure 1A**). After the colonies had redeveloped, they were routinely passaged with TrypLE™ Select. The reprogramming efficiency was calculated as the number of AP positive colonies divided by the total number of transfected cells (Setthawong et al., 2019).

Alkaline Phosphatase and Immunofluorescence Staining

The piPSCs and differentiated cells were fixed with 4% paraformaldehyde in phosphate-buffered saline (PBS) for 15 min and then washed three times with cold PBS. The piPSCs were subjected to the alkaline phosphatase (AP) assay by staining with a Leukocyte AP Kit (86R-1KT) according to the manufacturer's protocol. The immunofluorescence (IF) assay was used for detecting pluripotency and cardiac differentiation markers. In brief, the fixed cells were incubated with a cell permeabilization solution (0.25% Triton-X 100 in PBS) for 10 min and then incubated with a blocking solution (2% bovine serum albumin) for 1 h. Then, the cells were treated with the primary antibodies at 4°C overnight and subsequently incubated with the secondary antibodies at 37°C for 1 h (see **Supplementary Table 1** for the list of primary and secondary antibodies used). The cell nuclei were counterstained with 4′-6-diamidino-2-phenylindole. All cells were visualized using a Leica DMi8 inverted fluorescence microscope, and images were captured with an attached Leica DFC7000 camera (Leica Microsystems, Wetzlar, Germany). At least 30 z-stacks were obtained for each sample, with 0.6–0.7 μm intervals. Leica Application Suite X (LAS X) imaging software was used for the analysis of all images and for the quantitative measurement of the IF signals. The IF intensities of the immunoreactive pixels of OCT4, SOX2, LIN28, NANOG, stage-specific embryonic antigen (SSEA)-1, and SSEA-4 were measured in 20 randomly selected fields per piPSC line under ×400 magnification. At least three slides per group were scanned for the expression of these markers. Data are presented as the mean IF intensity value ± SEM after subtraction of the background signal.

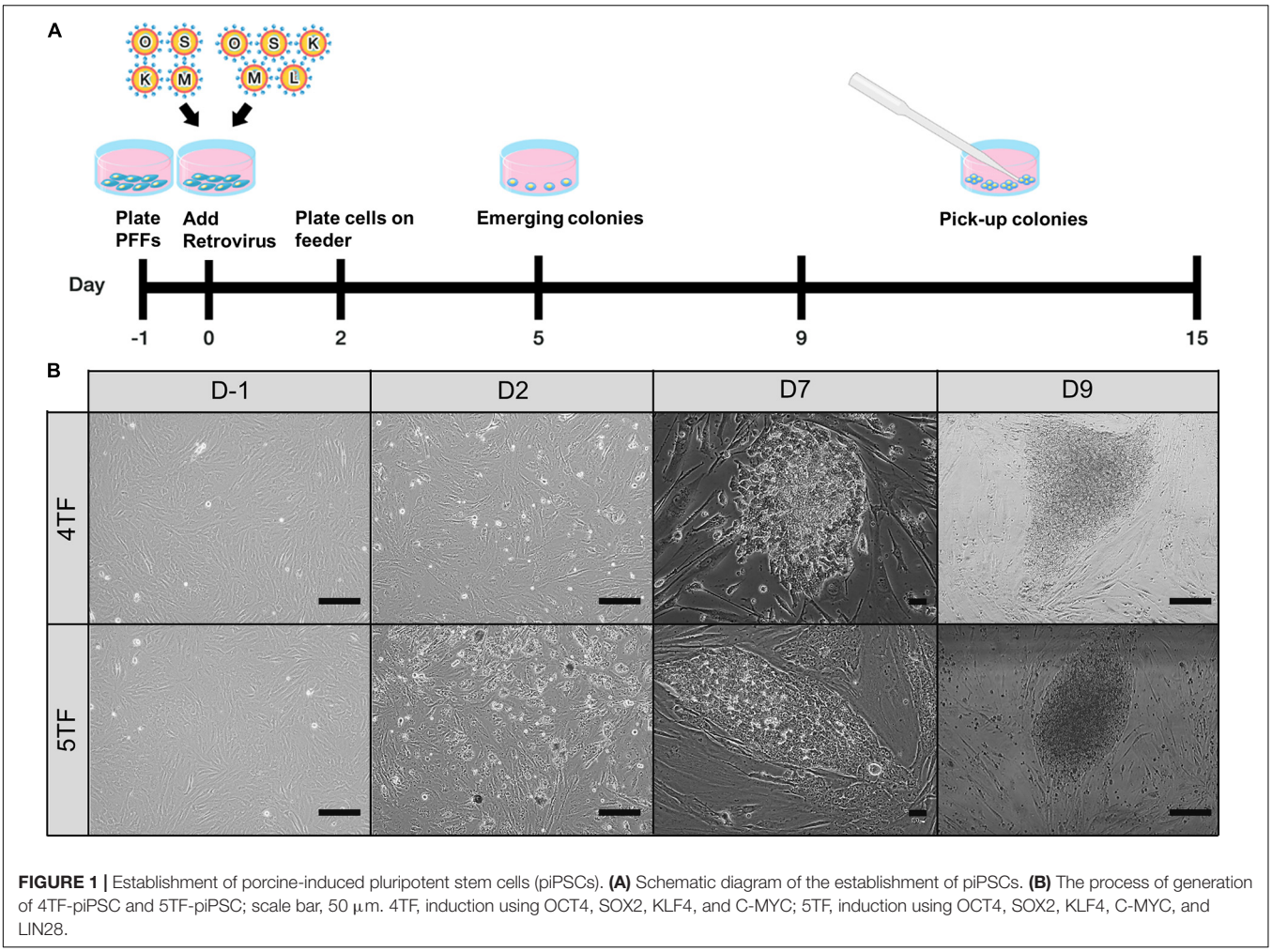

FIGURE 1 | Establishment of porcine-induced pluripotent stem cells (piPSCs). **(A)** Schematic diagram of the establishment of piPSCs. **(B)** The process of generation of 4TF-piPSC and 5TF-piPSC; scale bar, 50 μm. 4TF, induction using OCT4, SOX2, KLF4, and C-MYC; 5TF, induction using OCT4, SOX2, KLF4, C-MYC, and LIN28.

G-Banding Karyotype Analysis

Karyotype analysis was performed using a previously published protocol, with slight modifications (Phakdeedindan et al., 2019). In brief, the various piPSCs (passage 20) were incubated with 5 μg/mL colcemid (KaryoMAX^{TM} Colcemid^{TM} Solution in PBS) at 37°C for 1 h. Then, the cells were dissociated and treated with 75 M KCl at 37°C for 15 min. Thereafter, the cells were fixed three times in a cold fixative solution (1:3 acetic acid:methanol concentration) for 10 min each time with gentle inversion to allow mixing. The fixed cells were then dropped onto cold glass slides and incubated at 37°C overnight. Finally, the cells were observed under a Nikon Eclipse Ni microscope equipped with a DS-Ri2 camera (Nikon Instruments, Tokyo, Japan). In total, 50 G-banded metaphases per piPSC culture were analyzed using the LUCIA Cytogenetics System (Nikon Instruments).

Spontaneous Cardiogenic Differentiation of the piPSCs via Embryoid Body Formation

Spontaneous cardiogenic differentiation of the piPSCs was induced as described in a previously published report (Rungarunlert et al., 2013). In brief, floating embryoid bodies (EBs) were formed in the poly(2-hydroxyethyl methacrylate)-coated wells of 96-well plates using 5,000 piPSCs per well and maintained in differentiation medium for 21 days. On days 7 and 21 of culture, the floating EBs were collected for morphological characterization and for determination of their gene expression levels by reverse transcription polymerase chain reaction (RT-PCR) assay. To obtain adherent EBs, the EBs at day 3 were plated onto 0.1% gelatin-covered coverslips placed in the wells of a 24-well plate (1 EB/well) together with differentiation medium. The morphology of the differentiated cells and their cardiac beating were checked daily. Cells were collected at days 7, 14, and 21 for analysis of their gene expression profiles using RT-PCR. Additionally, cells were fixed with 4% paraformaldehyde for IF staining.

Teratoma Formation

For each piPSC line, two nude mice (8 weeks old) were subcutaneously injected with 8×10^6 cells into the right flank. After 35 days, the mice were euthanized and the teratomas were collected, fixed with PBS containing 10% neutral buffered formalin, and embedded in paraffin. Sections sliced from the

paraffin blocks were then stained with hematoxylin and eosin to confirm the capacity of the cells to differentiate into all three embryonic germ layers *in vivo*. Images of the teratomas were captured using an Axioskop 40 microscope equipped with an AxioCam MRc camera (Carl Zeiss, Oberkochen, Germany).

RT-PCR Analysis of Transgene and Endogenous Gene Expression

The expression of transgenes and endogenous genes by the various piPSCs and differentiated cells was examined by RT-PCR assay. Cells were lysed for RNA extraction using the RNeasy Mini Kit (Genaid Biotech Ltd., New Taipei City, Taiwan). Then, 1 μg of total RNA was reverse transcribed to cDNA using the SuperScript™ III First-Strand Synthesis System. The PCR mixture contained 50 ng of template cDNA, 12.5 μL of GoTaq PCR master mix (Promega, WI, United States), and 0.2 μM of each primer. The PCR-amplified products were separated on 2% agarose gels and then visualized with GelRed® nucleic acid staining (Biotium, Fremont, CA, United States). The primer oligonucleotide sequences are shown in **Supplementary Table 2**.

Capillary Western Blot Analysis

Cell samples were lysed by sonication in radioimmunoprecipitation assay buffer and the protein quantity was then detected using a protein assay kit (Bio-Rad Laboratory, Hercules, CA, United States). Next, capillary western blot analysis of the proteins was performed in 25 capillary cartridges according to the 12–230 kDa Jess and Wes Separation Module protocol (SM-W004, ProteinSimple, San Jose, CA, United States). In brief, a mixture of total protein with a fluorescent dye (4:1 ratio) was heated at 95°C for 5 min. After this denaturation step, the biotinylated ladder, protein sample, blocking reagent, primary antibodies (**Supplementary Table 1**), horseradish peroxidase-conjugated secondary antibodies, and chemiluminescent substrate were dispensed into a Jess assay plate according to the kit manual instructions. Thereafter, the separation and immunodetection of the proteins were performed with the Jess automated western blotting system (ProteinSimple). The results were analyzed using Compass for Simple Western version 5.0.1 software (Build 0911; ProteinSimple).

Flow Cytometric Analysis

The piPSCs were harvested and dissociated into single cells using 1% TrypLE™ Select. Thereafter, the cells were incubated with BD Cytofix/Cytoperm™ (BD Biosciences, Franklin Lakes, NJ, United States) at 4°C for 20 min and then washed three times with PBS. A blocking solution (3% bovine serum albumin) was then added and the cells were incubated for 30 min at ambient temperature. Then, the cells were stained with primary antibodies against the various markers at 4°C overnight. After washing with PBS, the cells were stained with fluorescence-labeled secondary antibodies at 37°C for 1 h. All samples were single-color stained, with 20,000 cells used for each marker. Samples incubated with IgG isotype antibodies were used as a negative control. The results were analyzed using FACScalibur and Cell Quest software (BD Biosciences). The list of primary and secondary antibodies used is shown in **Supplementary Table 1**.

Statistical Analysis

All experiments were repeated three times. Quantitative data are presented as the mean ± SEM from three independent experiments. One-way analysis of variance was used for the comparison of more than two groups, and Tukey's test was used as a *post hoc* test. All statistical analyses were performed using SPSS version 25.0 (IBM, Armonk, NY, United States), with statistical significance set at $P < 0.05$.

RESULTS

Establishment of the Various piPSC Lines

To test the role of LIN28 in cell reprogramming, PFFs were transduced with retroviral vectors designed to express either 4TF or 5TF. The schematic diagram of the establishment of the piPSCs is shown in **Figure 1A**. The ESC-like colonies generated through the 4TF and 5TF approaches were first observed on day 9 after retroviral transduction. On day 15 after transduction, the colonies were picked and mechanically passaged on iMEFs (**Figure 1B**). The 4TF− and 5TF-induced clones were designated as 4TF-piPSCs and 5TF-piPSCs, respectively. AP staining of the cells revealed the reprogramming efficiency (i.e., as reflected by the percentage of AP-positive colonies) of 4TF to be 0.33% and that of 5TF to be 0.17%. We obtained approximately fifteen 4TF-piPSC-like colonies from 4,500 initial transfected cells and three 5TF-piPSC-like colonies from 1,800 initial transfected cells (**Supplementary Table 3**). The percentage of cells maintaining self-renewal and pluripotency until passage 20 was 13.33% with the 4TF system but increased to 100% with 5TF induction. Moreover, the percentage of cells maintaining self-renewal and pluripotency until passage 40 increased from 6.67% with the 4TF system to 100% with 5TF induction. The induced day of 4TF and 5TF system was 11.5 ± 2.65 and 12 ± 3, respectively. In total, we generated three 5TF-piPSC and two 4TF-piPSC lines. We selected only two cell lines from each induction group based on their unlimited self-renewal ability and pluripotency (AP positive staining), namely, VSMUi001-A and VSMUi001-B from the 4TF group and VSMUi001-C and VSMUi001-E from the 5TF group as observed in **Figure 2A**. The discarded cell lines with limited self-renewal ability and pluripotency are shown in **Supplementary Figure 1** and on our previous publication (Chakritbudsabong et al., 2017).

Morphology and Proliferation of the piPSCs

Except for VSMUi001-A, all the 4TF-piPSC lines had flat-shaped colonies. By contrast, the VSMUi001-A colonies were tightly packed and dome-like in shape with clear edges and were indistinguishable from the 5TF-piPSC lines and mouse ESCs in terms of morphology. Moreover, the cells had a high nuclear-to-cytoplasm ratio, with dominant nucleoli (**Figure 2A**). VSMUi001-A and all the 5TF-piPSC lines were strongly positive

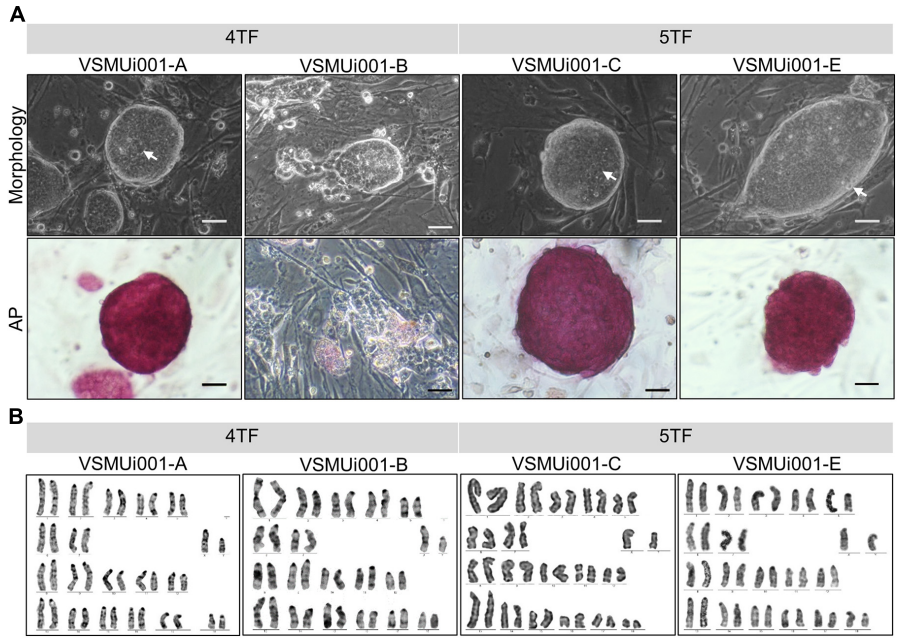

FIGURE 2 | Characterization of piPSCs. **(A)** Colony morphology and alkaline phosphatase (AP) staining of various piPSC lines; scale bar, 20 μm. **(B)** Karyotypes of the various piPSC lines. 4TF, induction using OCT4, SOX2, KLF4, and C-MYC; 5TF, induction using OCT4, SOX2, KLF4, C-MYC, and LIN28. AP, alkaline phosphatase; piPSCs, porcine-induced pluripotent stem cells.

for AP staining (**Figure 2A**), whereas the rest of the 4TF-piPSC lines were weakly positive in this regard. The proliferative activity of the piPSC lines was determined from their population doubling times, which were calculated by quantifying the cell count at every 12 h over a 48 h period. The VSMUi001-C cell line had the lowest population doubling time (∼9–10 h) compared with all the other piPSC lines (∼12 h) (**Supplementary Figure 2**). Moreover, only the VSMUi001-A and 5TF-piPSC lines could be passaged continuously for more than 40 passages (a maximum passages) as followed: VSMUi001-A (P47), VSMUi001-C (P42), and VSMUi001-E (P42). By contrast, all the other 4TF-piPSC lines could not be maintained beyond 20 passages owing to their low expansion rates and morphological changes. Both the 4TF-piPSCs and 5TF-piPSCs carried the normal porcine diploid karyotype (38, XY) throughout the extended culture periods (**Figure 2B**).

Pluripotency in the Various piPSC Lines

Reverse transcription polymerase chain reaction analysis confirmed the re-activation of the human exogenous genes and the activation of the porcine endogenous genes in the piPSCs. The 4TF-piPSCs displayed high expression levels of the endogenous pluripotency-associated transcription factors *pOCT4*, *pSOX2*, and *pNANOG*, whereas the 5TF-piPSCs expressed *pOCT4*, *pSOX2*, *pNANOG*, and *pLIN28* at a high level. By contrast, the PFFs and parent cells did not express any of the human exogenous and porcine endogenous pluripotency-associated genes (**Figure 3A**, **Supplementary Figure 3**). To confirm the RT-PCR data, capillary western blot analysis was performed to detect the endogenous OCT4, SOX2, and LIN28 proteins. Quantitative analysis of the protein levels relative to that of β-actin (an internal control) revealed that the expression of OCT4 was similar in the 4TF-piPSC and 5TF-piPSC lines (1.1 ± 0.14, 1 ± 0.11, 1.3 ± 0.12, and 1.1 ± 0.29 in VSMUi001-A, VSMUi001-B, VSMUi001-C, and VSMUi001-E, respectively). Moreover, in VSMUi001-A, VSMUi001-C, and VSMUi001-E, the expression levels of the SOX2 (0.29 ± 0.05, 0.21 ± 0.07, and 0.1 ± 0.03, respectively) and LIN28 proteins (0.06 ± 0.005, 0.045 ± 0.006, and 0.039 ± 0.006, respectively) were higher than those of VSMUi001-B. The PFFs expressed the lowest level of OCT4 (0.12 ± 0.006) and did not express SOX2 and LIN28 at all (**Figure 3B** and **Supplementary Figure 4**). After IF staining, only the VSMUi001-A and 5F-piPSC colonies were found to express proteomic pluripotency markers: OCT4, SOX2, NANOG, and LIN28 in their nuclei, and SSEA-1 on their surface. None of these colonies expressed SSEA-4. By contrast, a few colonies of VSMUi001-B expressed LIN28 and SSEA-1, and some also expressed OCT4 and SSEA-4 (**Figure 4A**). Additionally, the quantitative analysis of the IF staining under identical optical conditions confirmed that the mean fluorescence intensities of the immunoreactive pixels of OCT4, SOX2, LIN28, NANOG, and SSEA-1- were significantly brighter in the VSMUi001-A and 5TF-piPSC colonies than in the VSMUi001-B colonies. By contrast, that of SSEA-4 was significantly brighter in VSMUi001-B than in the other cell lines (**Figure 4B**). Furthermore, the flow cytometric analysis of the VSMUi001-A, VSMUi001-C, and VSMUi001-E cell lines revealed the percentage of $OCT4^+$ cells to be greater than 89% (88 ± 1.63, 91.3 ± 1.50, 91.1 ± 1.78%, respectively) and that of $SOX2^+$ cells to be greater than 80% (84.5 ± 1.49, 79.6 ± 2.15,

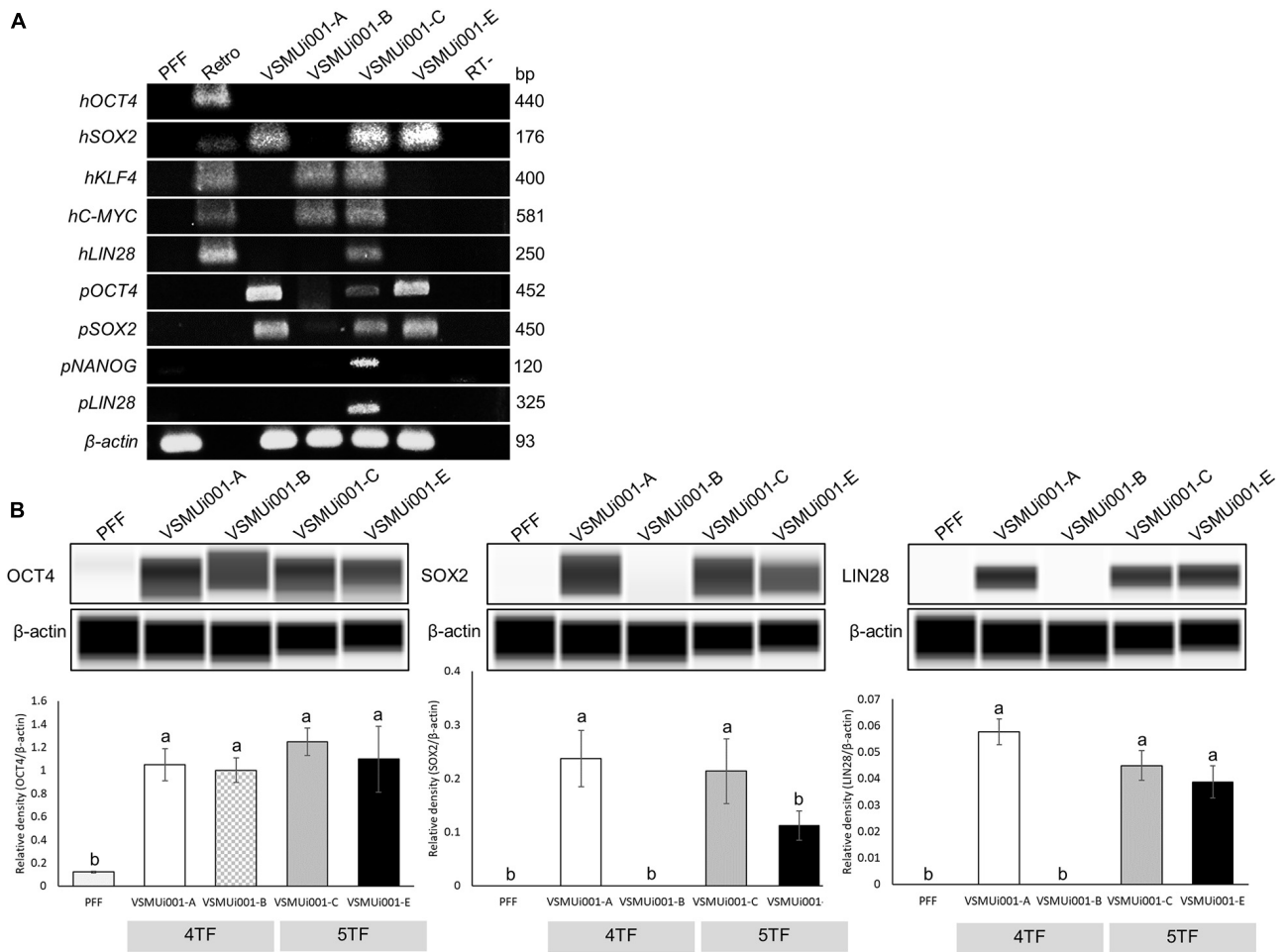

FIGURE 3 | Expression of pluripotency markers in various piPSC lines. **(A)** Expression of exogenous pluripotency genes (*hOCT4*, *hSOX2*, *hKLF4*, *hC-MYC*, and *hLIN28*) and endogenous pluripotency genes (*pOCT4*, *pSOX2*, *pNANOG*, and *pLIN28*) in the PFFs and various piPSC lines. **(B)** Western blot images of endogenous pluripotent protein (OCT4, SOX2, and LIN28) expression and quantification of the western blot results. β-Actin was used as an internal control. Means with different lowercase letters are significantly different at $P < 0.05$. PFF, porcine fetal fibroblast; piPSCs, porcine-induced pluripotent stem cells; *h*, exogenous human gene; *p*, endogenous porcine gene; *OCT4*, octamer-binding transcription factor 4; *SOX2*, SRY-box transcription factor 2; *KLF4*, Kruppel-like factor 4; *C-MYC*, MYC proto-oncogene, basic helix–loop–helix transcription factor; *LIN28*, Lin-28 homolog A; *NANOG*, Nanog homeobox.

77.1 ± 2.29%, respectively). By contrast, the percentage of $OCT4^+$ and $SOX2^+$ VSMUi001-B cells was significantly lower (69.3 ± 1.11 and 4.9 ± 0.13%, respectively). Moreover, the percentage of $LIN28^+$ cells was greater than 95% (96.9 ± 0.82, 97.9 ± 0.63, 96 ± 0.93%, respectively) and that of SSEA-1^+ cells was 92% (92.1 ± 1.90, 92.7 ± 2.39, 92.1 ± 0.80%, respectively) in the VSMUi001-A, VSMUi001-C, and VSMUi001-E cell lines. By contrast, in the VSMUi001-B cell line, the percentages of $LIN28^+$ and SSEA-1^+ cells were also significantly lower (67.2 ± 1.27 and 0.5 ± 0.07%, respectively), whereas the percentage of SSEA-4^+ cells (67.6 ± 0.67%) was significantly higher than that in the other cell lines (**Figure 5**).

Spontaneous Cardiogenic Differentiation

All four piPSC lines were tested for EB formation to determine their differentiation capability *in vitro*. VSMUi001-A and the two 5TF-piPSC lines were able to form floating EBs, which were homogeneous in size and shape on day 7 and displayed cystic cavities on day 21 (**Figure 6A**). These three cell lines were therefore evaluated for spontaneous cardiogenic differentiation. However, because VSMUi001-B could not form floating EBs after day 3 and the ones that it did form in the first 3 days showed a limited ability to differentiate (**Supplementary Figure 5**), it was not evaluated for spontaneous differentiation. Spontaneously beating cardiomyocytes were visible on day 6, with the VSMUi001-C line being significantly faster than the other two cell lines in developing into these cardiac cells, displaying 100% of cardiac beating on day 8 and maintaining this percentage until day 14 ($P < 0.01$). VSMUi001-A and VSMUi001-E showed approximately 80% of cardiac beating on day 10 (78 ± 2.78%) and day 12 (77.78 ± 11.11%), respectively (**Figure 6C**). Moreover, the area of spontaneous cardiac beating appeared to be smaller for VSMUi001-E than for VSMUi001-A and VSMUi001-C (2.58 ± 0.59 × 10^5,

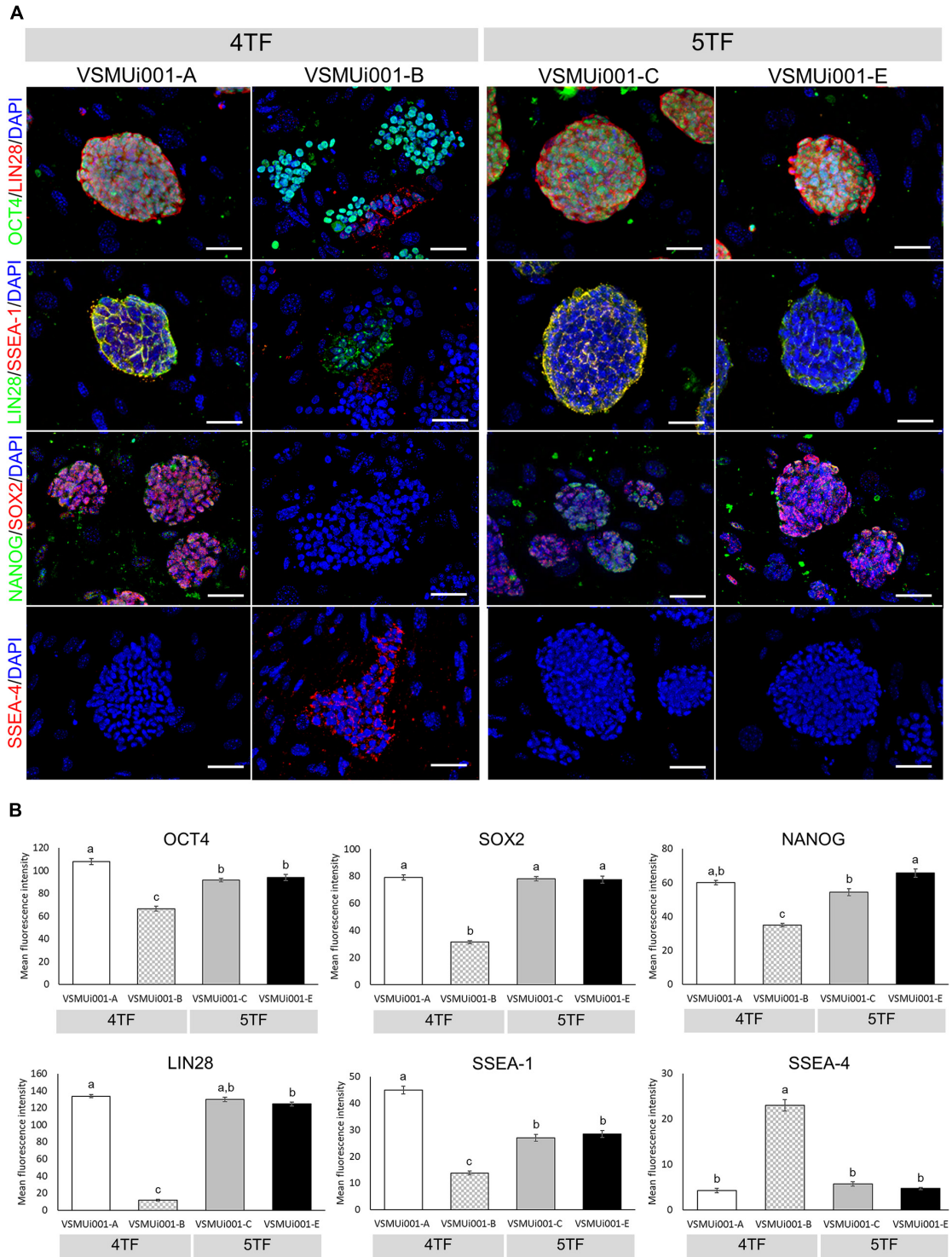

FIGURE 4 | Immunofluorescence analysis of pluripotency markers in various piPSC lines. **(A)** Detection of pluripotency markers in 4TF-piPSC and 5TF-piPSC lines using fluorescence microscopy; scale bar: 50 μm. **(B)** Quantitative analysis of the pluripotency markers in the various piPSC lines. The mean fluorescence signals for OCT4, SOX2, LIN28, NANOG, SSEA-1, and SSEA-4 were measured in 20 randomly selected fields per piPSC colony under identical optical settings. Means with different lowercase letters are significantly different at $P < 0.05$. 4TF, induction using OCT4, SOX2, KLF4, and C-MYC; 5TF, induction using OCT4, SOX2, KLF4, C-MYC, and LIN28. OCT4, octamer-binding transcription factor 4; SOX2, SRY-box transcription factor 2; LIN28, Lin-28 homolog A; NANOG, Nanog homeobox; SSEA, stage-specific embryonic antigen.

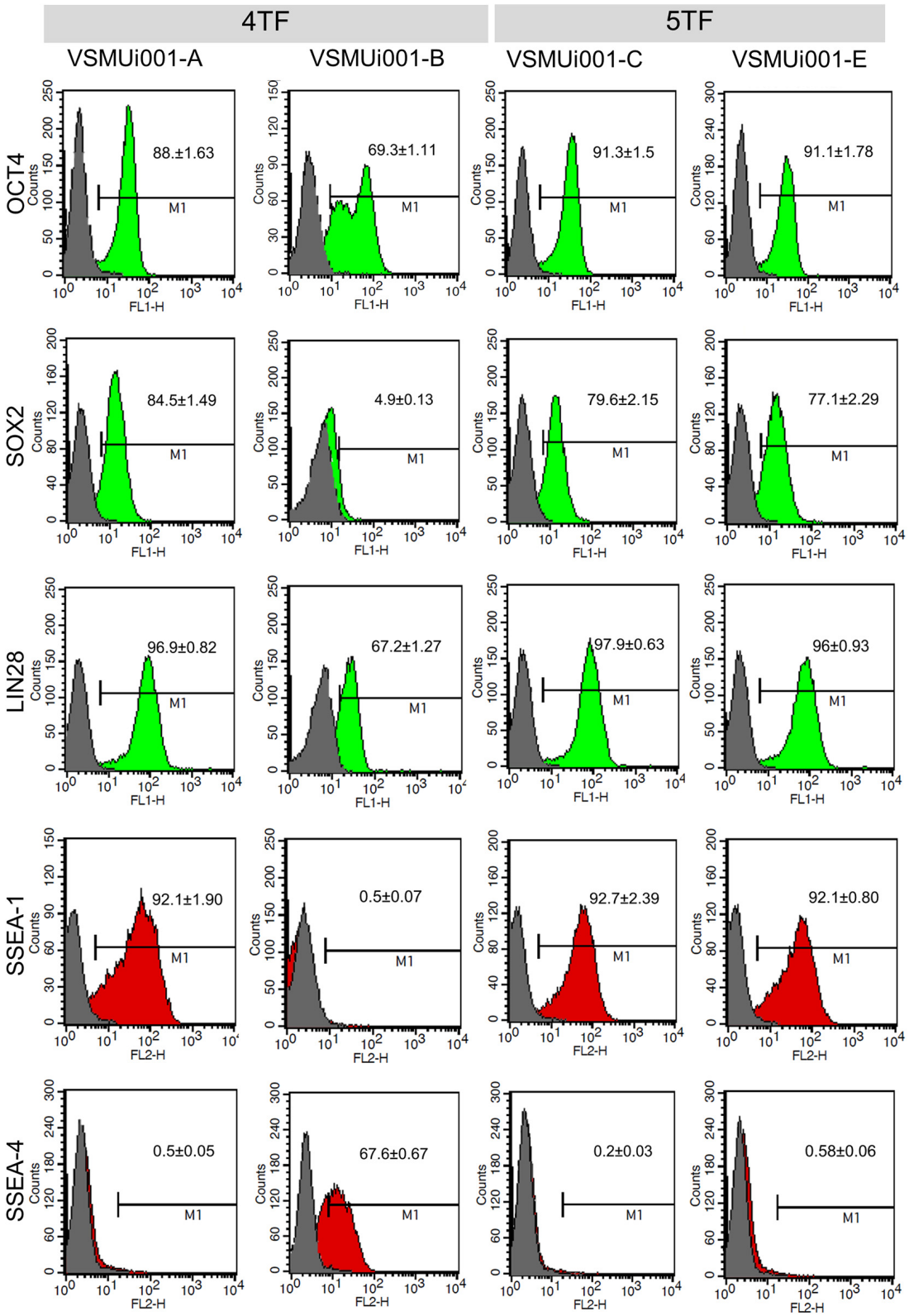

FIGURE 5 | Flow cytometric analysis of pluripotency markers expressed by various porcine-induced pluripotent stem cell lines. 4TF, induction using OCT4, SOX2, KLF4, and C-MYC; 5TF, induction using OCT4, SOX2, KLF4, C-MYC, and LIN28. OCT4, octamer-binding transcription factor 4; SOX2, SRY-box transcription factor 2; LIN28, Lin-28 homolog A; SSEA, stage-specific embryonic antigen.

$2.86 \pm 0.26 \times 10^5$, and $3.39 \pm 0.19 \times 10^5$ μm^2, respectively) (**Figures 6A,B**, and **Supplementary Videos 1–3**). All three piPSC lines expressed cardiac troponin T (cTnT), a specific cardiomyocyte marker (**Figure 6A**).

The abilities of VSMUi001-A, VSMUi001-C, and VSMUi001-E to express differentiation-related genes specific for the three germ layers were confirmed by RT-PCR. All three piPSC lines used for *in vitro* differentiation expressed the endogenous pluripotency markers *pOCT4*, *pSOX2*, and *pNANOG*. VSMUi001-A expressed the marker troponin T2, cardiac type (*TNNT2*) at day 7 and 21 of floating EB formation as well as at days 7, 14, and 21 of adherent EB formation. VSMUi001-C consistently expressed *pSOX2* at days 7 and 21 of floating EB formation and *pOCT4* at days 7 and 21 of floating EB formation and at days 14 and 21 of adherent EB formation. Moreover, VSMUi001-C also expressed differentiation-related gene markers for all three germ layers; namely, SRY-Box Transcription Factor 17 (*SOX17*) (endoderm) and Neuronal Differentiation 1 (*NEUROD1*) (ectoderm) at days 14 and 21 of adherent EB formation and Enolase 3 (*ENO3*), troponin T2, cardiac type (*TNNT2*) and troponin I1, slow skeletal type (*TNNI1*) (mesoderm) at days 7 and 21 of floating EB formation and days 7, 14, and 21 of adherent EB formation. By contrast, VSMUi001-E expressed only *pSOX2* at day 7 of floating EB formation and day 14 of adherent EB formation (**Figure 7A** and **Supplementary Figure 6**).

Teratoma Formation

VSMUi001-A, VSMUi001-C, and VSMUi001-E were tested for their abilities to form teratomas as part of their *in vivo* differentiation capability. VSMUi001-B was excluded as it was undergoing apoptosis. At 35 days after piPSC injection, all nude mice developed solid tumors in each of the three germ layers, as shown by hematoxylin and eosin staining (**Figure 7B**). The teratomas contained a broad range of tissue types, including keratinized squamous epithelia and immature neuroepithelia forming rosettes (ectoderm), cartilage and skeletal muscle (mesoderm), and respiratory-like epithelia (endoderm) (**Figure 7B**).

DISCUSSION

In this study, we successfully generated piPSC colonies *via* the induction of PFFs by both four and five reprogramming factors using retroviral biotechnology. The reprogramming efficiency of

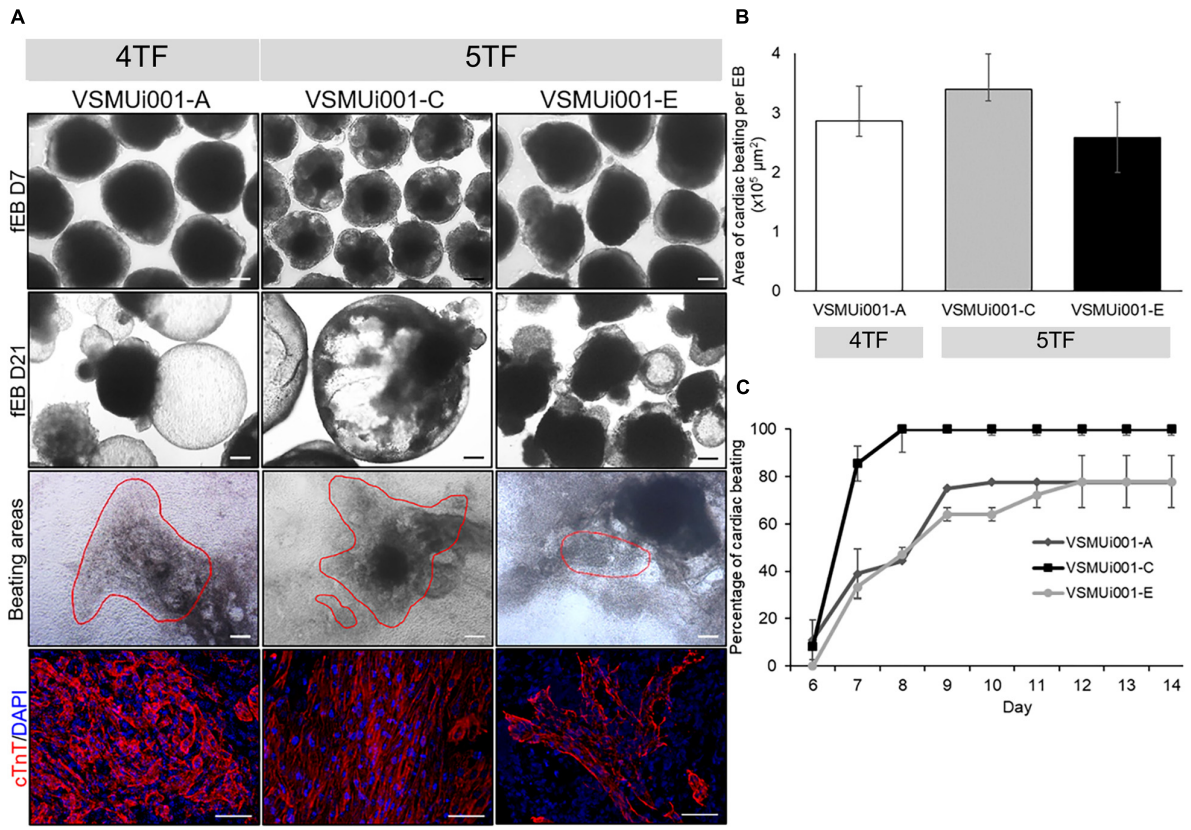

FIGURE 6 | *In vitro* cardiogenic differentiation of various porcine-induced pluripotent stem cell lines. **(A)** Morphology of floating embryoid bodies (fEB) at days 7 and 21, area of cardiac beating (scale bar, 100 μm), and cTnT expression of VSMUi001-A, VSMUi001-C, and VSMUi001-E; scale bar, 50 μm. **(B)** Area of cardiac beating per embryoid body. **(C)** Percentage of spontaneous cardiac beating. 4TF, induction using OCT4, SOX2, KLF4, and C-MYC; 5TF, induction using OCT4, SOX2, KLF4, C-MYC, and LIN28; cTnT, cardiac troponin T.

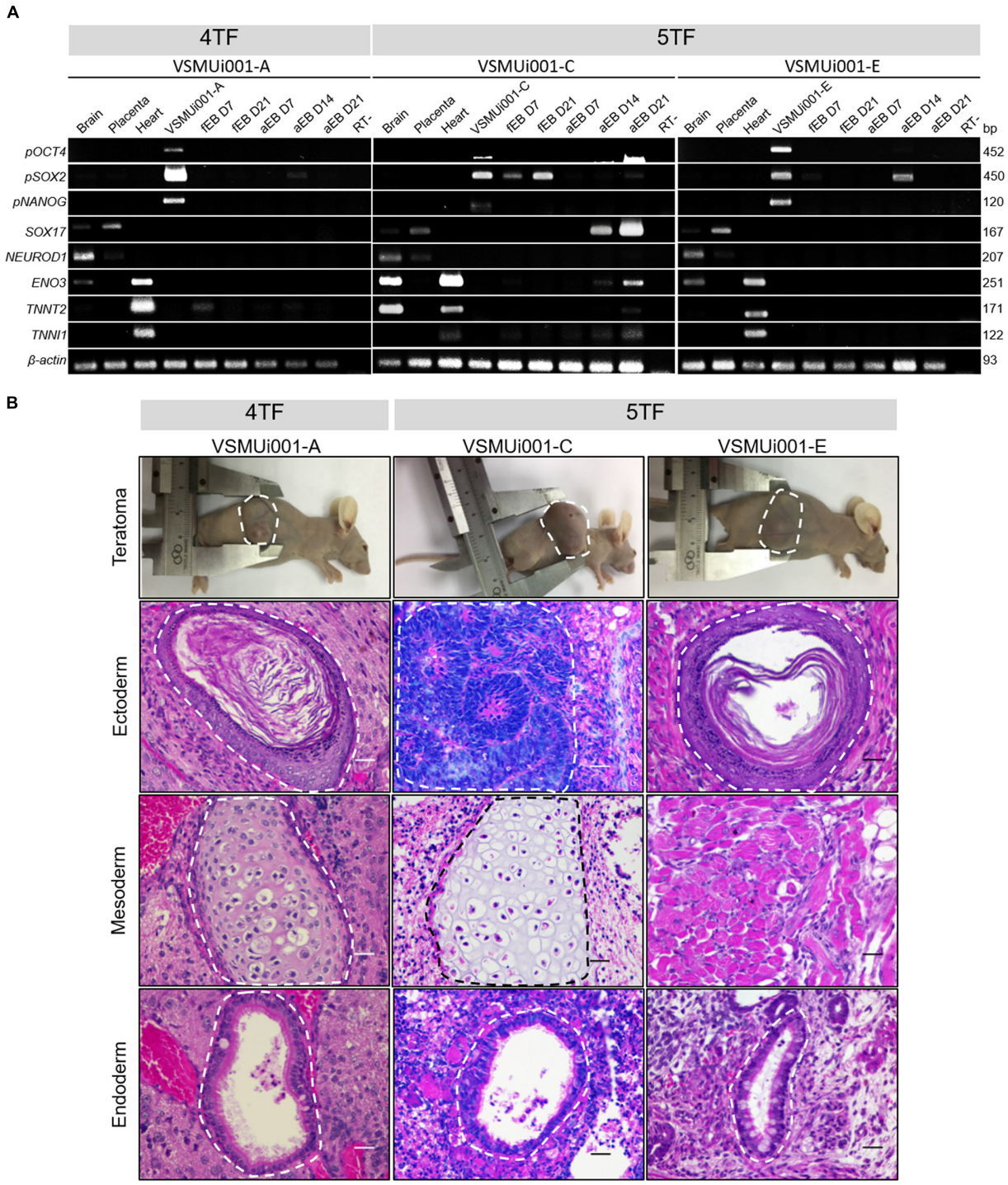

FIGURE 7 | Expression of differentiation-related genes and *in vivo* differentiation of the various porcine-induced pluripotent stem cell (piPSC) lines. **(A)** Expression of differentiation genes specific for the three germ layers: *pOCT4*, *pSOX2*, and *pNANOG* (pluripotency genes); *SOX17* (endoderm); *NEUROD1* (ectoderm); and *ENO3, TNNT2* and *TNNI1* (mesoderm). fEB, floating embryoid body; aEB, adherent embryoid body. **(B)** Teratoma formation; all nude mice developed teratomas. Hematoxylin and eosin staining of the teratoma section generated by piPSCs showing a broad range of tissues of the three germ layers: keratinized squamous epithelia (VSMUi001-A and VSMUi001-E) and immature neuroepithelia forming rosettes (VSMUi001-C; ectoderm), cartilage (VSMUi001-A and VSMUi001-C), and skeletal muscle (VSMUi001-E; mesoderm), and respiratory-like epithelia (VSMUi001-A, VSMUi001-C, and VSMUi001-E; endoderm); scale bar, 25 μm. 4TF, induction using OCT4, SOX2, KLF4, and C-MYC; 5TF, induction using OCT4, SOX2, KLF4, C-MYC, and LIN28; *pOCT4*, endogenous porcine octamer-binding transcription factor 4; *pSOX2*, endogenous porcine SRY-box transcription factor 2; *pNANOG*, endogenous porcine Nanog homeobox; *SOX17,* SRY-box transcription factor 17; *NEUROD1,* neuronal differentiation 1; *ENO3,* enolase 3; *TNNT2*, troponin T2, cardiac type; TNNI1, troponin I1, slow skeletal type.

the 4TF approach was quite low, resulting in only 0.002–2.7% AP-positive cells (Ruan et al., 2011; Gao et al., 2014; Setthawong et al., 2019). Furthermore, although the reprogramming efficiency of the 4TF system was higher than that of the 5TF system (0.33 versus 0.17%), its maintenance of self-renew and pluripotency (6.67%) was significantly lower than that of 5TF (100%). Taken together, this comparison study showed for the first time that the addition of Lin28 to OSKM TFs is more effective than OSKM alone for the following reasons: (1) 5TF can consistently establish self-renewal and pluripotency in all cell lines until passage 40 with 100% efficacy, whereas 4TF achieves this with 6.67% (1 out of 15 cell lines); and (2) further, all 5TF piPSC lines have the ability to differentiate into the three germ layers. Thus, the addition of LIN28 to 4TF was critical in enhancing the pluripotency and self-renewal capacity of piPSCs. In mammalian blastocysts, LIN28 is highly expressed in pluripotent cells of the inner cell mass and epiblast, which correlates with the intrinsic self-renewal ability of ESCs (Shyh-Chang and Daley, 2013). Moreover, LIN28 represses the maturation of *let-7* and prevents premature differentiation of the pluripotent cells of the inner cell mass and epiblast (Melton et al., 2010). Several studies have demonstrated that high LIN28 expression can improve the self-renewal capacity of ESCs *in vitro* (Bin et al., 2012; Shyh-Chang and Daley, 2013; Parisi et al., 2017; Mens and Ghanbari, 2018). Furthermore, models of LIN28 knockdown led to proliferative defects in mouse ESCs (Peng et al., 2011; Pan et al., 2018). LIN28, together with a cocktail of core reprogramming factors (OCT4, SOX2, and NANOG), was shown to promote hiPSC self-renewal (Hanna et al., 2009). In other studies, LIN28 promoted the self-renewal of mouse and human ESCs during reprogramming by upregulating numerous cell-cycle and cell growth regulators via *let-7* family repressors, such as Ras, Myc, high-mobility group A2 (Hmga2), insulin-like growth factor-2 mRNA-binding proteins (Igf2bps), and insulin–phosphoinositide 3-kinases (Pi3K)–mechanistic target of rapamycin (mTOR) pathways as well as other mRNAs encoding enzymes relevant to cell metabolism (Xu et al., 2009; Peng et al., 2011).

In this study, one of the 4TF-piPSC lines (VSMUi001-A) and two 5TF-piPSC lines revealed a typical mouse-like ESC morphology characterized by dome-shaped compact colonies with large nuclei and clear nucleoli and had SSEA-1 expression patterns similar to those reported in other piPSC studies (Cheng et al., 2012; Kwon et al., 2013; Zhang W. et al., 2015; Yuan et al., 2019) and our previous reports (Chakritbudsabong et al., 2017). As indicated in a previous report, LIN28 overexpression can enhance the derivation efficiency of miPSCs, where the loss of endogenous LIN28 facilitated the conversion of miPSCs from naïve to primed pluripotent cells through the induction of the FGF/activin signaling pathway (Zhang J. et al., 2016). Most of the 4TF-piPSCs exhibited low levels of SSEA-1 and LIN28, whereas they expressed high levels of SSEA-4. However, piPSCs have been shown to display varied expression patterns of the surface pluripotency markers SSEA-1, SSEA-3, and SSEA-4 (Ruan et al., 2011; Liu et al., 2012; Gao et al., 2014; Chakritbudsabong et al., 2017). This is of concern because it shows the high heterogeneity of the cells being generated by the different induction and maintenance methods (Koh and Piedrahita, 2014). Although the 4TF-piPSC line VSMUi001-A and the two 5TF-piPSC lines required both bFGF and LIF for maintaining pluripotency, the surface of all piPSCs expressed SSEA-1. Moreover, VSMUi001-A could express a high level of LIN28 as a result of the activation of core pluripotency TFs. OCT4, SOX2, and NANOG could regulate the transcription of LIN28 in mammalian ESCs (Marson et al., 2008) and SOX2 has been found to be the most critical factor for regulating LIN28A expression during iPSC reprogramming (Buganim et al., 2012). SOX2 is closely related to LIN28A in pluripotency because it binds directly to LIN28A to form a nuclear protein–protein complex (Cox et al., 2010).

In human and mouse iPSCs, retroviral vectors are transcriptionally silent as the endogenous genes maintain the pluripotent during iPSC induction, known as a fully reprogrammed iPSC state. On the contrary, partially reprogrammed iPSCs express both the viral transgenes and endogenous pluripotency genes (Maherali et al., 2007; Okita et al., 2007; Wernig et al., 2007; Hotta and Ellis, 2008). Substantial obstacles remain in the establishment of piPSCs, including the lack of transgene silencing of plasmid DNA integrated into the genome and the inability of cells to proliferate in the absence of transgene expression. These challenges suggest that reprogramming of these piPSCs is not fully complete (Esteban et al., 2009; Cheng et al., 2012; Liu et al., 2012; Zhang W. et al., 2015). Similarly, all piPSC lines in our study do not fully undergo reprogramming, expressing viral transgenes and endogenous pluripotency genes from the retrovirus-mediated gene delivery approach. Up to now, only one study in the literature has described silenced retroviral transgene expression (Zhang S. et al., 2015). To try to overcome this issue, researchers have made efforts to establish transgene-free piPSCs using integration-free reprogramming approaches such as episomal vectors (Telugu et al., 2010; Du et al., 2015; Li et al., 2018; Yuan et al., 2019). However, from these latter four reports, three demonstrated genome integration of the plasmid DNA into the piPSC genome (Telugu et al., 2010; Du et al., 2015; Yuan et al., 2019), and one described persistent exogenous gene expression in most piPSC lines with partial reprogramming (Li et al., 2018). Regarding reprogramming techniques using Sendai-viral vectors, only one study showed integration-free reprogramming though this group still reported strong exogenous transgene (*hsOCT4*) expression (Congras et al., 2016). Our reprogramming approach using monocistronic vectors can cause random expression of TFs in cells and partial reprogramming of piPSCs, which may potentially lead to partial reprogramming of piPSCs (Esteban et al., 2009). This is a limitation that can be overcome by using polycistronic vectors in future studies. Recently, polycistronic vectors have recently enabled the simultaneous delivery and expression of numerous genes, as well as the efficient co-expression of TFs (Shaimardanova et al., 2019).

Numerous previous studies have demonstrated that human and mouse TFs are capable of reprogramming porcine somatic cells to form piPSCs (Ma et al., 2014; Fukuda et al., 2017; Setthawong et al., 2019; Yuan et al., 2019). Similarly, in our study, piPSCs were successfully generated using factors associated with human reprogramming. Additionally, a previous report observed no differences in the morphology, AP staining, or

expression of pluripotency markers between piPSC generated from mouse or human TFs (Esteban et al., 2009). Contrary to other studies, only piPSCs reprogrammed with human TFs were capable of completely reprogramming porcine cells to piPSCs (Zhang S. et al., 2015) and developing live chimeric offspring (West et al., 2010). At the moment, the researchers are using porcine TFs to generate piPSCs. The reprogramming of piPSCs with porcine TFs has the potential to generate both embryonic and extraembryonic cells (Gao et al., 2019; Xu et al., 2019). In terms of DNA methylation, the previous study indicated that while piPSCs had a higher proportion of methylation at the OCT4 promoter, blastocyst and PFFs had a low rate of methylation. It demonstrated that the OCT4 gene was substantially expressed in piPSCs when compared to blastocysts and PFFs (Fujishiro et al., 2013). In this study, the methylation patterns in porcine OCT4 promoter region were not established using bisulfite sequencing as published previously (Choi et al., 2016) and require further assessment.

For *in vitro* differentiation, VSMUi001-A and the two 5TF-piPSC lines had the capability to differentiate into the three embryonic germ layers and toward a specific cardiac lineage, during which the *SOX2* gene was continuously upregulated. SOX2 is expressed not only in pluripotent stem cells but also in neural stem cells, which are maintained during the expansion of neural precursors throughout the development of the central nervous system and into adulthood (Pevny and Nicolis, 2010; Mercurio et al., 2019). Hence, the expression of SOX2 in the EBs as well as the *in vitro* spontaneous cardiogenic differentiation suggested that our piPSCs could also differentiate toward the neural lineage. For *in vivo* differentiation, teratoma development was slightly faster after 5TF-piPSC injection than after 4TF-piPSC injection. According to another study, high LIN28 expression generates higher-grade teratomas, whereas LIN28 knockdown induces smaller tumors (West et al., 2009). The chimera formation assay is the gold standard for determining the pluripotency of stem cells *in vivo*. Gao et al. (2019) generated extended pluripotent stem cells (EPSCs) that differentiate into both embryonic and extra-embryonic tissue in the pig blastocyst. Until now, this was the only report describing the production of a live chimeric pig in which piPSCs were discovered in the ears and tails (West et al., 2010).

Porcine iPSCs are a promising cellular source for the three-dimensional reconstruction of human-like organoids mimicking organ/system homeostasis or diseases, especially those related to the cardiovascular system. Cardiomyocytes derived from piPSCs can fulfill the application of PSCs in cardiac regenerative medicine and especially provide a porcine model for the evaluation of the efficiency, safety, and side effects of iPSC transplants (Zhou et al., 2012, 2014). Gu et al. (2012) revealed that piPSC-derived endothelial cells could induce neovascularization and important paracrine factors for myocardial healing, making them an effective treatment for myocardial infarction. However, there are not many studies that have reported the differentiation of piPSCs into cardiomyocytes (Montserrat et al., 2011; Chakritbudsabong et al., 2017). In this study, the cardiac lineage markers (TNNT2 and TNNI1) were visible since day 7 of floating EB formation. The three piPSC lines could differentiate into cells with mature cardiac phenotypes that expressed cTnT and cardiac contractile protein and displayed a high percentage of spontaneous cardiac beating. Xiang et al. (2019) have shown that LIN28 plays a critical role in the tumor necrosis factor receptor-2 (TNFR2)-mediated differentiation of hiPSC-derived cardiac stem cells by inducing the expression of TNFR2, which is usually found in mature cardiomyocytes, vascular endothelial cells, and hematopoietic cells. Conversely, LIN28 inhibition significantly reduced cardiac stem cell differentiation and activation (Xiang et al., 2019). In summary, our study demonstrated an effective method for inducing the spontaneous differentiation of piPSCs into cardiomyocytes *via* EB formation. In ongoing research, we aim to develop a robust biotechnology culture platform to (1) increase the number of piPSC-derived cardiomyocytes for future scalability, (2) develop organ-on-dish cardiac models for studying cardiovascular diseases and screening novel compounds for drug discovery; and (3) study the efficiency of piPSC-derived cardiomyocytes for use as a swine model for studying human cardiovascular diseases. Besides, these piPSCs are an innovative tool that can be used for study of disease pathologies and drug discovery for veterinary science.

CONCLUSION

The addition of LIN28 to the 4TF-induced reprogramming of piPSCs promoted the long-term maintenance of piPSC self-renewal and pluripotency and enhanced both the *in vitro* and *in vivo* differentiation capabilities of the cells toward all three embryonic germ layers and the cardiac lineage. Additionally, the spontaneous beating of the differentiated cardiomyocytes was augmented under the 5TF induction approach. This study proves that the vital role of LIN28 in the induction of pluripotency applies not only to hiPSCs but to piPSCs as well, thereby resolving the current challenges faced over the long-term maintenance of piPSC self-renewal and pluripotency. Importantly, our findings allow for the efficient scale-up of piPSC-derived cardiomyocytes for application in research studies on cardiovascular diseases and treatments. Further, the application of piPSCs and their differentiated cells are also great valuable in veterinary research.

DATA AVAILABILITY STATEMENT

The original contributions presented in the study are included in the article/**Supplementary Material**, further inquiries can be directed to the corresponding author.

ETHICS STATEMENT

The animal study was reviewed and approved by the Institutional Animal Care and Use Committee at the Faculty of Veterinary Science, Mahidol University, Thailand (Approval ID: VSMU-2012-57).

AUTHOR CONTRIBUTIONS

WC, JF, and SR designed the project and wrote the manuscript. WC, SC, and SR carried out most experiments, including the establishment and characterization of piPSC lines. LS performed molecular analysis. WC and SP conducted G-banding karyotype analysis. WC and PS performed immunofluorescence staining. WC and DG performed flow cytometry analysis. TT constructed pMXs plasmids. AD, JF, and SR revised the manuscript. All authors read and approved the final version submitted.

FUNDING

This research project was supported by Mahidol University (Basic Research Fund: fiscal year 2021), the Program Management Unit for Human Resources and Institutional Development, Research and Innovation, Thailand (Grant Number: B05F630046), and Mahidol University's Academic Development Scholarship. JF was supported by the following: Special Task Force for Activating Research for Exocrine Gland Biology and Regeneration Research Group, from Ratchadaphiseksomphot Endowment Fund at Chulalongkorn University (Grant Number: STF 6202432001-1) and a Mid-career Research Grant from the National Research Council of Thailand (Grant Number: NRCT5-RSA63001-12).

ACKNOWLEDGMENTS

We want to thank the following researchers and institutes for contributions: Nipon Chattipakorn and Siriporn C. Chattipakorn and the staff of the Cardiac Electrophysiology Research and Training (CERT) Center, Chiang Mai University, for cardiomyocyte characterization, and Phakhin Jantahiran for laboratory assistance. Moreover, we also want to thank Supath Tantivitayamas, Onvara Ritudomphol, and staff of Histocenter Thailand Co., Ltd. for a Leica DMi8 inverted fluorescent microscope with Leica DFC7000 camera, Utarat imsaard and staff of Hollywood International Ltd. for a DS-Ri2 Camera and the LUCIA Cytogenetics System, and Salaya Central Instrument Facility, Mahidol University for the flow cytometry machine and Jess automated western blotting system.

SUPPLEMENTARY MATERIAL

The Supplementary Material for this article can be found online at: https://www.frontiersin.org/articles/10.3389/fcell.2021.709286/full#supplementary-material

REFERENCES

Bin, G., Jiarong, Z., Shihao, W., Xiuli, S., Cheng, X., Liangbiao, C., et al. (2012). Aire promotes the self-renewal of embryonic stem cells through LIN28. *Stem Cells Dev.* 21, 2878–2890. doi: 10.1089/scd.2012.0097

Buganim, Y., Faddah, D. A., Cheng, A. W., Itskovich, E., Markoulaki, S., Ganz, K., et al. (2012). Single-cell expression analyses during cellular reprogramming reveal an early stochastic and a late hierarchic phase. *Cell* 150, 1209–1222. doi: 10.1016/j.cell.2012.08.023

Chakritbudsabong, W., Sariya, L., Pamonsupornvichit, S., Pronarkngver, R., Chaiwattanarungruengpaisan, S., Ferreira, J. N., et al. (2017). Generation of a pig induced pluripotent stem cell (piPSC) line from embryonic fibroblasts by incorporating LIN28 to the four transcriptional factor-mediated reprogramming: VSMUi001-D. *Stem Cell Res.* 24, 21–24. doi: 10.1016/j.scr.2017.08.005

Cheng, D., Guo, Y., Li, Z., Liu, Y., Gao, X., Gao, Y., et al. (2012). Porcine induced pluripotent stem cells require lif and maintain their developmental potential in early stage of embryos. *PLoS One* 7:e51778. doi: 10.1371/journal.pone.0051778

Choi, K. H., Park, J. K., Son, D., Hwang, J. Y., Lee, D. K., Ka, H., et al. (2016). Reactivation of endogenous genes and epigenetic remodeling are barriers for generating transgene-free induced pluripotent stem cells in pig. *PLoS One* 11:e0158046. doi: 10.1371/journal.pone.0158046

Congras, A., Barasc, H., Canale-Tabet, K., Plisson-Petit, F., Delcros, C., Feraud, O., et al. (2016). Non-integration strategy decrease chromosome instability and improves endogenous pluripotency genes reactivation porcine induced pluripotent-like stem cells. *Sci. Rep.* 6:27059. doi: 10.1038/srep27059

Cox, J. L., Mallanna, S. K., Luo, X., and Rizzino, A. (2010). Sox2 uses multiple domains to associate with proteins present in Sox2-protein complexes. *PLoS One* 5:e15486. doi: 10.1371/journal.pone.0015486

Du, X., Feng, T., Yu, D., Wu, Y., Zou, H., Ma, S., et al. (2015). Barriers for deriving transgene-free Pig iPS cells with episomal vectors. *Stem Cells* 33, 3228–3238. doi: 10.1002/stem.2089

Esteban, M. A., Xu, J., Yang, J., Peng, M., Qin, D., Li, W., et al. (2009). Generation of induced pluripotent stem cell lines from tibetan miniature pig. *J. Biol. Chem.* 284, 17634–17640. doi: 10.1074/jbc.M109.008938

Ezashi, T., Telugu, B. P., Alexenko, A. P., Sachdev, S., Sinha, S., and Roberts, R. M. (2009). Derivation of induced pluripotent stem cells from pig somatic cells. *Proc. Natl. Acad. Sci. U. S. A.* 106, 10993–10998. doi: 10.1073/pnas.0905284106

Fujishiro, S. H., Nakano, K., Mizukami, Y., Azami, T., Arai, Y., Matsunari, H., et al. (2013). Generation of naive-like porcine-induced pluripotent stem cells capable of contributing to embryonic and fetal development. *Stem Cells Dev.* 22, 473–482. doi: 10.1089/scd.2012.0173

Fukuda, T., Tani, T., Haraguchi, S., Donai, K., Nakajima, N., Uenishi, H., et al. (2017). Expression of six proteins causes reprogramming of porcine fibroblasts into induced pluripotent stem cells with both active X chromosomes. *J. Cell. Biochem.* 118, 537–553. doi: 10.1002/jcb.25727

Gao, X., Nowak-Imialek, M., Chen, X., Chen, D., Herrmann, D., Ruan, D., et al. (2019). Establishment of porcine and human expanded potential stem cells. *Nat. Cell Biol.* 21, 687–699. doi: 10.1038/s41556-019-0333-2

Gao, Y., Guo, Y., Duan, A., Cheng, D., Zhang, S., and Wang, H. (2014). Optimization of culture conditions for maintaining porcine induced pluripotent stem cells. *DNA Cell Biol.* 33, 1–11. doi: 10.1089/dna.2013.2095

Groenen, M. A., Archibald, A. L., Uenishi, H., Tuggle, C. K., Takeuchi, Y., Rothschild, M. F., et al. (2012). Analyses of pig genomes provide insight into porcine demography and evolution. *Nature* 491, 393–398. doi: 10.1038/nature11622

Gu, M., Nguyen, P. K., Lee, A. S., Hu, D. X., Plews, J. R., Han, L., et al. (2012). Microfluidic single-cell analysis shows that porcine induced pluripotent stem cell-derived endothelial cells improve myocardial function by paracrine activation. *Circ. Res.* 111, 882–893. doi: 10.1161/CIRCRESAHA.112.269001

Hall, V. (2008). Porcine embryonic stem cells: a possible source for cell replacement therapy. *Stem Cell Rev.* 4, 275–282. doi: 10.1007/s12015-008-9040-2

Hanna, J., Saha, K., Pando, B., Zon, J., Lengner, C. J., Creyghton, M. P., et al. (2009). Direct cell reprogramming is a stochastic process amenable to acceleration. *Nature* 462, 595–601. doi: 10.1038/nature08592

Harding, J., Robert, R. M., and Mirochnitchenko, O. (2013). Large animal models for stem cell therapy. *Stem Cell Res. Ther.* 4:23. doi: 10.1186/scrt171

Hotta, A., and Ellis, J. (2008). Retroviral vector silencing during iPS cell induction: an epigenetic beacon that signals distinct pluripotent states. *J. Cell. Biochem.* 105, 940–948. doi: 10.1002/jcb.21912

Koh, S., and Piedrahita, J. A. (2014). From "ES-like" cells to induced pluripotent stem cells: a historical perspective in domestic animals. *Theriogenology* 81, 103–111. doi: 10.1016/j.theriogenology.2013.09.009

Kwon, D. J., Jeon, H., Oh, K. B., Ock, S. A., Im, G. S., Lee, S. S., et al. (2013). Generation of leukemia inhibitory factor-dependent induced pluripotent stem cells from the Massachusetts General Hospital miniature pig. *Biomed. Res. Int.* 2013:140639. doi: 10.1155/2013/140639

Li, D., Secher, J., Hyttel, P., Ivask, M., Kolko, M., Hall, V. J., et al. (2018). Generation of transgene-free porcine intermediate type induced pluripotent stem cells. *Cell Cycle* 17, 2547–2563. doi: 10.1080/15384101.2018.1548790

Li, X., Zhang, F., Song, G., Gu, W., Chen, M., Yang, B., et al. (2013). Intramyocardial injection of pig pluripotent stem cells improves left ventricular function and perfusion: a study in a porcine model of acute myocardial infarction. *PLoS One* 8:e66688. doi: 10.1371/journal.pone.0066688

Liu, K., Ji, G., Mao, J., Liu, M., Wang, L., Chen, C., et al. (2012). Generation of porcine-induced pluripotent stem cells by using OCT4 and KLF4 porcine factors. *Cell Reprogram.* 14, 505–513. doi: 10.1089/cell.2012.0047

Ma, K., Song, G., An, X., Fan, A., Tan, W., Tang, B., et al. (2014). miRNAs promote generation of porcine-induced pluripotent stem cells. *Mol. Cell. Biochem.* 389, 209–218. doi: 10.1007/s11010-013-1942-x

Maherali, N., Sridharan, R., Xie, W., Utikal, J., Eminli, S., Arnold, K., et al. (2007). Directly reprogrammed fibroblasts show global epigenetic remodeling and widespread tissue contribution. *Cell Stem Cell* 1, 55–70. doi: 10.1016/j.stem.2007.05.014

Marson, A., Levine, S. S., Cole, M. F., Frampton, G. M., Brambrink, T., Johnstone, S., et al. (2008). Connecting microRNA genes to the core transcriptional regulatory circuitry of embryonic stem cells. *Cell* 134, 521–533. doi: 10.1016/j.cell.2008.07.020

Melton, C., Judson, R. L., and Blelloch, R. (2010). Opposing microRNA families regulate self-renewal in mouse embryonic stem cells. *Nature* 463, 621–626. doi: 10.1038/nature08725

Mens, M. M. J., and Ghanbari, M. (2018). Cell cycle regulation of stem cells by microRNAs. *Stem Cell Rev. Rep.* 14, 309–322. doi: 10.1007/s12015-018-9808-y

Mercurio, S., Serra, L., and Nicolis, S. K. (2019). More than just stem cells: functional roles of the transcription factor SOX2 in differentiated glia and neurons. *Int. J. Mol. Sci.* 20:4540. doi: 10.3390/ijms20184540

Montserrat, N., Bahima, E. G., Batlle, L., Häfner, S., Rodrigues, A. M., González, F., et al. (2011). Generation of pig iPS cells: a model for cell therapy. *J. Cardiovasc. Transl. Res.* 4, 121–130. doi: 10.1007/s12265-010-9233-3

Moradi, S., Mahdizadeh, H., Saric, T., Kim, J., Harati, J., Shahsavarani, H., et al. (2019). Research and therapy with induced pluripotent stem cells (iPSCs): social, legal and ethical considerations. *Stem Cell Res. Ther* 10, 341. doi: 10.1186/s13287-019-1455-y

Nguyen, L. H., and Zhu, H. (2015). Lin28 and let-7 in cell metabolism and cancer. *Transl. Pediatr.* 4, 4–11. doi: 10.3978/j.issn.2224-4336.2015.01.05

Okita, K., Ichisaka, T., and Yamanaka, S. (2007). Generation of germline-competent induced pluripotent stem cells. *Nature* 448, 313–317. doi: 10.1038/nature05934

Pan, P., Chen, T., Zhang, Y., Qi, Z., Qin, J., Cui, G., et al. (2018). Lin28A inhibits lysosome-associated membrane glycoprotein 1 protein expression in embryonic stem and bladder cancer cells. *Mol. Med. Rep.* 18, 399–406. doi: 10.3892/mmr.2018.8965

Parisi, S., Passaro, F., Russo, L., Musto, A., Navarra, A., Petrosino, G., et al. (2017). Lin28 is induced in primed embryonic stem cells and regulates let-7-independent events. *FASEB J.* 31, 1046–1058. doi: 10.1096/fj.201600848R

Peng, S., Chen, L. L., Lei, X. X., Yang, L., Lin, H., Carmichael, G. G., et al. (2011). Genome-wide studies reveal that lin28 enhances the translation of genes important for growth and survival of human embryonic stem cells. *Stem Cells* 29, 496–504. doi: 10.1002/stem.591

Pevny, L. H., and Nicolis, S. V. (2010). Sox2 roles in neural stem cells. *Int. J. Biochem. Cell Biol.* 42, 421–424. doi: 10.1016/j.biocel.2009.08.018

Phakdeedindan, P., Setthawong, P., Tiptanavattana, N., Rungarunlert, S., Ingrungruanglert, P., Israsena, N., et al. (2019). Rabbit induced pluripotent stem cells retain capability of in vitro cardiac differentiation. *Exp. Anim.* 68, 35–47. doi: 10.1538/expanim.18-0074

Ruan, W., Han, J., Li, P., Cao, S., An, Y., Lim, B., et al. (2011). A novel strategy to derive iPS cells from porcine fibroblasts. *Sci. China Life Sci.* 54, 553–559. doi: 10.1007/s11427-011-4179-5

Rungarunlert, S., Klincumhom, N., Tharasanit, T., Techakumphu, M., Pirity, M. K., and Dinnyes, A. (2013). Slow turning lateral vessel bioreactor improves embryoid body formation and cardiogenic differentiation of mouse embryonic stem cells. *Cell Reprogram.* 15, 443–458. doi: 10.1089/cell.2012.0082

Setthawong, P., Phakdeedindan, P., Tiptanavattana, N., Rungarunlert, S., Techakumphu, T., and Tharasanit, T. (2019). Generation of porcine induced-pluripotent stem cells from sertoli cells. *Theriogenology* 127, 32–40. doi: 10.1016/j.theriogenology.2018.12.033

Shaimardanova, A. A., Kitaeva, K. V., Abdrakhmanova, I. I., Chernov, V. M., Rutland, C. S., Rizvanov, A. A., et al. (2019). Production and application of multicistronic constructs for various human disease therapies. *Pharmaceutics* 11:580. doi: 10.3390/pharmaceutics11110580

Shyh-Chang, N., and Daley, G. Q. (2013). Lin28: primal regulator of growth and metabolism in stem cells. *Cell Stem Cell* 12, 395–406. doi: 10.1016/j.stem.2013.03.005

Singh, V. K., Kaisan, M., Kumar, N., Saini, A., and Chandra, R. (2015). Induced Pluripotent stem cells: applications in regenerative medicine, disease modeling, and drug discovery. *Front. Cell Dev. Biol.* 3:2. doi: 10.3389/fcell.2015.00002

Su, Y., Zhu, J., Salman, S., and Tang, Y. (2020). Induced pluripotent stem cells from farm animals. *J. Anim. Sci.* 98:skaa343. doi: 10.1093/jas/skaa343

Takahashi, K., Tanabe, K., Ohnuki, M., Narita, M., Ichisaka, T., Tomoda, K., et al. (2007). Induction of pluripotent stem cells from adult human fibroblasts by defined factors. *Cell* 131, 861–872. doi: 10.1016/j.cell.2007.11.019

Tanabe, K., Nakamura, M., Narita, M., Takahashi, K., and Yamanaka, Y. (2013). Maturation, not initiation, is the major roadblock during reprogramming toward pluripotency from human fibroblast. *Proc. Natl. Acad. Sci. U. S. A.* 110, 12172–12179. doi: 10.1073/pnas.1310291110

Telugu, B. P., Ezashi, T., and Roberts, R. M. (2010). Porcine induced pluripotent stem cells analogous to naïve and primed embryonic stem cells of the mouse. *Int. J. Dev. Biol.* 54, 1703–1711. doi: 10.1387/ijdb.103200bt

Tsialikas, J., and Romer-Seibert, J. (2015). LIN28: roles and regulation in development and beyond. *Development* 142, 2397–2404. doi: 10.1242/dev.117580

Vogt, E. J., Meglicki, M., Hartung, K. I., Borsuk, E., and Behr, R. (2012). Importance of the pluripotency factor LIN28 in the mammalian nucleolus during early embryonic development. *Development* 139, 4514–4523. doi: 10.1242/dev.083279

Wernig, M., Meissner, A., Foreman, R., Brambrink, T., Ku, M., Hochedlinger, K., et al. (2007). In vitro reprogramming of fibroblasts into a pluripotent es-cell-like state. *Nature* 448, 318–324. doi: 10.1038/nature05944

West, F. D., Terlouw, S. L., Kwon, D. J., Mumaw, J. L., Dhara, S. K., Hasneen, K., et al. (2010). Porcine induced pluripotent stem cells produce chimeric offspring. *Stem Cells Dev.* 19, 1211–1220. doi: 10.1089/scd.2009.0458

West, J. A., Viswanathan, S. R., Yabuuchi, A., Cunniff, K., Takeuchi, A., Park, I., et al. (2009). A role for Lin28 in primordial germ-cell development and germ-cell malignancy. *Nature* 460, 909–913. doi: 10.1038/nature08210

Wu, Z., Chen, J., Ren, J., Bao, L., Liao, J., Cui, C., et al. (2009). Generation of pig induced pluripotent stem cells with a drug-inducible system. *J. Mol. Cell Biol.* 1, 46–54. doi: 10.1093/jmcb/mjp003

Xiang, Q., Yang, B., Li, L., Qiu, B., Qiu, C., Gao, X. B., et al. (2019). Critical role of Lin28-TNFR2 signaling in cardiac stem cell activation and differentiation. *J. Cell. Mol. Med.* 23, 2943–2953. doi: 10.1111/jcmm.14202

Xu, B., Zhang, K., and Huang, Y. (2009). Lin28 modulates cell growth and associates with a subset of cell cycle regulator mRNAs in mouse embryonic stem cells. *RNA* 15, 357–361. doi: 10.1261/rna.1368009

Xu, J., Yu, L., Guo, J., Xiang, J., Zheng, Z., Gao, D., et al. (2019). Generation of pig induced pluripotent stem cells using an extended pluripotent stem cell culture system. *Stem Cell Res. Ther.* 10:193. doi: 10.1186/s13287-019-1303-0

Yang, D. H., and Moss, E. G. (2003). Temporally regulated expression of Lin-28 in diverse tissues of the developing mouse. *Gene Expr. Patterns* 3, 719–726. doi: 10.1016/s1567-133x(03)00140-6

Yu, J., Vodyanik, M. A., Smuga-Otto, K., Antosiewicz-Bourget, J., Frane, J. L., Tian, S., et al. (2007). Induced pluripotent stem cell lines derived from human somatic cells. *Science* 318, 1917–1920. doi: 10.1126/science.1151526

Yuan, Y., Park, J., Tian, Y., Choi, J., Pasquariello, R., Alexenko, A. P., et al. (2019). A six-inhibitor culture medium for improving naïve-type pluripotency of porcine pluripotent stem cells. *Cell Death Discov.* 5:104. doi: 10.1038/s41420-019-0184-4

Zhang, J., Ratanasirintrawoot, S., Chandrasekaran, S., Wu, Z., Ficarro, S. B., Yu, C., et al. (2016). LIN28 regulates stem cell metabolism and conversion to primed pluripotency. *Cell Stem Cell* 19, 66–80. doi: 10.1016/j.stem.2016.05.009

Zhang, S., Guo, Y., Cui, Y., Liu, Y., Yu, T., and Wang, H. (2015). Generation of intermediate porcine iPS cells under culture condition favorable for mesenchymal-to-epithelial transition. *Stem Cell Rev. Rep.* 11, 24–38. doi: 10.1007/s12015-014-9552-x

Zhang, W., Pei, Y., Zhong, L., Wen, B., Cao, S., and Han, J. (2015). Pluripotent and metabolic features of two types of porcine iPSCs derived from defined mouse and human es cell culture conditions. *PLoS One* 10:e0124562. doi: 10.1371/journal.pone.0124562

Zhou, Y., Wang, S., Yu, Z., Hoyt, R. F. Jr., Hunt, T., Kindzelski, B., et al. (2014). Induced pluripotent stem cell transplantation in the treatment of porcine chronic myocardial ischemia. *Ann. Thorac. Surg.* 98, 2130–2137. doi: 10.1016/j.athoracsur.2014.07.008

Zhou, Y., Wang, S., Yu, Z., Hoyt, R. F., Horvath, K. A., Singh, A. K., et al. (2012). Allogenic transplantation of induced pluripotent stem cells in a porcine model of chronic myocardial ischemia failed to stimulate myocyte differentiation. *Transplantation* 94:1014.

Conflict of Interest: AD is employed by BioTalentum Ltd., Hungary.

The remaining authors declare that the research was conducted in the absence of any commercial or financial relationships that could be construed as a potential conflict of interest.

frontiers in Cell and Developmental Biology

REVIEW
published: 28 July 2021
doi: 10.3389/fcell.2021.667765

Eccrine Sweat Gland and Its Regeneration: Current Status and Future Directions

*Yao Lin[1], Liyun Chen[1], Mingjun Zhang[1], Sitian Xie[1], Lijie Du[2], Xiang Zhang[2] and Haihong Li[1,2]**

[1] Department of Plastic Surgery and Burn Center, Second Affiliated Hospital of Shantou University Medical College, Shantou, China, [2] Department of Wound Repair and Dermatologic Surgery, Taihe Hospital, Hubei University of Medicine, Shiyan, China

Eccrine sweat glands (ESGs) play an important role in temperature regulation by secreting sweat. Insufficiency or dysfunction of ESGs in a hot environment or during exercise can lead to hyperthermia, heat exhaustion, heatstroke, and even death, but the ability of ESGs to repair and regenerate themselves is very weak and limited. Repairing the damaged ESGs and regenerating the lost or dysfunctional ESGs poses a challenge for dermatologists and bum surgeons. To promote and accelerate research on the repair and regeneration of ESGs, we summarized the development, structure and function of ESGs, and current strategies to repair and regenerate ESGs based on stem cells, scaffolds, and possible signaling pathways involved.

Keywords: eccrine sweat gland, regeneration, stem cells, scaffolds, signaling pathways, methods

OPEN ACCESS

Edited by:
Philip Iannaccone, Northwestern University, United States

Reviewed by:
Vasiliy Galat, Ann & Robert H. Lurie Children's Hospital of Chicago, United States
Yongan Xu, Zhejiang University, China

***Correspondence:**
Haihong Li
lihaihong1051@126.com

Specialty section:
This article was submitted to Stem Cell Research, a section of the journal Frontiers in Cell and Developmental Biology

Received: *14 February 2021*
Accepted: *09 July 2021*
Published: *28 July 2021*

Citation:
Lin Y, Chen L, Zhang M, Xie S, Du L, Zhang X and Li H (2021) Eccrine Sweat Gland and Its Regeneration: Current Status and Future Directions. Front. Cell Dev. Biol. 9:667765. doi: 10.3389/fcell.2021.667765

INTRODUCTION

As warm-blooded animals, humans regulate body temperature through various regulatory mechanisms. Among them, ESGs play an important role in cooling down body temperature by secreting primarily water that contains electrolytes (Saga, 2002). Human skin has two major types of sweat glands: eccrine and apocrine. The apocrine sweat glands are appendage of the hair follicle and release a cloudy, viscous fluid through the follicle orifice, which exclusively present in highly localized hairy axillary regions, and they are non-thermoregulatory (Sato et al., 1989). Some patients lack ESGs due to severe burns or genetic factors, while some patients suffered from congenital or acquired factors resulting in ESG dysfunction. If the human body has no way to sweat, it means that any hot weather or acute activity can cause them to get heatstroke or even die. Therefore, we focus on the wound repair and regeneration of ESGs in this review.

First, it is necessary to understand the normal structure and functions of ESGs. On the surface of the body, ESGs are small but very numerous (Sato et al., 1989), which directly open to the skin surface. During exercise, fever or hot environments, humans are able to dissipate heat through sweat to maintain body temperature within the optimal range (Shibasaki et al., 2006). In contrast, for most domestic mammals, most of their body surface lack ESGs. Mouse is the common model for ESG study because of the similarity of human ESG structure and function, which has ESGs solely present in the pads of their paws (Lu et al., 2012).

The ESGs are small tubular structures situated in epidermis and dermis. They comprise a relatively straight duct led to the skin surface and a secretory coil deep in the dermis. The duct of the ESG is a straight channel, and the secretory portion of the ESG is a distinctive, coiled tubular structure (**Figure 1**).

There are three types of cells in the secretory coil: clear cells, dark cells, and myoepithelial cells. Myoepithelial cells provide power support for sweat secretion and support the glands mechanically (Sato, 1977; Sato et al., 1989). The secretory cells can be classified into clear cells and dark cells based on their affinities to basic dyes and granule contents (Montagna et al., 1953; Munger, 1961). The clear cells are without secretory granules but have many mitochondria and membrane villi, which contribute to generate water, electrolytes, and inorganic substances in the sweat. By contrast, the dark cells contain many Schiff-reactive granules, which are mainly in charge of generating macromolecules such as glycoproteins (LobitzJr., and Dobson, 1961; Munger, 1961; Yanagawa et al., 1986). Furthermore, sweat also contains various proteolytic enzymes (Horie et al., 1986), IgA (Okada et al., 1988), active interleukin-1 (Sato and Sato, 1994) and several antimicrobial peptides (Schittek et al., 2001; Niyonsaba et al., 2009), which likely to be conducive to the barrier function of the skin.

The development of electron microscopy (EM) and the ultrastructure that it revealed accelerated the studies of ESGs. Ultrastructural observations on the development of ESG in human embryos have been reported since the 1960s (Hashimoto et al., 1965). From the perspective of embryonic development, at 3 about months, the epidermal ridges on the palms begin to form epithelial cell cords, which are the starting point for the development of ESGs, and at 5 about months, ESGs in other parts of the body begin to develop (Sato et al., 1989). By the eighth month of the fetus, ESGs are morphologically mature (Sato et al., 1989). In mice, ESG germs were spotted at E17.5 and the coiling of secretory portions was at P1, and ESG formation was in essence completed by P5 (Kunisada et al., 2009; **Figure 1**). In rats, ESG germs were first detected at E19.5, straight ducts first appeared at E21.5, and secretory coils began to form at P1 (Li et al., 2017). During the ESG morphogenesis, the progenitor properties change from multipotency to unipotency, and ultimately, they form four unipotent adult stem cell populations: basal duct, suprabasal duct, myoepithelial, and glandular luminal stem cells (Lu et al., 2012). Proliferation is almost undetectable in the mature glands and remain active only in the basal cells of the sweat duct and the epidermis of the paw skin (Lu et al., 2012).

FEASIBILITY OF REGENERATION OF ESG

Engineered skin is certainly developing rapidly today, while it still lacks skin appendages. As skin appendages, ESGs play important roles in the temperature regulation and maintenance of homeostasis (Huang et al., 2010). So far, patients with irreversible loss of functional ESGs still cannot receive effective treatment. Current strategies for repair and regeneration of ESGs are mainly based on stem cells, scaffolds, bioactive cytokine and growth factors, and involved signaling pathways (**Figures 2**, **3**).

ESG Regeneration by Stem Cells

Adult tissue-specific stem cells are distributed in various tissues and organs. In the skin, stem cells have long been found in the epidermis and hair follicles, but it was not known until recently that ESGs are also rich in stem cells (Lu et al., 2012). As judged from immunohistochemical staining of nucleotide analog incorporation and cell proliferation markers, proliferation occurs rarely in the secretory coil cells, but frequently in the basal cells of sweat ducts during homeostasis of adult ESGs (Morimoto and Saga, 1995; Li et al., 2008, 2016b; Chen et al., 2014). With the use of lineage tracing and pulse-chase studies, ESG stem cells have been identified from both developing and mature mouse ESGs by Lu et al. (2012). The multipotent $K14^+$ bud progenitors in the basal layer of embryonic ectoderm is the starting point of ESG formation, which then develops into transient multipotent $K14^+$ basal progenitors and $K18^+$/lowK14 suprabasal progenitors (Lu et al., 2012). Finally, in mature ESGs, the progenitor properties change from multipotency to unipotency in the form of four unipotent adult stem cell populations: basal duct, suprabasal duct, myoepithelial, and glandular luminal stem cells (Lu et al., 2012).

Basal cells in paw epidermis and sweat ducts proliferate can renew and replenish cells of scuffed suprabasal epidermis and intraepidermal duct during homeostasis (Lu et al., 2012; Chen et al., 2014; Li et al., 2016b). When epidermis is severely damaged or excised, neighboring basal cells of epidermis and sweat duct, not including secretory coil cells, rapidly proliferate to repair the injured area (Lu et al., 2012; Chen et al., 2014; Li et al., 2016b). The basal and suprabasal duct stem cells also contribute to repair the skin epidermis and epidermal sweat ducts wound (Lu et al., 2012; Chen et al., 2014; Li et al., 2016b).

There have been many studies that have shown the quiescent nature of both luminal and myoepithelial cells of the secretory coil in adult ESGs (Li et al., 2008, 2016b; Lu et al., 2012). Only when localized injury occurs, do myoepithelial and glandular luminal progenitors replenish their own descendants, and the remarkable thing is that they act as unipotent progenitors during repair (Lu et al., 2012). Luminal cells can proliferate to repair neighboring injured luminal cells, and myoepithelial cells can proliferate to repair neighboring injured myoepithelial cells (Lu et al., 2012). Many studies have shown that the myoepithelial cells of adult ESGs are quiescent (Li et al., 2008, 2016b; Lu et al., 2012).

There are also studies showing that ESG secretory cells not only participate in their own repair, but also participate in the repair of the epidermis, and their regeneration and repair ability is stronger than that of sweat duct luminal cells (Rittie et al., 2013; Pontiggia et al., 2014; Diao et al., 2019). As for myoepithelial cells, it is not clear whether they are involved in epidermal repair under physiological conditions. However, studies have shown that engrafting purified myoepithelial cells to back skin can generate epidermis (Lu et al., 2012). Investigators also isolated cells with typical characteristics of mesenchymal stem cells, from myoepithelial cells of secretory coils in adult human ESGs, which may contribute to the study of wound repair and ESG regeneration (Kurata et al., 2014; Ma Y. et al., 2018).

As is mentioned above, the stem cell populations in mature ESGs are unipotent. However, some unipotent stem cells tend to regain multipotency when leaving the original environment. Based on cell-surface markers, Lu et al. (2012) exploited fluorescent activating cell sorting (FACS), purified different cell populations from mouse secretory coils and sweat ducts, and

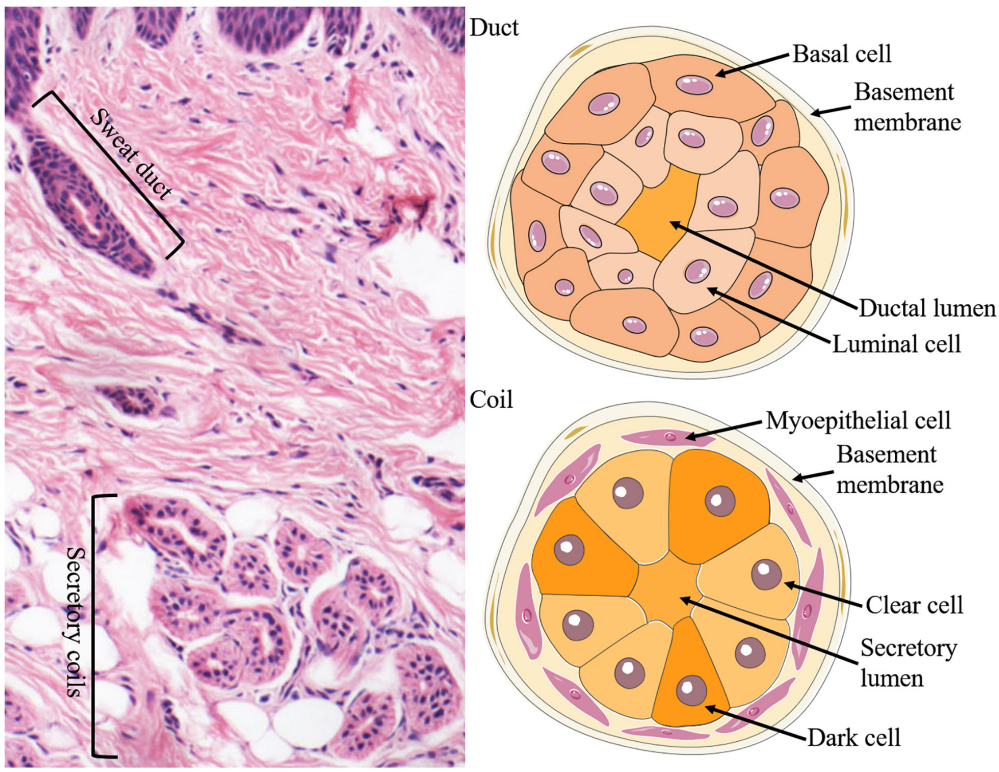

FIGURE 1 | Structure and cellular constituents of ESGs. The ESG is comprised of a relatively straight duct led to the skin surface and a secretory coil deep in the dermis (left panel). The duct is formed of two layers of cells: the basal (outer) and luminal (inner) cells, where ions are partially reabsorbed (right upper panel). There are three types of cells in the secretory coil: clear cells, dark cells, and myoepithelial cells (right lower panel).

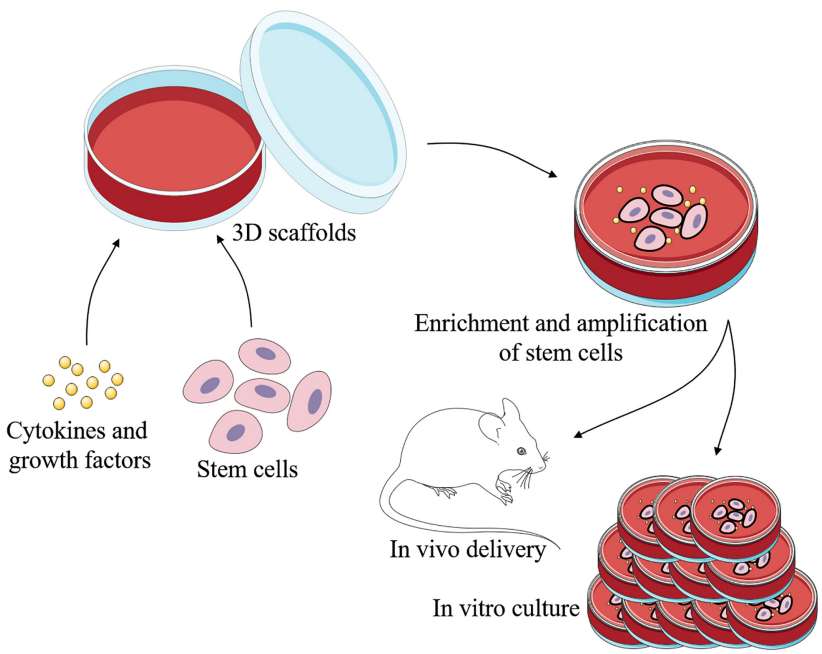

FIGURE 2 | Schematic representation of regeneration of ESGs. With the 3D scaffolds, specific cells can be induced by specific cytokines and growth factors to differeniate into sweat gland-like cells. There are three main types of cells that may be used to repair and regenerate ESGs: ESG-derived stem cells, non-sweat gland-derived stem cells, and induced pluripotent stem cells. This process can take place *in vivo* or *in vitro*.

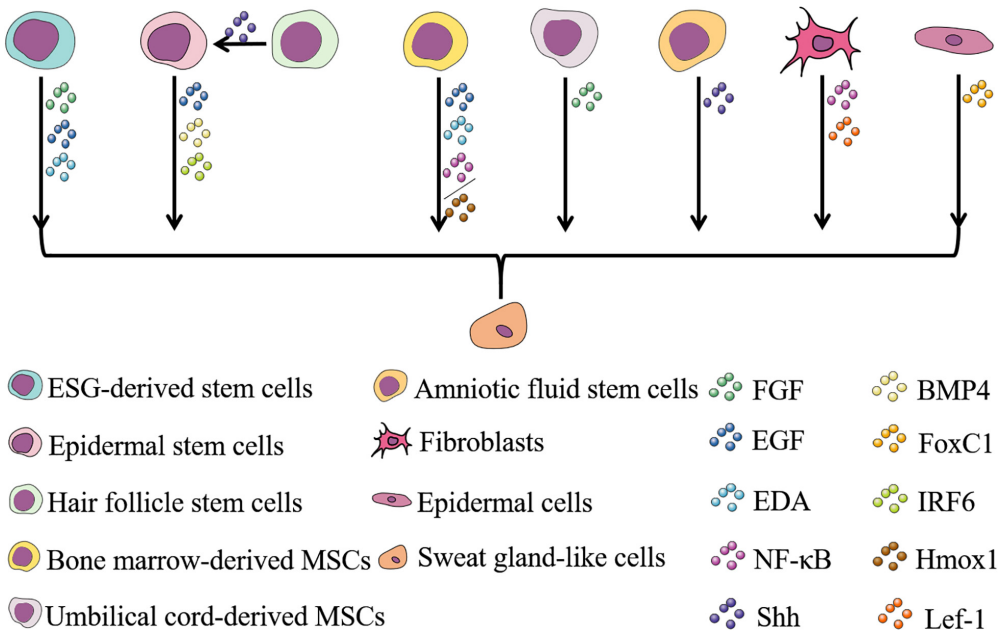

FIGURE 3 | Cells and factors involved in ESG regeneration and their relationships. Stem cells are often used in the study of wound repair and regeneration of various tissues due to their ability to self-renew and differentiate into multiple lineages. To date, eight types of cells have been reported to have the potential to regenerate ESGs (Shikiji et al., 2003; Li et al., 2006, 2015b; Nolte et al., 2008; Sheng et al., 2009; Vierbuchen et al., 2010; Lu et al., 2012; Xu et al., 2012, 2016; Wang et al., 2013, 2019; Hassan et al., 2014; Tao et al., 2014; Liang et al., 2016; Kolakshyapati et al., 2017; Sun et al., 2018; Yao et al., 2018, 2019, 2020; Chen et al., 2019; Hu et al., 2019). Cytokines and growth factors play a role in inducing cells directed to differentiate into sweat gland-like cells during the process of ESG regeneration, and the discovery of these factors involves research on the determination and development of ESGs (Shikiji et al., 2003; Cai et al., 2011; Zhao et al., 2015; Liang et al., 2016; Xu et al., 2016; Kolakshyapati et al., 2017; Sun et al., 2018; Yao et al., 2018, 2019, 2020; Chen et al., 2019; Hu et al., 2019; Wang et al., 2019). Selecting appropriate cells and appropriate factors to induce the differentiation of sweat gland-like cells makes the regeneration of ESGs possible.

studied their individual regenerative capacities in engraftment experiments. Grafting the myoepithelial or basal duct stem cells, but not luminal or suprabasal duct stem cells, into cleared mammary fat pads or shoulder fat pads can regenerate *de novo* ESGs (Lu et al., 2012). Notably, there have been many studies that have shown the quiescent nature of myoepithelial cells in adult ESGs (Li et al., 2008, 2016b; Lu et al., 2012; Leung et al., 2013). Based on these findings, it is interesting that adult progenitors show single-function nature in their native environmemt. Therefore, further experiments will be needed to analyze the molecular causes.

In a previous *in vitro* study, Li et al. (2013) demonstrated that human ESG cells cultured in Matrigel not only build three-dimensional (3D) tubular-like structures with lumens, but also express α-SMA, epithelial membrane antigen (EMA), CK7, and CK19, and then, they did *in vivo* experiment on this basis, Matrigel-embedded ESG cells were subcutaneously implanted into nude mice (Li et al., 2015a). Compared with ESGs formed *in vitro*, ESGs formed in nude mice were more similar to natural ones (Li et al., 2015a). Reconstituted 3D ESGs recapitulated the polarization at the appropriate time points during spheroid differentiation, and secreted fluid similar to native human ESGs (Li et al., 2016a). In addition to the above, the authors also demonstrated that the 3D-reconstituted ESGs were nourished by blood vessels and mediated by both cholinergic and adrenergic innervation (Zhang et al., 2018). Thus, the 3D-reconstituted ESGs have the completeness of structural components, the prerequisite for full functionality, from which the authors inferred that the 3D-reconstituted ESGs may function as the native ones do. However, the secretory function of the 3D-reconstituted ESGs remains to be fully established. All in all, it is an intriguing development in the process of questing treatments burn patients.

The difficulty of using isolated ESG cells to reconstruct sweat gland-like (SGL) structures is that ESG cells are dispersive in the dermis and difficult to gather. Further, with extensive severe burns, the ESGs of patients are destroyed and autologous mature ESG cells and ESG stem cells are insufficient. The optimized cell culture of Diao et al. (2019) can provid the appropriate cells in sufficient quantity for mouse ESGs and skin regeneration, and offers a new strategy for regenerating SGL structures.

In skin tissues, epidermal stem cells (EpiSCs), as the specific stem cell type, can regenerate skin tissue, repair wound and re-modeling (Boehnke et al., 2012). During embryonic development, both ESGs and hair follicles (HFs) originate from EpiSCs, so EpiSCs are the common progenitor cells of both ESGs and HFs. Research has shown that young human keratinocytes, including EpiSCs, can invade collagen gels and differentiate into/toward ESG duct-like structures *in vitro* with fibroblasts, epidermal growth factor (EGF) and fetal bovine serum (FBS) (Shikiji et al., 2003). EGF, interferon regulatory factor 6 (IRF6) and bone morphogenetic protein 4 (BMP4) have also been shown to play a role in inducing EpiSCs to transform into ESG cells

(Shikiji et al., 2003; Yao et al., 2018; Hu et al., 2019). Therefore, EpiSCs can be induced directly and differentiate into ESG cells, and is one of the most common means of ESG regeneration. However, in the adult body, the number of EpiSCs is limited, for merely 1–10 percent of basal stem cells (Cotsarelis et al., 1999). As a result, producing a large number of SGL cells (SGLCs) by epidermal cell reprogramming may be another method for ESG regeneration. Yao et al. (2019) showed that overexpressing the transcription factor FoxC1 can directly reprogram epidermal cells to induce functional SGLCs. Since the epidermis of patients with extensive severe traumatic burns is damaged and autologous mature epidermal cells and EpiSCs is scarce, this method of regeneration is more suitable for anhidrotic/hypohidrotic ectodermal dysplasia patients (Yao et al., 2019).

Bone marrow-derived MSCs (BM-MSCs) are characterized by lower immunogenicity and rarely destroyed in the event of skin damage, so they have great potential for development (Zhang et al., 2015). Although the mechanism of using BM-MSCs to regenerate ESGs remains unclear, multiple cytokines appear to play an important role in ESG regeneration and development. Li et al. (2006) directly co-culture BM-MSCs with heat-shocked ESG cells and found that it can differentiate BM-MSCs into SGLCs. Then, transplanting SGLCs into the wounds of nude mice showed a significantly promotion of damaged ESG repair and regeneration (Sheng et al., 2009). Li et al. (2015b) have also demonstrated that 3D co-culture of BM-MSCs and ESG cells in Matrigel can help the transdifferentiation of BM-MSCs into ESG cells, with the transdifferentiated BM-MSCs potentially able to function as ESG cells. There are other ways to directly induce BM-MSCs to differentiate into SGLCs, and involves various cytokines and scaffolds, which will be described in the following chapters. Even though there is a distinct advantage using BM-MSCs for ESG regeneration, the number of BM-MSCs is limited and it is difficult to maintain pluripotency after extensive passage (Zhang et al., 2015). Recently, investigators have reported that severely burned skin contains viable, undamaged cells that show characteristics of human MSCs, and can be used to promote wound healing without adverse side effects (Amini-Nik et al., 2018). These findings provide an ideal source of MSCs for treatment of severely burned patients.

3D Reconstitution Model of ESG *in vitro/vivo*

The extracellular matrix (ECM), often used to refer to all the substances surrounding cells in a multicellular organism except for circulating fluids, is a 3D structural scaffold made of non-cellular, fibrous, and non-fibrin proteins that exists in all tissues and is a major component of the cellular microenvironment (Theocharis et al., 2016). The ECM does more than provide physical support for organizational integrity and resilience: it is a dynamic structure that is constantly reshaped to control organizational homeostasis and organ development, as well as tissue repair and regeneration (Bonnans et al., 2014). A highly dynamic 3D ECM provides environmental signals that influence basic cell behaviors, such as cell proliferation, adhesion, migration and differentiation, impact cell mechanics, and regulate the fate of stem cells (Watt and Huck, 2013). Therefore, the ECM plays essential roles not only in embryonic development and homeostasis, but also in tissue engineering and regenerative medicine (Blankenship, 1990; Watt and Huck, 2013; Bonnans et al., 2014). 3D scaffolds are manufactured by removing cellular content from source tissues while retaining the original structural and functional molecular units of the ECM, and it has been widely applied to the field of tissue engineering and regenerative medicine (Costa et al., 2017).

So far, the studies on isolated sweat gland stem cells/progenitor cells cultured in traditional monolayers have always rapidly differentiated into keratinocytes and lost their specific phenotypic characteristics (Rittie et al., 2013; Pontiggia et al., 2014). Compared with the traditional 2D culture models, 3D culture models recapitulate the function and physiological architecture of the body (Kleinman and Martin, 2005; Kozowski et al., 2011). Under 2D culture conditions, cells undergo proliferation but have difficulty in inducing directional differentiation, but under 3D culture conditions, they could be induced directional differentiation (Petrakova et al., 2012; Li et al., 2015b). Therefore, culturing cells under 3D conditions is a useful model for studying cell proliferation and differentiation. To date, researchers have developed several kinds of 3D organoid culture matrices for ESG regeneration, aiming to achieve the enrichment and amplification of cells while maintaining the specific characteristics of ESG cells.

The Matrigel basement membrane matrix (abbreviated as Matrigel) is a dissolved basement membrane preparation that contains fetal collagens, laminin, entactin, heparan sulfate proteoglycans, and several matrix-bound growth factors, which help cell growth as organoids (Kleinman and Martin, 2005; Li et al., 2015a). Using 3D culture method to culture cells in a gel basement membrane matrix, many cells will differentiate into tissue-specific structures, and vascular endothelial cells are one of the earliest cell types showing morphological differentiation (Kleinman and Martin, 2005; Arnaoutova et al., 2009). The differentiation of endothelial cells in Matrigel mimics the process of angiogenesis *in vivo*, which indicates that Matrigel can be used to obtain a large amount of information about angiogenesis regulators, genes that play an important role in angiogenesis in endothelial cells, and the characterization/identification of endothelial progenitor cells (Auerbach et al., 2003). Besides this, Matrigel has been widely used to study tumor cell invasion, and an altered ECM has been shown to promote tumorigenesis (Bissell and Labarge, 2005). Salivary gland cell lines cultured on Matrigel are widely used to study cell differentiation, such as glandular-like morphogenesis, acinus formation and branching morphogenesis (Barka et al., 2005). Maria et al. (2011) obtained cells from parotid and submandibular glands, expanded *in vitro*, and then cultured on Matrigel. On Matrigel-coated substrates, cells formed 3D acinar-like units, adopting a large number of secreted granular acinar phenotypes, expressing α-amylase and the water channel protein, aquaporin-5. Experiments by Kozowski et al. (2011) show that the bovine mammary epithelial cell line BME-UV1 cultured on Matrigel could form 3D acinar structures with a hollow lumen in the center, which is similar to the mammary gland alveoli in a functionally active mammary gland. To study ESG progenitor/stem cells, Lu et al. (2012)

suspended four sorted ESG cells in Matrigel and injected them individually into cleared mammary or shoulder fat pads from female Nu/Nu mice. In rare cases, purified adult ductal basal cells produce glands and ducts, while purified myoepithelial cells continue to form ESGs, and luminal or suprabasal duct cells did not show this diverse behavior (Lu et al., 2012). Subsequently, Matrigel was applied to the regeneration of ESGs. Li et al. (2013, 2015a) inoculated ESG cells into the tissue structure formed by a Matrigel basement membrane matrix *in vitro* or in nude mice to simulate the growth microenvironment of natural ESGs, and successfully reconstructed SGL structures using the isolated ESG cells. These studies indicate that the interactions between Matrigel and ESG cells play important roles in the 3D reconstruction of SGL structures. On this basis, Diao et al. (2019) added some growth factors and small molecules, such as EGF, bFGF, and EDA, in order to increase the differentiation efficiency. Although there are some differences between the reconstructed SGL structures and the original ESGs, these studies demonstrated that Matrigel can induce ESG cells to reconstitute SGL structures. Maybe subsequent work could implant Matrigel-embedded ESG cells subcutaneously into burn victims to reconstitute ESGs. However, in practice, the implanted ESG cells do not reconstruct ESGs with complete structure and function as we had hoped. Therefore, in the following scientific research work, there are still many problems for us to explore and solve.

Three-dimensional bioprinting has become a promising technology for manufacturing complex tissue structures with tailor-made biological components and mechanical properties (Murphy and Atala, 2014). By using this revolutionary technology, bio-inks, including growth factors, cells, and hydrogels, can be precisely positioned to create 3D *in vitro* culture environments (Ma X. et al., 2018). Pati et al. (2014) decellularized adipose, cartilage and heart tissue to make bioink, and adopted a 3D bioprinting technique to construct a 3D structure *in vitro*, successfully inducing adipose-derived MSCs to express specific markers of cardiomyocytes and chondrocytes. By building 3D printing scaffolds that continuously release a variety of growth factors, Lee et al. (2014) successfully treated sheep with damaged menisci by inducing endogenous MSCs to differentiate into menisci *in vivo*. The findings strongly suggest that 3D bioprinting has great potential in simulating the microenvironment to induce stem cell differentiation and promote tissue regeneration. Through 3D bioprinting, Fu's research team successfully induced EpiSCs to differentiate into ESG cells using gelatin-alginate hydrogels and mouse ESG-ECM protein components (Huang et al., 2016; Liu et al., 2016; Li et al., 2018). They subsequently adopted 3D bioprinting to mimic the regenerative microenvironment to direct of MPCs or MSCs to specifically differentiate into ESGs, and ultimately guide the formation and function of glandular tissue (Wang et al., 2019; Yao et al., 2020). Alginate/gelatin hydrogel can serve as bio-ink due to its good cell compatibility, printability, and stable structure during long-term culture (Huang et al., 2009). Wang et al. (2019) used gelatin-alginate hydrogels to combine with ESG-ECM protein to form a characteristic bio-ink, which made it possible to induce the transformation of mammary progenitor cells to ESG cells (Yao et al., 2020). Although its mechanism still needs further exploration, it may be used as an effective tool to induce ideal cells or tissues *in vitro* through an engineered microenvironment in the future.

Gelatin is not only an irreversible form of denatured collagen, it has the ability to form a scaffold suitable for dermal regeneration without adding any other polymers, but also has the ability to control the release of growth factors for a long time (Shevchenko et al., 2014). Therefore, Huang et al. (2009, 2010) developed gelatin microspheres containing EGF as multifunctional vehicles on which ESG cells could be cultured, and delivered these ESG cell-microsphere complexes into an engineered skin for wound repair. Later, they delivered BM-MSCs by an EGF microsphere-based engineered skin model to repair ESGs and improve cutaneous wound healing (Huang et al., 2012). Analogously, Kolakshyapati et al. (2017) combined the collagen-chitosan porous scaffold with Lipofectamine 2000/pDNA-EGF complexes to yield a gene-activated scaffold (GAS) on which BM-MSCs are cultured. Such GAS/BM-MSCs could accelerate the wound healing and induce full-thickness skin regeneration with SGL structure *in situ* (Kolakshyapati et al., 2017). These engineered skin constructs are promising tools for ESG regeneration in skin repair and are a valuable engineering strategy for constructing engineered skin models containing appendages.

MECHANISM OF ESG DEVELOPMENT AND REGENERATION

Up to now, studies have revealed involvement of Wnt, EDA, Shh, BMP, and ERK signaling pathways in ESG determination and development (**Figure 4**). These findings lead to a series of explorations into the regeneration of ESG.

Wnt/β-Catenin Signaling Pathway

Wnt/β-catenin signaling pathway is a relatively conservative cell-cell communication system in evolution, which is very important for embryogenesis, stem cell renewal, cell proliferation and cell differentiation (Steinhart and Angers, 2018). When cytokines activate the Wnt signaling pathway, β-catenin accumulates and enters the nucleus, associates with DNA binding factors of the TCF/LEF family, and activates the expression of target genes (Xu et al., 2017). The Wnt/β-catenin signaling pathway is active in the appendages of embryonic ectoderm and is necessary for their formation. Whether the Wnt signaling is upstream or downstream of the EDA signaling is controversial in the basal formation process of the ectodermal appendage, but now, there is mounting evidence that Wnt signaling is an upstream regulator of EDA signaling (Cui et al., 2014). As ESG germs start to form, Wnt activity declines quickly in the dermis and rises strongly in the basal layer of epidermis, and then stays active at the tip of the growing ducts until it disappears when the sweat ducts starts to coil (Cui et al., 2014). According to reports, Wnt10a mutations account for 16% of human hyperhidrosis ectodermal dysplasia (HED) patients (Cluzeau et al., 2011). After further study, researchers have found that Wnt10a/β-catenin signaling is necessary for ESG germ development and postnatal ESG duct

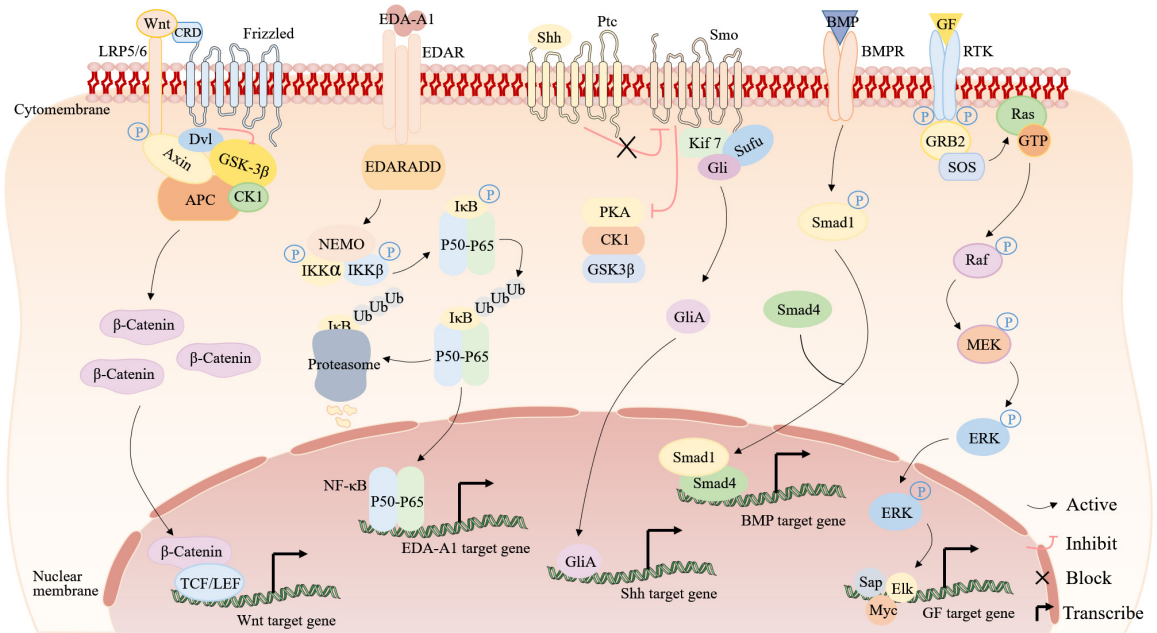

FIGURE 4 | The signaling pathways involved in ESG development and regeneration. From left to right are the Wnt, EDA-A1, Shh, BMP, and ERK signaling pathways. Wnt signaling pathway (Nusse and Clevers, 2017; Routledge and Scholpp, 2019): in the absence of Wnt signals, GSK-3β/Axin/APC/β-catenin/CK1 is a destruction complex. GSK-3β phosphorylates β-catenin, thereby inhibiting its activity and then β-catenin is degraded by ubiquitination. When Wnt proteins bind to a receptor complex, it induces the association of Axin and Dvl with LRP5/6 and Frizzled. Dvl inhibits GSK-3β and the destruction complex falls apart, and thus prevents the degradation of β-catenin, permitting β-catenin accumulation, leading to binding TCF/LEF in the nucleus to upregulate target genes. EDA signaling pathway (Oeckinghaus et al., 2011; Sisto et al., 2016): in the absence of EDA-A1 signals, NF-κB dimers (P50–P65) are bound to inhibitory IκB proteins, which sequester inactive NF-κB complexes in the cytoplasm. When EDA-A1 binds to EDAR, stimulation of EDAR leads to the binding of EDARADD, for IKK activation. Shh signaling pathway (Fattahi et al., 2018; Xin et al., 2018): in the absence of Shh signals, Ptc inhibits the activity of Smo by affecting its localization to the cell surface, and protein kinases (PKA, CK1, and GSK3β) constitutively phosphorylate Gli proteins to inhibit the Gli. The secreted active Shh ligand binds to Ptc and relieves the repressive effect of the Ptc on Smo, activating the Smo, which then translocates to the cell membrane to inhibit PKA, CK1, and GSK3, providing an assembly platform for the recruitment of Kif7, Sufu and Gli, thus activating the Gli. Subsequently, the activated Gli forms (GliAs) translocate into the nucleus and activate Shh target genes. BMP signaling pathway (Gonzalez and Medici, 2014): when BMPs bind to BMPRs, intracellular Smad1 becomes phosphorylated. The phosphorylated Smad1 binds to Smad4 and then translocates into the nucleus and activates BMP target genes. ERK signaling pathway (Calvo et al., 2010; Gallo et al., 2019): Phosphorylated RTK binds to GRB2, and GRB2 binds to SOS, which stimulates RAS. RAS initiates activation of the MEK-ERK cascade by converting a molecule from GDP to GTP.

development (Xu et al., 2017). It will be interesting in the future to apply Wnt10a to ESG regeneration.

EDA/EDAR/NF-κB Signaling Pathway

Hypohidrotic ectodermal dysplasia is a well-characterized human disease characterized by absent or malformed HFs, teeth, and ESGs (Cui and Schlessinger, 2006; Mikkola, 2009). Much of the information known about ESG determination and development related to signaling pathways originated from research on HED patients. As a member of the TNF family of signaling molecules, ectodysplasin-A (EDA) exists as two highly homologous isoforms, EDA1 and EDA2, and the EDA-A1 gene, specific for the type I transmembrane protein EDA receptor (EDAR), is one of the genes that regulates the determination and development of ESGs (Srivastava et al., 2001). The main axis of the pathway comprises EDA (encoded in mice by tabby), EDAR (encoded by downless), and EDAR-associated death domain (EDARADD, encoded by crinkled) (Srivastava et al., 1997; Monreal et al., 1999). Any mutation in the components of these pathways will cause HED, which is phenocopied in mice (Headon et al., 2001; Cui and Schlessinger, 2006). In addition, mice deficient for nuclear factor-κB (NF-κB) activity also showed a phenotype identical to HED, leading researchers to realize that EDA/EDAR sends signals through the NF-κB pathway during skin appendage development (Doffinger et al., 2001; Kumar et al., 2001; Schmidt-Ullrich et al., 2001). Studies have found that EDA mainly regulates ESG maturation through activating NF-κB after binding to EDAR in the early stages of embryonic development (Doffinger et al., 2001; Kumar et al., 2001).

The almost complete restoration of ectodermal appendages (including ESG) is caused by the transgenic expression of the mouse EDA-A1 isoform in Tabby (EDA-less) (Srivastava et al., 2001), but wild-type mice overexpressing EDA-A1 showed larger ESGs with greater activity (Mustonen et al., 2003). Furthermore, Gaide et al., found that treating pregnant Tabby mice with EDA-A1 recombinant protein can permanently rescue the tabby defect in the offspring (Gaide and Schneider, 2003). Thus, researchers have hypothesized that activation of the EDA gene could induce the regeneration of ESGs. In support of this, the reprogramming of BM-MSCs to SGLCs was successfully induced by the high expression of EDA gene in BM-MSC (Cai et al., 2011). In addition, the findings of Sun et al. (2018) demonstrate that

induction of EDA gene overexpression via transfection with an RNA-guided dCas9-effector could promote the transformation of BM-MSCs into SGLCs. These results indicate that the potential of EDA-modified MSCs for the repair and regeneration of ESGs.

As downstream effectors of EDA and EDAR signaling, IKK pathway activates the NF-κB transcription factors for development of skin appendages, and the activated NF-κB transcription factors can enter the nucleus to promote the expression of NF-κB target genes, such as keratins, cyclin D1, Shh and fox family genes (Schmidt-Ullrich et al., 2006). In different stages of ESG development, these genes are essential (Kunisada et al., 2009). Thus, researchers have sought to determine whether NF-κB could induce the regeneration of ESGs *in vitro*. Zhao et al. (2015) found that human fibroblasts could be directly reprogrammed into SGLCs by introducing NF-κB and Lef-1 (a downstream transcription factor of β-catenin signaling) genes into human fibroblasts. Chen et al. (2019) also noted increased expression of NF-κB during the reprogramming of BM-MSCs into SGLCs by determining the differential expression of miRNAs between BM-MSCs and SGLCs. These results indicate that EDA/EDAR/NF-κB signaling is not only associated with the occurrence and development of ESGs but also plays a vital role in ESG regeneration. However, many other aspects of the EDA/EDAR/NF-κB pathway for ESG regeneration still need to be thoroughly explored, such as receptor activation, ligand binding sites, desensitization, and transportation. It indicates that EDA/EDAR/NF-κB signaling are not only related to the determination and development of ESGs, but also important in ESGs regeneration.

Shh Signaling Pathway

The Shh signaling pathway plays a vital role in embryonic development and tissue regeneration (Xu et al., 2015). The Shh signaling pathway is downstream of the EDA/EDAR/NF-κB signaling pathway. Some studies have shown that Shh signaling is involved in the development of ESG, especially in the process of ESG induction and/or early development, but not in the process of maturation and/or maintenance (Kunisada et al., 2009; Lu and Fuchs, 2014; Lu et al., 2016). Conversely, many studies have also shown that Shh signaling inactivation does not affect the formation of ESG germ or subsequent ducts, but the secretory coil formation is still blocked in the primary stage (Cui et al., 2014; Cui and Schlessinger, 2015). In the process of ESG cells regeneration, it is unclear whether there is a specific connection between the two experimental results. Liang et al. (2016) reported that Shh is an important factor in conditioned medium that influences the differentiation and the formation of ESG tubule-like structures during the differentiation of amniotic fluid stem cells into SGLCs. However, the underlying mechanism is unknown and the exact role of Shh signaling in ESG morphogenesis remains to be clarified.

BMP Signaling Pathway

Bone morphogenetic proteins (BMPs) are multi-functional growth factors belonging to the transforming growth factor (TGF)-β superfamily (Botchkarev and Sharov, 2004). Previous experiments have shown that the ESGs in the mouse paws can be converted into HFs by suppressing the BMP signaling (Plikus et al., 2004). Lu et al. (2016) investigated it further and found that the selection of appendages depends on the antagonism between Shh signaling and BMP signaling in different skin areas in the mesenchyme after epidermal bud formation. When the BMP signaling is in the active state, it determines the formation of ESGs. When BMP signaling is weaker than Shh, it determines the formation of HFs. Hu et al. (2019) cocultured EpiSCs with embryonic paw pad tissue, which demonstrated glandular structure. Moreover, BMP4 concentration was detected in the medium and a BMP receptor inhibitor could effectively block the EpiSC differentiation to ESGs (Hu et al., 2019), implying the possibility of BMP4 application in the regeneration of ESGs.

ERK Signaling Pathway

Epidermal growth factor and FGF, as cytokines, can activate the ERK signaling pathway. EGF can specifically trigger proliferation or differentiation by leading to population-averaged transient or sustained ERK (Marshall, 1995; Santos et al., 2007). By activating ERK through FGFRs, FGF can regulate development, wound healing, and angiogenesis (Ornitz and Itoh, 2015). Some studies have shown that EGF or KGF (also called FGF7) could induce stem cell differentiation into SGLCs (Xu et al., 2016; Kolakshyapati et al., 2017). All of these show that the ERK pathway is important in ESG regeneration.

CONCLUSION AND FUTURE PERSPECTIVES

Recently, skin tissue engineering research has been greatly developed. However, current skin substitutes do not contain skin appendages. Therefore, current skin substitutes can only be used to cover the wound, but cannot play physiological functions of normal skin, which is far from enough for patients with severe burns. Studies on the development, structure and function of ESGs have been intensively conducted. On this basis, ESG regeneration has been studied and great advances have been made. The study of skin tissue engineering is often divided into several aspects of cells, scaffolds and biomolecules, and ESG regeneration research is also similar. In this review, ESG and its regeneration have been systematically reviewed. There are three main categories must be considered in ESG regeneration: stem cells, scaffolds, and possible signaling pathways involved.

It is clear from the works herein reviewed that ESG regeneration research involves combination of different types of stem cells, scaffolds, and signaling pathways. So far, researchers successfully reconstructed SGL structures via a variety of methods. However, whether the 3D-reconstituted ESGs can perform physiological functions needs further verification. In addition, the detailed mechanism of how a variety of biomolecules induces ESG differentiation remains to be further studied. Current methods of regenerating ESGs are inefficient, mainly due to the limited number of stem cells, low cell differentiation efficiency and other unpredictable factors. In conclusion, ESG regeneration research is still at a very early stage. We expect to be able to regenerate ESGs to compensate

for the inability of tissue-engineered skin to secrete sweat. With the development of stem cells study, molecular biology and biomaterials, ESG regeneration will be achieved in future.

AUTHOR CONTRIBUTIONS

HL conceived and presented the outline of the review. YL collected literature as well as wrote the review. LC, MZ, SX, LD, and XZ revised the manuscript, provided some relevant insights, and made some edits. All authors read and approved the final version of the manuscript.

FUNDING

This study was supported in part by the National Natural Science Foundation of China (81772102 and 81471882).

REFERENCES

Amini-Nik, S., Dolp, R., Eylert, G., Datu, A. K., Parousis, A., Blakeley, C., et al. (2018). Stem cells derived from burned skin - The future of burn care. *EBioMed.* 37, 509–520. doi: 10.1016/j.ebiom.2018.10.014

Arnaoutova, I., George, J., Kleinman, H. K., and Benton, G. (2009). The endothelial cell tube formation assay on basement membrane turns 20: state of the science and the art. *Angiogenesis* 12, 267–274. doi: 10.1007/s10456-009-9146-4

Auerbach, R., Lewis, R., Shinners, B., Kubai, L., and Akhtar, N. (2003). Angiogenesis assays: a critical overview. *Clin. Chem.* 49, 32–40. doi: 10.1373/49.1.32

Barka, T., Gresik, E. S., and Miyazaki, Y. (2005). Differentiation of a mouse submandibular gland-derived cell line (SCA) grown on matrigel. *Exp. Cell. Res.* 308, 394–406. doi: 10.1016/j.yexcr.2005.04.025

Bissell, M. J., and Labarge, M. A. (2005). Context, tissue plasticity, and cancer: are tumor stem cells also regulated by the microenvironment? *Cancer Cell.* 7, 17–23. doi: 10.1016/j.ccr.2004.12.013

Blankenship, M. L. (1990). Mite dermatitis other than scabies. *Dermatol. Clin.* 8, 265–275. doi: 10.1016/s0733-8635(18)30498-4

Boehnke, K., Falkowska-Hansen, B., Stark, H. J., and Boukamp, P. (2012). Stem cells of the human epidermis and their niche: composition and function in epidermal regeneration and carcinogenesis. *Carcinogenesis* 33, 1247–1258. doi: 10.1093/carcin/bgs136

Bonnans, C., Chou, J., and Werb, Z. (2014). Remodelling the extracellular matrix in development and disease. *Nat. Rev. Mol. Cell Biol.* 15, 786–801. doi: 10.1038/nrm3904

Botchkarev, V. A., and Sharov, A. A. (2004). BMP signaling in the control of skin development and hair follicle growth. *Diff. Res. Biol. Divers.* 72, 512–526. doi: 10.1111/j.1432-0436.2004.07209005.x

Cai, S., Pan, Y., Han, B., Sun, T. Z., Sheng, Z. Y., and Fu, X. B. (2011). Transplantation of human bone marrow-derived mesenchymal stem cells transfected with ectodysplasin for regeneration of sweat glands. *Chin. Med. J.* 124, 2260–2268.

Calvo, F., Agudo-Ibáñez, L., and Crespo, P. (2010). The Ras-ERK pathway: understanding site-specific signaling provides hope of new anti-tumor therapies. *Bioessays* 32, 412–421. doi: 10.1002/bies.200900155

Chen, L., Zhang, M., Li, H., Tang, S., and Fu, X. (2014). Distribution of BrdU label-retaining cells in eccrine sweat glands and comparison of the percentage of BrdU-positive cells in eccrine sweat glands and in epidermis in rats. *Arch. Dermatol. Res.* 306, 157–162. doi: 10.1007/s00403-013-1397-7

Chen, Y., Li, Q., Tan, Z., Zhang, C., and Fu, X. (2019). MicroRNA-mediated regulation of BM-MSCs differentiation into sweat gland-like cells: targeting NF-kappaB. *J. Mol. Histol.* 50, 155–166. doi: 10.1007/s10735-019-09814-2

Cluzeau, C., Hadj-Rabia, S., Jambou, M., Mansour, S., Guigue, P., Masmoudi, S., et al. (2011). Only four genes (EDA1, EDAR, EDARADD, and WNT10A) account for 90% of hypohidrotic/anhidrotic ectodermal dysplasia cases. *Hum. Mutat.* 32, 70–72. doi: 10.1002/humu.21384

Costa, A., Naranjo, J. D., Londono, R., and Badylak, S. F. (2017). Biologic Scaffolds. *Cold Spring Harb. Perspect. Med.* 7:a025676. doi: 10.1101/cshperspect.a025676

Cotsarelis, G., Kaur, P., Dhouailly, D., Hengge, U., and Bickenbach, J. (1999). Epithelial stem cells in the skin: definition, markers, localization and functions. *Exp. Dermatol.* 8, 80–88. doi: 10.1111/j.1600-0625.1999.tb00351.x

Cui, C. Y., and Schlessinger, D. (2006). EDA signaling and skin appendage development. *Cell Cycle* 5, 2477–2483. doi: 10.4161/cc.5.21.3403

Cui, C. Y., and Schlessinger, D. (2015). Eccrine sweat gland development and sweat secretion. *Exp. Dermatol.* 24, 644–650. doi: 10.1111/exd.12773

Cui, C. Y., Yin, M., Sima, J., Childress, V., Michel, M., Piao, Y., et al. (2014). Involvement of Wnt, Eda and Shh at defined stages of sweat gland development. *Development* 141, 3752–3760. doi: 10.1242/dev.109231

Diao, J., Liu, J., Wang, S., Chang, M., Wang, X., Guo, B., et al. (2019). Sweat gland organoids contribute to cutaneous wound healing and sweat gland regeneration. *Cell Death Dis.* 10:238. doi: 10.1038/s41419-019-1485-5

Doffinger, R., Smahi, A., Bessia, C., Geissmann, F., Feinberg, J., Durandy, A., et al. (2001). X-linked anhidrotic ectodermal dysplasia with immunodeficiency is caused by impaired NF-kappaB signaling. *Nat. Genet.* 27, 277–285. doi: 10.1038/85837

Fattahi, S., Pilehchian Langroudi, M., and Akhavan-Niaki, H. (2018). Hedgehog signaling pathway: Epigenetic regulation and role in disease and cancer development. *J. Cell. Physiol.* 233, 5726–5735. doi: 10.1002/jcp.26506

Gaide, O., and Schneider, P. (2003). Permanent correction of an inherited ectodermal dysplasia with recombinant EDA. *Nat. Med.* 9, 614–618. doi: 10.1038/nm861

Gallo, S., Vitacolonna, A., Bonzano, A., Comoglio, P., and Crepaldi, T. (2019). ERK: a Key Player in the Pathophysiology of Cardiac Hypertrophy. *Int. J. Mol. Sci.* 20:2164. doi: 10.3390/ijms20092164

Gonzalez, D. M., and Medici, D. (2014). Signaling mechanisms of the epithelial-mesenchymal transition. *Sci. Signal.* 7:re8. doi: 10.1126/scisignal.2005189

Hashimoto, K., Gross, B. G., and Lever, W. F. (1965). The ultrastructure of the skin of human embryos. I. The intraepidermal eccrine sweat duct. *J. Investig. Dermatol.* 45, 139–151. doi: 10.1038/jid.1965.110

Hassan, W. U., Greiser, U., and Wang, W. (2014). Role of adipose-derived stem cells in wound healing. *Wound Repair Regen.* 22, 313–325. doi: 10.1111/wrr.12173

Headon, D. J., Emmal, S. A., Ferguson, B. M., Tucker, A. S., Justice, M. J., Sharpe, P. T., et al. (2001). Gene defect in ectodermal dysplasia implicates a death domain adapter in development. *Nature* 414, 913–916. doi: 10.1038/414913a

Horie, N., Yokozeki, H., and Sato, K. (1986). Proteolytic enzymes in human eccrine sweat: a screening study. *Am. J. Physiol.* 250, R691–R698. doi: 10.1152/ajpregu.1986.250.4.R691

Hu, T., Xu, Y., Yao, B., Fu, X., and Huang, S. (2019). Developing a Novel and Convenient Model for Investigating Sweat Gland Morphogenesis from Epidermal Stem Cells. *Stem Cells Int.* 2019:4254759. doi: 10.1155/2019/4254759

Huang, S., Lu, G., Wu, Y., Jirigala, E., Xu, Y., Ma, K., et al. (2012). Mesenchymal stem cells delivered in a microsphere-based engineered skin contribute to cutaneous wound healing and sweat gland repair. *J. Dermatol. Sci.* 66, 29–36. doi: 10.1016/j.jdermsci.2012.02.002

Huang, S., Xu, Y., Wu, C., Sha, D., and Fu, X. (2010). In vitro constitution and in vivo implantation of engineered skin constructs with sweat glands. *Biomaterials* 31, 5520–5525. doi: 10.1016/j.biomaterials.2010.03.060

Huang, S., Yao, B., Xie, J., and Fu, X. (2016). 3D bioprinted extracellular matrix mimics facilitate directed differentiation of epithelial progenitors for sweat gland regeneration. *Acta Biomater.* 32, 170–177. doi: 10.1016/j.actbio.2015.12.039

Huang, S., Zhang, Y., Tang, L., Deng, Z., Lu, W., Feng, F., et al. (2009). Functional bilayered skin substitute constructed by tissue-engineered extracellular matrix

and microsphere-incorporated gelatin hydrogel for wound repair. *Tissue Eng. Part A* 15, 2617–2624. doi: 10.1089/ten.TEA.2008.0505

Kleinman, H. K., and Martin, G. R. (2005). Matrigel: basement membrane matrix with biological activity. *Semin. Cancer Biol.* 15, 378–386. doi: 10.1016/j.semcancer.2005.05.004

Kolakshyapati, P., Li, X., Chen, C., Zhang, M., Tan, W., Ma, L., et al. (2017). Gene-activated matrix/bone marrow-derived mesenchymal stem cells constructs regenerate sweat glands-like structure in vivo. *Sci. Rep.* 7:17630. doi: 10.1038/s41598-017-17967-x

Kozowski, M., Wilczak, J., Motyl, T., and Gajewska, M. (2011). Role of extracellular matrix and prolactin in functional differentiation of bovine BME-UV1 mammary epithelial cells. *Pol. J. Vet. Sci.* 14, 433–442. doi: 10.2478/v10181-011-0064-1

Kumar, A., Eby, M. T., Sinha, S., Jasmin, A., and Chaudhary, P. M. (2001). The ectodermal dysplasia receptor activates the nuclear factor-kappaB, JNK, and cell death pathways and binds to ectodysplasin A. *J. Biol. Chem.* 276, 2668–2677. doi: 10.1074/jbc.M008356200

Kunisada, M., Cui, C. Y., Piao, Y., Ko, M. S., and Schlessinger, D. (2009). Requirement for Shh and Fox family genes at different stages in sweat gland development. *Hum. Mol. Genet.* 18, 1769–1778. doi: 10.1093/hmg/ddp089

Kurata, R., Futaki, S., Nakano, I., Tanemura, A., Murota, H., Katayama, I., et al. (2014). Isolation and characterization of sweat gland myoepithelial cells from human skin. *Cell Struct. Funct.* 39, 101–112. doi: 10.1247/csf.14009

Lee, C. H., Rodeo, S. A., Fortier, L. A., Lu, C., Erisken, C., and Mao, J. J. (2014). Protein-releasing polymeric scaffolds induce fibrochondrocytic differentiation of endogenous cells for knee meniscus regeneration in sheep. *Sci. Transl. Med.* 6:266ra171. doi: 10.1126/scitranslmed.3009696

Leung, Y., Kandyba, E., Chen, Y. B., Ruffins, S., and Kobielak, K. (2013). Label retaining cells (LRCs) with myoepithelial characteristic from the proximal acinar region define stem cells in the sweat gland. *PLoS One* 8:e74174. doi: 10.1371/journal.pone.0074174

Li, H., Chen, L., Zeng, S., Li, X., Zhang, X., Lin, C., et al. (2015a). Matrigel basement membrane matrix induces eccrine sweat gland cells to reconstitute sweat gland-like structures in nude mice. *Exp. Cell Res.* 332, 67–77. doi: 10.1016/j.yexcr.2015.01.014

Li, H., Chen, L., Zhang, M., Tang, S., and Fu, X. (2013). Three-dimensional culture and identification of human eccrine sweat glands in matrigel basement membrane matrix. *Cell Tissue Res.* 354, 897–902. doi: 10.1007/s00441-013-1718-3

Li, H., Chen, L., Zhang, M., Xie, S., and Cheng, L. (2018). Expression and localization of Forkhead transcription factor A1 in the three-dimensional reconstructed eccrine sweat glands. *Acta Histochem.* 120, 520–524. doi: 10.1016/j.acthis.2018.06.003

Li, H., Chen, L., Zhang, M., and Zhang, B. (2017). Foxa1 gene and protein in developing rat eccrine sweat glands. *J. Mol. Histol.* 48, 1–7. doi: 10.1007/s10735-016-9700-5

Li, H., Fu, X., Ouyang, Y., Cai, C., Wang, J., and Sun, T. (2006). Adult bone-marrow-derived mesenchymal stem cells contribute to wound healing of skin appendages. *Cell Tissue Res.* 326, 725–736. doi: 10.1007/s00441-006-0270-9

Li, H., Li, X., Zhang, M., Chen, L., Zhang, B., Tang, S., et al. (2015b). Three-dimensional co-culture of BM-MSCs and eccrine sweat gland cells in Matrigel promotes transdifferentiation of BM-MSCs. *J. Mol. Histol.* 46, 431–438. doi: 10.1007/s10735-015-9632-5

Li, H., Zhang, M., Chen, L., Li, X., and Zhang, B. (2016a). Human eccrine sweat gland cells reconstitute polarized spheroids when subcutaneously implanted with Matrigel in nude mice. *J. Mol. Histol.* 47, 485–490. doi: 10.1007/s10735-016-9690-3

Li, H., Zhang, M., Li, X., Chen, L., Zhang, B., Tang, S., et al. (2016b). BrdU-label-retaining cells in rat eccrine sweat glands over time. *Acta Histochem.* 118, 74–79. doi: 10.1016/j.acthis.2015.11.009

Li, H. H., Fu, X. B., Zhang, L., and Zhou, G. (2008). Comparison of proliferating cells between human adult and fetal eccrine sweat glands. *Arch Dermatol. Res.* 300, 173–176. doi: 10.1007/s00403-007-0823-0

Liang, H., Sun, Q., Zhen, Y., Li, F., Xu, Y., Liu, Y., et al. (2016). The differentiation of amniotic fluid stem cells into sweat glandlike cells is enhanced by the presence of Sonic hedgehog in the conditioned medium. *Exp. Dermatol.* 25, 714–720. doi: 10.1111/exd.13062

Liu, N., Huang, S., Yao, B., Xie, J., Wu, X., and Fu, X. (2016). 3D bioprinting matrices with controlled pore structure and release function guide in vitro self-organization of sweat gland. *Sci. Rep.* 6:34410. doi: 10.1038/srep34410

Lobitz, W. C. Jr., and Dobson, R. L. (1961). Dermatology: the eccrine sweat glands. *Annu. Rev. Med.* 12, 289–298. doi: 10.1146/annurev.me.12.020161.001445

Lu, C., and Fuchs, E. (2014). Sweat gland progenitors in development, homeostasis, and wound repair. *Cold Spring Harb. Perspect. Med.* 4:a015222. doi: 10.1101/cshperspect.a015222

Lu, C. P., Polak, L., Keyes, B. E., and Fuchs, E. (2016). Spatiotemporal antagonism in mesenchymal-epithelial signaling in sweat versus hair fate decision. *Science* 354:aah6102. doi: 10.1126/science.aah6102

Lu, C. P., Polak, L., Rocha, A. S., Pasolli, H. A., Chen, S. C., Sharma, N., et al. (2012). Identification of stem cell populations in sweat glands and ducts reveals roles in homeostasis and wound repair. *Cell* 150, 136–150. doi: 10.1016/j.cell.2012.04.045

Ma, X., Liu, J., Zhu, W., Tang, M., Lawrence, N., Yu, C., et al. (2018). 3D bioprinting of functional tissue models for personalized drug screening and in vitro disease modeling. *Adv. Drug Del. Rev.* 132, 235–251. doi: 10.1016/j.addr.2018.06.011

Ma, Y., Li, M., Liu, J., Pang, C., Zhang, J., Li, Y., et al. (2018). Location, Isolation, and Identification of Mesenchymal Stem Cells from Adult Human Sweat Glands. *Stem Cells Int.* 2018:2090276. doi: 10.1155/2018/2090276

Maria, O. M., Maria, O., Liu, Y., Komarova, S. V., and Tran, S. D. (2011). Matrigel improves functional properties of human submandibular salivary gland cell line. *Int. J. Biochem. Cell Biol.* 43, 622–631. doi: 10.1016/j.biocel.2011.01.001

Marshall, C. J. (1995). Specificity of receptor tyrosine kinase signaling: transient versus sustained extracellular signal-regulated kinase activation. *Cell* 80, 179–185. doi: 10.1016/0092-8674(95)90401-8

Mikkola, M. L. (2009). Molecular aspects of hypohidrotic ectodermal dysplasia. *Am. J. Med. Genet. A* 149A, 2031–2036. doi: 10.1002/ajmg.a.32855

Monreal, A. W., Ferguson, B. M., Headon, D. J., Street, S. L., Overbeek, P. A., and Zonana, J. (1999). Mutations in the human homologue of mouse dl cause autosomal recessive and dominant hypohidrotic ectodermal dysplasia. *Nat. Genet.* 22, 366–369. doi: 10.1038/11937

Montagna, W., Chase, H. B., and Lobitz, W. C. Jr. (1953). Histology and cytochemistry of human skin. IV. The eccrine sweat glands. *J. Investig. Dermatol.* 20, 415–423. doi: 10.1038/jid.1953.52

Morimoto, Y., and Saga, K. (1995). Proliferating cells in human eccrine and apocrine sweat glands. *J. Histochem. Cytochem.* 43, 1217–1221. doi: 10.1177/43.12.8537637

Munger, B. L. (1961). The ultrastructure and histophysiology of human eccrine sweat glands. *J. Biophys. Biochem. cytol.* 11, 385–402. doi: 10.1083/jcb.11.2.385

Murphy, S. V., and Atala, A. (2014). 3D bioprinting of tissues and organs. *Nat. Biotechnol.* 32, 773–785. doi: 10.1038/nbt.2958

Mustonen, T., Pispa, J., Mikkola, M. L., Pummila, M., Kangas, A. T., Pakkasjarvi, L., et al. (2003). Stimulation of ectodermal organ development by Ectodysplasin-A1. *Dev. Biol.* 259, 123–136. doi: 10.1016/s0012-1606(03)00157-x

Niyonsaba, F., Suzuki, A., Ushio, H., Nagaoka, I., Ogawa, H., and Okumura, K. (2009). The human antimicrobial peptide dermcidin activates normal human keratinocytes. *Br. J. Dermatol.* 160, 243–249. doi: 10.1111/j.1365-2133.2008.08925.x

Nolte, S. V., Xu, W., Rennekampff, H. O., and Rodemann, H. P. (2008). Diversity of fibroblasts–a review on implications for skin tissue engineering. *Cells Tissues Organs.* 187, 165–176. doi: 10.1159/000111805

Nusse, R., and Clevers, H. (2017). Wnt/β-Catenin Signaling, Disease, and Emerging Therapeutic Modalities. *Cell* 169, 985–999. doi: 10.1016/j.cell.2017.05.016

Oeckinghaus, A., Hayden, M. S., and Ghosh, S. (2011). Crosstalk in NF-κB signaling pathways. *Nat. Immunol.* 12, 695–708. doi: 10.1038/ni.2065

Okada, T., Konishi, H., Ito, M., Nagura, H., and Asai, J. (1988). Identification of secretory immunoglobulin A in human sweat and sweat glands. *J. Investig. Dermatol.* 90, 648–651. doi: 10.1111/1523-1747.ep12560807

Ornitz, D. M., and Itoh, N. (2015). The Fibroblast Growth Factor signaling pathway. *Wiley Interdiscip. Rev. Dev. Biol.* 4, 215–266. doi: 10.1002/wdev.176

Pati, F., Jang, J., Ha, D. H., Won Kim, S., Rhie, J. W., Shim, J. H., et al. (2014). Printing three-dimensional tissue analogues with decellularized extracellular matrix bioink. *Nature communications*. 5, 3935. doi: 10.1038/ncomms4935

Petrakova, O. S., Ashapkin, V. V., Voroteliak, E. A., Bragin, E. Y., Shtratnikova, V. Y., Chernioglo, E. S., et al. (2012). Effect of 3D Cultivation Conditions on the Differentiation of Endodermal Cells. *Acta Nat.* 4, 47–57. doi: 10.32607/20758251-2012-4-4-47-57

Plikus, M., Wang, W. P., Liu, J., Wang, X., Jiang, T. X., and Chuong, C. M. (2004). Morpho-regulation of ectodermal organs: integument pathology and phenotypic variations in K14-Noggin engineered mice through modulation of bone morphogenic protein pathway. *Am. J. Pathol.* 164, 1099–1114. doi: 10.1016/s0002-9440(10)63197-5

Pontiggia, L., Biedermann, T., Bottcher-Haberzeth, S., Oliveira, C., Braziulis, E., Klar, A. S., et al. (2014). De novo epidermal regeneration using human eccrine sweat gland cells: higher competence of secretory over absorptive cells. *J. Investig. Dermatol.* 134, 1735–1742. doi: 10.1038/jid.2014.30

Rittie, L., Sachs, D. L., Orringer, J. S., Voorhees, J. J., and Fisher, G. J. (2013). Eccrine sweat glands are major contributors to reepithelialization of human wounds. *Am. J. Pathol.* 182, 163–171. doi: 10.1016/j.ajpath.2012.09.01

Routledge, D., and Scholpp, S. (2019). Mechanisms of intercellular Wnt transport. *Development* 146:dev176073. doi: 10.1242/dev.176073

Saga, K. (2002). Structure and function of human sweat glands studied with histochemistry and cytochemistry. *Prog. Histochem. Cytochem.* 37, 323–386. doi: 10.1016/s0079-6336(02)80005-5

Santos, S. D., Verveer, P. J., and Bastiaens, P. I. (2007). Growth factor-induced MAPK network topology shapes Erk response determining PC-12 cell fate. *Nat. Cell Biol.* 9, 324–330. doi: 10.1038/ncb1543

Sato, K. (1977). Pharmacology and function of the myoepithelial cell in the eccrine sweat gland. *Experientia* 33, 631–633. doi: 10.1007/bf01946542

Sato, K., Kang, W. H., Saga, K., and Sato, K. T. (1989). Biology of sweat glands and their disorders. I. Normal sweat gland function. *J. Am. Acad. Dermatol.* 20, 537–563. doi: 10.1016/s0190-9622(89)70063-3

Sato, K., and Sato, F. (1994). Interleukin-1 alpha in human sweat is functionally active and derived from the eccrine sweat gland. *Am. J. Physiol.* 266, R950–R959. doi: 10.1152/ajpregu.1994.266.3.R950

Schittek, B., Hipfel, R., Sauer, B., Bauer, J., Kalbacher, H., Stevanovic, S., et al. (2001). Dermcidin: a novel human antibiotic peptide secreted by sweat glands. *Nat. Immunol.* 2, 1133–1137. doi: 10.1038/ni732

Schmidt-Ullrich, R., Aebischer, T., Hülsken, J., Birchmeier, W., Klemm, U., and Scheidereit, C. (2001). Requirement of NF-kappaB/Rel for the development of hair follicles and other epidermal appendices. *Development* 128, 3843–3853. doi: 10.1242/dev.128.19.3843

Schmidt-Ullrich, R., Tobin, D. J., Lenhard, D., Schneider, P., Paus, R., and Scheidereit, C. (2006). NF-kappaB transmits Eda A1/EdaR signalling to activate Shh and cyclin D1 expression, and controls post-initiation hair placode down growth. *Development* 133, 1045–1057. doi: 10.1242/dev.02278

Sheng, Z., Fu, X., Cai, S., Lei, Y., Sun, T., Bai, X., et al. (2009). Regeneration of functional sweat gland-like structures by transplanted differentiated bone marrow mesenchymal stem cells. *Wound Repair Regen.* 17, 427–435. doi: 10.1111/j.1524-475X.2009.00474.x

Shevchenko, R. V., Eeman, M., Rowshanravan, B., Allan, I. U., Savina, I. N., Illsley, M., et al. (2014). The in vitro characterization of a gelatin scaffold, prepared by cryogelation and assessed in vivo as a dermal replacement in wound repair. *Acta Biomater.* 10, 3156–3166. doi: 10.1016/j.actbio.2014.03.027

Shibasaki, M., Wilson, T. E., and Crandall, C. G. (2006). Neural control and mechanisms of eccrine sweating during heat stress and exercise. *J. Appl. Physiol.* 100, 1692–1701. doi: 10.1152/japplphysiol.01124.2005

Shikiji, T., Minami, M., Inoue, T., Hirose, K., Oura, H., and Arase, S. (2003). Keratinocytes can differentiate into eccrine sweat ducts in vitro: involvement of epidermal growth factor and fetal bovine serum. *J. Dermatol. Sci.* 33, 141–150. doi: 10.1016/j.jdermsci.2003.09.004

Sisto, M., Barca, A., Lofrumento, D. D., and Lisi, S. (2016). Downstream activation of NF-κB in the EDA-A1/EDAR signalling in Sjögren's syndrome and its regulation by the ubiquitin-editing enzyme A20. *Clin. Exp. Immunol.* 184, 183–196. doi: 10.1111/cei.12764

Srivastava, A. K., Durmowicz, M. C., Hartung, A. J., Hudson, J., Ouzts, L. V., Donovan, D. M., et al. (2001). Ectodysplasin-A1 is sufficient to rescue both hair growth and sweat glands in Tabby mice. *Hum. Mol. Genet.* 10, 2973–2981. doi: 10.1093/hmg/10.26.2973

Srivastava, A. K., Pispa, J., Hartung, A. J., Du, Y., Ezer, S., Jenks, T., et al. (1997). The Tabby phenotype is caused by mutation in a mouse homologue of the EDA gene that reveals novel mouse and human exons and encodes a protein (ectodysplasin-A) with collagenous domains. *Proc. Natl. Acad. Sci. U. S. A.* 94, 13069–13074. doi: 10.1073/pnas.94.24.13069

Steinhart, Z., and Angers, S. (2018). Wnt signaling in development and tissue homeostasis. *Development* 145:dev146589. doi: 10.1242/dev.146589

Sun, S., Xiao, J., Huo, J., Geng, Z., Ma, K., Sun, X., et al. (2018). Targeting ectodysplasin promotor by CRISPR/dCas9-effector effectively induces the reprogramming of human bone marrow-derived mesenchymal stem cells into sweat gland-like cells. *Stem Cell Res. Ther.* 9:8. doi: 10.1186/s13287-017-0758-0

Tao, R., Sun, T. J., Han, Y. Q., Xu, G., Liu, J., and Han, Y. F. (2014). Epimorphin-induced differentiation of human umbilical cord mesenchymal stem cells into sweat gland cells. *Eur. Rev. Med. Pharmacol. Sci.* 18, 1404–1410.

Theocharis, A. D., Skandalis, S. S., Gialeli, C., and Karamanos, N. K. (2016). Extracellular matrix structure. *Adv. Drug Deliv. Rev.* 97, 4–27. doi: 10.1016/j.addr.2015.11.001

Vierbuchen, T., Ostermeier, A., Pang, Z. P., Kokubu, Y., Sudhof, T. C., and Wernig, M. (2010). Direct conversion of fibroblasts to functional neurons by defined factors. *Nature* 463, 1035–1041. doi: 10.1038/nature08797

Wang, R., Wang, Y., Yao, B., Hu, T., Li, Z., Liu, Y., et al. (2019). Redirecting differentiation of mammary progenitor cells by 3D bioprinted sweat gland microenvironment. *Burns Trauma* 7:29. doi: 10.1186/s41038-019-0167-y

Wang, Y., Liu, Z. Y., Zhao, Q., Sun, T. Z., Ma, K., and Fu, X. B. (2013). Future application of hair follicle stem cells: capable in differentiation into sweat gland cells. *Chin. Med. J.* 126, 3545–3552.

Watt, F. M., and Huck, W. T. (2013). Role of the extracellular matrix in regulating stem cell fate. *Nat. Rev. Mol. Cell Biol.* 14, 467–473. doi: 10.1038/nrm3620

Xin, M., Ji, X., De La Cruz, L. K., Thareja, S., and Wang, B. (2018). Strategies to target the Hedgehog signaling pathway for cancer therapy. *Med. Res. Rev.* 38, 870–913. doi: 10.1002/med.21482

Xu, M., Gong, A., Yang, H., George, S. K., Jiao, Z., Huang, H., et al. (2015). Sonic hedgehog-glioma associated oncogene homolog 1 signaling enhances drug resistance in CD44(+)/Musashi-1(+) gastric cancer stem cells. *Cancer Lett.* 369, 124–133. doi: 10.1016/j.canlet.2015.08.005

Xu, M., Horrell, J., Snitow, M., Cui, J., Gochnauer, H., Syrett, C. M., et al. (2017). WNT10A mutation causes ectodermal dysplasia by impairing progenitor cell proliferation and KLF4-mediated differentiation. *Nat. Commun.* 8:15397. doi: 10.1038/ncomms15397

Xu, Y., Hong, Y., Xu, M., Ma, K., Fu, X., Zhang, M., et al. (2016). Role of Keratinocyte Growth Factor in the Differentiation of Sweat Gland-Like Cells From Human Umbilical Cord-Derived Mesenchymal Stem Cells. *Stem Cells Transl. Med.* 5, 106–116. doi: 10.5966/sctm.2015-0081

Xu, Y., Huang, S., Ma, K., Fu, X., Han, W., and Sheng, Z. (2012). Promising new potential for mesenchymal stem cells derived from human umbilical cord Wharton's jelly: sweat gland cell-like differentiative capacity. *J. Tissue Eng. Regen. Med.* 6, 645–654. doi: 10.1002/term.468

Yanagawa, S., Yokozeki, H., and Sato, K. (1986). Origin of periodic acid-Schiff-reactive glycoprotein in human eccrine sweat. *J. Appl. Physiol.* 60, 1615–1622. doi: 10.1152/jappl.1986.60.5.1615

Yao, B., Song, W., Li, Z., Hu, T., Wang, R., Wang, Y., et al. (2018). Irf6 directs glandular lineage differentiation of epidermal progenitors and promotes limited sweat gland regeneration in a mouse burn model. *Stem Cell Res. Ther.* 9:179. doi: 10.1186/s13287-018-0929-7

Yao, B., Wang, R., Wang, Y., Zhang, Y., Hu, T., Song, W., et al. (2020). Biochemical and structural cues of 3D-printed matrix synergistically direct MSC differentiation for functional sweat gland regeneration. *Sci. Adv.* 6:eaaz1094. doi: 10.1126/sciadv.aaz1094

Yao, B., Xie, J., Liu, N., Hu, T., Song, W., Huang, S., et al. (2019). Direct reprogramming of epidermal cells toward sweat gland-like cells by defined factors. *Cell Death Dis.* 10:272. doi: 10.1038/s41419-019-1503-7

Zhang, C., Chen, Y., and Fu, X. (2015). Sweat gland regeneration after burn injury: is stem cell therapy a new hope? *Cytotherapy* 17, 526–535. doi: 10.1016/j.jcyt.2014.10.016

Zhang, M., Li, H., Chen, L., Fang, S., Xie, S., and Lin, C. (2018). Three-dimensional reconstructed eccrine sweat glands with vascularization and cholinergic and adrenergic innervation. *J. Mol. Histol.* 49, 339–345. doi: 10.1007/s10735-018-9773-4

Zhao, Z., Xu, M., Wu, M., Ma, K., Sun, M., Tian, X., et al. (2015). Direct reprogramming of human fibroblasts into sweat gland-like cells. *Cell Cycle* 14, 3498–3505. doi: 10.1080/15384101.2015.1093707

Conflict of Interest: The authors declare that the research was conducted in the absence of any commercial or financial relationships that could be construed as a potential conflict of interest.

Publisher's Note: All claims expressed in this article are solely those of the authors and do not necessarily represent those of their affiliated organizations, or those of the publisher, the editors and the reviewers. Any product that may be evaluated in this article, or claim that may be made by its manufacturer, is not guaranteed or endorsed by the publisher.

frontiers in Cell and Developmental Biology

REVIEW
published: 03 August 2021
doi: 10.3389/fcell.2021.609452

Current Trends and Research Topics Regarding Intestinal Organoids: An Overview Based on Bibliometrics

Meng-Meng Zhang[1,2†], Ke-Lu Yang[3†], Yan-Cheng Cui[1], Yu-Shi Zhou[1], Hao-Ran Zhang[1], Quan Wang[1,2], Ying-Jiang Ye[1,2], Shan Wang[1,2] and Ke-Wei Jiang[1,2]*

[1] Department of Gastroenterological Surgery, Peking University People's Hospital, Beijing, China, [2] Laboratory of Surgical Oncology, Beijing Key Laboratory of Colorectal Cancer Diagnosis and Treatment Research, Peking University People's Hospital, Beijing, China, [3] Evidence-Based Nursing Center, School of Nursing, Lanzhou University, Lanzhou, China

Currently, research on intestinal diseases is mainly based on animal models and cell lines in monolayers. However, these models have drawbacks that limit scientific advances in this field. Three-dimensional (3D) culture systems named organoids are emerging as a reliable research tool for recapitulating the human intestinal epithelium and represent a unique platform for patient-specific drug testing. Intestinal organoids (IOs) are crypt–villus structures that can be derived from adult intestinal stem cells (ISCs), embryonic stem cells (ESCs), or induced pluripotent stem cells (iPSCs) and have the potential to serve as a platform for individualized medicine and research. However, this emerging field has not been bibliometric summarized to date. Here, we performed a bibliometric analysis of the Web of Science Core Collection (WoSCC) database to evaluate 5,379 publications concerning the use of organoids; the studies were divided into four clusters associated with the current situation and future directions for the application of IOs. Based on the results of our bibliometric analysis of IO applications, we systematically summarized the latest advances and analyzed the limitations and prospects.

Keywords: organoid, intestinal stem cell, bibliometric analysis, overview, preclinical models

OPEN ACCESS

Edited by:
Philip Iannaccone, Northwestern University, United States

Reviewed by:
Bernat Soria, Miguel Hernández University of Elche, Spain
Hans Clevers, Hubrecht Institute (KNAW), Netherlands

***Correspondence:**
Ke-Wei Jiang
jiangkewei@pkuph.edu.cn

[†] These authors have contributed equally to this work

Specialty section:
This article was submitted to Stem Cell Research, a section of the journal Frontiers in Cell and Developmental Biology

Received: *23 September 2020*
Accepted: *08 June 2021*
Published: *03 August 2021*

Citation:
Zhang M-M, Yang K-L, Cui Y-C, Zhou Y-S, Zhang H-R, Wang Q, Ye Y-J, Wang S and Jiang K-W (2021) Current Trends and Research Topics Regarding Intestinal Organoids: An Overview Based on Bibliometrics. Front. Cell Dev. Biol. 9:609452. doi: 10.3389/fcell.2021.609452

INTRODUCTION

Recent progressive improvements in personalized medicine as a result of substantial developments in molecular biology and genetic research indicate the need for preclinical studies. Cell lines grown in monolayers, patient-derived tumor xenografts (PDTXs), and genetically engineered mouse models (GEMMs) are commonly used in experimental research. However, most of these models fail to phenocopy the response of diseases and drugs directly (see **Table 1**); human cell lines originate from a single type of cancer or embryonic cells due to strong selection bias (e.g., normal epithelium-derived cell lines are immortalized by virus transformation), which cannot recreate complex cell–cell interactions, heterogeneous environments, and gene mutations or chromosomal abnormalities (Bein et al., 2018; Fujii and Sato, 2021); the associated costs, animal ethics, and species differences between experimental animals and humans are major issues that must be resolved (Sato and Clevers, 2013; Hickman et al., 2014; Liu et al., 2016; Bein et al., 2018; Kapalczynska et al., 2018; Pereira et al., 2018; Yin et al., 2019). Thus, identifying simpler, more robust, and widely available preclinical models for basic gastrointestinal research has rapidly become a subject of interest in recent decades.

TABLE 1 | Advantages and disadvantages of research models.

Features	*In vitro*		*In vivo*	
	Cell lines	**Organoid**	**CDX/PDX**	**GEMM**
Advantages	• Homogenous • Ease of passage and maintenance • Simple media • Immortalization • High-throughput drug screens • Lowest cost	• 3D structure • Parental heterogeneity • Self-renew and self-organization • Original genetic and histological profiles • High-throughput drug screens • Fast expansion	• Tumor–stroma interaction • Angiogenesis • Integrated TME • Original genetic and histological profiles	• Amenable to relevant genetic modification • Immune competent • *In situ* cancer research
Disadvantages	• Fails to reflect the physiological environment • Tissue morphology • Lacks stromal and infiltrating cells andmicroenvironment • Does not represent heterogeneity • Gene mutation or chromosomal abnormality	• Only epithelial origin • Lacks tumor–stroma interaction	• Time- and resource-consuming • Immune suppression • Complex ethical issuesComplicated operation • Fail to reproduce species-specific effect of human • Large scale experiments not possible	

To address the associated challenges, Sato et al. (2009) cultured self-organizing three-dimensional (3D) epithelial-like structures termed intestinal organoids (IOs), which are also known as "enteroids" or "mini-gut." Upon suspension in a luminal-rich scaffold (namely, Matrigel) with a defined set of niche factors, organoids present long-term growth and expansion. The term organoid was first mentioned in a study on tumor mechanisms in 1946 (Smith and Cochrane, 1946). Subsequently, its meaning evolved to generally refer to tissues or structures that are similar to organs, and the term has been increasingly used for *in vitro* biology. IOs are derived from tissue-resident stem/progenitor cells, including embryonic stem cells (ESCs) or induced pluripotent stem cells (iPSCs), and they recapitulate many aspects of their functionality *in vitro* (Lancaster and Knoblich, 2014). Human organoid culture protocols have been established for several additional organs or tissues, such as the stomach, esophagus, colon, pancreas, breast, liver, prostate, retina, and thyroid (Barker et al., 2010; Huch et al., 2013a,b; Zhang et al., 2013; DeWard et al., 2014; Karthaus et al., 2014; Saito et al., 2018; Dorgau et al., 2019). Compared with 2D cell lines, IOs maintain all hallmarks of the original tissue in terms of architecture, cell type, and self-renewal dynamics. Moreover, organoids exhibit superior epithelial natural physiology and have stable phenotypic and genetic characteristics (Sato and Clevers, 2013; Toden et al., 2018). Overall, the development of organoids fills the gap between genetics and patient trials. In the future, they can be subcultured and cryopreserved for a long time (Sato et al., 2009; Sato and Clevers, 2013; Hickman et al., 2014; Liu et al., 2016), which represents ideal characteristics for future basic research and therapeutic development.

As a novel and bona fide research model, IOs have raised hopes for research on disease modeling, therapeutic development, host–microbe interactions, biomolecule delivery, and intestinal biology and development. At present, a significant number of academic publications related to this relevant topic are contributed from worldwide institutions and laboratories. Since these publications are scattered, a robust conclusion of the research in IOs is needed to pull the literature together in a coherent way. Here, we first performed a bibliometric analysis to form a network map using keywords from publications on IOs and provided an in-depth and comprehensive understanding of IO research involved based on a large-scale publication. This technology-based review outlines dynamic topics in biomedical and clinical research over recent decades and focused on the limitations and strengths of IOs.

VISUALIZATION OF IOS BASED ON BIBLIOMETRICS

Current Developmental Trends of IO Headings

First, we performed a search query using "organoid" or "organoids" on the Web of Science Core Collection (WoSCC) database from 2009 (which was when the first report on organoids was published) to December 31, 2019, and 5,379 publications were found. Next, we conducted another search using the following terms: "intestinal organoids" or "mini-gut" or "enteroids" and identified 750 publications in all. These studies could be classified into 10 study types (see **Figure 1C**). Original articles (71.3%) were the most dominant type of publications throughout the whole period, and reviews accounted for 13.2% of articles. We used the polynomial model (see **Figure 1D**) to identify the number of publications on IO research in various research fields. The successful development of IOs was first reported in 2009, and the next 5 years showed slow and steady progress in the field. After 2015, the number of papers continued to show a growth trajectory, with a year-to-year increase in studies. Most research has mainly focused on cell biology and oncology in the fields of gastroenterology and hepatology. In addition, the number of papers published in immunology, pharmacology/pharmacy and chemistry, materials science and engineering, and infectious diseases and metabolism per year steadily increased. A similar trend of annual development was

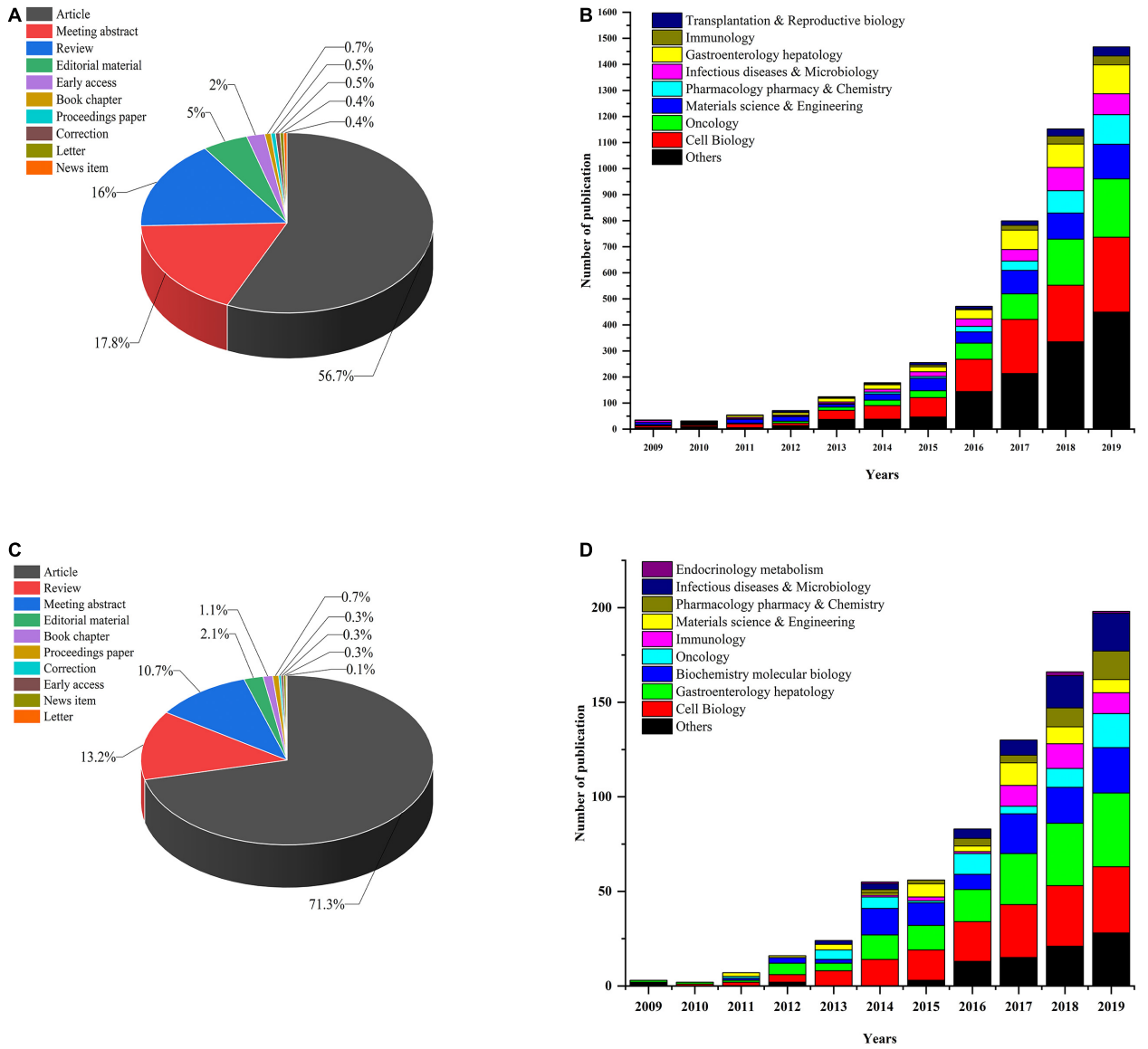

FIGURE 1 | (A) Organoid research papers by document type percentage; **(B)** distribution of different research fields and number of papers for organoids per year in 2009–2019. **(C)** IO research papers by document type percentage; **(D)** distribution of different research fields and number of papers for IOs per year since 2009.

observed for both the studies on organoids and IOs (see **Figure 1**).

Network Analysis of Research Topics

The network map of keywords was visualized by VOSveiwer 1.6.11 (Leiden University, Leiden, Netherlands). The node size in the network map represents the frequency of keywords, the links between nodes represent their co-occurrence, and the differences in node color indicate different clusters (Xie, 2015; Gao et al., 2019). Network analysis based on high-frequency keywords (see **Figure 2**) showed that the keywords from published papers could be clustered into four groups. The red region (Cluster #1, entitled "The formation of IO") included the main terms associated with stem cell and organoid formation, including stem cells, IOs, pluripotent stem cells, pathogenesis, human colon, enteroids, culture, and disease. The green region (Cluster #2, entitled "IO as a disease model") described the application of organoids in various fields, such as disease models and drug screening. The terms in the figure (Crohn's disease, tumorigenesis, homeostasis, colitis, microbiota, etc.) represent the current, relatively mature field of organoids. The blue area (Cluster #3, summarized as "IO for drug research") indicated that tissue-engineered intestine, including tissue transplantation and regeneration, could represent a new era in IO applications. Another interesting finding from these network maps was the yellow cluster, which was related to engineered biomaterials used in organoid systems (Cluster #4, indicated by "IO in organ regeneration and transplantation"), representing potential ways

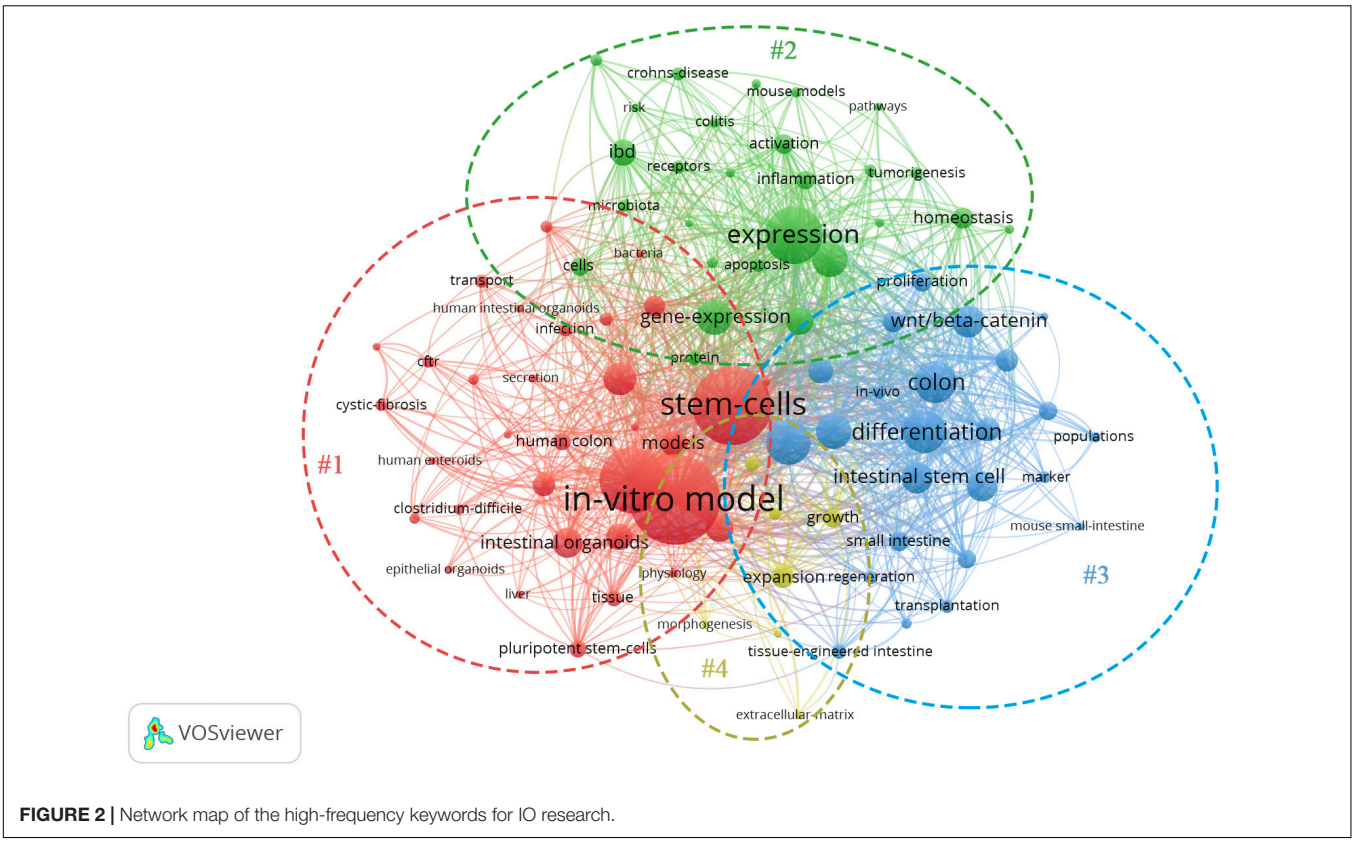

FIGURE 2 | Network map of the high-frequency keywords for IO research.

for overcoming the shortcomings of organoid systems. Although there are few studies on this topic at present, we believe that this topic will become the next hot spot in organoid research.

Based on the bibliometric findings, we will highlight recent advances and divide them into four research topics related to the application of IOs over the past decades with the expectation of more valuable conclusions in future follow-up studies (see **Figure 3**).

APPLICATIONS OF IOS ACCORDING TO THE FOUR CLUSTERS OF THE NETWORK ANALYSIS

The Formation of IOs

The gastrointestinal tract is an essential part of the human body responsible for digestion, nutrient absorption, and waste excretion (Okamoto and Watanabe, 2016). The intestinal epithelium is a single-cell layer that establishes a natural barrier against the external environment through a highly regulated self-renewal and differentiation process (Snijder and Pelkmans, 2011; Yui et al., 2012; Barker, 2014). Crypts are proliferative areas that harbor stem and progenitor cells at the base, and villi are differentiated regions that protrude into the lumen and consist of various terminally differentiated cell types; these two areas constitute the basic structure of self-renewing epithelial cells. Intestinal stem cells (ISCs) are indispensable at the start of the canonical crypt-to-villus hierarchical migratory hypothesis (Hendry and Potten, 1974; Bjerknes and Cheng, 2006). Two subgroups of ISCs can be identified: ISCs reside on the bottom of the crypt and are also referred to as crypt base columnar (CBC) cells, while +4 region cells stay in a quiescent state (Scoville et al., 2008). The intestinal epithelium maintains regenerative capacity and can be replaced every 3–4 days in mice and every week in humans. The specialized ISC population in the CBC is the main driving force of intestinal self-renewal (Sato et al., 2009; Kwon et al., 2020). For the sustainable maintenance of the intestinal epithelium, CBC cells that strongly express leucine-rich repeat-containing G protein-coupled receptor 5 (Lgr5) (Barker et al., 2007) provide progenitor cells during self-renewal (see **Figure 3**). Generally, Lgr5 + CBC cells differentiate into transit-amplifying (TA) cells, which migrate upward along the crypt–villus axis and further lose their proliferative ability, and finally generate mature epithelial cells, such as enterocytes, goblet cells, enteroendocrine cells, Paneth cells, and Tuft cells (Sato et al., 2011b; Yui et al., 2012).

Sato et al. (2009) utilized this self-organizing and self-renewal characteristic of ISCs to develop the first IO culture system from a single Lgr5 + ISC in mice. Accordingly, niche-mimicking and defined growth factors are added to the culture medium to either stimulate or inhibit signaling pathways involved in sustaining the self-renewal capabilities of the Lgr5 + ISCs (van der Flier and Clevers, 2009; Sato et al., 2011b; Clevers et al., 2014; van Rijn et al., 2016). The important ingredients of the small IO culture medium include R-spondin

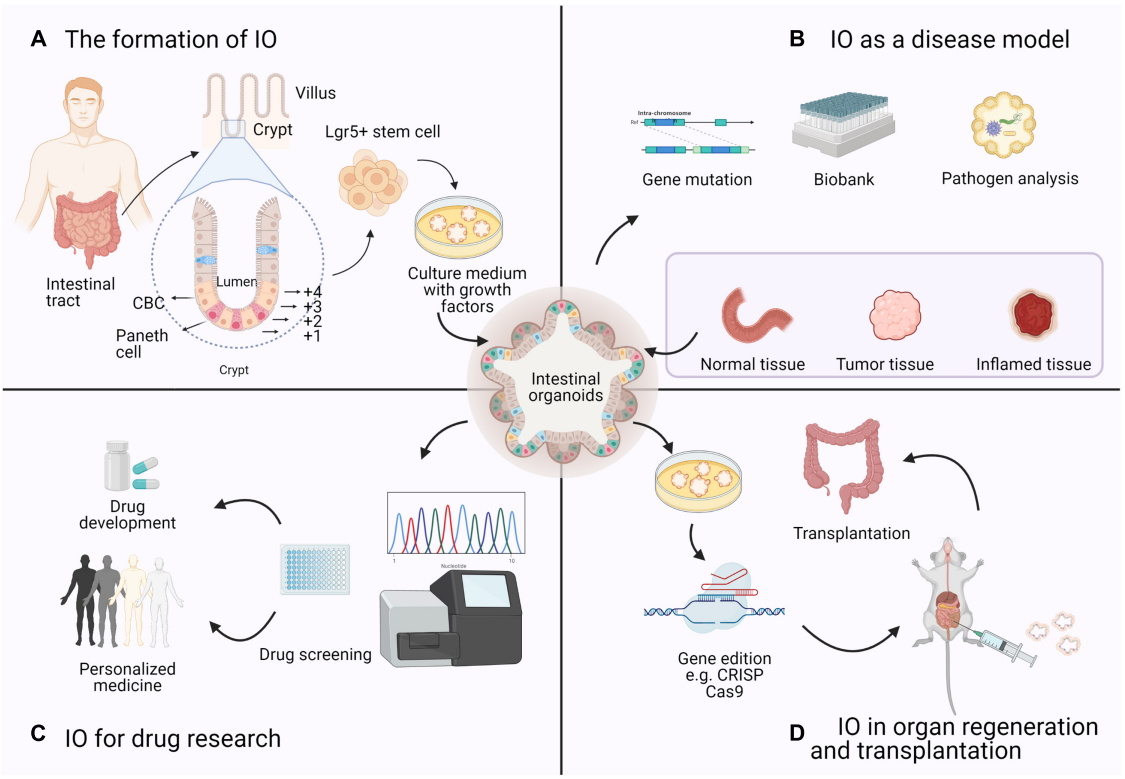

FIGURE 3 | Four research topics on the application of IOs based on bibliometrics. **(A)** The formation of IO: Organoids are derived from a single Lgr5 + ISC. ISCs reside either at the crypt base, between Paneth cells, as CBCs, or at position +4 from the bottom of the crypt. **(B)** IO as a disease model: Intestinal diseased organoids use samples from biopsies or resection and preserved as a biobank in basic research. **(C)** IO for drug research: Based on the sequencing results and gene–drug association links, high-throughput drug screening of candidate drugs can be performed in IOs to determine effective therapeutic strategies. **(D)** IO in organ regeneration and transplantation: Many studies of organoid transplantation and maturation are in progress, which means that organoids can be used as a source of cells or tissues with genetic mutations for regenerative medicine purposes.

1; Holmberg et al., 2017; Qi et al., 2017), epidermal growth factor (EGF), bone morphogenic protein (BMP) antagonist Noggin, and ROCK inhibitor Y-27632. R-spondin 1 is a Wnt agonist that induces marked crypt hyperplasia *in vivo* (Barker et al., 2007). An expansion in the number of crypts is induced by Noggin's transgene expression (Haramis et al., 2004). The Rho kinase inhibitor Y-27632 can inhibit anoikis of ESCs (Zhang et al., 2019), whereas WNT3A supplementation is necessary for colonic organoid cultures (Sato et al., 2009, 2011a). To reduce the commercial burden of these defined factors and simplify the media formulation for organoid culture, Miyoshi and Stappenbeck (2013) inverted a novel conditioned medium (CM) from the supernatant of L-WRN cells, which are derived from mouse L cells and secrete Wnt3aA, R-spondin 3, and noggin. Compared with recombinant media, L-WRN CM is relatively inexpensive and provides complete high-titer proteins to activate Wnt signaling pathways.

Morphologically, IOs recapitulate intestinal epithelial structures *in vivo*: single Lgr5 + ISCs initially form villus-like spherical structures with a closed-loop hollow lumen, and then the cyst buds up, differentiates into a crypt-like structure, and finally forms a mature organoid structure; subsequently, ISCs stay at the bottom of the budding domains, while other differentiated intestinal epithelial cells (IECs) migrate to the central cyst (Sato et al., 2009; Date and Sato, 2015). Moreover, IOs can maintain stable genetic characteristics and biological behavior after repeated freezing and passaging and require passaging at 1:3–1:4 every 3 days (VanDussen et al., 2015).

IOs as a Disease Model

Spence et al. (2011) generated an organoid system to mimic embryonic intestinal development. This system recapitulates the differentiation from human pluripotent stem cells (hPSCs) to polarized intestinal epithelium that is patterned into villus-like structures and crypt-like proliferative zones and contains all major epithelial cell types. This breakthrough demonstrates that human intestinal organoids (HIOs) can be used to study early events in intestinal disease development and identify unique disease preventive agents. Finkbeiner et al. (2015) demonstrated that HIOs closely resemble the fetal intestine and found that the ISC marker OLFM4 was expressed at extraordinarily low levels in the fetal intestine and HIOs but expressed at high levels in adult crypts, indicating that HIOs can be used to model fetal-to-adult gut maturation. A dysfunctional mutation in NEUROG3 induces congenital malabsorptive diarrhea because of the lack of enteroendocrine cells. Furthermore, knocking down

the NEUROG3 transcript *via* short hairpin RNA in hPSC-derived organoids has been reported to result in a reduction in intestinal enteroendocrine cells, suggesting that NEUROG3 expression can directly affect the development of intestinal enteroendocrine cells (Spence et al., 2011).

Over past decades, IOs have been widely used to study the pathophysiology of various human diseases, including colorectal carcinoma (CRC), gastrointestinal inflammation (such as inflammatory bowel disease, IBD), infectious diseases (such as those related to *Helicobacter* and *Salmonella*), malignancy, and genetic diseases (such as cystic fibrosis, CF).

Intestinal Carcinoma

Colorectal carcinoma is a heterogeneous disease that consists of genomic and epigenetic alterations (IJspeert et al., 2015). Organoids cultured from human CRC cells are more accurate models of CRC that present stable passage, easy operation, and indefinite expansion features. Correspondingly, transcriptomic profiling has shown that these "patients in the lab" can carry over the complete genotypic and biological characteristics of the original tumor (van de Wetering et al., 2015; Vlachogiannis et al., 2018; Lau et al., 2020).

Methods have been developed to culture CRC organoids originating from both surgery specimens and endoscopic biopsy tissues. Multiple collections of patient-derived organoid (PDO) cultures have been established. van de Wetering et al. (2015) collected tissue from 22 consecutive primary CRC patients and 19 normal controls to establish the first living organoid biobank, with a 90% success rate. Compared with normal hIOs, over 94% of IOs derived from CRC patients showed aberrant activation of the Wnt signaling pathway caused by mutations (Cancer Genome Atlas Network, 2012); therefore, Wnt and R spondin withdrawal culture medium was used to selectively expand tumor organoids with high purity (van de Wetering et al., 2015). Intestinally, further testing showed that in addition to Wnt activators, an optimal oxygen concentration and a p38 inhibitor were essential for the long-term passage of CRC organoids (Fujii et al., 2016). With improved culture conditions, living organoid biobanks representing rare histological subtypes (e.g., mucinous adenocarcinoma and neuroendocrine tumor), premalignant subtypes (e.g., hyperplastic polyps, sessile serrated adenoma/polyps, and tubulovillous adenoma), and metastatic CRC have been successfully established (Fujii et al., 2016). Another study (Vlachogiannis et al., 2018) obtained 110 biopsy specimens from patients with advanced colorectal and gastroesophageal cancer tissues and constructed 71 PDOs. According to the comparison of the drug response (including that of target therapies and chemotherapies) observed in patients and the *ex vivo* response in the respective PDOs, these PDOs have higher specificity and more accurate predictions than other models, indicating that they have the potential to be implemented in personalized medicine programs.

Sixty percent of all CRC cases arise from adenomatous polyps following the adenoma-carcinoma sequence (also named the conventional pathway) (Lau et al., 2020; Shaashua et al., 2020). Wnt signaling is continuously activated in the intestinal organs of APC-deficient mice, which interferes with the differentiation process. Transplanting APC gene-deficient organs into immunodeficient mice can cause subcutaneous tumor formation and activate the Kras signaling pathway to promote tumorigenesis (Onuma et al., 2013). Cao et al. (2015) established IOs derived from CRC-prone $Apc^{Min/+}$ mice to screen for epigenetically active compounds responsible for increasing organoid differentiation [including histone deacetylase (HDAC) inhibitors, sirtuin (SIRT) modulators, and methyltransferase inhibitors]. Xu et al. (2014) used $Apc^{Min/+}$ mouse intestinal epithelium to form APC gene-deficient heterozygous organs to mimic familial adenomatous polyposis and found that Rad21 is a crucial regulator of APC gene deficiency and plays a key role in the pathogenesis of colon cancer. Nadauld et al. (2014) found that TGFBR2 loss induces metastatic gastric cancer *via* shRNA knockdown in $Cdh1^{-/-}$ $Tp53^{-/-}$ murine organoids. With similar shRNA strategies, the Apc, p53, $Kras^{G12D}$, and Smad4 genes were knocked down in murine CRC organoids. These organoids exhibited an invasive adenocarcinoma-like histological structure and had tumorigenic tumors *in vivo* (Li et al., 2014). In 2018, scientists (Sakai et al., 2018) transplanted intestinal tumor-derived organoids carrying mutations in APC, $Kras^{G12D}$, and TGFBR2 into mice, and these organoids promoted intravasation and efficient liver metastasis.

Efficient genome cleavage by the CRISPR-Cas9 system in organoids contributes to defined gene defects mimicking the effect of tumors. By knocking out tumor suppressor factors, such as APC, TP53, and SMAD4, as well as overexpressing oncogenes, such as Kras and PI3K, by CRISP/Cas9, direct conversion of healthy human colon organoids into homologous cancerous organoids has been realized (Drost et al., 2015; Matano et al., 2015). Deleting certain DNA repair genes to simulate mismatch repair deficiency in human CRC organoids and dissecting predominant mutation signatures could be performed to systematically determine their molecular origins (Drost et al., 2017). Serrated colon adenoma is a precursor CRC subtype that is characterized by a serrated histopathological morphology and initiated by oncogene $BRAF^{V600E}$ mutations. Scientists have demonstrated that $BRAF^{V600E}$ mutations in combination with microenvironmental transforming growth factor-β (TGFβ) signaling drive the transformation from serrated colon adenoma to mesenchymal CRC in engineered $BRAF^{V600E}$-expressing human organoid cultures (Fessler et al., 2016). CRISPR-Cas9-based orthotopic transplantation models of organoids have also been established (O'Rourke et al., 2017; Roper et al., 2017). Organoids harboring Apc/Trp53 deletion were directly injected into the colonic epithelium for primary tumor and hepatic metastasis formation in mice without cancer-predisposing mutations. To promote high-throughput genetic testing and the functional characterization of tumor drivers, the latest studies developed a screening platform that uses a combined CRISPR-Cas9 library in PDOs from CRC patients, and it can identify tumor suppressor genes *in vivo* and *in vitro*. The platform is paired with a unique molecular identifier (UMI) to establish a CRISPR-UMI screening library for patient-specific functional genomics, thus allowing phenotypic research at a clonal level (Michels et al., 2020). Accordingly, organoids derived from a single cell that capture the intratumor heterogeneity of genetic

mutations can be a powerful tool to improve therapeutic strategies against CRC. Notably, in the PDO system, multiple passages should be avoided to ensure that the genetic features of the original tumors are maintained and prevent the continuous accrual of chromosome mis-segregations or replication errors in organoids with chromosomal instability.

Inflammatory Bowel Disease

Inflammatory bowel disease can cause damage to the epithelium of the small intestine (Crohn's disease, CD) and colon (ulcerative colitis, UC). The lack of an appropriate model for the intestinal epithelium in IBD has hindered studies on the possible mechanisms and drug development. Dotti et al. (2017) established UC epithelial organoids first and identified differential gene sets between UC and normal organoids. Interestingly, the genes upregulated in UC, including WNT3, EGF, DLL4, and BMP2, are key niche factors of Paneth cells in the murine small intestine. Another study used PDOs taken from the active lesions of CD patients and examined them *via* microfluid-based single-cell multiplex gene expression analysis (Suzuki et al., 2018). The results showed that the active lesion presents a distinct expression pattern of ISC marker genes, suggesting that small ISC properties are modified by unidentified factors in the inflammatory environment. These studies indicated that the inflammatory microenvironment in the ISC niche leads to a disrupted epithelial barrier and suggested that impaired epithelial regeneration could be a potential cause of the pathogenesis of UC.

Previous studies have re-established the inflammatory milieu in IO culture systems. Mutation of the autophagy-related gene ATG16L1 can cause necrotic apoptosis of the intestinal epithelium and Paneth cell dysfunction related to IBD. Stimulation with tumor necrosis factor-α (TNF-α) or its combination with interferon-γ induced Paneth cell loss and programmed necrosis in ATG16L1-deficient IOs. The cytoprotective function of ATG16L1 is related to the role of autophagy in promoting mitochondrial homeostasis, indicating the role of ATG16L1 in protecting IECs (Matsuzawa-Ishimoto et al., 2017; Pott et al., 2018). ATG16L1 deficiency also sensitizes mouse ileal organoids to the cytokine interleukin (IL)-22, a Crohn's disease-related cytokine that is associated with epithelial proliferation, tissue regeneration, inflammatory response, and transcriptional program regulation (Tsai et al., 2017; Powell et al., 2020). Studies have used the organoid survival rate as a determinant for ISC survival and organoid size as a measure of ISC proliferation, and they demonstrated that increased IL22 expression limits ISC expansion by controlling progenitor cell numbers and expansion (Zwarycz et al., 2019). Powell et al. (2020) analyzed transcriptomic data of PDOs from a large cohort of patients with active CD and found that IL22-responsive transcripts are highly correlated with the endoplasmic reticulum (ER) stress response transcription module of the colonic epithelium in active colitis patients. Both IL22 and ER stress are highly enriched in the colonic epithelium of active colitis patients and are positively correlated with the severity of colitis, suggesting that the IL22/ER stress axis plays an essential role in chronic inflammation development. *Via* whole-exome sequencing of uninflamed and inflamed organoids from the same UC patient, a recent study demonstrated that the inflamed epithelium of UC accumulates somatic mutations related to the IL-17–NF-κB signaling pathway. Notably, some of these mutations could exacerbate IBD but are irrelevant to tumorigenesis (Nanki et al., 2020). Khaloian et al. (2020) found that ileal crypts from inflamed $TNF^{\Delta ARE}$ mice with mitochondrial dysfunction caused by knocking out Hsp60 in Lgr5 + ISCs failed to grow mature organoids. Mitochondrial respiratory dysfunction resulted in lower Lgr5 expression in ISCs and promoted their differentiation into abnormal Paneth cells to influence the ISC niche. Taken together, these findings indicate that the IO model can be effectively used to provide insights into the mechanism of IBD according to pathways specific to the epithelium and genotype, and that it can also be used to identify new therapeutic targets.

Cystic Fibrosis

Intestinal organoid technology has had impressive impacts on research for the autosomal recessive disorder, CF, which is caused by mutations in the CF transmembrane conductance regulator (CFTR) gene that contribute to aberrant function of the chloride channel (Ratjen and Doring, 2003). Patients with CF suffer from the buildup of highly viscous mucus, and the main complications are persistent lung and gastrointestinal tract infections (Dekkers et al., 2016). Because various CFTR mutations (up to 2,000) are implicated in a broad spectrum of phenotypes, cell lines and animal models cannot faithfully mimic the self-renewal of CF-related cells (Dekkers et al., 2013). Because of the absence of well-defined molecular targets, CF patients lack effective treatment options.

The earliest use of IOs in CF was reported in 2012 (Liu et al., 2012): researchers used murine intestinal crypt cultures for physiological studies of crypt epithelium by focusing on the transport activity of the CFTR. Subsequently, Dekkers et al. (2013) collected ISCs from rectal biopsy specimens to generate organoids and developed a sophisticated microscopic assay called the forskolin-induced swelling (FIS) assay to model CFTR function. CFTR is the only channel that opens in a cAMP-dependent manner in the intestine. Forskolin increases the intracellular cyclic AMP concentration, thereby inducing the robust swelling of wild-type organoids. Correspondingly, swelling does not occur in CF organoids with abnormally functioning CFTR, is attenuated in organoids expressing CFTR-F508del (F508del is the most dominant CFTR mutation), and is totally lost in CFTR-deleted organoids. By applying PDO technology and FIS assays, this team demonstrated that cotreatment with the CFTR potentiator VX-770 and the CFTR corrector VX-809 was superior to a single treatment in restoring the function of CFTR-F508del (Dekkers et al., 2016). In addition, Clevers' team (Schwank et al., 2013) modified the CFTR locus by homologous recombination *via* CRISPR/Cas9 technology, wherein a normal CFTR gene was inserted into organoids from CF patients. The morphology, function, and gene expression of these PDOs were consistent with those of healthy organoids, and FIS was restored after repair. If these repaired organoids are reintroduced into the source patient, they may cure CF.

Thus, organoid technology provides a new scope for personalized treatment for CF patients.

Infectious Diseases

The human gastrointestinal epithelium is the prime interface for interactions with microorganisms. The healthy intestinal mucosal barrier is a finely tuned ecosystem of microbiota that maintains the balance between host–microbe interactions. Intestinal cell lines and animal models cannot accurately imitate gastrointestinal infectious diseases *in vitro* because of poor phenotypic, genetic, and epigenetic characteristics (Yin et al., 2015). Increasing studies are focusing on explaining the relationship between host–pathogen interactions in IO models. 3D enteric pathogen organoid models, including bacteria, viruses, and parasites, have been successfully established to explore the physiological role or pathogenic mechanism of the intestinal infectious diseases. Instances of such infectious agents include *Salmonella typhi* (Zhang et al., 2014; Wilson et al., 2015), enterohemorrhagic *Escherichia coli* (EHEC) (Foulke-Abel et al., 2014; In et al., 2016), *Clostridium difficile* (Engevik et al., 2015; Leslie et al., 2015), rotavirus (Saxena et al., 2016), norovirus (Ettayebi et al., 2016), enteroviruses (Drummond et al., 2017), and *Cryptosporidium* (Heo et al., 2018).

Many of the pathogens that infect humans fail to grow in 2D cultures. Although several attempts have been made over many years, scientists are still unsure how to grow human norovirus (HuNov) *ex vivo* because of the lack of a reproducible cultivation system. Research has used microinjections to mimic enteric infections, and this approach is more beneficial for the intestinal lumenal structure (Engevik et al., 2015). Ettayebi et al. (2016) established an ISC-derived organoid system to support HuNov replication *in vitro* and demonstrated that some variants (such as GII.3) replicate only in the environment of the intestinal cellular milieu constructed by bile, suggesting that IOs might be used as antivirals against norovirus. Rotaviruses are a common cause of acute, dehydrating, often fatal, gastroenteritis in infants and young children. Finkbeiner et al. (2012) tested that induced hIOs derived from differentiated stem cell lines can support replication of rotaviruses directly from stool samples. Compared with traditional cell line models, most rotavirus strains have about 10 times higher viral replication power, which supports the use of HIO as a new tool for human rotavirus research. Meanwhile, Heo et al. (2018) infected intestinal and lung organoids derived from healthy human donors with *Cryptosporidium parvum*. Of note, *Cryptosporidium* propagates within IOs, especially in differentiated organoids rather than expanding organoids, and recapitulates its complex life cycle with asexual and sexual stages *in vitro*. Present studies confirm that IO can also be a promising model for vaccines and antivirals. Yin et al. (2015) demonstrated that compared with 2D Caco-2 (immortalized human colonic adenocarcinoma) cell lines, hIOs are highly permissive to rotavirus infection. Furthermore, treatment of interferon-alpha or ribavirin that inhibited viral replication in organoids showed more sensitive and diverse antiviral effects. Next, this team testified the effects of PI3K–Akt–mTOR signaling on maintenance of rotavirus infection within hIOs, and the mTOR inhibitor, rapamycin, induced autophagy machinery to inhibit rotavirus replication, which may indicate that new therapeutic targets for antiviral drugs.

The threat caused by severe acute respiratory syndrome coronavirus 2 (SARS-CoV-2) is challenging health systems globally. Regarding the ongoing coronavirus disease 19 (COVID-19) pandemic, human organoids are also being utilized against SARS-CoV-2 infections (Hou et al., 2020; Wang et al., 2020; Zhou et al., 2020; Geurts et al., 2021). Compared with many cell lines, human organoids can be infected with SARS-CoV-2 easily without inducing the addition of key host factors, such as ACE2, which allows the examination of pathogen interactions with primary epithelial cells directly. These unanticipated findings provide new insight into enteroviral infection using IOs that provide a robust model system for studying rotavirus–host interactions and assessing antiviral medications.

IOs for Drug Research

The intestinal epithelium contains several drug-metabolism enzymes that play a vital role in the assessment of the pharmacokinetics of oral drugs, the metabolism of drugs, and the expression of uptake and efflux transporters (Onozato et al., 2018). The development of novel drugs is difficult, and the translation of innovative science into effective therapies has been seen as a major bottleneck in new drug research. Compared with the traditional drug screening model, IOs predict drug toxicity and human efficacy more accurately, thus making them an important alternative in drug screening and development that can provide perspective and highlight emerging opportunities.

Regarding pharmacokinetic functions, IOs generated from murine intestinal cells were successfully used to evaluate the function of the efflux transporter ATP-binding cassette, subfamily B, member 1/multidrug resistance 1 (ABCB1/MDR1) (Hilgendorf et al., 2007; International Transporter Consortium et al., 2010). In recent years, studies quantifying the excretion function of ABCB1/MDR1 using 3D IOs have been reported, and these organoids are expected to be applied to a P-gp inhibitor screening system (Mizutani et al., 2012; Zhang et al., 2016; Zhao et al., 2017). Onozato et al. (2018) successfully induced human iPSC differentiation in pharmacokinetically functional IOs by using A-83-01, PD98059, 5-azacytidine, and dual antiplatelet therapy (A/PD/5-aza/DAPT). This result indicates that human iPSC-derived IOs can serve as useful *in vitro* experimental systems in pharmacokinetic studies and accelerate the pace of mechanistic research.

Grabinger et al. (2014) found that IOs were 10–30 times more sensitive to 5-fluorouracil treatment than 2D cell lines *via* a modified MTT assay, suggesting that *ex vivo* IOs may reflect the sensitivity of intestinal crypt cells more closely *in vivo*. Next, they cultured IOs from mice with deletion of the pro-apoptotic Bcl-2 homolog Bim ($Bim^{-/-}$ mice) and wild-type mice and treated them with cisplatin, revealing that the sensitivity of IOs from $Bim^{-/-}$ knockout mice to cisplatin was significantly decreased and indicating that Bim is necessary for IO apoptosis induced by cisplatin. Another study (Lavitrano et al., 2020) used drug-resistant TP53-null colon cancer PDOs and demonstrated that silencing or chemical inhibition of p65BTK, a novel oncogenic isoform of Bruton's tyrosine kinase (BTK), helped overcome the

5-fluorouracil resistance of PDOs and significantly slowed the growth of xenografted tumors. Targeting p65BTK can restore the apoptotic response in drug-resistant CRC cells, suggesting that the combination of BTK inhibitors with 5-fluorouracil is a novel therapeutic approach for CRC patients.

High-throughput screening of 83 types of compounds and 22 types of living organoids from biobanks was applied to identify the most potent drugs for each organoid, and then the drug sensitivity was correlated with the genomic data to accurately detect the molecular markers related to drug effects and lesions. This organoid drug screening assay generates reproducible high-quality drug-sensitivity data. Vlachogiannis et al. (2018) collected 67 metastatic CRC biopsy samples from 61 patients and cultured 40 PDOs. These PDOs could be used to predict the patient response to irinotecan (I) and I + 5-fluorouracil (FI) combination therapy, which demonstrated that a response to FI combination therapy in a PDO indicated longer progression-free survival in the corresponding patient. This report was the first to show the prognostic value of PDOs in personalized medicine *via* a biobank of PDOs. Moreover, Buzzelli et al. (2018) validated that CRC liver metastasis organoids recapitulated the morphological characteristics and pathological stage of the corresponding tumor. These organoids were collected from patients who did not respond to oxaliplatin treatment or capecitabine therapy. The cultures were pretreated with three rounds of chemotherapy drugs for 4 days, and the loss of distinct lumen-like structures in the culture morphology was observed after chemotherapy. The results demonstrated that CRC liver metastasis organoids acquire chemotherapy resistance patterns and can be used as surrogates for drug testing. Furthermore, an additional study (Toden et al., 2018) using PDOs demonstrated that oligomeric proanthocyanidins (OPCs) in CRC protect against chemotherapy-induced toxicity by targeting cancer stem cells. Another study involving an organoid culture assay revealed that apigenin (Xu et al., 2016) suppresses CRC cell proliferation, migration, and invasion *via* inhibition of the Wnt/β-catenin signaling pathway. The results discussed above indicate that IOs can recapitulate the histological and genetic features of CRC tissues and may serve as useful drug screening models.

Organoids help bridge the gap between preclinical and clinical research by providing a relevant *in vitro* model of human diseases. The combination of newly established 3D patient organoid culture systems with personalized high-throughput drug screening and genomic analysis of patient-derived tumor samples offers a unique opportunity to stratify and identify effective cancer therapies for individual patients (Kriston-Vizi and Flotow, 2017).

IOs in Organ Regeneration and Transplantation

Organ transplantation is currently the best method for treating end-stage organ diseases. However, multiple problems, such as organ source, postoperative graft rejection, and complications, remain to be solved. Proof-of-concept studies have demonstrated the feasibility of expanding organoids from single stem cells and subsequent safe transplantation into animals.

Transplanting functional colonic organoids into a dextran sulfate-induced acute colitis mouse model can repair the damaged colonic epithelium, suggesting that organoids can expand from single adult colonic stem cells *in vitro* (Yui et al., 2012). Sugimoto et al. (2018) transplanted human colon organoids *in situ* into the submucosa of mouse colons and observed their growth in mice. Interestingly, the xenografts retained the original human characteristics rather than acquiring those of the mouse host; these features included the crypt–villus structure and Paneth cells. Patients with IBD who fail to respond to physical medication have to undergo enterectomy, which leads to a substantial reduction in quality of life. Yui et al. (2012) grafted mouse-derived colon organoids to cover the epithelial-defective region in mice with colitis. Four weeks later, the organoid-based xenografts had formed a single-layered epithelium that restored normal intestinal function and histology. A clinical trial (Shimizu et al., 2019) established an orthotopic xenograft system for IBD patients *via* organoids derived from colonoscopy biopsy samples. In the trial, the generated grafts enriched in ISCs were used to cover the wound, thus enabling the restoration of mucosal barrier integrity and local immune abnormalities. Therefore, ISC transplantation represents a potential therapeutic tool for IBD patients who do not respond to medication and refuse surgery. Nakamura and Sato (2018) proposed the use of tubular scaffolds to culture IOs into a tubular structure *in vitro* and showed subsequent anastomosis to the intestinal defect site *in vivo* after induction of differentiation. Furthermore, a panel of immunosuppressants was screened using human mini-guts to confirm that mycophenolic acid potently inhibits rotavirus infection by inhibiting inosine-50-monophosphate dehydrogenase (IMPDH) in the host, which indicates the possible dual benefits of mycophenolic acid in preventing organ rejection in transplantation patients and combatting rotavirus infection (Yin et al., 2016). In addition, various reports have described the development of transplantation procedures for gene-edited organoids that enable the generation of metastatic mouse models of CRC (see section "Intestinal Carcinoma"). These methods reveal the potential therapeutic applications of IOs in regenerative medicine; however, they are only theoretically feasible and need to be supported by clinical trial results.

Nonetheless, successful *in vivo* organoid-based engraftment of epithelial cultures remains challenging because of the lack of a supporting mesenchyme. Researchers in Ohio transplanted ESC-derived or iPSC-derived IOs into immunodeficient mice, and these HIOs not only formed mature human intestinal epithelium but also generated a laminated human mesenchyme (Watson et al., 2014). This research paved the way for future bioengineering studies. Recently, scientists (Gjorevski et al., 2016; Cruz-Acuna et al., 2017) performed decellularization, lyophilization, and grinding; radiation sterilization; digestion and neutralization; and other treatments on porcine small intestinal mucosa to produce extracellular matrix (ECM), which can retain nutrients such as collagen, elastin, and mucopolysaccharides. The mechanical properties and 3D structure were comparable to those of commercial Matrigel, and it has been verified that the characteristics of the ECM proteome are similar to those of human endoderm stem cell-differentiated tissues,

which can successfully cultivate human and mouse endoderm-like organoids (such as stomach, liver, pancreas, and small intestine). In addition to the ECM from animal tissue, the growing demand for non-xenobiotic materials is desirable for the application of human organoids. Gjorevski et al. (2016) established a new protocol by facilitating the required minimal adhesion by adding proteins such as RGD and laminin-111 to a poly ethylene glycol (PEG) hydrogel backbone. Poling et al. (2018) confirmed the importance of dynamic mechanical forces in HIO morphogenesis. A nitinol spring covered by a degradable capsule was implanted inside the HIOs, and it resulted in a significant increase in villus height, crypt depth, and crypt fission compared with that of the control HIOs. In addition to the similarity of the combination of the spring and HIOs to the human jejunum in morphology, the ISC compartment, vilification process, and smooth muscle thickness in the organoids plus spring group were significantly increased, indicating better barrier functions and smooth muscle motility. This new method is expected to accelerate the application of intestinal transplantation technology. These developments in biomaterials reveal the potential for the clinical application of human organoids.

In summary, IOs have been established from a range of different diseases, which lays a foundation for more studies on drug development and precision medicine. Of note, while autologous cell therapy transplantation is highly promising in the organoid field, its efficacy, safety, and immunogenicity are still pending evaluation.

LIMITATIONS AND DEVELOPMENT

Compared with traditional models, IO technology opens new horizons for disease research in areas including organogenesis, cellular differentiation, genomic analysis, cell–cell interaction, and physiological functions (see **Table 1**). This novel research tool has sufficient data support for large-scale experimental research. However, several shortcomings remain. First, an important inherent limitation of organoid culture is the lack of a mesenchymal structure, vasculature factors, and immune cells; accordingly, co-culture systems should be explored in the context of organoids. Second, although Matrigel-based IO culture systems can largely simulate the human intestinal epithelium, their spherical structure prevents external stimuli from entering the apical region, thus limiting their high-throughput testing, drug interactions, and microbial–epithelial interactions (Altay et al., 2019). Third, the enclosed lumen structure limits the secretion of materials, leads to the shedding of apoptotic cells from the luminal region, and influences the efficacy of drugs.

New insights have been reported regarding the abovementioned concerns. Ettayebi et al. (2016) first established human intestinal enteroid monolayer cultures that were inoculated with HuNov. In addition, a method of culturing organoids in a "hanging drop" without embedding them in Matrigel has attracted great interest, and this technique physically enhances cell-to-cell interactions due to the lack of rigid support (a glass or plastic surface) or a solidified ECM scaffold (Foty, 2011). Ueda et al. (2010) used mouse iPSCs to organize an enteric organoid with motor functions *in vitro* by a hanging drop culture system, which exhibited spontaneous contraction and highly coordinated peristalsis accompanied by the transportation of contents. Polish scientists (Panek et al., 2018) also formed organoids derived from chicken embryo intestines by applying a hanging drop system without embedding; this culture technique presents cost savings because it uses a smaller quantity of culture media and Matrigel. In addition, the solidification step of Matrigel is skipped, increasing the speed of the cell seeding process.

To overcome the obstacles in mimicking *in vivo* physiological coupling, a microfluidic-based 3D system called organ-on-a-chip has been developed (Bhatia and Ingber, 2014; Bein et al., 2018; Mittal et al., 2019). Organ-on-a-chip allows for two parallel hollow microchannels to be separated by a porous ECM-coated membrane. Kasendra et al. (2018) established a chip wherein human enteroids were cultured on an ECM-coated (Matrigel-type I collagen) membrane, and differential cells exposed their apical surfaces to an open lumen and interface with endothelium. In addition, this chip was reported to replicate normal intestinal functions, including nutrient absorption and mucus secretion. Recently, Liu et al. (2015) successfully mimicked the tumor microenvironment (TME) by co-culturing cancer cells and four TME-related cell types (fibroblasts, macrophages, human umbilical vein endothelial cells, and stromal cells) in a microfluidic device. The TME characteristics of paracrine interactions and macrophage migration were simulated in this system to enable the prediction of the effects of neoadjuvant chemotherapy. Taken together, these findings indicate that this novel technology can help better improve the efficacy and function of IOs.

Despite the remaining challenges, the future application of hIOs is still promising. The feasibility of using IOs as an accurate and high-throughput preclinical tool for precision medicine is being confirmed continuously. Given their comparable structure and behavior, IOs may serve as a relevant surrogate system for *in vitro* testing of intestinal epithelium-damaging drugs and toxins and for investigating cell death pathways, which will provide information on treatments that are ineffective for the patient, thus conserving valuable time for the development of effective therapeutic approaches for specific patients. The efficient culture of organoids makes it possible to screen individualized drugs within a clinical treatment time window and then to apply them to translational medicine and individualized treatment. It is believed that with an increased understanding and further innovations in organoid-related research, organoid culture will play an increasingly important role in scientific research.

The long-term IO model from single stem cells was first developed in 2009. In recent years, a growing body of literature has demonstrated that organoid technology has expanded to embrace genetic editing, omics-based drug screening analyses, and diverse co-culture systems with immune cells, viruses, bacteria, and parasites. Although IO culture protocols *in vitro* are relatively mature, the most urgent problems to be solved are how to characterize and verify that the established organoids present high fidelity with human biology and how to translate them

from human organoids *in vitro* to regenerative transplantation approaches *in vivo*. Deep profiling of the organoids using spatially resolved single-cell RNA sequencing could be a powerful tool for revealing the subgroups, differentiation degree, and state of cells. The "Organoid Cell Atlas" pilot project is currently ongoing to address the problems mentioned above (Bock et al., 2021). We believe that human organoid systems will provide unprecedented opportunities to improve human health.

AUTHOR CONTRIBUTIONS

M-MZ, Y-CC, SW, and K-WJ designed the review. K-LY and QW performed the literature search and analyzed the bibliometric data. Y-SZ and H-RZ assisted in publication searching and screening. M-MZ and K-LY wrote the manuscript. Y-CC, Y-JY, SW, and K-WJ reviewed and edited the manuscript. All authors contributed to the article and approved the submitted version.

REFERENCES

Altay, G., Larranaga, E., Tosi, S., Barriga, F. M., Batlle, E., Fernandez-Majada, V., et al. (2019). Self-organized intestinal epithelial monolayers in crypt and villus-like domains show effective barrier function. *Sci. Rep.* 9:10140. doi: 10.1038/s41598-019-46497-x

Barker, N. (2014). Adult intestinal stem cells: critical drivers of epithelial homeostasis and regeneration. *Nat. Rev. Mol. Cell Biol.* 15, 19–33.

Barker, N., Huch, M., Kujala, P., van de Wetering, M., Snippert, H. J., van Es, J. H., et al. (2010). Lgr5(+ve) stem cells drive self-renewal in the stomach and build long-lived gastric units in vitro. *Cell Stem Cell* 6, 25–36. doi: 10.1016/j.stem.2009.11.013

Barker, N., van Es, J. H., Kuipers, J., Kujala, P., van den Born, M., Cozijnsen, M., et al. (2007). Identification of stem cells in small intestine and colon by marker gene Lgr5. *Nature* 449, 1003–1007. doi: 10.1038/nature06196

Bein, A., Shin, W., Jalili-Firoozinezhad, S., Park, M. H., Sontheimer-Phelps, A., Tovaglieri, A., et al. (2018). Microfluidic organ-on-a-chip models of human intestine. *Cell. Mol. Gastroenterol. Hepatol.* 5, 659–668. doi: 10.1016/j.jcmgh.2017.12.010

Bhatia, S. N., and Ingber, D. E. (2014). Microfluidic organs-on-chips. *Nat. Biotechnol.* 32, 760–772. doi: 10.1038/nbt.2989

Bjerknes, M., and Cheng, H. (2006). Intestinal epithelial stem cells and progenitors. *Methods Enzymol.* 419, 337–383. doi: 10.1016/S0076-6879(06)19014-X

Bock, C., Boutros, M., Camp, J. G., Clarke, L., Clevers, H., Knoblich, J. A., et al. (2021). The organoid cell atlas. *Nat. Biotechnol.* 39, 13–17. doi: 10.1038/s41587-020-00762-x

Buzzelli, J. N., Ouaret, D., Brown, G., Allen, P. D., and Muschel, R. J. (2018). Colorectal cancer liver metastases organoids retain characteristics of original tumor and acquire chemotherapy resistance. *Stem Cell Res.* 27, 109–120. doi: 10.1016/j.scr.2018.01.016

Cancer Genome Atlas Network. (2012). Comprehensive molecular characterization of human colon and rectal cancer. *Nature* 487, 330–337. doi: 10.1038/nature11252

Cao, L., Kuratnik, A., Xu, W., Gibson, J. D., Kolling, F., Falcone, E. R., et al. (2015). Development of intestinal organoids as tissue surrogates: cell composition and the epigenetic control of differentiation. *Mol. Carcinog.* 54, 189–202. doi: 10.1002/mc.22089

Clevers, H., Loh, K. M., and Nusse, R. (2014). Stem cell signaling. an integral program for tissue renewal and regeneration: wnt signaling and stem cell control. *Science* 346:1248012. doi: 10.1126/science.1248012

Cruz-Acuna, R., Quiros, M., Farkas, A. E., Dedhia, P. H., Huang, S., Siuda, D., et al. (2017). Synthetic hydrogels for human intestinal organoid generation and colonic wound repair. *Nat. Cell Biol.* 19, 1326–1335. doi: 10.1038/ncb3632

Date, S., and Sato, T. (2015). Mini-gut organoids: reconstitution of the stem cell niche. *Annu. Rev. Cell Dev. Biol.* 31, 269–289. doi: 10.1146/annurev-cellbio-100814-125218

Dekkers, J. F., Berkers, G., Kruisselbrink, E., Vonk, A., de Jonge, H. R., Janssens, H. M., et al. (2016). Characterizing responses to CFTR-modulating drugs using rectal organoids derived from subjects with cystic fibrosis. *Sci. Transl. Med.* 8:344ra384. doi: 10.1126/scitranslmed.aad8278

Dekkers, J. F., van der Ent, C. K., and Beekman, J. M. (2013). Novel opportunities for CFTR-targeting drug development using organoids. *Rare Dis.* 1:e27112. doi: 10.4161/rdis.27112

DeWard, A. D., Cramer, J., and Lagasse, E. (2014). Cellular heterogeneity in the mouse esophagus implicates the presence of a nonquiescent epithelial stem cell population. *Cell Rep.* 9, 701–711. doi: 10.1016/j.celrep.2014.09.027

Dorgau, B., Felemban, M., Hilgen, G., Kiening, M., Zerti, D., Hunt, N. C., et al. (2019). Decellularised extracellular matrix-derived peptides from neural retina and retinal pigment epithelium enhance the expression of synaptic markers and light responsiveness of human pluripotent stem cell derived retinal organoids. *Biomaterials* 199, 63–75. doi: 10.1016/j.biomaterials.2019.01.028

Dotti, I., Mora-Buch, R., Ferrer-Picon, E., Planell, N., Jung, P., Masamunt, M. C., et al. (2017). Alterations in the epithelial stem cell compartment could contribute to permanent changes in the mucosa of patients with ulcerative colitis. *Gut* 66, 2069–2079. doi: 10.1136/gutjnl-2016-312609

Drost, J., van Boxtel, R., Blokzijl, F., Mizutani, T., Sasaki, N., Sasselli, V., et al. (2017). Use of CRISPR-modified human stem cell organoids to study the origin of mutational signatures in cancer. *Science* 358, 234–238. doi: 10.1126/science.aao3130

Drost, J., van Jaarsveld, R. H., Ponsioen, B., Zimberlin, C., van Boxtel, R., Buijs, A., et al. (2015). Sequential cancer mutations in cultured human intestinal stem cells. *Nature* 521, 43–47. doi: 10.1038/nature14415

Drummond, C. G., Bolock, A. M., Ma, C., Luke, C. J., Good, M., and Coyne, C. B. (2017). Enteroviruses infect human enteroids and induce antiviral signaling in a cell lineage-specific manner. *Proc. Natl. Acad. Sci. U.S.A.* 114, 1672–1677. doi: 10.1073/pnas.1617363114

Engevik, M. A., Engevik, K. A., Yacyshyn, M. B., Wang, J., Hassett, D. J., Darien, B., et al. (2015). Human clostridium difficile infection: inhibition of NHE3 and microbiota profile. *Am. J. Physiol. Gastrointest. Liver Physiol.* 308, G497–G509. doi: 10.1152/ajpgi.00090.2014

Ettayebi, K., Crawford, S. E., Murakami, K., Broughman, J. R., Karandikar, U., Tenge, V. R., et al. (2016). Replication of human noroviruses in stem cell-derived human enteroids. *Science* 353, 1387–1393. doi: 10.1126/science.aaf5211

Fessler, E., Drost, J., van Hooff, S. R., Linnekamp, J. F., Wang, X., Jansen, M., et al. (2016). TGFbeta signaling directs serrated adenomas to the mesenchymal colorectal cancer subtype. *EMBO Mol. Med.* 8, 745–760. doi: 10.15252/emmm.201606184

Finkbeiner, S. R., Hill, D. R., Altheim, C. H., Dedhia, P. H., Taylor, M. J., Tsai, Y. H., et al. (2015). Transcriptome-wide analysis reveals hallmarks of human intestine development and maturation *in vitro* and *in vivo*. *Stem Cell Rep.* 4, 1140–1155. doi: 10.1016/j.stemcr.2015.04.010

Finkbeiner, S. R., Zeng, X. L., Utama, B., Atmar, R. L., Shroyer, N. F., and Estes, M. K. (2012). Stem cell-derived human intestinal organoids as an infection model for rotaviruses. *mBio* 3:e00159. doi: 10.1128/mBio.00159-12

Foty, R. (2011). A simple hanging drop cell culture protocol for generation of 3D spheroids. *J. Vis. Exp.* 51:2720. doi: 10.3791/2720

Foulke-Abel, J., In, J., Kovbasnjuk, O., Zachos, N. C., Ettayebi, K., Blutt, S. E., et al. (2014). Human enteroids as an ex-vivo model of host-pathogen interactions in the gastrointestinal tract. *Exp. Biol. Med.* 239, 1124–1134. doi: 10.1177/1535370214529398

Fujii, M., and Sato, T. (2021). Somatic cell-derived organoids as prototypes of human epithelial tissues and diseases. *Nat. Mater.* 20, 156–169. doi: 10.1038/s41563-020-0754-0

Fujii, M., Shimokawa, M., Date, S., Takano, A., Matano, M., Nanki, K., et al. (2016). A colorectal tumor organoid library demonstrates progressive loss of niche factor requirements during tumorigenesis. *Cell Stem Cell* 18, 827–838. doi: 10.1016/j.stem.2016.04.003

Gao, Y., Shi, S., Ma, W., Chen, J., Cai, Y., Ge, L., et al. (2019). Bibliometric analysis of global research on PD-1 and PD-L1 in the field of cancer. *Int. Immunopharmacol.* 72, 374–384. doi: 10.1016/j.intimp.2019.03.045

Geurts, M. H., van der Vaart, J., Beumer, J., and Clevers, H. (2021). The organoid platform: promises and challenges as tools in the fight against COVID-19. *Stem Cell Rep.* 16, 412–418. doi: 10.1016/j.stemcr.2020.11.009

Gjorevski, N., Sachs, N., Manfrin, A., Giger, S., Bragina, M. E., Ordonez-Moran, P., et al. (2016). Designer matrices for intestinal stem cell and organoid culture. *Nature* 539, 560–564. doi: 10.1038/nature20168

Grabinger, T., Luks, L., Kostadinova, F., Zimberlin, C., Medema, J. P., Leist, M., et al. (2014). Ex vivo culture of intestinal crypt organoids as a model system for assessing cell death induction in intestinal epithelial cells and enteropathy. *Cell Death Dis.* 5:e1228. doi: 10.1038/cddis.2014.183

Haramis, A. P., Begthel, H., van den Born, M., van Es, J., Jonkheer, S., Offerhaus, G. J., et al. (2004). De novo crypt formation and juvenile polyposis on BMP inhibition in mouse intestine. *Science* 303, 1684–1686. doi: 10.1126/science.1093587

Hendry, J. H., and Potten, C. S. (1974). Cryptogenic cells and proliferative cells in intestinal epithelium. *Int. J. Radiat. Biol. Relat. Stud. Phys. Chem. Med.* 25, 583–588. doi: 10.1080/09553007414550771

Heo, I., Dutta, D., Schaefer, D. A., Iakobachvili, N., Artegiani, B., Sachs, N., et al. (2018). Modelling cryptosporidium infection in human small intestinal and lung organoids. *Nat. Microbiol.* 3, 814–823. doi: 10.1038/s41564-018-0177-8

Hickman, J. A., Graeser, R., de Hoogt, R., Vidic, S., Brito, C., Gutekunst, M., et al. (2014). Three-dimensional models of cancer for pharmacology and cancer cell biology: capturing tumor complexity in vitro/ex vivo. *Biotechnol. J.* 9, 1115–1128. doi: 10.1002/biot.201300492

Hilgendorf, C., Ahlin, G., Seithel, A., Artursson, P., Ungell, A. L., and Karlsson, J. (2007). Expression of thirty-six drug transporter genes in human intestine, liver, kidney, and organotypic cell lines. *Drug Metab. Dispos.* 35, 1333–1340. doi: 10.1124/dmd.107.014902

Holmberg, F. E., Seidelin, J. B., Yin, X., Mead, B. E., Tong, Z., Li, Y., et al. (2017). Culturing human intestinal stem cells for regenerative applications in the treatment of inflammatory bowel disease. *EMBO Mol. Med.* 9, 558–570. doi: 10.15252/emmm.201607260

Hou, Y. J., Okuda, K., Edwards, C. E., Martinez, D. R., Asakura, T., Dinnon, K. H. III, et al. (2020). SARS-CoV-2 reverse genetics reveals a variable infection gradient in the respiratory tract. *Cell* 182, 429–446. doi: 10.1016/j.cell.2020.05.042

Huch, M., Bonfanti, P., Boj, S. F., Sato, T., Loomans, C. J., van de Wetering, M., et al. (2013a). Unlimited in vitro expansion of adult bi-potent pancreas progenitors through the Lgr5/R-spondin axis. *EMBO J.* 32, 2708–2721. doi: 10.1038/emboj.2013.204

Huch, M., Dorrell, C., Boj, S. F., van Es, J. H., Li, V. S., van de Wetering, M., et al. (2013b). In vitro expansion of single Lgr5+ liver stem cells induced by Wnt-driven regeneration. *Nature* 494, 247–250. doi: 10.1038/nature11826

IJspeert, J. E., Vermeulen, L., Meijer, G. A., and Dekker, E. (2015). Serrated neoplasia-role in colorectal carcinogenesis and clinical implications. *Nat. Rev. Gastroenterol. Hepatol.* 12, 401–409. doi: 10.1038/nrgastro.2015.73

In, J., Foulke-Abel, J., Zachos, N. C., Hansen, A. M., Kaper, J. B., Bernstein, H. D., et al. (2016). Enterohemorrhagic *Escherichia coli* reduce mucus and intermicrovillar bridges in human stem cell-derived colonoids. *Cell. Mol. Gastroenterol. Hepatol.* 2, 48–62. doi: 10.1016/j.jcmgh.2015.10.001

International Transporter Consortium, Giacomini, K. M., Huang, S. M., Tweedie, D. J., Benet, L. Z., Brouwer, K. L., et al. (2010). Membrane transporters in drug development. *Nat. Rev. Drug Discov.* 9, 215–236. doi: 10.1038/nrd3028

Kapalczynska, M., Kolenda, T., Przybyla, W., Zajaczkowska, M., Teresiak, A., Filas, V., et al. (2018). 2D and 3D cell cultures - a comparison of different types of cancer cell cultures. *Arch. Med. Sci.* 14, 910–919. doi: 10.5114/aoms.2016.63743

Karthaus, W. R., Iaquinta, P. J., Drost, J., Gracanin, A., van Boxtel, R., Wongvipat, J., et al. (2014). Identification of multipotent luminal progenitor cells in human prostate organoid cultures. *Cell* 159, 163–175. doi: 10.1016/j.cell.2014.08.017

Kasendra, M., Tovaglieri, A., Sontheimer-Phelps, A., Jalili-Firoozinezhad, S., Bein, A., Chalkiadaki, A., et al. (2018). Development of a primary human Small Intestine-on-a-chip using biopsy-derived organoids. *Sci. Rep.* 8:2871. doi: 10.1038/s41598-018-21201-7

Khaloian, S., Rath, E., Hammoudi, N., Gleisinger, E., Blutke, A., Giesbertz, P., et al. (2020). Mitochondrial impairment drives intestinal stem cell transition into dysfunctional paneth cells predicting crohn's disease recurrence. *Gut* 69, 1939–1951. doi: 10.1136/gutjnl-2019-319514

Kriston-Vizi, J., and Flotow, H. (2017). Getting the whole picture: high content screening using three-dimensional cellular model systems and whole animal assays. *Cytometry A* 91, 152–159. doi: 10.1002/cyto.a.22907

Kwon, O., Han, T. S., and Son, M. Y. (2020). Intestinal morphogenesis in development, regeneration, and disease: the potential utility of intestinal organoids for studying compartmentalization of the crypt-villus structure. *Front. Cell Dev. Biol.* 8:593969. doi: 10.3389/fcell.2020.593969

Lancaster, M. A., and Knoblich, J. A. (2014). Organogenesis in a dish: modeling development and disease using organoid technologies. *Science* 345:1247125. doi: 10.1126/science.1247125

Lau, H. C. H., Kranenburg, O., Xiao, H., and Yu, J. (2020). Organoid models of gastrointestinal cancers in basic and translational research. *Nat. Rev. Gastroenterol. Hepatol.* 17, 203–222. doi: 10.1038/s41575-019-0255-2

Lavitrano, M., Ianzano, L., Bonomo, S., Cialdella, A., Cerrito, M. G., Pisano, F., et al. (2020). BTK inhibitors synergise with 5-FU to treat drug-resistant TP53-null colon cancers. *J. Pathol.* 250, 134–147. doi: 10.1002/path.5347

Leslie, J. L., Huang, S., Opp, J. S., Nagy, M. S., Kobayashi, M., Young, V. B., et al. (2015). Persistence and toxin production by clostridium difficile within human intestinal organoids result in disruption of epithelial paracellular barrier function. *Infect. Immun.* 83, 138–145. doi: 10.1128/IAI.02561-14

Li, X., Nadauld, L., Ootani, A., Corney, D. C., Pai, R. K., Gevaert, O., et al. (2014). Oncogenic transformation of diverse gastrointestinal tissues in primary organoid culture. *Nat. Med.* 20, 769–777. doi: 10.1038/nm.3585

Liu, F., Huang, J., Ning, B., Liu, Z., Chen, S., and Zhao, W. (2016). Drug discovery via human-derived stem cell organoids. *Front. Pharmacol.* 7:334. doi: 10.3389/fphar.2016.00334

Liu, J., Walker, N. M., Cook, M. T., Ootani, A., and Clarke, L. L. (2012). Functional CFTR in crypt epithelium of organotypic enteroid cultures from murine small intestine. *Am. J. Physiol. Cell Physiol.* 302, C1492–C1503. doi: 10.1152/ajpcell.00392.2011

Liu, P. F., Cao, Y. W., Zhang, S. D., Zhao, Y., Liu, X. G., Shi, H. Q., et al. (2015). A bladder cancer microenvironment simulation system based on a microfluidic co-culture model. *Oncotarget* 6, 37695–37705. doi: 10.18632/oncotarget.6070

Matano, M., Date, S., Shimokawa, M., Takano, A., Fujii, M., Ohta, Y., et al. (2015). Modeling colorectal cancer using CRISPR-Cas9-mediated engineering of human intestinal organoids. *Nat. Med.* 21, 256–262. doi: 10.1038/nm.3802

Matsuzawa-Ishimoto, Y., Shono, Y., Gomez, L. E., Hubbard-Lucey, V. M., Cammer, M., Neil, J., et al. (2017). Autophagy protein ATG16L1 prevents necroptosis in the intestinal epithelium. *J. Exp. Med.* 214, 3687–3705. doi: 10.1084/jem.20170558

Michels, B. E., Mosa, M. H., Streibl, B. I., Zhan, T., Menche, C., Abou-El-Ardat, K., et al. (2020). Pooled in vitro and in vivo CRISPR-Cas9 screening identifies tumor suppressors in human colon organoids. *Cell Stem Cell* 26, 782–792. doi: 10.1016/j.stem.2020.04.003

Mittal, R., Woo, F. W., Castro, C. S., Cohen, M. A., Karanxha, J., Mittal, J., et al. (2019). Organ-on-chip models: implications in drug discovery and clinical applications. *J. Cell. Physiol.* 234, 8352–8380. doi: 10.1002/jcp.27729

Miyoshi, H., and Stappenbeck, T. S. (2013). In vitro expansion and genetic modification of gastrointestinal stem cells in spheroid culture. *Nat. Protoc.* 8, 2471–2482. doi: 10.1038/nprot.2013.153

Mizutani, T., Nakamura, T., Morikawa, R., Fukuda, M., Mochizuki, W., Yamauchi, Y., et al. (2012). Real-time analysis of P-glycoprotein-mediated drug transport across primary intestinal epithelium three-dimensionally cultured in vitro. *Biochem. Biophys. Res. Commun.* 419, 238–243. doi: 10.1016/j.bbrc.2012.01.155

Nadauld, L. D., Garcia, S., Natsoulis, G., Bell, J. M., Miotke, L., Hopmans, E. S., et al. (2014). Metastatic tumor evolution and organoid modeling implicate TGFBR2 as a cancer driver in diffuse gastric cancer. *Genome Biol.* 15:428. doi: 10.1186/s13059-014-0428-9

Nakamura, T., and Sato, T. (2018). Advancing intestinal organoid technology toward regenerative medicine. *Cell. Mol. Gastroenterol. Hepatol.* 5, 51–60. doi: 10.1016/j.jcmgh.2017.10.006

Nanki, K., Fujii, M., Shimokawa, M., Matano, M., Nishikori, S., Date, S., et al. (2020). Somatic inflammatory gene mutations in human ulcerative colitis epithelium. *Nature* 577, 254–259. doi: 10.1038/s41586-019-1844-5

O'Rourke, K. P., Loizou, E., Livshits, G., Schatoff, E. M., Baslan, T., Manchado, E., et al. (2017). Transplantation of engineered organoids enables rapid generation of metastatic mouse models of colorectal cancer. *Nat. Biotechnol.* 35, 577–582. doi: 10.1038/nbt.3837

Okamoto, R., and Watanabe, M. (2016). Role of epithelial cells in the pathogenesis and treatment of inflammatory bowel disease. *J. Gastroenterol.* 51, 11–21. doi: 10.1007/s00535-015-1098-4

Onozato, D., Yamashita, M., Nakanishi, A., Akagawa, T., Kida, Y., Ogawa, I., et al. (2018). Generation of intestinal organoids suitable for pharmacokinetic studies from human induced pluripotent stem cells. *Drug Metab. Dispos.* 46, 1572–1580. doi: 10.1124/dmd.118.080374

Onuma, K., Ochiai, M., Orihashi, K., Takahashi, M., Imai, T., Nakagama, H., et al. (2013). Genetic reconstitution of tumorigenesis in primary intestinal cells. *Proc. Natl. Acad. Sci. U.S.A.* 110, 11127–11132. doi: 10.1073/pnas.1221926110

Panek, M., Grabacka, M., and Pierzchalska, M. (2018). The formation of intestinal organoids in a hanging drop culture. *Cytotechnology* 70, 1085–1095. doi: 10.1007/s10616-018-0194-8

Pereira, I., Lechanteur, A., and Sarmento, B. (2018). 3D model replicating the intestinal function to evaluate drug permeability. *Methods Mol. Biol.* 1817, 107–113. doi: 10.1007/978-1-4939-8600-2_11

Poling, H. M., Wu, D., Brown, N., Baker, M., Hausfeld, T. A., Huynh, N., et al. (2018). Mechanically induced development and maturation of human intestinal organoids in vivo. *Nat. Biomed. Eng.* 2, 429–442. doi: 10.1038/s41551-018-0243-9

Pott, J., Kabat, A. M., and Maloy, K. J. (2018). Intestinal epithelial cell autophagy is required to protect against TNF-induced apoptosis during chronic colitis in mice. *Cell Host Microbe* 23, 191–202. doi: 10.1016/j.chom.2017.12.017

Powell, N., Pantazi, E., Pavlidis, P., Tsakmaki, A., Li, K., Yang, F., et al. (2020). Interleukin-22 orchestrates a pathological endoplasmic reticulum stress response transcriptional programme in colonic epithelial cells. *Gut* 69, 578–590. doi: 10.1136/gutjnl-2019-318483

Qi, Z., Li, Y., Zhao, B., Xu, C., Liu, Y., Li, H., et al. (2017). BMP restricts stemness of intestinal Lgr5(+) stem cells by directly suppressing their signature genes. *Nat. Commun.* 8:13824. doi: 10.1038/ncomms13824

Ratjen, F., and Doring, G. (2003). Cystic fibrosis. *Lancet* 361, 681–689. doi: 10.1016/S0140-6736(03)12567-6

Roper, J., Tammela, T., Cetinbas, N. M., Akkad, A., Roghanian, A., Rickelt, S., et al. (2017). In vivo genome editing and organoid transplantation models of colorectal cancer and metastasis. *Nat. Biotechnol.* 35, 569–576. doi: 10.1038/nbt.3836

Saito, Y., Onishi, N., Takami, H., Seishima, R., Inoue, H., Hirata, Y., et al. (2018). Development of a functional thyroid model based on an organoid culture system. *Biochem. Biophys. Res. Commun.* 497, 783–789. doi: 10.1016/j.bbrc.2018.02.154

Sakai, E., Nakayama, M., Oshima, H., Kouyama, Y., Niida, A., Fujii, S., et al. (2018). Combined mutation of Apc, Kras, and Tgfbr2 effectively drives metastasis of intestinal cancer. *Cancer Res.* 78, 1334–1346. doi: 10.1158/0008-5472.CAN-17-3303

Sato, T., and Clevers, H. (2013). Growing self-organizing mini-guts from a single intestinal stem cell: mechanism and applications. *Science* 340, 1190–1194. doi: 10.1126/science.1234852

Sato, T., Stange, D. E., Ferrante, M., Vries, R. G., Van Es, J. H., Van den Brink, S., et al. (2011a). Long-term expansion of epithelial organoids from human colon, adenoma, adenocarcinoma, and Barrett's epithelium. *Gastroenterology* 141, 1762–1772. doi: 10.1053/j.gastro.2011.07.050

Sato, T., van Es, J. H., Snippert, H. J., Stange, D. E., Vries, R. G., van den Born, M., et al. (2011b). Paneth cells constitute the niche for Lgr5 stem cells in intestinal crypts. *Nature* 469, 415–418. doi: 10.1038/nature09637

Sato, T., Vries, R. G., Snippert, H. J., van de Wetering, M., Barker, N., Stange, D. E., et al. (2009). Single Lgr5 stem cells build crypt-villus structures in vitro without a mesenchymal niche. *Nature* 459, 262–265. doi: 10.1038/nature07935

Saxena, K., Blutt, S. E., Ettayebi, K., Zeng, X. L., Broughman, J. R., Crawford, S. E., et al. (2016). Human intestinal enteroids: a new model to study human rotavirus infection, host restriction, and pathophysiology. *J. Virol.* 90, 43–56. doi: 10.1128/JVI.01930-15

Schwank, G., Koo, B. K., Sasselli, V., Dekkers, J. F., Heo, I., Demircan, T., et al. (2013). Functional repair of CFTR by CRISPR/Cas9 in intestinal stem cell organoids of cystic fibrosis patients. *Cell Stem Cell* 13, 653–658. doi: 10.1016/j.stem.2013.11.002

Scoville, D. H., Sato, T., He, X. C., and Li, L. (2008). Current view: intestinal stem cells and signaling. *Gastroenterology* 134, 849–864. doi: 10.1053/j.gastro.2008.01.079

Shaashua, L., Mayer, S., Lior, C., Lavon, H., Novoselsky, A., and Scherz-Shouval, R. (2020). Stromal expression of the core clock gene period 2 is essential for tumor initiation and metastatic colonization. *Front. Cell Dev. Biol.* 8:587697. doi: 10.3389/fcell.2020.587697

Shimizu, H., Suzuki, K., Watanabe, M., and Okamoto, R. (2019). Stem cell-based therapy for inflammatory bowel disease. *Intest. Res.* 17, 311–316. doi: 10.5217/ir.2019.00043

Smith, E., and Cochrane, W. J. (1946). Cystic organoid teratoma: (report of a case). *Can. Med. Assoc. J.* 55, 151–152.

Snijder, B., and Pelkmans, L. (2011). Origins of regulated cell-to-cell variability. *Nat. Rev. Mol. Cell Biol.* 12, 119–125. doi: 10.1038/nrm3044

Spence, J. R., Mayhew, C. N., Rankin, S. A., Kuhar, M. F., Vallance, J. E., Tolle, K., et al. (2011). Directed differentiation of human pluripotent stem cells into intestinal tissue in vitro. *Nature* 470, 105–109. doi: 10.1038/nature09691

Sugimoto, S., Ohta, Y., Fujii, M., Matano, M., Shimokawa, M., Nanki, K., et al. (2018). Reconstruction of the human colon epithelium in vivo. *Cell Stem Cell* 22, 171–176. doi: 10.1016/j.stem.2017.11.012

Suzuki, K., Murano, T., Shimizu, H., Ito, G., Nakata, T., Fujii, S., et al. (2018). Single cell analysis of Crohn's disease patient-derived small intestinal organoids reveals disease activity-dependent modification of stem cell properties. *J. Gastroenterol.* 53, 1035–1047. doi: 10.1007/s00535-018-1437-3

Toden, S., Ravindranathan, P., Gu, J., Cardenas, J., Yuchang, M., and Goel, A. (2018). Oligomeric proanthocyanidins (OPCs) target cancer stem-like cells and suppress tumor organoid formation in colorectal cancer. *Sci. Rep.* 8:3335. doi: 10.1038/s41598-018-21478-8

Tsai, P. Y., Zhang, B., He, W. Q., Zha, J. M., Odenwald, M. A., Singh, G., et al. (2017). IL-22 upregulates epithelial claudin-2 to drive diarrhea and enteric pathogen clearance. *Cell Host Microbe* 21, 671–681.e4. doi: 10.1016/j.chom.2017.05.009

Ueda, T., Yamada, T., Hokuto, D., Koyama, F., Kasuda, S., Kanehiro, H., et al. (2010). Generation of functional gut-like organ from mouse induced pluripotent stem cells. *Biochem. Biophys. Res. Commun.* 391, 38–42. doi: 10.1016/j.bbrc.2009.10.157

van de Wetering, M., Francies, H. E., Francis, J. M., Bounova, G., Iorio, F., Pronk, A., et al. (2015). Prospective derivation of a living organoid biobank of colorectal cancer patients. *Cell* 161, 933–945. doi: 10.1016/j.cell.2015.03.053

van der Flier, L. G., and Clevers, H. (2009). Stem cells, self-renewal, and differentiation in the intestinal epithelium. *Annu. Rev. Physiol.* 71, 241–260. doi: 10.1146/annurev.physiol.010908.163145

van Rijn, J. M., Schneeberger, K., Wiegerinck, C. L., Nieuwenhuis, E. E., and Middendorp, S. (2016). Novel approaches: tissue engineering and stem cells–in vitro modelling of the gut. *Best Pract. Res. Clin. Gastroenterol.* 30, 281–293. doi: 10.1016/j.bpg.2016.03.005

VanDussen, K. L., Marinshaw, J. M., Shaikh, N., Miyoshi, H., Moon, C., Tarr, P. I., et al. (2015). Development of an enhanced human gastrointestinal epithelial culture system to facilitate patient-based assays. *Gut* 64, 911–920. doi: 10.1136/gutjnl-2013-306651

Vlachogiannis, G., Hedayat, S., Vatsiou, A., Jamin, Y., Fernandez-Mateos, J., Khan, K., et al. (2018). Patient-derived organoids model treatment response of metastatic gastrointestinal cancers. *Science* 359, 920–926. doi: 10.1126/science.aao2774

Wang, M., Cao, R., Zhang, L., Yang, X., Liu, J., Xu, M., et al. (2020). Remdesivir and chloroquine effectively inhibit the recently emerged novel coronavirus (2019-nCoV) in vitro. *Cell Res.* 30, 269–271. doi: 10.1038/s41422-020-0282-0

Watson, C. L., Mahe, M. M., Munera, J., Howell, J. C., Sundaram, N., Poling, H. M., et al. (2014). An in vivo model of human small intestine using pluripotent stem cells. *Nat. Med.* 20, 1310–1314. doi: 10.1038/nm.3737

Wilson, S. S., Tocchi, A., Holly, M. K., Parks, W. C., and Smith, J. G. (2015). A small intestinal organoid model of non-invasive enteric pathogen-epithelial cell interactions. *Mucosal Immunol.* 8, 352–361. doi: 10.1038/mi.2014.72

Xie, P. (2015). Study of international anticancer research trends via co-word and document co-citation visualization analysis. *Scientometrics* 105, 611–622. doi: 10.1007/s11192-015-1689-0

Xu, H., Yan, Y., Deb, S., Rangasamy, D., Germann, M., Malaterre, J., et al. (2014). Cohesin Rad21 mediates loss of heterozygosity and is upregulated via WNT promoting transcriptional dysregulation in gastrointestinal tumors. *Cell Rep.* 9, 1781–1797. doi: 10.1016/j.celrep.2014.10.059

Xu, M., Wang, S., Song, Y. U., Yao, J., Huang, K., and Zhu, X. (2016). Apigenin suppresses colorectal cancer cell proliferation, migration and invasion via inhibition of the Wnt/beta-catenin signaling pathway. *Oncol. Lett.* 11, 3075–3080. doi: 10.3892/ol.2016.4331

Yin, Y., Bijvelds, M., Dang, W., Xu, L., van der Eijk, A. A., Knipping, K., et al. (2015). Modeling rotavirus infection and antiviral therapy using primary intestinal organoids. *Antiviral Res.* 123, 120–131. doi: 10.1016/j.antiviral.2015.09.010

Yin, Y., Wang, Y., Dang, W., Xu, L., Su, J., Zhou, X., et al. (2016). Mycophenolic acid potently inhibits rotavirus infection with a high barrier to resistance development. *Antiviral Res.* 133, 41–49. doi: 10.1016/j.antiviral.2016.07.017

Yin, Y. B., de Jonge, H. R., Wu, X., and Yin, Y. L. (2019). Mini-gut: a promising model for drug development. *Drug Discov. Today* 24, 1784–1794. doi: 10.1016/j.drudis.2019.06.006

Yui, S., Nakamura, T., Sato, T., Nemoto, Y., Mizutani, T., Zheng, X., et al. (2012). Functional engraftment of colon epithelium expanded in vitro from a single adult Lgr5(+) stem cell. *Nat. Med.* 18, 618–623. doi: 10.1038/nm.2695

Zhang, X., Claerhout, S., Prat, A., Dobrolecki, L. E., Petrovic, I., Lai, Q., et al. (2013). A renewable tissue resource of phenotypically stable, biologically and ethnically diverse, patient-derived human breast cancer xenograft models. *Cancer Res.* 73, 4885–4897. doi: 10.1158/0008-5472.CAN-12-4081

Zhang, X., Qin, J., Xie, Z., Liu, C., Su, Y., Chen, Z., et al. (2019). Y-27632 preserves epidermal integrity in a human skin organ-culture (hSOC) system by regulating AKT and ERK signaling pathways. *J. Dermatol. Sci.* 96, 99–109. doi: 10.1016/j.jdermsci.2019.10.006

Zhang, Y., Zeng, Z., Zhao, J., Li, D., Liu, M., and Wang, X. (2016). Measurement of rhodamine 123 in three-dimensional organoids: a novel model for p-glycoprotein inhibitor screening. *Basic Clin. Pharmacol. Toxicol.* 119, 349–352. doi: 10.1111/bcpt.12596

Zhang, Y. G., Wu, S., Xia, Y., and Sun, J. (2014). *Salmonella*-infected crypt-derived intestinal organoid culture system for host-bacterial interactions. *Physiol. Rep.* 2:e12147. doi: 10.14814/phy2.12147

Zhao, J., Zeng, Z., Sun, J., Zhang, Y., Li, D., Zhang, X., et al. (2017). A novel model of P-glycoprotein inhibitor screening using human small intestinal organoids. *Basic Clin. Pharmacol. Toxicol.* 120, 250–255. doi: 10.1111/bcpt.12680

Zhou, J., Li, C., Liu, X., Chiu, M. C., Zhao, X., Wang, D., et al. (2020). Infection of bat and human intestinal organoids by SARS-CoV-2. *Nat. Med.* 26, 1077–1083. doi: 10.1038/s41591-020-0912-6

Zwarycz, B., Gracz, A. D., Rivera, K. R., Williamson, I. A., Samsa, L. A., Starmer, J., et al. (2019). IL22 inhibits epithelial stem cell expansion in an ileal organoid model. *Cell. Mol. Gastroenterol. Hepatol.* 7, 1–17. doi: 10.1016/j.jcmgh.2018.06.008

Conflict of Interest: The authors declare that the research was conducted in the absence of any commercial or financial relationships that could be construed as a potential conflict of interest.

Publisher's Note: All claims expressed in this article are solely those of the authors and do not necessarily represent those of their affiliated organizations, or those of the publisher, the editors and the reviewers. Any product that may be evaluated in this article, or claim that may be made by its manufacturer, is not guaranteed or endorsed by the publisher.

frontiers in Cell and Developmental Biology

ORIGINAL RESEARCH
published: 13 August 2021
doi: 10.3389/fcell.2021.710159

Hair Cell Generation in Cochlear Culture Models Mediated by Novel γ-Secretase Inhibitors

Silvia T. Erni[1,2,3,4], John C. Gill[5], Carlotta Palaferri[1,2,3], Gabriella Fernandes[1,2,3], Michelle Buri[1,2,3], Katherine Lazarides[5], Denis Grandgirard[1,2], Albert S. B. Edge[6,7,8†], Stephen L. Leib[1,2†] and Marta Roccio[2,3,9,10†]*

[1] Neuroinfection Laboratory, Institute for Infectious Diseases, University of Bern, Bern, Switzerland, [2] Cluster for Regenerative Neuroscience, Department for BioMedical Research (DBMR), University of Bern, Bern, Switzerland, [3] Laboratory of Inner Ear Research, Department for BioMedical Research (DBMR), University of Bern, Bern, Switzerland, [4] Graduate School for Cellular and Biomedical Sciences, University of Bern, Bern, Switzerland, [5] Audion Therapeutics B.V., Amsterdam, Netherlands, [6] Massachusetts Eye and Ear, Boston, MA, United States, [7] Harvard Medical School, Boston, MA, United States, [8] Harvard Stem Cell Institute, Cambridge, MA, United States, [9] Department of Otorhinolaryngology, Head and Neck Surgery, University Hospital Zurich, Zurich, Switzerland, [10] Department of Otorhinolaryngology, University of Zurich, Zurich, Switzerland

OPEN ACCESS

Edited by:
Lon J. Van Winkle,
Rocky Vista University, United States

Reviewed by:
Ramasamy Palaniappan,
Sree Balaji Medical College and Hospital, India
Pierfrancesco Pagella,
Linköping University, Sweden

***Correspondence:**
Marta Roccio
marta.roccio@usz.ch

† These authors have contributed equally to this work

Specialty section:
This article was submitted to Stem Cell Research, a section of the journal Frontiers in Cell and Developmental Biology

Received: 15 May 2021
Accepted: 26 July 2021
Published: 13 August 2021

Citation:
Erni ST, Gill JC, Palaferri C, Fernandes G, Buri M, Lazarides K, Grandgirard D, Edge ASB, Leib SL and Roccio M (2021) Hair Cell Generation in Cochlear Culture Models Mediated by Novel γ-Secretase Inhibitors. Front. Cell Dev. Biol. 9:710159. doi: 10.3389/fcell.2021.710159

Sensorineural hearing loss is prevalent within society affecting the quality of life of 460 million worldwide. In the majority of cases, this is due to insult or degeneration of mechanosensory hair cells in the cochlea. In adult mammals, hair cell loss is irreversible as sensory cells are not replaced spontaneously. Genetic inhibition of Notch signaling had been shown to induce hair cell formation by transdifferentiation of supporting cells in young postnatal rodents and provided an impetus for targeting Notch pathway with small molecule inhibitors for hearing restoration. Here, the oto-regenerative potential of different γ-secretase inhibitors (GSIs) was evaluated in complementary assay models, including cell lines, organotypic cultures of the organ of Corti and cochlear organoids to characterize two novel GSIs (CPD3 and CPD8). GSI-treatment induced hair cell gene expression in all these models and was effective in increasing hair cell numbers, in particular outer hair cells, both in baseline conditions and in response to ototoxic damage. Hair cells were generated from transdifferentiation of supporting cells. Similar findings were obtained in cochlear organoid cultures, used for the first time to probe regeneration following sisomicin-induced damage. Finally, effective absorption of a novel GSI through the round window membrane and hair cell induction was attained in a whole cochlea culture model and *in vivo* pharmacokinetic comparisons of transtympanic delivery of GSIs and different vehicle formulations were successfully conducted in guinea pigs. This preclinical evaluation of targeting Notch signaling with novel GSIs illustrates methods of characterization for hearing restoration molecules, enabling translation to more complex animal studies and clinical research.

Keywords: drug therapy, sensorineural hearing loss, cochlear organoids, hair cell regeneration, Notch signaling, gamma secretase inhibitor

INTRODUCTION

Hair cells are the sensory receptors of the vestibular and the auditory system in the inner ear. In the cochlea there are two types of auditory hair cells: inner hair cells (IHCs), which are the primary sound detectors and outer hair cells (OHCs), which act as acoustic pre-amplifiers (Fettiplace and Hackney, 2006). Hair cells are organized in rows, intercalated by different types of supporting cells, which exert supporting, trophic and barrier functions. Degeneration of hair cells is the most common reason for sensorineural hearing loss and can be caused by acoustic overstimulation, ototoxic drugs, aging, genetic disorders or infections (Muller and Barr-Gillespie, 2015; Bommakanti et al., 2019). Disabling hearing loss affects the quality of life of 5% of the world population, with high social and economic costs (Wilson et al., 2017).

Non-mammalian vertebrates regenerate damaged or lost vestibular as well as auditory hair cells throughout life and thereby restore sensory functions (Corwin, 1981, 1985; Corwin and Cotanche, 1988; Ryals and Rubel, 1988; Weisleder and Rubel, 1993). This is mediated by the activity of supporting cells in the sensory patches, which give rise to new hair cells either through cell division or transdifferentiation. In mammals, some degree of spontaneous hair cell regeneration has been reported for the vestibular organs (Forge et al., 1993; Warchol et al., 1993; Sayyid et al., 2019; Wang et al., 2019). For the cochlear auditory epithelium, similar responses have been detected only in early postnatal stages, prior to hearing onset (Atkinson et al., 2015). Specifically, spontaneous regeneration has been observed in mice when hair cells were genetically ablated in a perinatal window of 4 days (Cox et al., 2014). Fate-mapping showed that the novel hair cells were generated from supporting cells by mitotic regeneration and direct transdifferentiation (Bramhall et al., 2014; Cox et al., 2014; Hu et al., 2016). Despite the limited extent of spontaneous regeneration, these findings have directed attention toward chemical and genetic modifications that might promote and extend the permissive window for regeneration.

The Notch and the Wnt signaling pathways have been recently targeted to enhance this regenerative potential (Roccio et al., 2019; Samarajeewa et al., 2019). A subset of supporting cells within the postnatal cochlear epithelium expresses the Wnt co-receptor and target Lgr5 (Chai et al., 2011; Chai et al., 2012; Shi et al., 2012; Zak et al., 2016), a marker of stem cells in several epithelial organs (Barker et al., 2013). Lgr5+ cells display enhanced Wnt responsiveness and forced activation of Wnt in these cells, through genetic modification or chemical stimulation, causes their proliferation (Jacques et al., 2012; Roccio et al., 2015; Samarajeewa et al., 2018) as well as their differentiation into hair cells (Bramhall et al., 2014; Shi et al., 2014; Hu et al., 2016). *LGR5* expression and Wnt responsiveness have also been confirmed in human fetal cochleas and cochlear organoid cultures (Roccio et al., 2018).

The Notch signaling pathway controls hair cell and supporting cell specification and plays a role in tissue regeneration. During cochlear development, hair cells and supporting cells arise from a common precursor within the cochlear prosensory domain (Kelley, 2006; Groves and Fekete, 2012). Notch ligand-receptor interaction between prosensory progenitors defines the mosaic organization of hair cells and supporting cells (Kelley, 2006; Kiernan, 2013). Binding of Notch ligands triggers the cleavage of the Notch receptor, allowing the translocation of the intracellular domain to the nucleus, which transcriptionally regulates developmental gene programs and inner ear cell patterning (Kopan and Ilagan, 2009; Bray, 2016). Notch activation leads to the repression of Atoh1, a key transcription factor controlling hair cell differentiation (Bermingham et al., 1999; Chen et al., 2002; Woods et al., 2004), and otic progenitor cell fate is directed to supporting cell lineage in the absence of Atoh1 (Zheng et al., 2000; Zine et al., 2001; Hayashi et al., 2008; Doetzlhofer et al., 2009). Chemical or genetic inactivation of Notch signaling can induce hair cell formation by conversion of supporting cells (Korrapati et al., 2013; Mizutari et al., 2013; Li et al., 2015; Maass et al., 2015; Ni et al., 2016b). This has been made evident also in human prosensory cell-derived organoid cultures as chemical inhibition of Notch signaling enhanced hair cell differentiation, supporting the presence of similar mechanisms in human inner ear specification (Roccio et al., 2018).

Notch receptors are cleaved in the intracellular domain by enzymes known as γ-secretases (Kopan and Ilagan, 2009; Andersson and Lendahl, 2014; Bray, 2016). Pharmacological γ-secretase inhibitors (GSIs) have been tested in postnatal animal models as a strategy to induce hair cell differentiation and hearing restoration *in vivo* (Mizutari et al., 2013; Tona et al., 2014; Maass et al., 2015). In adult animals deafened by noise overexposure, inhibition of Notch signaling by local delivery of a single dose of the GSI LY411575 resulted in new hair cell formation and small improvements in the cochlear function in the low frequency regions that were correlated with increased expression of Atoh1 (Mizutari et al., 2013).

The aim of this study was to evaluate and characterize two novel GSI compounds, hereafter CPD3 and CPD8, and their efficacy to modify hair cell gene expression and direct *de novo* hair cell differentiation. The results reported are based on a series of *in vitro* models, including Notch-dependent cell lines, explants of the organ of Corti (OC), novel whole cochlea cultures and cochlear organoids derived from the mouse and rat inner ear. GSIs were also evaluated in models of ototoxic damage, in order to probe the regenerative potential after hair cell loss. Finally, we evaluated different GSI-containing formulations for their permeability through the round window membrane and performed pharmacokinetic studies to quantify local concentrations in the perilymph. These preclinical data supported the advancement of CPD3 to clinical trial. The assays presented in this study illustrate furthermore a potential pipeline for *ex vivo* characterization of hearing restoration molecules.

MATERIALS AND METHODS

Animals

Animal studies (*in vivo* or *ex vivo*) were all approved by either the Animal Care and Experimentation Committee of the Canton of Bern, Switzerland [license BE 142/16 (SLL); BE119/12 (MR)] and followed the Swiss national guidelines for

the performance of animal experiments, or performed under an approved institutional protocol according to National Institutes of Health guidelines, or under animal protocols approved by the Animal Studies Committee of Languedoc Roussillon that comply with French legislation and European Directives.

Female albino Hartley guinea pigs, 250 g, from Charles River (France), housed in macrolon cages (2/cage; Innocage Rat Static-Innovive, Paris) with filter air, were maintained at 22 ± 2°C on a 12-h light cycle with standard A04C (UAR) diet and water "*ad libitum*." Lgr5-GFP mice containing an EGFP-IRES-CreERT2 knock-in allele at the Lgr5 locus were obtained from the Jackson Labs (Stock 008875, C57BL/6J/RccHsd background). Atoh1-nGFP transgenic mice (C57Bl/6J background) were from Jane Johnson (Lumpkin et al., 2003). Wistar rats were obtained from Charles River.

Pharmacokinetics in the Inner Ear

γ-secretase inhibitors pharmacokinetic studies tested CPD3, CPD8 (Eli Lilly) or LY411575 (Stemcell Technologies) each formulated at 3.4 mg/ml in the following vehicles, 10% Poloxamer 338 (Sigma), 20% Poloxamer 338, 70% PEG400 (Sigma) or 1% hyaluronic acid (HA-700; Lifecore, Chaska, MN, United States) all prepared with PBS (pH 6.2). A single 70 μl injection of the formulated compound (total dose, 870 μg/kg) was delivered to the middle ear space of isoflurane-anesthetized guinea pigs by transtympanic administration. Perilymph from treated animals (perilymph volumes, >2 μl) was collected at time points up to 48 h post-administration (CILcare, Montpellier, France). Briefly, concentrations of each compound in perilymph and plasma, as well as controls prepared in artificial perilymph, were measured by LC-MS/MS on an AB Sciex, API 4000 mass spectrometer using an Onyx C18 5 μm 50*2.0 mm separation column (Oroxcell, Romainville, France).

Cell Lines and Tissue Culture

The human colon cancer cell line LS174T (CL-188; ATCC) was cultured without antibiotics in 1% FBS/Eagle's Minimum Essential Medium (MEM; Thermo Fisher) (Asakura et al., 2018). The cells were exposed to GSIs or vehicle for 4 days, prior to analysis.

Otic Sphere Assay

The generation of otic spheres followed previously described protocols (Oshima et al., 2009) with modifications during differentiation phase to test GSIs. Briefly, OCs were dissociated and single cells were deposited in ultralow-cluster plates (Corning) and expanded in "full otic medium" consisting of DMEM/F12, supplemented with N2, B27 (Thermo Fisher), EGF (20 ng/ml; Chemicon), bFGF (10 ng/ml; Chemicon), IGF-1 (50 ng/ml; Chemicon), and heparan sulfate (50 ng/ml; Sigma-Aldrich). After culturing for 3–4 days at 37°C, spheres were collected, plated in cell culture-treated 96 well-plate and cultured in DMEM/F12, supplemented with N2, B27 with/without GSIs for 7 days after which they were lysed for RNA extraction.

Dissection and Isolation of Organ of Corti for Sensory Epithelium Explant Culture

OC explants were isolated from postnatal day 2 (P2) Wistar rats, P0-P2 mice (Lgr5-GFP or Atoh1-nGFP mice). Dissection of the cochlea under a stereomicroscope (Nikon SMZ800, Japan) allowed OC separation from stria vascularis and modiolus, and the sensory epithelium was plated with hair cells facing up on Cell-Tak (Corning, United States)-coated transwell-clear inserts (6-well format, 0.4 μm pore, Corning, United States). Dissection medium was exchanged for 1.5 ml full otic medium supplemented with 10% FBS (Invitrogen) and 0.01% Ampicillin (Sigma), added under the insert membrane, maintaining the OC under a thin film of medium during culture at 37°C. 5-ethyl-2′-deoxyuridine (EdU, 5 μM, Life Technologies) was added directly in the medium when indicated.

GSI-Treatment of Organotypic Cultures

Concentrations of small molecule GSIs {LY411575, CPD3, CPD8, DAPT (N-[N-(3,5-Difluorophenacetyl)-L-alanyl]-*S*-phenylglycine t-butyl ester; Sigma)} were prepared in DMSO and are indicated in Figure Legends and Results. DMSO included as Control. Treatment groups were assigned randomly.

Ototoxic Insults in Organotypic Cultures

To induce ototoxic damage, medium was removed from the OC cultures on the day after dissection and either 200 μM sisomicin (Sigma) in full otic medium, or 10^8 cfu/ml *Streptococcus pneumoniae* (described below) in ampicillin-free and FBS-free otic medium were added under the transwell membrane (lower compartment) of the cultivation system. After 2 h of exposure to the ototoxic insult, OCs were carefully washed 3 times and culture was continued for 4 days in fresh full otic medium.

Streptococcus pneumoniae Inoculum

A clinical isolate of *S. pneumoniae,* serotype 3 was used as previously described (Leib et al., 2000; Perny et al., 2017). Briefly, bacteria were cultured overnight (ON) in brain-heart infusion medium and diluted 1:10 in fresh medium the following day. Bacteria were grown until the logarithmic phase was reached (after approximately 5 h). The culture was centrifuged for 10 min at 3,100 *g* at 4°C and the pellet was resuspended in 0.85% NaCl and centrifuged again. Bacteria were diluted to the desired optical density ($OD_{570\ nm}$) and the final inoculum concentration was determined by plating serial dilutions on Columbia sheep blood agar.

Ex vivo Whole Cochlea Culture

To culture the intact cochlea of P0–P1 mice, the entire otic capsule (cochlea and semicircular canals) was carefully dissected. Connective tissues and nerves were removed to clear the round window niche and the capsule was positioned with the round window facing up in a sterile 35 mm dish. A surgical sponge was employed to blot dry the interior of the round window niche, which was then filled with 2 μl of the formulated drug and applied with a small pipette tip. Following 2 h of drug treatment at 37°C with 5% CO2, the tissue was transferred to a

50 ml conical tube containing 10 ml medium (DMEM, 5%FBS, 5% horse serum and ampicillin) and the tube was sparged with 95% O_2/5% CO_2 for 5–10 min and incubated for 2 days at 37°C, rotating on a roller/rocker (SCILOGEX MX-T6-S Analog Tube Roller) at 15–17 rpm.

Dissection and Isolation of Organ of Corti Cells for Organoid Culture

On day 0, the cochlear sensory epithelium was dissected and the OC was separated from the modiolus and stria vascularis, as described above, from either Wistar rat pups (P2), Lgr5-GFP mice (P0–P2) or Atoh1-GFP mice (P0–P2). To separate the sensory epithelial layer from underlying mesenchyme and neurons, the OC was placed in a 100 μl drop of Matrisperse Cell Recovery Solution (Corning) for 1 h at RT, then delaminated with the aid of forceps. Gentle enzymatic dissociation of hair cells and supporting cells followed with 100 μl drop of TrypLE (Gibco), 20 min at 37°C, then mechanical trituration in DMEM/F12. The cell suspension was centrifuged for 5 min at 500 *g* at 4°C and resuspended in DMEM/F12 medium supplemented with B27 and N2 (Invitrogen), EGF (50 ng/ml), bFGF (50 ng/ml), IGF (25 ng/ml), CHIR99021 (GSK-3β inhibitor, 3 μM, Merck), valproic acid (HDAC inhibitor, 1 mM, Sigma), 2-phospho-L-ascorbic acid (280 μM, Stemcell Technologies) and 0.01% ampicillin (Sigma). Cells were plated at 2,000 cells per well on 96 wells plate (Corning Costar; ultra-low attachment, round-bottom) to allow aggregation at 37°C. On day 1, Matrigel (GF-depleted, Corning; 2% stock) was added to a final concentration of 0.18 mg/ml. On day 3, cells were transferred to 24 wells plate (ultra-low attachment; Corning Costar), pooling the organoid aggregates from 4 to 5 wells (96 well-plate) to one 24-well, culturing at 37°C and exchanging half medium and Matrigel every other day, On day 10, organoids were differentiated by replacing medium with DMEM/F12 supplemented with B27, N2, CHIR99021 (3 μM), and Notch inhibitors CPD3 (5 μM) or LY411575 (5 μM), and culture was continued as above for another 10 days.

Organoid Ototoxic Treatment

On day 20, differentiated organoids were exposed to sisomicin for 2 h at the concentration of 500 μM. The medium was then washed and replaced with differentiation medium with/without GSI for an additional 4 or 7 days. For propidium iodide (PI) uptake, on day 24 of *in vitro* differentiation, cells were incubated in the presence of PI (5 μg/ml) for 5 min and subsequently washed and fixed. Immunostaining was then performed as indicated below.

Gene Expression by RT-PCR

Cells or tissue were lysed using RLT Lysis Buffer (Qiagen) and high purity RNA was prepared on the MagNA Pure instrument using MagNA Pure 96 Cellular RNA LV Kit (Roche). Reagents from Thermo Fisher were used for cDNA synthesis by reverse transcription using random hexamers. Resulting cDNA was RNAse H treated and amplified by TaqMan GEX mastermix and PCR primers and probes for human ATOH1 (Hs00944192_s1) and TBP (Hs00427620_m1), mouse Tbp (Mm00446971_m1), Atoh1 (Mm00476035_s1), Hes5 (Mm00439311_g1), Pouf4s (Mm04213795_s1), and Myo7a (Mm01274015_m1) on the Applied Biosystems QuantStudio 7 Flex Real-Time PCR System. Normalized to Tbp, relative gene expression fold-change was quantified and compared between experimental and control conditions by $\Delta\Delta Ct$ calculation.

Immunohistochemistry and Imaging of Organ of Corti Explants

Following culture, explants were washed (PBS) and fixed for 10 min at room temperature (RT) with 4% paraformaldehyde (PFA). Samples were permeabilized with 3% Triton X-100 for 30 min at RT and blocked with blocking buffer containing 2% bovine serum albumin (BSA) and 0.01% Triton X-100 for 1 h at RT.

Dividing cells were labeled with, 5-ethyl-2′-deoxyuridine (EdU) and detected with Click-it Plus kit (Life Technologies). Primary antibodies [mouse anti-Pou4f3 (1:200; Santa Cruz Biotechnology, United States) and rabbit anti-Sox2 (1:200; Cell Signalling Tech, United States)] were incubated in blocking buffer ON at 4°C. Samples were washed and incubated for 2 h at RT with secondary antibodies [goat anti-mouse Alexa Fluor 488 and goat anti-rabbit Alexa Fluor 555 (1:500 dilution, Invitrogen, United States)], as well as Phalloidin-Alexa Fluor 647 (Sigma). Explants were washed and mounted on glass slides with Fluoroshield containing DAPI (Sigma).

Explants were visualized with a Nikon Eclipse Ti-E for overview purposes. Individual *z*-planes at an interval of 5 μm were acquired with a confocal laser-scanning microscope (Zeiss LSM710, Plan-Apochromat 20×/0.8 NA objective) to ensure visualization of all hair cells.

Image processing was performed with the open-source image processing software FIJI, version 2.0 (Schindelin et al., 2012). Hair cells were quantified by counting Pou4f3 or Myo7a positive cells of the organ of Corti at three random microscopic fields for each cochlear region (base, middle, and apex) covering in total at least 1,200 μm. The number of hair cells (IHCs and OHCs) is expressed as unit per 100 μm.

Immunofluorescent Staining and Imaging of Cochlear Organoids

For staining and imaging, organoids were allowed to adhere ON onto transwell-permeable support membranes (Corning) in 12-well plates coated with 100% Matrigel. The next day, they were fixed with 4% PFA (10 min). Cells were permeabilized with 3% Triton-X 100 for 10 min and incubated ON with blocking buffer containing 2% BSA and 0.01% Triton-X 100. Primary antibodies were incubated ON at 4°C (1:200 dilution). Anti-Sox2 (mouse, BD Bioscience), anti-Pou4f3/Brn-3c (mouse, Santa Cruz Biotechnology) anti-Myo7a (rabbit, Enzo Life Sciences) and anti-p27/Kip1 (rabbit, Abcam). Organoids were then rinsed and incubated ON with the secondary antibodies as described above. For FM1-43 uptake, organoids were first incubated with Hoechst (10 μg/ml), 30 min at 37°C, then a brief incubation FM1-43 (5 μM; Life Technologies) for 30 s, and washed twice before fixation (4% PFA). To image organoids, inserts were placed

face down in a 24 well glass bottom plate (MatTek) and imaged on a Zeiss LSM710 laser scanning microscope (5 μm *Z*-stacks intervals). Compiled *Z*-projections were processed (FIJI, ver2.0) and hair cells quantified on individual planes with manual cell counter plugin, by evaluation of cytosolic expression and nuclear exclusion of Myo7a. Organoid volumes were estimated from the sum of the product of the area of the organoid (at each plane) and the *Z* stack height.

Immunofluorescent Staining of Inner Ear Whole Mounts

For whole-mount immunohistochemistry, whole cochleae were fixed (4% PFA) ON at 4°C, then incubated in primary antibodies (72 h, rocking at 4°C), goat anti-GFP polyclonal Ab (AbCam, ab6673) and rabbit anti-Sox2 polyclonal IgG (GenTex, GTX101506) in 4% normal donkey serum. Following extended washes (over 24 h), cochlea were incubated for 24 h in secondary antibodies donkey anti-goat Alexa 488 (Thermo Fisher, A11055) and donkey anti-rabbit Alexa 647 (Thermo Fisher, A31573) and extensively washed. The intact OC were then microdissected from cochleae and mounted on a coverslip for confocal imaging. A LSM 510 Confocal Microscope (Zeiss) utilizing 63X Zeiss Plan-APOCHROMAT DIC oil, 1.4NA and Zen 2009 LSM imaging software was used to optically scan mid-apex regions of OCs. Cellular quantification and image analysis computation were performed with Imaris 8.2.1 software (Bitplane).

Data Analysis and Statistics

Statistical analysis was performed with GraphPad Prism software (Prism9; GraphPad Software Inc., San Diego, CA, United States). For explant cultures, when the number of explants/replicates was not sufficient to test for Gaussian distribution normal distribution of the data was assumed based on previous experiments (Perny et al., 2017; Erni et al., 2019). Alternatively, the distribution of the datasets was tested by D'Agostino and Pearson normality test. Unpaired *t*-tests were used to compare parametric data sets of two groups. Welch's correction was applied if variances were not equal. For non-parametric data, the Mann–Whitney test was adopted. One-way ANOVA was used to determine the difference in means among multiple groups and multiple comparison correction was tested. Graphs indicate the single data point, the mean values ± standard deviation. IC50s were calculated by non-linear regression of data normalized by percent change from controls to compare multiple experiments. Differences in IC50s from Best fit data were compared by Least Squares (*F*-test; Extra sum of squares; alpha = 0.05). The number of technical and biological replicates are indicated in Figure Legends.

RESULTS

Activity and Inner Ear Pharmacokinetics of GSIs Examined in This Study

To measure the relative potency between different GSIs, a pharmacological assay was initially used to identify the dose ranges effective to induce *ATOH1* expression. The cell line LS174T, a human colorectal adenocarcinoma, was used to evaluate Notch-dependent expression of *ATOH1* (Kazanjian et al., 2010). Two compounds from Eli Lilly, designated LY3056480 (CPD3) and LY3056359 (CPD8) (**Figures 1A,B**) were compared with the commercially available GSIs LY411575 and DAPT. *ATOH1* expression was upregulated by GSI treatment in a dose-dependent manner after 72 h. IC50s for the 4 GSIs were 17.3 nM (CPD3; *open circles*), 62.0 nM (CPD8; *filled diamonds*), 0.4 nM (LY411575; *open triangles*) and 1.4 μM (DAPT; *open squares*). These IC50s ranked the potency for CPD3 and CPD8 intermediate between that of LY411575 and DAPT, with the CPD3 IC50 measured as significantly lower than that of CPD8 (**Figure 1C**; $p < 0.05$). The intermediate potency of CPD3 and 8 was likely to be adequate to achieve levels above the IC50 after dilution into perilymph in the inner ear.

To verify this, *in vivo* compound concentrations were measured in perilymph of guinea pigs after intratympanic delivery of GSIs into the middle ear. Initially, four vehicle formulations, with different physical properties, were tested, poloxamer 338 (POX; at 10% or 20%), hyaluronic acid (HA), or polyethylene glycol 400 (PEG). For this comparison only one GSI was prepared in each formulation (CPD3, 3.4 mg/ml) and a single dose was injected into the middle ear. Perilymph and plasma were sampled for 48 h (**Figure 1D**). The highest perilymph concentrations were achieved in 10% POX and 20% POX formulations, respectively. The mean, maximal perilymph concentration for these formulations was reached at 0.5 h post-dosing and declined over time. Detectable CPD3 remained in perilymph throughout the test, and at 48 h concentrations between 485 ng/ml (1.0 μM) and 1,000 ng/ml (2.1 μM) indicated sufficient residence times and concentrations for GSI activity. Next, using only 10% POX as vehicle, inner ear adsorption was compared between CPD3, CPD8, and LY411575 by transtympanic injections (**Figure 1D**, *inset*). Perilymph concentrations were sampled at 0.5, 1, and 6 h post-dosing, with concentrations of CPD3, CPD8, and LY411575 quantifiable at all time points. Each compound achieved levels several folds above their respective IC50s. The mean maximal perilymph concentration of CPD3 at 0.5 h post-dosing was 85,489 ng/ml (183 μM), then declined at 1 h to 12,928 ng/ml (27.7 μM), and at 6 h to 12,652 ng/ml (27.1 μM). GSIs in plasma samples were not detected (data not shown).

GSI-Mediated Induction of Hair Cell Gene Expression and *de novo* Generation of Hair Cells in the Neonatal Cochlear Sensory Epithelium

CPD3 and CPD8 were further compared for their potency to induce hair cell gene expression in otic sphere assays (Oshima et al., 2009). Cells were first expanded in presence of growth factors, and in a second step differentiated by growth factor removal and GSI treatment. Both CPD3 and CPD8 significantly induced *Atoh1*, *Pou4f3,* and *Myo7a* expression in dose-responsive manner ($p < 0.05$; two-way ANOVA). However, CPD3 (IC50 = 6.7 nM) was more potent in *Atoh1* upregulation than CPD8 (IC50 = 302.8 nM; $p < 0.05$; two-way ANOVA). This

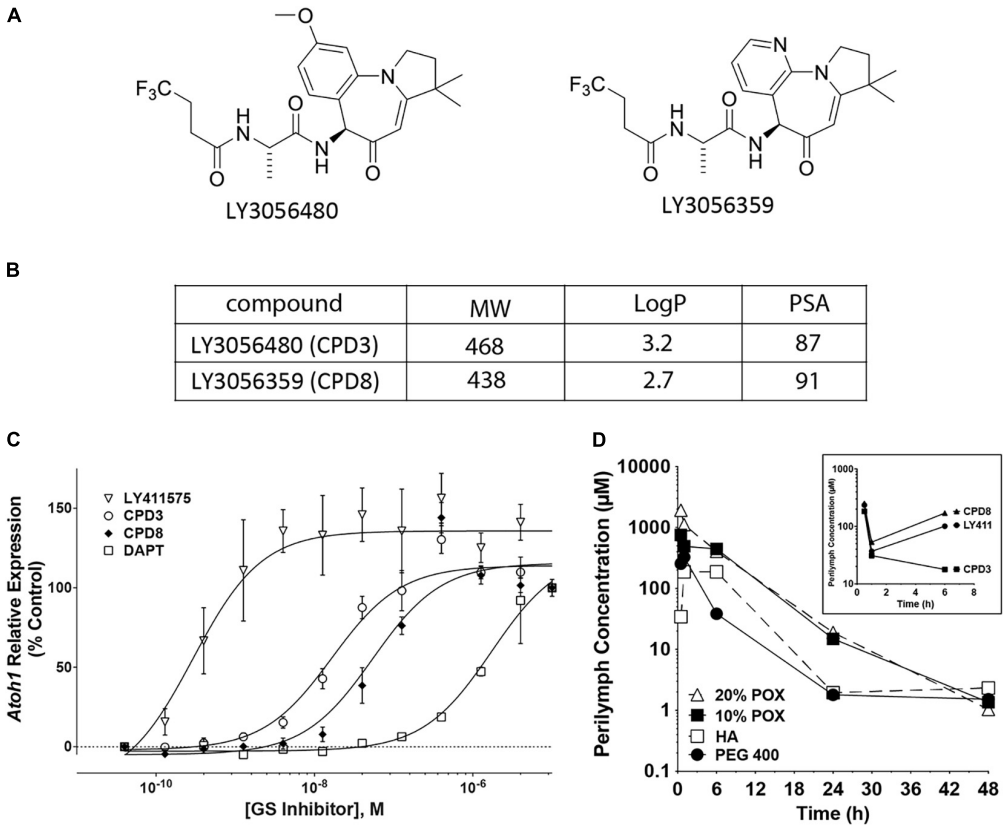

compound	MW	LogP	PSA
LY3056480 (CPD3)	468	3.2	87
LY3056359 (CPD8)	438	2.7	91

FIGURE 1 | γ-secretase inhibitors (GSI) characterization. **(A)** Structures of the two novel GSIs tested in these studies. **(B)** Properties of the two GSIs (CPD3 and CPD8). Molecular weights (MW), logarithms of the octanol-water partition coefficients (logP), and polar surface areas (PSA). **(C)** Dose-response curves for CPD3, CPD8, DAPT, and LY411575 in the human intestinal epithelial cell line LS174T. Fold-change of human *ATOH1* expression in response to GSI treatment after 72 h. IC50s for the 4 GSIs were 17.3 nM (CPD3; *open circles*), 62.0 nM (CPD8; *filled diamonds*), 0.4 nM (LY411575; *open triangles*), and 1.4 μM (DAPT; open squares). Atoh1 expression is reported as fold-change relative to carrier control [0.05% dimethyl sulfoxide (DMSO)]. Duplicate measurements are from 4 separate experiments (total $n = 8$). **(D)** Inner ear pharmacokinetic study in albino Hartley guinea pigs. A single transtympanic dose of CPD3 in [20% poloxamer (POX; *open triangle*), 10% POX; *closed square*], hyaluronic acid (HA; *open square*), or PEG 400 (*closed circle*) resulted in detectable CPD3 concentrations in the perilymph up to 48 h post-dosing. A single transtympanic dose of CPD3 (*squares*), CPD8 (*triangles*), and LY411575 (*circles*) in 10% POX resulted in perilymph levels shown at 0.5, 1, and 6 h post-dosing (*inset graph*).

indicated a modest advantage of CPD3 in eliciting expression of the early hair cell marker *Atoh1*, but similar potency on expression of some later markers of HC differentiation, *Pou4f3* and *Myo7a* (**Figure 2A**). From the results of two screening assays, CPD3 was selected for additional characterization studies based on its lower IC50 to induce *Atoh1*/*ATOH1* expression in the otic spheres and LS174T cells, respectively.

Subsequently, the analysis of gene expression changes induced by CPD3 was assessed in OC explants. As control GSIs, LY411575 and DAPT were used. CPD3 (1 μM) increased the expression levels of several hair cell genes: *Atoh1* (3.7 ± 0.54-fold; $p < 0.005$), *Pou4f3* (2.04 ± 0.35-fold; $p < 0.05$) and *Myo7a* (1.73 ± 0.33-fold; ns, one-way ANOVA with multiple comparison). Similar inductions were observed for LY411575 (5 μM): *Atoh1* (4.34 ± 0.82-fold; $p < 0.001$), *Pou4f3* (1.46 ± 0.26-fold, ns), and *Myo7a* (1.42 ± 0.31-fold; ns, one-way ANOVA with multiple comparison), as well as for DAPT (5 μM): *Atoh1* (2.36 ± 0.39-fold, ns) *Myo7a* (1.59 ± 0.21-fold, ns), and *Pou4f3* (2.14 ± 0.36-fold, ns) (**Figure 2B**).

In order to evaluate the potency of the compounds to induce *de novo* hair cell formation, OC explant cultures of the early postnatal organs were exposed to GSIs and hair cell numbers were quantified in cultures of mouse (**Figure 2C**) and rat tissue (**Figures 2D,E**). In both species, the GSIs increased OHC counts, whereas IHC counts remained unchanged. Here, OHC induction by CPD3 was moreover limited to the apical region ($p < 0.05$, unpaired *t*-test; **Figure 2E**).

To assess the regenerative potential of CPD3 in response to hair cell damage, treatment with CPD3 was tested in rat OC explants in two ototoxicity models: aminoglycoside exposure, specifically using sisomicin (Huth et al., 2015), and exposure to living *S. pneumoniae* (Perny et al., 2017; Erni et al., 2019). As reported previously, sisomicin caused a dramatic loss of hair cells, in particular OHCs, in the basal cochlear domain (**Figure 3A**) (Perny et al., 2017; Erni et al., 2019). Hair cell numbers in the apex remained comparable to control explants (dashed line/yellow shaded area), and increased OHC numbers elicited from CPD3 were not statistically significant, possibly due to this blunted

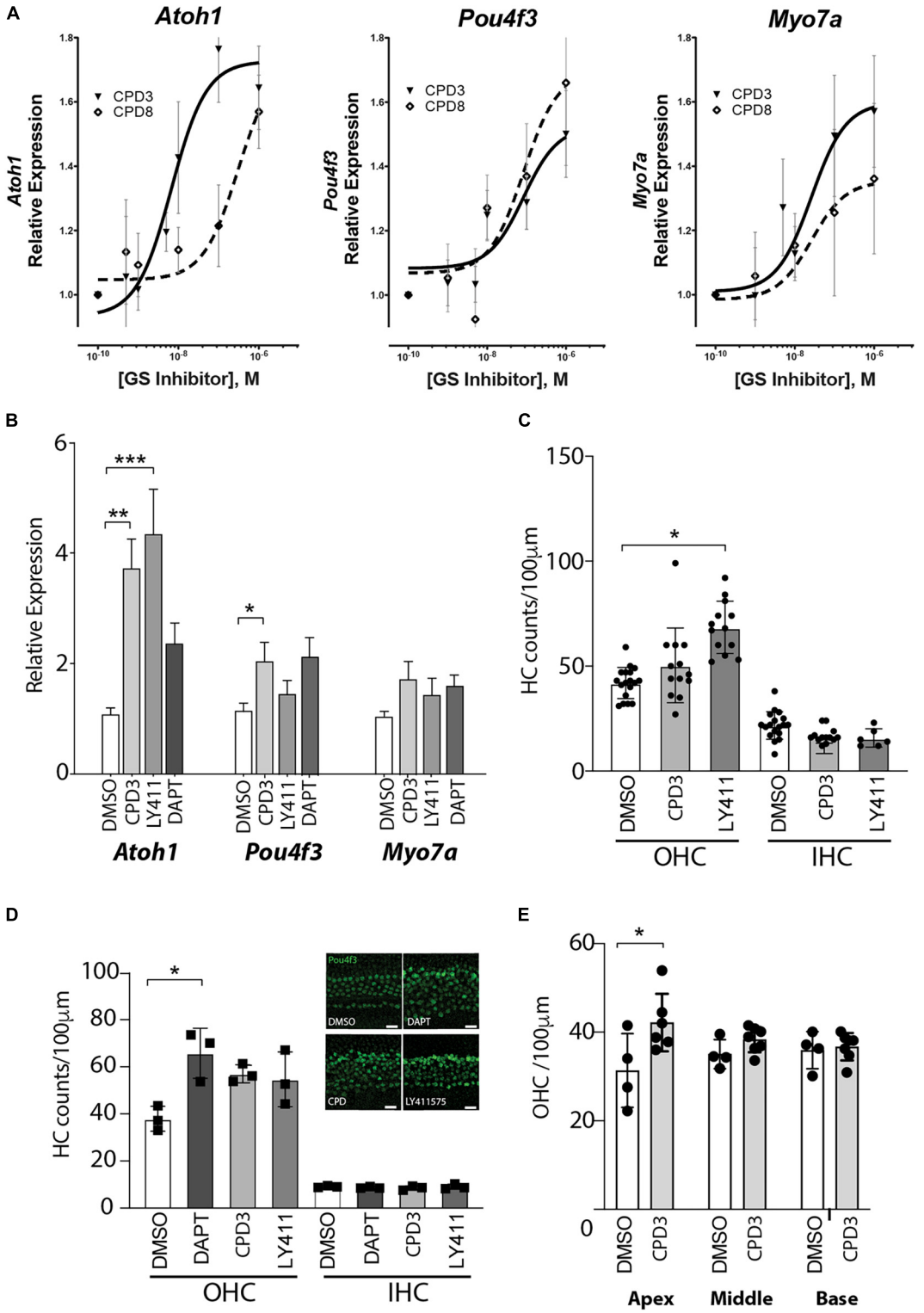

FIGURE 2 | GSI-mediated induction of hair cell gene expression and *de novo* generation of hair cells in the neonatal cochlear sensory epithelium. **(A)** Gene expression changes of *Atoh1, Pou4f3,* and *Myo7a* in response to Notch pathway inhibition by CPD3 (*solid lines, triangles*) and CPD8 (*dashed lines, open square*) in otic spheres. Gene expression is reported as fold-change relative to carrier control-treated (DMSO, 0.05%). (n = 9–12). EC50 values are significantly different for Atoh1 ($p < 0.05$, F-Test). **(B)** Gene expression analysis for the hair cell genes *Atoh-1, Myo7a,* and *Pou4f3*. DMSO control n = 13, CPD3 n = 12, LY411575 n = 9, DAPT n = 6 from 2–4 independent experiments. OC explants were cultured for 4 days with/without GSI prior to lysis and analysis. One-way ANOVA with

(Continued)

FIGURE 2 | Continued
Dunnett's multiple comparison test, each condition compared to DMSO control. (*$p < 0.05$, **$p < 0.005$, ***$p < 0.001$). **(C)** Cell counts of Atoh1 positive HCs (OHC left, IHC right) in the mouse cochlear sensory epithelium in the mid-apex region after 7 days in culture with different γ-secretase inhibitors. One-way ANOVA Dunnett's multiple comparison test, each condition compared to DMSO control. (*$p < 0.05$; n = 3–5 independent experiments). **(D)** Quantification of Pou4f3 positive HCs (OHC left, IHC right) in the cochlear sensory epithelium from P2 rats in the apical domain after 8 days in culture with different γ-secretase inhibitors. One-way ANOVA with Dunnett's multiple comparison test, each condition compared to DMSO control (*$p < 0.05$, n = 3). Representative immunohistological images of the apical domain after 8 days incubation (*inset*). scale bar = 20 μm. **(E)** Quantification of Pou4f3 positive OHCs in the apex, middle and basal domain of organ of Corti explants from rats after 4 days of CPD3 treatment compared to DMSO (*$p < 0.05$, unpaired t-test) n = 4–6 explants from 2 independent experiments.

baseline of damage (**Figure 3B**). Interestingly, an increase in Pou4f3+/Sox2+ double-positive cells at the apical side of the organ of Corti was detected, where 3rd Deiters' and Hensen's cells are located (**Figure 3C**). These double positive cells lacked hair bundles (*F*-actin) (**Figure 3C**, arrows), suggesting they were newly generated. Pou4f3/Sox2 double-positive cells were observed only in the apical domain of explants treated with CPD3 (**Figure 3D**) ($p = 0.057$, Unpaired t-test with Welch's correction).

For bacteria-induced ototoxicity, the damage was moderate in these experiments (**Figures 3E,F**). Explants that were subsequently treated with CPD3 for 4 days showed more OHCs in all turns of the organ of Corti, compared to DMSO-treated organs, with a density similar to that of undamaged explants (**Figure 3F**). Again, some cells co-expressed Pou4f3 and Sox2, possibly indicating a process of direct transdifferentiation. This was supported by the lack of EdU incorporation (**Figures 3E–G**). Quantification of Pou4f3/Sox2 double-positive cells showed increased occurrence when explants were treated with CPD3 after damage, however, only in the apical domain. These effects did not reach statistical significance (**Figure 3H**).

Hair Cell Formation in Whole Cochlea Culture

To assess the permeability of the compounds across the round window membrane, a novel *ex vivo* model was devised to compare drug entry, after delivery to the exterior of the cochlear capsule, to resemble middle ear application. Specifically, CPD3 application was tested in organotypic culture of the entire otic capsule (**Figure 4**). CPD3, formulated at two different concentrations (1 and 7.2 mM) in 70% PEG400 or 10% POX338 (POX), was applied at the round window niche. Drug formulations were allowed to absorb briefly into the cochlea prior to the 48 h culture. Confocal microscope images of stained cells in four landmark regions (Base, Mid-Base, Mid-Apex, and Apex) revealed a dose-dependent increase in hair cell number (Atoh1-GFP positive cells) upon GSI treatment (**Figures 4A–D**). The total number of Atoh1+ hair cells, independent of the anatomical location, showed robust increases over control vehicles in both formulations. In the PEG400 formulation, CPD3 stimulated a 60.1% increase in Atoh1+ hair cells at 7.2 mM (87 ± 15 hair cells/100 μm) above vehicle-only (54 ± 5 hair cells/100 μm; $p < 0.001$, One-way ANOVA with Multiple comparison), but no change at the lower dose (1 mM; 54 ± 7 hair cells/100 μm). In the POX338 formulation, CPD3 stimulated Atoh1+ hair cell significant increases both in the low dose (23.3%) and at the high dose (**Figure 4D**, *green dots*; 54.4%; from 59 ± 6 hair cells/100 μm in vehicle-only, 72 ± 11 hair cells/100 μm at 1 mM and 90 ± 20 hair cells/100 μm at 7.2 mM; *$p < 0.05$; ***$p < 0.001$, one-way ANOVA with multiple comparison). For the POX338 formulation, we further characterized the number of Sox2+ supporting cells in the sensory epithelium. A significant decrease in supporting cell (Sox2+) counts was concomitant to the increase in Atoh1+ hair cells (**Figures 4C,D**, *red dots*; ***$p < 0.001$, one-way ANOVA with multiple comparison), in agreement with a previously reported transdifferentiation mechanism (Bramhall et al., 2014). Also in this model, we observed a trend for new hair cells to be greater toward the apex than the base in agreement with the results obtained with the OC organotypic culture and indicated GSI exposure was throughout the entire length of the organ of Corti length during the culture period.

CDP3-Induced Hair Cell Differentiation in Cochlear Organoids

CPD3 was then tested in cochlear organoid culture (McLean et al., 2017; Lenz et al., 2019). In this model, supporting cells/progenitors are first expanded and subsequently differentiated to hair cells by growth factors withdrawal and addition of CHIR99021, to activate Wnt signaling, and inhibition of Notch, by GSI. Previously, LY411575 was used in similar experiments (McLean et al., 2017; Lenz et al., 2019). The use of Lgr5-GFP reporter mice enabled verification of Lgr5 induction during expansion (**Figure 5A**). Within 10 days of differentiation, cells of hair cell phenotypes were observed (**Figure 5B**), which also displayed uptake of the styryl dye FM1-43, an indirect readout for functional hair cells (**Figures 5C,D**).

Evaluating CPD3 efficacy to induce hair cell formation during the differentiation phase was assessed by gene expression changes of hair cell and supporting cell specific genes by RT-PCR. For this specific set of experiments, Atoh1-nGFP mice were used to facilitate the verification of hair cell induction prior to cell lysis for RNA isolation (data not shown). While hair cell genes (*Atoh1; Pou4f3*; and *Myo7a*) were upregulated, supporting cell genes (*Hes5* and *Lgr5*) were as expected downregulated. Sox2 mRNA expression was, however, not changed in this time-frame (**Supplementary Figure 1**). CPD3 (5 μM) induced Atoh1 expression (8.07 ± 5.6-fold; $p < 0.0001$, unpaired t-test), Pou4f3 expression (12.65 ± 11.07-fold; $p < 0.0005$, unpaired t-test) and Myo7a (9.9 ± 10.5-fold; $p < 0.005$, unpaired t-test) compared to untreated samples. Hes5 expression was downregulated fourfold (0.24% ± 0.4; $p < 0.05$ unpaired t-test) (**Figure 5E**). When compared to LY411575, comparable effects were observed for hair cells and supporting cell gene markers (**Supplementary Figure 1**).

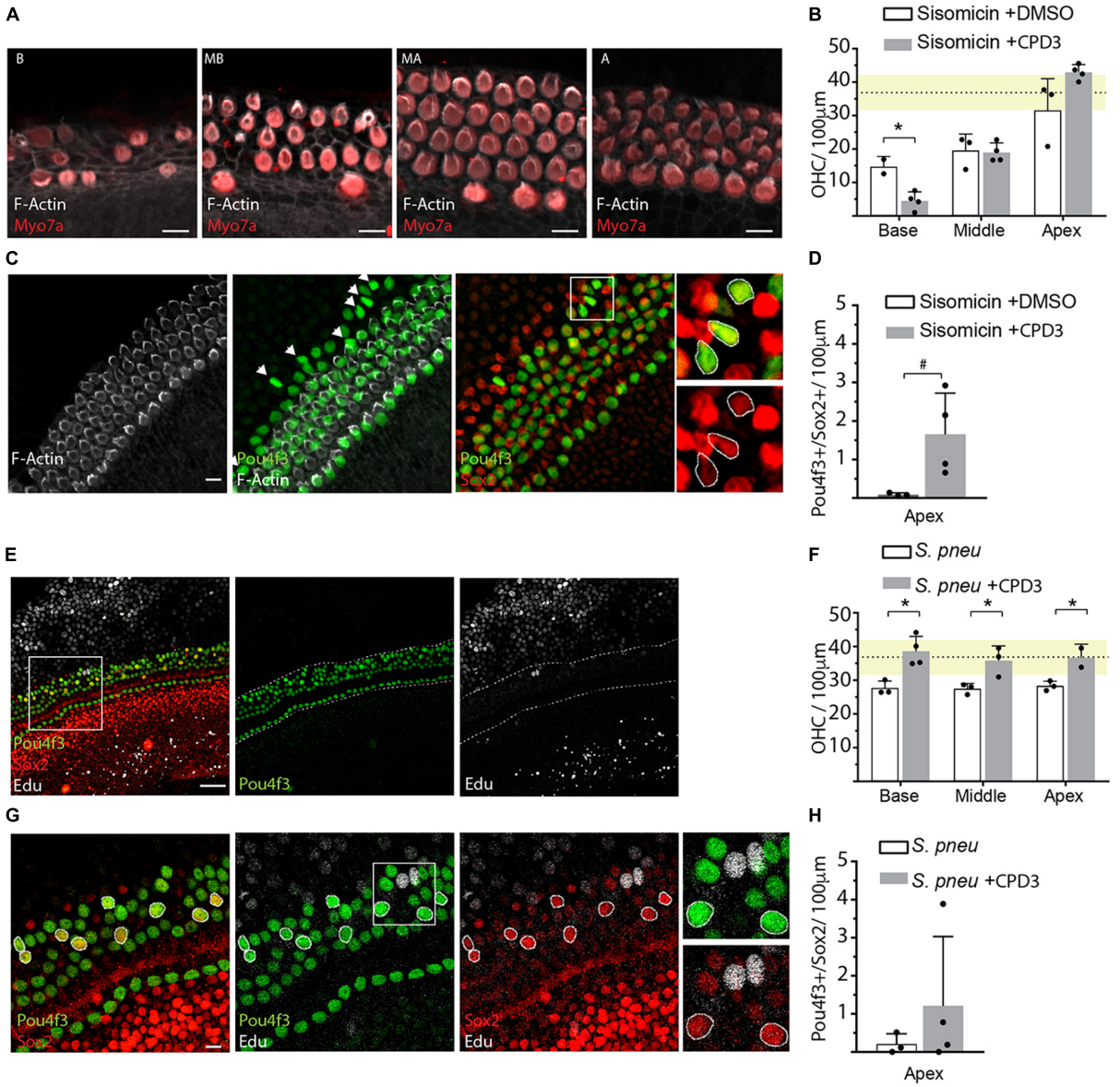

FIGURE 3 | GSI treatment after ototoxic damage. **(A)** Representative immunohistological pictures of the base (B), midbase (MB), midapex (MA), and apex (A) of a sisomicin treated explant stained for hair cells (Myo7a), hair bundles (*F*-actin). Scale bars: 10 μm. **(B)** Quantification of OHCs in sisomicin-treated explants (2 h; 200 μM), 4 days after ototoxic insult, and cultured in presence or absence of CPD3. Dashed line shows the mean of the undamaged control explants with SD in yellow (n = 3–4 explants). **(C)** Immunohistological images of an apical OC turn after ototoxic damage with sisomicin and subsequent treatment with CPD3. Some cells co-expressed hair cell marker Pou4f3 and supporting cell marker Sox2 but did not show *F*-actin positive hair bundles (arrows). Scale bars = 10 μm. Boxed area is enlarged in the panels on the right showing merged and single channels. **(D)** Quantification of Pou4f3/Sox2 double-positive cells in the apex of sisomicin-exposed explants, treated with CPD3 or DMSO (ns, n = 3–4 explants). **(E)** Representative immunohistological images of the apical turn of the organ of Corti 4 days after exposure to *S. pneumoniae* and treatment with CPD3. Scale bar = 50 μm. **(F)** OHC quantification after bacteria-induced damage. Dashed line shows the mean of the undamaged control explants with SD in yellow. (n = 3,4 explants per condition). ($p < 0.05$, unpaired t-test, between CPD3 ± and each location). **(G)** Immunostaining of the organ of Corti apical domain for Pou4f3 and Sox2. Double-positive cells are highlighted with circles. EdU (*white*). Scale bar = 10 μm. **(H)** Quantification of Pou4f3/Sox2 double-positive cells in the apex after exposure to *S. pneumoniae*. (n = 3–4 explants per condition. ns, unpaired t-test with Welch's correction). *$p < 0.05$.

Cochlear organoids derived from the rat sensory epithelium allowed corroboration of CPD3 to induce hair cell formation in another species model (**Figures 5F–J** and **Supplementary Figure 2**). As above, successful proliferation of Sox2+ progenitors (**Supplementary Figure 2**) was followed by cellular differentiation to generate Myo7a+ hair cells (**Figures 5F–H**). Hair cells demonstrated the ability to incorporate FM1-43, suggesting their functional differentiation in rat organoids also (**Figure 5H**). Interestingly, a subset of organoids contained cells double positive for Myo7a and Sox2, suggesting intermediate

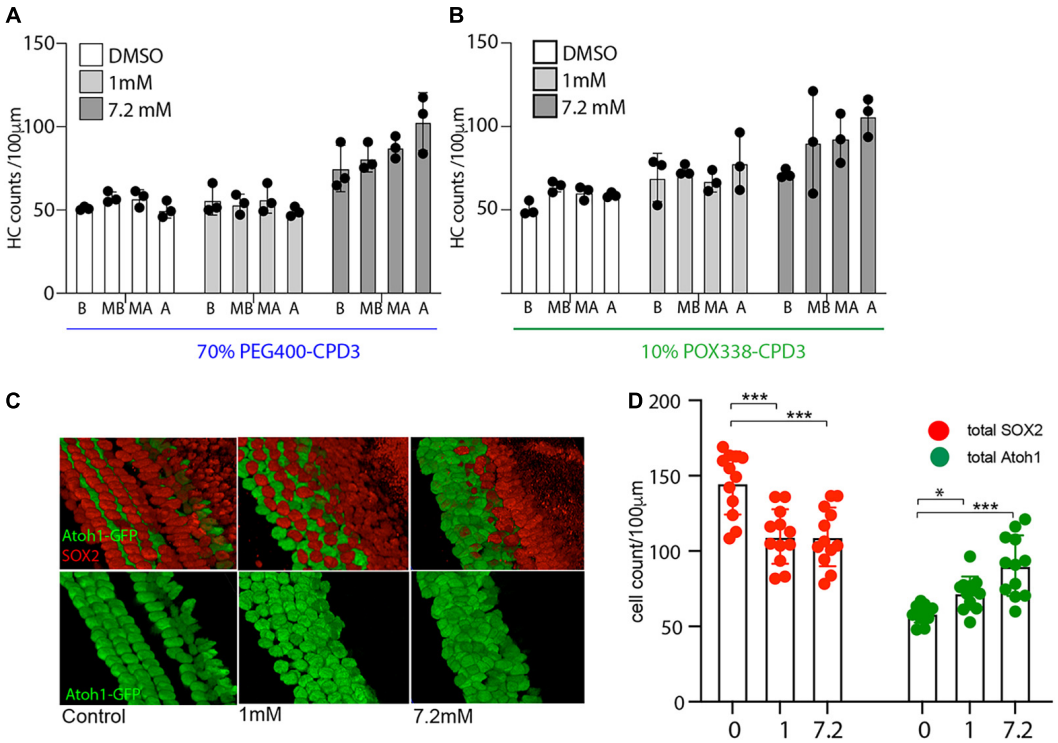

FIGURE 4 | Hair cell quantification in whole cochlea culture. **(A)** Hair cell counts from whole cochea culture with directly applied CPD3 in 70% PEG400 (1 mM or 7.2 mM). *Atoh1*-GFP positive hair cells in different organ of Corti regions (*B*, base; *MB*, mid-base; *MA*, mid-apex; *A*, apex) ($n = 3$ independent experiments). **(B)** Hair cell counts from whole cochea culture with directly applied CPD3 in 10% POX338 (1 mM;, or 7.2 mM). *Atoh1*-GFP positive hair cells in different organ of Corti regions (*B*, base; *MB*, mid-base; *MA*, mid-apex; *A*, apex; $n = 3$ independent experiments). **(C)** Immunostained inner ear sensory epithelia following whole cochlea culture with direct application of CPD3 (1 and 7.2 mM; Vehicle, 10% POX338). 3D projections of confocal stacks at mid-base region of organ of Corti, Atoh1-GFP (hair cells, *green*) and Sox2 (supporting cells, *red*). **(D)** Quantification of *Atoh1*-GFP-positive (*green dots*) and Sox2-positive cells (*red dots*) after direct application of CPD3 (1 or 7.2 mM), or vehicle formulated in 10% POX338. (*$p < 0.05$; ***$p < 0.001$, one-way ANOVA with multiple comparison; $n = 12$; 3 independent experiments; all regions-base to apex).

phenotypes during the transdifferentiation from supporting cells or immaturity (**Figure 5G**). The addition of CPD3 significantly increased hair cell numbers during differentiation ($p < 0.05$ Welch's test) (**Figure 5I**), and CPD3 was then compared to LY411575 in the differentiation phase. For both compounds, higher numbers of hair cells per organoid could be differentiated relative to vehicle-treated samples, however, this did not reach statistical significance (**Figure 5J**). Some hair cells could also be identified when no GSI was added to the differentiation medium (DMSO group), with numbers comparable to what was obtained at the end of the expansion phase. To adjust for variation in size of the organoids, hair cell counts are expressed as relative to the organoid volume.

Cochlear Organoids Hair Cells Are Sensitive to Sisomicin-Induced Damage

Finally, the regenerative potential of CPD3 was assessed with rat cochlear organoids testing the efficacy of CPD3 to transdifferentiate any remaining supporting cells after ototoxic damage. Sisomicin (500 µM) was applied for 2 h at day 20 of differentiation, followed by 4–7 days culture in absence or in presence of GSIs. Qualitative assessment of the ototoxic effect of the aminoglycoside showed features of damage, including abnormal morphologies, cell shrinkage and uptake of propidium iodide in Myo7a positive cells, consistent with sisomicin-induced cell death (**Figures 6A–C**). A decrease in Myo7a+ hair cells was detected 7 days following sisomicin damage (**Figure 6D**). From the baseline of sisomicin-treated hair cell numbers, a significant increase in Myo7a+ hair cells was restored in organoids that were cultured in presence of CPD3 ($p < 0.001$, unpaired *t*-test with Welch's correction) (**Figure 6D**). While the total number of Sox2 positive cells in the organoid did not change in response to CPD3 (**Figure 6E**), the number of Myo7a+/Sox2+ hair cells did increase ($p < 0.001$, unpaired *t*-test with Welch's correction) (**Figure 6F**). Together these data indicated that, GSI treatment did induce *de novo* hair cell formation from supporting cells in the sisomicin-damage organoid model.

DISCUSSION

Reactivation of signaling pathways that contribute to hair cell development during embryonic and fetal stages is one of the approaches under investigation to trigger tissue regeneration of the inner ear sensory epithelia. This strategy targets supporting

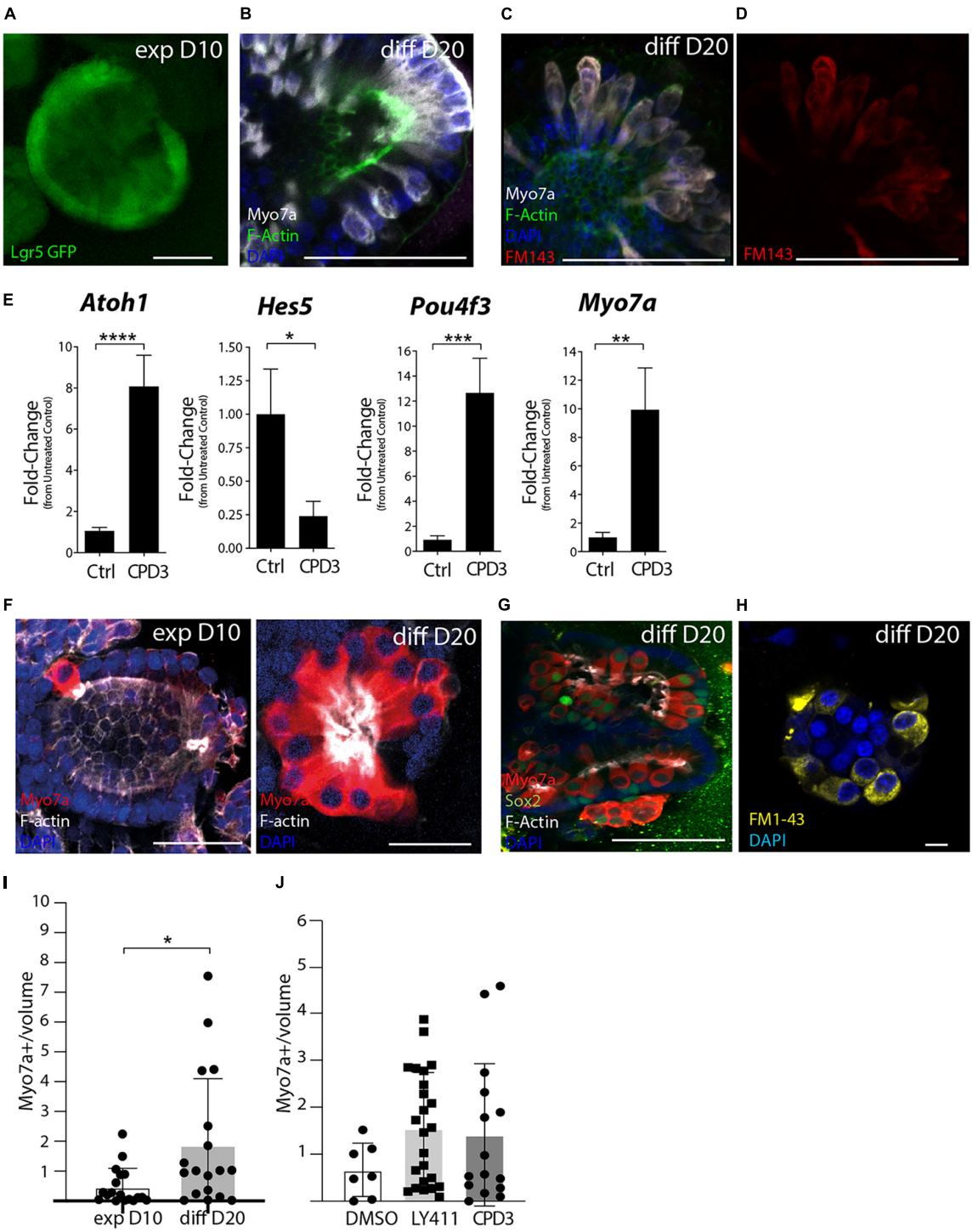

FIGURE 5 | Assessment of GSI effects in cochlear organoid culture. **(A)** Representative example of Lgr5-GFP organoids after 10 days expansion (*exp D10*). Scale bar = 50 μm. **(B)** Immunostaining Lgr5-GFP organoids at 20 days of differentiation (*diff D20*) for Myo7a (*white*) and *F*-Actin (Phalloidin, *green*). Scale bar = 50 μm. **(C,D)** Incorporation of FM1-43-FX in organoid exposed to the dye for 30 s, subsequently fixed and immunostained for Myo7a (*white*) and *F*-Actin (*green*). Scale bar = 50 μm. **(E)** Gene expression analysis by RT-PCR of hair cell genes (*Atoh1, Pou4f3*, and *Myo7a*) and supporting cell gene (*Hes5*) in organoids derived from Atoh1-GFP mice at the end of differentiation. Ctrl (DMSO) and CPD3 (5 μM; $^{*}p < 0.05$, $^{**}p < 0.005$, $^{***}P < 0.0005$, $^{****}p < 0.0001$; Unpaired *t*-test; $n = 14$). **(F)** Representative example of organoids derived from the P2 rats cochlear sensory epithelium immunostained for the hair cell markers Myo7a (*red*) and *F*-Actin (*Phalloidin, white*) at day 10 of expansion (*exp D10*) and after day 10 of differentiation (*diff D20*). Scale bar = 25 μm. **(G)** Representative immunostaining at day 20 of differentiation for Myo7a, Sox2, and *F*-Actin. single *Z* stack. Scale bar = 50 μm. **(H)** FM1-43 uptake (*yellow*) at day 20 of differentiation. Scale bar = 10 μm. **(I)** Quantification of hair cell numbers *in vitro* (normalized for the volume of the organoids in mm^3 ($\times 10^{-5}$) at 10 days of expansion (*exp D10*) or at 20 days of

(Continued)

FIGURE 5 | Continued
differentiation in the presence of CPD3 (*diff D20*) $n = 18$ per group ($p < 0.05$; unpaired *t*-test with Welch's correction). **(J)** Relative hair cells at the end of differentiation (normalized for organoid size). Total hair cells per organoid prior to normalization: DMSO (9.4 ± 11.2; $n = 7$), CPD3 (22.8 ± 18.0; $n = 24$), and LY411575 (17.17 ± 20.9; $n = 15$).

cells, given the common developmental origin, and aims to force their *de novo* differentiation to hair cells (Roccio et al., 2019). With this rationale, Notch signaling was manipulated in a set of experiments to characterized the *in vitro* responses of the cochlear sensory epithelium to chemical Notch inhibition.

The activities of two novel GSIs were assessed in this study and compared to the commercially available inhibitors. The new compounds displayed intermediate potency to previously reported GSIs in terms of IC50 for *ATOH1* induction. Still they induced comparable levels of hair cell generation *ex vivo* in all the tested models. *De novo* hair cell induction appeared to be driven by the transdifferentiation of supporting cells. Using *ex vivo* culture and pharmacokinetic studies, it was possible to evaluate their permeability through the round window membrane, assess different formulations, and determine the local concentration of these compounds into the inner ear. Ultimately, CPD3 was further selected as the new chemical entity for a phase1/2 clinical trial for mild-moderate SNHL (REGAIN trial[1]).

Gamma secretases have additional cellular targets other than Notch receptors, including the amyloid precursor protein (APP), for which they were initially designed, ERBB4, *E*-cadherin and others (Andersson and Lendahl, 2014). Specifically for the inner ear, the GSI effects observed in early postnatal stages are comparable to genetic Notch suppression (Ni et al., 2016a,b). In a direct comparison between GSI treatment (DAPT) and Notch blocking antibody *ex vivo*, similar levels of hair cell gene expression and *de novo* hair cell induction were reported (Maass et al., 2015). GSIs such as LY411575 have greater potency than the older transition state analogs and DAPT-type peptidomimetics (Han and Shen, 2012). However, the increased potency comes with some off-target effects, such as non-selectivity toward proteases and can result in inhibition of signal peptidases (Weihofen et al., 2003) or the proteasome (Han and Shen, 2012). The choice of the novel molecules assessed in this study was primarily based on the ability to inhibit Notch signaling and reduce potential off target effects. The intermediate potency of CPD3 and CPD8 and their concentration in perilymph, notably higher than the IC50 for *ATOH1* induction, were therefore positively evaluated. Finally, local delivery to the inner ear has the advantage to likely minimize systemic side effects (Andersson and Lendahl, 2014).

The initial pharmacology of the different GSIs was characterized in a human cell line that responds to Notch inhibition and allows for quantitative comparisons of IC50 for the upregulation of *ATOH1*. The phenotypic assays that followed were performed in inner ear tissues intended to increasingly represent targets of therapeutic treatment. In each of the assays, the concentration ranges used were based on the concentrations achieved in pharmacokinetic tests (**Figure 1**). Using organotypic cultures, CPD3 upregulated the expression of hair cell genes in the tissue and resulted in an increased number of hair cells, in particular OHCs in the apical region of the sensory epithelium, in agreement with previously reported GSI studies (Korrapati et al., 2013; Li et al., 2015; Maass et al., 2015; Ni et al., 2016b). CPD3 increased hair cells in undamaged cultures and also after ototoxic damage induced by sisomicin. In the case of *S. pneumoniae* exposure, we observed higher numbers of putative novel hair cells, co-expressing *Pou4f3* and *Sox2* in the apical domain. However, hair cell counts were increased in all cochlear regions after GSI treatment. It remains unclear which mechanism may contribute to this increase and whether GSIs may exert some partial otoprotective function in this model.

While the reason for the higher regenerative potential of the apical domain of the cochlear sensory epithelium in early postnatal ears is likely related to the younger age of these cells relative to the hair cells at the base (Driver and Kelley, 2020), these differences in plasticity are unlikely to hold for the adult. This regional effect may pose a problem for hair cell regeneration as OHCs in the base are most vulnerable to damage (Liberman, 1990; Sha et al., 2001; Perny et al., 2016; Perny et al., 2017) resulting in predominant high-frequency hearing loss.

The *in vitro* findings with rat explant cultures supported a model where hair cells are generated by transdifferentiation of supporting cells as immature hair cells expressing both Pou4f3 and Sox2, lacking hair bundles were identified, but these cells did not incorporate EdU (**Figure 3**). This is in contrast with mitogenic responses observed with murine tissue by us (Roccio et al., unpublished data) and others (Li et al., 2015; Ni et al., 2016b). Further, different supporting cell types responded to GSI treatment and damage. In explants exposed to sisomicin, newly-formed hair cells were detected adjacent to the 3rd row of hair cells and therefore likely originated from transdifferentiation of the 3rd Deiters' cells/Hensen's cells. In explants exposed to live *S. pneumoniae*, newly-formed hair cells were located at different locations across the medial-lateral axis of the sensory epithelium. It is therefore plausible that different ototoxic damage models may activate different supporting cell types, modifying their response to regenerative molecules. Interestingly, ectopic hair cells were not observed in the greater epithelial ridge, nor in the inner hair cell region after GSI exposure.

Transdifferentiation of supporting cells to hair cells without replenishment of the supporting cell pool may alter the epithelial organization and therefore *per se,* impact the organ functionality. Different studies have focused on simultaneous induction of proliferation and differentiation of supporting cells to mimic a regenerative response (Ni et al., 2016a,b; Shu et al., 2019). Restoration of the original cellular organization remains a major challenge to be solved in order to enable proper restoration of organ function.

[1] https://www.regainyourhearing.eu/

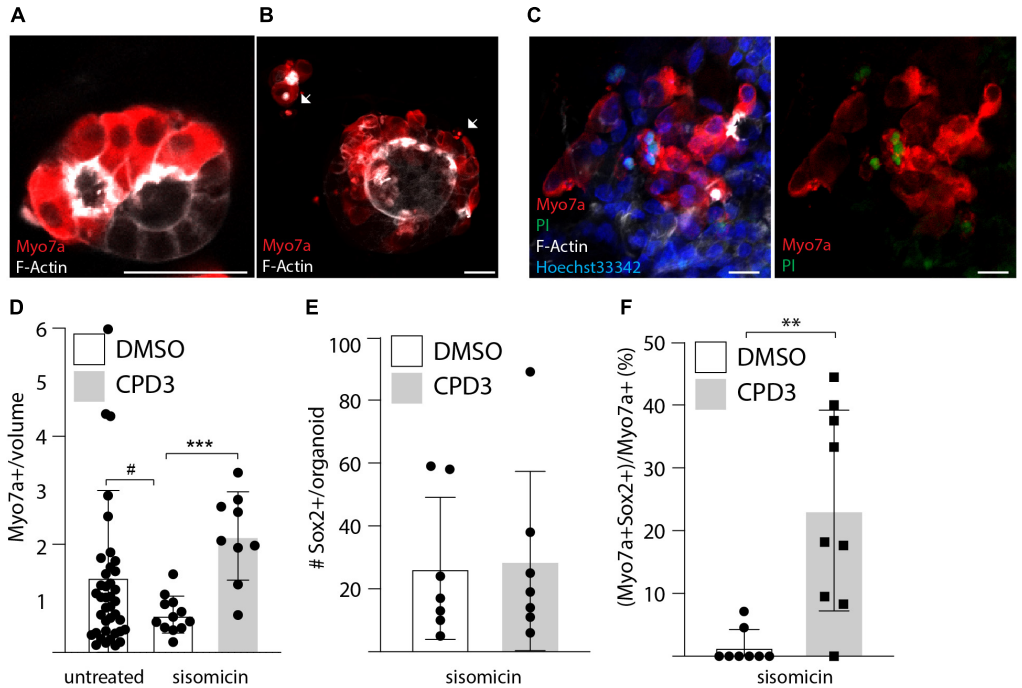

FIGURE 6 | Ototoxic assay in cochlear organoid. **(A)** Immunostaining of untreated organoids for Myo7a and *F*-Actin at day 24. **(B)** Immunostaining of organoids for Myo7a and *F*-Actin at day 24 after exposure for 2 h to sisomicin (500 μM) on day 20. Cells presenting signs of apoptosis are labeled with arrows. **(C)** Propidium Iodide incorporation at day 24 is seen in a subset of hair cells after exposure to sisomicin. Scale bar: 25 μm. **(D)** Quantitative analysis of hair cells survival 1 week after sisomicin exposure [HC number relative to the organoid volume in mm^3 ($\times 10^{-5}$)]. Control: $n = 40$; sisomicin: $n = 12$; sisomicin + CPD3; $n = 9$ ($^{\#}p = 0.052$; $^{***}p < 0.001$; unpaired *t*-test with Welch's correction). **(E)** Quantification of Sox2 positive cells after sisomicin damage and CPD3 exposure ($n = 7$). **(F)** CPD3 effects on the percentage of Myo7a positive cells co-expressing Sox2 ($^{**}p < 0.001$, unpaired *t*-test with Welch's correction; $n = 8$–9).

Organotypic cultures of the postnatal organ of Corti are well-established and widely used tools to evaluate *in vitro* responses to drugs as they can be directly exposed to selected concentrations of compounds under controlled conditions. They also enable the assessment of the anatomical location and the type of cells that are affected by the treatment. However, any approach for *in vivo* delivery will likely not match the high and precise doses that can be tested *in vitro*. In order to complement the pharmacological data, a different *ex vivo* model of the whole cochlea from mice was established. The model aimed to demonstrate that CPD3 could induce an increase in hair cell number by local delivery and to corroborate the preclinical pharmacokinetic tests documenting drug absorption into the perilymph. CPD3 was tested in two vehicle formulations: 70% PEG (Mizutari et al., 2013) and 10% POX (Gausterer et al., 2020), designed to increase the residence time *in vivo*. In both cases, the highest concentration of the compound led to a basal-to-apical gradient of increased hair cell number. A decrease of Sox2+ cells reaffirmed that GSI entered the cochlea and induced hair cell formation, predominantly through transdifferentiation. The data reported here are obtained from P1–2 mice. While the model provides an initial, complementary approach to test drug permeability and efficacy, it remains highly challenging to establish similar *ex vivo* culture systems from older animals.

Finally, cochlear organoid models (McLean et al., 2017) were successfully employed to compare the effectiveness of GSI in a range of experiments testing hair cell regeneration. The culture methods rely on a primary phase of cochlear progenitor expansion followed by differentiation to hair cells by concomitant Wnt activation and Notch inhibition (McLean et al., 2017; Roccio et al., 2018; Lenz et al., 2019). This enabled a side-by-side comparison of GSIs. In this case, the efficacy of hair cell induction of CPD3 was comparable to LY411575, both in terms of upregulation of hair cell genes, as well as the number of derived hair cells at the end of the differentiation period. Comparable findings were obtained from mouse and rat cultures. While a direct comparison was not conducted, rat cochlear organoids seemed to have a higher proportion of Sox2+ cells at the end of differentiation. Hence, this provided a convenient model to test supporting cell-dependent hair cell regeneration. The sensitivity to sisomicin in rat organoids suggested a functional cochlear hair cell phenotype. Interestingly, hair cells lost from the ototoxic insult were replenished after CPD3 treatment (**Figure 6**).

Organoid culture models have the drawback that they lack information concerning the precise cell type and anatomical location where damage and regeneration occur, as supporting cells derived from the entire cochlear duct are isolated, pooled and cultured in homogeneous conditions. Furthermore, the media composition has been selected to maximize the proliferative and stem-like features of these cells, and findings obtained *in vitro* may not be representative of *in vivo* responses obtained in intact organs with single drugs. It is, however,

possible to maintain these cultures for a prolonged time. Here, we tested up to 1 month (20 days of differentiation 7 days after damage). Optimization of the conditions may enable further maturation to late postnatal stages. In contrast, *ex vivo* cultures of the OC tend to lose tissue organization once cultured for a prolonged time, and late postnatal tissue cannot be directly isolated undamaged from the ossified inner ear. Benchmarking *in vitro* derived hair cells and supporting cells from the organoid cultures against primary tissue from late postnatal and adult organs will be pivotal to better understand the advantages and limitations of this model (Burns et al., 2015; Ranum et al., 2019; Yu et al., 2019; Hoa et al., 2020).

Furthermore, validation of these strategies on human tissue may further provide robust evidence for their clinical translation. While human fetal and adult (postmortem or surgically derived material) can be used for important validation studies, their limited accessibility in fact strongly hampers the use in routine or high throughput experimental settings (Chen et al., 2007; Roccio et al., 2018; Taylor et al., 2018). Generation of human cell types using stem cell technologies may provide alternative and scalable tools for *in vitro* testing of drug therapies (Koehler et al., 2017; Roccio, 2020). In conclusion, while the tested GSI reliably enhanced *de novo* hair cell formation *in vitro* in all the presented assays, a major future hurdle will be to generate advanced models that are representative of mature or aged tissues to study disease and regeneration in these settings prior to the translation to more complex *in vivo* models.

DATA AVAILABILITY STATEMENT

The original contributions generated for this study are included in the article/**Supplementary Material**, further inquiries can be directed to the corresponding authors.

ETHICS STATEMENT

The animal study was reviewed and approved by the Animal Care and Experimentation Committee of the Canton of Bern, Switzerland [license BE 142/16 (SL); BE119/12 (MR)] and followed the Swiss national guidelines for the performance of animal experiments, or under an approved institutional protocol according to National Institutes of Health guidelines, or under animal protocols approved by the Animal Studies Committee of Languedoc Roussillon that comply with French legislation and European Directives.

AUTHOR CONTRIBUTIONS

SE, CP, GF, MB, JG, KL, and MR planned and executed experiments and collected and analyzed data. SE and JG performed statistical analysis and contributed significantly to manuscript writing. DG, SL, AE, and MR study design, project supervision, funding, and manuscript writing. All authors contributed to the article and approved the submitted version.

FUNDING

This work was supported by the Innosuisse (Swiss Innovation Agency), the Rijksdienst voor Ondernemend Nederland (The Netherlands Enterprise Agency) and co-funded by the European Union's Horizon 2020 Framework Programme under the Eurostars E!10491 HEARit project, and by the Swiss National Science Foundation (grants 162583 and 189136).

ACKNOWLEDGMENTS

The authors acknowledge the contribution of Dr. Helmuth van Es (Audion Therapeutics B.V.) for compound selections and study design.

SUPPLEMENTARY MATERIAL

The Supplementary Material for this article can be found online at: https://www.frontiersin.org/articles/10.3389/fcell.2021.710159/full#supplementary-material

REFERENCES

Andersson, E. R., and Lendahl, U. (2014). Therapeutic modulation of Notch signalling — are we there yet? *Nat. Rev. Drug. Disc.* 13, 357–378. doi: 10.1038/nrd4252

Asakura, A., Zeng, X., Kirkpatrick, R., Hofmann, G., Grillot, D., Linhart, V., et al. (2018). Screen for modulators of atonal homolog 1 gene expression using notch pathway-relevant gene transcription based cellular assays. *PLoS One* 13:e0207140. doi: 10.1371/journal.pone.0207140

Atkinson, P. J., Huarcaya Najarro, E., Sayyid, Z. N., and Cheng, A. G. (2015). Sensory hair cell development and regeneration: similarities and differences. *Development* 142, 1561–1571. doi: 10.1242/dev.114926

Barker, N., Tan, S., and Clevers, H. (2013). Lgr proteins in epithelial stem cell biology. *Development* 140, 2484–2494. doi: 10.1242/dev.083113

Bermingham, N. A., Hassan, B. A., Price, S. D., Vollrath, M. A., Ben-Arie, N., Eatock, R. A., et al. (1999). Math1: an essential gene for the generation of inner ear hair cells. *Science* 284, 1837–1841. doi: 10.1126/science.284.5421.1837

Bommakanti, K., Iyer, J. S., and Stankovic, K. M. (2019). Cochlear histopathology in human genetic hearing loss: state of the science and future prospects. *Hear. Res.* 382:107785. doi: 10.1016/j.heares.2019.107785

Bramhall, N. F., Shi, F., Arnold, K., Hochedlinger, K., and Edge, A. S. (2014). Lgr5-positive supporting cells generate new hair cells in the postnatal cochlea. *Stem Cell Rep.* 2, 311–322. doi: 10.1016/j.stemcr.2014.01.008

Bray, S. J. (2016). Notch signalling in context. *Nat. Rev. Mol. Cell Biol.* 17, 722–735. doi: 10.1038/nrm.2016.94

Burns, J. C., Kelly, M. C., Hoa, M., Morell, R. J., and Kelley, M. W. (2015). Single-cell RNA-Seq resolves cellular complexity in sensory organs from the neonatal inner ear. *Nat. Commun.* 6:8557.

Chai, R., Kuo, B., Wang, T., Liaw, E. J., Xia, A., Jan, T. A., et al. (2012). Wnt signaling induces proliferation of sensory precursors in the postnatal mouse cochlea. *Proc. Natl. Acad. Sci. U.S.A.* 109, 8167–8172. doi: 10.1073/pnas.1202774109

Chai, R., Xia, A., Wang, T., Jan, T. A., Hayashi, T., Bermingham-McDonogh, O., et al. (2011). Dynamic expression of Lgr5, a Wnt target gene, in the developing

and mature mouse cochlea. *J. Assoc. Res. Otolaryngol.* 12, 455–469. doi: 10.1007/s10162-011-0267-2

Chen, P., Johnson, J. E., Zoghbi, H. Y., and Segil, N. (2002). The role of Math1 in inner ear development: uncoupling the establishment of the sensory primordium from hair cell fate determination. *Development* 129, 2495–2505. doi: 10.1242/dev.129.10.2495

Chen, W., Cacciabue-Rivolta, D. I., Moore, H. D., and Rivolta, M. N. (2007). The human fetal cochlea can be a source for auditory progenitors/stem cells isolation. *Hear. Res.* 233, 23–29. doi: 10.1016/j.heares.2007.06.006

Corwin, J. T. (1981). Postembryonic production and aging in inner ear hair cells in sharks. *J. Comp. Neurol.* 201, 541–553. doi: 10.1002/cne.902010406

Corwin, J. T. (1985). Perpetual production of hair cells and maturational changes in hair cell ultrastructure accompany postembryonic growth in an amphibian ear. *Proc. Natl. Acad. Sci. U.S.A.* 82, 3911–3915. doi: 10.1073/pnas.82.11.3911

Corwin, J. T., and Cotanche, D. A. (1988). Regeneration of sensory hair cells after acoustic trauma. *Science* 240, 1772–1774. doi: 10.1126/science.3381100

Cox, B. C., Chai, R., Lenoir, A., Liu, Z., Zhang, L., Nguyen, D. H., et al. (2014). Spontaneous hair cell regeneration in the neonatal mouse cochlea in vivo. *Development* 141, 816–829. doi: 10.1242/dev.103036

Doetzlhofer, A., Basch, M. L., Ohyama, T., Gessler, M., Groves, A. K., and Segil, N. (2009). Hey2 regulation by FGF provides a Notch-independent mechanism for maintaining pillar cell fate in the organ of Corti. *Dev. Cell* 16, 58–69. doi: 10.1016/j.devcel.2008.11.008

Driver, E. C., and Kelley, M. W. (2020). Development of the cochlea. *Development* 147:dev162263.

Erni, S. T., Fernandes, G., Buri, M., Perny, M., Rutten, R. J., van Noort, J. M., et al. (2019). Anti-inflammatory and oto-protective effect of the small heat shock protein alpha b-crystallin (HspB5) in experimental pneumococcal meningitis. *Front. Neurol.* 10:570. doi: 10.3389/fneur.2019.00570

Fettiplace, R., and Hackney, C. M. (2006). The sensory and motor roles of auditory hair cells. *Nat. Rev. Neurosci.* 7, 19–29. doi: 10.1038/nrn1828

Forge, A., Li, L., Corwin, J. T., and Nevill, G. (1993). Ultrastructural evidence for hair cell regeneration in the mammalian inner ear. *Science* 259, 1616–1619. doi: 10.1126/science.8456284

Gausterer, J. C., Saidov, N., Ahmadi, N., Zhu, C., Wirth, M., Reznicek, G., et al. (2020). Intratympanic application of poloxamer 407 hydrogels results in sustained N-acetylcysteine delivery to the inner ear. *Eur. J. Pharmaceutics Biopharmaceutics* 150, 143–155. doi: 10.1016/j.ejpb.2020.03.005

Groves, A. K., and Fekete, D. M. (2012). Shaping sound in space: the regulation of inner ear patterning. *Development* 139, 245–257. doi: 10.1242/dev.067074

Han, J., and Shen, Q. (2012). Targeting γ-secretase in breast cancer. *Breast Cancer: Targets Ther.* 4, 83–90.

Hayashi, T., Kokubo, H., Hartman, B. H., Ray, C. A., Reh, T. A., and Bermingham-McDonogh, O. (2008). Hesr1 and Hesr2 may act as early effectors of Notch signaling in the developing cochlea. *Dev. Biol.* 316, 87–99. doi: 10.1016/j.ydbio.2008.01.006

Hoa, M., Olszewski, R., Li, X., Taukulis, I., Gu, S., DeTorres, A., et al. (2020). Characterizing adult cochlear supporting cell transcriptional diversity using Single-Cell RNA-Seq: validation in the adult mouse and translational implications for the adult human cochlea. *Front. Mol. Neurosci.* 13:13. doi: 10.3389/fnmol.2020.00013

Hu, L., Lu, J., Chiang, H., Wu, H., Edge, A. S., and Shi, F. (2016). Diphtheria toxin-induced cell death triggers wnt-dependent hair cell regeneration in neonatal mice. *J. Neurosci.* 36, 9479–9489. doi: 10.1523/jneurosci.2447-15.2016

Huth, M. E., Han, K. H., Sotoudeh, K., Hsieh, Y. J., Effertz, T., Vu, A. A., et al. (2015). Designer aminoglycosides prevent cochlear hair cell loss and hearing loss. *J. Clin. Invest.* 125, 583–592. doi: 10.1172/jci77424

Jacques, B. E., Puligilla, C., Weichert, R. M., Ferrer-Vaquer, A., Hadjantonakis, A. K., Kelley, M. W., et al. (2012). Function for canonical Wnt/beta-catenin signaling in the developing mammalian cochlea. *Development* 139, 4395–4404. doi: 10.1242/dev.080358

Kazanjian, A., Noah, T., Brown, D., Burkart, J., and Shroyer, N. F. (2010). Atonal homolog 1 is required for growth and differentiation effects of Notch/γ-Secretase inhibitors on normal and cancerous intestinal epithelial cells. *Gastroenterology* 139, 918.e6–928.e6.

Kelley, M. W. (2006). Regulation of cell fate in the sensory epithelia of the inner ear. *Nat. Rev. Neurosci.* 7, 837–849. doi: 10.1038/nrn1987

Kiernan, A. E. (2013). Notch signaling during cell fate determination in the inner ear. *Semin. Cell. Dev. Biol.* 24, 470–479. doi: 10.1016/j.semcdb.2013.04.002

Koehler, K. R., Nie, J., Longworth-Mills, E., Liu, X. P., Lee, J., Holt, J. R., et al. (2017). Generation of inner ear organoids containing functional hair cells from human pluripotent stem cells. *Nat. Biotechnol.* 35, 583–589. doi: 10.1038/nbt.3840

Kopan, R., and Ilagan, M. X. (2009). The canonical Notch signaling pathway: unfolding the activation mechanism. *Cell* 137, 216–233. doi: 10.1016/j.cell.2009.03.045

Korrapati, S., Roux, I., Glowatzki, E., and Doetzlhofer, A. (2013). Notch signaling limits supporting cell plasticity in the hair cell-damaged early postnatal murine cochlea. *PLoS One* 8:e73276. doi: 10.1371/journal.pone.0073276

Leib, S. L., Leppert, D., Clements, J., and Tauber, M. G. (2000). Matrix metalloproteinases contribute to brain damage in experimental pneumococcal meningitis. *Infect. Immun.* 68, 615–620. doi: 10.1128/iai.68.2.615-620.2000

Lenz, D. R., Gunewardene, N., Abdul-Aziz, D. E., Wang, Q., Gibson, T. M., and Edge, A. S. B. (2019). Applications of Lgr5-Positive cochlear progenitors (LCPs) to the study of hair cell differentiation. *Front. Cell Dev. Biol.* 7:14. doi: 10.3389/fcell.2019.00014

Li, W., Wu, J., Yang, J., Sun, S., Chai, R., Chen, Z. Y., et al. (2015). Notch inhibition induces mitotically generated hair cells in mammalian cochleae via activating the Wnt pathway. *Proc. Natl. Acad. Sci. U.S.A.* 112, 166–171. doi: 10.1073/pnas.1415901112

Liberman, M. C. (1990). Quantitative assessment of inner ear pathology following ototoxic drugs or acoustic trauma. *Toxicol. Pathol.* 18, 138–148. doi: 10.1177/019262339001800119

Lumpkin, E. A., Collisson, T., Parab, P., Omer-Abdalla, A., Haeberle, H., Chen, P., et al. (2003). Math1-driven GFP expression in the developing nervous system of transgenic mice. *Gene Exp. Patterns* 3, 389–395. doi: 10.1016/s1567-133x(03)00089-9

Maass, J. C., Gu, R., Basch, M. L., Waldhaus, J., Lopez, E. M., Xia, A., et al. (2015). Changes in the regulation of the Notch signaling pathway are temporally correlated with regenerative failure in the mouse cochlea. *Front. Cell Neurosci.* 9:110. doi: 10.3389/fncel.2015.00110

McLean, W. J., Yin, X., Lu, L., Lenz, D. R., McLean, D., Langer, R., et al. (2017). Clonal expansion of Lgr5-positive cells from mammalian cochlea and high-purity generation of sensory hair cells. *Cell Rep.* 18, 1917–1929. doi: 10.1016/j.celrep.2017.01.066

Mizutari, K., Fujioka, M., Hosoya, M., Bramhall, N., Okano, H. J., Okano, H., et al. (2013). Notch inhibition induces cochlear hair cell regeneration and recovery of hearing after acoustic trauma. *Neuron* 77, 58–69. doi: 10.1016/j.neuron.2012.10.032

Muller, U., and Barr-Gillespie, P. G. (2015). New treatment options for hearing loss. *Nat. Rev. Drug. Discov.* 14, 346–365. doi: 10.1038/nrd4533

Ni, W., Lin, C., Guo, L., Wu, J., Chen, Y., Chai, R., et al. (2016a). Extensive supporting cell proliferation and mitotic hair cell generation by in vivo genetic reprogramming in the neonatal mouse cochlea. *J. Neurosci.* 36, 8734–8745. doi: 10.1523/jneurosci.0060-16.2016

Ni, W., Zeng, S., Li, W., Chen, Y., Zhang, S., Tang, M., et al. (2016b). Wnt activation followed by Notch inhibition promotes mitotic hair cell regeneration in the postnatal mouse cochlea. *Oncotarget* 7, 66754–66768. doi: 10.18632/oncotarget.11479

Oshima, K., Senn, P., and Heller, S. (2009). Isolation of sphere-forming stem cells from the mouse inner ear. *Methods Mol. Biol.* 493, 141–162. doi: 10.1007/978-1-59745-523-7_9

Perny, M., Roccio, M., Grandgirard, D., Solyga, M., Senn, P., and Leib, S. L. (2016). The severity of infection determines the localization of damage and extent of sensorineural hearing loss in experimental pneumococcal meningitis. *J. Neurosci.* 36, 7740–7749. doi: 10.1523/jneurosci.0554-16.2016

Perny, M., Solyga, M., Grandgirard, D., Roccio, M., Leib, S. L., and Senn, P. (2017). Streptococcus pneumoniae-induced ototoxicity in organ of Corti explant cultures. *Hear. Res.* 350, 100–109. doi: 10.1016/j.heares.2017.04.012

Ranum, P. T., Goodwin, A. T., Yoshimura, H., Kolbe, D. L., Walls, W. D., Koh, J. Y., et al. (2019). Insights into the biology of hearing and deafness revealed by single-cell RNA sequencing. *Cell Rep.* 26, 3160.e3-3171.e3.

Roccio, M. (2020). Directed differentiation and direct reprogramming: applying stem cell technologies to hearing research. *Stem Cells* 39, 375–388. doi: 10.1002/stem.3315

Roccio, M., Hahnewald, S., Perny, M., and Senn, P. (2015). Cell cycle reactivation of cochlear progenitor cells in neonatal FUCCI mice by a GSK3 small molecule inhibitor. *Sci. Rep*. 5:17886.

Roccio, M., Perny, M., Ealy, M., Widmer, H. R., Heller, S., and Senn, P. (2018). Molecular characterization and prospective isolation of human fetal cochlear hair cell progenitors. *Nat. Commun.* 9:4027.

Roccio, M., Senn, P., and Heller, S. (2019). Novel insights into inner ear development and regeneration for targeted hearing loss therapies. *Hear. Res.* 397:107859. doi: 10.1016/j.heares.2019.107859

Ryals, B. M., and Rubel, E. W. (1988). Hair cell regeneration after acoustic trauma in adult Coturnix quail. *Science* 240, 1774–1776. doi: 10.1126/science.3381101

Samarajeewa, A., Jacques, B. E., and Dabdoub, A. (2019). Therapeutic potential of Wnt and notch signaling and epigenetic regulation in mammalian sensory hair cell regeneration. *Mol. Ther.* 27, 904–911. doi: 10.1016/j.ymthe.2019.03.017

Samarajeewa, A., Lenz, D. R., Xie, L., Chiang, H., Kirchner, R., Mulvaney, J. F., et al. (2018). Transcriptional response to Wnt activation regulates the regenerative capacity of the mammalian cochlea. *Development* 145:dev166579.

Sayyid, Z. N., Wang, T., Chen, L., Jones, S. M., and Cheng, A. G. (2019). Atoh1 directs regeneration and functional recovery of the mature mouse vestibular system. *Cell Rep.* 28, 312.e4–324.e4.

Schindelin, J., Arganda-Carreras, I., Frise, E., Kaynig, V., Longair, M., Pietzsch, T., et al. (2012). Fiji: an open-source platform for biological-image analysis. *Nat. Methods* 9, 676–682. doi: 10.1038/nmeth.2019

Sha, S. H., Taylor, R., Forge, A., and Schacht, J. (2001). Differential vulnerability of basal and apical hair cells is based on intrinsic susceptibility to free radicals. *Hear. Res.* 155, 1–8. doi: 10.1016/s0378-5955(01)00224-6

Shi, F., Hu, L., Jacques, B. E., Mulvaney, J. F., Dabdoub, A., and Edge, A. S. (2014). beta-Catenin is required for hair-cell differentiation in the cochlea. *J. Neurosci.* 34, 6470–6479. doi: 10.1523/jneurosci.4305-13.2014

Shi, F., Kempfle, J. S., and Edge, A. S. (2012). Wnt-responsive Lgr5-expressing stem cells are hair cell progenitors in the cochlea. *J. Neurosci.* 32, 9639–9648. doi: 10.1523/jneurosci.1064-12.2012

Shu, Y., Li, W., Huang, M., Quan, Y. Z., Scheffer, D., Tian, C., et al. (2019). Renewed proliferation in adult mouse cochlea and regeneration of hair cells. *Nat. Commun.* 10:5530.

Taylor, R. R., Filia, A., Paredes, U., Asai, Y., Holt, J. R., Lovett, M., et al. (2018). Regenerating hair cells in vestibular sensory epithelia from humans. *Elife* 7:e34817.

Tona, Y., Hamaguchi, K., Ishikawa, M., Miyoshi, T., Yamamoto, N., Yamahara, K., et al. (2014). Therapeutic potential of a gamma-secretase inhibitor for hearing restoration in a guinea pig model with noise-induced hearing loss. *BMC Neurosci.* 15:66. doi: 10.1186/1471-2202-15-66

Wang, T., Niwa, M., Sayyid, Z. N., Hosseini, D. K., Pham, N., Jones, S. M., et al. (2019). Uncoordinated maturation of developing and regenerating postnatal mammalian vestibular hair cells. *PLoS Biol.* 17:e3000326. doi: 10.1371/journal.pbio.3000326

Warchol, M. E., Lambert, P. R., Goldstein, B. J., Forge, A., and Corwin, J. T. (1993). Regenerative proliferation in inner ear sensory epithelia from adult guinea pigs and humans. *Science* 259, 1619–1622. doi: 10.1126/science.8456285

Weihofen, A., Lemberg, M. K., Friedmann, E., Rueeger, H., Schmitz, A., Paganetti, P., et al. (2003). Targeting presenilin-type aspartic protease signal peptide peptidase with γ-Secretase inhibitors. *J. Biol. Chem.* 278, 16528–16533. doi: 10.1074/jbc.m301372200

Weisleder, P., and Rubel, E. W. (1993). Hair cell regeneration after streptomycin toxicity in the avian vestibular epithelium. *J. Comp. Neurol.* 331, 97–110. doi: 10.1002/cne.903310106

Wilson, B. S., Tucci, D. L., Merson, M. H., and O'Donoghue, G. M. (2017). Global hearing health care: new findings and perspectives. *Lancet* 390, 2503–2515. doi: 10.1016/s0140-6736(17)31073-5

Woods, C., Montcouquiol, M., and Kelley, M. W. (2004). Math1 regulates development of the sensory epithelium in the mammalian cochlea. *Nat. Neurosci.* 7, 1310–1318. doi: 10.1038/nn1349

Yu, K. S., Frumm, S. M., Park, J. S., Lee, K., Wong, D. M., Byrnes, L., et al. (2019). Development of the mouse and human cochlea at single cell resolution. *BioRxiv [preprint]* doi: 10.1101/739680

Zak, M., van Oort, T., Hendriksen, F. G., Garcia, M. I., Vassart, G., and Grolman, W. (2016). LGR4 and LGR5 regulate hair cell differentiation in the sensory epithelium of the developing mouse cochlea. *Front. Cell Neurosci.* 10:186. doi: 10.3389/fncel.2016.00186

Zheng, J. L., Shou, J. Y., Guillemot, F., Kageyama, R., and Gao, W. Q. (2000). Hes1 is a negative regulator of inner ear hair cell differentiation. *Development* 127, 4551–4560. doi: 10.1242/dev.127.21.4551

Zine, A., Aubert, A., Qiu, J., Therianos, S., Guillemot, F., Kageyama, R., et al. (2001). Hes1 and Hes5 activities are required for the normal development of the hair cells in the mammalian inner ear. *J. Neurosci.* 21, 4712–4720. doi: 10.1523/jneurosci.21-13-04712.2001

Conflict of Interest: JG and KL are employed by Audion Therapeutics. AE is a founder and consultant to the company. Part of the study at the University of Bern was sponsored by Audion Therapeutics.

The remaining authors declare that the research was conducted in the absence of any commercial or financial relationships that could be construed as a potential conflict of interest.

frontiers in Cell and Developmental Biology

REVIEW
published: 07 October 2021
doi: 10.3389/fcell.2021.737429

Unraveling Human Brain Development and Evolution Using Organoid Models

Sarah Fernandes[1,2], *Davis Klein*[1,3] *and Maria C. Marchetto*[1,4]*

[1] *Laboratory of Genetics, The Salk Institute for Biological Studies, La Jolla, CA, United States,* [2] *Department of Biological Sciences, University of California, San Diego, San Diego, CA, United States,* [3] *Department of Chemistry and Biochemistry, San Diego State University, San Diego, CA, United States,* [4] *Department of Anthropology, Center for Academic Research and Training in Anthropogeny (CARTA), University of California, San Diego, San Diego, CA, United States*

Brain organoids are proving to be physiologically relevant models for studying human brain development in terms of temporal transcriptional signature recapitulation, dynamic cytoarchitectural development, and functional electrophysiological maturation. Several studies have employed brain organoid technologies to elucidate human-specific processes of brain development, gene expression, and cellular maturation by comparing human-derived brain organoids to those of non-human primates (NHPs). Brain organoids have been established from a variety of NHP pluripotent stem cell (PSC) lines and many protocols are now available for generating brain organoids capable of reproducibly representing specific brain region identities. Innumerous combinations of brain region specific organoids derived from different human and NHP PSCs, with CRISPR-Cas9 gene editing techniques and strategies to promote advanced stages of maturation, will successfully establish complex brain model systems for the accurate representation and elucidation of human brain development. Identified human-specific processes of brain development are likely vulnerable to dysregulation and could result in the identification of therapeutic targets or disease prevention strategies. Here, we discuss the potential of brain organoids to successfully model human-specific processes of brain development and explore current strategies for pinpointing these differences.

Keywords: neurodevelopment, evolution, brain disorders, disease modeling, non-human primates, neocortex, transcriptomics, brain organoids

OPEN ACCESS

Edited by:
Lon J. Van Winkle,
Rocky Vista University, United States

Reviewed by:
In-Hyun Park,
Yale University, United States
Yuhua Sun,
Institute of Hydrobiology, Chinese Academy of Sciences (CAS), China

***Correspondence:**
Maria C. Marchetto
mcmarchetto@ucsd.edu

Specialty section:
This article was submitted to Stem Cell Research, a section of the journal Frontiers in Cell and Developmental Biology

Received: *06 July 2021*
Accepted: *14 September 2021*
Published: *07 October 2021*

Citation:
Fernandes S, Klein D and Marchetto MC (2021) Unraveling Human Brain Development and Evolution Using Organoid Models. Front. Cell Dev. Biol. 9:737429. doi: 10.3389/fcell.2021.737429

INTRODUCTION

There exists human (*Homo sapiens*)-specific molecular and cellular processes of brain development that are not shared even with our closest Hominidae relatives like chimpanzees (*Pan troglodytes*). While mammalian neurodevelopment mutually exhibits apicobasal organization of radial glia cells (RGs), timed cellular specification, and maturation of heterogeneous cell populations resulting in functional neural circuits (Campbell and Götz, 2002; Bakken et al., 2016), there are primate-specific characteristics of cortex development and maturation. These primate-specific features include delayed and extended periods of myelination, increased excessive synapse production, and postponed and protracted synaptic pruning (Petanjek et al., 2011; Miller et al., 2012). Furthermore,

primates uniquely demonstrate expanded progenitor populations of the inner subventricular (iSVZ) and outer subventricular zones (oSVZ) which, together, comprise the subventricular zone (SVZ) (Giandomenico and Lancaster, 2017). It has been proposed that the advent of outer radial glial cells (oRGs) and the oSVZ led to the dramatic expansion of the cortex by giving rise to neurons of superficial layers and resulted in gyrification of the cortices of carnivores and primates, including humans (Stahl et al., 2013). Yet, recent findings in macaques support the hypothesis that, after embryonic day (E)92 and around the time of gyrification between E100 and E125, the oSVZ primarily functions as a source of astrocytes and oligodendrocytes rather than neurons (Rash et al., 2019). The complete coordination of neocortical expansion and gyrification is poorly understood as it is a complex process likely requiring the cumulative effect of several processes including neuronal growth, dendritic branching, epigenetic regulation, and the expansion of cortical neuropil (Hirabayashi and Gotoh, 2010; Rash et al., 2019).

Although primates commonly display features of brain development not observed in other mammals, it has been further suggested that approximately 9% of genes in humans have different developmental trajectories that could be contributing to delayed brain maturation when compared to rhesus monkeys (*Macaca mulatta*) (Bakken et al., 2016). Neoteny is thought to be central for the emergence of human-specific brain anatomy responsible for unique cognitive abilities by allowing for extended periods of neural remodeling, plasticity, and fine-tuning (Langer, 1996; Johnson, 2001). Pre- and postnatal transcriptomic analyses of human brain development have revealed neotenic gene expression patterns in humans when compared to macaques and chimpanzees; however, prenatal studies on neoteny are limited and increased sample distribution across age and developing brain regions are required to gain a more complete understanding of human neotenic brain development (Somel et al., 2009; Li et al., 2020). The timing of postnatal neotenic shifts in gene expression seem to correspond to the duration of gray-matter volume reduction which is associated with synapse elimination and remodeling (Somel et al., 2009). Synaptogenesis and the subsequent elimination of excessive synaptic spines are essential for optimal refinement of neuronal circuitry and cognitive skills while dysregulation of these processes have been linked to late-onset neuropsychiatric disorders (Petanjek et al., 2011). Studies suggest that both pre and postnatal human cortex development demonstrates regional differences and extended rates of synaptogenesis when compared to that of rhesus monkeys which exhibit uniform, simultaneous synaptogenesis (Rakic et al., 1986; Huttenlocher and Dabholkar, 1997). Humans are also born with reduced amounts of myelinated axons compared to chimpanzees and exhibit no adultlike neocortical myelination unlike chimpanzees (Miller et al., 2012). Additionally, dopaminergic (DAergic) axons, labeled by tyrosine hydroxylase (TH), show much higher innervation in layers V/VI of areas 9 and 32 of the human and chimpanzee cortex when compared to those of macaques (*Macaca*) (Raghanti et al., 2011). Altogether, human-specific aspects of neurodevelopment and maturation likely contribute to our differences in cellular and laminar organization, interconnectivity of various brain regions, hemispheric asymmetry, and overall encephalization resulting in species-specific cognitive abilities. Nonetheless, further research is needed to illuminate human-specific features of neurodevelopment and their correlation to distinctly human cognition (Preuss, 2011; Sakai et al., 2013; **Table 1**).

Uniquely human features of neocortical development and maturation are not only intriguing for their implications in human-specific cognitive abilities, but they are also vulnerable to dysregulation which could cause or contribute to distinctly human brain disorder pathophysiology. The human cerebral cortex is essential for both cognition and emotional processing and dysregulation of these processes of the cortex are associated with a wide range of brain disorders including schizophrenia (SZ), autism spectrum disorder (ASD), Parkinson's disease (PD), and Alzheimer's disease (AD) (Berman and Weinberger, 1991; Rubenstein, 2011; Xu et al., 2019). Much remains to be learned about the mechanisms governing cortical expansion and responses to pathogenesis between human and non-human primates (NHPs) (Otani et al., 2016). Understanding these differences could shed light on the underlying mechanisms responsible for human-specific brain disorders and lead to the identification of key targets for the development of effective therapies.

Subtle differences observed by comparing human neurodevelopment to that of our closest evolutionary relatives could reveal underlying mechanisms, including genomic or transcriptional differences, contributing to varied phenotypes (Pollen et al., 2019). Human-specific responses to pathogenesis might be elucidated in a similar manner; by comparing brain pathophysiology of humans to our non-human primate counterparts (Hof et al., 2004). Although rodent models have taught us much about basic mammalian brain development and disorders (Fernando and Robbins, 2011), comparing governing processes and responses to species more closely related to humans can reduce the number of variables allowing for the identification of specific mechanisms responsible for observed deviations. Studies analyzing induced pluripotent stem cells (iPSCs) derived from humans, chimpanzees, and bonobos (*Pan paniscus*) show large sets of differentially expressed genes between human and NHP iPSCs. Perhaps the most compelling differentially expressed genes are those related to increased long interspersed element-1 (LINE-1) mobility in chimpanzees and bonobos, which could have implications on the rates of genetic divergence among species, and alternative mechanisms of pluripotency maintenance in chimpanzees (Marchetto et al., 2013; Gallego Romero et al., 2015). Furthermore, when human and NHP iPSCs were differentiated to neurons, they displayed distinctive migratory patterns at the neural progenitor cell (NPC) stage followed by contrasting morphology and timing of maturation in neurons (Marchetto et al., 2019). Despite the ability of two-dimensional (2D) PSC-derived neural cultures to demonstrate basic organization and transcriptomic changes of early brain development (Yan et al., 2013), while retaining the genetic background of the somatic cells from which they are reprogrammed, they lack the ability to develop complex cytoarchitecture, recapitulate advanced spatiotemporal transcriptomics, and brain region interconnectivity (including

TABLE 1 | Summary of some of the known and unknown aspects of human and NHP brain development and anatomy.

	Differences in Brain Development and Anatomy	Unknowns of Brain Development and Anatomy
Unique to humans	Neotenic gene expression patterns compared to NHPs	Complete map of neotenic gene expression patterns compared to NHPs, Systematic understanding of neoteny in humans compared to NHPs across age and developing brain regions, How neoteny gives rise to human-specific cognitive abilities
	Regional differences in rates of synaptogenesis in developing cortex (compared to rhesus monkeys)	How regional differences in rates of synaptogenesis differ in human when compared to NHP species other than rhesus monkeys
	Reduced amounts of myelinated axons at birth and no adultlike neocortical myelination at birth (compared to chimpanzees)	Developmental timing of axon myelination in human when compared to NHP species other than chimpanzees and across brain regions
	Higher innervation of dopaminergic axons (labeled by TH) in layers V/VI of areas 9 and 32 of the human cortex when compared to chimpanzees and macaques	While the involvement of DA in cognitive processes is well documented, how DAergic innervation corresponds to NHP differences in cognition and emotional processing is less understood
Unique to primates or other gyrencephalic species	Expanded regions and progenitor cell populations of the iSVZ and oSVZ	How expanded iSVZs and oSVZs contribute to expanded cortices and cognitive abilities
	oRGs comprising the oSVZ	The complete mechanisms by which oRGs contribute to cortical expansion and gyrification
	Denser, more extensive DAergic innervation with fibers in all cortical layers when compared to rodents	The specific mechanisms governing DAergic axon innervation in primates and humans during brain development

migration and axon guidance) of ensuing primate brain development (Soldner and Jaenisch, 2019). Intricate cellular heterogeneity, complex architecture, and interconnectivity of neurodevelopment, in addition to pathogenic responses, could be observed by comparing human and NHP brain tissues; however, ethical concerns and the inaccessibility of pre- and postnatal primate brain tissues limits the feasibility of such studies.

While brain organoids might be a long way from forming or sharing thoughts with us, they could still teach us much about ourselves. Brain organoids are three-dimensional (3D), PSC-derived structures that display complex radial organization of expanding neuroepithelium following embedding in an extracellular matrix like Matrigel and can recapitulate some subsequent processes of neurodevelopment including neurogenesis, gliogenesis, synaptogenesis, heterogenous cytoarchitecture, cell and axon migration, myelination of axons, and spontaneously-active neuronal networks (Lancaster et al., 2013; Bagley et al., 2017; Birey et al., 2017; Quadrato et al., 2017; Xiang et al., 2017; Marton et al., 2019; Shaker et al., 2021). It is likely that all these features of neurodevelopment are governed by some degree of specifies-specific dynamics. Brain organoids can be generated from human and NHP PSCs and, since some pathways regulating neural induction and brain region specification are well conserved in primates, both unguided cerebral organoids and guided brain region specific organoids can be generated (Mora-Bermúdez et al., 2016; Field et al., 2019; Kanton et al., 2019). Additional protocols have been established for the derivation of brain region specific organoids from human PSCs (hPSCs), including dorsal forebrain, ventral forebrain, midbrain, thalamus, basal ganglia, cerebellum, and telencephalic organoids (Muguruma et al., 2015; Sakaguchi et al., 2015; Jo et al., 2016; Bagley et al., 2017; Birey et al., 2017; Watanabe et al., 2017; Xiang et al., 2017, 2019; Qian et al., 2018). With some modifications, these methods could prove to be successful in establishing brain region-specific organoids from a variety of NHP PSC lines allowing for the reproducible comparison of homogeneous, human-specific neurodevelopment and brain disorder pathophysiology in brain regions beyond the cortex.

In this review we discuss the application of human and NHP-derived brain organoids, and the implementation of genome editing technologies in these model systems, to investigate human brain evolution and pinpoint human-specific processes of neurodevelopment and maturation vulnerable to dysregulation (**Figure 1**). We further consider the application of brain organoid technologies to reveal distinctly human responses to pathogenesis. Our goal is to provide insight into methods for identifying uniquely human mechanisms driving brain disorder pathophysiology which could illuminate potential therapeutic targets.

BRAIN ORGANOIDS MODEL HUMAN SPECIFIC BRAIN DEVELOPMENT AND EVOLUTION

Brain organoids are paving the way for *in vitro* access to elaborate, physiological relevant model systems of human-specific neurodevelopmental. Brain organoids have the advantage of retaining the species-specific genetic background of the PSCs from which they are derived while supporting the orchestration of dynamic processes of neurodevelopment as transcriptomic changes occur in a 3D space. PSCs have been established from a variety of NHP species including chimpanzee, bonobo, gorilla (*Gorilla gorilla*), orangutan (*Pongo abelii*), and rhesus monkey (Liu et al., 2008; Marchetto et al., 2013; Gallego Romero et al., 2015; Mostajo-Radji et al., 2020). Access to these cell lines sets the stage for creative brain organoid development and analysis representing several combinations of species, brain

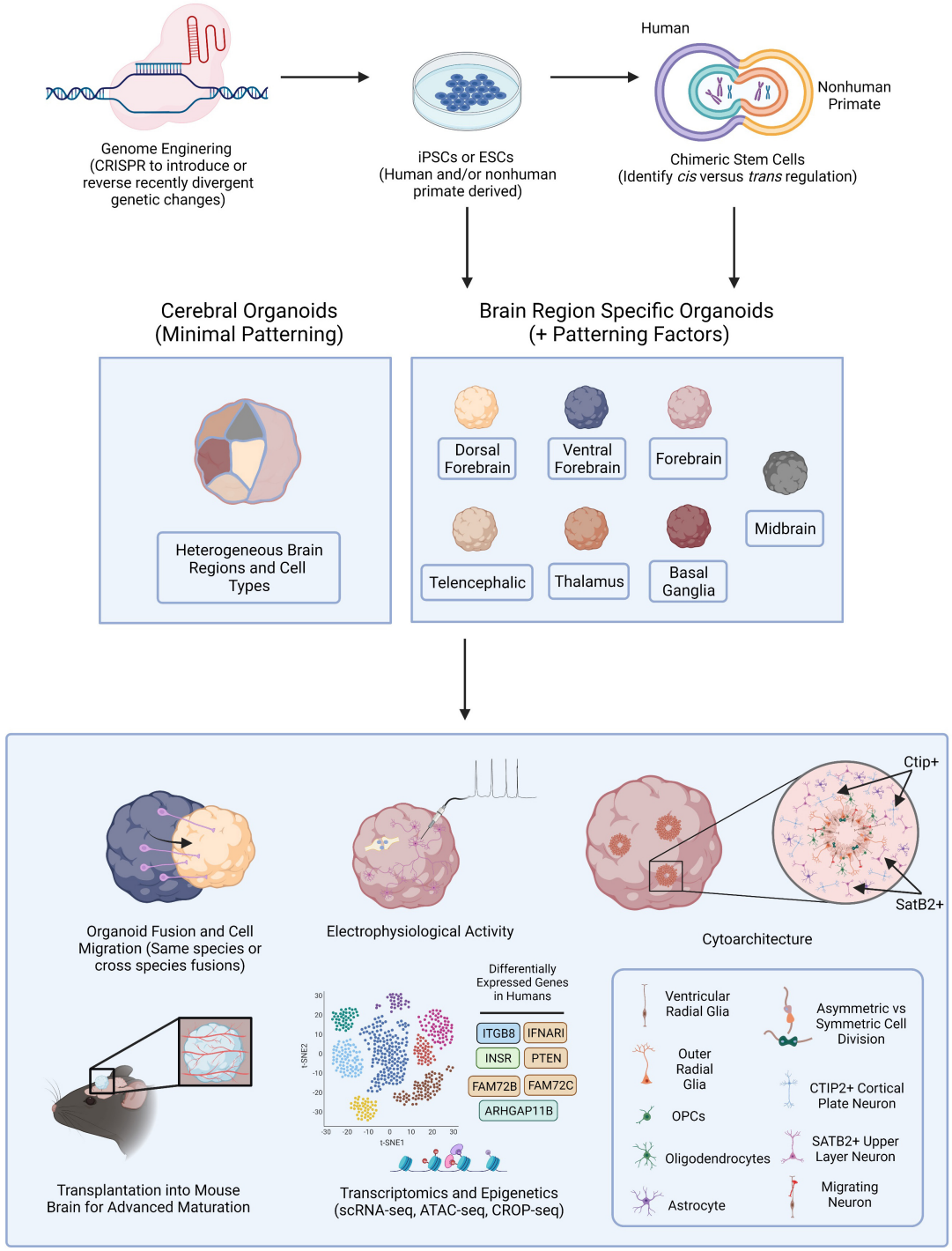

FIGURE 1 | Brain Organoid Based Models to Identify Human-Specific Processes of Brain Development. Schematic outlining the possible methods for establishing brain organoids from PSCs and various means of analysis and downstream processes to compare resulting phenotypes. PSCs can be obtained from either human or NHPs and CRISPR-Cas9, or other gene editing technologies, can be employed to introduce genetic perturbations into the PSCs. Cerebral or brain region specific organoids can then be directly generated from PSCs or human and NHP PSCs can first be fused forming tetraploid hybrid PSCs for the identification of *cis* vs. *trans* regulatory elements and then be applied for the generation of brain organoids. Cerebral organoids or several different types of brain region specific organoids can be produced from a variety of human and NHP PSCs. Different combinations of organoids can then be fused to observe neuronal migratory patterns important for establishing healthy brain connectivity. Resulting organoids can be implanted into the mouse brain for subsequent vascularization allowing for oxygen and glucose penetration into the organoid and advanced cellular maturation. Human specific phenotypes, including complex, functional cytoarchitectural differences or differentially expressed genes can then be identified through different means of analysis including monitoring of electrophysiological activity using MEA or with high-throughput omic analyses like scRNA-seq or ATAC-seq.

regions, and genomic and epigenomic modifications. Here, we discuss strategies to develop and analyze complex brain organoid model systems for the elucidation of distinctly human brain development and to provide insight into human brain evolution.

Transcriptomics and Omics

The human brain is an immensely complex organ, with the prenatal cortex alone developing at a rate of approximately 3.86 million new neurons per hour including about 42.3 million synapses per minute, and requires over two decades to fully form into a structure containing approximately 84.6 billion communicating neurons (NeuN-positive cells) and 84.6 billion non-neuronal (NeuN-negative) cells (Azevedo et al., 2009; Silbereis et al., 2016). Although some inherent variation in human brain size and shape might occur, brain development is reproducibly accomplished through complex molecular and cellular processes that are governed by elegant regulation of a genetic blueprint (Silbereis et al., 2016; Reardon et al., 2018). These processes give rise to systematic transcriptional signatures that are expressed in consistent spatiotemporal patterns throughout neurodevelopment. How reliably brain organoids can recapitulate temporal cellular specification and maturation of brain development, indicated by changes in transcriptomics, is an ongoing conversation.

Bulk RNA-sequencing is useful for obtaining a sense of gene expression patterns and regulation across tissue or organoid samples; however, it is unable to discern transcriptomic trends at the single-cell level. Advances in single cell sequencing technology allow for transcriptome analysis with single cell resolution, providing detailed snapshots of transcriptomic changes and cellular heterogeneity during development or other dynamic tissue processes (Tang et al., 2009). Several platforms for single-cell RNA sequencing (scRNA-seq) are now available which can vary in sensitivity, accuracy, and precision (Ziegenhain et al., 2017). Beginning in 2015, various groups have employed scRNA-seq platforms to compare different brain organoid generation protocols among themselves and against human fetal brain tissues (Atamian et al., 2021). The earliest study used SMART-seq to contrast 226 single-cell transcriptomes from 12 and 13-week human neocortex against 333 single-cell transcriptomes from five cerebral organoids ranging from days 33 to 65. They found comparable gene expression profiles in over 80% of genes associated with neocortex disease or evolution between cerebral organoids and neocortical tissues (Camp et al., 2015). Following studies aimed to determine the reproducibility of the cellular composition of organoids by employing droplet-based single-cell mRNA sequencing (Drop-seq) to analyze about 67,000 cells from 19 optimized cerebral organoids isolated from four different bioreactors at 6 months. They reported a diversity of cell types in organoids closely related to those observed during *in vivo* brain development; however, although some cell types were reproducible generated, others appeared inconsistently which was partially attributed to bioreactor-based batch effects (Quadrato et al., 2017). More recently, researchers have used BD Rhapsody and 10X Genomics to analyze dorsal forebrain organoids, cortical spheroids, and human cortical organoids established *via* alternative directed differentiation protocols. While some groups noted an increase in apoptotic, glycolysis, and ER stress genes, they all cited the presence of reproducible cellular subtypes and aspects of development (Velasco et al., 2019; Yoon et al., 2019; Bhaduri et al., 2020; Tanaka et al., 2020).

scRNA-seq has led to a general consensus that brain organoids reliably recapitulate broad and some specific cell types present during neurodevelopment, transcriptional signatures of early to mid-fetal human cortex, and some degree of cellular maturation (Kelava and Lancaster, 2016; Sloan et al., 2017; Velasco et al., 2019). A recent study has reported the establishment of human cortical organoid protocols capable of achieving some epigenetic and transcriptional milestones up to postnatal days 250 and 300 (Gordon et al., 2021). These studies have laid the foundation for transcriptional comparisons of human and NHP derived organoids to elucidate evolutionary differences in gene expression patterns during brain development. Early reports describing the establishment of cerebral organoids from chimpanzee iPSCs turned to scRNA-seq to assist in characterizing the developed organoids. One group found populations of cells in chimpanzee organoids like those previously described in human cerebral organoids and with gene expression patterns correlated to those observed in human organoids and fetal cerebral cortex. The identified groups of cells in the chimpanzee cerebral organoids represented the cerebral cortex, hindbrain, ventral midbrain, and peripheral mesenchyme in addition to those in various stages of maturation (Camp et al., 2015; Mora-Bermúdez et al., 2016). Further analysis of the scRNA-seq transcriptome reads suggested that genes required for membrane structure, like integrin beta 8 (ITGB8), and intercellular signaling, including insulin receptor (INSR), were greatly upregulated in human organoid apical progenitor cells (APs) and neurons (Mora-Bermúdez et al., 2016).

More recent studies performed scaled-up scRNA-seq experiments with increasing numbers of brain organoid samples, cells, species, and timepoints. Using scRNA-seq (10X Genomics) to analyze human, chimpanzee, and macaque cerebral organoids at several timepoints from the PSC stage to 4 months of organoid development, researchers found that human neuronal development occurs at a protracted rate compared to chimpanzees and macaques and differentially expressed genes related to proliferation, neuronal migration, and neurite formation are enriched in human radial glial cells (RGs), intermediate progenitors (IPs), and neurons. Furthermore, accessible chromatin profiling demonstrated that differential chromatin accessibility corresponded to human-specific gene expression. Four of the 23 differentially expressed genes were specific to G2M phase progenitors of the telencephalon and included ARHGAP11B, FAM72B, FAM72C, and FAM72D (Kanton et al., 2019). An additional large-scale transcriptomic comparison of primary human and macaque telencephalon found 1,258 differentially expressed genes and, when these genes were contrasted with differentially expressed genes between human and chimpanzee telencephalon organoids using Fluidigm C1, 261 genes overlapped suggesting human-specific expression of these genes during cortical development. They identified upregulated gene co-expression modules in humans related to transcription during G1/S transition, neuronal apoptosis,

and mTOR pathway genes (both activators, including INSR, ITGB8, and IFNAR1, and repressors like PTEN) implicated in stemness and long-term self-renewal (Pollen et al., 2019). Finally, cerebral cortex organoids were derived from human embryonic stem cells (ESCs), rhesus monkey ESCs, chimpanzee iPSCs, and orangutan iPSCs (Eiraku et al., 2008). Focusing on long non-coding RNAs (lncRNAs), associated with gene regulation, imprinting, and stem cell maintenance, the authors observed 920 human lncRNAs conserved in all species with transiently expressed lncRNAs in specific cell types as indicated through scRNA-seq (Field et al., 2019). Studies analyzing 33 brain regions from the postmortem tissue of humans, chimpanzees, bonobos, and macaques using bulk-RNA-sequencing and single nuclei RNA-sequencing (snRNA-seq) found that human-specific gene expression differences were not uniform across brain regions or cell types suggesting that even more cellular- and regionally-specified organoids could be advantageous in translating these evolutionary differences to function and brain development across species (Khrameeva et al., 2020).

scRNA-seq is powerful in characterizing known and unknown cell types, comparing tissue compositions, and understanding evolutionary differences at the cellular level; nevertheless, it requires the loss of spatial information which is necessary for elucidating the effects of transcriptomic differences on function and complex, physical cellular interactions as cells must be dissociated from their location in tissues. Through scRNA-sequencing analysis of four different lobes of the human neocortex, researchers found asynchronous cell development and a priority for regional maturation in the different areas emphasizing the importance of spatial resolution in conjugation with transcriptomic information (Fan et al., 2020). Furthermore, a large-scale study applying scRNA-seq to analyze 314 human microglia samples from 115 donors suggested that there are transcriptional differences among microglia from different brain regions and throughout aging (de Paiva Lopes et al., 2020). Although neurons in cortical and cerebral organoids do not seem to acquire spatial organization, progenitor and other cell types could and other brain organoid types might (Bhaduri et al., 2020; Libby et al., 2021). Neurons have been shown to display transcriptomic signatures of areal identity and considering these expression patterns could too be advantageous in analyzing transcriptomic information from organoids (Bhaduri et al., 2020). Spatial transcriptomic (ST) technologies are allowing researchers to merge transcriptomic and spatial information by employing glass slides printed with spatially barcoded oligo(dT) probes or bead arrays (high-definition ST) that permit mRNA hybridization to the probes after tissue slices are applied and enzymatically permeabilized (Vickovic et al., 2016, 2019; Larsson et al., 2021). Not only are ST technologies useful in relating transcriptomic changes to functional processes of brain development but they are also helpful in correlating transcriptomic changes that might occur during disease progression to cellular processes in response to pathogenesis. Utilizing the 5XFAD mouse model of AD, researchers implemented ST techniques to find that genes spatially associated with amyloid plaques had been previously identified as being functionally related to Amyloid-β (Choi et al., 2021). Implementing similar ST strategies to investigate AD and other brain disorders in organoid models derived from patients' PSCs could reveal human-specific transcriptomic changes and their contribution to cell-specific responses to pathogenesis.

While evolutionary differences in gene expression have been analyzed primarily at the transcription level, understanding the influence of gene regulatory modalities at the epigenetic, protein, and microRNA level could illuminate processes governing human-specific neurodevelopmental phenotypes. Brain organoids have been demonstrated to cluster with fetal brain tissue and separately from adult brain tissue based on transcriptomes and histone marks (Amiri et al., 2018). They have also been shown to recapitulate transcriptomics and the epigenetic landscape of early to mid-fetal development (Luo et al., 2016). Researchers found that inhibition of G9a-mediated H3K9me2 modification in human cerebral organoids resulted in increased NPC proliferation causing organoid expansion, and G9a is likely regulated by the hominoid-specific protein TBC1D3 (Hou et al., 2021). These findings suggest an epigenetic regulatory mechanism for neocortical expansion and possibly ensuing gyrification. To understand how chromatin state varies in cells across tissues or organoids and influences gene expression in spatial patterns, researchers could implement high-spatial-resolution chromatin modification state profiling by sequencing (hsrChST-seq) which exploits DNA barcoding and Under Targets and Tagmentation (CUT&Tag) chemistry (Deng et al., 2021). Furthermore, applying multimodal omics analysis with combinations of techniques like single-cell ATAC-seq (scATAC-seq) with scRNA-seq, pooled CRISPR-Cas9 to introduce genetic perturbations followed by scRNA-seq or scATAC-seq, or simultaneous introduction of genetic perturbations with scRNA-seq (CROP-seq) could allow for the elucidation of regulatory relationship evolution during brain development (Datlinger et al., 2017; Efremova and Teichmann, 2020). Pooled CRISPR nuclease (CRISPRn) can target many genes introducing DNA breaks causing deletions or insertions that disrupt gene function while pooled CRISPR interference (CRISPRi) or CRISPR activation (CRISPRa) take advantage of nuclease dead Cas9 (dCas9) to interact with activator or repressor domains in DNA, modulating gene expression (Gilbert et al., 2013; Kampmann, 2017; Tian et al., 2019). Subsequent effects of such genetic perturbations during brain development can be compared between human and NHP species to elucidate human specific mechanisms of neurodevelopment. Additional regulatory elements of interest in human brain evolution include miRNA-mRNA interactions, in particular is the interaction between ORC4 (enriched in RGs) and miR-2115 (an miRNA specific to great apes), which is implicated in RG proliferation rates during human brain development (Nowakowski et al., 2018). Furthermore, researchers have developed a platform to divulge the influence of *cis* and *trans* acting regulation on gene expression. Human and chimpanzee iPSCs were fused so that the tetraploid genomic information contributed by each species shared the same nuclear space. Neural organoids were then established from the hybrid iPSCs and allele specific expression in hybrid organoids was compared to chimpanzee and human organoids to reveal *cis* regulatory divergences.

Human somatostatin receptor 2 gene (SSTR2), responsible for neuronal calcium signaling regulation and associated with neuropsychiatric disorders, was found to be upregulated in these studies (Romero-Grimaldi and Moreno-López, 2008). Lastly, high-throughput mass spectrometry can be employed to obtain high resolution of the proteome of developed brain organoids and provide insight into the regulation of genes during neurodevelopment at the protein expression level (Bauernfeind et al., 2015; Mostajo-Radji et al., 2020).

Cytoarchitecture

Much focus has been given to primate specific differences in neocortical development, yet there is less information on, but likely existing, primate and human specific differences in alternate brain regions that occur during development and maturation. For example, recent studies using computational neuroanatomy to reconstruct Neanderthal (*Homo neanderthalensis*) and early *Homo sapiens* brains found that Neanderthals, when averaged, had smaller cerebellar hemispheres than *Homo sapiens* which could have influences on cognition and social functions (Kochiyama et al., 2018). Human brains are not the largest on earth suggesting that evolutionary changes in brain structure, including the laminar organization of cells in the cortex, are particularly important in understanding species-specific cognition (Preuss, 2011; Sakai et al., 2013). Cellular organization and connectivity in the cortex and beyond vary among hominid species and are relevant in understanding differences in brain organization and function (Semendeferi and Damasio, 2000; Barger et al., 2007; Marchetto et al., 2019). Contributing to distinct brain cytoarchitecture and connectivity are unique cellular morphologies and subtypes like human and chimpanzee-specific varicose projection astrocytes, human-specific morphology of cortical pyramidal neurons, and primate-specific expression of TMEM14B in oRGs (Oberheim et al., 2009; Bianchi et al., 2013; Liu et al., 2017). Here, we discuss the current state and future applications of brain organoid-based models to recapitulate primate-specific brain regions, cytoarchitecture, and interconnectivity.

Unguided, cerebral organoid generation protocols promote the self-organization and expansion of developing neuroepithelium resulting in heterogeneous structures that represent several brain region identities. VZ-like structures of cerebral organoids are comprised of RGs with some oblique and vertical orientations which might be more indicative of human brain tissues than rodents. VZ-like zones also contain dividing cells at the apical surface. Additionally, $TBR1^+$ cells show radial migration to developing preplate-like regions above an intermediate zone-like layer while $TBR2^+$ cells indicate IP localization in SVZ-like structures (Lancaster et al., 2013). Expanded progenitor pools within these regions are thought to contribute to the diversified architecture of the developing cortex of primates and are valuable regions of interest in the identification of primate-specific processes of neocortical development (Giandomenico and Lancaster, 2017).

While cerebral organoid brain region heterogeneity could be applied to investigate brain region interconnectivity, cerebral organoids exhibit high amounts of variability among represented brain regions and more strictly guided protocols are often employed to achieve increased reproducibility and homogeneity. Forebrain and cortical organoids recapitulate some amount of timed NPC migration and neuronal subtype layering although they do not represent all six distinct layers of the primate cortex. Like cerebral organoids, forebrain organoids contain VZ-, SVZ-, preplate-, and $CTIP2^+$ neuron-containing cortical plate (CP)-like structures; however, cortical organoid protocols have further demonstrated more distinct oSVZ-like regions and upper and deep cortical layers containing neurons and astrocytes reminiscent of third trimester human neocortical development (Lancaster et al., 2013; Kadoshima et al., 2014; Pasca et al., 2015; Qian et al., 2018, 2020). Neuronal migration events have been compared using human, chimpanzee, and macaque iPSC derived cortical organoids. Researchers observed the presence of abundant $SATB2^+$ upper-layer neurons in macaque organoids at day 60 whereas human and chimpanzee organoids did not exhibit large populations of $SATB2^+$ neurons in upper-layers until approximately day 80 of development corroborating their findings in 2D rosette systems (Otani et al., 2016). Furthermore, mitosis of APs at the ventricular surface of human iPSC-derived cerebral organoids were observed to experience a 40–60% increase in the time spent in metaphase when compared to chimpanzee and orangutan APs and it was determined that this phenomenon could be a feature of an earlier phase of cortical development. Additionally, S-phase was about 5 h longer in human APs than those of chimpanzees and orangutans (Mora-Bermúdez et al., 2016). Finally, immunohistochemical staining for the mTOR effector phosphorylated ribosomal protein S6 (pS6) in human, macaque, and chimpanzee-derived organoids revealed that oRGs of oSVZ-like regions of human organoids expressed higher amounts of pS6 indicating human-specific differences in mTOR signaling (Pollen et al., 2019). It is likely that observing primate-specific TMEM14B expression in oRGs of SVZ-like regions of human and NHP derived brain organoids could provide insight into cortical thickening and gyrification. It has been demonstrated that expressing TMEM14B in embryonic mouse NPCs induces thickening of the cortex and gyrification in the otherwise lissencephalic organism (Liu et al., 2017).

Brain Region Specification

Brain organoids representative of additional brain regions and enriched with brain region specific cell types could illuminate evolutionary divergence in cellular morphology and dynamic processes of brain development. Researchers have applied what is known about *in vivo* brain development and *in vitro* 2D neural differentiation protocols to direct the differentiation of brain organoids *via* transcriptional regulation. Currently, brain region specific protocols are available for the development of midbrain, hypothalamus, hippocampus, cerebellum, and basal ganglionic organoids (Muguruma et al., 2015; Sakaguchi et al., 2015; Jo et al., 2016; Watanabe et al., 2017; Qian et al., 2018). Recently, caudalizing factors have been implemented during organoid generation to promote axial elongation similar to neural tube development. Remarkably, these hindbrain and neural tube organoids demonstrate regionalized gene expression and spatially distinct cellular organization showing

promise that more definite cellular regionalization could be obtained in alternative brain region specific organoid models (Libby et al., 2021). Dorsal forebrain organoids enriched with excitatory glutamatergic pyramidal neurons and ventral forebrain organoids predominately containing inhibitory GABAergic cortical interneurons have also been established. By fusing dorsal and ventral forebrain organoids, researchers can observe the migration of ventral inhibitory neurons to targets in dorsal forebrain organoids (Bagley et al., 2017; Birey et al., 2017). This neuronal migratory event occurs during mid-to-late gestation and is essential for the integration and maturation of cortical circuits (Birey et al., 2017). Generating dorsal and ventral organoids from human and NHP PSCs and fusing both same species and cross species organoids could provide insight into evolutionary differences driving this significant process of brain development and maturation. Human-specific differences in pyramidal cell function and behavior, in addition to already observed morphological differences, might also be revealed by studying dorsal forebrain organoids enriched with excitatory pyramidal neurons (Marchetto et al., 2019). Furthermore, it could be possible to establish brain organoids enriched in DAergic, TH^+ axons and observe potential human-specific patterns of DAergic axon innervation into fused cortical organoids (Raghanti et al., 2011). It is foreseeable that numerous combinations of human and NHP cerebral and brain region specific organoids could be developed and fused to elucidate the evolutionary differences responsible for brain interconnectivity and synchronization.

Human brain development is a prolonged process that continues well beyond prenatal events and into early adulthood (Silbereis et al., 2016). Implementing strategies that allow for long-term culture of complex brain organoid-based model systems are essential for obtaining a complete understanding of the processes responsible for the fabrication of the uniquely human brain. A reported lack of regional separation of neurons with areal identities and reduced neuronal maturation in brain organoids has been attributed to increases in oxidative and metabolic stress observed during *in vitro* culture (Bhaduri et al., 2020). Modifications to early cerebral organoid protocols, including seeding embryoid bodies with a reduced number of cells, incorporating a two-step neural induction phase, and supplementing final differentiation media with brain-derived neurotrophic factor (BDNF), allowed for progressive development of cerebral organoids over 9 months and advanced maturation of neurons with dendritic spines that formed spontaneously active neural networks (Quadrato et al., 2017). Other groups had found that the addition of recombinant leukemia inhibitory factor (LIF) during organoid generation increased the size of SVZ-like regions, allowed for increased separation of deep and upper layer neurons of the cortex, and maintained organoid structure to 22 weeks (Watanabe et al., 2017). More recently, researchers have accomplished brain organoid maintenance for up to 300 days demonstrating the ability to recapitulate later events of *in vivo* brain development like birth (Gordon et al., 2021). Since brain organoids lack a vascular network, overcoming hypoxic stress and reduced nutrient delivery into deeper layers of brain organoid structures has been an ongoing challenge. By culturing slices of forebrain organoids, researchers have achieved a reduction in the commonly occurring necrotic core of organoids, reduced apoptosis, more distinct separation of upper and lower cortical layers, and retention of VZ, oSVZ, and CP-like regions through days 100–150 (Qian et al., 2020). Additionally, developing organoids with a PSC derived perfusable vascular-like network, engineering organoids to develop an endogenous perfusable vascular-like network, or the transplantation of organoids into the mouse brain resulting in *in vivo* vascularization has greatly reduced apoptosis and cellular stress allowing for the development of organoids into the third trimester and advanced cellular maturation (Mansour et al., 2018; Pham et al., 2018; Cakir et al., 2019). Supporting the long-term culture of brain organoids could allow for the modeling of later processes of human-specific brain development, including overproduction of synapses followed by vigorous remodeling through synaptic pruning and delayed myelination of axons (Petanjek et al., 2011; Miller et al., 2012).

Gliogenesis, like neurogenesis, occurs both pre- and postnatally; however, the ability to model gliogenesis in brain organoid systems is limited due to reduced glial progenitor cell (GPC) populations when compared to primary neocortex tissue and the continued loss of GPCs as organoids develop (Stiles and Jernigan, 2010; Rusznák et al., 2016; Bhaduri et al., 2020). Preserving and enriching GPC populations in human brain organoids is necessary for the development of more representative models of human-specific brain development, as approximately half of adult brain volume consists of glial cells (Barres, 2008). Bioengineered neuronal organoids with induced neuro- and gliogenesis using FGF-2 for increased NPC proliferation, TGFb1 to promote gliogenesis, and DAPT for neuronal differentiation are enriched with astrocytes by day 60 and oligodendrocytes by day 150 (Zafeiriou et al., 2020). Astrocytes have also been reported in cortical spheroids, cerebral organoids, and forebrain organoids beginning between days 75 and 90; yet, the astrocytes typically do not represent the quantities found *in vivo* (Pasca et al., 2015; Quadrato et al., 2017; Renner et al., 2017; Sloan et al., 2017; Bhaduri et al., 2020). Observing astrocytes in glial-enriched organoids that exhibit advanced stages of maturation can reveal primate- and human-specific astrocyte, including chimp- and human-specific varicose projection astrocytes, influence on brain development and maturation (Oberheim et al., 2009).

Oligodendrocytes play a central role in healthy brain function by facilitating the electrical properties of neurons through the myelination of axons which occurs later and over a drawn out period of time in human development compared to chimpanzees (Barres, 2008; Miller et al., 2012). Oligodendrocytes are the last major neural cell type formed during human brain development; nonetheless, they have been established in brain organoids through both spontaneous formation and directed protocols that enrich for oligodendrocyte progenitor cells (OPCs) (Monzel et al., 2017; Renner et al., 2017; Matsui et al., 2018; Kim et al., 2019; Marton et al., 2019; Zafeiriou et al., 2020). Mature, functional oligodendrocytes have been identified in organoids *via* the expression of the mature oligodendrocyte marker, myelin

basic protein (MBP), and the pinpointing of axons that are insulated by 2′,3′-cyclic nucleotide 3′-phosphodiesterase (CNP) positive oligodendrocyte myelin sheets (Monzel et al., 2017; Zafeiriou et al., 2020; Shaker et al., 2021).

However, the enrichment of GPCs might not result in the presence of microglia in organoids since microglia are derived from the mesoderm germ layer and likely migrate to the cerebrum sometime between the 4th and 24th week of development (Kierdorf et al., 2013; Menassa and Gomez-Nicola, 2018). Instead, the modification of organoid generation protocols to increase the number of mesodermal progenitors with already existing neuroectodermal progenitors has resulted in functional microglia with ramified morphology, a characteristic inflammatory response, and phagocytic ability including the capacity to perform synaptic pruning (Kierdorf et al., 2013; Menassa and Gomez-Nicola, 2018). Other options for incorporating microglia into brain organoids involve the coculture of primary microglia obtained from postmortem brain tissue or those derived from iPSCs. Implementing microglia derived from primary tissue or from the iPSCs of human and NHPs can help researchers to elucidate the behavior and influence of species-specific microglia interactions during development and could reveal species-specific microglia behaviors (Abud et al., 2017). For example, microglia from chimpanzees can be introduced into human brain organoids and the resulting effects on neuronal development can be compared to human organoids that contain human microglia to disentangle microglia influenced effects from cell autonomous effects. The significant roles that glial cells play in healthy brain development and maturation are just beginning to be appreciated and brain organoids might assist in further defining these elusive roles (Barres, 2008; Rusznák et al., 2016).

Connectivity

Once complete brain organoid models are established, containing representative amounts of maturing cell types found in the developing brain under minimal cellular stresses, their electrophysiological activity can be monitored throughout development to observe oscillatory events during spontaneous network formation. While researchers have demonstrated spontaneous electrophysiological activity in cerebral organoids, it has only recently been suggested that human cortical organoids display oscillatory activity comparable to that recorded in preterm human electroencephalography (Quadrato et al., 2017; Trujillo et al., 2019). Previous works have applied multielectrode array (MEA) analysis to observe firing rates of human, chimpanzee, and bonobo iPSC-derived neurons at 2 and 6 weeks. They found increased firing rates of chimpanzee and bonobo derived neurons at 1.5 weeks when compared to human neurons, while human-derived neural cultures showed increased firing rates at 5 weeks (Marchetto et al., 2019). However, studies remain to be performed comparing human and NHP-derived brain organoid oscillatory activity to corroborate the finding of delayed functional maturation of human iPSC-derived 2D neurons compared to chimpanzee and bonobo neurons.

Extinct Ancestral Modeling

Current work has brought us closer to our most recent non-living hominin relatives. Like discovering the DNA of an extinct species locked in amber, CRISPR-Cas9 has provided access to the past and opened possibilities for the interrogation of humans' most recent divergences in brain evolution. Researchers identified neuro-oncological ventral antigen 1 (NOVA1) as a gene with differences between human and archaic hominin genomes that could play a role in human-specific neurodevelopment. Using CRISPR-Cas9, they replaced the human allele of NOVA1 in hiPSCs with an ancestral allele associated with Neanderthals and Denisovans. They then generated cortical organoids from edited hiPSCs with the archaic variant ($NOVA1^{Ar/Ar}$) and from unedited isogenic control hiPSCs ($NOVA1^{Hu/Hu}$). $NOVA1^{Ar/Ar}$ organoids were smaller in diameter than $NOVA1^{Hu/Hu}$ organoids during the proliferation and maturation stages and demonstrated increased surface rugosity. Additionally, $NOVA1^{Ar/Ar}$ organoids had less VZ- and SVZ-like areas, increased apoptotic cells, and slower proliferation compared to $NOVA1^{Hu/Hu}$ organoids. The researchers then performed RNA sequencing and found 277 genes differentially expressed between $NOVA1^{Hu/Hu}$ organoids and $NOVA1^{Hu/Hu}$ organoids with the top three differentially expressed genes being FEZF1, PAX6, and LHX5. Single-nucleus RNA-seq then revealed differences in cell-type proportions at one and 2 months of development and variations in gene splicing. Finally, $NOVA1^{Ar/Ar}$ organoids had lower levels of pre- and postsynaptic proteins with less colocalized synaptic puncta likely resulting in reduced synchrony and increased variability based on observed firing rate and coefficient variation when evaluated by MEA (Trujillo et al., 2021).

Until very recently, Neanderthals and Denisovans (*Denisova hominins*) were thought to be our closest evolutionary relatives. The discovery of *Homo longi*, suspected to be an even closer extinct relative of humans than Neanderthals, could open the possibility for a new understanding of divergence in human brain evolution (Ji et al., 2021). Deviating genes might be identified from *Homo longi* that, 1 day, could be genome edited into human iPSCs for the development of different versions of ancestral organoids. Accurate cellular modeling of ancestral species will require recapitulation of ancestral genome mutations *via* introduction of multiple DNA edits in the same cell. Current CRISPR/Cas9 technology allows for multiple guide sequences to be encoded into a single CRISPR array to enable simultaneous editing of several sites within the primate genome (Cong et al., 2013). It remains to be seen if full recapitulation of ancestral mutations in a human neuron will change its physiology to a more ancient "Neanderthal-like" state.

BRAIN ORGANOID DISEASE MODELING FROM AN EVOLUTIONARY PERSPECTIVE

Many of the previously discussed human-specific processes of brain development are vulnerable to dysregulation and

could be at the root of human brain disorder pathophysiology or detrimental responses to pathogenesis (**Table 2**). Here we identify some potentially human-specific features of and responses to brain diseases and explore methods that might assist in elucidating therapeutic targets and protective strategies (**Figure 2**).

TABLE 2 | Overview of primary literature employing human, NHP, and ancestral gene edited brain organoids to elucidate human-specific processes of brain development and implicated brain disorders.

	Compared Species	Model	Findings	Implicated Brain Disorders	Citation
Cortex development	• Chimpanzee • Macaque • Human	Brain organoids and 2D neural rosettes	Different rates of NPC proliferation; Differences in neurogenesis output; Cell autonomous regulation of neurogenesis	• Epilepsy • ASD • HD • TS • FXS	Otani et al., 2016
	• Chimpanzee • Human	Cerebral organoids	Similar cytoarchitecture, cell type composition, and neurogenic gene expression programs; Lengthening of prometaphase-metaphase of AP mitosis; Differential AP gene expression associated with prolonged proliferative capacity; Less BPs in humans	• Microcephaly • Lissencephaly • Heteropias	Mora-Bermúdez et al., 2016
	• Chimpanzee • Gorilla • Human	Cerebral (telencephalic) organoids	Protracted neuroepithelial differentiation in apes; Larger human organoids; Shorter cell cycles in humans; Differential gene expression of cell morphogenesis factors (ZEB2); Newly identified NPC transition morphotype state	• Mowat–Wilson syndrome (syndromic form of Hirschprung's disease)	Benito-Kwiecinski et al., 2021
Gene expression	• Chimpanzee • Macaque • Human	Cerebral organoids	Identified 216 differentially expressed genes in human vs. chimpanzees and macaque cortex (including regulators of PI3K/AKT/mTOR signaling); Increased activation of PI3K/AKT/mTOR pathway in human RGs dependent on two upregulated receptors in humans (INSR and ITGB8); Increase in almost all genes in the SMN1 and ARL17A loci in the developing human cortex of humans compared to chimpanzee and macaque	mTOR: • ASD • Focal cortical dysplasia • Glioblastoma multiforme	Pollen et al., 2019
	• Chimpanzee • Macaque • Human	Cerebral oganoids	Human neuronal development happens at a slower pace; Identified 23 differentially expressed duplicated or rearranged genes in humans, four specific to G2M phase NPCs of the telencephalon (ARHGAP11B, FAM72B, FAM72C, and FAM72D); found 98 differentially expressed genes in RGs, IPs, and neurons and are associated with proliferation of RGs, neuron migration, and neurite formation; Differential accessibility in NPCs and neurons of humans and chimpanzees showed 7% increase and 9% decrease in accessibility in humans.	• ASD • Microcephaly • Lissencephaly • Heteropias	Kanton et al., 2019
	• Chimpanzee • Human	Hybrid human-chimpanzee, human, and chimpanzee PSC derived cortical spheroids	Thousands of genes with human vs. chimpanzee divergent *cis* regulation; Set of astrocyte related genes with evidence of selection; Upregulation of SSTR2 gene expression; Pharmacological induced species-specific calcium signaling	• Schizophrenia • Dementia in patients with AD Calcium signaling: • AD • PD • HD • ALS • Spinocerebellar ataxias	Agoglia et al., 2021
	• Neanderthal • Human	CRISPR-Cas9 replaced human NOVA1 allele with ancestral NOVA1 allele in iPSCs, derived cortical organoids from archaic NOVA1 iPSCs and human iPSCs	Changes in alternative splicing of genes related to neurodevelopment, proliferation, and neural network formation; Archaic NOVA1 organoids had excitatory synaptic changes compared to human organoids; Smaller archaic NOVA1 organoids during the proliferation and maturation stages; Archaic NOVA1 organoids has less VZ- and SVZ-like areas, increased apoptotic cells, and slower proliferation; 277 differentially expressed genes between archaic NOVA1 organoids and human organoids (top three were FEZF1, PAX6, and LHX5)	• ASD • HD • SZ • Depression • Cocaine addiction	Trujillo et al., 2021

List of implicated brain disorders is based on findings and is not exhaustive. ASD, autism spectrum disorder; HD, Huntington's disease; SZ, schizophrenia; PD, Parkinson's disease; AD, Alzheimer's disease; TS, Timothy syndrome; FXS, fragile X syndrome.

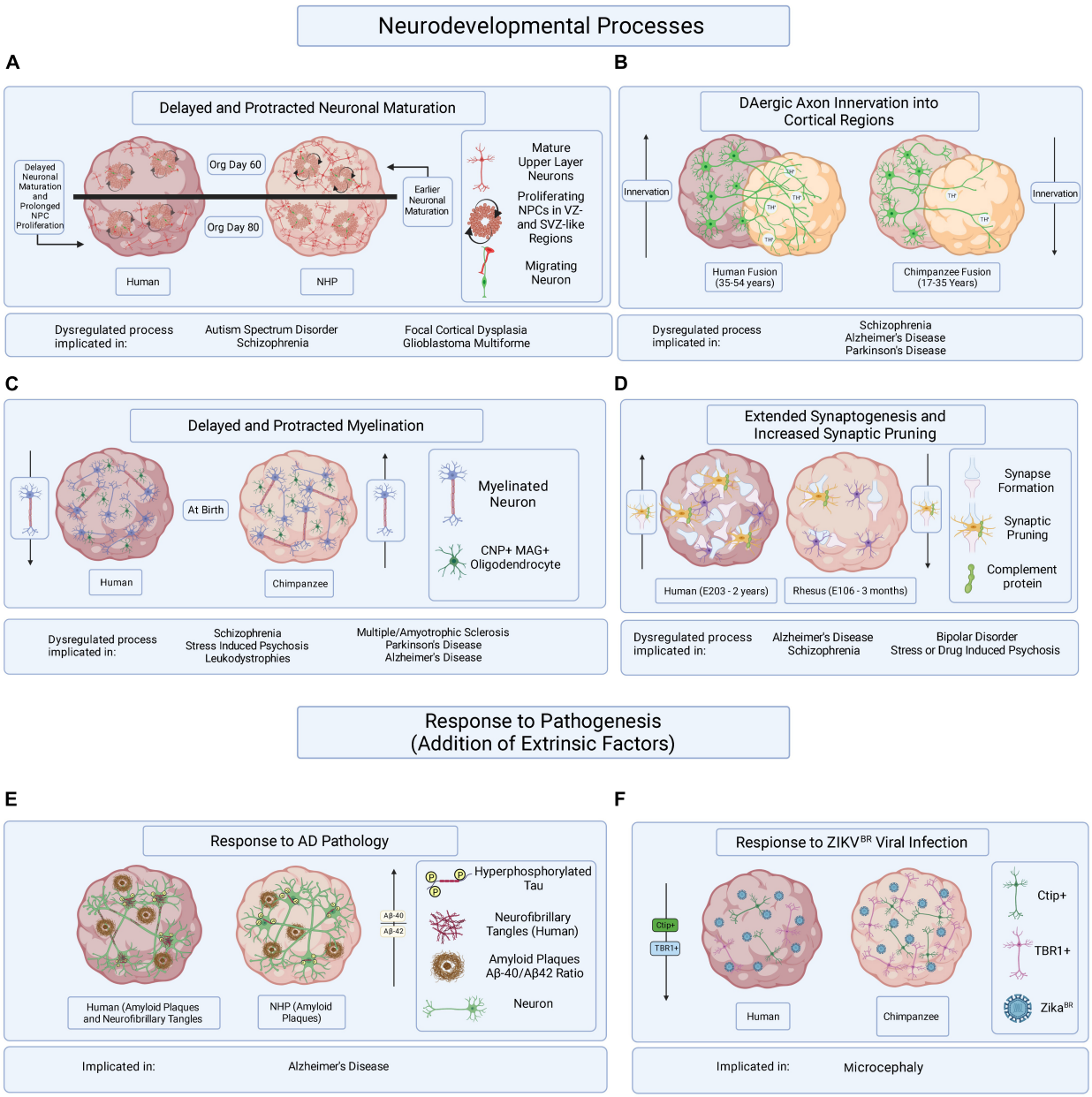

FIGURE 2 | Hypothesized brain organoid-based models of human specific processes implicated in brain disease etiology and progression. Schematic illustrating multiple processes of human-specific brain development or responses to pathogenesis compared to those of NHPs and represented in brain organoids. **(A)** Delayed neuronal maturation and prolonged NPC proliferation have been observed in human brain organoids when compared to chimpanzee derived brain organoids. The dysregulation of NPC proliferation and neuronal maturation during brain developed has been linked to ASD, SZ, focal cortical dysplasia, and glioblastoma multiforme. Org is organoid. **(B)** It might be possible to observe differences in DAergic axon innervation between human and NHPs by fusing cortical organoids to organoids enriched in dopaminergic neurons. The disruption of DA regulation systems has been implicated in SZ, AD, and PD. Timepoints reflect observations of DAergic axon innervation in certain regions of the cortex comparing human and chimpanzee postmortem tissue samples. **(C)** Delayed and protracted myelination has been observed in human when compared to chimpanzee pre- and postnatal postmortem tissues and the disruption of axonal myelination is linked to SZ, stress induced psychosis, leukodystrophies, MS, PD, and AD. Axonal myelination might be compared in primate organoids containing CNP/MAG^{+} oligodendrocytes. **(D)** Observing periods of synaptogenesis followed by the pruning of excessive synapses in organoids containing microglia could reveal species-specific mechanisms of neuronal maturation when comparing primate organoids. Dysregulated synaptogenesis and synaptic pruning are implicated in AD, SZ, BD and stress and drug induced psychosis. E is embryonic day and timepoints correspond to observations in postmortem tissue. **(E)** It has been suggested that some aging NHPs develop amyloid-beta plaque deposits but only develop NFTs in rare cases. The overexpression of hyperphosphorylated tau, a precursor of NFT accumulation, in brain organoids derived from humans and NHPs could allow for the identification of species-specific responses to the disease burden. **(F)** Neurotrophic viral infection, like ZIKV^{BR} infection, can and has been compared among primate species by establishing human and NHP derived brain organoids, infecting them with neurotrophic viruses, and observing resulting differences in pathogenic responses or viral mechanisms of infection. The mentioned implicated brain disorders or processes are not all-encompassing.

Oligodendrocytes and Myelination

Contrasting human- and NHP-derived brain organoids that are optimized to model processes of human brain development vulnerable to dysregulation could allow researchers to elucidate the mechanisms governing those processes providing insight into brain disease etiology and potential therapeutic targets. For example, decreases in neocortical myelin development and myelin-related gene expression resulting in dysregulated CNP and myelin-associated protein (MAG) levels have been observed in patients with schizophrenia (SZ) (Hakak et al., 2001; Dracheva et al., 2006; McCullumsmith et al., 2007; Mitkus et al., 2008). Additionally, oligodendrocyte and astrocyte dysfunction has been associated with decreased myelination in multiple sclerosis, amyotrophic lateral sclerosis, PD, AD, Down syndrome (DS), and leukodystrophies (Salameh et al., 2015; Wasseff and Scherer, 2015; Domingues et al., 2016; McKenzie et al., 2017; Reiche et al., 2019; Shaker et al., 2021). It has been suggested that the extended period of myelination in humans, in addition to the metabolic burden of myelinating the large quantities of neurons in humans, increases our susceptibility to these brain diseases; however, the mechanisms responsible for the dysregulation of oligodendrocytes and their ability to maintain appropriate amounts of myelination for healthy brain function are unclear (Bove, 2018). Generating oligodendrocyte and astrocyte containing organoids capable of myelination from human and NHP PSCs could allow for the examination of species-specific molecular mechanisms governing myelination (Madhavan et al., 2018; Kim et al., 2019; Shaker et al., 2021). Investigating axon myelination through perturbations of the processes of myelination, like increasing metabolic stress or altering CNP and MAG gene expression, in both human and NHP organoids could reveal species-specific mechanisms of myelination homeostasis.

Synaptogenesis

Additionally, synaptogenesis is a process of brain development with uniquely human features like high quantities of excessive synapse formation in the cerebral cortex followed by extended periods of synapse remodeling *via* pruning (Petanjek et al., 2011). The dysregulation of synaptic pruning by astrocyte and complement protein responsive microglia has been implicated in SZ, bipolar disorder (BD), and stress- or drug-induced psychosis (Feinberg, 1982; Stevens et al., 2007; Eroglu and Barres, 2010; Paolicelli et al., 2011; Petanjek et al., 2011; Sellgren et al., 2019). Incorporating microglia derived from human and NHP PSCs into brain organoids, establishing both same species and cross species microglia enriched organoid co-cultures, and inducing neuroinflammation *via* cytokine activation might reveal human-specific complement guided microglia responses during organoid development and synaptic pruning (Stevens et al., 2007; Severance et al., 2014; Abud et al., 2017). Microglia are also implicated in AD pathology and coordinate activities with astrocytes and other neural cells (Hong et al., 2016; Menassa and Gomez-Nicola, 2018). Transplanting brain organoids into the mouse brain has resulted in the colonization of the transplanted human brain organoids with ramified mouse microglia, and it might be feasible to inject PSC-derived human and NHP microglia into mouse brains containing AD patient iPSC-derived brain organoids to identify human-specific microglia, astrocyte, and blood brain barrier (BBB) interactions in an AD pathophysiological relevant environment (Abud et al., 2017; Mansour et al., 2018, 2021; Hasselmann et al., 2019; Park et al., 2021; **Figure 1**).

Radial Glia and Neural Progenitor Cell Proliferation and Migration

Proliferating cells of the VZ-, SVZ-, and oSVZ-like regions of brain organoids could be of notable importance when investigating human-specific disease etiology. NPCs differentiated from the hiPSCs of SZ patients conserved a large amount of the gene signature of SZ hiPSC-derived neurons and demonstrated aberrant migration patterns compared to control NPCs which was observed in neurosphere outgrowth and microfluidic chamber migration assays (Brennand et al., 2015). Furthermore, brain organoids developed from the hiPSCs of patients with autism spectrum disorder (ASD) showed no difference in the ability of RGs to establish $TBR1^+$ cortical neurons yet revealed increased thickness of CP-like regions and transcriptional dysregulation related to cortical neuron development. However, circumventing the NSC stage using direct iPSC to induced neuron conversion rescued abnormal neural fate specification and neurite branching (Schafer et al., 2019). Deviating migration patterns have been revealed in hiPSC-derived NPCs when compared to bonobo and chimpanzee NPCs in 2D cultures and evidence suggests that cortical progenitor cells play a key role in primate-specific cortical size through differences in the duration of cortical progenitor cell expansion (Otani et al., 2016; Marchetto et al., 2019). It has also been suggested that increased INSR and ITGB8 may be related to human-specific differences in mTOR signaling pathway activation in RGs, particularly oRGs, and mutations related to mTOR signaling have been linked to ASD, focal cortical dysplasia, and glioblastoma multiforme (Ceccarelli et al., 2016; Mora-Bermúdez et al., 2016; Pollen et al., 2019). These findings provide a platform for understanding the mechanisms regulating NPC proliferation, migration, and overall contributions to healthy human brain development through primate-derived brain organoid models.

DISCUSSION

Brain organoids provide unparalleled access to human-specific processes of neurodevelopment and these processes can be further highlighted by contrasting them with those of our closest NHP and extinct ancestral relatives. However, our access to ESCs and primary cells of some NHPs, including several species of lemurs, monkeys, and great apes, is limited due to declining species numbers (Gray et al., 2013; Estrada et al., 2017). Additionally, protocols to reprogram human somatic cells to PSCs, and to direct the differentiation of PSCs to neural and brain region specific lineages, could lack consistent translation to NHPs. Although early processes of transcriptional regulation during development are often well conserved across species, obtaining NHP brain organoids with increasing brain-region

specification could pose a challenge and require species-specific optimization (Acampora et al., 1998; Godenschwege et al., 2006; Castells-Nobau et al., 2019). Cerebral and cortical brain organoids have been derived from chimpanzee, bonobo, rhesus monkey, and orangutan ESCs and iPSCs using protocols originally established for human PSC organoid derivation with minimal optimization (Mora-Bermúdez et al., 2016; Otani et al., 2016; Kanton et al., 2019; Pollen et al., 2019). Reconstructing and identifying diverging ancestral genes to introduce into human brain organoids for the modeling of evolutionary divergences in brain development is also challenging since ancestral DNA is often poorly preserved, fragmented, contaminated by other DNA molecules, and contains post-mortem mutations. Remarkably, recent progress in high-throughput sequencing technologies are transforming ancient DNA research by providing access to entire genome sequences from ancient DNA fragments (Orlando et al., 2015). Once brain organoids are developed from human and NHP PSCs, high-throughput scRNA-seq, scATAC-seq, CROP-seq, pooled CRISPR screens, and tandem mass spectrometry are revolutionizing our understanding of transcriptional, translational, and epigenetic regulations during human brain development and our ability to validate brain organoid model systems (Bakken et al., 2016; Amiri et al., 2018; Tian et al., 2019; Atamian et al., 2021). Eventually, the application of technologies like seqFISH might provide spatial-temporal resolution of dynamic transcriptional changes and cell lineage tracing in brain organoid models (Shah et al., 2018; Atamian et al., 2021).

Non-human primates brain organoid disease modeling could provide insight into human-specific brain disease etiology and pathogenesis. We have learned much from rodent models of human neurodevelopment and disease, including the idea that physiological differences between species could result in erroneous conclusions (Van Fernando and Robbins, 2011; Kariya and Ishikawa, 2019; Norman, 2019). However, modeling and comparing these physiological differences in species more closely related to us could help elucidate the human-specific processes implicated in brain disease progression. Human and NHP brain organoid-based models of AD could be exceptionally informative due to the unique susceptibility that humans seem to exhibit for developing AD, which could be related to genetic differences, cerebral structural differences, and increased lifespan (Walker and Jucker, 2017). Although aged NHPs, like chimpanzees, orangutans, rhesus monkeys, squirrel monkeys (*Samiri sciureus*), and gorillas, demonstrate diffuse amyloid plaques, neuritic amyloid plaques, and vascular amyloid, in addition to hyperphosphorylated tau expression in neurons, they most often do not present with tau positive neurofibrillary tangles (NFTs) or neuropil threads and very few NHPs have been reported with both amyloid beta pathology in combination with NFTs (Perez et al., 2013, 2016; Edler et al., 2017). The identification of cellular mechanisms providing NHPs with the capability of preventing or clearing NFT formation might be accomplished by challenging human- and NHP-derived brain organoids with over-expression of the shortest human brain tau isoform (T44) in neurons (Ishihara et al., 1999). This comparison could reveal potential therapeutic targets in AD. Additionally, it is unclear whether the response of astrocytes and microglia of AD patients is protective or detrimental to the neuroinflammatory pathogenesis of AD (Cai et al., 2017; Ahmad et al., 2019). Microglia and astrocyte activation are early responses to AD pathology that increase oxidative stress and the production of inflammatory cytokines, some of which exhibit neurotoxic effects (Heneka et al., 2014). By implementing previously discussed strategies to enrich brain organoids with astrocytes and microglia, one could investigate the complex astrocyte, microglia, and neuronal interactions in the context of AD related neuroinflammation. GFAP expression suggesting astrogliosis in chimpanzee brains does not appear to increase during aging as it does in humans suggesting lower levels of oxidative stress, and, while astrogliosis is observed in cortex layer I and the hippocampus of chimpanzees exhibiting AD pathology, it is not as widely spread throughout the cortex as has been observed in human postmortem AD tissues (Munger et al., 2020). It could be hypothesized that organisms with increasing brain complexity and resulting increased metabolic demand demonstrate greater susceptibility to oxidative stress during aging making them more inclined to develop age-related neurodegenerative diseases like AD, although more research is required to determine if there is a connection between brain complexity, metabolic demand, and oxidative stress handling. The lack of vascularization and hyper- and hypoxic conditions during *in vitro* brain organoid culture has been shown to cause increased metabolic, oxidative, and cellular stress compared to *in vivo* conditions resulting in increases in apoptosis and necrosis (Bhaduri et al., 2020). While this does present a challenge in establishing many physiological relevant brain organoid model systems, it remains to be tested if this effect might turn out to be an advantage by facilitating the exacerbation and early onset of disease phenotypes in brain organoids (Park et al., 2021).

In addition to the genetic and molecular basis of brain disease, the influence of external factors on brain development might also be compared in human- and NHP-derived brain organoids. For example, researchers infected human and chimpanzee cerebral organoids with the Brazilian Zika virus ($ZIKV^{BR}$) and found a reduction in both $TBR1^{+}$ and $CTIP2^{+}$ cortical neurons, and a subsequent reduction in the size of the CP-like structure of human organoids following infection, but they did not observe these effects in chimpanzee organoids after $ZIKV^{BR}$ infection suggesting human-specific neurotropism adaptations of $ZIKV^{BR}$ (Cugola et al., 2016). These studies indicate that brain organoid models can be implemented in the study of neurotropic viral infections and subsequent influence on brain development. It is foreseeable that similar models might be applied to understand additional viruses suspected of reaching the brain and influencing brain development like Sars-cov2, HIV (through HIV-1 infected microglia), or cerebral malaria (Harbuzariu et al., 2019; Dos Reis et al., 2020; Ramani et al., 2020). Finally, toxicology screenings in human- and NHP-derived brain organoids could reveal compounds that have a species-specific influence on brain development and potentially identify the protective effect provided by the non-susceptible primate (Quadrato et al., 2016). Human and NHP-derived organoids can teach us much about ourselves and the world around us, from human-specific processes of brain development and disease to evolutionary differences and neurotropic viral mechanisms,

possibly providing insight into the development of effective therapies and protective strategies against brain dysregulation.

AUTHOR CONTRIBUTIONS

SF wrote the manuscript. DK designed and generated the figures. MM conceived and supervised the work. All authors listed have made a substantial, direct and intellectual contribution to the work, and approved it for publication.

FUNDING

We are grateful for the funding provided to MM by the Larry L. Hillblom Foundation and to SF by the T32 Ruth L. Kirschstein Institutional National Research Service Award (Grant No. 1T32GM133351-01) through the National Institutes of Health and distributed by UCSD's Pathways in Biological Sciences (PiBS) training program. DK is funded by the California Institute for Regenerative Medicine (CIRM) Bridges through SDSU.

ACKNOWLEDGMENTS

We would like to thank Fred Gage and all the members of the Gage laboratory for their insightful conversions and all their support. The UCSD biology and anthropology departments and SDSU chemistry and biochemistry department for all the guidance, training, and support. We would like to thank the University of California Center for Academic Research and Training in Anthropogeny (CARTA). Figures were created with Biorender.com.

REFERENCES

Abud, E. M., Ramirez, R. N., Martinez, E. S., Healy, L. M., Nguyen, C. H. H., Newman, S. A., et al. (2017). IPSC-derived human microglia-like cells to study neurological diseases. *Neuron* 94, 278–293. doi: 10.1016/j.neuron.2017.03.042

Acampora, D., Avantaggiato, V., Tuorto, F., Barone, P., Reichert, H., Finkelstein, R., et al. (1998). Murine Otx1 and drosophila OTD genes share conserved genetic functions required in invertebrate and vertebrate brain development. *Development* 1702, 1691–1702. doi: 10.1242/dev.125.9.1691

Agoglia, R. M., Sun, D., Birey, F., Yoon, S., Miura, Y., Sabatini, K., et al. (2021). Primate cell fusion disentangles gene regulatory divergence in neurodevelopment. *Nature* 592, 421–427. doi: 10.1038/s41586-021-03343-3

Ahmad, M. H., Fatima, M., and Mondal, A. C. (2019). Influence of microglia and astrocyte activation in the neuroinflammatory pathogenesis of Alzheimer's disease: rational insights for the therapeutic approaches. *J. Clin. Neurosci.* 59, 6–11. doi: 10.1016/j.jocn.2018.10.034

Amiri, A., Coppola, G., Scuderi, S., Wu, F., Roychowdhury, T., Liu, F., et al. (2018). Transcriptome and epigenome landscape of human cortical development modeled in organoids. *Science* 362:eaat6720. doi: 10.1126/science.aat6720

Atamian, A., Cordón-Barris, L., and Quadrato, G. (2021). Taming human brain organoids one cell at a time. *Semin. Cell Dev. Biol.* 111, 23–31. doi: 10.1016/j.semcdb.2020.05.022

Azevedo, F. A. C., Carvalho, L. R. B., Grinberg, L. T., Farfel, J. M., Ferretti, R. E. L., Leite, R. E. P., et al. (2009). Equal numbers of neuronal and nonneuronal cells make the human brain an isometrically scaled-up primate brain. *J. Comp. Neurol.* 513, 532–541. doi: 10.1002/cne.21974

Bagley, J. A., Reumann, D., Bian, S., évi-Strauss, J. L., and Knoblich, J. A. (2017). Fused dorsal-ventral cerebral organoids model complex interactions between diverse brain regions. *Nat. Methods* 14, 743–751. doi: 10.1038/nmeth.4304. Fused

Bakken, T. E., Miller, J. A., Lin Ding, S., Sunkin, S. M., Smith, K. A., Ng, L., et al. (2016). A comprehensive transcriptional map of primate brain development. *Nature* 535, 367–375. doi: 10.1038/nature18637

Barger, N., Stefanacci, L., and Semendeferi, K. (2007). A comparative volumetric analysis of the amygdaloid complex and basolateral division in the human and ape brain. *Am. J. Phys. Anthropol.* 134, 392–403. doi: 10.1002/ajpa.20684

Barres, B. A. (2008). The mystery and magic of glia: a perspective on their roles in health and disease. *Neuron* 60, 430–440. doi: 10.1016/j.neuron.2008.10.013

Bauernfeind, A. L., Reyzer, M. L., Caprioli, R. M., Ely, J. J., Babbitt, C. C., Wray, G. A., et al. (2015). High spatial resolution proteomic comparison of the brain in humans 640 and chimpanzees. *J. Comp. Neurol.* 523, 2043–2061. doi: 10.1002/cne.23777

Benito-Kwiecinski, S., Giandomenico, S. L., Sutcliffe, M., Riis, E. S., Freire-Pritchett, P., Kelava, I., et al. (2021). An early cell shape transition drives evolutionary expansion of the human forebrain. *Cell* 184, 2084–2102. doi: 10.1016/j.cell.2021.02.050

Berman, K. F., and Weinberger, D. R. (1991). Chapter 26 the prefrontal cortex in schizophrenia and other neuropsychiatric diseases: in vivo physiological correlates of cognitive deficits. *Prog. Brain Res.* 85, 521–537. doi: 10.1016/S0079-6123(08)62698-9

Bhaduri, A., Andrews, M. G., Mancia Leon, W., Jung, D., Shin, D., Allen, D., et al. (2020). Cell stress in cortical organoids impairs molecular subtype specification. *Nature* 578, 142–148. doi: 10.1038/s41586-020-1962-0

Bianchi, S., Stimpson, C. D., Bauernfeind, A. L., Schapiro, S. J., Baze, W. B., McArthur, M. J., et al. (2013). Dendritic morphology of pyramidal neurons in the chimpanzee neocortex: regional specializations and comparison to humans. *Cereb. Cortex* 23, 2429–2436. doi: 10.1093/cercor/bhs239

Birey, F., Andersen, J., Makinson, C. D., Islam, S., Wei, W., Huber, N., et al. (2017). Assembly of functionally integrated human forebrain spheroids. *Nature* 545, 54–59. doi: 10.1038/nature22330

Bove, R. M. (2018). Why monkeys do not get multiple sclerosis (spontaneously): an evolutionary approach. *Evol. Med. Public Health* 2018, 43–59. doi: 10.1093/emph/eoy002

Brennand, K., Savas, J. N., Kim, Y., Tran, N., Simone, A., Hashimoto-Torii, K., et al. (2015). Phenotypic differences in HiPSC NPCs derived from patients with schizophrenia. *Mol. Psychiatry* 20, 361–368. doi: 10.1038/mp.2014.22

Cai, Z., Wan, Q. C., and Liu, Z. (2017). Astrocyte and Alzheimer's disease. *J. Neurol.* 264, 2068–2074. doi: 10.1007/s00415-017-8593-x

Cakir, B., Xiang, Y., Tanaka, Y., Kural, M. H., Parent, M., Jin Kang, Y., et al. (2019). Engineering of human brain organoids with a functional vascular-like system. *Nat. Methods* 16, 1169–1175. doi: 10.1038/s41592-019-0586-5

Camp, J. G., Badsha, F., Florio, M., Kanton, S., Gerber, T., Wilsch-Bräuninger, M., et al. (2015). Human cerebral organoids recapitulate gene expression programs of fetal neocortex development. *Proc. Natl. Acad. Sci. U.S.A.* 112, 15672–15677. doi: 10.1073/pnas.1520760112

Campbell, K., and Götz, M. (2002). Radial glia: multi-purpose cells for vertebrate brain development. *Trends Neurosci.* 25, 235–238. doi: 10.1016/S0166-2236(02)02156-2

Castells-Nobau, A., Eidhof, I., Fenckova, M., Brenman-Suttner, D. B., Scheffer-De Gooyert, J. M., Christine, S., et al. (2019). Conserved regulation of neurodevelopmental processes and behavior by FoxP in *Drosophila*. *PLoS One* 14:e0211652. doi: 10.1371/journal.pone.0211652

Ceccarelli, M., Barthel, F. P., Malta, T. M., Sabedot, T. S., Salama, S. R., Murray, B. A., et al. (2016). Molecular profiling reveals biologically discrete subsets and pathways of progression in diffuse glioma. *Cell* 164, 550–563. doi: 10.1016/j.cell.2015.12.028

Choi, H., Lee, E. J., Shin, J. S., Kim, H., Bae, S., and Lee, D. S. (2021). Spatiotemporal characterization of glial cell activation in an Alzheimer's disease model by spatially resolved transcriptome. *Biorxiv* [Preprint] doi: 10.1101/2021.06.28.450154 bioRxiv: 29450154,

Cong, L., Ran, F. A., Cox, D., Lin, S., Barretto, R., Hsu, P. D., et al. (2013). Multiplex genome engineering using CRISPR/Cas Systems. *Science* 339, 819–823. doi: 10.1126/science.1231143.Multiplex

Cugola, F. R., Fernandes, I. R., Russo, F. B., Freitas, B. C., Dias, J. L. M., Guimarães, K. P., et al. (2016). The brazilian zika virus strain causes birth defects in experimental models. *Nature* 534, 267–271. doi: 10.1038/nature18296

Datlinger, P., Rendeiro, A. F., Schmidl, C., Krausgruber, T., Traxler, P., Klughammer, J., et al. (2017). Pooled CRISPR screening with single-cell transcriptome readout. *Nat. Methods* 14, 297–301. doi: 10.1038/nmeth.4177

de Paiva Lopes, K., Snijders, G. J. L., Humphrey, J., Allan, A., Sneeboer, M., Navarro, E., et al. (2020). Atlas of genetic effects in human microglia transcriptome across brain regions, aging and disease pathologies. *BioRxiv* [Preprint] doi: 10.1101/2020.10.27.356113

Deng, Y., Zhang, D., Liu, Y., Su, G., Enninful, A., Bai, Z., et al. (2021). Spatial epigenome sequencing at tissue scale and cellular level. *BioRxiv* [preprint] doi: 10.1101/2021.03.11.434985

Domingues, H. S., Portugal, C. C., Socodato, R., and Relvas, J. B. (2016). Oligodendrocyte, astrocyte, and microglia crosstalk in myelin development, damage, and repair. *Front. Cell Dev. Biol.* 4:71. doi: 10.3389/fcell.2016.00071

Dos Reis, R. S., Sant, S., Keeney, H., Wagner, M. C. E., and Ayyavoo, V. (2020). Modeling HIV-1 neuropathogenesis using three-dimensional human brain organoids (HBORGs) with HIV-1 infected microglia. *Sci. Rep.* 10:15209. doi: 10.1038/s41598-020-72214-0

Dracheva, S., Davis, K. L., Chin, B., Woo, D. A., Schmeidler, J., and Haroutunian, V. (2006). Myelin-associated MRNA and protein expression deficits in the anterior cingulate cortex and hippocampus in elderly schizophrenia patients. *Neurobiol. Dis.* 21, 531–540. doi: 10.1016/j.nbd.2005.08.012

Edler, M. K., Sherwood, C. C., Meindl, R. S., Hopkins, W. D., Ely, J. J., Erwin, J. M., et al. (2017). Aged chimpanzees exhibit pathologic hallmarks of Alzheimer's disease. *Neurobiol. Aging* 59, 107–120. doi: 10.1016/j.neurobiolaging.2017.07.006

Efremova, M., and Teichmann, S. A. (2020). Computational methods for single-cell omics across modalities. *Nat. Methods* 17, 14–17. doi: 10.1038/s41592-019-0692-4

Eiraku, M., Watanabe, K., Matsuo-Takasaki, M., Kawada, M., Yonemura, S., Matsumura, M., et al. (2008). Self-organized formation of polarized cortical tissues from ESCs and its active manipulation by extrinsic signals. *Cell Stem Cell* 3, 519–532. doi: 10.1016/j.stem.2008.09.002

Eroglu, C., and Barres, B. A. (2010). Regulation of synaptic connectivity by glia. *Nature* 468, 223–231. doi: 10.1038/nature09612

Estrada, A., Garber, P. A., Rylands, A. B., Roos, C., Fernandez-Duque, E., Di Fiore, A., et al. (2017). Impending extinction crisis of the world's primates: why primates matter. *Sci. Adv.* 3:e1600946. doi: 10.1126/sciadv.1600946

Fan, X., Fu, Y., Zhou, X., Sun, L., Yang, M., Wang, M., et al. (2020). Single-cell transcriptome analysis reveals cell lineage specification in temporal-spatial patterns in human cortical development. *Sci. Adv.* 6:eaaz2978. doi: 10.1126/sciadv.aaz2978

Feinberg, I. (1982). Schizophrenia: caused by a fault in programmed synaptic elimination during adolescence? *J. Psychiatr. Res.* 17, 319–334. doi: 10.1016/0022-3956(82)90038-3

Fernando, A. B. P., and Robbins, T. W. (2011). Animal models of neuropsychiatric disorders. *Annu. Rev. Clin. Psychol.* 7, 39–61. doi: 10.1146/annurev-clinpsy-032210-104454

Field, A. R., Jacobs, F. M. J., Fiddes, I. T., Phillips, A. P. R., Reyes-Ortiz, A. M., LaMontagne, E., et al. (2019). Structurally conserved primate LncRNAs are transiently expressed during human cortical differentiation and influence cell-type-specific genes. *Stem Cell Rep.* 12, 245–257. doi: 10.1016/j.stemcr.2018.12.006

Gallego Romero, I., Pavlovic, B. J., Hernando-Herraez, I., Zhou, X., Ward, M. C., Banovich, N. E., et al. (2015). A panel of induced pluripotent stem cells from chimpanzees: a resource for comparative functional genomics. *Elife* 4:e07103. doi: 10.7554/elife.07103

Giandomenico, S. L., and Lancaster, M. A. (2017). Probing human brain evolution and development in organoids. *Curr. Opin. Cell Biol.* 44, 36–43. doi: 10.1016/j.ceb.2017.01.001

Gilbert, L. A., Larson, M. H., Morsut, L., Liu, Z., Brar, G. A., Torres, S. E., et al. (2013). XCRISPR-mediated modular RNA-guided regulation of transcription in eukaryotes. *Cell* 154:442. doi: 10.1016/j.cell.2013.06.044

Godenschwege, T. A., Kristiansen, L. V., Uthaman, S. B., Hortsch, M., and Murphey, R. K. (2006). A conserved role for drosophila neuroglian and human L1-CAM in central-synapse formation. *Curr. Biol.* 16, 12–23. doi: 10.1016/j.cub.2005.11.062

Gordon, A., Yoon, S., Tran, S. S., Makinson, C. D., Park, J. Y., Andersen, J., et al. (2021). Long-term maturation of human cortical organoids matches key early postnatal transitions. *Nat. Neurosci.* 24, 331–342. doi: 10.1038/s41593-021-00802-y

Gray, M., Roy, J., Vigilant, L., Fawcett, K., Basabose, A., Cranfield, M., et al. (2013). Genetic census reveals increased but uneven growth of a critically endangered mountain gorilla population. *Biol. Conserv.* 158, 230–238. doi: 10.1016/j.biocon.2012.09.018

Hakak, Y., Walker, J. R., Li, C., Hung Wong, W., Davis, K. L., Buxbaum, J. D., et al. (2001). Genome-wide expression analysis reveals dysregulation of myelination-related genes in chronic schizophrenia. *Proc. Natl. Acad. Sci. U.S.A.* 98, 4746–4751. doi: 10.1073/pnas.081071198

Harbuzariu, A., Pitts, S., Cespedes, J. C., Harp, K. O., Nti, A., Shaw, A. P., et al. (2019). Modelling heme-mediated brain injury associated with cerebral malaria in human brain cortical organoids. *Sci. Rep.* 9:19162. doi: 10.1038/s41598-019-55631-8

Hasselmann, J., Coburn, M. A., England, W., Figueroa Velez, D. X., Kiani Shabestari, S., Tu, C. H., et al. (2019). Development of a chimeric model to study and manipulate human microglia in vivo. *Neuron* 103, 1016–1033. doi: 10.1016/j.neuron.2019.07.002

Heneka, M. T., Kummer, M. P., and Latz, E. (2014). Innate immune activation in neurodegenerative disease. *Nat. Rev. Immunology* 14, 463–477. doi: 10.1038/nri3705

Hirabayashi, Y., and Gotoh, Y. (2010). Epigenetic control of neural precursor cell fate during development. *Nat. Rev. Neurosci.* 11, 377–388. doi: 10.1038/nrn2810

Hof, P. R., Gilissen, E. P., Sherwood, C. C., Duan, H., Lee, P. W. H., Delman, B. N., et al. (2004). Comparative neuropathology of brain aging in primates. *Aging Nonhum. Primates* 31, 130–154. doi: 10.1159/000061462

Hong, S., Hong, S., Beja-glasser, V. F., Nfonoyim, B. M., Frouin, A., Li, S., et al. (2016). Complement and microglia mediate early synapse loss in Alzheimer mouse models. *Science* 8373, 712–716. doi: 10.1126/science.aad8373

Hou, Q. Q., Xiao, Q., Sun, X. Y., Ju, X. C., and Luo, Z. G. (2021). TBC1D3 promotes neural progenitor proliferation by suppressing the histone methyltransferase G9a. *Sci. Adv.* 7:eaba8053. doi: 10.1126/sciadv.aba8053

Huttenlocher, P. R., and Dabholkar, A. S. (1997). Regional differences in synaptogenesis in human cerebral cortex. *J. Comp. Neurol.* 387, 167–178. doi: 10.1002/(SICI)1096-9861(19971020)387:2<167::AID-CNE1<3.0.CO;2-Z

Ishihara, T., Bin Zhang, M. H., Nakagawa, Y., Lee, M. K., Trojanowski, J. Q., and Lee, V. M. Y. (1999). Age-dependent emergence and progression of a tauopathy in transgenic mice overexpressing the shortest human tau isoform. *Neuron* 24, 751–762. doi: 10.1016/S0896-6273(00)81127-7

Ji, Q., Wu, W., Ji, Y., Li, Q., and Ni, X. (2021). Late middle pleistocene harbin cranium represents a new homo species. *Innovation* 2:100132. doi: 10.1016/j.xinn.2021.100132

Jo, J., Xiao, Y., Sun, A. X., Cukuroglu, E., Tran, H. D., Göke, J., et al. (2016). Midbrain-like organoids from human pluripotent stem cells contain functional dopaminergic and neuromelanin-producing neurons. *Cell Stem Cell* 19, 248–257. doi: 10.1016/j.stem.2016.07.005

Johnson, M. H. (2001). Functional brain development in humans. *Nat. Rev. Neurosci.* 2, 475–483. doi: 10.1038/35081509

Kadoshima, T., Sakaguchi, H., Nakano, T., Soen, M., Ando, S., Eiraku, M., et al. (2014). Erratum: self-organization of axial polarity, inside-out layer pattern, and species-specific progenitor dynamics in human ES cell-derived neocortex. *Proc. Natl. Acad. Sci. U.S.A.* 111:7498. doi: 10.1073/pnas.1407159111

Kampmann, M. (2017). A CRISPR approach to neurodegenerative diseases. *Trends Mol. Med.* 23, 483–485. doi: 10.1016/j.molmed.2017.04.003

Kanton, S., Boyle, M. J., He, Z., Santel, M., Weigert, A., Sanchís-Calleja, F., et al. (2019). Organoid single-cell genomic atlas uncovers human-specific features of brain development. *Nature* 574, 418–422. doi: 10.1038/s41586-019-1654-9

Kariya, T., and Ishikawa, K. (2019). The art of war in drug development. *JACC Basic Transl. Sci.* 4, 715–716. doi: 10.1016/j.jacbts.2019.09.002

Kelava, I., and Lancaster, M. A. (2016). Dishing out mini-brains: current progress and future prospects in brain organoid research. *Dev. Biol.* 420, 199–209. doi: 10.1016/j.ydbio.2016.06.037

Khrameeva, E., Kurochkin, I., Han, D., Guijarro, P., Kanton, S., Santel, M., et al. (2020). Single-cell-resolution transcriptome map of human, chimpanzee, bonobo, and macaque brains. *Genome Res.* 30, 776–789. doi: 10.1101/gr.256958.119

Kierdorf, K., Erny, D., Goldmann, T., Sander, V., Schulz, C., Perdiguero, E. G., et al. (2013). Microglia emerge from erythromyeloid precursors via Pu.1-and Irf8-dependent pathways. *Nat. Neurosci.* 16, 273–280. doi: 10.1038/nn.3318

Kim, H., Xu, R., Padmashri, R., Dunaevsky, A., Liu, Y., Dreyfus, C. F., et al. (2019). Pluripotent stem cell-derived cerebral organoids reveal human oligodendrogenesis with dorsal and ventral origins. *Stem Cell Rep.* 12, 890–905. doi: 10.1016/j.stemcr.2019.04.011

Kochiyama, T., Ogihara, N., Tanabe, H. C., Kondo, O., Amano, H., Hasegawa, K., et al. (2018). Reconstructing the neanderthal brain using computational anatomy. *Sci. Rep.* 8:6296. doi: 10.1038/s41598-018-24331-0

Lancaster, M. A., Renner, M., Martin, C.-A., Wenzel, D., Bicknell, L. S., Hurles, M. E., et al. (2013). Cerebral organoids model human brain development and microcephaly. *Nature* 501, 373–379. doi: 10.1038/nature12517

Langer, J. (1996). "Heterochrony and the evolution of primate cognitive development," in *Reaching into Thought: The Minds of the Great Apes*, eds A. E. Russon, K. A. Bard, and S. T. Parker (Cambridge: Cambridge University Press), 257–277.

Larsson, L., Frisén, J., and Lundeberg, J. (2021). Spatially resolved transcriptomics adds a new dimension to genomics. *Nat. Methods* 18, 15–18. doi: 10.1038/s41592-020-01038-7

Li, M. L., Li, M. L., Tang, H., Shao, Y., Shao, Y., Wang, M. S., et al. (2020). Evolution and transition of expression trajectory during human brain development. *BMC Evol. Biol.* 20:72. doi: 10.1186/s12862-020-01633-4

Libby, R. G. A., Joy, D. A., Edler, N. H., Bulger, E. A., Krakora, M. Z., Gaylord, E. A., et al. (2021). Axial elongation of caudalized human organoids mimics aspects of neural tube development. *Development* 148:dev198275. doi: 10.1242/dev.198275

Liu, H., Zhu, F., Yong, J., Zhang, P., Hou, P., Li, H., et al. (2008). Generation of induced pluripotent stem cells from adult rhesus monkey fibroblasts. *Cell Stem Cell* 3, 587–590. doi: 10.1016/j.stem.2008.10.014

Liu, J., Liu, W., Yang, L., Wu, Q., Zhang, H., Fang, A., et al. (2017). The primate-specific gene TMEM14B marks outer radial glia cells and promotes cortical expansion and folding. *Cell Stem Cell* 21, 635–649. doi: 10.1016/j.stem.2017.08.013

Luo, C., Lancaster, M. A., Castanon, R., Nery, J. R., Knoblich, J. A., and Ecker, J. R. (2016). Cerebral organoids recapitulate epigenomic signatures of the human fetal brain. *Cell Rep.* 17, 3369–3384. doi: 10.1016/j.celrep.2016.12.001

Madhavan, M., Nevin, Z. S., Shick, H. E., Garrison, E., Clarkson-Paredes, C., Karl, M., et al. (2018). Induction of myelinating oligodendrocytes in human cortical spheroids. *Nat. Methods* 15, 700–706. doi: 10.1038/s41592-018-0081-4

Mansour, A. A., Tiago Gonçalves, J., Bloyd, C. W., Li, H., Fernandes, S., Quang, D., et al. (2018). An in vivo model of functional and vascularized human brain organoids. *Nat. Biotechnol.* 36, 432–441. doi: 10.1038/nbt.4127

Mansour, A. A. F., Schafer, S. T., and Gage, F. H. (2021). Cellular complexity in brain organoids: current progress and unsolved issues. *Semin. Cell Dev. Biol.* 111, 32–39. doi: 10.1016/j.semcdb.2020.05.013

Marchetto, M. C., Hrvoj-Mihic, B., Kerman, B. E., Yu, D. X., Vadodaria, K. C., Linker, S. B., et al. (2019). Species-specific maturation profiles of human, chimpanzee and bonobo neural cells. *Elife* 8:e37527. doi: 10.7554/eLife.37527

Marchetto, M. C. N., Narvaiza, I., Denli, A. M., Benner, C., Lazzarini, T. A., Nathanson, J. L., et al. (2013). Differential L1 regulation in pluripotent stem cells of humans and apes. *Nature* 503, 525–529. doi: 10.1038/nature12686

Marton, R. M., Miura, Y., Sloan, S. A., Li, Q., Revah, O., Levy, R. J., et al. (2019). Differentiation and maturation of oligodendrocytes in human three-dimensional neural cultures. *Nat. Neurosci.* 22, 484–491. doi: 10.1038/s41593-018-0316-9

Matsui, T. K., Matsubayashi, M., Sakaguchi, Y. M., Hayashi, R. K., Zheng, C., Sugie, K., et al. (2018). Six-month cultured cerebral organoids from human es cells contain matured neural cells. *Neurosci. Lett.* 670, 75–82. doi: 10.1016/j.neulet.2018.01.040

McCullumsmith, R. E., Gupta, D., Beneyto, M., Kreger, E., Haroutunian, V., Davis, K. L., et al. (2007). Expression of transcripts for myelination-related genes in the anterior cingulate cortex in schizophrenia. *Schizophr. Res.* 90, 15–27. doi: 10.1016/j.schres.2006.11.017

McKenzie, A. T., Moyon, S., Wang, M., Katsyv, I., Song, W. M., Zhou, X., et al. (2017). Multiscale network modeling of oligodendrocytes reveals molecular components of myelin dysregulation in Alzheimer's disease. *Mol. Neurodegener.* 12:82. doi: 10.1186/s13024-017-0219-3

Menassa, D. A., and Gomez-Nicola, D. (2018). Microglial dynamics during human brain development. *Front. Immunol.* 9:1014. doi: 10.3389/fimmu.2018.01014

Miller, D. J., Duka, T., Stimpson, C. D., Schapiro, S. J., Baze, W. B., McArthur, M. J., et al. (2012). Prolonged myelination in human neocortical evolution. *Proc. Natl. Acad. Sci. U.S.A.* 109, 16480–16485. doi: 10.1073/pnas.1117943109

Mitkus, S. N., Hyde, T. M., Vakkalanka, R., Kolachana, B., Weinberger, D. R., Kleinman, J. E., et al. (2008). Expression of oligodendrocyte-associated genes in dorsolateral prefrontal cortex of patients with schizophrenia. *Schizophr. Res.* 98, 129–138. doi: 10.1016/j.schres.2007.09.032

Monzel, A. S., Smits, L. M., Hemmer, K., Hachi, S., Moreno, E. L., Wuellen, T. V., et al. (2017). Derivation of human midbrain-specific organoids from neuroepithelial stem cells. *Stem Cell Rep.* 8, 1144–1154. doi: 10.1016/j.stemcr.2017.03.010

Mora-Bermúdez, F., Badsha, F., Kanton, S., Camp, J. G., Vernot, B., Köhler, K., et al. (2016). Differences and similarities between human and chimpanzee neural progenitors during cerebral cortex development. *Elife* 5:e18683. doi: 10.7554/eLife.18683

Mostajo-Radji, M. A., Schmitz, M. T., Montoya, S. T., and Pollen, A. A. (2020). Reverse engineering human brain evolution using organoid models. *Brain Res.* 1729:146582. doi: 10.1016/j.brainres.2019.146582

Muguruma, K., Nishiyama, A., Kawakami, H., Hashimoto, K., and Sasai, Y. (2015). Self-organization of polarized cerebellar tissue in 3d culture of human pluripotent stem cells. *Cell Rep.* 10, 537–550. doi: 10.1016/j.celrep.2014.12.051

Munger, E. L., Edler, M. K., Hopkins, W. D., Ely, J. J., Erwin, J. M., Perl, D. P., et al. (2020). Pathology in chimpanzees. *J. Comp. Neurol.* 527, 1179–1195. doi: 10.1002/cne.24610.Astrocytic

Norman, G. A. V. (2019). Limitations of animal studies for predicting toxicity in clinical trials: is it time to rethink our current approach? *JACC Basic to Transl. Sci.* 4, 845–854. doi: 10.1016/j.jacbts.2019.10.008

Nowakowski, T. J., Rani, N., Golkaram, M., Zhou, H. R., Alvarado, B., Huch, K., et al. (2018). Regulation of cell-type-specific transcriptomes by MicroRNA networks during human brain development. *Nat. Neurosci.* 21, 1784–1792. doi: 10.1038/s41593-018-0265-3

Oberheim, N. A., Takano, T., Han, X., He, W., Lin, J. H. C., Wang, F., et al. (2009). Uniquely hominid features of adult human astrocytes. *J. Neurosci.* 29, 3276–3287. doi: 10.1523/JNEUROSCI.4707-08.2009

Orlando, L., Gilbert, M. T. P., and Willerslev, E. (2015). Reconstructing ancient genomes and epigenomes. *Nat. Rev. Genet.* 16, 395–408. doi: 10.1038/nrg3935

Otani, T., Marchetto, M. C., Gage, F. H., Simons, B. D., and Livesey, F. J. (2016). 2D and 3D stem cell models of primate cortical development identify species-specific differences in progenitor behavior contributing to brain size. *Cell Stem Cell* 18, 467–480. doi: 10.1016/j.stem.2016.03.003

Paolicelli, R. C., Bolasco, G., Pagani, F., Maggi, L., Scianni, M., Panzanelli, P., et al. (2011). Synaptic pruning by microglia is necessary for normal brain development. *Science* 333, 1456–1458. doi: 10.1126/science.1202529

Park, J. C., Jang, S. Y., Lee, D., Lee, J., Kang, U., Chang, H., et al. (2021). A logical network-based drug-screening platform for Alzheimer's disease representing pathological features of human brain organoids. *Nat. Commun.* 12:280. doi: 10.1038/s41467-020-20440-5

Pasca, A. M., Sloan, S. A., Clarke, L. E., Tian, Y., Makinson, C. D., Huber, N., et al. (2015). Functional cortical neurons and astrocytes from human pluripotent stem cells in 3D Culture. *Nat. Methods* 12, 671–678. doi: 10.1038/nmeth.3415

Perez, S. E., Raghanti, M. A., Hof, P. R., Kramer, L., Ikonomovic, M. D., Lacor, P. N., et al. (2013). Alzheimer's disease pathology in the neocortex and hippocampus of the western lowland gorilla (*Gorilla Gorilla* Gorilla). *J. Comp. Neurol.* 521, 4318–4338. doi: 10.1002/cne.23428

Perez, S. E., Sherwood, C. C., Cranfield, M. R., Erwin, J. M., Mudakikwa, A., Hof, P. R., et al. (2016). Early Alzheimer's disease-type pathology in the frontal cortex of wild mountain gorillas (Gorilla Beringei Beringei). *Neurobiol. Aging* 39, 195–201. doi: 10.1016/j.neurobiolaging.2015.12.017

Petanjek, Z., Judaš, M., Šimiæ, G., Rašin, M. R., Uylings, H. B. M., Rakic, P., et al. (2011). Extraordinary neoteny of synaptic spines in the human prefrontal cortex. *Proc. Natl. Acad. Sci. U.S.A.* 108, 13281–13286. doi: 10.1073/pnas.1105108108

Pham, M. T., Pollock, K. M., Rose, M. D., Cary, W. A., Stewart, H. R., Zhou, P., et al. (2018). Generation of human vascularized brain organoids. *Neuroreport* 29, 588–593. doi: 10.1097/WNR.0000000000001014

Pollen, A. A., Bhaduri, A., Andrews, M. G., Nowakowski, T. J., Meyerson, O. S., Mostajo-Radji, M. A., et al. (2019). Establishing cerebral organoids as models of human-specific brain evolution. *Cell* 176, 743–756. doi: 10.1016/j.cell.2019.01.017

Preuss, T. M. (2011). The human brain: rewired and running hot. *Ann. N. Y. Acad. Sci.* 1225(Suppl. 1), 182–191. doi: 10.1111/j.1749-6632.2011.06001.x

Qian, X., Jacob, F., Song, M. M., Nguyen, H. N., Song, H., and Ming, G.-L. (2018). Generation of human brain region–specific organoids using a miniaturized spinning bioreactor. *Nat. Protoc.* 13, 565–580. doi: 10.1038/nprot.2017.152

Qian, X., Su, Y., Adam, C. D., Deutschmann, A. U., Pather, S. R., Goldberg, E. M., et al. (2020). Sliced human cortical organoids for modeling distinct cortical layer formation. *Cell Stem Cell* 26, 766–781. doi: 10.1016/j.stem.2020.02.002

Quadrato, G., Brown, J., and Arlotta, P. (2016). The promises and challenges of human brain organoids as models of neuropsychiatric disease. *Nat. Med.* 22, 1220–1228. doi: 10.1038/nm.4214

Quadrato, G., Nguyen, T., Macosko, E. Z., Sherwood, J. L., Yang, S. M., Berger, D. R., et al. (2017). Cell diversity and network dynamics in photosensitive human brain organoids. *Nature* 545, 48–53. doi: 10.1038/nature22047

Raghanti, M. A., Stimpson, C. D., Marcinkiewicz, J. L., Erwin, J. M., Hof, P. R., and Sherwood, C. C. (2011). NIH public access. *Neuroscience* 155, 203–220. doi: 10.1016/j.neuroscience.2008.05.008.Cortical

Rakic, P., Bourgeois, J. P., Eckenhoff, M. F., Zecevic, N., and Goldman-Rakic, P. S. (1986). Concurrent overproduction of synapses in diverse regions of the primate cerebral cortex. *Science* 232, 232–235. doi: 10.1126/science.3952506

Ramani, A., Müller, L., Ostermann, P. N., Gabriel, E., Abida-Islam, P., Müller-Schiffmann, A., et al. (2020). SARS -CoV-2 targets neurons of 3D human brain organoids. *EMBO J.* 39:e106230. doi: 10.15252/embj.2020106230

Rash, B. G., Duque, A., Morozov, Y. M., Arellano, J. I., Micali, N., and Rakic, P. (2019). Gliogenesis in the outer subventricular zone promotes enlargement and gyrification of the primate cerebrum. *Proc. Natl. Acad. Sci. U.S.A.* 116, 7089–7094. doi: 10.1073/pnas.1822169116

Reardon, P. K., Seidlitz, J., Vandekar, S., Liu, S., Patel, R., Park, M. T. M., et al. (2018). Normative brain size variation and brain shape diversity in humans. *Science* 360, 1222–1227. doi: 10.1126/science.aar2578

Reiche, L., Küry, P., and Göttle, P. (2019). Aberrant oligodendrogenesis in down syndrome: shift in gliogenesis? *Cells* 8:1591. doi: 10.3390/cells8121591

Renner, M., Lancaster, M. A., Bian, S., Choi, H., Ku, T., Peer, A., et al. (2017). Self-organized developmental patterning and differentiation in cerebral organoids. *EMBO J.* 36, 1316–1329. doi: 10.15252/embj.201694700

Romero-Grimaldi, C., and Moreno-López, B. (2008). Age-dependent effect of nitric oxide on subventricular zone and olfactory bulb. *J. Comp. Neurol.* 346, 339–346. doi: 10.1002/cne

Rubenstein, J. L. R. (2011). Annual research review: development of the cerebral cortex: implications for neurodevelopmental disorders. *J. Child Psychol. Psychiatry* 52, 339–355. doi: 10.1111/j.1469-7610.2010.02307.x

Rusznák, Z., Henskens, W., Schofield, E., Kim, W. S., and Fu, Y. H. (2016). Adult neurogenesis and gliogenesis: possible mechanisms for neurorestoration. *Exp. Neurobiol.* 25, 103–112. doi: 10.5607/en.2016.25.3.103

Sakaguchi, H., Kadoshima, T., Soen, M., Narii, N., Ishida, Y., Ohgushi, M., et al. (2015). Generation of functional hippocampal neurons from self-organizing human embryonic stem cell-derived dorsomedial telencephalic tissue. *Nat. Commun.* 6:8896. doi: 10.1038/ncomms9896

Sakai, T., Matsui, M., Mikami, A., Malkova, L., Hamada, Y., Tomonaga, M., et al. (2013). Developmental patterns of chimpanzee cerebral tissues provide important clues for understanding the remarkable enlargement of the human brain. *Proc. R. Soc. B Biol. Sci.* 280:20122398. doi: 10.1098/rspb.2012.2398

Salameh, J. S., Brown, R. H., and Berry, J. D. (2015). Amyotrophic lateral sclerosis: review. *Semin. Neurol.* 35, 469–476. doi: 10.1055/s-0035-1558984

Schafer, S. T., Paquola, A. C. M., Stern, S., Gosselin, D., Ku, M., Pena, M., et al. (2019). Pathological priming causes developmental gene network heterochronicity in autistic subject-derived neurons. *Nat. Neurosci.* 22, 243–255. doi: 10.1038/s41593-018-0295-x

Sellgren, C. M., Gracias, J., Watmuff, B., Biag, J. D., Thanos, J. M., Whittredge, P. B., et al. (2019). Increased synapse elimination by microglia in schizophrenia patient-derived models of synaptic pruning. *Nat. Neurosci.* 22, 374–385. doi: 10.1038/s41593-018-0334-7

Semendeferi, K., and Damasio, H. (2000). The brain and its main anatomical subdivisions in living hominoids using magnetic resonance imaging. *J. Hum. Evol.* 38, 317–332. doi: 10.1006/jhev.1999.0381

Severance, E. G., Gressitt, K. L., Buka, S. L., Cannon, T. D., and Yolken, R. H. (2014). Maternal complement c1q and increased odds for psychosis in adult offspring. *Schizophr. Res.* 159, 14–19. doi: 10.1016/j.schres.2014.07.053

Shah, S., Takei, Y., Zhou, W., Lubeck, E., Yun, J., Linus Eng, C. H., et al. (2018). Dynamics and spatial genomics of the nascent transcriptome by intron SeqFISH. *Cell* 174, 363–376. doi: 10.1016/j.cell.2018.05.035

Shaker, M. R., Pietrogrande, G., Martin, S., Lee, J. H., Sun, W., and Wolvetang, E. J. (2021). Rapid and efficient generation of myelinating human oligodendrocytes in organoids. *Front. Cell. Neurosci.* 15:631548. doi: 10.3389/fncel.2021.631548

Silbereis, J. C., Pochareddy, S., Zhu, Y., Li, M., and Sestan, N. (2016). The cellular and molecular landscapes of the developing human central nervous system. *Neuron* 89:248. doi: 10.1016/j.neuron.2015.12.008

Sloan, S. A., Darmanis, S., Huber, N., Khan, T. A., Birey, F., Caneda, C., et al. (2017). Human astrocyte maturation captured in 3d cerebral cortical spheroids derived from pluripotent stem cells. *Neuron* 95, 779–790. doi: 10.1016/j.neuron.2017.07.035

Soldner, F., and Jaenisch, R. (2019). Stem cells, genome editing, and the path to translational medicine. *Cell* 175, 615–632. doi: 10.1016/j.cell.2018.09.010.Stem

Somel, M., Franz, H., Yan, Z., Lorenc, A., Guo, S., Giger, T., et al. (2009). Transcriptional neoteny in the human brain. *Proc. Natl. Acad. Sci. U.S.A.* 106, 5743–5748. doi: 10.1073/pnas.0900544106

Stahl, R., Walcher, T., Juan Romero, C. D., Pilz, G. A., Cappello, S., Irmler, M., et al. (2013). Trnp1 regulates expansion and folding of the mammalian cerebral cortex by control of radial glial fate. *Cell* 153, 535–549. doi: 10.1016/j.cell.2013.03.027

Stevens, B., Allen, N. J., Vazquez, L. E., Howell, G. R., Christopherson, K. S., Nouri, N., et al. (2007). The classical complement cascade mediates CNS synapse elimination. *Cell* 131, 1164–1178. doi: 10.1016/j.cell.2007.10.036

Stiles, J., and Jernigan, T. L. (2010). The basics of brain development. *Neuropsychol. Rev.* 20, 327–348. doi: 10.1007/s11065-010-9148-4

Tanaka, Y., Cakir, B., Xiang, Y., Sullivan, G. J., and Park, I. H. (2020). Synthetic analyses of single-cell transcriptomes from multiple brain organoids and fetal brain. *Cell Rep.* 30, 1682–1689. doi: 10.1016/j.celrep.2020.01.038

Tang, F., Barbacioru, C., Wang, Y., Nordman, E., Lee, C., Xu, N., et al. (2009). MRNA-seq whole-transcriptome analysis of a single cell. *Nat. Methods* 6, 377–382. doi: 10.1038/nmeth.1315

Tian, R., Gachechiladze, M. A., Ludwig, C. H., Laurie, M. T., Hong, J. Y., Nathaniel, D., et al. (2019). CRISPR interference-based platform for multimodal genetic screens in human IPSC-derived neurons. *Neuron* 104, 239–255. doi: 10.1016/j.neuron.2019.07.014

Trujillo, C. A., Gao, R., Negraes, P. D., Gu, J., Buchanan, J., Preissl, S., et al. (2019). Complex oscillatory waves emerging from cortical organoids model early human brain network development. *Cell Stem Cell* 25, 558–569. doi: 10.1016/j.stem.2019.08.002

Trujillo, C. A., Rice, E. S., Schaefer, N. K., Chaim, I. A., Emily, C., Madrigal, A. A., et al. (2021). Reintroduction of the archaic variant of NOVA1 in cortical organoids alters neurodevelopment. *Science* 371:eaax2537. doi: 10.1126/science.aax2537.Reintroduction

Velasco, S., Kedaigle, A. J., Simmons, S. K., Nash, A., Rocha, M., Quadrato, G., et al. (2019). Individual brain organoids reproducibly form cell diversity of the human cerebral cortex. *Nature* 570, 523–527. doi: 10.1038/s41586-019-1289-x

Vickovic, S., Eraslan, G., Salmén, F., Klughammer, J., Stenbeck, L., Schapiro, D., et al. (2019). High-definition spatial transcriptomics for in situ tissue profiling. *Nat. Methods* 16, 987–990. doi: 10.1038/s41592-019-0548-y

Vickovic, S., Magnusson, J., Giacomello, S., Asp, M., Westholm, J. O., Huss, M., et al. (2016). Visualization and analysis of gene expression in tissue sections by spatial transcriptomics patrik. *Science* 353, 78–82.

Walker, L. C., and Jucker, M. (2017). The exceptional vulnerability of humans to Alzheimer's disease. *Trends Mol. Med.* 23, 534–545. doi: 10.1016/j.molmed.2017.04.001

Wasseff, S. K., and Scherer, S. S. (2015). Activated immune response in an inherited leukodystrophy disease caused by the loss of oligodendrocyte gap junctions. *Neurobiol. Dis.* 82, 86–98. doi: 10.1016/j.nbd.2015.05.018

Watanabe, M., Buth, J. E., Vishlaghi, N., de la Torre-Ubieta, L., Taxidis, J., Khakh, B. S., et al. (2017). Self-organized cerebral organoids with human-specific features predict effective drugs to combat Zika Virus infection. *Cell Rep.* 21, 517–532. doi: 10.1016/j.celrep.2017.09.047

Xiang, Y., Tanaka, Y., Cakir, B., Patterson, B., Kim, K. Y., Sun, P., et al. (2019). HESC-derived thalamic organoids form reciprocal projections when fused with cortical organoids. *Cell Stem Cell* 24, 487–497. doi: 10.1016/j.stem.2018.12.015

Xiang, Y., Tanaka, Y., Patterson, B., Kang, Y. J., Govindaiah, G., Roselaar, N., et al. (2017). Fusion of regionally specified HPSC-derived organoids models human brain development and interneuron migration. *Cell Stem Cell* 21, 383–398. doi: 10.1016/j.stem.2017.07.007

Xu, P., Chen, A., Li, Y., Xing, X., and Lu, H. (2019). Medial prefrontal cortex in neurological diseases. *Physiol. Genom.* 51, 432–442.

Yan, Y., Shin, S., Jha, B. S., Liu, Q., Sheng, J., Li, F., et al. (2013). Efficient and rapid derivation of primitive neural stem cells and generation of brain subtype neurons from human pluripotent stem cells. *Stem Cells Transl. Med.* 2, 862–870. doi: 10.5966/sctm.2013-0080

Yoon, S. J., Elahi, L. S., Paşca, A. M., Marton, R. M., Gordon, A., Revah, O., et al. (2019). Reliability of human cortical organoid generation. *Nat. Methods* 16, 75–78. doi: 10.1038/s41592-018-0255-0

Zafeiriou, M. P., Bao, G., Hudson, J., Halder, R., Blenkle, A., Schreiber, M. K., et al. (2020). Developmental GABA polarity switch and neuronal plasticity in bioengineered neuronal organoids. *Nat. Commun.* 11:3791. doi: 10.1038/s41467-020-17521-w

Ziegenhain, C., Vieth, B., Parekh, S., Reinius, B., Guillaumet-Adkins, A., Smets, M., et al. (2017). Comparative analysis of single-cell RNA sequencing methods. molecular. *Cell* 65, 631–643. doi: 10.1016/j.molcel.2017.01.023

Conflict of Interest: The authors declare that the research was conducted in the absence of any commercial or financial relationships that could be construed as a potential conflict of interest.

Publisher's Note: All claims expressed in this article are solely those of the authors and do not necessarily represent those of their affiliated organizations, or those of the publisher, the editors and the reviewers. Any product that may be evaluated in this article, or claim that may be made by its manufacturer, is not guaranteed or endorsed by the publisher.

frontiers in Cell and Developmental Biology

MINI REVIEW
published: 04 November 2021
doi: 10.3389/fcell.2021.709824

Generation of Skin Organoids: Potential Opportunities and Challenges

Hui Sun[1,2,3], *Yi-Xuan Zhang*[1,2,3] *and Yu-Mei Li*[1,2,3]*

[1]*Institute of Regenerative Medicine, Affiliated Hospital of Jiangsu University, Jiangsu University, Zhenjiang, China,* [2]*Department of Dermatology, Affiliated Hospital of Jiangsu University, Jiangsu University, Zhenjiang, China,* [3]*School of Medicine, Jiangsu University, Zhenjiang, China*

Although several types of human skin substitutes are currently available, they usually do not include important skin appendages such as hair follicles and sweat glands, or various skin-related cells, such as dermal adipocytes and sensory neurons. This highlights the need to improve the *in vitro* human skin generation model for use as a tool for investigating skin diseases and as a source of cells or tissues for skin regeneration. Skin organoids are generated from stem cells and are expected to possess the complexity and function of natural skin. Here, we summarize the current literatures relating to the "niches" of the local skin stem cell microenvironment and the formation of skin organoids, and then discuss the opportunities and challenges associated with multifunctional skin organoids.

Keywords: skin organoid, skin stem cell niches, 3D culture, single-cell RNA sequencing, skin generation

OPEN ACCESS

Edited by:
Philip Iannaccone, Northwestern University, United States

Reviewed by:
Johannes Boltze, University of Warwick, United Kingdom
Lon J Van Winkle, Rocky Vista University, United States

***Correspondence:**
Yu-Mei Li
yumeili@ujs.edu.cn

Specialty section:
This article was submitted to Stem Cell Research, a section of the journal Frontiers in Cell and Developmental Biology

Received: *14 May 2021*
Accepted: *21 October 2021*
Published: *04 November 2021*

Citation:
Sun H, Zhang Y-X and Li Y-M (2021) Generation of Skin Organoids: Potential Opportunities and Challenges. Front. Cell Dev. Biol. 9:709824. doi: 10.3389/fcell.2021.709824

INTRODUCTION

The skin is a very complex organ that comprises various stem cell populations as well as numerous other cell types (Clevers et al., 2014; Chen et al., 2018). The skin plays an essential role in maintaining the stability of the body's internal environment, protecting the body from daily attrition, and regulating the body's temperature and perception. The outer boundary of the skin, known as the epidermis, is maintained by epidermal stem cells that reside in the basal layer, while the dermis, the layer under the epidermis, is rich in dermal fibroblasts that produce extracellular matrix components, such as collagen and elastic fibers, that give the skin its elasticity. Under the dermis lies subcutaneous fat, which functions as padding, insulation, and energy storage (Takeo et al., 2015; Gravitz, 2018). However, the current *in vitro*-generated skin models lack many of the normal and necessary skin structures, so we should find new alternative cells and functional models for skin diseases and regeneration.

The continuous and rapid development of stem cell biology can provide new insights into the basic biology of human diseases, thereby driving innovation in the diagnosis and treatment of a variety of conditions. Human pluripotent stem cells (hPSCs), including human embryonic stem cells (hESCs) and human induced pluripotent stem cells (hiPSCs), have become a valuable tool for modeling human diseases, complementing traditional animal research models (Takahashi and Yamanaka, 2006; Takahashi et al., 2007; Shi et al., 2017). Under specific induction conditions, hPSCs can differentiate into any cell or tissue type of the human body. They can also be used to generate three-dimensional (3D) *in vitro* models, i.e., organoids, containing various cell types that can be used for modeling organogenesis and developmental disorders (Dutta et al., 2017; Rossi

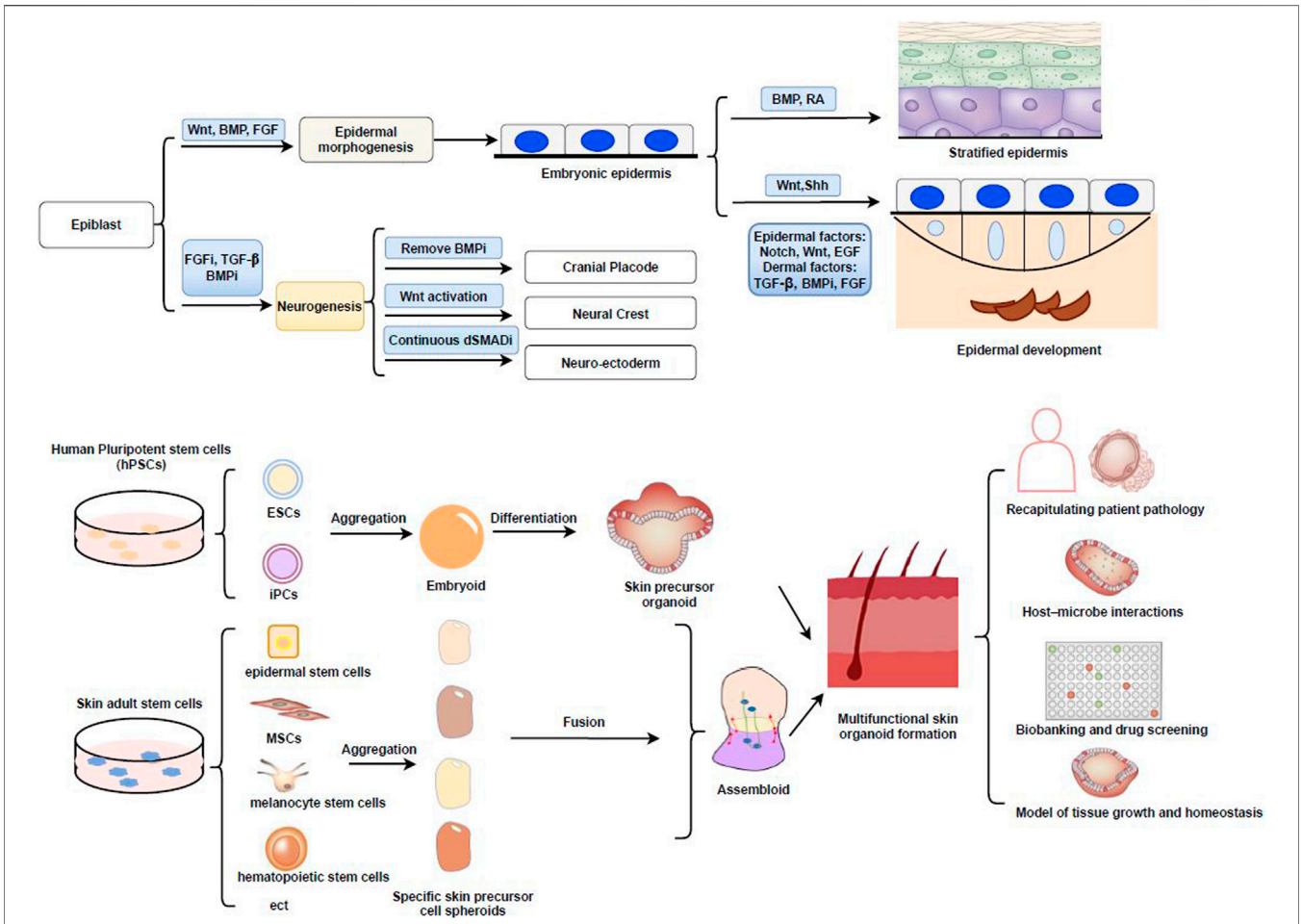

FIGURE 1 | (A) Early signaling of skin development. Wnt signaling blocks the ability of early ectodermal progenitor cells, allowing them to respond to BMP signaling and adopt an epidermal fate. Representation of the border model and important signaling pathways such as mall molecules termed as dual SMAD inhibition (dSMADi) that inhibit the BMP and TGFβ signaling pathways, respectively and influence particular cell fates in neurogenesis as well as CP, NC, NE. While Wnt/Shh activating signals produce the hair placode and additional dermal messages further instruct the placodes to make the hair follicle. **(B)** Schematic illustration of skin organoid formation and its application. This figure summarizes how integration of skin organoid technology with PSC/ASC approaches (including EB formation and fusion assembloids with different skin precursor cells) allowed the understanding of various applications in skin diseases. Cranial placode, CP; dual SMAD inhibition, dSMADi; Embryoid-body, EB; Neural crest, NC; Neuroectoderm, NE; Retinoic acid, RA.

et al., 2018). Skin organoids are derived from hPSCs and can self-assemble to form an organized, skin-like structure composed of skin progenitor cells and hair follicles resembling fetal skin (Lee et al., 2018; Kim and Ju, 2019; Lee et al., 2020).

In this review, we first evaluate recent advances in skin formation in the field of stem cells and regenerative medicine. Then, we discuss the origins of skin cells and skin organoid culture systems and offer feasible suggestions for future directions and methods to generate ideal skin organoids using the latest technologies, such as 3D culture. Despite their tremendous promise, current skin organoid models still have limitations. Therefore, in this review, we also aim to provide an impartial view of the opportunities and challenges relating to skin organoids. Only when current models are fully understood can skin organoids help shed light on our understanding of human skin biology and skin diseases.

SKIN DEVELOPMENT AND MICROENVIRONMENT

Different types of skin-resident cells perform different functions; thus, we must first fully understand the mechanisms involved in skin development as well as the microenvironment. Importantly, multiple types of skin stem cells, such as epidermal stem cells, as well as other types of progenitor cells that reside in the skin and its appendages (e.g., hair bulbs and sweat glands), are required for the development, continuous renewal, and regeneration of the body's skin, activities that are controlled by the "niches" within the local stem cell microenvironment (Fuchs, 2007; Yin et al., 20132011; Mahmoudi and Brunet, 2012). With the development of genetic and imaging tools, our understanding of the relationship between skin stem cells and their progeny, as well as the interaction between skin stem cells and their niches, has increased over recent years (Gravitz, 2018). Wnt signaling

emanating from the niches has been proposed to act as a cue for stem cell self-renewal in a variety of mammalian tissues (Clevers et al., 2014) (**Figure 1A**). At the same time, lineage analysis demonstrated heterogeneity among the cells in stem or progenitor cells are stochastic. In addition, stem cells and their downstream progenitors exploit the full advantages of their own environment according to detailed areas as niches (Ito et al., 2007; Yang et al., 2017). Therefore, skin stem cells, their niches, and associated signals are essential for skin development and differentiation. In addition, the maintenance and function of adult skin stem cells require different microenvironments within the niches, including the presence of a variety of allogeneic cells and associated stem cell lineages (Lane et al., 2014; Gonzales and Fuchs, 2017).

The skin originates from two major tissue types, namely, the ectoderm (epidermis) and mesenchyme (dermis, hypodermis, and mesodermal connective tissue). Sensory nerve endings and melanocytes (neural crest) are also present in the skin (Quarto et al., 2010). In the early embryo, Wnt/β-catenin signaling plays a key role in skin development (Siebel and Lendahl, 2017; Lim and Nusse, 2013). During gastrulation, the ectoderm invaginates along the midline for development, and then the ectodermal cells proliferate and migrate downwards from the center (Tchieu et al., 2017). Three primary cell layers (germ layers) are formed in the gastrula: ectoderm, mesoderm, and endoderm. The ectodermal layer lies on the surface of the embryo, and whether or not the ectoderm develops into skin is dependent on Wnt signaling (Fuchs, 2007). In the absence of FGF signaling, ectodermal cells express bone morphogenetic protein (BMP) and develop into epidermis (Tchieu et al., 2017). Additionally, in the absence of Wnt signaling, FGF signaling is activated, BMP expression is weakened, and ectodermal cells can also adopt a neural crest fate (**Figure 1A**) (Ji et al., 2019; Girgin et al., 2021). By precisely modulating the activities of the FGF, BMP, Wnt, and transforming growth factor β (TGF-β) pathways using different substrates and a chemically defined medium, reproducible derivations of neuroectoderm, neural crest, cranial placode, and non-neural ectoderm can be achieved (Tchieu et al., 2017) (**Figure 1A**).

During early skin development, within several days, cell divisions become first oblique, and then more perpendicular, leading to asymmetric fates, as well as the differentiation and stratification of the epidermis (Matsumura et al., 2021). When morphogenesis is complete, progenitor cells of the epidermis and appendages maintain their contact with the basement membrane and express markers that identify them as keratinocytes (Green et al., 2003).

To conclude, skin formation is a multistep process, involving the growth of the dermis and epidermis, as well as skin appendages. Skin appendages such as hair placodes form from the congregation of Wnt^{high} cells in the basal layer (Gonzales and Fuchs, 2017). These cells begin to divide perpendicular to the basement membrane, leading to asymmetrically fated daughters. Wnt^{high} cells produce sonic hedgehog (Shh), but only neighboring cells can respond to this signal. Shh signaling induces the underlying mesenchyme to organize into a dermal condensate and simultaneously produce BMP inhibitors. Shh signaling also prompts the covering daughter cells that lose contact with the basement membrane to dampen Wnt signaling (Wnt^{low}) and divide symmetrically. These Wnt^{low} daughters will generate the outer root sheath, which can develop a niche (bulges) of stem cells, while the Wnt^{high} daughters may generate the inner root sheath or hair shaft (Hsu and Fuchs, 2012; Gonzales and Fuchs, 2017).

Knowledge about the early stages of human melanocyte and skin appendage fate specification is limited to basic histological studies (Xie et al., 2016; Wang et al., 2020). Lineage tracing using single-cell sequencing has identified important differences in regenerative and developmental strategies among skin stem cells (e.g., bulge stem cells) or normal cells (e.g., adipocytes, melanocytes) (Guerrero-Juarez et al., 2019; Kim et al., 2020; Solé-Boldo et al., 2020). Epithelial and mesenchymal structures form from several types of fate-restricted progenitors. The skin appendage, a functional mini organ, develops in a dynamic environment influenced by a variety of molecular signals (Lim and Nusse, 2013).

Different signaling patterns at different stages of development ensure the growth and progression of the corium and its derivatives (Fuchs, 2007; Hsu and Fuchs, 2012). Every step of epidermal development is closely related to the development of the dermis and the substratum, while differences in the dermis can lead to regional heterogeneity of the overlying epidermis (Zhu et al., 20141004). A variety of cells interact during skin formation (**Figure 1A**).

SOURCES OF SKIN CELLS AND THE GENERATION OF SKIN ORGANOIDS

The management of skin defects, both local and full thickness, remains a considerable clinical challenge. The current treatment option consists mainly of medium-thickness skin grafts, but this is constrained by donor site limitations (Meuli et al., 2019). Cell transplantation is a novel treatment that involves isolating cells from small skin biopsies and seeding them in collagen hydrogels (Meuli et al., 2019; Shpichka et al., 2019). While new skin substitutes provide safe coverage of skin defects, traditional skin tissue engineering methods reduce the complexity of skin tissue to two main parts (epidermis and dermis), which does not allow the function of the patient's skin to be reproduced (Weng et al., 2020). Meanwhile, keratinocyte culture *in vitro* is time-consuming and labor-intensive, and the generated skin substitutes lack appendages (Tjin et al., 2020; Weng et al., 2020).

Stem cells are the foundation of all mammalian life. The establishment of 3D culture systems (or organoids, where an organ is in a dish) is revolutionizing the way human biology is studied (Kaluthantrige Don and Huch, 2021). Organoids are generated *via* the 3D culture of isolated tissue progenitor cells or PSCs and need an appropriate environmental background for development (Lei et al., 2017).

Stem cells are the main source of cells for the construction of organoids (Yin et al., 2016). There are two main types of stem cells. One is adult stem cells (ASCs), with each organ having its own specialized ASCs, which usually reside in "niches" that

TABLE 1 | Overview of current skin organoid methods. A summary of important parameters in skin organoids, including types of stem cells, species, skin organoid identity, source of starting materials, intrinsic patterning or extrinsic signaling molecules, extracellular scaffold and/or bioreactor, whether to use high-throughput sequencing and special considerations for skin modeling. ASCs, Adult stem cells; BMP4, Bone Morphogenetic Protein 4; CDB, Clustering-dependent embryoid body; DP, Dermal papilla; EBs, Embryonic bodies; EEM, Epidermal expansion medium; PSCs, Pluripotent stem cells; RA, Retinoic Acid; TGF-βi, TGF-β signaling inhibitor; 3D, three-dimensional;

Types of stem cells	Species	Organoid identity	Starting cells	Intrinsic patterning or extrinsic signaling molecules	Extracellular scaffold and/or bioreactor	High-throughput analysis	Special considerations for skin modeling	References
ASCs	Mouse	Murine epidermal organoid	Murine epidermal stem cells	EEM, Noggin, R-spondin 1, Forskolin, and FGF1	Basement membrane extract (Cultrex)	Whole mRNA transcriptome analysis	Serving as a model to study adult epidermal homeostasis and disease *in vitro*	Boonekamp et al. (2019)
	Human	Organoid model of dermal papilla of human hair follicle	DP fibroblasts	Contextual human hair induction assay using dermal papillae implanted into human skin	Cultured as 3D dermal papilla fibroblast spheroids	Affymetrix microarray analysis	When grown as spheroids, human dermal papilla cells induce *de novo* hair follicles in skin	Higgins et al. (2013)
	Mouse	Sweat gland organoid	Sweat gland cells	EGF, bFGF, EDA, TGF-βi, FSK, BMP4	Matrigel tailored for sweat glands formed epithelial organoids	NA	A new strategy for regenerating functional sweat gland-like structures	Diao et al. (2019)
	Mouse	3D skin organoid	Newborn mouse skin cells	PKC inhibition IGF2, VEGF, Wnt3a, Wnt10b, and MMP14	Epidermal cells and dermal cells in one droplet	Whole transcriptome RNA-seq	Functional perturbation with inhibitors of the key molecules at each phase-transition stage can suppress or accelerate the phase-transition process to form skin	Lei et al. (2017)
PSCs	Human	Induced pluripotent stem cell-derived skin organoid	iPSC-derived fibroblasts iPSC-derived keratinocytes	RA, BMP4, and EGF.	Embryonic bodies Coating with type I collagen for fibroblasts Coating with type IV collagen Transwell plate	NA	Using CBMC-iPSCs as a novel tool for *in vitro* and *in vivo* dermatological research	Kim et al. (2018), Kim and Ju (2019)
	Mouse	Integumentary organ system (IOS)	iPSCs	A mitomycin C–treated SNLP feeder layer Wnt10b a novel *in vivo* transplantation model	CDB	NA	Establishing a novel non-animal assay system, including appendages such as hair follicles and sebaceous glands, for cosmetics and quasi-drug testing	Takagi et al. (2016), Toyoshima et al. (2019)
	Mouse	PSC-derived skin organoid	ESCs iPSCs	TGF-β inhibitor BMP4 FGF-2 BMP inhibitor	Matrigel	NA	Studying minimal cellular and microenvironmental requirements for hair follicle induction, evaluating hair follicle growth-promoting/ inhibitory drugs, or modeling skin diseases	Lee et al. (2018)
	Human	Hair-bearing human skin organoid	ESCs iPSCs	BMP4 bFGF TGFβ inhibitor BMP inhibitor	Matrigel Orbital shaker	Single-cell RNA-seq to gain insight into the cell lineages arising in skin organoids	Establishing a model for investigating the cellular dynamics of developing human skin and its appendages	Lee et al. (2020), Lee and Koehler (2021)

provide distinct microenvironments for stem cell maintenance and function (Mahmoudi and Brunet, 2012). The skin contains a variety of ASCs, including epidermal, hair follicle, dermal mesenchymal (MSCs), melanocyte, endothelial, and hematopoietic stem cells, among others (**Figure 1B**) (Hsu et al., 2014). These ASCs can replace tissue lost through daily attrition, trauma, or disease. Numerous studies have reported on ASC-derived skin organoids, such as those related to the epidermis, sweat glands, and hair follicles (Higgins et al., 2013; Boonekamp et al., 2019; Diao et al., 2019). In addition, the other type is PSCs, including ESCs and iPSCs (Takahashi and Yamanaka, 2006; Mora et al., 2017). Recent studies have shown that iPSCs can be well controlled and optimized to generate embryoid bodies and then differentiate into

fibroblasts and keratinocytes under specific condition in the early stage (Kim et al., 2018). However, the derivation of iPSCs by ectopic expression of core pluripotency factors adds the concerns for PSC tumorigenesis (Lee et al., 2013). Cord blood mononuclear cells (CBMCs) have also become a source of replacement cells, and CBMC-derived iPSCs have been differentiated into keratinocytes and fibroblasts, as well as into 3D skin organoids. The derived keratinocytes and fibroblasts have characteristics similar to those of the original cell lines (Kim and Ju, 2019).

Recently, Lei et al. demonstrated *in vitro* skin organoids to form skin with hairs from dissociated cells (Lei et al., 2017), while Lee et al. reported a skin organoid culture system that produces complex skin from human PSCs (iPS/ES) (**Table 1**) (Lee et al., 2020). Within spherical cell aggregates, non-neuroectodermal and neural crest cells were induced by the stepwise regulation of the TGF-β and FGF signaling pathways. During the 45-months incubation period, the existing skin organoid had developed stratified epidermis, fat-rich dermis, and pigmented hair follicles with sebaceous glands. A network of sensory neurons and Schwann cells that formed neuro-like bundles could also be seen. Additionally, when transplanted into nude mice, these organoids formed flat, hairy, and almost completely natural skin.

Skin organoids can produce skin appendages, especially hair follicles, which grow radially and receive innervation from sensory neurons (Lee et al., 2020). Additionally, the hair follicles of skin organoids can reach a level of maturity that is roughly equivalent to second-trimester fetal hair and exhibit the cellular components required for further maturation. However, long-term culture is needed to determine whether xenografted skin organoid-derived follicles can convert to a terminal hair fate or maintain a growth cycle *in vivo* (Lee et al., 2020).

Capillarization is very important for the development of skin organoids. Recent studies showed that human brain organoids transplanted into the adult mouse brain developed a vasculature and incorporated into local tissues [e.g., blood–brain barrier (BBB)] (Mansour et al., 2018; Grebenyuk and Ranga, 2019). Ebner-Peking et al. reported the 3D self-assembly of adult and induced pluripotent stem cell (iPSC)-derived fibroblasts, keratinocytes, and endothelial progenitors into a novel type of floating spheroid skin organoid. Multi-cell transplant self-organization facilitates the development of skin regeneration strategies using cell suspension transplantation in combination with human platelet factors (Ebner-Peking et al., 2021). We deem that these novel platforms could be leveraged to seed skin organoids with pericytes and endothelial cells, thereby facilitating the investigation of the role of angiogenesis in skin maturation or to derive vascularized skin grafts in the future.

Single-cell RNA sequencing analysis of two strains of PSC-derived skin organoids further showed that they came from anatomically different groups of ectodermal cells. Nevertheless, no immune cells, such as Langerhans cells (LCs), were detected in these skin organoids. It is possible to improve our understanding of different cell types and states, as well as their specific pathways, by mining large datasets of single-cell gene expression profiles in this research (Lee et al., 2018; Lee et al., 2020; Lee and Koehler, 2021). A recent single-cell analysis identified new subpopulations of basal cells located at the top or bottom of the reticular dermis and reported that cell fate specification is determined by the expression of lineage-specific transcription factors (Matsumura et al., 2021). Direct reprogramming techniques can convert adult cells from one type to another. The technology of fused assembloids is ripe to build different brain regions in cerebral organoids and this scheme is expected to bring new hope for reasonable source of functional skin (**Figure 1B**) (Soufi et al., 2012; Iacovides et al., 2016; Qian et al., 2019).

One goal of generating skin organoids is to reconstruct fully functional skin from PSCs or ASCs *in vitro*. Research has shown that dissociated human fetal skin can reconstitute hair-bearing skin in a nude mouse model because of the specific microenvironment (Yang et al., 2014). Studies on hair follicle generation from hPSC-derived cells have relied on complex bioengineering approaches or chimeric methods using human/mouse epidermal/skin cells xenografting onto nude mice to promote skin cell development and folliculogenesis (Lee et al., 2018; Kageyama et al., 2021). The ability to induce substantial vascularization and morphological maturation in skin organoids is conducive to the maturation of skin cells to obtain an adult-like skin (Ebner-Peking et al., 2021). Skin organoids represent a platform for gaining a more in-depth understanding of skin development and formation. Nevertheless, a substantial amount of work must be undertaken to improve the skin organoid system to allow the wide-spread adoption of this technology in this field.

THE APPLICATIONS OF MULTIFUNCTIONAL SKIN ORGANOIDS

Currently available skin constructs are mainly skin grafts, including cultured epidermal autografts, that can be cultured from skin-derived stem cells. They can effectively support skin wound healing and are also a valuable supplement to traditional skin transplantation methods. In addition, combining biomaterials can enhance the stability and functionality of skin grafts. Nevertheless, the high manufacturing costs and lack of skin appendages (e.g., glands, hair) currently limit the therapeutic application of these products (Brockmann et al., 2018; Ebner-Peking et al., 2021). Skin organoids may provide solutions of therapeutic value and clinical applicability of skin grafts and can also be used to identify new regenerative drugs, or for gene therapy. These organoids are similar to primary skin tissues in terms of composition and structure and are easily manipulated and cryopreserved (Boonekamp et al., 2019; Diao et al., 2019). Notably, more complex biotechnologies are currently available, ranging from organoids to multi-physiological systems or organs-on-chips. Some of these models perform at least as well as animal-based models (Park et al., 2019; Horejs, 2021). The overexpression of FOXC1 is sufficient to induce the reprogramming of epidermal cells to functional sweat gland-like cells, which is beneficial for wound healing and sweat gland regeneration (Yao et al., 2019). Furthermore, recent studies have reported the use of cutaneous organ models to investigate the occurrence, development, and resistance to treatment of skin tumors, such as basal cell carcinoma, squamous cell carcinoma, melanoma, and Merkel cell carcinoma (Rebecca et al., 2020). Skin

organoids could similarly be used for disease modeling applications and drug screening (Yang et al., 2020; Han et al., 2021). Alternatively, patient-sourced or gene-edited donor hiPSCs could be used to simulate inherited skin diseases. For example, genetically modified autologous epidermal cells could provide a lasting treatment for vesicular skin diseases. Several studies have shown that it is possible to correct epidermolysis bullosa, a genetic skin disorder, by CRISPR/Cas9-based targeted genome editing (Itoh et al., 2011; Hirsch et al., 2017; Jacków et al., 2019). hiPSCs can become ideal sources of cells for generating skin organoids. Thus, it is evident that being able to recapitulate skin tissues in a dish has considerably broadened the scope of skin organoid applications, including the study of human skin development, disease modeling, drug testing, investigating skin barrier biology, the development of cell/gene therapies, and toxicological assessments (Niehues et al., 2018; Lee and Koehler, 2021) (**Figure 1B**).

hiPSC-derived skin organoids can be instantly generated from available spheroids or assembloids (Vogt, 2021) (**Figure 1B**), allowing their application for high-content screening and drug testing. The push for non-animal testing as laid down in European legislation, particularly regarding European cosmetics regulation, has brought animal-free regulatory testing one step closer. Skin models, such as skin organoids containing a variety of skin structures, could deliver the accuracy required for increased applicability in predicting toxicological effects on the skin (Niehues et al., 2018; Riebeling et al., 2018). Skin organoids might provide novel options for identifying promising targets for future research on the pleiotropic effects of devastating skin injuries sustained in chemical warfare (e.g., resulting from exposure to sulfur mustard) (Rose et al., 2018). Skin organoids generated through the self-organizational abilities of stem/progenitor cells will aid in the development of new strategies targeting skin regeneration and wound healing (Lee et al., 2020).

The EU H2020 HCA Organoid project has now been launched, aiming to provide a practically useful and readily extensible initial version of the Organoid Cell Atlas within 2 years. The Organoid Cell Atlas represents a basic biology and biomedical application that will enable researchers to functionally dissect and systematically perturb human biological systems, including the skin (Bock et al., 2021). Hence, skin organoids may provide an unprecedented framework to study the molecular and cellular mechanisms of skin biology, including skin diseases, while at the same time opening numerous possibilities for identifying new patient-specific therapeutic approaches.

LIMITATIONS

Although many challenges have been surmounted, many bottlenecks remain to be overcome, and there is still a large gap between the current state of skin organoid technology and the reality of how these organoids develop and function in the body. First, as the body's first line of defense, the skin is equipped with an impressive array of immune cells, such as LCs. However, it is not enough to simulate the structure of skin, as excluding connective tissues, blood vessels, and immune cells does not allow to recapitulate the physiological environment of normal tissues and organs (Lee et al., 2018; Lee et al., 2020).

Secondly, potential sources of skin cells (e.g., keratinocytes) are scarce, and culturing skin cells *in vitro* is difficult with current technology (Kim et al., 2018). Cell reprogramming techniques, which can help to regenerate skin cells, are still inefficient *in vitro* (Chen et al., 2014), and the cells are prone to aging (Mahmoudi and Brunet, 2012). Thus, skin organoid culture systems need to be optimized to allow for their clinical application. Systems for the *in vitro* culture of potential cells should also continue to be optimized, while more effective reprogramming techniques, such as small molecule-induced chemical reprogramming or genetic reprogramming of genes delivered by biomaterials, should be identified. The 3D regeneration of skin organoids requires better external safety, including controllability, and internal stability, as well as the non-toxicity of the biological materials used. Additionally, whether the function of regenerated skin organoids is normal and how long they could be maintained in the body also need further investigation. Other problems that need to be overcome include the heterogeneity among cell lines and differences among batches.

SUMMARY AND FUTURE PERSPECTIVES

To conclude, stem and progenitor cells have great potential for future cell transplantation applications and may prove to be a sustainable alternative source of skin cells. Although the production of PSCs is time-consuming and laborious, HLA homozygous iPS cells have been proposed as an alternative way to solve this problem, in that a small number of cells can be used in large numbers of patients (Okita et al., 2011; Xu et al., 2019). In addition, 3D bioprinting technology enables a much more precise simulation of biophysical properties, including organoid size, cell number, and conformation, and modification of the latter can substantially increase starting cell numbers (Lawlor et al., 2021). Although many problems and obstacles remain, patient-derived organoids should further improve our understanding of disease and heterogeneity in patients, which may lead to personalized therapies for the treatment of a variety of diseases (Dutta et al., 2017).

The generation of skin organoids represents a new hope for skin regeneration and is expected to provide a novel scheme for the diagnosis and treatment of skin diseases. Skin organoids can be used to investigate physiological functions, such as cutaneous nerve sensation and microbiome–skin interactions, as well as for exploratory research into models of cutaneous viral–bacterial co-infections, makeup testing, and high-throughput drug screening (**Figure 1B**). Overall, we believe that skin organoids represent a huge breakthrough that should facilitate the advancement of both basic and clinical research.

AUTHOR CONTRIBUTIONS

This review paper was written by HS, revised by Y-XZ, and guided by Y-ML.

FUNDING

This work was supported by the National Natural Science Foundation of the People's Republic of China (Grant Nos 81573053).

ACKNOWLEDGMENTS

The authors would like to thank Yun-Wen Zheng and Li-Ping Liu for discussions about the idea, Meng-Xue Xu for proofreading the draft.

REFERENCES

Bock, C., Boutros, M., Boutros, M., Camp, J. G., Clarke, L., Clevers, H., et al. (2021). The Organoid Cell Atlas. *Nat. Biotechnol.* 39 (1), 13–17. Epub 2021/01/02PubMed PMID: 33384458; PubMed Central PMCID: PMCPMC7801253. doi:10.1038/s41587-020-00762-x

Boonekamp, K. E., Kretzschmar, K., Wiener, D. J., Asra, P., Derakhshan, S., Puschhof, J., et al. (2019). Long-term Expansion and Differentiation of Adult Murine Epidermal Stem Cells in 3D Organoid Cultures. *Proc. Natl. Acad. Sci. USA* 116 (29), 14630–14638. Epub 2019/06/30PubMed PMID: 31253707; PubMed Central PMCID: PMCPMC6642409. doi:10.1073/pnas.1715272116

Brockmann, I., Ehrenpfordt, J., Sturmheit, T., Brandenburger, M., Kruse, C., Zille, M., et al. (2018). Skin-Derived Stem Cells for Wound Treatment Using Cultured Epidermal Autografts: Clinical Applications and Challenges. *Stem Cell Int.* 2018, 1–9. Epub 2018/05/17PubMed PMID: 29765411; PubMed Central PMCID: PMCPMC5889868. doi:10.1155/2018/4623615

Chen, Y. E., Fischbach, M. A., and Belkaid, Y. (2018). Skin Microbiota-Host Interactions. *Nature* 553 (7689), 427–436. Epub 2018/01/25PubMed PMID: 29364286; PubMed Central PMCID: PMCPMC6075667. doi:10.1038/nature25177

Chen, Y., Mistry, D. S., and Sen, G. L. (2014). Highly Rapid and Efficient Conversion of Human Fibroblasts to Keratinocyte-like Cells. *J. Invest. Dermatol.* 134 (2), 335–344. Epub 2013/08/08PubMed PMID: 23921950; PubMed Central PMCID: PMCPMC3875612. doi:10.1038/jid.2013.327

Clevers, H., Loh, K. M., and Nusse, R. (2014). An Integral Program for Tissue Renewal and Regeneration: Wnt Signaling and Stem Cell Control. *Science*, 346(6205). New York, NY, 1248012. Epub 2014/10/04PubMed PMID: 25278615. doi:10.1126/science.1248012

Diao, J., Liu, J., Wang, S., Chang, M., Wang, X., Guo, B., et al. (2019). Sweat Gland Organoids Contribute to Cutaneous Wound Healing and Sweat Gland Regeneration. *Cell Death Dis* 10 (3), 238. Epub 2019/03/13PubMed PMID: 30858357; PubMed Central PMCID: PMCPMC6411741. doi:10.1038/s41419-019-1485-5

Dutta, D., Heo, I., and Clevers, H. (2017). Disease Modeling in Stem Cell-Derived 3D Organoid Systems. *Trends Mol. Med.* 23 (5), 393–410. Epub 2017/03/28PubMed PMID: 28341301. doi:10.1016/j.molmed.2017.02.007

Ebner-Peking, P., Krisch, L., Wolf, M., Hochmann, S., Hoog, A., Vári, B., et al. (2021). Self-assembly of Differentiated Progenitor Cells Facilitates Spheroid Human Skin Organoid Formation and Planar Skin Regeneration. *Theranostics* 11 (17), 8430–8447. Epub 2021/08/11PubMed PMID: 34373751; PubMed Central PMCID: PMCPMC8344006. doi:10.7150/thno.59661

Fuchs, E. (2007). Scratching the Surface of Skin Development. *Nature* 445 (7130), 834–842. Epub 2007/02/23PubMed PMID: 17314969; PubMed Central PMCID: PMCPMC2405926. doi:10.1038/nature05659

Girgin, M. U., Broguiere, N., Mattolini, L., and Lutolf, M. P. (2021). Gastruloids Generated without Exogenous Wnt Activation Develop Anterior Neural Tissues. *Stem Cel. Rep.* 16, 1143–1155. Epub 2021/04/24PubMed PMID: 33891872. doi:10.1016/j.stemcr.2021.03.017

Gonzales, K. A. U., and Fuchs, E. (2017). Skin and its Regenerative Powers: An Alliance between Stem Cells and Their Niche. *Dev. Cel.* 43 (4), 387–401. Epub 2017/11/22PubMed PMID: 29161590; PubMed Central PMCID: PMCPMC5797699. doi:10.1016/j.devcel.2017.10.001

Gravitz, L. (2018). Skin. *Nature* 563 (7732), S83. Epub 2018/11/23PubMed PMID: 30464282. doi:10.1038/d41586-018-07428-4

Grebenyuk, S., and Ranga, A. (2019). Engineering Organoid Vascularization. *Front. Bioeng. Biotechnol.* 7, 39. Epub 2019/04/04PubMed PMID: 30941347; PubMed Central PMCID: PMCPMC6433749. doi:10.3389/fbioe.2019.00039

Green, H., Easley, K., and Iuchi, S. (2003). Marker Succession during the Development of Keratinocytes from Cultured Human Embryonic Stem Cells. *Proc. Natl. Acad. Sci.* 100 (26), 15625–15630. Epub 2003/12/10PubMed PMID: 14663151; PubMed Central PMCID: PMCPMC307618. doi:10.1073/pnas.0307226100

Guerrero-Juarez, C. F., Dedhia, P. H., Jin, S., Ruiz-Vega, R., Ma, D., Liu, Y., et al. (2019). Single-cell Analysis Reveals Fibroblast Heterogeneity and Myeloid-Derived Adipocyte Progenitors in Murine Skin Wounds. *Nat. Commun.* 10 (1), 650. Epub 2019/02/10PubMed PMID: 30737373; PubMed Central PMCID: PMCPMC6368572. doi:10.1038/s41467-018-08247-x

Han, Y., Duan, X., Yang, L., Nilsson-Payant, B. E., Wang, P., Duan, F., et al. (2021). Identification of SARS-CoV-2 Inhibitors Using Lung and Colonic Organoids. *Nature* 589 (7841), 270–275. Epub 2020/10/30PubMed PMID: 33116299; PubMed Central PMCID: PMCPMC8034380. doi:10.1038/s41586-020-2901-9

Higgins, C. A., Chen, J. C., Cerise, J. E., Jahoda, C. A. B., and Christiano, A. M. (2013). Microenvironmental Reprogramming by Three-Dimensional Culture Enables Dermal Papilla Cells to Induce De Novo Human Hair-Follicle Growth. *Proc. Natl. Acad. Sci.* 110 (49), 19679–19688. Epub 2013/10/23PubMed PMID: 24145441; PubMed Central PMCID: PMCPMC3856847. doi:10.1073/pnas.1309970110

Hirsch, T., Rothoeft, T., Teig, N., Bauer, J. W., Pellegrini, G., De Rosa, L., et al. (2017). Regeneration of the Entire Human Epidermis Using Transgenic Stem Cells. *Nature* 551 (7680), 327–332. Epub 2017/11/17PubMed PMID: 29144448; PubMed Central PMCID: PMCPMC6283270. doi:10.1038/nature24487

Horejs, C. (2021). Organ Chips, Organoids and the Animal Testing Conundrum. *Nat. Rev. Mater.* 6, 372–373. PubMed PMID: 33936776; PubMed Central PMCID: PMCPMC8072732. Epub 2021/05/04. doi:10.1038/s41578-021-00313-z

Hsu, Y.-C., and Fuchs, E. (2012). A Family Business: Stem Cell Progeny Join the Niche to Regulate Homeostasis. *Nat. Rev. Mol. Cel Biol* 13 (2), 103–114. Epub 2012/01/24PubMed PMID: 22266760; PubMed Central PMCID: PMCPMC3280338. doi:10.1038/nrm3272

Hsu, Y.-C., Li, L., and Fuchs, E. (2014). Emerging Interactions between Skin Stem Cells and Their Niches. *Nat. Med.* 20 (8), 847–856. Epub 2014/08/08PubMed PMID: 25100530; PubMed Central PMCID: PMCPMC4358898. doi:10.1038/nm.3643

Iacovides, D., Rizki, G., Lapathitis, G., and Strati, K. (2016). Direct Conversion of Mouse Embryonic Fibroblasts into Functional Keratinocytes through Transient Expression of Pluripotency-Related Genes. *Stem Cel Res Ther* 7 (1), 98. Epub 2016/07/31PubMed PMID: 27473056; PubMed Central PMCID: PMCPMC4966867. doi:10.1186/s13287-016-0357-5

Ito, M., Yang, Z., Andl, T., Cui, C., Kim, N., Millar, S. E., et al. (2007). Wnt-dependent De Novo Hair Follicle Regeneration in Adult Mouse Skin after Wounding. *Nature* 447 (7142), 316–320. Epub 2007/05/18PubMed PMID: 17507982. doi:10.1038/nature05766

Itoh, M., Kiuru, M., Cairo, M. S., and Christiano, A. M. (2011). Generation of Keratinocytes from normal and Recessive Dystrophic Epidermolysis Bullosa-Induced Pluripotent Stem Cells. *Proc. Natl. Acad. Sci.* 108 (21), 8797–8802. Epub 2011/05/11PubMed PMID: 21555586; PubMed Central PMCID: PMCPMC3102348. doi:10.1073/pnas.1100332108

Jacków, J., Guo, Z., Hansen, C., Abaci, H. E., Doucet, Y. S., Shin, J. U., et al. (2019). CRISPR/Cas9-based Targeted Genome Editing for Correction of Recessive Dystrophic Epidermolysis Bullosa Using iPS Cells. *Proc. Natl. Acad. Sci. USA* 116 (52), 26846–26852. Epub 2019/12/11PubMed PMID: 31818947; PubMed Central PMCID: PMCPMC6936361. doi:10.1073/pnas.1907081116

Ji, Y., Hao, H., Reynolds, K., McMahon, M., and Zhou, C. J. (2019). Wnt Signaling in Neural Crest Ontogenesis and Oncogenesis. *Cells* 8 (10), 1173. Epub 2019/10/02, PubMed PMID: 31569501; PubMed Central PMCID: PMCPMC6829301. doi:10.3390/cells8101173

Kageyama, T., Chun, Y.-S., and Fukuda, J. (2021). Hair Follicle Germs Containing Vascular Endothelial Cells for Hair Regenerative Medicine. *Sci. Rep.* 11 (1), 624. Epub 2021/01/14PubMed PMID: 33436760; PubMed Central PMCID: PMCPMC7804392. doi:10.1038/s41598-020-79722-z

Kaluthantrige Don, F., and Huch, M. (2021). Organoids, where We Stand and where We Go. *Trends Mol. Med.* 27, 416–418. doi:10.1016/j.molmed.2021.03.001

Kim, D., Chung, K. B., and Kim, T.-G. (2020). Application of Single-Cell RNA Sequencing on Human Skin: Technical Evolution and Challenges. *J. Dermatol. Sci.* 99 (2), 74–81. Epub 2020/07/01PubMed PMID: 32593488. doi:10.1016/j.jdermsci.2020.06.002

Kim, Y., and Ju, J. H. (2019). Generation of 3D Skin Organoid from Cord Blood-Derived Induced Pluripotent Stem Cells. *JoVE* (146). Epub 2019/05/07PubMed PMID: 31058887. doi:10.3791/59297

Kim, Y., Park, N., Rim, Y. A., Nam, Y., Jung, H., Lee, K., et al. (2018). Establishment of a Complex Skin Structure via Layered Co-culture of Keratinocytes and Fibroblasts Derived from Induced Pluripotent Stem Cells. *Stem Cel Res Ther* 9 (1), 217. Epub 2018/08/15PubMed PMID: 30103800; PubMed Central PMCID: PMCPMC6090613. doi:10.1186/s13287-018-0958-2

Lane, S. W., Williams, D. A., and Watt, F. M. (2014). Modulating the Stem Cell Niche for Tissue Regeneration. *Nat. Biotechnol.* 32 (8), 795–803. Epub 2014/08/06PubMed PMID: 25093887; PubMed Central PMCID: PMCPMC4422171. doi:10.1038/nbt.2978

Lawlor, K. T., Vanslambrouck, J. M., Higgins, J. W., Chambon, A., Bishard, K., Arndt, D., et al. (2021). Cellular Extrusion Bioprinting Improves Kidney Organoid Reproducibility and Conformation. *Nat. Mater.* 20 (2), 260–271. Epub 2020/11/25PubMed PMID: 33230326; PubMed Central PMCID: PMCPMC7855371. doi:10.1038/s41563-020-00853-9

Lee, A. S., Tang, C., Rao, M. S., Weissman, I. L., and Wu, J. C. (2013). Tumorigenicity as a Clinical Hurdle for Pluripotent Stem Cell Therapies. *Nat. Med.* 19 (8), 998–1004. Epub 2013/08/08PubMed PMID: 23921754; PubMed Central PMCID: PMCPMC3967018. doi:10.1038/nm.3267

Lee, J., Böscke, R., Tang, P.-C., Hartman, B. H., Heller, S., and Koehler, K. R. (2018). Hair Follicle Development in Mouse Pluripotent Stem Cell-Derived Skin Organoids. *Cel Rep.* 22 (1), 242–254. Epub 2018/01/04PubMed PMID: 29298425; PubMed Central PMCID: PMCPMC5806130. doi:10.1016/j.celrep.2017.12.007

Lee, J., and Koehler, K. R. (2021). Skin Organoids: A New Human Model for Developmental and Translational Research. *Exp. Dermatol.* 30 (4), 613–620. Epub 2021/01/29PubMed PMID: 33507537. doi:10.1111/exd.14292

Lee, J., Rabbani, C. C., Gao, H., Steinhart, M. R., Woodruff, B. M., Pflum, Z. E., et al. (2020). Hair-bearing Human Skin Generated Entirely from Pluripotent Stem Cells. *Nature* 582 (7812), 399–404. Epub 2020/06/05PubMed PMID: 32494013; PubMed Central PMCID: PMCPMC7593871. doi:10.1038/s41586-020-2352-3

Lei, M., Schumacher, L. J., Lai, Y.-C., Juan, W.-T., Yeh, C.-Y., Wu, P., et al. (2017). Self-organization Process in Newborn Skin Organoid Formation Inspires Strategy to Restore Hair Regeneration of Adult Cells. *Proc. Natl. Acad. Sci. USA* 114 (34), E7101–E7110. Epub 2017/08/12PubMed PMID: 28798065; PubMed Central PMCID: PMCPMC5576784. doi:10.1073/pnas.1700475114

Lim, X., and Nusse, R. (2013). Wnt Signaling in Skin Development, Homeostasis, and Disease. *Cold Spring Harbor Perspect. Biol.* 5 (2), a008029. Epub 2012/12/05PubMed PMID: 23209129; PubMed Central PMCID: PMCPMC3552514. doi:10.1101/cshperspect.a008029

Mahmoudi, S., and Brunet, A. (2012). Aging and Reprogramming: a Two-Way Street. *Curr. Opin. Cel. Biol.* 24 (6), 744–756. Epub 2012/11/14PubMed PMID: 23146768; PubMed Central PMCID: PMCPMC3540161. doi:10.1016/j.ceb.2012.10.004

Mansour, A. A., Gonçalves, J. T., Bloyd, C. W., Li, H., Fernandes, S., Quang, D., et al. (2018). An *In Vivo* Model of Functional and Vascularized Human Brain Organoids. *Nat. Biotechnol.* 36 (5), 432–441. Epub 2018/04/17PubMed PMID: 29658944; PubMed Central PMCID: PMCPMC6331203. doi:10.1038/nbt.4127

Matsumura, H., Liu, N., Nanba, D., Ichinose, S., Takada, A., Kurata, S., et al. (2021). Distinct Types of Stem Cell Divisions Determine Organ Regeneration and Aging in Hair Follicles. *Nat. Aging* 1 (2), 190–204. doi:10.1038/s43587-021-00033-7

Meuli, M., Hartmann-Fritsch, F., Hüging, M., Marino, D., Saglini, M., Hynes, S., et al. (2019). A Cultured Autologous Dermo-Epidermal Skin Substitute for Full-Thickness Skin Defects. *Plast. Reconstr. Surg.* 144 (1), 188–198. Epub 2019/06/28PubMed PMID: 31246829. doi:10.1097/prs.0000000000005746

Mora, C., Serzanti, M., Consiglio, A., Memo, M., and Dell'Era, P. (2017). Clinical Potentials of Human Pluripotent Stem Cells. *Cell Biol Toxicol* 33 (4), 351–360. Epub 2017/02/09PubMed PMID: 28176010. doi:10.1007/s10565-017-9384-y

Niehues, H., Bouwstra, J. A., El Ghalbzouri, A., Brandner, J. M., Zeeuwen, P. L. J. M., and van den Bogaard, E. H. (2018). 3D Skin Models for 3R Research: The Potential of 3D Reconstructed Skin Models to Study Skin Barrier Function. *Exp. Dermatol.* 27 (5), 501–511. Epub 2018/03/09PubMed PMID: 29518287. doi:10.1111/exd.13531

Okita, K., Matsumura, Y., Sato, Y., Okada, A., Morizane, A., Okamoto, S., et al. (2011). A More Efficient Method to Generate Integration-free Human iPS Cells. *Nat. Methods* 8 (5), 409–412. Epub 2011/04/05PubMed PMID: 21460823. doi:10.1038/nmeth.1591

Park, S. E., Georgescu, A., and Huh, D. (2019). Organoids-on-a-chip. *Science*, 364(6444). New York, NY, 960–965. Epub 2019/06/07PubMed PMID: 31171693; PubMed Central PMCID: PMCPMC7764943. doi:10.1126/science.aaw7894

Qian, X., Song, H., and Ming, G.-l. (2019). Brain Organoids: Advances, Applications and Challenges. *Development*, 146(8). Cambridge, England. Epub 2019/04/18PubMed PMID: 30992274; PubMed Central PMCID: PMCPMC6503989. doi:10.1242/dev.166074

Quarto, N., Wan, D. C., Kwan, M. D., Panetta, N. J., Li, S., and Longaker, M. T. (2010). Origin Matters: Differences in Embryonic Tissue Origin and Wnt Signaling Determine the Osteogenic Potential and Healing Capacity of Frontal and Parietal Calvarial Bones. *J. Bone Mineral Res.* 25 (7), 091123192917092–42. Epub 2009/11/26PubMed PMID: 19929441; PubMed Central PMCID: PMCPMC3154006. doi:10.1359/jbmr.091116

Rebecca, V. W., Somasundaram, R., and Herlyn, M. (2020). Pre-clinical Modeling of Cutaneous Melanoma. *Nat. Commun.* 11 (1), 2858. Epub 2020/06/07PubMed PMID: 32504051; PubMed Central PMCID: PMCPMC7275051. doi:10.1038/s41467-020-15546-9

Riebeling, C., Luch, A., and Tralau, T. (2018). Skin Toxicology and 3Rs-Current Challenges for Public Health protection. *Exp. Dermatol.* 27 (5), 526–536. Epub 2018/03/27PubMed PMID: 29575089. doi:10.1111/exd.13536

Rose, D., Schmidt, A., Brandenburger, M., Sturmheit, T., Zille, M., and Boltze, J. (2018). Sulfur Mustard Skin Lesions: A Systematic Review on Pathomechanisms, Treatment Options and Future Research Directions. *Toxicol. Lett.* 293, 82–90. Epub 2017/12/06PubMed PMID: 29203275. doi:10.1016/j.toxlet.2017.11.039

Rossi, G., Manfrin, A., and Lutolf, M. P. (2018). Progress and Potential in Organoid Research. *Nat. Rev. Genet.* 19 (11), 671–687. Epub 2018/09/20PubMed PMID: 30228295. doi:10.1038/s41576-018-0051-9

Shi, Y., Inoue, H., Wu, J. C., and Yamanaka, S. (2017). Induced Pluripotent Stem Cell Technology: a Decade of Progress. *Nat. Rev. Drug Discov.* 16 (2), 115–130. Epub 2016/12/17PubMed PMID: 27980341; PubMed Central PMCID: PMCPMC6416143. doi:10.1038/nrd.2016.245

Shpichka, A., Butnaru, D., Bezrukov, E. A., Sukhanov, R. B., Atala, A., Burdukovskii, V., et al. (2019). Skin Tissue Regeneration for Burn Injury. *Stem Cel Res Ther* 10 (1), 94. Epub 2019/03/17PubMed PMID: 30876456; PubMed Central PMCID: PMCPMC6419807. doi:10.1186/s13287-019-1203-3

Siebel, C., and Lendahl, U. (2017). Notch Signaling in Development, Tissue Homeostasis, and Disease. *Physiol. Rev.* 97 (4), 1235–1294. Epub 2017/08/11PubMed PMID: 28794168. doi:10.1152/physrev.00005.2017

Solé-Boldo, L., Raddatz, G., Schütz, S., Mallm, J.-P., Rippe, K., Lonsdorf, A. S., et al. (2020). Single-cell Transcriptomes of the Human Skin Reveal Age-Related Loss of Fibroblast Priming. *Commun. Biol.* 3 (1), 188. Epub 2020/04/25PubMed PMID: 32327715; PubMed Central PMCID: PMCPMC7181753 financial interests: F.L. received consultation fees from Beiersdorf AG. The other authors have no competing financial interests. doi:10.1038/s42003-020-0922-4

Soufi, A., Donahue, G., and Zaret, K. S. (2012). Facilitators and Impediments of the Pluripotency Reprogramming Factors' Initial Engagement with the Genome. *Cell* 151 (5), 994–1004. Epub 2012/11/20PubMed PMID: 23159369; PubMed Central PMCID: PMCPMC3508134. doi:10.1016/j.cell.2012.09.045

Takagi, R., Ishimaru, J., Sugawara, A., Toyoshima, K.-e., Ishida, K., Ogawa, M., et al. (2016). Bioengineering a 3D Integumentary Organ System from iPS Cells Using an *In Vivo* Transplantation Model. *Sci. Adv.* 2 (4), e1500887. Epub 2016/04/

07PubMed PMID: 27051874; PubMed Central PMCID: PMCPMC4820374. doi:10.1126/sciadv.1500887

Takahashi, K., Tanabe, K., Ohnuki, M., Narita, M., Ichisaka, T., Tomoda, K., et al. (2007). Induction of Pluripotent Stem Cells from Adult Human Fibroblasts by Defined Factors. *Cell* 131 (5), 861–872. Epub 2007/11/24PubMed PMID: 18035408. doi:10.1016/j.cell.2007.11.019

Takahashi, K., and Yamanaka, S. (2006). Induction of Pluripotent Stem Cells from Mouse Embryonic and Adult Fibroblast Cultures by Defined Factors. *Cell* 126 (4), 663–676. Epub 2006/08/15PubMed PMID: 16904174. doi:10.1016/j.cell.2006.07.024

Takeo, M., Lee, W., and Ito, M. (2015). Wound Healing and Skin Regeneration. *Cold Spring Harbor Perspect. Med.* 5 (1), a023267. Epub 2015/01/07PubMed PMID: 25561722; PubMed Central PMCID: PMCPMC4292081. doi:10.1101/cshperspect.a023267

Tchieu, J., Zimmer, B., Fattahi, F., Amin, S., Zeltner, N., Chen, S., et al. (2017). A Modular Platform for Differentiation of Human PSCs into All Major Ectodermal Lineages. *Cell stem cell* 21 (3), 399–410. e7. Epub 2017/09/09PubMed PMID: 28886367; PubMed Central PMCID: PMCPMC5737635. doi:10.1016/j.stem.2017.08.015

Tjin, M. S., Chua, A. W. C., and Tryggvason, K. (2020). Chemically Defined and Xenogeneic-free Culture Method for Human Epidermal Keratinocytes on Laminin-Based Matrices. *Nat. Protoc.* 15 (2), 694–711. Epub 2020/01/17PubMed PMID: 31942079. doi:10.1038/s41596-019-0270-3

Toyoshima, K.-e., Ogawa, M., and Tsuji, T. (2019). Regeneration of a Bioengineered 3D Integumentary Organ System from iPS Cells. *Nat. Protoc.* 14 (5), 1323–1338. Epub 2019/04/10PubMed PMID: 30962607. doi:10.1038/s41596-019-0124-z

Vogt, N. (2021). Assembloids. *Nat. Methods* 18 (1), 27. Epub 2021/01/08PubMed PMID: 33408387. doi:10.1038/s41592-020-01026-x

Wang, S., Drummond, M. L., Guerrero-Juarez, C. F., Tarapore, E., MacLean, A. L., Stabell, A. R., et al. (2020). Single Cell Transcriptomics of Human Epidermis Identifies Basal Stem Cell Transition States. *Nat. Commun.* 11 (1), 4239. Epub 2020/08/28PubMed PMID: 32843640; PubMed Central PMCID: PMCPMC7447770. doi:10.1038/s41467-020-18075-7

Weng, T., Wu, P., Zhang, W., Zheng, Y., Li, Q., Jin, R., et al. (2020). Regeneration of Skin Appendages and Nerves: Current Status and Further Challenges. *J. Transl Med.* 18 (1), 53. Epub 2020/02/06PubMed PMID: 32014004; PubMed Central PMCID: PMCPMC6996190. doi:10.1186/s12967-020-02248-5

Xie, J., Yao, B., Han, Y., Huang, S., and Fu, X. (2016). Skin Appendage-Derived Stem Cells: Cell Biology and Potential for Wound Repair. *Burns & trauma* 4, 38. Epub 2016/11/02PubMed PMID: 27800498; PubMed Central PMCID: PMCPMC5082359. doi:10.1186/s41038-016-0064-6

Xu, H., Wang, B., Ono, M., Kagita, A., Fujii, K., Sasakawa, N., et al. (2019). Targeted Disruption of HLA Genes via CRISPR-Cas9 Generates iPSCs with Enhanced Immune Compatibility. *Cell stem cell* 24 (4), 566–578. e7. Epub 2019/03/12PubMed PMID: 30853558. doi:10.1016/j.stem.2019.02.005

Yang, H., Adam, R. C., Ge, Y., Hua, Z. L., and Fuchs, E. (2017). Epithelial-Mesenchymal Micro-niches Govern Stem Cell Lineage Choices. *Cell* 169 (3), 483–496. e13. Epub 2017/04/18PubMed PMID: 28413068; PubMed Central PMCID: PMCPMC5510744. doi:10.1016/j.cell.2017.03.038

Yang, L., Han, Y., Nilsson-Payant, B. E., Gupta, V., Wang, P., Duan, X., et al. (2020). A Human Pluripotent Stem Cell-Based Platform to Study SARS-CoV-2 Tropism and Model Virus Infection in Human Cells and Organoids. *Cell stem cell* 27 (1), 125–136. e7. Epub 2020/06/25PubMed PMID: 32579880; PubMed Central PMCID: PMCPMC7303620. doi:10.1016/j.stem.2020.06.015

Yang, R., Zheng, Y., Burrows, M., Liu, S., Wei, Z., Nace, A., et al. (2014). Generation of Folliculogenic Human Epithelial Stem Cells from Induced Pluripotent Stem Cells. *Nat. Commun.* 5, 3071. Epub 2014/01/29PubMed PMID: 24468981; PubMed Central PMCID: PMCPMC4049184. doi:10.1038/ncomms4071

Yao, B., Xie, J., Liu, N., Hu, T., Song, W., Huang, S., et al. (2019). Direct Reprogramming of Epidermal Cells toward Sweat Gland-like Cells by Defined Factors. *Cel Death Dis* 10 (4), 272. Epub 2019/03/22PubMed PMID: 30894517; PubMed Central PMCID: PMCPMC6426881. doi:10.1038/s41419-019-1503-7

Yin, H., Price, F., and Rudnicki, M. A. (20132011). Satellite Cells and the Muscle Stem Cell Niche. *Physiol. Rev.* 93 (1), 23–67. Epub 2013/01/11PubMed PMID: 23303905; PubMed Central PMCID: PMCPMC4073943. doi:10.1152/physrev.0004310.1152/physrev.00043.2011

Yin, X., Mead, B. E., Safaee, H., Langer, R., Karp, J. M., and Levy, O. (2016). Engineering Stem Cell Organoids. *Cell stem cell* 18 (1), 25–38. Epub 2016/01/11PubMed PMID: 26748754; PubMed Central PMCID: PMCPMC4728053. doi:10.1016/j.stem.2015.12.005

Zhu, X.-J., Liu, Y., Dai, Z.-M., Zhang, X., Yang, X., Li, Y., et al. (201410046). BMP-FGF Signaling axis Mediates Wnt-Induced Epidermal Stratification in Developing Mammalian Skin. *Plos Genet.* 10 (10), e1004687. Epub 2014/10/21PubMed PMID: 25329657; PubMed Central PMCID: PMCPMC4199507. doi:10.1371/journal.pgen10.1371/journal.pgen.1004687

Conflict of Interest: The authors declare that the research was conducted in the absence of any commercial or financial relationships that could be construed as a potential conflict of interest.

Publisher's Note: All claims expressed in this article are solely those of the authors and do not necessarily represent those of their affiliated organizations, or those of the publisher, the editors and the reviewers. Any product that may be evaluated in this article, or claim that may be made by its manufacturer, is not guaranteed or endorsed by the publisher.

frontiers in Cell and Developmental Biology

REVIEW
published: 13 December 2021
doi: 10.3389/fcell.2021.749822

Research Progress on the Treatment of Premature Ovarian Failure Using Mesenchymal Stem Cells: A Literature Review

*Jing Wang[1], Wanru Liu[1], Dehai Yu[2], Zongxing Yang[3], Sijie Li[4] and Xiguang Sun[5]**

[1]Department of Reproductive Medicine, Department of Prenatal Diagnosis, The First Hospital of Jilin University, Changchun, China, [2]The Laboratory of Cancer Precision Medicine, The First Hospital of Jilin University, Changchun, China, [3]Department of Clinical Laboratory, The First Hospital of Jilin University, Changchun, China, [4]Department of Breast Surgery, The First Hospital of Jilin University, Changchun, China, [5]Hand Surgery Department, The First Hospital of Jilin University, Changchun, China

Premature ovarian failure (POF) has become one of the main causes of infertility in women of childbearing age and the incidence of POF is increasing year by year, seriously affecting the physical and mental health of patients and increasing the economic burden on families and society as a whole. The etiology and pathogenesis of POF are complex and not very clear at present. Currently, hormone replacement therapy is mainly used to improve the symptoms of low estrogen, but cannot fundamentally solve the fertility problem. In recent years, stem cell (SC) transplantation has become one of the research hotspots in the treatment of POF. The results from animal experiments bring hope for the recovery of ovarian function and fertility in patients with POF. In this article, we searched the published literature between 2000 and 2020 from the PubMed database (https://pubmed.ncbi.nlm.nih.gov), and summarized the preclinical research data and possible therapeutic mechanism of mesenchymal stem cells (MSCs) in the treatment of POF. Our aim is to provide useful information for understanding POF and reference for follow-up research and treatment of POF.

Keywords: mesenchymal stem cells, fertility, premature ovarian failure (POF), ovarian dysfunction, reproductive medicine

OPEN ACCESS

Edited by:
Rebecca Ryznar,
Rocky Vista University, United States

Reviewed by:
Sina Naserian,
Hôpital Paul Brousse, France
Mohammad Ghasemzadeh-H,
University of Glasgow,
United Kingdom

****Correspondence:***
Xiguang Sun
xgsun@jlu.edu.cn

Specialty section:
This article was submitted to Stem Cell Research, a section of the journal Frontiers in Cell and Developmental Biology

Received: *30 July 2021*
Accepted: *29 November 2021*
Published: *13 December 2021*

Citation:
Wang J, Liu W, Yu D, Yang Z, Li S and Sun X (2021) Research Progress on the Treatment of Premature Ovarian Failure Using Mesenchymal Stem Cells: A Literature Review. Front. Cell Dev. Biol. 9:749822. doi: 10.3389/fcell.2021.749822

INTRODUCTION

POF is a kind of ovarian dysfunction characterized by menstrual disorder, ovarian atrophy, decreased sexual life and decreased fertility in women between puberty and 40 years old, which seriously affects female reproductive health and endocrine balance and is one of the main causes of female infertility (Sheikhansari et al., 2018). Approximately 1% of women under the age of 40 suffer from premature ovarian failure (Huhtaniemi et al., 2018). Under the influence of high pressure and a fast paced life, the incidence of POF is increasing and manifesting at younger ages, and it has affected more than 10% of women in recent years (Thakur et al., 2018).

POF treatment is extremely difficult. Although assisted reproductive technology has become an effective treatment, it is not ideal, and fertility loss and low estrogen status have become a great threat to female reproductive health (Laven, 2016). POF has become one of the most severe problems threatening the reproductive health of women of normal childbearing age. Its occurrence may be related to an insufficient reserve of primordial follicular cistern, accelerated follicular atresia, changes

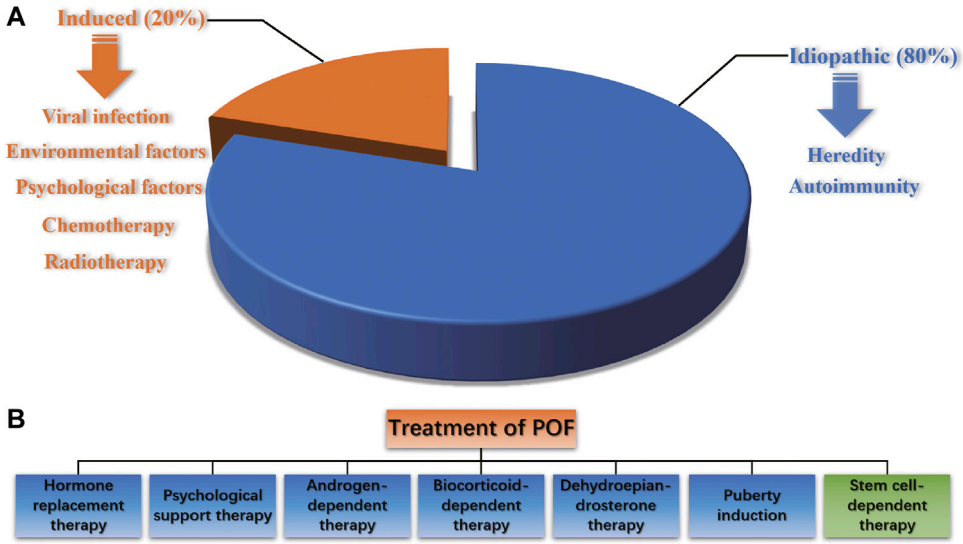

FIGURE 1 | The pathogenic factors and treatment options of POF.

of dominant follicular recruitment, follicular maturation disorders and so on (Xiang et al., 2019). In view of the limitations of conventional treatment, clinical and scientific research work has focused on improving ovarian function and restoring fertility in patients with POF. In recent years, MSC transplantation has opened up a new direction for the treatment of POF, but this is still in the stage of preclinical research (Lai et al., 2015; Sun et al., 2017; Zhang et al., 2018; Liu S. et al., 2019; Zheng et al., 2019), and there are few clinical studies so far. The mechanism by which MSCs improve ovarian function has also not been completely elucidated. At present, there is no clear and effective treatment to restore the reproductive function of ovaries. In this paper, we reviewed the preclinical research data of the treatment of POF using MSCs and the possible therapeutic mechanisms to provide a reference for follow-up research and treatment of POF.

THE CURRENT SITUATION OF POF TREATMENT

POF is a reproductive endocrine disease that occurs before the age of 40 and is characterized by increased gonadotropin levels and decreased estrogen levels, accompanied by primary or secondary amenorrhea. It is also one of the common diseases leading to female infertility. POF is a highly heterogeneous condition. Abnormal follicular development in all stages can lead to POF, and such damage to ovarian function is irreversible. The pathogenic factors of POF include heredity, autoimmunity, viral infection, iatrogenic factors, and environmental and psychological factors, and approximately eighty percent of POF cases are idiopathic (Webber et al., 2016) (**Figure 1A**). It has been reported that radiotherapy, chemotherapy and bone marrow transplantation of cancer can result in POF (Dolmans and Donnez, 2021; Imai et al., 2008). The traditional treatment of POF includes hormone replacement therapy (HRT), psychological support therapy, androgen-dependent therapy, biocorticoid-dependent therapy, dehydroepiandrosterone therapy and puberty induction (**Figure 1B**). However, HRT can only relieve low estrogen symptoms such as vaginal dryness, hot flashes and genitourinary tract atrophy, but has no essential effect on improving ovarian reproductive function. Long-term use of HRT is controversial because it increases the risk of endometrial and ovarian cancer (Ali, 2013; Lee et al., 2020). Since the etiology of POF infertility is complex, the current treatment efficacy is unsatisfactory, and the pregnancy rate and carrying to term rates are still quite low after treatments. Therefore, for women with fertility requirements, it is necessary to strengthen early prevention, early detection and early treatment to delay the development of POF and improve the live birth rate.

The results from animal experiments of MSC transplantation has brought hope to the recovery of ovarian function and fertility in patients with POF. In the following, we will introduce advances in the treatment of POF with MSCs.

MSCS AND FERTILITY PROTECTION

MSCs were the first type of adult stem cell discovered in bone marrow. They originate from mesoderm and are distributed in almost all connective tissue and organ stroma of the entire body. They have the potential for multidirectional differentiation of stem cells and also have a strong migration ability to damaged tissues. Since MSCs have low immunogenicity and fewer disputes in bioethics than fetal-derived stem cells, they are widely applied in clinical research and medical bioengineering (Pers et al., 2016; Badawy et al., 2017; Mu et al., 2018). Currently, MSCs have been used to treat diseases related to the blood, nervous, motor, cardiovascular and skin systems, showing good curative effects (Zaher et al., 2014).

The reproductive capacity of most female mammals is mainly affected by the primordial follicular pool. Under normal

TABLE 1 | Advances in the treatment of POF with MSCs.

Research category	Type of MSCs	Method	Outcome of MSC treatment	Molecular mechanism	Biological effect	References
Preclinical research/ animal experiment	Mouse menSCs	Injection by the tail vein	Repairing ovarian injury, improving ovarian function and stimulating regeneration	MenSCs produce high level of FGF2, which is essential for angiogenesis and the proliferation and remodeling of endometrial cells that plays important roles in repairing and regenerating the damaged tissues	MenSCs increase the follicular numbers, return sex hormone level, repair oocyte function and protect ovary damage	Wang et al. (2017)
Preclinical research/ animal experiment	Human PMSCs	Injected subcutaneously	Restoring ovarian function	PMSCs activate the PI3K/ Akt pathway, reduce Th17 cells percentage and increase Treg cells percentage	PMSCs increase serum levels of E2 and AMH and decrease FSH, LH and AZPAb levels	Yin et al. (2018b)
Preclinical research/ animal experiment	Human AMSCs	Intraperitoneal injection and intragastric administration	Improving injured ovarian tissue structure and function	AMSC transplantation elevate serum oestrogen level and decrease FSH secretions	AMSCs promote follicular development, granulosa cell proliferation and secretion function by improving the local microenvironment of POF mouse ovary	Liu et al. (2019b)
Preclinical research/ animal experiment	Mouse ADSCs	Intravenous injection	Improving ovarian function	Expression levels of ZCCHC11, ANGPTL and ONECUT2 are upregulated	ADSCs increase follicle number, ovulation and inhibit cell apoptosis in POF ovaries	Sun et al. (2013)
Preclinical research/ laboratory research	Human BMSCs	Collection of MSC conditioned media	—	BMSCs conditioned media increase angiogenesis marker including VEGF, VEGFR, Endoglin, Tie-2 and VE-Cadherin through the PI3K/ALK pathway	MSC conditioned media stimulates the proliferation of HOVEC cells	Park et al. (2019)
Preclinical research/ animal experiment	Human BMSCs	Intraovarian injection	Restoring ovarian hormone production and reactivating folliculogenesis	BMSCs decrease FSH level and increase AMH level	BMSCs induce follicle growth and increase the pregnancy rate	Mohamed et al. (2018)
Preclinical research/ animal experiment	Human UCMSC	Intraovarian injection	UCMSC transplantation preserved ovarian function of POF mice	UCMSC transplantation increase estrogen (E2) and AMH levels, and increase the expression of CD31	UCMSCs increase ovarian volume and the number of antral follicles, and promote granulosa cell proliferation and ovarian angiogenesis	Yang et al. (2019b)
Clinical research	Human UCMSC	Intraovarian injection	Two POF patients conceived naturally within 1 year after UCMSC transplantation	UCMSCs activate primordial follicles via phosphorylation of FOXO3a and FOXO1	UCMSCs rescue ovarian function, elevate estradiol concentrations, improve follicular development and increase the number of antral follicles	Ding et al. (2018)
Clinical research	Human autologousBMSC	Laparoscopic intraovarian injection	BMSC treatment revealed promising improvement of POF.	—	BMSCs elevate serum estrogen level, increase volume of the treated ovaries and improve menopausal symptoms	Igboeli et al. (2020)
Clinical research	Human autologous BMSC	Intraovarian instillation	Perimenopausal woman delivered a healthy baby	BMSCs increase AMH level	BMSCs improve follicular development	Gupta et al. (2018)
Clinical research	Human autologous BMSC	Intraarterial catheterization to ovarian artery	5/15 poor responders conceived and 3 healthy babies were born after the stem cell administration	BMSCs increase AMH level and antral follicular count	BMSCs increase the number of antral follicles and retrieve oocytes	Herraiz et al. (2018)
Clinical research	Human autologous ADSCs	Intraovarian injection	Menstruation resumption	BMSCs decreased FSH level	—	Mashayekhi et al. (2021)
Clinical research	Human UCMSC	Intraovarian injection	UCMSC transplantation improved the injured ovarian function, and 4/61 POI patients obtained clinical delivery	—	UCMSCs increase follicular development and improve egg collection	Yan, et al. (2020)

circumstances, to avoid depletion of the follicular pool, most primordial follicles in the ovary are maintained in a resting phase. Primordial follicles undergo follicular activation and a series of developmental processes and finally develop into mature follicles. Various molecules are involved in regulating follicular activation, growth and atresia. Ovarian function recovery is based on oocyte production and follicular quantity/quality recovery (Woods and Tilly, 2012; Truman et al., 2017). Several studies have shown that MSCs can directly differentiate into oocyte-like cells, and transplantation of MSCs is conducive to restoring ovarian function and reproductive capacity (Bahrehbar et al., 2020; Yoon et al., 2020; Taheri et al., 2021). Therefore, MSCs are considered a new choice for the treatment of POF.

The effectiveness of MSCs in the treatment of reproductive system diseases has been confirmed by preclinical and clinical research, which has brought great hope to POF infertility and improved female reproductive health (Herraiz et al., 2019; Fu et al., 2021; Li et al., 2021). MSCs used for the treatment of POF include BMSCs, UCMSCs, PMSCs, AMSCs, AFMSCs, MenSCs and ADMSCs. MSCs originating from different sources have some common characteristics, which make them an ideal treatment choice for POF. A number of animal experiments and clinical trials have confirmed that ovarian function can be improved by MSC homing, inhibiting the apoptosis of OGC and promoting ovarian angiogenesis (Esfandyari et al., 2020). For example, Yan et al. transplanted MSCs to 61 patients with POF and found that the number of follicles in each developmental stage, including antral follicles, dominant follicles and mature follicles, increased significantly (Yan et al., 2020). Other researchers have found that autologous MSC transplantation can trigger menstruation to resume, relieve menopausal symptoms, improve ovarian function and help patients become pregnant (Bukovsky and Caudle, 2012; Igboeli et al., 2020; Mashayekhi et al., 2021; Ulin et al., 2021). Ling *et al.* treated POF mice with MSCs and found that MSC transplantation could significantly restore their hormone secretion ability, improve follicular growth and GC survival, and recover the ovarian function that was destroyed by chemotherapy used to create the POF mice (Ling et al., 2019). A meta-analysis of POF indicated that MSCs could decrease the level of FSH, increase the level of E2 and promote the proliferation of follicles, thus improving the quality of ovaries in POF animals and humans (Chen et al., 2018). Interestingly, Bahrehbar et al. proved that MSC-transplanted POF mice can produce offspring (Bahrehbar et al., 2020).

Table 1 summarizes the preclinical and clinical trials that indicate the validity of treating POF with MSCs. However, the underlying molecular and cellular mechanisms are still controversial and need to be further clarified. Additionally, current clinical research is still insufficient, and there is still a long way to go before the large-scale clinical application of MSCs.

THE MECHANISM OF TREATING POF WITH MSCS

The mechanism of treating POF with MSCs can be summarized as follows (**Figure 2**): 1) MSCs have a "homing" effect; 2) MSCs can promote the growth and development of follicles at all developmental stages; 3) MSCs may induce and differentiate into primordial germ cells (uncertain); 4) MSCs can directly differentiate into GCs or inhibit the apoptosis of GCs; 5) MSCs can promote the formation of ovarian blood vessels; 6) MSCs have immunomodulatory and anti-inflammatory effects and 7) MSCs can reduce oxidative stress.

Homing Effect of MSCs

The homing capacity of MSCs is an important determinant of effective MSC-based therapy (Li et al., 2017; Lin et al., 2017). Homing refers to the process by which MSCs migrate to damaged tissues and promote their recovery. Therefore, enhancing the homing efficiency of MSCs is essential for optimizing the therapeutic outcome of POF. Noory *et al.* reported the application of MenSC transplantation as a treatment modality in a rat model of POF and observed that MSCs can survive in ovarian stroma at 2 months after MSC transplantation and directly differentiated into GCs (Noory et al., 2019). Experiments from Liu et al., Jalalie, et al., Lai et al., Song et al. and Park et al. also demonstrated that after transplantation, MSCs home to damaged tissue and reach the site of injured ovaries (Liu et al., 2014; Lai et al., 2015; Jalalie et al., 2019; Park et al., 2021). However, studies have also shown that although MSCs have a homing effect, they cannot directly differentiate into oocytes but do localize in the ovarian matrix, secrete various cytokines and improve ovarian reserve function through the paracrine pathway (Takehara et al., 2013; Gabr et al., 2016; Li et al., 2017). A study by Taheri et al. demonstrated that MSC isolated from follicular fluid cultured in human recombinant BMP15 medium may differentiate into oocyte-like cells *in vitro*, but they did not investigate whether such MSCs can differentiate into oocytes *in vivo* (Taheri et al., 2021). Therefore, whether MSCs can directly differentiate into oocytes remains unclear, and more in-depth laboratory experiments are still necessary to solve this scientific problem.

Effects of MSCs on Follicular Development

Folliculogenesis is an important part of ovarian function, as it provides oocytes for reproduction (Hua et al., 2015). A large number of genes/proteins have been identified to be associated with follicular development, growth, ovulation and atresia processes. It has been reported that PMSC transplantation can increase the secretion of growth factors, angiogenic factors, pleiotropic cytokines, chemotactic cytokines and extracellular matrix proteins, which are all essential for folliculogenesis (Kupcova Skalnikova, 2013). In POF treatment, the widely discussed follicular development related genes are *Nanos3*, *Nobox* and *Lhx8*. Lai et al. proved that SMSC transplantation could reactivate injured mouse ovaries, with increased expression of the folliculogenesis marker genes *Nobox*, *Nanos3*, and *Lhx8* in the ovaries of SMSC-treated mice (Lai et al., 2014). Kim et al. showed that three-dimensional cultured PDMSC spheres could upregulate the expression level of *Nanos3*, *Nobox* and *Lhx8*, and resume ovulation through regulation of the follicular microenvironment and stimulation of follicular development (Kim et al., 2018). Peng et al. also showed that the mRNA levels of these three genes in POF mice treated with BMSCs

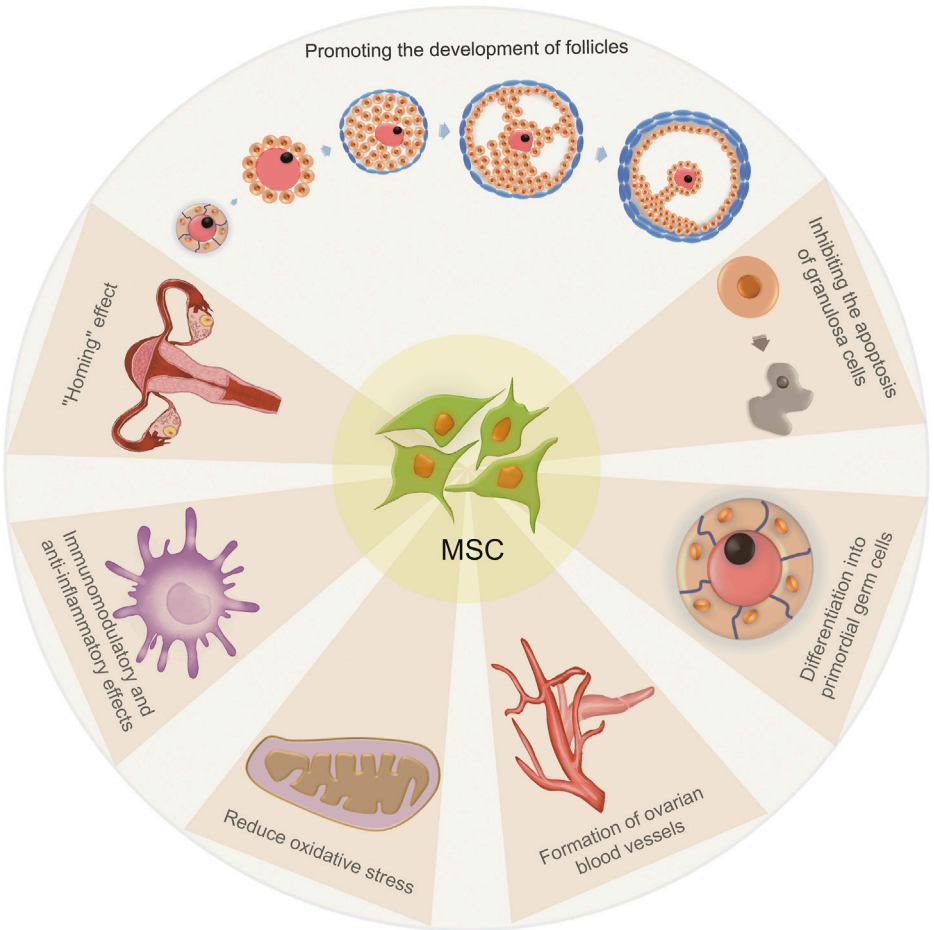

FIGURE 2 | The mechanisms of treating POF with MSCs.

were significantly higher than those in the untreated group (Peng et al., 2018). Other follicular development-related genes include *Foxo3a* and *Foxo1*. Ding *et al.* found that UCMSCs on a collagen scaffold can activate primordial follicles *in vitro via* phosphorylation of FOXO3a and FOXO1, and transplantation of collagen/UCMSCs to the ovaries of POF patients can elevate estradiol concentrations, improve follicular development and increase the number of antral follicles (Ding et al., 2018).

Cytokines are critical regulators of folliculogenesis and ovulation. They contribute to creating an environment supporting follicle selection and growth, regulating cellular proliferation/differentiation, follicular survival/atresia and oocyte maturation (Field et al., 2014). The most important cytokines in POF treatments are TGF-β and IFN-γ. TGF-β superfamily members, including TGF-βs, AMH, activins, inhibins, BMPs and GDFs, impact several stages of follicular development (Trombly et al., 2009; Sanfins et al., 2018). According to Knight et al., the positive TGF-β regulators of preantral follicle growth, include GDF-9 and BMP-15 of oocyte origin, activins of granulosal origin, BMP-4 and BMP-7 of thecal origin and TGF-β from theca and GCs; in contrast, AMH plays a negative role in preantral follicle development (Knight and Glister, 2006). However, the existing research conclusions are not consistent with each other. El-Derany et al. transplanted BMSCs to a γ-ray induced POF rats model and reported that BMSCs recovered the folliculogenesis process, upregulating *Foxo1*, *Gdf-9* and *Fst* gene expression accompanied by downregulating TGF-β (El-Derany et al., 2021), whereas Song et al. and Yin et al. found that MSC transplantation could increase the level of TGF-β and decrease the level of IFN-γ in POF models (Yin et al., 2018a; Song et al., 2018). Additionally, Ling et al. reported that amnion-derived mesenchymal stem cell transplantation can inhibit granulosa cell apoptosis and that the expression levels of AMH were significantly increased in the treatment group compared to the POF group (Ling et al., 2017). Zhang et al. and Mohamed et al. also found that after MSC transplantation, AMH expression in ovarian tissue was significantly higher than that in the POF group (Mohamed et al., 2018; Zhang et al., 2018).

Although the mechanism of MSCs on follicular development is not completely clear, most research agrees that MSC transplantation can promote the development and formation of primordial follicles, eggs and reduce the apoptosis of GCs. All of the involved genes and their correlated mechanisms are listed in **Table 2**.

TABLE 2 | The effects of MSCs on follicular development.

Related gene/hormones/ cytokines	Regulation of expression	Outcome of MSC treatment	References
Nanos3 Nobox Lhx8	Up Up Up	Reducing atretic follicle and increasing antral follicle and secondary follicle	Lai et al. (2014)
Nanos3 Nobox Lhx8	Up Up Up	Stimulating follicular development and resuming ovulation	Kim et al. (2018)
TGF-β GDF-9 BMP-15 BMP-4 BMP-7	Up Up Up Up Up	Inhibiting follicular atresia and reducing the apoptosis of GCs in secondary follicles and cystic follicles	Knight and Glister (2006)
Foxo1 Gdf-9 Fst	Up Up Up	Recovering the suppressed folliculogenesis process and promoting egg formation	El-Derany et al. (2021)
TGF-β IFN-γ AMH AMH	Up Down Up Up	Promoting follicular growth Inhibiting granulosa cell apoptosis Increasing the number of follicles Promoting follicular growth	Song et al. (2018) Zhao et al. (2018a) Ling et al. (2017) Mohamed et al. (2018)
FOXO3a FOXO1	Up Up	Promoting follicular development and maturation	Ding et al. (2018)

MSCs and PGCs

Multiple studies have shown that MSCs can be induced and differentiate into PGCs. Fang et al. and Li et al. proved that CD61 could promote the differentiation of ADMSC into PGC-like cells through activation of the TGF-β pathway (Li et al., 2016; Fang et al., 2017). Wei et al. found that AMSC can be induced into PGC-like cells by BMP4 (Wei et al., 2016). Ge et al. found that when hfSDSCs were cultured in porcine follicle fluid, they may differentiate into both male and female germ cell-like cells (Ge et al., 2015). Park et al. proved that female mouse skin-derived stem cells could differentiate into ovarian-cell-like cells that are consistent with female germ, and ovarian follicle somatic cells. When ovarian cell-like cells are transplanted into ovariectomized mice, they restore the estrus cycle and serum estradiol levels (Park et al., 2014). Unfortunately, no *in vivo* research has reported whether MSC-differentiated germ cells can be fertilized and form embryos, and studies in this area are still lacking.

MSCs Can Promote the Proliferation of GCs

OGCs are the most important stromal cells in the ovary, providing necessary nutrition for oocyte development and follicle maturation, participating in the regulation of gonadotropins that modulate oocyte development and maintaining the microenvironment of oocyte maturation through autocrine and paracrine mechanisms. GCs play an important role in all developmental stages of follicles. GCs abnormalities can lead to abnormal hormone secretion, follicular development disorders and even follicular atresia (Lai et al., 2014). Chemotherapy induces GC apoptosis by damaging DNA and activating apoptosis pathways, thus leading POF. Therefore, enhancing GC function and inhibiting GC apoptosis may effectively prevent POF (Bedoschi et al., 2016). Studies have shown that GCs and MSCs express some similar surface markers (Dzafic et al., 2014; Maleki et al., 2014). Transplanted MSCs are mainly located in the GC layer around follicles, suggesting that MSCs have a significant effect on follicle formation and ovulation (Manshadi et al., 2019).

MSCs can inhibit GC apoptosis and promote GC proliferation by releasing cytokines and hormones, upregulating proliferation-related genes and inhibiting apoptosis-related genes (He et al., 2018; Wang et al., 2020). Zhang et al. showed that PMSC transplantation could upregulate the expression of AMH and FSHR in GCs of POF mice, inhibit GC apoptosis and follicular atresia, and thus restore ovarian function (Zhang et al., 2018). Fu et al. also found that BMSC transplantation may reduce GC apoptosis and improve ovarian function by releasing VEGF, HGF, and IGF-1 and upregulating Bcl-2 expression (Fu et al., 2008). Ding et al. showed that coculturing of AMSCs and GCs might inhibit the apoptosis of GCs, and transplantation of AMSCs may improve ovarian function during natural aging by secreting HGF and EGF (Ding et al., 2018).

The underlying mechanism of MSC treatment of POF may be related to exosome-mediated microRNA modulation. Multiple studies have highlighted the potential therapeutic advantages of using exosomal miRNAs from MSCs for the treatment of various diseases and injuries, including POF. Yang *et al.* demonstrated that BMSC-derived exosomes prevent ovarian follicular atresia in POF rats via the delivery of miR-144-5p, which can decrease GC apoptosis by targeting the PTEN pathway (Yang et al., 2020). Xiao et al. found that miR-146a and miR-10a are rich in exosomes secreted by AFSCs. miR-146a can restore ovarian function by downregulating IRAK1 and TRAF632 expression and miR-10a can inhibit GC apoptosis and prevent follicular atresia by suppressing Bim and caspase-9 expression (Xiao et al., 2016). Sun et al. found that exosomes derived from UCMSCs may prevent and treat chemotherapy-induced OGC apoptosis *in vitro* by upregulating the expression level of Bcl-2 and downregulating the expression levels of caspase-3, Bax, cleaved

caspase-3 and cleaved PARP (Sun et al., 2017). miR-21 is related to apoptosis. Studies have shown that MSC treatment suppresses the expression of PTEN and PDCD4 through upregulation of miR-21 and inhibiting the apoptosis of GCs (Fu et al., 2017). Sun et al. reported that miR-644-5p carried by MSC exosomes could regulate p53 signaling and inhibit GC apoptosis (Sun et al., 2019).

MSCs Promote Angiogenesis

The establishment and remodeling of the ovarian vascular system is the basis of ovarian development and functional recovery. The follicles and corpus luteum can obtain nutritional support through ovarian blood vessels and transport hormones to target organs. Some researchers observed the distribution of BMSCs in ovaries by labeling specific markers of BMSCs and found that BMSCs were mainly distributed in the blood vessels of damaged ovaries (Liu et al., 2014), implying that BMSCs may play a role in ovarian blood vessels construction. Angiogenesis-related factors secreted by MSCs, such as VEGF, HGF, IGF and FGF, are increased in MSC-transplanted POF ovaries. VEGF and HGF have a synergistic effect and synergistically promote angiogenesis (Golocheikine et al., 2010). The combination of VEGF and HGF leads to an increased vascular diameter (Beilmann et al., 2004); VEGF promotes the length, area and branch point number of the induced vessels, while HGF contributes to vascular area growth (He et al., 2018). Wang et al. showed that MSCs could promote ovarian angiogenesis and reduce interstitial fibrosis by secreting VEGF, IGF-1, GCSF and HGF (Wang et al., 2017). Xia et al. demonstrated that MSC transplantation could enhance the expression levels of VEGF, FGF2 and angiogenin, significantly stimulate neovascularization and increase blood perfusion of the grafts in ovarian tissue (Xia et al., 2015). Zhang et al., Cho et al. and Park et al., also proved that MSC transplantation could repair damaged POF ovaries and promote ovarian development and function through angiogenesis (Zhang et al., 2017; Park et al., 2019; Cho et al., 2021).

Microvesicles are cell-derived membrane and cytoplasmic components. There are three subtypes of EVs: exosomes, microvesicles and apoptotic bodies. Exosomes and microvesicles can transfer mRNA, protein and lipids to target cells through surface-expressed ligands and surface receptors, thus affecting the phenotype and function of the target cells (Bidarimath et al., 2017). EVs have a therapeutic effect on female reproductive disorders, such as repairing injured endometrium, suppressing fibrosis of the endometrium, regulating immunity and anti-inflammation, and repressing the apoptosis of GCs in ovaries (Liao et al., 2021). Several studies have shown that MSC-derived microvesicles contain multiple pro-angiogenic proteins, such as VEGF and HGF (Merino-Gonzalez et al., 2016; Pakravan et al., 2017; Han et al., 2019; Shi et al., 2019). Yang et al. showed that UCMSC microvesicles transplantation in POI mice could induce angiogenesis by activating the PI3K/Akt signaling pathway and improve ovarian function (Yang Z. et al., 2019). Sun et al. found that miR-644-5p carried by BMSC-derived exosomes inhibited the apoptosis of ovarian GCs by targeting the p53 pathway (Sun et al., 2019); Zhang et al. also found that UCMSC-derived microvesicles can inhibit the apoptosis of GSs by downregulating the expression level of caspase-3 and upregulating the ratio of Bcl-2/Bax (Zhang J. et al., 2020).

Anti-inflammatory and Immunomodulatory Effect of MSCs

POF is an autoimmune disease. Autoimmune dysfunction is one of the most important pathogeneses of POF, causing inflammatory reactions of the ovary, destroying the ultrastructure of follicular cells (such as zona pellucida damage, gap link rupture and mitochondrial swelling), causing apoptosis of ovarian cells, affecting the maturation and atresia of follicles and inducing a decline in ovarian function (Nelson, 2001; Luo et al., 2017). It has been reported that certain types of immune cells will expand in ovaries with POF and infiltrate into the ovarian tissue, indicating that they are involved in the inflammation associated with POF (van Kasteren et al., 2000; Chernyshov et al., 2001; La Marca et al., 2010; Wang et al., 2018).

The anti-inflammatory effect is a critical mechanism by which MSCs restore ovarian function. MSCs may inhibit the activation and proliferation of lymphocytes, inhibit the secretion of proinflammatory cytokines, inhibit the function of antigen-presenting cells, and convey regulatory messages to immune cells (Zhou et al., 2019). In contrast, since the ovaries of most POF patients are in inflammatory conditions, the presence of inflammatory cytokines is also crucial for the regulation of MSC immunological and regenerative functions. Beldi et al. proved that the tumor TNF-α-TNFR2 axis is necessary for MSCs to produce anti-inflammatory mediators (such as IL-10, TGFβ and NO) and sustain regenerative functions such as wound healing, complex tube formation and endothelial pro-angiogenic support (Beldi et al., 2020a; Beldi et al., 2020b). IFN-γ and MSCs have a synergistic effect on immunosuppression. They upregulate PGE2, HGF, IL-6 and TGF-1 in MSCs and induce MSCs to express IDO, promoting GC proliferation and increasing the number of follicles (Najar et al., 2016; Liang et al., 2018). Yin et al. showed that the level of proinflammatory IFN-γ increased and the level of anti-inflammatory TGF-β decreased in POF mice, whereas PMSC transplantation reversed this situation and improved ovarian function (Yin et al., 2018a). A study also showed that PMSCs increase the secretion of IL-10 by inhibiting NF-κB-mediated pro-inflammatory reactions and thus promote tissue repair (Wang et al., 2016).

Immune cells (Treg cells, NK cells, Th cells, etc.) are important pathogenic factors in several models of autoimmune diseases (Alvarez Arias et al., 2014; Gianchecchi et al., 2018; Zhang X.-M. et al., 2020; Sakaguchi et al., 2020). These results indicate that the interaction of MSCs and immune cells plays a critical role in regulating the inflammatory microenvironment of POF. Yin et al. showed that PMSC transplantation might restore the ovarian function of POF mice by balancing the ratios of Th17/Tc17 and Th17/Treg cells (Yin et al., 2018b). Lu et al. reported that the serum levels of IL-2 and IFN-γ secreted by Th1 cells increased, while IL-4 secreted by Th2 cells decreased in POF mice; however, after UMSC transplantation, the amounts of these cytokines were reversed (Lu et al., 2019). Yin et al. showed that UCMSC

TABLE 3 | Factors involved in the process of MSC treatment of POF.

Issues	Factors	Function	References
Follicular development	TGF-βs, AMH, BMPs, GDFs	Promoting follicular development.	Sanfins et al. (2018)
	TGF-β, GDF-9, BMP-15, BMP-4, BMP-7, AMH	Reducing GC apoptosis and promoting GC proliferation.	Knight and Glister (2006)
	TGF-β	Recovering the suppressed folliculogenesis process.	El-Derany et al. (2021)
	TGF-β, IFN-γ	Promoting follicular growth.	Song et al. (2018)
	AMH	Inhibiting GC apoptosis and promoting follicular growth.	Ling et al. (2017)
Primordial germ cells	CD61, TGF-β	Promoting MSCs different into PGC-like cells.	Fang et al. (2017)
	BMP4	Inducing MSC into PGC-like cells	Wei et al. (2016)
Proliferation of GC	AMH	Inhibiting GC apoptosis.	Zhang et al. (2018)
	VEGF, HGF, IGF-1, Bcl-2	Reducing GC apoptosis and improving ovarian function.	Fu et al. (2008)
	HGF, EGF	Reducing apoptosis of ovarian GC.	Ding et al. (2018)
	PARP	Inhibiting ovarian follicular atresia and reducing GC apoptosis.	Sun et al. (2017)
	Bcl-2, AMH, FSHR, caspase-3	Promoting GC proliferation and inhibiting GC apoptosis.	Wang et al. (2020)
Angiogenesis	VEGF, HGF	Promoting ovarian angiogenesis.	Golocheikine et al. (2010)
	VEGF, HGF	Increasing vascular diameter.	Beilmann et al. (2004)
	VEGF, IGF-1, GCSF, HGF	Promoting ovarian angiogenesis and reducing interstitial fibrosis.	Wang et al. (2017)
	VEGF, FGF2	Stimulating neovascularization and increasing blood perfusion of the grafts.	Xia et al. (2015)
Immunomodulatory effect	IL-2, IFN-γ, IL-4	Reducing GC apoptosis.	Lu et al. (2019)
Anti-inflammatory effect	PGE2, HGF, IL-6, TGF-1	Promoting GC proliferation.	Liang et al. (2018)
	IFN-γ, TGF-β	Improving ovarian function	Yin et al. (2018a)
Oxidative stress	HGF, IL-6, IL-8, VEGF, BDNF, LIF	Increasing the production of antioxidant enzymes and inhibiting ROS production.	Amoroso et al. (2017)

transplantation into POF mice upregulates the ratio of $CD8^+$ Treg cells, which have a typical immunosuppressive function and can reduce immune rejection (Su et al., 2014; Yin et al., 2020).

The Effect of MSCs on Oxidative Stress

Oxidative stress is a phenomenon of imbalance between the oxidative system and the antioxidant system caused by excessive ROS produced in cells. Reduction of ROS can protect the structure and function of ovarian mitochondria, increase the levels of antioxidant and antiapoptotic enzymes, and reduce apoptosis and oxidative damage of the ovary (He et al., 2018). Abumaree et al. indicated that cocultured PMSCs could reverse the destructive effect of OS on H_2O_2-treated endothelial cells and increase cell proliferation and migration (Abumaree et al., 2017). One study showed that ROS inhibit the expression and activity of TERT and induce POF (Jiang et al., 2018). MSCs can increase the production of antioxidant enzymes and inhibit ROS production through secretion of HGF, IL-6, IL-8, VEGF, BDNF and LIF and activation of the FOXO, NOQ1/MAPK, PI3K/Akt and Nrf2-ARE pathways (Amoroso et al., 2017). One study indicated that fMSCs upregulate MT1, JNK1, PCNA and AMPK levels and enhance antioxidant effects (Huang et al., 2019). Recently, it has been found that PMSC transplantation can reduce the levels of UCP-2, SOD1, reactive oxygen species and 8-hydroxydeoxyguanosine in POF rats, improving mitochondrial function *in vivo*, inhibiting oxidative stress and improving ovarian function (Zhang et al., 2016).

Using MSCs to treat POF is a sophisticated project. To better understand the mechanism by which MSCs improves ovarian functions, we summarized the cytokines and regulatory factors involved in the homing effect, follicular development, cell proliferation/apoptosis, angiogenesis, immunomodulation and oxidative stress processes, as shown in **Table 3**.

PERSPECTIVE

MSCs possess multiple differentiation potentials and homing and immunomodulatory functions. They can be used as seed cells to participate in the regeneration and reconstruction of tissues and organs in various diseases, such as rheumatoid arthritis, amyotrophic lateral sclerosis, systemic lupus erythematosus and other degenerative diseases (spinal cord injury, Parkinson's disease, Alzheimer's disease). At present, more than ten kinds of stem cell preparations have been used to treat graft-versus-host disease (Zhao et al., 2019), acute myocardial infarction (Cho et al., 2017), osteoarthritis (Matas et al., 2019), etc. The clinical application of MSCs has brought great hope to the treatment of POF infertility and the improvement of female reproductive health, and a large number of clinical studies are actively being carried out. However, with increasing age, the number and function of MSCs decrease accordingly. The senescence of MSCs may be related to telomere shortening, DNA damage, epigenetics and immunological characteristics (Trachana et al., 2017; Wagner, 2019). At present, senescence of MSC is still the bottleneck of stem cell tissue engineering and clinical applications. Therefore, how to deeply understand the molecular mechanism of MSC senescence and delay or prevent MSC senescence efficiently through reasonable gene manipulation

or drug intervention, has crucial practical significance and important economic value.

CONCLUSION

MSCs derived from different sources have similar curative effects in the treatment of POF through multiple mechanisms. MSCs have attractive clinical transformation and application prospects in the restoration of reproductive function in POF patients, even in older women with POF. Therefore, understanding the molecular mechanism of POF is still a key scientific problem for comprehensively and deeply evaluating the safety and effectiveness of MSC transplantation, especially the long-term impact on parents and offspring.

AUTHOR CONTRIBUTIONS

XS and JW contributed to the conception and design of the article. JW and WL drafted the article. ZY, DY, and SL drafted the figures. All authors have read and approved the final manuscript.

FUNDING

This work was supported in part by the National Natural Science Foundation of China Grant (No. #81801227 to XS), the Subject Arrangement Program from Science and Technology Department of Jilin Province (Nos. #20200201123JC to DY and #20190201209JC to SL), and Clinical-Translational Medicine Project from the First Hospital of Jilin University (No. #JDYYJCHX2020013 and #2020-ZL-13 to XS and DY).

REFERENCES

Abumaree, M. H., Hakami, M., Abomaray, F. M., Alshabibi, M. A., Kalionis, B., Al Jumah, M. A., et al. (2017). Human Chorionic Villous Mesenchymal Stem/Stromal Cells Modify the Effects of Oxidative Stress on Endothelial Cell Functions. *Placenta* 59, 74–86. doi:10.1016/j.placenta.2017.05.001

Ali, A. T. (2013). Risk Factors for Endometrial Cancer. *Ceska Gynekol* 78, 448–459.

Alvarez Arias, D. A., Kim, H.-J., Zhou, P., Holderried, T. A. W., Wang, X., Dranoff, G., et al. (2014). Disruption of CD8+ Treg Activity Results in Expansion of T Follicular Helper Cells and Enhanced Antitumor Immunity. *Cancer Immunol. Res.* 2, 207–216. doi:10.1158/2326-6066.cir-13-0121

Amoroso, M. R., Matassa, D. S., Agliarulo, I., Avolio, R., Maddalena, F., Condelli, V., et al. (2017). Stress-Adaptive Response in Ovarian Cancer Drug Resistance. *Adv. Protein Chem. Struct. Biol.* 108, 163–198. doi:10.1016/bs.apcsb.2017.01.004

Badawy, A., Sobh, M., Ahdy, M., and Abdelhafez, M. (2017). Bone Marrow Mesenchymal Stem Cell Repair of Cyclophosphamide-Induced Ovarian Insufficiency in a Mouse Model. *Int. J. women's Health* 9, 441–447. doi:10.2147/ijwh.s134074

Bahrehbar, K., Valojerdi, M. R., Esfandiari, F., Fathi, R., Hassani, S.-N., and Baharvand, H. (2020). Human Embryonic Stem Cell-Derived Mesenchymal Stem Cells Improved Premature Ovarian Failure. *World J. Stem Cell* 12, 857–878. doi:10.4252/wjsc.v12.i8.857

Bedoschi, G., Navarro, P. A., and Oktay, K. (2016). Chemotherapy-Induced Damage to Ovary: Mechanisms and Clinical Impact. *Future Oncol.* 12, 2333–2344. doi:10.2217/fon-2016-0176

Beilmann, M., Birk, G., and Lenter, M. C. (2004). Human Primary Co-Culture Angiogenesis Assay Reveals Additive Stimulation and Different Angiogenic Properties of VEGF and HGF. *Cytokine* 26, 178–185. doi:10.1016/j.cyto.2004.03.003

Beldi, G., Bahiraii, S., Lezin, C., Nouri Barkestani, M., Abdelgawad, M. E., Uzan, G., et al. (2020a). TNFR2 Is a Crucial Hub Controlling Mesenchymal Stem Cell Biological and Functional Properties. *Front. Cel Dev. Biol.* 8, 596831. doi:10.3389/fcell.2020.596831

Beldi, G., Khosravi, M., Abdelgawad, M. E., Salomon, B. L., Uzan, G., Haouas, H., et al. (2020b). TNFα/TNFR2 Signaling Pathway: An Active Immune Checkpoint for Mesenchymal Stem Cell Immunoregulatory Function. *Stem Cel Res Ther* 11, 281. doi:10.1186/s13287-020-01740-5

Bidarimath, M., Khalaj, K., Kridli, R. T., Kan, F. W., Koti, M., and Tayade, C. (2017). Extracellular Vesicle Mediated Intercellular Communication at the Porcine Maternal-Fetal Interface: A New Paradigm for Conceptus-Endometrial Cross-Talk. *Sci. Rep.* 7, 40476. doi:10.1038/srep40476

Bukovsky, A., and Caudle, M. R. (2012). Immunoregulation of Follicular Renewal, Selection, POF, and Menopause *In Vivo*, vs. Neo-Oogenesis *In Vitro*, POF and Ovarian Infertility Treatment, and a Clinical Trial. *Reprod. Biol. Endocrinol.* 10, 97. doi:10.1186/1477-7827-10-97

Chen, L., Guo, S., Wei, C., Li, H., Wang, H., and Xu, Y. (2018). Effect of Stem Cell Transplantation of Premature Ovarian Failure in Animal Models and Patients: A Meta-Analysis and Case Report. *Exp. Ther. Med.* 15, 4105–4118. doi:10.3892/etm.2018.5970

Chernyshov, V. P., Radysh, T. V., Gura, I. V., Tatarchuk, T. P., and Khominskaya, Z. B. (2001). Immune Disorders in Women with Premature Ovarian Failure in Initial Period. *Am. J. Reprod. Immunol.* 46, 220–225. doi:10.1034/j.1600-0897.2001.d01-5.x

Cho, D. I., Kang, W. S., Hong, M. H., Kang, H. J., Kim, M. R., Kim, M. C., et al. (2017). The Optimization of Cell Therapy by Combinational Application with Apicidin-Treated Mesenchymal Stem Cells after Myocardial Infarction. *Oncotarget* 8, 44281–44294. doi:10.18632/oncotarget.17471

Cho, J., Kim, T.-H., Seok, J., Jun, J. H., Park, H., Kweon, M., et al. (2021). Vascular Remodeling by Placenta-Derived Mesenchymal Stem Cells Restores Ovarian Function in Ovariectomized Rat Model via the VEGF Pathway. *Lab. Invest.* 101, 304–317. doi:10.1038/s41374-020-00513-1

Ding, C., Zou, Q., Wang, F., Wu, H., Chen, R., Lv, J., et al. (2018). Human Amniotic Mesenchymal Stem Cells Improve Ovarian Function in Natural Aging through Secreting Hepatocyte Growth Factor and Epidermal Growth Factor. *Stem Cel Res Ther* 9, 55. doi:10.1186/s13287-018-0781-9

Ding, L., Yan, G., Wang, B., Xu, L., Gu, Y., Ru, T., et al. (2018). Transplantation of UC-MSCs on Collagen Scaffold Activates Follicles in Dormant Ovaries of POF Patients with Long History of Infertility. *Sci. China Life Sci.* 61, 1554–1565. doi:10.1007/s11427-017-9272-2

Dolmans, M.-M., and Donnez, J. (2021). Fertility Preservation in Women for Medical and Social Reasons: Oocytes vs Ovarian Tissue. *Best Pract. Res. Clin. Obstet. Gynaecol.* 70, 63–80. doi:10.1016/j.bpobgyn.2020.06.011

Dzafic, E., Stimpfel, M., Novakovic, S., Cerkovnik, P., and Virant-Klun, I. (2014). Expression of Mesenchymal Stem Cells-Related Genes and Plasticity of Aspirated Follicular Cells Obtained from Infertile Women. *Biomed. Res. Int.* 2014, 508216. doi:10.1155/2014/508216

El-Derany, M. O., Said, R. S., and El-Demerdash, E. (2021). Bone Marrow-Derived Mesenchymal Stem Cells Reverse Radiotherapy-Induced Premature Ovarian Failure: Emphasis on Signal Integration of TGF-β, Wnt/β-Catenin and Hippo Pathways. *Stem Cel Rev Rep* 17, 1429–1445. doi:10.1007/s12015-021-10135-9

Esfandyari, S., Chugh, R. M., Park, H. S., Hobeika, E., Ulin, M., and Al-Hendy, A. (2020). Mesenchymal Stem Cells as a Bio Organ for Treatment of Female Infertility. *Cells* 9, 2253. doi:10.3390/cells9102253

Fang, J., Wei, Y., Lv, C., Peng, S., Zhao, S., and Hua, J. (2017). CD61 Promotes the Differentiation of Canine ADMSCs into PGC-like Cells through Modulation of TGF-β Signaling. *Sci. Rep.* 7, 43851. doi:10.1038/srep43851

Field, S. L., Dasgupta, T., Cummings, M., and Orsi, N. M. (2014). Cytokines in Ovarian Folliculogenesis, Oocyte Maturation and Luteinisation. *Mol. Reprod. Dev.* 81, 284–314. doi:10.1002/mrd.22285

Fu, X., He, Y., Xie, C., and Liu, W. (2008). Bone Marrow Mesenchymal Stem Cell Transplantation Improves Ovarian Function and Structure in Rats with

Chemotherapy-Induced Ovarian Damage. *Cytotherapy* 10, 353–363. doi:10.1080/14653240802035926

Fu, X., He, Y., Wang, X., Peng, D., Chen, X., Li, X., et al. (2017). Overexpression of miR-21 in Stem Cells Improves Ovarian Structure and Function in Rats with Chemotherapy-Induced Ovarian Damage by Targeting PDCD4 and PTEN to Inhibit Granulosa Cell Apoptosis. *Stem Cel Res Ther* 8, 187. doi:10.1186/s13287-017-0641-z

Fu, Y. X., Ji, J., Shan, F., Li, J., and Hu, R. (2021). Human Mesenchymal Stem Cell Treatment of Premature Ovarian Failure: New Challenges and Opportunities. *Stem Cel Res. Ther.* 12, 161. doi:10.1186/s13287-021-02212-0

Gabr, H., Rateb, M. A., El Sissy, M. H., Ahmed Seddiek, H., and Ali Abdelhameed Gouda, S. (2016). The Effect of Bone Marrow-Derived Mesenchymal Stem Cells on Chemotherapy Induced Ovarian Failure in Albino Rats. *Microsc. Res. Tech.* 79, 938–947. doi:10.1002/jemt.22725

Ge, W., Ma, H. G., Cheng, S. F., Sun, Y. C., Sun, L. L., Sun, X. F., et al. (2015). Differentiation of Early Germ Cells from Human Skin-Derived Stem Cells without Exogenous Gene Integration. *Sci. Rep.* 5, 13822. doi:10.1038/srep13822

Gianchecchi, E., Delfino, D. V., and Fierabracci, A. (2018). NK Cells in Autoimmune Diseases: Linking Innate and Adaptive Immune Responses. *Autoimmun. Rev.* 17, 142–154. doi:10.1016/j.autrev.2017.11.018

Golocheikine, A., Tiriveedhi, V., Angaswamy, N., Benshoff, N., Sabarinathan, R., and Mohanakumar, T. (2010). Cooperative Signaling for Angiogenesis and Neovascularization by VEGF and HGF Following Islet Transplantation. *Transplantation* 90, 725–731. doi:10.1097/tp.0b013e3181ef8a63

Gupta, S., Lodha, P., Karthick, M. S., and Tandulwadkar, S. R. (2018). Role of Autologous Bone Marrow-Derived Stem Cell Therapy for Follicular Recruitment in Premature Ovarian Insufficiency: Review of Literature and a Case Report of World's First Baby with Ovarian Autologous Stem Cell Therapy in a Perimenopausal Woman of Age 45 Year. *J. Hum. Reprod. Sci.* 11, 125–130. doi:10.4103/jhrs.JHRS_57_18

Han, Y., Ren, J., Bai, Y., Pei, X., and Han, Y. (2019). Exosomes from Hypoxia-Treated Human Adipose-Derived Mesenchymal Stem Cells Enhance Angiogenesis through VEGF/VEGF-R. *Int. J. Biochem. Cel Biol.* 109, 59–68. doi:10.1016/j.biocel.2019.01.017

He, Y., Chen, D., Yang, L., Hou, Q., Ma, H., and Xu, X. (2018). The Therapeutic Potential of Bone Marrow Mesenchymal Stem Cells in Premature Ovarian Failure. *Stem Cel Res Ther* 9, 263. doi:10.1186/s13287-018-1008-9

Herraiz, S., Romeu, M., Buigues, A., Martínez, S., Díaz-García, C., Gómez-Seguí, I., et al. (2018). Autologous Stem Cell Ovarian Transplantation to Increase Reproductive Potential in Patients Who Are Poor Responders. *Fertil. sterility* 110, 496–505. doi:10.1016/j.fertnstert.2018.04.025

Herraiz, S., Pellicer, N., Romeu, M., and Pellicer, A. (2019). Treatment Potential of Bone Marrow-Derived Stem Cells in Women with Diminished Ovarian Reserves and Premature Ovarian Failure. *Curr. Opin. Obstet. Gynecol.* 31, 156–162. doi:10.1097/gco.0000000000000531

Hua, J., Xu, B., Yang, Y., Ban, R., Iqbal, F., Cooke, H. J., et al. (2015). Follicle Online: an Integrated Database of Follicle Assembly, Development and Ovulation. *Database* 2015, bav036. doi:10.1093/database/bav036

Huang, B., Qian, C., Ding, C., Meng, Q., Zou, Q., and Li, H. (2019). Fetal Liver Mesenchymal Stem Cells Restore Ovarian Function in Premature Ovarian Insufficiency by Targeting MT1. *Stem Cel Res Ther* 10, 362. doi:10.1186/s13287-019-1490-8

Huhtaniemi, I., Hovatta, O., La Marca, A., Livera, G., Monniaux, D., Persani, L., et al. (2018). Advances in the Molecular Pathophysiology, Genetics, and Treatment of Primary Ovarian Insufficiency. *Trends Endocrinol. Metab.* 29, 400–419. doi:10.1016/j.tem.2018.03.010

Igboeli, P., El Andaloussi, A., Sheikh, U., Takala, H., ElSharoud, A., McHugh, A., et al. (2020). Intraovarian Injection of Autologous Human Mesenchymal Stem Cells Increases Estrogen Production and Reduces Menopausal Symptoms in Women with Premature Ovarian Failure: Two Case Reports and a Review of the Literature. *J. Med. Case Rep.* 14, 108. doi:10.1186/s13256-020-02426-5

Imai, A., Furui, T., and Yamamoto, A. (2008). Preservation of Female Fertility during Cancer Treatment. *Reprod. Med. Biol.* 7, 17–27. doi:10.1111/j.1447-0578.2007.00197.x

Jalalie, L., Rezaie, M. J., Jalili, A., Rezaee, M. A., Vahabzadeh, Z., Rahmani, M. R., et al. (2019). Distribution of the CM-Dil-Labeled Human Umbilical Cord Vein Mesenchymal Stem Cells Migrated to the Cyclophosphamide-Injured Ovaries in C57BL/6 Mice. *Iranian Biomed. J.* 23, 200–208. doi:10.29252/ibj.23.3.200

Jiang, H. L., Cao, L. Q., and Chen, H. Y. (2018). Protective Effects ROS Up-Regulation on Premature Ovarian Failure by Suppressing ROS-TERT Signal Pathway. *Eur. Rev. Med. Pharmacol. Sci.* 22, 6198–6204. doi:10.26355/eurrev_201810_16025

Kim, T. H., Choi, J. H., Jun, Y., Lim, S. M., Park, S., Paek, J. Y., et al. (2018). 3D-Cultured Human Placenta-Derived Mesenchymal Stem Cell Spheroids Enhance Ovary Function by Inducing Folliculogenesis. *Sci. Rep.* 8, 15313. doi:10.1038/s41598-018-33575-9

Knight, P. G., and Glister, C. (2006). TGF-β Superfamily Members and Ovarian Follicle Development. *Reproduction* 132, 191–206. doi:10.1530/rep.1.01074

Kupcova Skalnikova, H. (2013). Proteomic Techniques for Characterisation of Mesenchymal Stem Cell Secretome. *Biochimie* 95, 2196–2211. doi:10.1016/j.biochi.2013.07.015

La Marca, A., Brozzetti, A., Sighinolfi, G., Marzotti, S., Volpe, A., and Falorni, A. (2010). Primary Ovarian Insufficiency: Autoimmune Causes. *Curr. Opin. Obstet. Gynecol.* 22, 277–282. doi:10.1097/gco.0b013e32833b6c70

Lai, D., Wang, F., Dong, Z., and Zhang, Q. (2014). Skin-Derived Mesenchymal Stem Cells Help Restore Function to Ovaries in a Premature Ovarian Failure Mouse Model. *PloS one* 9, e98749. doi:10.1371/journal.pone.0098749

Lai, D., Wang, F., Yao, X., Zhang, Q., Wu, X., and Xiang, C. (2015). Human Endometrial Mesenchymal Stem Cells Restore Ovarian Function through Improving the Renewal of Germline Stem Cells in a Mouse Model of Premature Ovarian Failure. *J. Transl Med.* 13, 155. doi:10.1186/s12967-015-0516-y

Laven, J. (2016). Primary Ovarian Insufficiency. *Semin. Reprod. Med.* 34, 230–234. doi:10.1055/s-0036-1585402

Lee, A. W., Wu, A. H., Wiensch, A., Mukherjee, B., Terry, K. L., Harris, H. R., et al. (2020). Estrogen Plus Progestin Hormone Therapy and Ovarian Cancer. *Epidemiology* 31, 402–408. doi:10.1097/ede.0000000000001175

Li, B., Liu, W., Zhuang, M., Li, N., Wu, S., Pan, S., et al. (2016). Overexpression of CD61 Promotes hUC-MSC Differentiation into Male Germ-like Cells. *Cell Prolif.* 49, 36–47. doi:10.1111/cpr.12236

Li, J., Mao, Q., He, J., She, H., Zhang, Z., and Yin, C. (2017). Human Umbilical Cord Mesenchymal Stem Cells Improve the Reserve Function of Perimenopausal Ovary via a Paracrine Mechanism. *Stem Cel. Res. Ther.* 8 (1), 55. doi:10.1186/s13287-017-0514-5

Li, Z., Zhang, M., Tian, Y., Li, Q., and Huang, X. (2021). Mesenchymal Stem Cells in Premature Ovarian Insufficiency: Mechanisms and Prospects. *Front. Cel Dev. Biol.* 9, 718192. doi:10.3389/fcell.2021.718192

Liang, C., Jiang, E., Yao, J., Wang, M., Chen, S., Zhou, Z., et al. (2018). Interferon-γ Mediates the Immunosuppression of Bone Marrow Mesenchymal Stem Cells on T-Lymphocytes *In Vitro*. *Hematology* 23, 44–49. doi:10.1080/10245332.2017.1333245

Liao, Z., Liu, C., Wang, L., Sui, C., and Zhang, H. (2021). Therapeutic Role of Mesenchymal Stem Cell-Derived Extracellular Vesicles in Female Reproductive Diseases. *Front. Endocrinol.* 12, 665645. doi:10.3389/fendo.2021.665645

Lin, W., Xu, L., Zwingenberger, S., Gibon, E., Goodman, S. B., and Li, G. (2017). Mesenchymal Stem Cells Homing to Improve Bone Healing. *J. orthopaedic translation* 9, 19–27. doi:10.1016/j.jot.2017.03.002

Ling, L., Feng, X., Wei, T., Wang, Y., Wang, Y., Zhang, W., et al. (2017). Effects of Low-Intensity Pulsed Ultrasound (LIPUS)-pretreated Human Amnion-Derived Mesenchymal Stem Cell (hAD-MSC) Transplantation on Primary Ovarian Insufficiency in Rats. *Stem Cel Res Ther* 8, 283. doi:10.1186/s13287-017-0739-3

Ling, L., Feng, X., Wei, T., Wang, Y., Wang, Y., Wang, Z., et al. (2019). Human Amnion-Derived Mesenchymal Stem Cell (hAD-MSC) Transplantation Improves Ovarian Function in Rats with Premature Ovarian Insufficiency (POI) at Least Partly through a Paracrine Mechanism. *Stem Cel Res Ther* 10, 46. doi:10.1186/s13287-019-1136-x

Liu, J., Zhang, H., Zhang, Y., Li, N., Wen, Y., Cao, F., et al. (2014). Homing and Restorative Effects of Bone Marrow-Derived Mesenchymal Stem Cells on Cisplatin Injured Ovaries in Rats. *Mol. Cell* 37, 865–872. doi:10.14348/molcells.2014.0145

Liu, S., Wang, J., Han, R., Meng, M., Wang, W., Zhao, Y., et al. (2019a). Therapeutic Effect of Transplanted Umbilical Cord Mesenchymal Stem Cells in a Cynomolgus Monkey Model of Multiple Sclerosis. *Am. J. Transl Res.* 11, 2516–2531.

Liu, R., Zhang, X., Fan, Z., Wang, Y., Yao, G., Wan, X., et al. (2019b). Human Amniotic Mesenchymal Stem Cells Improve the Follicular Microenvironment to Recover Ovarian Function in Premature Ovarian Failure Mice. *Stem Cel Res Ther* 10, 299. doi:10.1186/s13287-019-1315-9

Lu, X., Cui, J., Cui, L., Luo, Q., Cao, Q., Yuan, W., et al. (2019). The Effects of Human Umbilical Cord-Derived Mesenchymal Stem Cell Transplantation on Endometrial Receptivity Are Associated with Th1/Th2 Balance Change and uNK Cell Expression of Uterine in Autoimmune Premature Ovarian Failure Mice. *Stem Cel Res Ther* 10, 214. doi:10.1186/s13287-019-1313-y

Luo, Q., Yin, N., Zhang, L., Yuan, W., Zhao, W., Luan, X., et al. (2017). Role of SDF-1/CXCR4 and Cytokines in the Development of Ovary Injury in Chemotherapy Drug Induced Premature Ovarian Failure Mice. *Life Sci.* 179, 103–109. doi:10.1016/j.lfs.2017.05.001

Maleki, M., Ghanbarvand, F., Behvarz, M. R., Ejtemaei, M., and Ghadirkhomi, E. (2014). Comparison of Mesenchymal Stem Cell Markers in Multiple Human Adult Stem Cells. *Int. J. Stem Cell* 7, 118–126. doi:10.15283/ijsc.2014.7.2.118

Manshadi, M. D., Navid, S., Hoshino, Y., Daneshi, E., Noory, P., and Abbasi, M. (2019). The Effects of Human Menstrual Blood Stem Cells-derived Granulosa Cells on Ovarian Follicle Formation in a Rat Model of Premature Ovarian Failure. *Microsc. Res. Tech.* 82, 635–642. doi:10.1002/jemt.23120

Mashayekhi, M., Mirzadeh, E., Chekini, Z., Ahmadi, F., Eftekhari-Yazdi, P., Vesali, S., et al. (2021). Evaluation of Safety, Feasibility and Efficacy of Intra-ovarian Transplantation of Autologous Adipose Derived Mesenchymal Stromal Cells in Idiopathic Premature Ovarian Failure Patients: Non-Randomized Clinical Trial, Phase I, First in Human. *J. ovarian Res.* 14, 5. doi:10.1186/s13048-020-00743-3

Matas, J., Orrego, M., Amenabar, D., Infante, C., Tapia-Limonchi, R., Cadiz, M. I., et al. (2019). Umbilical Cord-Derived Mesenchymal Stromal Cells (MSCs) for Knee Osteoarthritis: Repeated MSC Dosing Is Superior to a Single MSC Dose and to Hyaluronic Acid in a Controlled Randomized Phase I/II Trial. *STEM CELLS Translational Med.* 8, 215–224. doi:10.1002/sctm.18-0053

Merino-González, C., Zuñiga, F. A., Escudero, C., Ormazabal, V., Reyes, C., Nova-Lamperti, E., et al. (2016). Mesenchymal Stem Cell-Derived Extracellular Vesicles Promote Angiogenesis: Potencial Clinical Application. *Front. Physiol.* 7, 24. doi:10.3389/fphys.2016.00024

Mohamed, S. A., Shalaby, S. M., Abdelaziz, M., Brakta, S., Hill, W. D., Ismail, N., et al. (2018). Human Mesenchymal Stem Cells Partially Reverse Infertility in Chemotherapy-Induced Ovarian Failure. *Reprod. Sci.* 25, 51–63. doi:10.1177/1933719117699705

Mu, Y., Wu, X., and Hao, Z. (2018). Comparative Evaluation of Mesenchymal Stromal Cells from Umbilical Cord and Amniotic Membrane in Xeno-free Conditions. *BMC Cel Biol* 19, 27. doi:10.1186/s12860-018-0178-8

Najar, M., Raicevic, G., Fayyad-Kazan, H., Bron, D., Toungouz, M., and Lagneaux, L. (2016). Mesenchymal Stromal Cells and Immunomodulation: A Gathering of Regulatory Immune Cells. *Cytotherapy* 18, 160–171. doi:10.1016/j.jcyt.2015.10.011

Nelson, L. (2001). Autoimmune Ovarian Failure: Comparing the Mouse Model and the Human Disease. *J. Soc. Gynecol. Investig.* 8, S55–S57. doi:10.1016/s1071-5576(00)00110-6

Noory, P., Navid, S., Zanganeh, B. M., Talebi, A., Borhani-Haghighi, M., Gholami, K., et al. (2019). Human Menstrual Blood Stem Cell-Derived Granulosa Cells Participate in Ovarian Follicle Formation in a Rat Model of Premature Ovarian Failure *In Vivo*. *Cell Reprogramming* 21, 249–259. doi:10.1089/cell.2019.0020

Pakravan, K., Babashah, S., Sadeghizadeh, M., Mowla, S. J., Mossahebi-Mohammadi, M., Ataei, F., et al. (2017). MicroRNA-100 Shuttled by Mesenchymal Stem Cell-Derived Exosomes Suppresses *In Vitro* Angiogenesis through Modulating the mTOR/HIF-1α/VEGF Signaling axis in Breast Cancer Cells. *Cell Oncol.* 40, 457–470. doi:10.1007/s13402-017-0335-7

Park, B.-W., Pan, B., Toms, D., Huynh, E., Byun, J.-H., Lee, Y.-M., et al. (2014). Ovarian-Cell-Like Cells from Skin Stem Cells Restored Estradiol Production and Estrus Cycling in Ovariectomized Mice. *Stem Cell Dev.* 23, 1647–1658. doi:10.1089/scd.2014.0029

Park, H. S., Ashour, D., Elsharoud, A., Chugh, R. M., Ismail, N., El Andaloussi, A., et al. (2019). Towards Cell Free Therapy of Premature Ovarian Insufficiency: Human Bone Marrow Mesenchymal Stem Cells Secretome Enhances Angiogenesis in Human Ovarian Microvascular Endothelial Cells. *HSOA J. Stem Cell Res Dev Ther* 5, 19. doi:10.24966/srdt-2060/100019

Park, H. S., Chugh, R. M., Elsharoud, A., Ulin, M., Esfandyari, S., Aboalsoud, A., et al. (2021). Safety of Intraovarian Injection of Human Mesenchymal Stem Cells in a Premature Ovarian Insufficiency Mouse Model. *Cel Transplant.* 30, 963689720988502. doi:10.1177/0963689720988502

Peng, J., Xiao, N., and Cheng, L. (2018). Therapeutic Potential of BMSCs for Premature Ovarian Failure in Mice. *Zhong nan da Xue Xue Bao Yi Xue ban = J. Cent. South Univ. Med. Sci.* 43, 7–13. doi:10.11817/j.issn.1672-7347.2018.01.002

Pers, Y.-M., Rackwitz, L., Ferreira, R., Pullig, O., Delfour, C., Barry, F., et al. (2016). Adipose Mesenchymal Stromal Cell-Based Therapy for Severe Osteoarthritis of the Knee: A Phase I Dose-Escalation Trial. *Stem Cell translational Med.* 5, 847–856. doi:10.5966/sctm.2015-0245

Sakaguchi, S., Mikami, N., Wing, J. B., Tanaka, A., Ichiyama, K., and Ohkura, N. (2020). Regulatory T Cells and Human Disease. *Annu. Rev. Immunol.* 38, 541–566. doi:10.1146/annurev-immunol-042718-041717

Sanfins, A., Rodrigues, P., and Albertini, D. F. (2018). GDF-9 and BMP-15 Direct the Follicle Symphony. *J. Assist. Reprod. Genet.* 35, 1741–1750. doi:10.1007/s10815-018-1268-4

Sheikhansari, G., Aghebati-Maleki, L., Nouri, M., Jadidi-Niaragh, F., and Yousefi, M. (2018). Current Approaches for the Treatment of Premature Ovarian Failure with Stem Cell Therapy. *Biomed. Pharmacother.* 102, 254–262. doi:10.1016/j.biopha.2018.03.056

Shi, Y., Shi, H., Nomi, A., Lei-Lei, Z., Zhang, B., and Qian, H. (2019). Mesenchymal Stem Cell-Derived Extracellular Vesicles: A New Impetus of Promoting Angiogenesis in Tissue Regeneration. *Cytotherapy* 21, 497–508. doi:10.1016/j.jcyt.2018.11.012

Song, K., Cai, H., Zhang, D., Huang, R., Sun, D., and He, Y. (2018). Effects of Human Adipose-Derived Mesenchymal Stem Cells Combined with Estrogen on Regulatory T Cells in Patients with Premature Ovarian Insufficiency. *Int. Immunopharmacology* 55, 257–262. doi:10.1016/j.intimp.2017.12.026

Su, J., Xie, Q., Xu, Y., Li, X. C., and Dai, Z. (2014). Role of CD8(+) Regulatory T Cells in Organ Transplantation. *Burns Trauma* 2, 18–23. doi:10.4103/2321-3868.126086

Sun, M., Wang, S., Li, Y., Yu, L., Gu, F., Wang, C., et al. (2013). Adipose-Derived Stem Cells Improved Mouse Ovary Function after Chemotherapy-Induced Ovary Failure. *Stem Cel Res Ther* 4, 80. doi:10.1186/scrt231

Sun, L., Li, D., Song, K., Wei, J., Yao, S., Li, Z., et al. (2017). Exosomes Derived from Human Umbilical Cord Mesenchymal Stem Cells Protect against Cisplatin-Induced Ovarian Granulosa Cell Stress and Apoptosis *In Vitro*. *Sci. Rep.* 7, 2552. doi:10.1038/s41598-017-02786-x

Sun, B., Ma, Y., Wang, F., Hu, L., and Sun, Y. (2019). miR-644-5p Carried by Bone Mesenchymal Stem Cell-Derived Exosomes Targets Regulation of P53 to Inhibit Ovarian Granulosa Cell Apoptosis. *Stem Cel Res Ther* 10, 360. doi:10.1186/s13287-019-1442-3

Taheri, M., Saki, G., Nikbakht, R., and Eftekhari, A. R. (2021). Bone Morphogenetic Protein 15 Induces Differentiation of Mesenchymal Stem Cells Derived from Human Follicular Fluid to Oocyte-Like Cell. *Cell Biol Int* 45, 127–139. doi:10.1002/cbin.11475

Takehara, Y., Yabuuchi, A., Ezoe, K., Kuroda, T., Yamadera, R., Sano, C., et al. (2013). The Restorative Effects of Adipose-Derived Mesenchymal Stem Cells on Damaged Ovarian Function. *Lab. Invest.* 93, 181–193. doi:10.1038/labinvest.2012.167

Thakur, M., Feldman, G., and Puscheck, E. E. (2018). Primary Ovarian Insufficiency in Classic Galactosemia: Current Understanding and Future Research Opportunities. *J. Assist. Reprod. Genet.* 35, 3–16. doi:10.1007/s10815-017-1039-7

Trachana, V., Petrakis, S., Fotiadis, Z., Siska, E. K., Balis, V., Gonos, E. S., et al. (2017). Human Mesenchymal Stem Cells with Enhanced Telomerase Activity Acquire Resistance against Oxidative Stress-Induced Genomic Damage. *Cytotherapy* 19, 808–820. doi:10.1016/j.jcyt.2017.03.078

Trombly, D. J., Woodruff, T. K., and Mayo, K. E. (2009). Roles for Transforming Growth Factor Beta Superfamily Proteins in Early Folliculogenesis. *Semin. Reprod. Med.* 27, 14–23. doi:10.1055/s-0028-1108006

Truman, A. M., Tilly, J. L., and Woods, D. C. (2017). Ovarian Regeneration: The Potential for Stem Cell Contribution in the Postnatal Ovary to Sustained Endocrine Function. *Mol. Cell. Endocrinol.* 445, 74–84. doi:10.1016/j.mce.2016.10.012

Ulin, M., Cetin, E., Hobeika, E., Chugh, R. M., Park, H.-S., Esfandyari, S., et al. (2021). Human Mesenchymal Stem Cell Therapy and Other Novel Treatment Approaches for Premature Ovarian Insufficiency. *Reprod. Sci.* 28, 1688–1696. doi:10.1007/s43032-021-00528-z

van Kasteren, Y. M., von Blomberg, M., De Koning, C., Lambalk, N., Van Montfrans, J., Schoemaker, J., et al. (2000). Incipient Ovarian Failure and Premature Ovarian Failure Show the Same Immunological Profile. *Am. J. Reprod. Immunol.* 43, 359–366. doi:10.1111/j.8755-8920.2000.430605.x

Wagner, W. (2019). The Link Between Epigenetic Clocks for Aging and Senescence. *Front. Genet.* 10, 303. doi:10.3389/fgene.2019.00303

Wang, H., Chen, L., Liu, Y., Luo, B., Xie, N., Tan, T., et al. (2016). Implantation of Placenta-Derived Mesenchymal Stem Cells Accelerates Murine Dermal Wound Closure through Immunomodulation. *Am. J. Transl Res.* 8, 4912–4921.

Wang, Z., Wang, Y., Yang, T., Li, J., and Yang, X. (2017). Study of the Reparative Effects of Menstrual-Derived Stem Cells on Premature Ovarian Failure in Mice. *Stem Cel Res Ther* 8, 11. doi:10.1186/s13287-016-0458-1

Wang, P., Lu, Y., Chen, S., Chen, Y., Hu, C., and Zuo, Y. (2018). Protective Function of Bu Shen Huo Xue Formula on the Immunity of B6AF1 Mice with Experimental Autoimmune Premature Ovarian Failure. *Exp. Ther. Med.* 15, 3302–3310. doi:10.3892/etm.2018.5804

Wang, Z., Wei, Q., Wang, H., Han, L., Dai, H., Qian, X., et al. (2020). Mesenchymal Stem Cell Therapy Using Human Umbilical Cord in a Rat Model of Autoimmune-Induced Premature Ovarian Failure. *Stem Cell Int* 2020, 3249495. doi:10.1155/2020/3249495

Webber, L., Webber, L., Davies, M., Anderson, R., Bartlett, J., Braat, D., et al. (2016). ESHRE Guideline: Management of Women with Premature Ovarian Insufficiency. *Hum. Reprod.* 31, 926–937. doi:10.1093/humrep/dew027

Wei, Y., Fang, J., Cai, S., Lv, C., Zhang, S., and Hua, J. (2016). Primordial Germ Cell-like Cells Derived from Canine Adipose Mesenchymal Stem Cells. *Cel Prolif.* 49, 503–511. doi:10.1111/cpr.12271

Woods, D. C., and Tilly, J. L. (2012). The Next (Re)generation of Ovarian Biology and Fertility in Women: Is Current Science Tomorrow's Practice? *Fertil. Sterility* 98, 3–10. doi:10.1016/j.fertnstert.2012.05.005

Xia, X., Yin, T., Yan, J., Yan, L., Jin, C., Lu, C., et al. (2015). Mesenchymal Stem Cells Enhance Angiogenesis and Follicle Survival in Human Cryopreserved Ovarian Cortex Transplantation. *Cel Transpl.* 24, 1999–2010. doi:10.3727/096368914x685267

Xiang, J., Jiang, T., Zhang, W., Xie, W., Tang, X., and Zhang, J. (2019). Human Umbilical Cord-Derived Mesenchymal Stem Cells Enhanced HK-2 Cell Autophagy through MicroRNA-145 by Inhibiting the PI3K/AKT/mTOR Signaling Pathway. *Exp. Cel. Res.* 378, 198–205. doi:10.1016/j.yexcr.2019.03.019

Xiao, G. Y., Cheng, C. C., Chiang, Y. S., Cheng, W. T., Liu, I. H., and Wu, S. C. (2016). Exosomal miR-10a Derived from Amniotic Fluid Stem Cells Preserves Ovarian Follicles after Chemotherapy. *Sci. Rep.* 6, 23120. doi:10.1038/srep23120

Yan, L., Wu, Y., Li, L., Wu, J., Zhao, F., Gao, Z., et al. (2020). Clinical Analysis of Human Umbilical Cord Mesenchymal Stem Cell Allotransplantation in Patients with Premature Ovarian Insufficiency. *Cell Prolif* 53, e12938. doi:10.1111/cpr.12938

Yang, Z., Du, X., Wang, C., Zhang, J., Liu, C., Li, Y., et al. (2019a). Therapeutic Effects of Human Umbilical Cord Mesenchymal Stem Cell-Derived Microvesicles on Premature Ovarian Insufficiency in Mice. *Stem Cel Res Ther* 10, 250. doi:10.1186/s13287-019-1327-5

Yang, Y., Lei, L., Wang, S., Sheng, X., Yan, G., Xu, L., et al. (2019b). Transplantation of Umbilical Cord-Derived Mesenchymal Stem Cells on a Collagen Scaffold Improves Ovarian Function in a Premature Ovarian Failure Model of Mice. In Vitro *Cell.Dev.Biol.-Animal* 55, 302–311. doi:10.1007/s11626-019-00337-4

Yang, M., Lin, L., Sha, C., Li, T., Zhao, D., Wei, H., et al. (2020). Bone Marrow Mesenchymal Stem Cell-Derived Exosomal miR-144-5p Improves Rat Ovarian Function after Chemotherapy-Induced Ovarian Failure by Targeting PTEN. *Lab. Invest.* 100, 342–352. doi:10.1038/s41374-019-0321-y

Yin, N., Zhao, W., Luo, Q., Yuan, W., Luan, X., and Zhang, H. (2018a). Restoring Ovarian Function with Human Placenta-Derived Mesenchymal Stem Cells in Autoimmune-Induced Premature Ovarian Failure Mice Mediated by Treg Cells and Associated Cytokines. *Reprod. Sci.* 25, 1073–1082. doi:10.1177/1933719117732156

Yin, N., Wang, Y., Lu, X., Liu, R., Zhang, L., Zhao, W., et al. (2018b). hPMSC Transplantation Restoring Ovarian Function in Premature Ovarian Failure Mice Is Associated with Change of Th17/Tc17 and Th17/Treg Cell Ratios through the PI3K/Akt Signal Pathway. *Stem Cel Res Ther* 9, 37. doi:10.1186/s13287-018-0772-x

Yin, N., Wu, C., Qiu, J., Zhang, Y., Bo, L., Xu, Y., et al. (2020). Protective Properties of Heme Oxygenase-1 Expressed in Umbilical Cord Mesenchymal Stem Cells Help Restore the Ovarian Function of Premature Ovarian Failure Mice through Activating the JNK/Bcl-2 Signal Pathway-Regulated Autophagy and Upregulating the Circulating of CD8+CD28− T Cells. *Stem Cel Res Ther* 11, 49. doi:10.1186/s13287-019-1537-x

Yoon, S. Y., Yoon, J. A., Park, M., Shin, E.-Y., Jung, S., Lee, J. E., et al. (2020). Recovery of Ovarian Function by Human Embryonic Stem Cell-Derived Mesenchymal Stem Cells in Cisplatin-Induced Premature Ovarian Failure in Mice. *Stem Cel Res Ther* 11, 255. doi:10.1186/s13287-020-01769-6

Zaher, W., Harkness, L., Jafari, A., and Kassem, M. (2014). An Update of Human Mesenchymal Stem Cell Biology and Their Clinical Uses. *Arch. Toxicol.* 88, 1069–1082. doi:10.1007/s00204-014-1232-8

Zhang, J., Xiong, J., Fang, L., Lu, Z., Wu, M., Shi, L., et al. (2016). The Protective Effects of Human Umbilical Cord Mesenchymal Stem Cells on Damaged Ovarian Function: A Comparative Study. *Biosci. Trends* 10, 265–276. doi:10.5582/bst.2016.01125

Zhang, Y., Xia, X., Yan, J., Yan, L., Lu, C., Zhu, X., et al. (2017). Mesenchymal Stem Cell-Derived Angiogenin Promotes Primodial Follicle Survival and Angiogenesis in Transplanted Human Ovarian Tissue. *Reprod. Biol. Endocrinol.* 15, 18. doi:10.1186/s12958-017-0235-8

Zhang, H., Luo, Q., Lu, X., Yin, N., Zhou, D., Zhang, L., et al. (2018). Effects of hPMSCs on Granulosa Cell Apoptosis and AMH Expression and Their Role in the Restoration of Ovary Function in Premature Ovarian Failure Mice. *Stem Cel Res Ther* 9, 20. doi:10.1186/s13287-017-0745-5

Zhang, J., Yin, H., Jiang, H., Du, X., and Yang, Z. (2020a). The Protective Effects of Human Umbilical Cord Mesenchymal Stem Cell-Derived Extracellular Vesicles on Cisplatin-Damaged Granulosa Cells. *Taiwanese J. Obstet. Gynecol.* 59, 527–533. doi:10.1016/j.tjog.2020.05.010

Zhang, X.-M., Liu, C.-Y., and Shao, Z.-H. (2020b). Advances in the Role of Helper T Cells in Autoimmune Diseases. *Chin. Med. J.* 133, 968–974. doi:10.1097/cm9.0000000000000748

Zhao, L., Chen, S., Yang, P., Cao, H., and Li, L. (2019). The Role of Mesenchymal Stem Cells in Hematopoietic Stem Cell Transplantation: Prevention and Treatment of Graft-Versus-Host Disease. *Stem Cel Res Ther* 10, 182. doi:10.1186/s13287-019-1287-9

Zheng, Q., Fu, X., Jiang, J., Zhang, N., Zou, L., Wang, W., et al. (2019). Umbilical Cord Mesenchymal Stem Cell Transplantation Prevents Chemotherapy-Induced Ovarian Failure via the NGF/TrkA Pathway in Rats. *Biomed. Res. Int.* 2019, 6539294. doi:10.1155/2019/6539294

Zhou, Y., Yamamoto, Y., Xiao, Z., and Ochiya, T. (2019). The Immunomodulatory Functions of Mesenchymal Stromal/Stem Cells Mediated via Paracrine Activity. *J. Clin. Med.* 8, 1025. doi:10.3390/jcm8071025

Conflict of Interest: The authors declare that the research was conducted in the absence of any commercial or financial relationships that could be construed as a potential conflict of interest.

Publisher's Note: All claims expressed in this article are solely those of the authors and do not necessarily represent those of their affiliated organizations, or those of the publisher, the editors and the reviewers. Any product that may be evaluated in this article, or claim that may be made by its manufacturer, is not guaranteed or endorsed by the publisher.

GLOSSARY

ADMSC adipose-derived stem cells
AFMSC amniotic fluid mesenchymal stem cells
akt protein kinase B
AMH anti-mullerian hormone
AMPK adenosine 5'-monophosphate (AMP)-activated protein kinase
AMSC amniotic mesenchymal stem cells
ARE antioxidant response element
AZPAb anti-Zona pellucida antibody
Bax Bcl-2 associated X protein
Bcl-2 B-cell lymphoma-2
b-FGF basic fibroblast growth factor
BDNF brain-derived neurotrophic factor
Bim Bcl-2 interacting mediator of cell death
BMP bone morphogenetic protein
BMSC bone marrow stem cells
CD cluster of differentiation
EGF epidermal growth factorepidermal growth factor
E2 estrogen
EGF epidermal growth factorepidermal growth factor
FGF fibroblast growth factor
FOXO forkhead box O
FSH follicle stimulating hormone
FSHR follicle stimulating hormone receptor
fst homo sapiens follistatin
GC ovarian granulosa cellsgranulosa cells
GC ovarian granulosa cellsgranulosa cells
GCSF granulocyte colony stimulating factor
Gdf growth differentiation factor
HGF hepatocyte growth factor
HOVEC human ovarian endothelial cell
HRT hormone replacement therapy
IDO indoleamine 2,3-dioxygenase
IGF-1 insulin-like growth factors-1
IFN-γ interferon γ
IRAK1 interleukin 1 receptor associated Kinase 1
IL interleukin-10
JNK1 jun n-terminal kinase1
LH luteinizing hormone
LIF interleukin 6 family cytokine
MAPK mitogen-activated protein kinase
MCP monocyte chemotactic protein
Mensc menstrual-derived stem cell
MSC mesenchymal stem cells
MVs microvesicles
MT1 melatonine receptor1
Nanos3 nanos C2HC-type Zinc finger 3
NF-κB nuclear factor kappa-light-chain-enhancer of activated B cells
NK natural killer cell
Nobox NOBOX oogenesis homeobox
NO nitric oxide
NOQ1 NAD(P)H quinone dehydrogenase 1
Nrf2 NF-E2-related factor 2
OGCs ovarian granulosa cells
PARP poly ADP-ribose polymerase
PCNA proliferating cell nuclear antigen
PDCD4 programmed cell death 4
PDMSC placenta-derived mesenchymal stem cells
PGF placental growth factor
PGE2 prostaglandin E2
PGC primordial germ cell
PMSC placenta-derived mesenchymal stem cell
POF premature ovarian failure
PTEN phosphatase and tensin homolog
PI3K phosphatidylinositol-3-kinase
ROS reactive oxygen species
SC stem cell
SOD1 superoxide dismutase 1
TERT telomerase reverse transcriptase
TGF transforming growth factor
th helper T cell
TNF-α tumor necrosis factor-α
TRAF632 receptor associated factor 632
UCMSC umbilical cord mesenchymal stem cells
UCP-2 uncoupling protein-2
VEGF vascular endothelial growth factor
VEGFR vascular endothelial growth factor

Advantages of publishing in Frontiers

OPEN ACCESS
Articles are free to read for greatest visibility and readership

FAST PUBLICATION
Around 90 days from submission to decision

HIGH QUALITY PEER-REVIEW
Rigorous, collaborative, and constructive peer-review

TRANSPARENT PEER-REVIEW
Editors and reviewers acknowledged by name on published articles

Frontiers
Avenue du Tribunal-Fédéral 34
1005 Lausanne | Switzerland

Visit us: www.frontiersin.org
Contact us: frontiersin.org/about/contact

REPRODUCIBILITY OF RESEARCH
Support open data and methods to enhance research reproducibility

DIGITAL PUBLISHING
Articles designed for optimal readership across devices

FOLLOW US
@frontiersin

IMPACT METRICS
Advanced article metrics track visibility across digital media

EXTENSIVE PROMOTION
Marketing and promotion of impactful research

LOOP RESEARCH NETWORK
Our network increases your article's readership